

**A Network-Based Design Synthesis of Distributed Ship Services
Systems for a Non Nuclear Powered Submarine in Early Stage Design**

by

Muhammad Hary Mukti

A thesis submitted for the degree of Doctor of Philosophy

Department of Mechanical Engineering, UCL

2022

Declaration

I, Muhammad Hary Mukti confirm that the work presented in this thesis is my own. Where information has been derived from other sources, I confirm that this has been indicated in the thesis.

Signed:

Abstract

Even though the early-stage design of a complex vessel is where the important decisions are made, the synthesis of the distributed ship service systems (DS3) often relies on “past practice” and simple vessel displacement based weight algorithms. Such an approach inhibits the ability of the concept designer to consider the impact of different DS3 options. It also reduces the ability to undertake Requirements Elucidation, especially regarding the DS3. Given the vital role the many DS3 provide to a submarine, this research considers whether there is a better way to synthesise DS3 without resorting to the detailed design of the distributed systems, which is usually inappropriate at the exploratory stages of design.

The research proposes a new approach, termed the Network Block Approach (NBA), combining the advantages of the 3D physical based synthesis UCL Design Building Block (DBB) approach with the Virginia Tech Architectural Flow Optimisation (AFO) method, when applied to submarine DS3 design. Utilising a set of novel frameworks and the Paramarine CASD tool, the proposed approach also enabled the development of the submarine concept design at different levels of granularities, ranging from modelling individual spaces to various DS3 components and routings. The proposed approach also allowed the designer to balance the energy demands of various distributed systems, performing a steady-state flow simulation, and visualising the complexity of the submarine DS3 in a 3D multiplex network configuration. Such 3D based physical and network syntheses provide potential benefits in early-stage submarine DS3 design.

The overall aim of proposing and demonstrating a novel integrated DS3 synthesis approach applicable to concept naval submarine design was achieved, although several issues and limitations emerged during both the development and the implementation of the approach. Through identification of the research limitations, areas for future work aimed at improving the proposal have been outlined.

Impact Statement

Designing vital distributed ship service systems (DS3), which are quite complex, are very challenging if undertaken in submarine Early Stage Design. The proposed Network Block Approach (NBA) has been demonstrated to enable a network based DS3 synthesis without losing the benefits of a 3D architecturally centred submarine and DS3 synthesis, and the 3D informed dialogue that Paramarine-SURFCON provides. Such a 3D informed dialogue has the potential to greatly improve communicating the design of submarine DS3 to the wider world (stakeholders - wider Navy, Defence, the rest of government and to parliament, the media and the public). This is essential if requirements elucidation is to be achieved in projects producing naval vessels, which are directly funded by public money, unlike most commercial projects.

Although the initial comparison to the broadly realistic but unclassified submarine design data provided has been undertaken, validating the accuracy of sizing of the various DS3 using the proposed approach would require comparison of the sizing results with several real submarine designs. However, given the lack of such detailed data in the public domain due to military or commercially sensitivity, the level of effort to perform such validation would have been significant, if at all possible, in an academic environment. However, in industry, such validation could be undertaken using weight and space breakdown data from previous real submarine designs available to government or other submarine designers to builders.

The proposed NBA has been shown to improve the DS3 synthesis in terms of its 3D physical and logical definitions, which were considered to unlock many potential benefits with regard to aspects of DS3 integrity, maintainability, and supportability of future submarines or complex vessels. At least ten distinct publications could be derived from this research. Three have already been accepted for presentation at forthcoming prestigious conferences in the field of marine design.

As the research was sponsored by the Indonesia Presidential Scholarship, the candidate was felt obliged to comment on the recent submarine sinking in Indonesia. Accordingly, the candidate has published an article in a highly reputable national newspaper and has been interviewed on a national television programme to educate a wider audience about submarine design in Indonesia.

Acknowledgements

I have received support from innumerable people during the course of my PhD, and I would like to specially recognise:

My mother and father for making me the person I am today. My wife, Astrie, and my son, Ansel, for making me feel loved and gave me the confidence that I needed to believe that I could achieve any goal. The infinite support from my sister and my big family in Indonesia.

My primary supervisor, Prof David Andrews, for the wealth of knowledge and making sure I could transform from a professional into an expert in the field of engineering design. My secondary supervisor, Dr Rachel Pawling, for inspiring me by having a strong net presence in the field of warship design. The support from Prof Catriona Savage at the beginning of my PhD journey.

Prof Alan Brown and Prof John van Griethuysen for lending their time and expertise in naval ship design and making the viva examination possible.

NICOP researchers at ONR, Virginia Tech, TU Delft, and the University of Michigan, for the face-to-face meeting at the UCL back then before the COVID pandemic, sharpening my research in the field of naval distributed ship service systems.

Dr Nick Bradbeer and Dr Tom Peach for the opportunity to develop my teaching experience at both the undergraduate and postgraduate levels. My officemates and colleagues in the department of mechanical engineering UCL, the UCL Design Research Centre, and, in particular, the UK MoD marine engineering staff.

Lastly, funding for the research concerning this thesis was provided by the UCL joint scholarship programme and the Indonesia Presidential Scholarship, whose support is gratefully acknowledged.

Table of Contents

Declaration	2
Abstract	3
Impact Statement	4
Acknowledgements	6
Table of Contents	7
List of Figures	13
List of Tables	18
Nomenclature	21
List of Symbols	25
Chapter 1 Introduction	28
1.1 Background	28
1.2 Research Scope and Aim	33
1.3 Outline of the Thesis	34
Chapter 2 State of the Art Design for Distributed Systems	36
2.1 Relevant Distributed Systems Attributes	37
2.1.1 Distributed Systems Framework	37
2.1.2 Design Style in Submarine Systems	40
2.2 Approaches in Submarine Concept Design	42
2.2.1 Decision-Making Process for Complex Vessels	42
2.2.2 A Generic Initial Design Procedure for Submarine	44
2.2.3 The UCL Design Building Block Approach	48
2.3 Approaches in Submarine Distributed Systems Design	53
2.3.1 Traditional Numerical Synthesis	53
2.3.2 Sizing from First Principles	55

2.3.3	Smart Ship Systems Design	55
2.3.4	Network Theory.....	56
2.4	Conclusion and Gap Analysis	65
2.5	Research Aim.....	66
2.6	Research Objectives	67
Chapter 3 Development of the Approach		70
3.1	Network Flow Optimisation Approach	70
3.1.1	Mathematical Description of the Network.....	71
3.1.2	Operational Matrix for the Network Flow Optimisation	72
3.1.3	Edge Loss Scenario in the Network Flow Optimisation.....	82
3.1.4	Conclusion from the Network Flow Optimisation Approach	83
3.2	Initial Implementation of Network to Distributed Systems.....	86
3.2.1	Case Study 3.2.1 Setup	86
3.2.2	Proposed Style Framework.....	88
3.2.3	Traditional Numerical Synthesis of the Case Study	89
3.2.4	Semantic Network Applied to the Case Study.....	93
3.2.5	SUBFLOW Applied to the Case Study	95
3.2.6	Conclusion from the Case Study.....	108
3.3	The Initial DS3 Synthesis Approach.....	109
3.3.1	Case Study 3.3.1 Setup	109
3.3.2	The Initial DS3 Synthesis Approach.....	110
3.3.3	Defining the Problem.....	112
3.3.4	Selection of DS3 Styles.....	113
3.3.5	Submarine DS3 Synthesis	117
3.3.6	Evaluation of the DS3 Candidate Architecture	125
3.3.7	Selecting A DS3 Solution	136

3.3.8	Feedback and Conclusion from the Initial DS3 Synthesis	137
3.4	Conclusion from the Initial Implementation.....	140
Chapter 4	The Network Block Approach	141
4.1	Introduction to the Proposed Approach	142
4.2	Physical Loop Method	146
4.2.1	The Structure of Physical Loop Method	146
4.2.2	Design Granularity and Design Fidelity	149
4.2.3	Types of Design Building Block Objects.....	152
4.2.4	Design Building Block Hierarchical Breakdown.....	153
4.2.5	Distributed Systems Routing Model	156
4.2.6	Naming Convention for Design Building Blocks	158
4.3	Logical Loop Method	163
4.3.1	The Structure of Logical Loop Method	164
4.3.2	SUBFLOW Network Model	165
4.3.3	SUBFLOW Operational Matrix	166
4.3.4	SUBFLOW Multiplex Visualisation	169
4.4	Summary of the Proposed Approach	171
Chapter 5	The Approach Applied to a Submarine Study	173
5.1	Case Study 5.1 Setup	174
5.2	Design Development	175
5.3	Power System	190
5.3.1	Fuel System	191
5.3.2	Electrical System.....	194
5.4	Systems for Hydrodynamic Control	203
5.4.1	Propulsion System	203
5.4.2	Hydraulic System	207

5.5	Systems for Hydrostatic Control	213
5.5.1	High-Pressure Air System	214
5.5.2	Low-Pressure Air System	221
5.5.3	Trim and Ballast System	225
5.6	Information Data System	230
5.7	Heat Removal System	234
5.8	Summary of the Application	249
5.9	Numerical Validation of DS3 Sizing Results	258
Chapter 6 Design Experiments		261
6.1	Effect of Varying an Aspect of Ship Performance	262
6.1.1	Case Study 6.1.1 Setup	262
6.1.2	Results from the Performance Study	264
6.2	Effect of Varying Micro Styles on Overall Design	275
6.2.1	Case Study 6.2.1 Setup	275
6.2.2	Results from the Micro Style Study	278
6.3	Effect of Varying Main Styles on Overall Design	287
6.3.1	Case Study 6.3.1 Setup	287
6.3.2	Results from the Main Style Study	291
6.4	Conclusion from Sensitivity Analyses	308
Chapter 7 Discussion		309
7.1	Meeting the Research Aim	309
7.1.1	Improving the Submarine Concept Design	312
7.1.2	Enabling DS3 Synthesis Approach	315
7.2	DS3 Synthesis in the Initial Submarine Design	318
7.2.1	Alternative Design Tools: 2.5D	319
7.2.2	Alternative Design Tools: An Automated Approach	320

7.2.3	The Strategy of the Proposed Approach	323
7.2.4	The Design Building Block Object and the Network Theory ...	326
7.3	The Novel Network Block Approach.....	333
7.3.1	Responsiveness to Design Flexibility	334
7.3.2	Space Reservation for DS3 Routing	337
7.3.3	The Inside-Out Early Submarine Design.....	339
7.3.4	Findings from the Sensitivity Analyses.....	340
7.3.5	Various DS3 Based on Functional Group	341
7.3.6	Basic Taxonomy of Design Detail in the Proposed Approach	343
7.4	Emergent Issues in the Proposed Network Block Approach	345
7.5	The Nature of DS3 Synthesis in Concept Design.....	348
7.6	DS3 Synthesis and Network Optimisation.....	351
Chapter 8 Conclusions and Recommendations		358
References		362
Appendix 1 Body of Knowledge.....		375
Appendix 2 Estimation of Propulsion System		387
Appendix 3 RINA IJME 2021 Journal Paper		392
Appendix 4 Physical Model of DS3 Synthesis		413
A 4.1	Space Model.....	413
A 4.2	Equipment Model.....	414
A 4.3	Connection Model.....	416
A 4.4	Further Design Development.....	420
Appendix 5 Programs in the Network Block Approach		421
A 5.1	Development of the Input Data Centre Tool	421
A 5.1.1	Physical Loop Method.....	421
A 5.1.2	Logical Loop Method.....	426

A 5.2 Description of the Input Data Centre Tool.....	428
A 5.2.1 Main Menu Program.....	428
A 5.2.2 Hull Granularity Program.....	429
A 5.2.3 Volume Granularity Program.....	430
A 5.2.4 Weight Granularity Program.....	432
A 5.2.5 Equipment Database Program.....	432
A 5.2.6 Component Granularity Program	433
A 5.2.7 System Preamble Program	436
A 5.2.8 System Connection Program	438
Appendix 6 Codes	441
A 6.1 VBA Codes	441
A 6.2 MATLAB Codes.....	458
Appendix 7 Analyses of Case Study 5.1.....	475
A 7.1 Stability	475
A 7.1.1 Weight and Space Balance	475
A 7.1.2 Longitudinal Moment and Vertical Stability	482
A 7.1.3 Submerged Equilibrium Analysis	489
A 7.2 Speed	490
A 7.3 Strength	492
A 7.4 Manoeuvrability	494
Appendix 8 Initial Results and System Diagrams.....	495
Appendix 9 Derivation of DS3 of Case Study 5.1.....	506

List of Figures

Figure 1.1: Naval vessels are highly complex products	28
Figure 1.2: Submarine design for different “objectives”	29
Figure 1.3: Example of the complexity of selected distributed systems runs	30
Figure 1.4: Representation of the importance of the front-end design.....	32
Figure 1.5: Overall structure of the thesis	35
Figure 2.1: Schematic of Chapter 2	36
Figure 2.2: Distributed systems framework and its application.....	37
Figure 2.3: The decision making sequence for complex vessels.....	43
Figure 2.4: Traditional numerical initial synthesis for a military submarine	45
Figure 2.5: Logic of the Design Building Block implementation.....	50
Figure 2.6: Gulfs of Execution and Evaluation	51
Figure 2.7: Adjacency matrix definition of a simplex and multiplex network	59
Figure 3.1: Schematic of Chapter 3	70
Figure 3.2: Examples of undirected and directed -weighted networks	71
Figure 3.3: The basic NSMCF network problem	74
Figure 3.4: A network flow solution of the NSCMF network problem.....	81
Figure 3.5: Proposed style framework	88
Figure 3.6: Semantic network of diesel powering sizing algorithm	93
Figure 3.7: Development of the SUBFLOW process.....	96
Figure 3.8: Network sketch of an SSK power system	97
Figure 3.9: SUBFLOW solution for an SSK power system.....	105
Figure 3.10: An overview of an early version of the DS3 synthesis approach	111
Figure 3.11: Energy flow diagram of a typical DC electric drive	114
Figure 3.12: Illustration of different distribution styles for electrical systems	115
Figure 3.13: Energy flow diagram of the PPS study.....	116
Figure 3.14: Submarine DS3 synthesis implementation in Paramarine.....	118

Figure 3.15: Case Study 3.3.1 design progression diagram.....	119
Figure 3.16: A functional group philosophy	123
Figure 3.17: Initial SSK design of Case Study 3.3.1.....	125
Figure 3.18: PPS architecture displayed in Paramarine.....	126
Figure 3.19: Nodes labelling to the PPS architecture.....	128
Figure 3.20: A 3D model and a sketch of the PPS cableway arrangement	131
Figure 3.21: Visualisation of the PPS arcs sizing results	138
Figure 4.1: Schematic of Chapter 4	141
Figure 4.2: The logic of the proposed Network Block Approach.....	143
Figure 4.3: The detailed breakdown of the input data centre	144
Figure 4.4: The structure of the Physical Loop method.....	148
Figure 4.5: Framework of design granularity and fidelity	150
Figure 4.6: A traditional Design Building Block (DBB) hierarchy	154
Figure 4.7: A proposed Design Building Block (DBB) hierarchy.....	154
Figure 4.8: A feature to expand a design building block object	155
Figure 4.9: Example of initial highways visualisation and setup	158
Figure 4.10: The high level tasks performed in the Logical Loop method.....	164
Figure 4.11: Types of nodes and arcs in the Network Block Approach	165
Figure 4.12: Partial London tube network	170
Figure 4.13: Summary of the proposed Network Block Approach.....	172
Figure 5.1: Schematic of Chapter 5	173
Figure 5.2: The logic of the proposed Network Block Approach (NBA)	176
Figure 5.3: Design progress of Case Study 5.1	178
Figure 5.4: Overall DS3 network logic for Case Study 5.1	182
Figure 5.5: Multiplex 3D network of the overall DS3 for Case Study 5.1	183
Figure 5.6: Initial routing in the second step of the Physical Loop method	185
Figure 5.7: The schematic of performing 3D layout arrangement of DS3.....	187
Figure 5.8: Initial highways of Case Study 5.1	188

Figure 5.9: Refined DS3 model in the third step	189
Figure 5.10: Network visualisation of the fuel oil 'FO' system	192
Figure 5.11: SUBFLOW solution of the fuel oil 'FO' system	193
Figure 5.12: The initial model of the fuel oil 'FO' system	193
Figure 5.13: Network visualisation of the electrical 'EL' system	196
Figure 5.14: SUBFLOW solution of the electrical 'EL' system in the snort	199
Figure 5.15: SUBFLOW solution of the electrical 'EL' system in the sprint.....	200
Figure 5.16: The initial model of the electrical 'EL' system.....	202
Figure 5.17: Network visualisation of the mechanical 'ME' system	204
Figure 5.18: SUBFLOW solution of the electrical 'ME' system.....	205
Figure 5.19: The initial model of the mechanical 'ME' system.....	206
Figure 5.20: Network visualisation of the hydraulic 'HY' system.....	210
Figure 5.21: The initial model of the hydraulic 'HY' system	212
Figure 5.22: Network visualisation of the high-pressure air 'HP' system	217
Figure 5.23: The initial model of the high-pressure air 'HP' system.....	220
Figure 5.24: Network visualisation of the low-pressure air 'LP' system	222
Figure 5.25: The initial model of the low-pressure air 'LP' system.....	224
Figure 5.26: Network visualisation of the trim ballast and bilge 'TB' system.....	227
Figure 5.27: The initial model of the trim and ballast 'TB' system.....	229
Figure 5.28: Network visualisation of the data 'DT' system	231
Figure 5.29: The initial model of the information data 'DT' system	233
Figure 5.30: High level relationship between various cooling mediums.....	235
Figure 5.31: Network visualisation of the heat removal system.....	237
Figure 5.32: Parametric cooling demand and volume	239
Figure 5.33: SUBFLOW solution of the air intake 'HV IN' system	241
Figure 5.34: SUBFLOW solution of the exhaust 'HV EX' system	242
Figure 5.35: SUBFLOW solution of the chilled water 'CW' system.....	243
Figure 5.36: SUBFLOW solution for the 'LO' and 'FW' systems.....	244

Figure 5.37: SUBFLOW solution for the seawater cooling 'SW' system.....	245
Figure 5.38: HVHE connection size vs air velocity.....	246
Figure 5.39: The initial model of the heat removal system	248
Figure 5.40: DS3 network response in the snorting operating condition.....	250
Figure 5.41: DS3 network response in the sprint submerged.....	251
Figure 5.42: Multiplex DS3 network response in the snorting	252
Figure 5.43: Multiplex DS3 network response in the sprint submerged.....	253
Figure 5.44: Detailed proposed Network Block Approach (NBA) procedure	256
Figure 5.45: Summary of the output in the Physical Loop method	257
Figure 6.1: Schematic of Chapter 6	261
Figure 6.2: SUBFLOW simulation result for design Variant 6.1.1.A	265
Figure 6.3: SUBFLOW simulation result for Variant 6.1.1.B.....	266
Figure 6.4: SUBFLOW simulation result for design Variant 6.1.1.C	267
Figure 6.5: Physical Loop method result of design Variant 6.1.1.A	271
Figure 6.6: Network comparison of Case Study 6.2.1	277
Figure 6.7: SUBFLOW simulation result for design Variant 6.2.1.B snort.....	280
Figure 6.8: SUBFLOW simulation result for design Variant 6.2.1.B sub.....	281
Figure 6.9: The physical architecture of Case Study 6.2.1	283
Figure 6.10: Node modelling of the Stirling AIP system	287
Figure 6.11: Node modelling of the PEMFC AIP system.....	288
Figure 6.12: The physical architecture of design Variant 6.3.1.B	292
Figure 6.13: The physical architecture of design Variant 6.3.1.C	294
Figure 6.14: SUBFLOW simulation result for design Variant 6.3.1.B snort.....	297
Figure 6.15: SUBFLOW simulation result for design Variant 6.3.1.B sprint.....	298
Figure 6.16: SUBFLOW simulation result for design Variant 6.3.1.B sub.....	299
Figure 6.17: SUBFLOW simulation result for design Variant 6.3.1.C snort	302
Figure 6.18: SUBFLOW simulation result for design Variant 6.3.1.C sprint.....	303
Figure 6.19: SUBFLOW simulation result for design Variant 6.3.1.C sub.....	304

Figure 7.1: A simplified nature of the Computer Aided Ship Design tool	322
Figure 7.2: Decision making CAD processes vs human designer	323
Figure 7.3: A depiction of data flow problem	324
Figure 7.4: A proposed strategy for data flow	325
Figure 7.5: Illustrative types of data	327
Figure 7.6: Hierarchical network of Case Study 3.3.1	327
Figure 7.7: Illustrative 3D network hierarchy of Case Study 3.3.1	328
Figure 7.8: Commonalities between DBB objects and network.....	329
Figure 7.9: Visualisation of numerical sizing relationship	331
Figure 7.10: Major variables	332
Figure 7.11: Illustrative output of the proposed Network Block Approach	334
Figure 7.12: DS3 components arrangement in the 3D layout.....	336
Figure 7.13: DS3 connections in the 3D layout.....	338
Figure 7.14: Illustrative energy flow of various DS3	342
Figure 7.15: Taxonomy of design granularity and design fidelity.....	344

List of Tables

Table 1.1: Description of terminologies.....	31
Table 2.1: Listing of style topics relevant to submarine design	41
Table 2.2: Summary of network theory applications.....	58
Table 2.3: Research objectives.....	67
Table 3.1: The adjacency matrix.....	74
Table 3.2: Node properties of the NSCMF network problem.....	75
Table 3.3: Arc properties of the NSCMF network problem	75
Table 3.4: Linear programming formulation and realisation	77
Table 3.5: The Operational Matrix of the basic NSCMF example.....	80
Table 3.6: Results comparison of an NSCMF network problem	85
Table 3.7: The realisation for Case Study 3.2.1	87
Table 3.8: Baseline submarine payload equipment.....	87
Table 3.9: Summary of calculated prerequisite variables for diesel sizing.....	92
Table 3.10: Summary of variables and algorithms for diesel sizing.....	92
Table 3.11: Nodes properties for an SSK power system network	99
Table 3.12: Arcs properties for an SSK power system network	100
Table 3.13: The adjacency matrix of an SSK power system	101
Table 3.14: The Operational Matrix of an SSK power system.....	104
Table 3.15: Properties of nodes of the SUBFLOW solution	107
Table 3.16: Properties of arcs of the SUBFLOW solution	107
Table 3.17: The realisation for Case Study 3.3.1	110
Table 3.18: An example of power types for various service loads.....	114
Table 3.19: The physical architecture properties of PPS	126
Table 3.20: The adjacency matrix of the PPS study.....	128
Table 3.21: The Operational Matrix of the PPS study	130
Table 3.22: The summary of the power commodity	135

Table 3.23: Sizing results of the PPS study	139
Table 4.1: Summary of programs in the Network Block Approach	145
Table 4.2: Example of numerical data for different types of DBB objects	153
Table 4.3: Naming convention framework as design granularity identifier	159
Table 4.4: Naming convention for weight granularity	160
Table 4.5: Naming convention for volume granularity	161
Table 4.6: Naming convention for component granularity	162
Table 4.7: Two possible ways of using SUBFLOW	163
Table 4.8: The pseudo-Operational Matrix of SUBFLOW	168
Table 5.1: The realisation for Case Study 5.1	174
Table 5.2: List of volume objects of Case Study 5.1	179
Table 5.3: Shape and colour coding for different types of nodes.....	184
Table 5.4: Colour coding and description of arcs	184
Table 5.5: List of nodes for the fuel oil (FO) system.....	192
Table 5.6: List of nodes for the electrical system	195
Table 5.7: List of nodes for the mechanical system	204
Table 5.8: List of nodes for the hydraulic system	209
Table 5.9: List of nodes for the high-pressure air system.....	216
Table 5.10: List of nodes for the low-pressure air system	221
Table 5.11: List of nodes for the trim and ballast 'TB' system	226
Table 5.12: List of nodes of the data system	230
Table 5.13: List of nodes for the heat removal system.....	236
Table 5.14: Weight results for the 2500 data vs Network Block Approach	260
Table 6.1: Scheme for compiling the sensitivity analysis	263
Table 6.2: Summary of Results for Case Study 6.1.1	273
Table 6.3: Normalised results for Case Study 6.1.1	274
Table 6.4: Scheme for compiling the sensitivity analysis	276
Table 6.5: Summary of results for Case Study 6.2.1.....	285

Table 6.6: Normalised results for Case Study 6.2.1	286
Table 6.7: Scheme for compiling the sensitivity analysis	290
Table 6.8: Summary of results for Case Study 6.3.1	306
Table 6.9: Normalised results for Case Study 6.3.1	307
Table 7.1: First part of the strategic view	312
Table 7.2: Second part of the strategic view	315
Table 7.3: Tailored design guidance.....	350

Nomenclature

AC	Alternating Current
ACH	Air Changes per Hour
AFO	Architecture Flow Optimisation
AIP	Air Independent Propulsion
AMS	Auxiliary Machinery Space
ANCR	Advanced Naval Concepts Research
ATG	Automatic Topology Generator
ATP	Air Turbine Pump
ATU	Air Treatment Unit
BB	Building Block
BG	Buoyancy-Gravity (distance between the vertical CoB and the CoG)
BIBS	Built in Breathing System
BPS	Bow Passive Sonar
C	Communications fit
C&RE	Concept and Requirements Exploration
CAD	Computer Aided Design
CASD	Computer Aided Ship Design
CGP	Component Granularity Program
CMS	Command/Combat Management Systems
CoB	Centre of Buoyancy
CoG	Centre of Gravity
CoP	Coefficient of Performance
CPLEX	The IBM CPLEX Optimiser tool
CPU	Central Processing Unit
CW	Chilled Water (system)
DAFO	Dynamic Architecture Flow Optimisation
DAP	Design Analysis Program
DAPO	Design Analysis Program Output
DB	Database (granularity identifier)
DBB	Design Building Block
DC	Direct Current
DDD	Deep Diving Depth
DDSTP	Design/Deep Diving System Test Pressure
DG	Diesel Generator
DGSM	Director General Submarines
DPP	Design Preamble Program
DPPO	Design Preamble Program Output
DRC	Design Research Centre
DS3	Distributed Ship Service Systems
DSSCA	Diving System Self Contained Compressed Air
DT	Data (information system)
DV	Dry Variables (types of volumes)
EDP	Equipment Database Program
EDPO	Equipment Database Program Output

EL	Electrical (system)
EPLA	Electric Power Load Analysis
ESD	Early-Stage Design
ESRDC	Electric Ship Research and Development Consortium
ESSD	Early Stage of Ship Design
EW	Electronic Warfare
FAS	Flank Array Sonar
FF	Free Floods (type of volumes)
FH	Fight (functional group)
FL	Float (functional group)
FMFI	Fight Move Float Infrastructure
FO	Fuel Oil (system)
FPSO	Floating Production Storage and Offloading
FW	Fresh Water (cooling system)
GRC	Graphic Research Corporation
HGP	Hull Granularity Program
HGPO	Hull Granularity Program Output
HP	High-Pressure (air system)
HPAC	High-Pressure Air Compressor
HVAC	Heating Ventilation and Air Conditioning
HVEX	HVAC Exhaust (air exhaust system)
HVHE	HVAC Heat (air heat cooling system)
HVIN	HVAC Intake (air intake system)
HY	Hydraulic (system)
IA	Infrastructure (functional group)
ICABA	Internal Compressed Air Breathing Apparatus
IEP	Integrated Engineering Plant
IFEP	Integrated Full Electric Propulsion
IMDC	International Marine Design Conference
IR	Indiscretion Ratio
KCL	Kernel Command Language
KG	Keel-Gravity (distance between the keel and the vertical CoG)
LCB	Longitudinal Centre Buoyancy
LCG	Longitudinal Centre Gravity
L-PAT	Logical-Physical Architecture Translation
LO	Lubricant Oil (cooling system)
LOX	Liquid Oxidant (tank)
LP	Low-pressure (air system)
M-1	Minus One
MATLAB	Matrix Laboratory (programming language)
MB	Main Ballast (type of volumes)
MBB	Master Building Block
MBT	Main Ballast Tank
MCC	Machinery Control Console
MCD	Minimum Collapse Depth
MCR	Maximum Continuous Rating
ME	Mechanical (propulsion system)

MED	Maximum Excursion Depth
MEL	Machinery Equipment List
MILP	Mixed Integer Linear Programming
MIT	Massachusetts Institute of Technology
MMP	Main Menu Program
MMPO	Main Menu Program Output
MOD	Ministry of Defence
MV	Move (functional group)
MVDC	Medium Voltage DC
NAME	Naval Architecture and Marine Engineering
NAVSEA	Naval Sea Systems Command
NBA	Network Block Approach
NCR	Nominal Continuous Rating
NFO	Network Flow Optimisation
NICOP	Naval International Cooperative Opportunities Program
NL	Numerical (granularity identifier)
NSMCF	Non-Simultaneous Multi Commodity Flow
NSMCPCF	Non-Simultaneous Multi Constraints Parallel Commodity Flow
OD	Outer Diameter
ONR	Office of Naval Research
PCM	Power Conversion Module
PDM	Power Distribution Module
PEMFC	Proton Exchange Membrane Fuel Cell
PG	Power Generation
PGM	Power Generation Module
PH	Pressure Hull
PID	Piping Instrumentation Diagram
PL	Plexus
PM	Propulsion Motor
PMM	Power Motor Module
PPS	Power and Propulsion Systems
PRS	Passive Ranging Sonar
PSD	Preliminary Ship Design
R	Radar
RFOM	Relative Figure of Merit
RM	Room (type of volumes)
RN	(UK) Royal Navy
RNLN	Royal Netherlands Navy
S3D	Smart Ship Systems Design
SBB	Super Building Block
SCC	Ship Control Console
SCP	System Connection Program
SDAC	Submarine Design and Acquisition Course
SDB	Submarine Data Book
SED	Stored Energy Device
SFC	Specific Fuel Consumption
SP	Sonar Passive

SPP	System Preamble Program
SPPO	System Preamble Program Output
SRE	Safety & Rescue Equipment
SSK	Submarine Submarine Killer (non nuclear powered attack submarine)
SSM	Ship Synthesis Model
SSN	Ship Submersible Nuclear (nuclear powered attack submarine)
SUBCODE	Submarine Concept Design
SUBFLOW	Submarine Flow
SUPERB	Submarine Preliminary Exploration of Requirements
SURFCON	Surface Concept
SW	Saltwater (cooling system)
SWBS	Ship Work Breakdown System
TB	Trim and Ballast (systems or type of volumes)
UCL	University College London
UK	United Kingdom
UNDEX	Underwater Explosion
USN	United States Navy
UUV	Unmanned Underwater Vehicles
VAC	Volts Alternating Current (AC)
VAFO	Vulnerability Architecture Flow Optimisation
VBA	Visual Basic for Applications (programming language)
VCB	Vertical Centre Buoyancy
VCG	Vertical Centre of Gravity (CoG) or KG
VGP	Volume Granularity Program
VL	Volume
WGP	Weight Granularity Program
WV	Wet Variable (type of volumes)

List of Symbols

α	Coefficient of the objective function for a cable type A
ACH_{RM}	Air change (per) hour requirement
β	Coefficient of the objective function for a cable type B
b_i	Specific amount of commodity of a node i
\overline{BG}	Distance between the CoB and the vertical CoG or VCG
cp_{air}	Specific heat of air
CoP	Coefficient of performance
$\delta_{i,j}$	Binary variable of an arc i,j
ΔT_{air}	Normal temperature difference between hot and cold sides
D	Battery drain
η_{ME}	Mechanical system efficiency
E	Energy available of each battery cell
$E_{chpercell}$	Energy charging per battery cell
E_n	Energy at a node n
e	Energy coefficient
γ_p	Power flow produced by a path node
γ_s	Power flow produced by a source node
γ_t	Power flow produced by a sink node
H_{pay}	Hotel load for payload equipment
H_{snort}	Hotel load snorting
H_{sub}	Hotel load submerged
$i \in n$	A node I as a subset of a set of nodes a
$(i, j) \in a$	An arc i,j as a subset of a set of arcs a
I_{max}	Maximum current lead/acid battery
$k \in K$	Indexed scenario k as a subset of scenarios K
k_{BAT}	Energy density lead/acid battery
\overline{KG}	Distance between the keel and the vertical CoG or VCG
$\lambda_{i,j}$	Power to volume ratio of an arc i,j
$L(i, j)$	Distance between nodes i and j
$\mu_{i,j}$	Coefficient of the objective function of an arc i,j
m	Margin battery
m_{ch}	Power margin in charging the battery
$k \in K$	Indexed damage scenario m as a subset of scenarios M
\overline{LCB}	Distance between the CoB to the aft perpendicular
\overline{LCG}	Distance between the CoG to the aft perpendicular
LF	Load factor
n	Empirical value lead/acid battery
N_c	Number of cells
$OF_{i,j}$	Objective function value of an arc i,j
P_{Batt}	Stored energy
P_{Conv}	Power converter
P_{DIES}	Diesel generator
P_{Fuel}	Fuel oil
$P_{i,j}$	Power of an arc i,j

P_{HO}	Hotel load
PH_{vol}	Volume of pressure hull
P'_{Motor}	Motor snort
P''_{Motor}	Motor submerged
P_n	Power at a node n
P'_S	Propulsion power at snort speed
P''_S	Propulsion power at submerged speed endurance
P''_{SS}	Propulsion power at sprint submerged speed
$P_{VV_TK}^{snort}$	Power at the fuel nodes in the snorting condition
$P_{VV_TK}^{sprint}$	Power at the fuel nodes in the sprint submerged condition
$P_{EE_SM}^{snort}$	Power required to charge the energy storage or battery in the snorting condition
$P_{SA_DC}^{snort}$	Power demand at the search periscope node in the snorting condition
$P_{AK_DC}^{snort}$	Power demand at the attack periscope node in the snorting condition
$P_{CN_DC}^{snort}$	Power demand at the comms mast node in the snorting condition
$P_{EW_DC}^{snort}$	Power demand at the EW mast node in the snorting condition
$P_{RA_DC}^{snort}$	Power demand at the radar mast node in the snorting condition
$P_{CO_AC_a}^{snort/sprint}$	Power demand at the aft command console nodes in the snorting condition or the sprint submerged condition
$P_{CO_AC_f}^{snort/sprint}$	Power demand at the forward command console nodes in the snorting condition or the sprint submerged condition
$P_{PU_AC}^{snort/sprint}$	Power demand at the CPU nodes in the snorting condition or the sprint submerged condition
$P_{SO_DC}^{snort/sprint}$	Power demand at the sonar nodes in the snorting condition or the sprint submerged condition
$P_{HO_AN}^{snort/sprint}$	Hotel load at the aft node in the snorting condition or the sprint submerged condition
$P_{HO_MN}^{snort/sprint}$	Hotel load at the mid node in the snorting condition or the sprint submerged condition
$P_{HO_FN}^{snort/sprint}$	Hotel load at the forward node in the snorting condition or the sprint submerged condition
$P_{VL_LD}^{snort}$	Power demand at the numerical velocity load node in the snorting condition
$P_{VL_LD}^{sprint}$	Power demand at the numerical velocity load node in the sprint submerged condition
$P_{HY_PT}^{snort/sprint}$	Power demand at the hydraulic plant nodes in the snorting condition or the sprint submerged condition
p_{HY}	Hydraulic working pressure
$P_{HP_CM}^{snort}$	Power demand at the high-pressure air compressor nodes in the snorting condition
$P_{LP_BR}^{snort}$	Power demand at the low-pressure air blower node in the snorting condition
$P_{TB_PP}^{snort/sprint}$	Power demand at the trim and ballast pump nodes in the snorting condition or the sprint submerged condition
p_{DDSTP}	Hydrostatic pressure at the DDSTP depth
p_{loss}	Loss of pressure due to the pipe friction

$P_{HV_HE_RM}^{snort/sprint}$	Heat load at the room nodes in the snorting condition or the sprint submerged condition
$P_{HV_HE_AT_p/s}^{snort/sprint}$	Power demand at the ATU nodes in the snorting condition or the sprint submerged condition
$P_{LO_PT_HX}^{snort}$	Power demand at the LO heat exchangers in the snorting condition or the sprint submerged condition
$P_{CW_PT_HX_p/s}^{snort/sprint}$	Power demand at the CW heat exchangers in the snorting condition or the sprint submerged condition (port or starboard)
$P_{FW_SW_HX_p/s}^{snort/sprint}$	Power demand at the FW-SW heat exchangers in the snorting condition or the sprint submerged condition (port or starboard)
$P_{hub_node}^{snort/sprint}$	Power at hub nodes in the snorting condition or the sprint submerged condition
T_{ch}	Charging time
T_{chmin}	Minimum time to recharge lead/acid battery
T_{DIS}	Discharge time
T_{ops}	Operational time
T_{sub}	Submerged time
$U_{i,j}$	Flow capacity of an arc i,j
\dot{V}_{PT}	Required hydraulic capacity
\dot{V}_{PP}	Volume flow rate required for the trim and ballast pumps
$V_{i,j}$	Volume of an arc i,j
V_{RM}	Volume of the compartment or room
\overline{VCB}	Distance between the VCB and the keel
\overline{VCG}	Distance between the VCG and the keel
x	Margin energy/ power margin during battery discharge
$x_{i,j}$	Flow variable of an arc i,j
$x_{i,n}$	Flow variable from a node i to node n
$x_{n,j}$	Flow variable from a node n to node j
Y_s	Power flow capacity of a source node

Chapter 1

Introduction

1.1 Background

In the product development process, complexity can arise from several intertwining domains. These domains include how requirements are to be met, how the product is to be designed and developed, how organisations involved in the product's design interact and what tools and technologies are incorporated in the design and the product (Danilovic and Browning, 2007). As the size of these domains grows, so does the complexity of the product. Figure 1.1 shows naval vessels are not just complex systems but also physically large (Andrews, 2012).

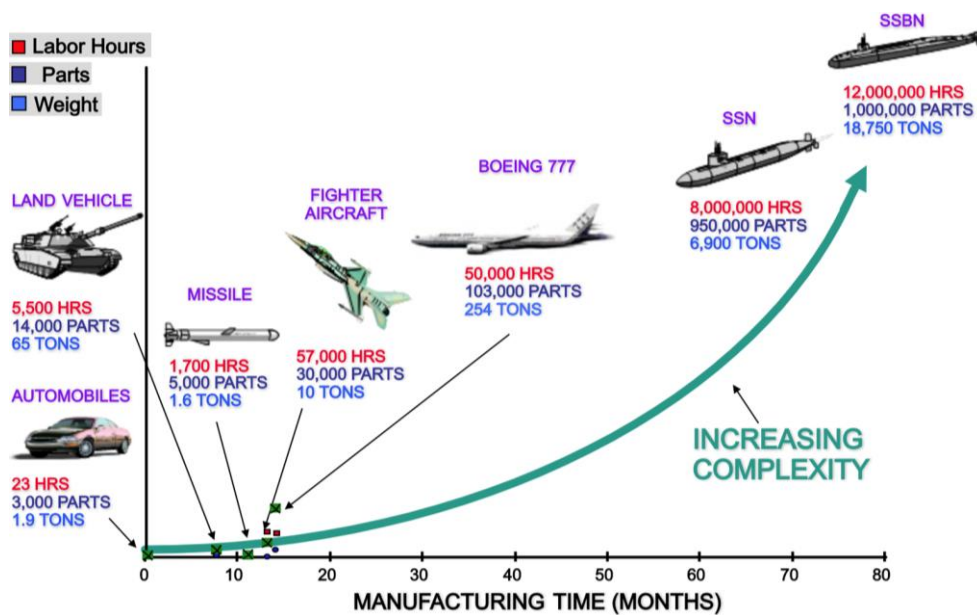


Figure 1.1: Naval vessels are highly complex products (Morais et al., 2018)

The submarine, as a sophisticated naval vessel requires an extremely high quantity of labour hours, parts, and systems with around 350,000 parts, two million design hours, and 700,000 construction hours for a diesel submarine to be assembled (Budell, 2014). The shipbuilder must perform concurrent detailed design, construction, and equipment procurement (Morais et al., 2018). While this can also be the case with large civil and chemical plant construction, naval industries and process are distinctly different to such commercial industries.

Standards for acceptability are important and draw on the demands of the stakeholders (Elliott and Deasley, 2007). Thus, these can be based on how the product (the vessel) would perform and accomplish tasks in the vessel's life. Unlike most commercial projects, all naval projects are funded by public money. Many more stakeholders contribute to formulating the requirements for naval vessels. Often, the requirements for naval vessels are not clear at the beginning of design development (Andrews, 2018b). Besides, there is no absolute measure in warships acquisition which adequately reflects the complexity in the requirements development of naval projects (Andrews, 1981).

Submarines, as a particular demanding example of the naval project, must be designed to satisfy different design stakeholders to meet (sometimes) conflicting requirements (Andrews, 1998). An amusing depiction in Figure 1.2 shows many of the stakeholders in submarine design have conflicting visions, which must be compromised in the submarine designer's eventual design solution. A submarine designer can then be seen as the integrating engineer at the whole boat level who need to understand, appreciate, and balance various sub-specialists engineering disciplines to meet the emergent requirements.

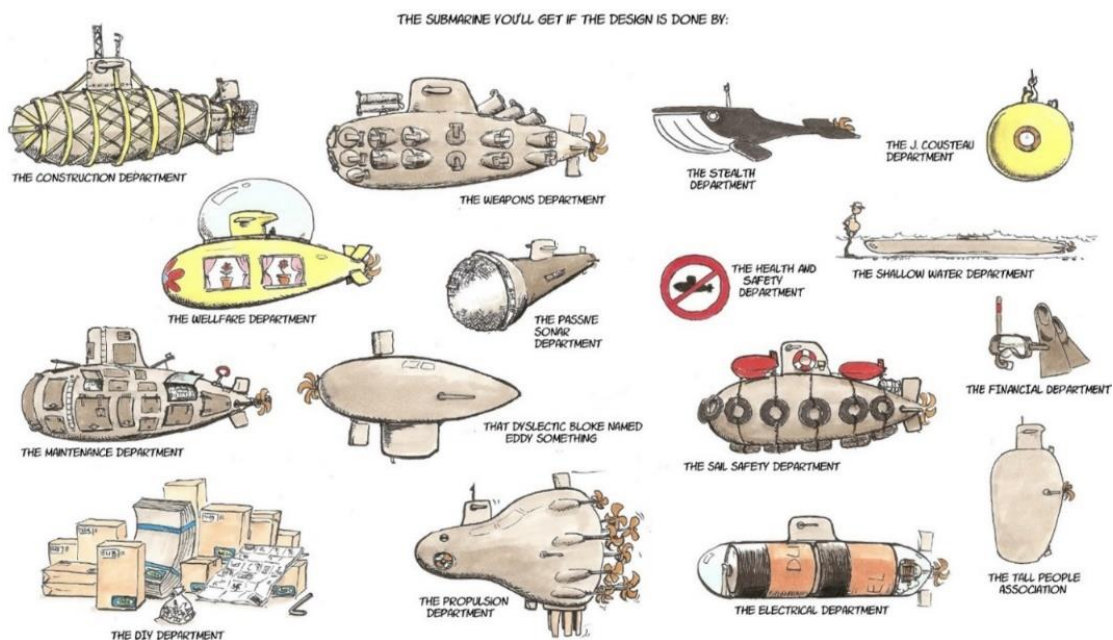


Figure 1.2: Submarine design for different “objectives” due to Commander Boomstra RNLN (Duchateau, 2016)

Part of submarine design complexity is that they are typified by extensive and densely engineered distributed systems (Andrews, 2017) (see Figure 1.3). Submarine systems, distributed systems, or service systems are termed in this thesis as distributed ship service system(s) (DS3), which is “a collection of connected components that provide a service from one or multiple sources to multiple users, via connections throughout the ship, directed towards defined functions, supporting specific operations of the vessel” (Mukti et al., 2021). Therefore, DS3 is composed of two main parts: components and connections.

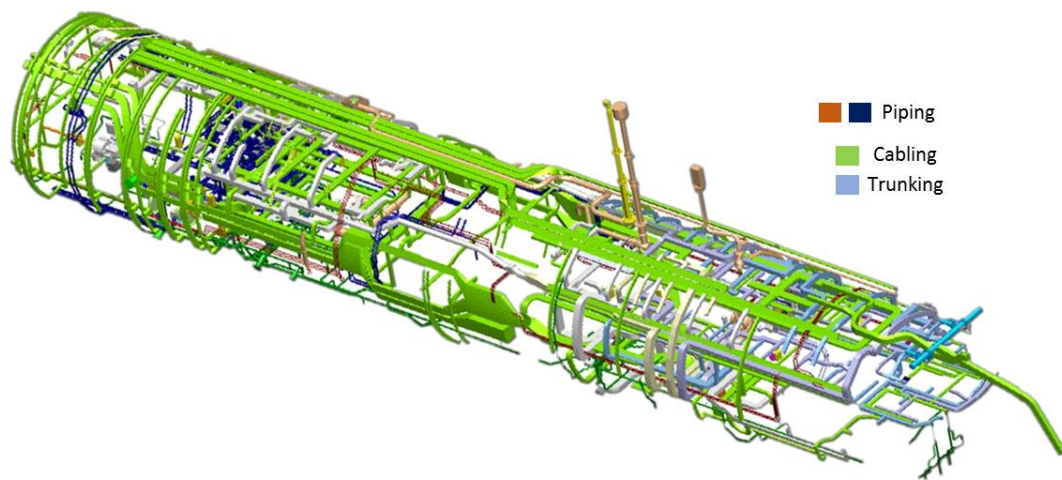


Figure 1.3: Example of the complexity of selected distributed systems runs on the RN ASTUTE Class submarines (Morris and Spinney, 2017), legend added by the candidate (see Figure A.2 and Figure A.3 in Appendix 1 for other examples)

Figure 1.3 shows three different (physical) connections based on the type of commodities distributed: cabling for power, degaussing, and data or information services; trunking or Heating Ventilation and Air Conditioning (HVAC) for atmosphere control; and pipework for many fluid based (liquid or gas) systems, such as hydraulics, high-pressure air system, and water distribution systems. Compared to surface vessels, submarines rely on the quality standards for the DS3 that are akin to those required in high-performance aircraft, yet on a physically larger scale and without prototypes (Andrews, 2017).

Given the importance of the submarine DS3 to safe and effective vessel performance, this raises a major design question. When should aspects important to DS3 be addressed in the overall submarine design?

The submarine design process (as a warship design) generally encompasses various design phases, which may be conducted by different organisation entities (see Table 1.1). The design phases comprise concept, assessment or feasibility, followed by contract or project definition to fix price and check that the selected design remains balanced. This especially applies to the buoyancy and stability balance, even it is more demanding in submarine design than for surface ships, which needs to be done before proceeding to the detailed design (Andrews, 1994). Therefore, as the design progresses, the design knowledge increases along with the confidence in the design.

Table 1.1: Description of terminologies used to describe the stages in warship design (Andrews, 1994)

Terminology	Organisation	Description
Concept Phase	Government led	The exploration of design solution space, the investigation of design drivers, and trade-off studies to meet the initial outline requirements
Feasibility	Government led	One (or occasionally two) solutions are developed to a sufficient level of detail to assess its technical viability, addressing all major technical issues
Ship design and contract definition	Government-Industry	The design is developed to sufficient detail to form the technical content of a contract
Detailed design	Industry	Overlapping with the construction, which involves producing the working definition (drawings, etc.)

In the detailed design phase, the design work is typically conducted by shipbuilders (depending on the contract) and is heavily constrained (Koenig, 2017; Shin, 2017). Detailed design work is a phase where detailed information on DS3 components becomes clear and ready to be manufactured, procured, installed, and tested (Lee et al., 2012). Consequently, in the detailed design phase, it is too late for a submarine design project to conduct trade-off studies, especially for those related to DS3, as it may require significant design changes and thus costly redesign (Tupper, 2013). For that reason, DS3 aspects are best explored, and options are considered when the design is still fluid during the Concept Phase or Early Stage of Ship Design (ESSD). ESSD or Early-Stage Design (ESD) is a generic term that replaces Preliminary Ship Design (PSD), used in earlier UCL papers, as the latter clashes with USN practice where PSD is used for the (UK) Feasibility Assessment Phase.

The main objective of the ESSD of naval vessels is not about producing a preferred solution to meet operational requirements, but rather how to bottom out the problem and to understand what is really wanted and what can be afforded by design stakeholders (Andrews, 2018c). Hence, unlike other design phases, ESSD is an important stage in not only finding design solutions that meet the requirements but also defining the requirements themselves, which has therefore been termed the Requirement Elucidation process (Andrews, 2011). The importance of this process is depicted in Figure 1.4, where design decision making in ESSD has the most significant impact, while the greatest uncertainty, minimum information, and elucidating design requirements between design stakeholders takes place (Andrews, 2018a).

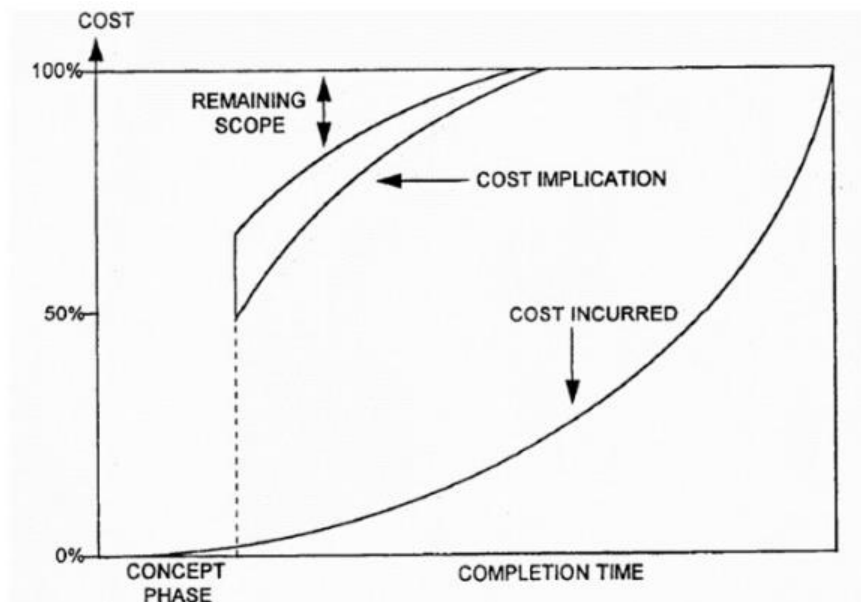


Figure 1.4: Representation of the importance of the front-end design (Andrews, 1993)

ESSD, encompassing three overlapping stages defined by Andrews (1994), aims to achieve the Requirement Elucidation process: Concept Exploration; Concept Studies; and Concept Design. Concept Exploration is a stage where a wide-ranging divergent phase of exploration in which initial ideas on solutions to meet the initial outline requirements should be explored. Such an exploration could be based on the design solution space, in which Andrews (2018c) would have three main axes: capability, related to the S^4 performance (Brown and

Andrews, 1980); packaging, the operational capacity of the vessel; and technology, the overall technology incorporated in the design. Then some selected designs are developed in a sufficient level of detail to conduct Concept Studies to investigate issues that are likely to be significant size or cost drivers in the design (see different types of cost in Figure A.1, Appendix 1). Before the Feasibility Phase, Concept Design is conducted to be working up the selected baseline design or possibly two distinct competing options by performing trade-off studies of cost-capability and highlighting design risks.

Even though the ESSD of the complex vessel is the phase to address major DS3 choices in the design process, in the initial sizing and submarine synthesis, reliance is often made on “past practice” and simple vessel displacement based weight algorithms. Such a type ship approach not only inhibits the ability of the concept designer to consider the impact of different DS3 options but also ignores the opportunity (or necessity) to undertake Requirements Elucidation, more specifically for DS3 (Andrews, 2018c). Thus, the time has to come to consider whether advances in CASD will enable greater consideration of DS3, given they are a crucial design feature of submarines. However, this does not mean the ESSD must ‘bottom out the preferred design’ for DS3 synthesis. Therefore, this research aims to propose a novel approach that allows DS3 synthesis to be addressed in ESSD without resorting to the detailed design of the distributed ship service systems, which is usually inappropriate at the exploratory stages of design.

1.2 Research Scope and Aim

Applicability of the Research

The research into CASD outlined in this thesis is focused on the issues of synthesising DS3 in ESSD, when a wide-ranging set of solutions may be investigated. However, without the Requirement Elucidation interactions in a real design environment, this research study cannot constitute a fully realised concept phase as described by Andrews (1994). Furthermore, this thesis does not encompass the downstream issues of DS3 procurement or detailed

engineering design, where the selected design solution is developed to a very high level of detail. Although the proposed approach may have applicability to submarine design in general, the first demonstration is limited to a specific style choice, which is the non nuclear powered submarine design (Mukti and Randall, 2017). Hence, this thesis specifies a proposed approach that would improve the submarine DS3 synthesis process in ESSD.

Research Approach

The proposed Network Block Approach has been demonstrated to fill the gap by providing a less constraining approach and combining the advantages of the sophisticated 3D based architecturally centred submarine synthesis and the 3D network based DS3 synthesis approach. Thus, with the proposed approach, conducting 3D submarine design studies were plausible in a practical timeframe and there was improved flexibility provided by the DS3 network based synthesis. This then permitted a more radical ideas exploration in the future submarine concept design as part of elucidating requirement intent.

Thesis Aim

The main aim of this thesis is to demonstrate a novel approach that improves the traditional DS3 synthesis in ESSD to allow a more effective Requirement Elucidation process. It also describes the nature of the DS3 synthesis process that results from this demonstration and proposes directions for future development, which could enhance the effectiveness of the proposed approach to improve submarine ESD.

1.3 Outline of the Thesis

The thesis is divided into eight chapters with separate appendices providing additional material relevant to specific sections, as shown in Figure 1.5. This includes, at Appendix 3, a published journal paper, which the candidate co-authored with his supervisors. The first chapter provides the background of the research and relevant diagrams outlined in Appendix 1. Chapter 2 provides the State-of-the-Art Review in the field of submarine design and DS3 synthesis,

which ended by the justified aim and the (sub) objectives as the key performance indicators of the research. Appendix 1 is not only a supplement to Chapters 1 and 2 but also to Appendix 8 for developing a set of DS3 baseline designs. Chapter 3 presents an investigation of existing approaches to synthesising DS3 through some case studies, which are supported by three Appendices (2, 3, and 4). This leads into Chapter 4, which outlines the proposed approach. The proposed approach was first applied to a baseline design as demonstrated in Chapter 5 and then applied to a range of design options in Chapter 6. Supporting appendices (7, 8, and 9) are given to provide a full demonstration of the proposed approach. The discussion in Chapter 7 brings together the issues raised in Chapter 2 with the proposed approach from Chapter 4, and the experience of demonstrating the proposed approach in Chapters 5 and 6. From these discussions, conclusions are drawn in Chapter 8, including recommended future work.

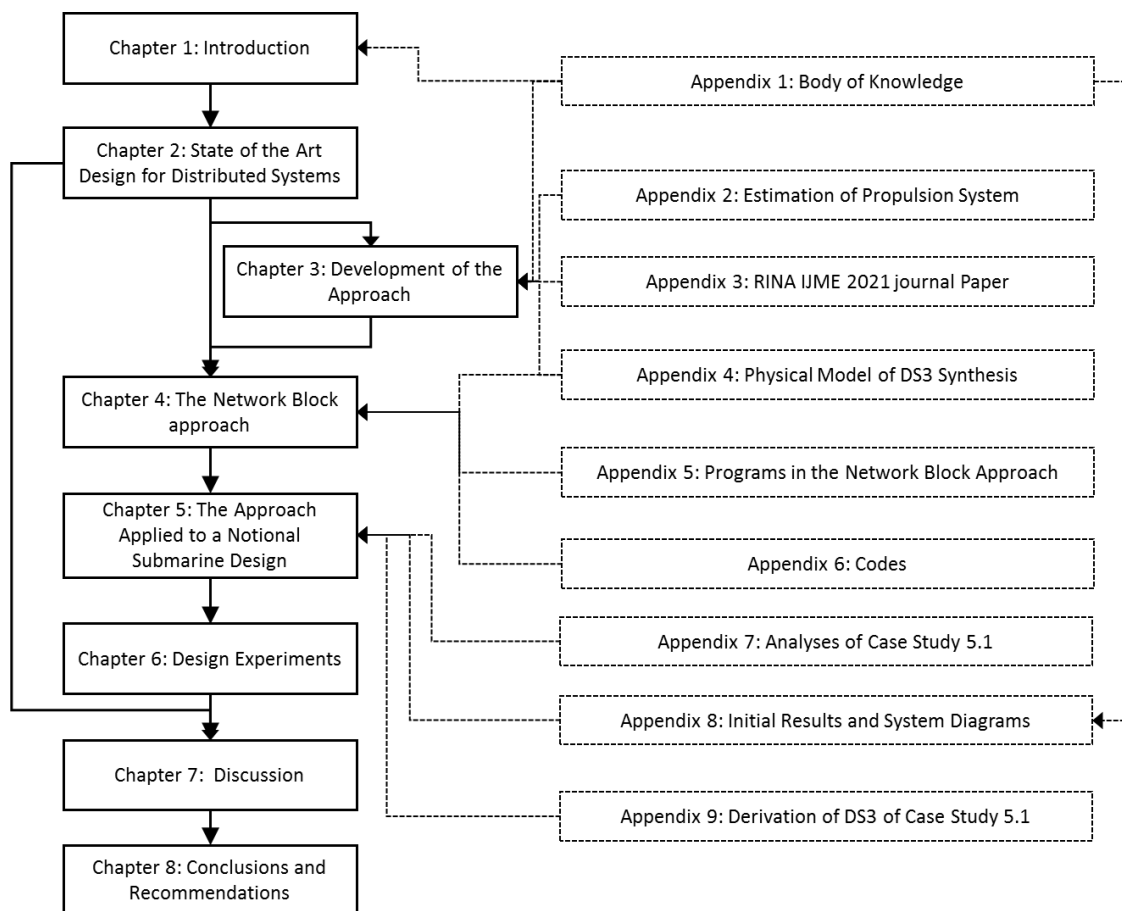


Figure 1.5: Overall structure of the thesis

Chapter 2

State of the Art Design for Distributed Systems

The novel problem specified in the introduction implies that the development of an approach to DS3 synthesis for submarines is the primary goal of this research. To answer such a problem, the state of the art is reviewed in the two main parts of this chapter (see Figure 2.1). The first four sections of this chapter give an overview of the investigations carried out to justify the overall aim of the research. The last two sections outline the justified aim and the (sub) objectives as the key performance indicators of the research.

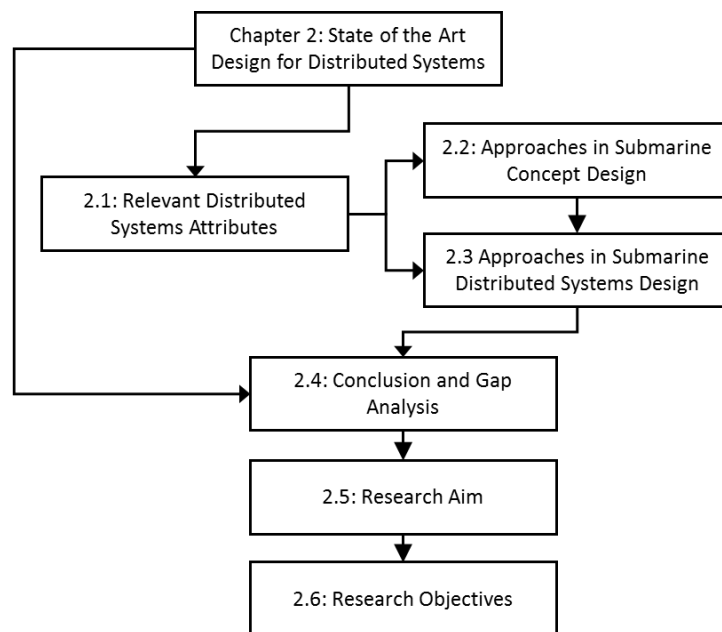


Figure 2.1: Schematic of Chapter 2

Section 2.1 discusses the aspects important to submarine systems that are relevant and able to be investigated early in the design process. Section 2.2 investigates how those aspects could be considered through adopting various design synthesis approaches. Section 2.3 evaluates different methods specific to designing submarine systems that are commensurate with doing so in ESSD. Lastly, Sections 2.4 to 2.6 highlight the knowledge gap in the design for distributed systems research as well as some potential approaches that could be developed to aid DS3 synthesis much earlier in the submarine design Concept Phase.

2.1 Relevant Distributed Systems Attributes

This section is devoted to specifying what aspects are important to the development of submarine systems as previously stated to be the main concern of the research. It is divided into two subsections. Subsection 2.1.1 discusses an approach to define different views of DS3 while Subsection 2.1.2 outlines the issue of design style as a governing attribute in any consideration of DS3.

2.1.1 Distributed Systems Framework

The Naval International Cooperative Opportunities Program (NICOP), funded by the US Navy Office of Naval Research (ONR), involved the University of Michigan, TU Delft, Virginia Tech, and UCL in a five-year collaborative research project started in 2015 and focused on naval surface ships distributed ship services survivability (Pawling et al., 2013). The team proposed an architectural framework for DS3 (Brefort et al., 2018). The framework is given in Figure 2.2 (left) and the example of its application to a surface ship, Figure 2.2 (right).

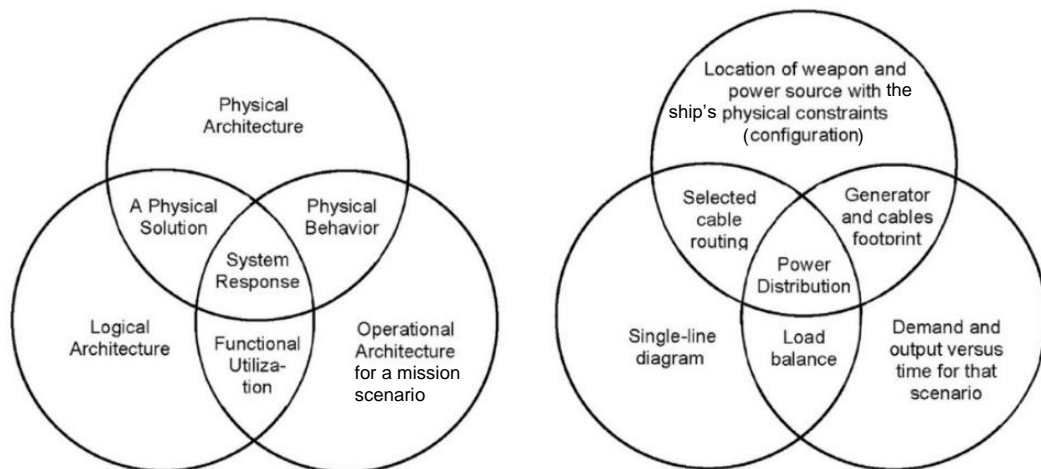


Figure 2.2: Distributed systems framework and its application for a typical surface ship naval combatant for a given DS3 in a given operational scenario, after (Brefort et al., 2018).

In Figure 2.2, there are three types of architectures:

- *Physical Architecture* gives DS3 volumes and locations, i.e., the physical definition of the system in the vessel's design layout. This representation

shows the interaction of distributed systems with the vessel's spatial definition;

- *Logical Architecture* defines the functional relationship of DS3 components, i.e., how various DS3 components are connected towards functions, for example, a system line diagram or a logic similar to the system topology defined by de Vos (2018). The interaction between the distributed systems is depicted by this architecture;
- *Operational Architecture* focuses on temporal relationships i.e., functions of the various DS3 with respect to time to meet the capacity demands or produced for a specific operational scenario.

In Figure 2.2, there are also interactions between the three logics above. *Physical Solution* being the medium or way for the transported service on the vessel, such as cable routing for power. *Physical Behaviour* is the resultant of DS3 components and connections due to the specific system demand for a particular scenario. An example of this is the size of the generator and the size of the cables driven by power demand for that operational scenario. *Functionalisation* gives the balance indication in the context of supply-demand of service between its DS3 components, such as electrical load balance for the case of distributed ship electrical power in a specific (action) scenario. Finally, *System Response* provides the flow configuration of a specific DS3 (electrical power) in response to an operational scenario. The power distribution (flow) in a specific operational scenario is the instance of the specific *System Response* in Figure 2.2 (right).

Nonetheless, there is an issue related to this framework, namely as to whether the physical architecture is that which constrains the DS3 through the architecture of the whole ship, or is just describing the physical architecture of DS3 dependant on the ship's architecture. How these architectures combine in a scenario remains unclear and thus the NICOP team are pursuing this logic further. In this research, the main three architectures, more specifically, physical architecture and logical architecture were considered applicable to broadly describe DS3 components and connections of a submarine for the three different views of abstraction.

The physical architecture of the DS3 in submarine design is one of the most important aspects to ensure not only space and weight (numerical) balance, but also to ensure achievement of submarine's stability at the Concept Phase, e.g., vertical balance and longitudinal balance. Any changes in DS3 size and locations would also change the Centre of Gravity ($\overline{KG/LCG}$) as well as the \overline{BG} (distance between the centre of buoyancy $\overline{LCB/VCB}$ and overall $\overline{KG/LCG}$), and thus makes submarine design 'highly tuned', i.e., highly sensitive compared to surface ship design (Andrews, 2017a). This suggests that the physical architecture of the submarine's DS3 could affect the size of the whole submarine design as well as its performance to a more significant degree than is the case in most surface vessels.

In parallel, the logical architecture of the DS3 in submarine design can capture the configuration of the submarine's DS3 in a higher 'helicopter' view not obvious from physical models, revealing the complexity of the interactions between different distributed systems on a submarine. In this architecture, a certain DS3 configuration, such as a ring main configuration, typically adopted for a submarine's high-pressure air system (Burcher and Rydill, 1994), can be visualised in a more direct manner. It also allows a clear representation of the DS3 level of redundancy without resorting to a more detailed DS3 layout (physical architecture), which could overwhelm the focus at the submarine Concept Phase, since the submarine design is broadly some three times more densely engineered than most surface vessels (Andrews, 2017a).

The size of the submarine's DS3 will be driven by the operational architecture, which defines how much power demand and output of DS3 components in a given operational scenario appropriate to that distributed system. One of the approaches to derive this information is in the case of distributed electrical power where use is made of an Electric Power Load Analysis (EPLA), which analyses the load factors based on per cent time in operation (Wolfe and Roa, 2017). Due to the inadequacy of such information for submarines in the open literature, it was concluded that the electrical load factors for a submarine's DS3 components needed to be assumed or, better, derived from surface ship practice.

The discussion above suggests that the physical architecture, logical architecture, and operational architecture of the submarine's various DS3 can play an important role in Early Stage submarine design and thus need to be considered concurrently at these earliest design stages. All three architectures are also driven by what has been termed as 'style' (Brown and Andrews, 1980) decisions relevant to individual DS3, which are made by the designer at the ESSD as is discussed in the next subsection.

2.1.2 Design Style in Submarine Systems

In the initial sizing of complex vessels, there are front-end decisions that are traditionally implicit but should be included in a properly conducted Requirement Elucidation process (Andrews, 2018c). These decisions are very important because they will drive the final chosen design solutions (Andrews, 2018c). It can also influence the ship design 'traditional naval architecture' S⁴ primary concerns (Brown and Andrews, 1980): Speed, Strength, Stability, and Seakeeping (although manoeuvrability is a more appropriate concern for the submarine design than that of Seakeeping). Brown & Andrews (1980) saw this gap and thus introduced the term 'style' to be the 5th S with the S⁴ to accommodate such important decisions in the Requirement Elucidation dialogue appropriate to the design of complex vessels. Andrews (2018a) has then proposed different style decisions, which are categorised into several levels: transversal; macro; major; and micro. There is also a non-design driven choice, i.e., a government selection, which is classified as a "Mega Style" choice (Andrews, 2021).

The transversal style decision, as proposed by Andrews (2017b), is a decision that cuts across the engineering disciplines involved in a ship design, for example, the level of survivability. The macro style decision denotes the overall style of a design, such as the configuration of the hull design (Andrews, 2018c). Going down to major level was seen by Andrews to cover a set of aspects as specified examples in six categories (see Table 2.1) for these aspects, many of which are not readily quantifiable (Andrews, 2012), including the micro style decision, which could encompass many style choices on DS3. This suggests

that a framework of style decisions needs to be developed, given there are many style decisions related to DS3.

Table 2.1: Listing of style topics relevant to submarine design (Andrews, 2021)

Stealth	Protection	Human Factors	Sustainability	Margins	Design style
Acoustic signature	Underwater weapon effect	Accommodation & Escape	Mission duration	Space	Robustness
Magnetic	Fire	Access	Watches	Weight	Adaptability
Infra-red	Shock	Maintenance levels	Stores	Vertical & Longitudinal centre of gravity	Modularity
Radar cross section	Damage control	Operation automation	Maintenance cycles	Power	Operational serviceability
Visual	Collision	Ergonomics	Refit philosophy	Services	Producibility
	Above water Weapon effect		Upkeep by exchange	Board Margin (future upgrades)	
	Corrosion				

Harbour (2001) presented an evaluation and comparison of various choices on electric propulsion motors (and their associated components) in terms of quantitative attributes (space and weight) and qualitative attributes (reliability and technology risk) using a nuclear submarine as the baseline design. Although this research only considered the propulsion system of a specific submarine design style (nuclear), it does suggest that the style choice at the systems components level can potentially give a significant impact on the whole submarine size. Although it is not obvious whether these numbers only refer to the components or the compartments to contain the components that are useful to the designer in designing submarine, Harbour quotes more than 40% weight and 16% volume reduction due to incorporation of electric based rather than mechanical based propulsion systems in the nuclear submarine design example. Therefore, the ability to consider the impact of different DS3 style choices in submarine Concept Design could be said to be doubly important. The next section, in turn, discusses how existing design approaches could facilitate this.

2.2 Approaches in Submarine Concept Design

This section reviews various approaches to ship design synthesis and how they could not only allow DS3 synthesis but could also enable aspects important to DS3 to be considered in ESSD. The first subsection discusses the whole ship design process for complex vessels. Moving on, a design procedure specific to submarine design is outlined. This is followed by a review of sophisticated design synthesis, the UCL Design Building Block (DBB) approach (Andrews et al., 1996), which has put architecture at the centre of the process. Each design approach is discussed while focusing on how it could tackle the early design of distributed systems as outlined in Section 2.1.

2.2.1 Decision-Making Process for Complex Vessels

Having specified in Subsections 2.1.1 and 2.1.2 the aspects important to DS3, this has shown that many important submarine design decisions are made either consciously or unconsciously in the Concept Phase. However, the issue is that such major design decisions are often not questioned nor acknowledged by design stakeholders, furthermore such decisions should be subject to investigation in a properly conducted Requirement Elucidation process (Andrews, 2018c). Andrews (2018c), in turn, has long proposed the whole ship design process given in Figure 2.3, which does not just list sequential tasks in the ship design process but also encapsulates major decisions the designer must take to undertake those tasks.

Figure 2.3 shows the approach commenced by the need to build a new ship. For naval vessels, it could be originated from the identification of a gap in the Navy's operational capability (Chalfant, 2015). This Step 1 is followed directly by a formulation of a set of putative and broad requirements to begin the design process (Step 2), which can include some initial whole ship performance, such as design or Deep Diving Depth (DDD), accommodation, and patrol endurance. The third step of the approach for a given distinct design option is the selection of relevant style, as discussed in Subsection 2.1.2. Next, the selection of major equipment can be derived in Step 4. Step 4 also indicates the importance of the quality of the (equipment) database, especially those related to major

equipment. The initial set of broad requirements from Step 2 can then be derived to select the traditional naval architecture S⁴ measures as well as Step 5 for the next level of style (more specific of major style choices). Step 6 is the selection of the synthesis model based on the type of ship design in terms of design novelty (e.g., simple synthesis or architectural synthesis see Table 3 in (Andrews, 2018c)).

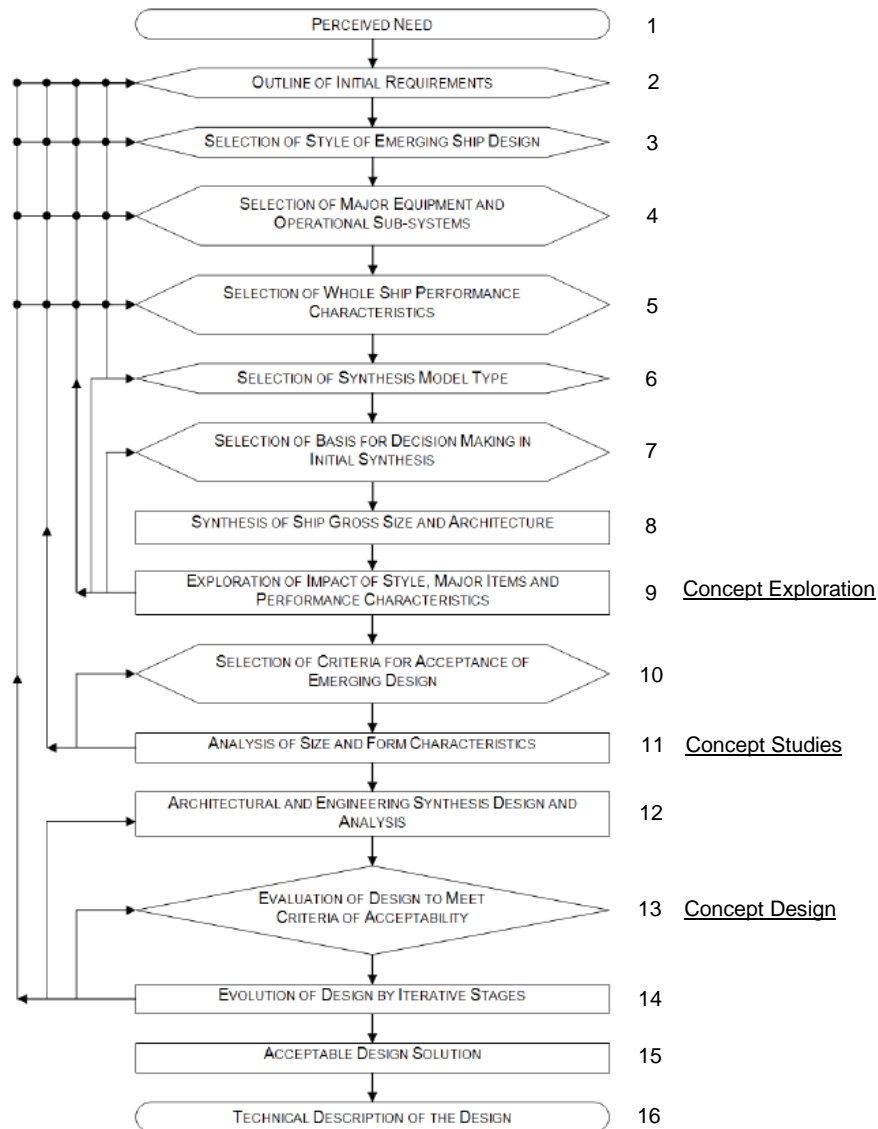


Figure 2.3: The decision making sequence for complex vessels outlined in detail in Figure 4 and Appendix A of (Andrews, 2018c) in a similar manner to the submarine example in Figure 4 of (Andrews, 2021)

Before one or more design studies or options (e.g., nuclear or non nuclear) or variants (e.g., the number of torpedo tubes) are produced in Step 8, the basis

of decision making in initial synthesis has to be made in Step 7 and this should be beyond numerical weight and space balance, as strongly proposed by Andrews (2018c). Such a broad decision making or selection also determines how detailed the design needs to be to inform such issues, which should emerge from the Requirement Elucidation dialogue with the requirement owner and preferably design stakeholders. As already discussed in the introductory chapter (Section 1.1), the Concept Exploration is indicated in Step 9 of Figure 2.3, while the Concept Studies and Concept Design are reflected in Steps 11 and 13, respectively. The rest of the steps of Figure 2.3 highlight the full Concept Phase activities and even go beyond the Concept Phase (see Table 1.1 on page 31).

The first nine steps in the ‘decision making’ approach summarised in Figure 2.3 cover the ESD scope of the research, as stated in Section 1.2. The next subsection discusses design approaches that could potentially accommodate both the synthesis of the whole submarine as well as that for the DS3. This leads to a discussion of the selection of the synthesis model type, which is Step 6 in the ‘decision making’ approach (Figure 2.3).

2.2.2 A Generic Initial Design Procedure for Submarine

The approach to initial submarine synthesis used at UCL for the annual post-MSc submarine design and acquisition course (SDAC) (UCL, 2021) was adopted from a sequential design procedure given by Burcher & Rydill (1994). The procedure, as is shown in Figure 2.4, begins with an initial set of broad requirements to initiate the process. From these initial requirements, a set of payload equipment can be selected, which then gives a first numerical indication of likely submarine size. As such it can then be used to parametrically estimate the size of component design features based on mathematical relationships with coefficients suggested by Burcher and Rydill (1994) or scale based on the UCL submarine data (UCL-NAME, 2014). The UCL submarine data consists of fictitious but not unrealistic submarine data and declassified equipment database from the UK MoD - Director General Submarines (DGSM) (UCL-NAME, 2014).

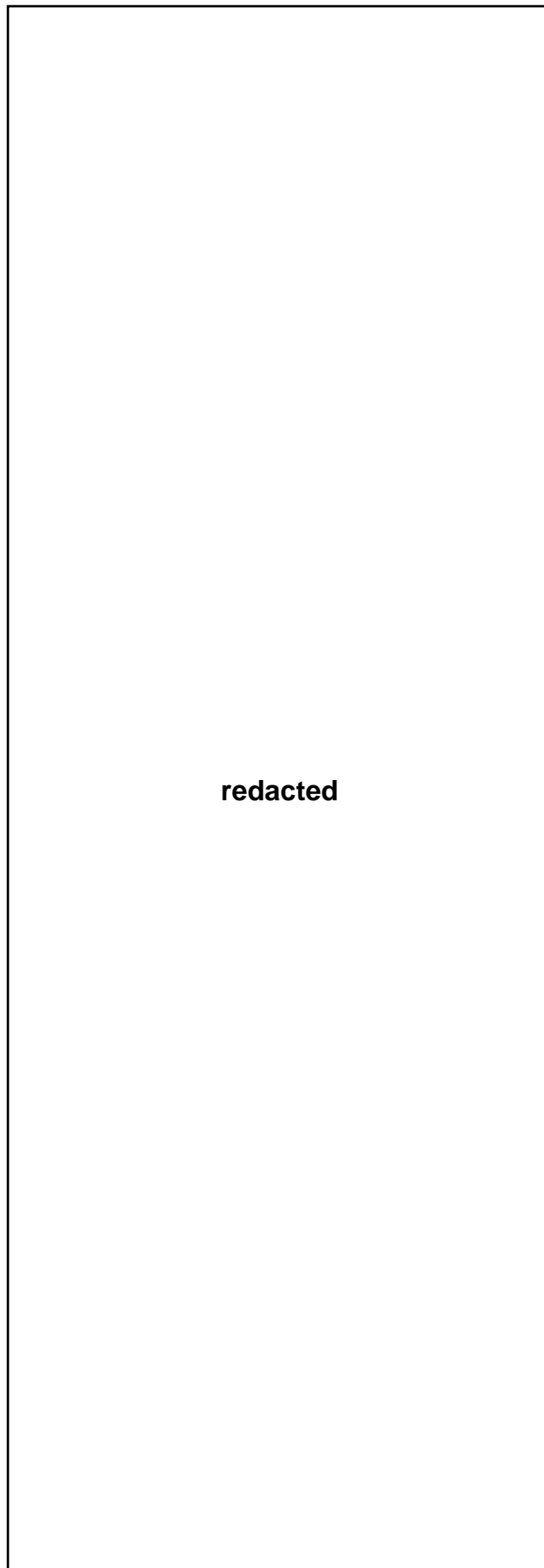


Figure 2.4: Traditional numerical initial synthesis for a military submarine, proposed by Burcher & Rydill (1994)

The steps between the 'Calculate Payload' step to 'Select Margins' in Figure 2.4 can be directly influenced by the initial set of broad requirements related to the whole ship performance characteristics, for example, the Deep Diving Depth (DDD) is a driver of the weight for the structure in the 'Estimate Structure' step or the top speed during short period submerged is a determinant of the size of the propulsion system in the 'Estimate Propulsion System' step.

Once the initial sizing process is done, a verification of 'gross' weight and volume, giving a first 'numerically' balanced design ('Total Volume & Space Required' in Figure 2.4), is produced to check whether there is enough volume and buoyancy to accommodate the space and weight demand on the vessel. The term 'numerical' here refers to 'crude' (or 'gross') initial estimation of weight and space (budget) of the submarine design, which does not reflect more (architectural) detail. Therefore, this first numerically balanced design implies the longitudinal moment and vertical balance have yet to be addressed.

After the initial numerical balance, as shown in the 'Estimate Cost' box in Figure 2.4, the initial submarine cost estimation using parametric cost per tonne (UCL-NAME, 2014) can be calculated to see if the design is still within the budget, otherwise, the initial set of requirements needs to be altered. This cost loop is coherent with the aim of the ESSD, which is to elucidate what is wanted and what can be afforded as essential to Requirement Elucidation (Andrews, 2018c). At this point, the design can proceed with more specific design choices and calculations (see the third part of Figure 2.4).

The inclusion of DS3 in the procedure shown in the first part of Figure 2.4 can be seen in the "Estimate other systems" step, which, as previously mentioned, can be initially estimated either via crude scaling weight equation or scaling from the UCL submarine data (UCL-NAME, 2014). Such an initial DS3 size can then be broken down to include a line diagram in the "Design System" step defining the logical architecture of DS3 (see Subsection 2.1.1), which is to be conducted through slightly more detailed calculations (in the third part of Figure 2.4) towards the end of this initial sizing process.

The procedure in Figure 2.4 was considered 'generic' because it is not bound to a specific submarine design style. It can be used to design a nuclear or a diesel-powered submarine and even to design an unorthodox submarine configuration, such as an unmanned vehicle mothersub (Purton, 2016). This is because the design procedure given by Burcher and Rydill is not too rigid to allow the introduction of innovation and new ideas that is the essence of the ESSD (Burcher and Rydill, 1994). Consequently, it is unclear when exactly the architectural aspect (i.e., the general layout or arrangement of the submarine) needs to be considered within this procedure, although some are necessary to ensure the longitudinal and vertical balance is readily achievable. Such a balance is dominated by interacting physical demands, which makes the submarine design Requirement Elucidation process more detailed than that for most surface ships (Andrews, 2017a).

Their outline of a sequential submarine design procedure by Burcher and Rydill (1994) also provides some possible design algorithms with coefficients, which may be developed based upon 'rules of thumb' drawn from their hands-on submarine design experience within the UK Royal Navy, suggesting such rules of thumb are likely to be different from navy to navy (e.g., US Navy (Arentzen and Mandel, 1960) and MIT professional summer programme (Jackson, 1992)). This, in turn, implies the 'traditional' characteristic of the procedure. Likewise, if such algorithms are largely used in the design procedure, it reflects a narrow evolutionary design approach or even a type ship approach (Andrews, 2018c). Such a crude numerical based synthesis sizing cannot reflect how the spaces onboard are configured beyond the 'type ship' design style.

Additionally, as there is no arrow between the 'Calculate Payload step to 'Select Margins' in Figure 2.4, the precise order of these steps can be debated. For example, there should not be a direct line between the 'Calculate Payload' to 'Estimate Structure' step as this would only be possible if the size of the pressure hull is already selected. Burcher and Rydill produced this procedure, which was appropriate for teaching. Whether it is exactly what would be followed in a real case is probably debatable, what is useful for the designer is that this was a basis for starting a submarine design synthesis.

Therefore, it was considered that the adoption of just this procedure was insufficient and could not deal with the physical architecture of DS3 (see Subsection 2.1.1). The submarine design needs to incorporate the 'architectural' or the configurational aspect of the submarine to enable the physical architecture of DS3 to be considered early in the design process, as is discussed in the next subsection.

2.2.3 The UCL Design Building Block Approach

The limitation of the traditional numerical synthesis in addressing requirements elucidation was first raised in the 1980s by Andrews (1981), who then demonstrated an architecturally driven ship synthesis (Andrews, 1984), which was subsequently fully integrated in the early 90s to the submarine case with the architecture and weight organised functionally (e.g., Fight, Move, Float, and Infrastructure), as opposed to the traditional weight breakdown structure (Andrews et al., 1996). This approach, known as the UCL Design Building Block (DBB) approach (Andrews and Dicks, 1997), is now a proven design method and was implemented as the Surface Concept (SURFCON) module (for both surface ships and submarines) in the sophisticated fully three-dimensional (3D), commercially available naval architectural Computer-Aided Design (CAD) software Paramarine™ (Qinetiq, 2019), coded by Graphic Research Corporation (GRC) (Andrews and Pawling, 2003).

The architecturally centred DBB approach has been developed for more than two decades, many "Proof of Concept" studies have been completed, demonstrating that the inside-out, DBB approach can expand the scope of ESSD beyond the traditional naval architecture S⁴ concerns, such as design for production, design for survivability, design for support, and design for personnel movement (Andrews, 2018c). This is because the DBB approach puts the architecture, the arrangement, the layout, or the configuration of the ship at the centre of the process. By focusing on the submarine's configuration, the initial hull form sizing can better accommodate the demands of the layout and features beyond gross weight and space, i.e., inside-out.

Since the DBB implementation has been designer-led, decisions are made by the designer, as opposed to highly automated approaches. In a previous submarine design research at UCL, Purton created an automated design tool that he called Submarine Preliminary Exploration of Requirements by Blocks (SUPERB) (Purton et al., 2015). This used high level input and sizing algorithms provided by the UCL design procedure to arrive at crude numerical syntheses. The numerically balanced Pareto Front solutions were then assessed, and the front 'lowered' from more detailed consideration (Purton, 2016). Prior to this UCL work, the US submarine builder, Electric Boat and US Navy's Naval Sea Systems Command (NAVSEA) also developed Submarine Concept Design (SUBCODE) using one hundred Microsoft® Excel® workbooks (Microsoft, 2021a) to automate the early stages of submarine design (Mahonen et al., 2007). More recent work is the application of the packing approach model (pioneered by (van Oers, 2011) and, subsequently, (Duchateau, 2016)) for the conceptual design of submarines (Cieraad et al., 2017).

Automated approaches hardcode many design algorithms and their assumptions for sizing often implying, but not limited to, how the spaces are arranged within the vessel. This, in turn, makes the software program follow several design decisions automatically every time an unbalanced condition occurs in the design. This can then allow hundreds of concept designs to be generated quickly by the computer(s), but all based on 'hidden' configurational assumptions. Such an automated approach is consequently difficult to be assessed, i.e., is not revealed easily (if at all) to the designer and thus is a 'black box' synthesis. The danger of such black box approaches is that it is not only do they inhibit creativity and the introduction of innovations, but also could constrain the overall ship design size early in the design process. Whereas Andrews (2011) has strongly argued, any design solution should emerge from a proper Requirement Elucidation dialogue with requirement owners or stakeholders. Such a dialogue aims to balance different visions or objectives across multiple design stakeholders in the eventual complex vessel design as already depicted in Figure 1.2 on page 29. This requires an approach like the UCL DBB approach that is human-centred (glass box) rather than computer-centred (black box) and thus architecturally driven.

The Implementation of the DBB approach in Paramarine™ (Qinetiq, 2019) provides an object-oriented and top-down approach that allows discrete objects to be modelled and manipulated in different levels of granularity. These objects can be attached information in a form of string and numerical data, such as weight and geometry and even can be assigned different sizing algorithms (Pawling, 2007). One can start to develop a small number of coarse models as indicated by ‘Space (Geometry) Definition’ in Figure 2.5. These models can be based on equipment databases, including new equipment that is under development, reflecting the technology and configurational innovations implicit in commencing the process through fostering ‘Radical Ideas’ (see Figure 2.5). As the design progresses, the coarse model of a few, termed as Super Building Blocks (SBB), not fully populating the enclosed volume is expanded, broken down into more detailed definitions as necessary as reflected in the building block design phases for ship design (e.g., topside and major feature design phase and SBB based design phase) (Andrews and Pawling, 2008). From these assembled blocks the ship design can be manipulated and assessed under a block called a Master Building Block (MBB) (Andrews and Pawling, 2003) until the design is balanced i.e., reach an acceptable performance that can go beyond S⁴ concerns (Andrews, 2018c).

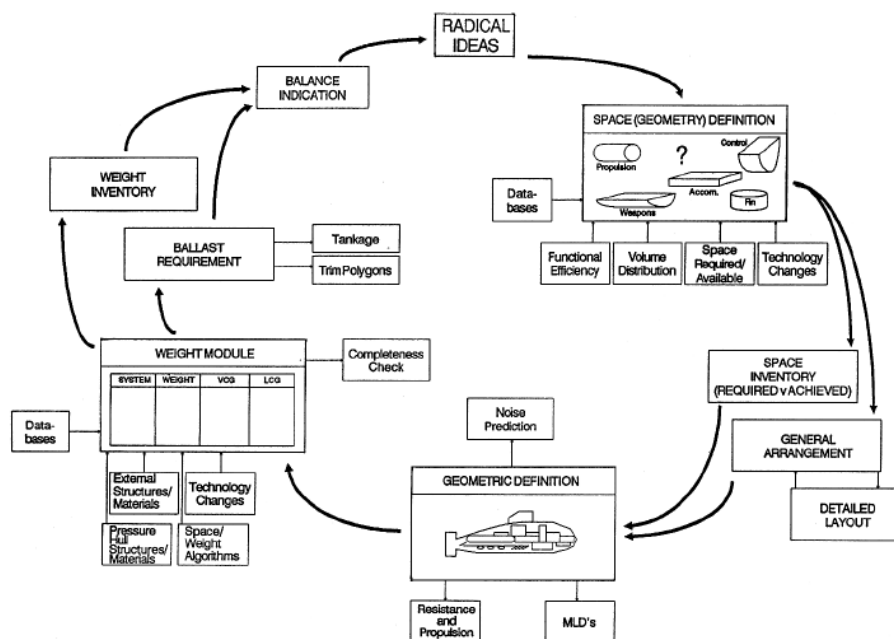


Figure 2.5: Logic of the Design Building Block implementation to submarine design in SUBCON (Andrews et al., 1996)

The objects in the SURCON module of the Paramarine suite could also be used to store numerical DS3 demands and thus, for example, the aggregate power demand was able to be assessed when selecting a set of power plants. Paramarine can also model systems routing or connections that were not exploited in the previous UCL DBB research (e.g., (Pawling, 2007; Piperakis, 2013; Purton, 2016)). This capability was seen to potentially aid the designer to address the physical architecture of DS3 (Subsection 2.1.1) in a more comprehensive manner.

However, there were several drawbacks in implementing such a sophisticated (fully 3-D) and high-capability Computer-Aided Ship Design (CASD) modelling tool in ESSD, such as the difficulties due to effort in modelling or creating each of the numerous features and placing them individually. The latter can be considered laborious and demanding, especially if detailed modelling must be carried out after each design change and iteration (Andrews et al., 2009). Such modelling effort can be referred as to the Gulfs of Execution and Evaluation (see Figure 2.6), which highlights the overall effort required in making a system perform the desired task correctly (Norman, 2013).

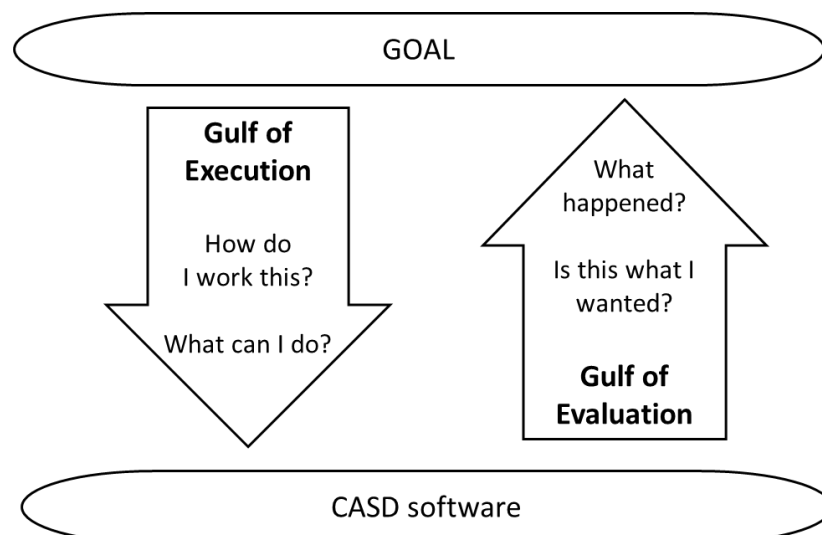


Figure 2.6: Gulfs of Execution and Evaluation for Computer Aided Ship Design (CASD) development, after (Norman, 2013)

Therefore, the 3D based synthesis was then reduced by the UCL ship design research team to be what is called '2.5D', to allow a simpler architecturally oriented design tool to be developed in-house, for specifically surface ship

research and education, referred as to the UCL JavaScript layout exploration tool (Pawling et al., 2015; Kouriampalis et al., 2021). In the current research, an alternative solution needed to be developed without creating a further separate or standalone design tool like the UCL JavaScript tool. That tool sacrificed many advantages from using a 3D based synthesis and a 3D informed dialogue, which Paramarine facilitated and was seen to be necessary for exploring the submarine DS3 in ESSD.

Thus, although the synthesis of the whole submarine design could have been developed using the sophisticated 3D based synthesis UCL DBB approach, it was seen to be sensible to consider in the next section design issues and existing approaches specific to designing DS3. Some of these were seen as aiding the designer in developing DS3 beyond the physical architecture level of abstraction (see Subsection 2.1.1) in ESSD.

2.3 Approaches in Submarine Distributed Systems Design

Designing DS3 are quite complex and relevant information may not be addressable during initial submarine sizing (Burcher and Rydill, 1994). Furthermore, each DS3 technology may require different design methods. To address DS3 design issues, this section reviews different approaches to synthesising distributed ship service systems at ESSD. It is divided into four major subsections. The first subsection discusses the utilisation of the traditional numerical approach for sizing DS3 at ESSD. Subsection 2.3.2 presents sizing from a first principle approach while Subsection 2.3.3 reviews a recent development of a systems design tool. The last section analyses recent network theory based studies for the design of distributed systems, particularly for naval surface vessels. Each investigation highlights how each approach performs and how it might be applied to the submarine's DS3 synthesis problem.

2.3.1 Traditional Numerical Synthesis

As already discussed in Subsection 2.2.2, the traditional numerical synthesis approach sizes DS3 via simple weight equations (i.e., they are parametrically scaled from previous design data). The scaling can be either direct or based upon some design parameters, such as submerged displacement, hull volume, endurance, personnel size, propulsion power, or a mix of parameters. Thus, for example, the volume size for systems and auxiliary machinery can be taken as equal to $K \times \text{Hull Volume}$ where K is a factor based upon existing design solutions (Burcher and Rydill, 1994). This approach assumes most of the equipment procured from the vendors remains invariant and or the new design is a direct derivative of an existing design with the same DS3 style, this approach thus implies a very narrow evolutionary approach to early stage DS3 design.

Despite its evolutionary nature, the parametric approach can aid the designer in estimating the DS3 using information that is uncertain or unclear in the initial sizing of the submarine (Burcher and Rydill, 1994). To accommodate such uncertainty at ESSD, design practice is to employ design margins, which can

be seen as part of the style decisions (Subsection 2.1.2). In general UK Defence Equipment and Support (2007) make use of design margin based upon a quantitatively defined maturity level, which reveals the more accurate that specific DS3 component information, the lesser design margin is required. However, the issue is that at best only early maturity levels can be applied at ESDD.

Traditional numerical synthesis works well for an evolutionary design, but it cannot be appropriate to design anything significantly new, arising from technology advancements, or innovations resulting from new items of equipment, and or notable departure in physical arrangement (Andrews, 2017). Traditional numerical algorithms, which may use parametric curves (Thornton, 1994) or regression analysis on existing design solutions, could also be considered a 'black box' method, as the rationale behind the factor used in a parametric sizing is not assessable easily by the designer using the algorithm (Hu, 2016). Rigterink (2014) argued that a small set of parameters cannot capture DS3 design, which is vastly different from ship type to ship type. Likewise, reliance on these parametric methods is unable to capture different possible design styles, including those for DS3. If the scaling approach is used to fix the size of the submarine hull and then followed by the development of the physical architecture and logical architecture of DS3 (see Subsection 2.1.1), this implies an outside-in approach with the latter invariably constrained by the gross sizing decisions or constraints.

Although the scaling based approach, without potentially excessive margins, will not provide an accurate DS3 size as in the detailed design or production stage and will not be able to capture specifically different style DS3 choices, parametric sizing has been a convenient approach as it requires little effort to provide a quick numerical sizing that can accommodate the 'first principles' sizing approach (see the next subsection). Therefore, the parametric approach was considered suitable to size some 'straight forward' DS3 with limited style options or seen to have little impact on the overall submarine size, such as sanitary system and domestic plumbing.

2.3.2 Sizing from First Principles

Sizing from the first principles or detailed sizing may give a more accurate sizing than the whole vessel scaling, or rules of thumb approach. This is because, such an approach predicts the whole dimension of a (DS3) component or a machine using relevant first principle relationships, for example, the diameter of a diesel engine cylinder can be sized based upon basic physical first principle parameters, such as power output, torque, and angular velocity of the machine (Stapersma and de Vos, 2015). While sizing from the first principle is desirable, it can be time consuming. More importantly, the detailed component design information may not be available at the earliest design phases and this is quite distracting from the essence of ESSD Requirements Elucidation (Andrews, 2018c). Furthermore, such sizing from the first principle is largely limited to particular numerical calculations or even the demand parameters, which to be appropriate are likely to require the input of the different DS3 architectures (physical, logical, and operational architectures, see Subsection 2.1.1) to be able to be solved at ESSD. Hence, the next subsection highlights a recent development of a systems design tool that could potentially tackle those three architectures in the Concept Phase of ship design.

2.3.3 Smart Ship Systems Design

As summarised in the 2018 IMDC state of the art report on design methodology (Andrews et al., 2018), there are other projects than the ONR NICOP (Brefort et al., 2018), which are considered relevant to DS3. One of them is the Electric Ship Research and Development Consortium (ESRDC) also funded by the US Navy (ONR-ESRDC, 2018). This focused on future electric surface warships using high-energy weapons (Chalfant et al., 2017) and developed a collaborative analysis tool called Smart Ship Systems Design (S3D) (Smart et al., 2017). This enabled specialist engineers to be involved much earlier in the design phase (Langland et al., 2015). Further relevant work has provided specific ship design inputs from the simulation based environment to evaluate thermal cooling system design (Babaei et al., 2015), machinery (Jurkiewicz et al., 2013), and power distribution system (Chalfant and Chrysostomidis, 2011).

Nevertheless, the collaboration between specialist engineers in designing ship systems can result in excessive design detail at ESSD, which was considered inappropriate. This is because, as Andrews argued, one should not fix large portions of the design since the overall design should still be subject to big decisions as part of Requirement Elucidation, and hence undertaking detailed design is either nugatory or curtailing choice (Andrews, 2013). The next subsection considers a more likely approach to synthesise DS3 in ESSD for submarine Concept Design requirements elucidation, which invariably leads to revisiting high level (pre-Initial Gate) decision points well into design and each construction (Andrews, 2003).

2.3.4 Network Theory

Lying between detailed distributed ship service systems (DS3) sizing and the traditional numerical approach is network theory. This requires fewer assumptions than detailed sizing but is seen to demand more inputs than a parametric approach when applied to DS3. A set of DS3, as already defined in the introductory chapter (Section 1.1), is an assembly of connected individual components and thus appropriates to be studied using a network or graph. A network is a collection of points connected by lines usually known as arcs or edges (Newman, 2010). Modelling connected entities as in a DS3 as a network has been considered as a means to new insights (Newman, 2004). Not only can a DS3 be modelled as a network, but also relationships between spaces within a ship arrangement (Gillespie, 2012; Pawling and Andrews, 2018), as well as variables within design algorithms (Collins et al., 2015).

At UCL, one of the types of network theory called a knowledge based approach or semantic networks (Sowa, 1983) is being applied to a nuclear submarine design (Collins et al., 2015). Semantic networks typically have not been used to store numerical data, but rather contextual (string) data (Sowa, 1983). The use of the semantic network by Collins et al (2015) captures the domain knowledge in submarine sizing through modelling constants, coefficients, and variables in traditional numerical based algorithms, rather than the physical entities of DS3 in the design. This ongoing investigation into a semantic network approach has the potential to reduce the 'black box' nature of the parametric

approach by revealing the rationale and assumptions behind the traditional vessel sizing process. However, so far this has been limited to selected design algorithms in exploring major design and has not set out to capture distributed ship service systems (DS3) design style choice.

Due to a paucity of network theory applications specific to submarine systems, applications of network theory to surface ship design were also investigated. Table 2.2 summarises and provides a high level comparison of how network theory has been applied to naval surface ship distributed systems design. Table 2.2 also indicates that all the current approaches require the logical architecture (see Subsection 2.1.1) of the systems as well as the physical architecture or network of the overall ship layout as the main input. A network of the ship can model the spaces within a ship (physical architecture) while nodes in the distributed system's logical architecture can be assigned to those nodes in the physical architecture. Each approach used a different optimisation technique for systems routing, which varied from the shortest path algorithm (Dijkstra, 1959) to the Network Flow Optimisation (Trapp, 2015), discussed further in this subsection.

Table 2.2: Summary of network theory applications to ship service distributed systems, taken from various sources as specified in the header of the table

	(A) The L-PAT approach (Shields et al., 2017)	(B) The early routing approach (Duchateau et al., 2018)	(C) The Architecture Flow Optimisation approach (Robinson, 2018)																																							
1	System model for the L-PAT algorithm application (total of five logics including personnel movement) (Shields et al., 2017)	Power system network as the input of the early routing approach (Duchateau et al., 2018)	Mechanical plex logical architecture that provides a list of components required for a specific distributed system (Brown, 2020)																																							
Logical Architecture																																										
2	System model nodes (1A) are assigned to vessel arrangement (Shields et al., 2017)	Routing adjacency network for naval vessel compartments and superstructure defining the decks and hull envelope (Duchateau et al., 2018)	Subdivision block of a generic naval combatant produced from Synthesis Model of the Virginia Tech where the blocks are defined by decks, watertight bulkhead, and hull extent (Robinson, 2018)																																							
Physical Architecture	<table border="1"> <thead> <tr> <th>System Component</th> <th>Watertight Bulkhead</th> <th>Def_3</th> <th>Bridge</th> <th>Radar</th> <th>Structural Zones</th> </tr> </thead> <tbody> <tr> <td>Def_1</td> <td></td> <td>CIC_2</td> <td>CIC_1</td> <td>Comm</td> <td>Def_2</td> </tr> <tr> <td></td> <td></td> <td>Hotel_1</td> <td></td> <td>Hotel_2</td> <td></td> </tr> <tr> <td>Mach_1</td> <td></td> <td></td> <td></td> <td></td> <td>Mach_2</td> </tr> <tr> <td></td> <td></td> <td>PR_MVR</td> <td>MAIN</td> <td>AUX</td> <td>Chiller</td> </tr> <tr> <td></td> <td>BH_1</td> <td>BH_2</td> <td>BH_3</td> <td>BH_4</td> <td>BH_5</td> <td>BH_6</td> <td>BH_7</td> <td>BH_8</td> </tr> </tbody> </table> <p>Label: main (MAIN) and auxiliary (AUX) machinery, prime mover (PR_MVR), defence system component (Def) (e.g., radar, bridge, combat information centre (CIC)), mechanical component (Mech/Mach) (e.g., hotel load centre, chiller, and communications centre (Comm))</p>	System Component	Watertight Bulkhead	Def_3	Bridge	Radar	Structural Zones	Def_1		CIC_2	CIC_1	Comm	Def_2			Hotel_1		Hotel_2		Mach_1					Mach_2			PR_MVR	MAIN	AUX	Chiller		BH_1	BH_2	BH_3	BH_4	BH_5	BH_6	BH_7	BH_8		
System Component	Watertight Bulkhead	Def_3	Bridge	Radar	Structural Zones																																					
Def_1		CIC_2	CIC_1	Comm	Def_2																																					
		Hotel_1		Hotel_2																																						
Mach_1					Mach_2																																					
		PR_MVR	MAIN	AUX	Chiller																																					
	BH_1	BH_2	BH_3	BH_4	BH_5	BH_6	BH_7	BH_8																																		
3	The output of the L-PAT approach in 2D representation showing different routing densities (0 to 5): 0 indicates no connection; 5.0 means the connection contains all systems in 1A (Shields et al., 2017)	The output of the early routing approach shows power (orange and blue), cooling (yellow), and data (purple and light blue) for a generic naval combatant (Duchateau et al., 2018)	The output of the Architecture Flow Optimisation approach shows mechanical (grey), electrical (red), chill water (blue), and seawater (green) for a generic naval combatant (Robinson, 2018)																																							
Physical Solution																																										

(A) The L-PAT Approach

The research produced by the University of Michigan’s Advanced Naval Concepts Research (ANCR) group applied network theory (Newman, 2010) to naval ship design general arrangements (Gillespie and Singer, 2013) for a better understanding of the relationship between DS3 and ship’s arrangements (Rigterink et al., 2014). The Logical-Physical Architecture Translation (L-PAT) algorithm was proposed to provide the designer with knowledge of physical solutions (see Subsection 2.1.1 and Figure 2.2) using network approaches (Shields et al., 2017). In this approach, DS3 routing was developed from logical architecture, via simplex (Shields et al., 2017) and multiplex network (Gomez et al., 2013), which could be said to be similar to a multislice network representation (Mucha et al., 2010). Figure 2.7 (right) shows that a multiplex network can be composed of multiple simplex networks while Figure 2.7 (left) shows the multiplex network is a 3D network consisting of multiple 2D simplex networks.

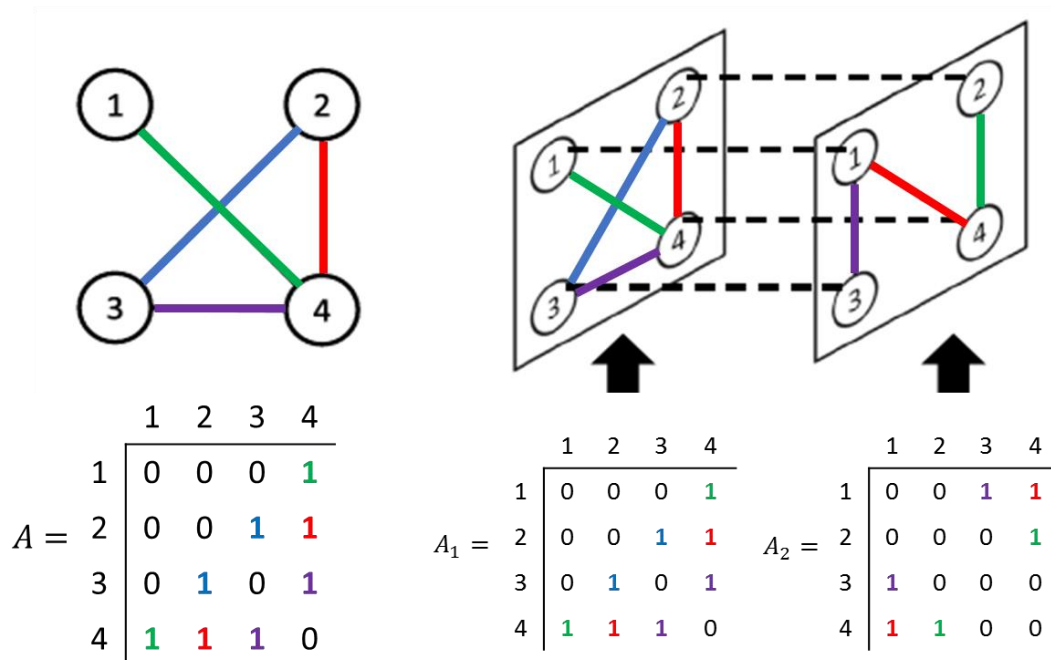


Figure 2.7: Adjacency matrix definition of a simplex and multiplex network, left and right, respectively, after (Shields et al., 2017)

DS3 components, their individual locations, and their interrelationships, including those defined through an initial vessel synthesis, must be known

beforehand to use the L-PAT approach. L-PAT can be initialised by modelling the logical architecture of DS3 as is shown in Table 2.2 (1A). Then the physical architecture of the vessel was modelled into a network description. This network consisted of nodes that model geometric representation of a section of the vessel containing compartments, zones, or decks and edges as the adjacency definitions between compartments. Thus, the multiplex, representing the logical architecture of a set of DS3, could be assigned to geometric nodes (see Table 2.2 (2A)). Using the shortest path algorithm (Dijkstra, 1959) for routing, L-PAT could produce a physical solution (see Subsection 2.1.1).

Once a DS3 routing had been produced, a quantitative measurement, such as routing density could be calculated in the following manner, which quantified how many types of DS3 were routed within an edge in an undirected network. For example, if the routing density value of an edge was 5.0, it meant there were five different types of DS3 routed to that edge. This routing density could be useful to physically size that edge. L-PAT could be applied to 2D networks (see Table 2.2 (3A)), or to 2.5D networks by adding transverse space to the port and starboard sides of a 2D routing arrangement (Goodrum et al., 2017). The extension of this work provided a more general method, which was seen to be independent of the shortest-path algorithm (Shields et al., 2018) and was able to account for the physical architecture of the relevant DS3 components (Donohue et al., 2019).

The L-PAT tool from the University of Michigan could give insights into a DS3 physical solution (routing), by indicating where in the vessel the DS3 physical solution could be located without requiring excessively detailed 3D modelling. However, the process behind making the minimum input information (e.g., the size of DS3 major components and the vessel's physical architecture) ready for such an analysis remained questionable and thus was not seen to be very helpful in understanding the starting process for synthesising DS3 components for submarines. Hence, it was concluded that research was necessary on how to use networks to give insight directly into DS3 architecture, as a precursor to initial sizing information for submarine distributed systems.

(B) The Early Routing Approach

TU Delft, another member of the NICOP group, also undertook DS3 related work using an extension of Delft's automated bin packing approach (van Oers, 2011). TU Delft used a genetic algorithm (GA) (Deb et al., 2002) and Pareto Front representation to reduce the number of solutions in design space explorations of DS3 in ESSD. The first attempt at Delft explored different 2D routings using genetic algorithm and Pareto Front representation, based on two different drivers or objectives, (a) shortest routing length and (b) the number of components available after hits by removing the hit compartment (van Oers, 2012). The extension of the 2D routing to 3D was done by Duchateau et al. (2018). Their work included design space explorations of logical architecture (exploring myriad systems topologies, in the order of 10^3 - 10^5). Using such a genetic algorithm and a Pareto Front approach, a tool called Automatic Topology Generator (ATG) was created to assist a system designer in the decision making in the early design of a ship's DS3 (de Vos, 2018).

In this routing proposal, the process was started by translating a 3D CAD ship model into subdivision and adjacency networks (see Table 2.2 (2B)). Unlike L-PAT (Goodrum et al., 2017), the Automatic Topology Generator (ATG) could depict multiple DS3 in a simplex form (see Table 2.2 (1B)), and the location of relevant DS3 components imposed on the 3D CAD model of the selected ship's arrangement. The routing began by coupling Yen's routing algorithm (Yen, 1971) to a specific genetic algorithm (Deb et al., 2002). Yen's algorithm (Yen, 1971) gave not only the shortest possible routing but also considered when an arc was removed from the network. A typical example of the routing is shown in Table 2.2 (3B).

The TU Delft's ATG showed that the routing of DS3 could be done using an automated and optimisation based approach, where many options could be explored using a network representation. However, the optimisation was done only at the logical architecture level of abstraction. Furthermore, particular ship's systems must be known before ATG could function, as the number of components was a chosen input to be made before the ATG could be run. This

would seem to be a process like the University of Michigan's L-PAT tool, which was more suitable for outside-in ship design approaches. The output of ATG was seen only to explore the number of connections and was considered not sufficiently sensitive to varying DS3 components for (say) redundancy as part of a more style driven approach and thus was rejected as attractive in the current research.

(C) The Architecture Flow Optimisation Approach

The Network Flow Optimisation (NFO) approach combined network theory and linear programming (Trapp, 2015). In the NFO approach, nodes and arcs were modelled as a set of mathematical variables describing the necessary constraints, bounds, and objective functions for linear programming to be undertaken. The NFO approach was applied to model shipboard Integrated Engineering Plant (IEP) by Trapp (2015) via Mixed-Integer Linear Programming (MILP), which he called Non-Simultaneous Multi-Commodity Flow (NSMCF). A follow up to this was the development of Non-Simultaneous Multi-Constraint Parallel-Commodity Flow (NSMPCF) or Architecture Flow Optimisation (AFO) by the research team at Virginia Tech led by Brown (Robinson, 2018). Since then, AFO had been significantly enhanced and developed to be the Dynamic AFO (DAFO) and Vulnerability AFO (VAFO) (Parsons et al., 2020a).

Unlike a semantic network (Sowa, 1983), AFO was used to model the actual physical objects representing a total ship, all systems in a putative large and complex naval combatant (Parsons et al., 2020b). Although this was not feasible without recourse to a significant 'machinery equipment list', i.e., equipment database (Parsons et al., 2020a), AFO allowed a direct representation of decisions made for different DS3 style choices in a ship design. AFO could provide numerical data, such as energy, which could then be used to scale the size of baseline DS3 components (Stinson, 2019) and thus unlike other network applications, AFO had been applied to design and size distributed naval ships systems. Such conversion to space and weight input for the relevant DS3 was only possible provided that the ratios for converting the energy data into space and weight input were known or assumed, which meant

the approach was also dependent on the quality of the database of DS3 components.

For the design input, AFO departed from the Ship Synthesis Model (SSM) part of Concept and Requirements Exploration (C&RE) that were developed by Brown's research team at Virginia Tech and MIT over more than two decades (Stinson, 2019). This synthesis model allowed the designer to synthesise ship geometry using relatively few inputs, such as overall length, length to beam ratio, and minimum volume of deckhouse as 'design variables' (Parsons et al., 2020a). The ship geometry could then be represented by a set of subdivision block(s) to obtain a simple 2.5D ship representation (extent of port and starboard, see Table 2.2 (2C)). This representation could be said to be akin to the ship network L-PAT (Shields et al., 2017) but without edges, which would model the adjacency between compartments.

In the AFO approach, the logical architecture for a distributed system could be developed in several ways: built from scratch; automatically generated using the Automatic Topology Generator (de Vos, 2018); making use of templates developed by the ESRDC team (Chalfant and Chryssostomidis, 2017); or using plexus (Brown, 2020). Plexus was produced by Brown (Brown, 2020) to mimic systems on a typical naval combatant. An example of a plexus is shown in Table 2.2 (1C), as a pre-defined vital component listing for a twin-screw propulsion system and connected to a series directed network. The volume and weight information of the vital components must be known before using the AFO (Stinson, 2019). The use of pre-defined plexus in the AFO allowed the inclusion of multiple DS3 for a ship through linear programming optimisation early in the design process.

Like the L-PAT approach (Shields et al., 2017), the plexus based logical architecture was assigned to the vessel's subdivisions block (Robinson, 2018). However, since the volumes of the subdivision blocks were known from the ship synthesis model, this had been considered as a hard constraint to define where possible DS3 components were fitted into that particular subdivision block (Parsons et al., 2020a) and thus this could also be considered as an outside-in

approach with the design constraints that then apply. Using damaged scenarios (Robinson, 2018), the AFO tool could produce 2.5D whole ship physical solutions (see Table 2.2 (3C)). Instead of tracking various commodities in the network flow, as was done using Trapp's NSMCF approach (Trapp, 2015), AFO only tracked energy flow in a steady state condition (i.e., no varying load requirements in a given operating condition (Robinson, 2018)). Assuming a linear relationship, the energy flow was then used as the basis for scaling up or down the size of DS3 (Stinson, 2019).

The approach in using the AFO tool was that the definition of the wider system's (the vessel) physical architecture should be kept as simple as possible (Parsons et al., 2020b). This also applied to the approaches from the University of Michigan (Table 2.2 (2A)) and the TU Delft (Table 2.2 (2B)). Thus, the volume of a space, such as a typical ship's compartment, could be represented by a single node. This enabled such a network tool to be easily used without the need for 3D physical modelling as in the Paramarine-SURFCON implementation of the UCL Design Building Block (DBB) approach (Andrews, 2018c). However, the AFO process had been devised to work specifically with the Virginia Tech's ship design process, which was different from the inside-out UCL DBB approach. Likewise, the surface ship applications of AFO were limited to ship procurement cost and survivability formulation and thus as they stood were not considered applicable to submarine's DS3 ESD without further work. Thus, an investigation on applying the Network Flow Optimisation approach to submarine DS3 design became one of the focuses of the current research.

2.4 Conclusion and Gap Analysis

It was considered to be an important contribution to advancing the submarine Concept Design to be able to undertake the synthesis of vital DS3, where explicit style choices could be integrated into the whole submarine design, within a practical timeframe. Thus, the eventual solution of submarine Concept Design could emerge from the Requirement Elucidation dialogue, which included investigating feasible and appropriate DS3 style choices. None of the existing approaches was considered to be able to fulfil such an aim without further work. Therefore, this research aimed to fill this gap in the following manner.

Firstly, the submarine design concept process must retain a large degree of flexibility, avoiding too mechanistic an approach, and must be able to reflect the importance of style decisions. These must include those for DS3 that are then open to revisions, thus meeting the overall concept necessity to assist in Requirement Elucidation. For that reason, the first nine steps in the 'decision making' approach in Figure 2.3 on page 43 were adopted as a basis to develop DS3 synthesis.

Secondly, the design procedure must be generic, i.e., not limited to certain design styles to allow a comprehensive exploration of the design solution space. Thus, the generic submarine design procedure proposed by Burcher and Rydill was used with an inside-out philosophy (Andrews, 2018c). Thirdly, to inform submarine concept balance and understand the impact of DS3 style choices on the overall submarine design, the design process needs to incorporate an architecturally centred approach, namely the UCL Design Building Block approach, which could also enable a 3D informed dialogue of the physical architecture of set of vital submarine DS3.

Thirdly, different approaches in synthesising DS3 have been considered ranging from the simple traditional parametric sizing (Subsection 2.3.1) to the collaborative systems modelling (Subsection 2.3.3). The applications of network theory to the design of distributed ship service systems were

considered to fit between these two extremes, i.e., it is more accurate than the type ship or rule of thumb scaling approach, yet not too detailed as would be the collaborative systems modelling approach. Most importantly, the proposed approach could aid the early capture of the complexity of interrelated DS3 in terms of logical architecture.

However, it was considered that most of the current network theory applications to surface ship distributed systems depend on optimisation schemes, which constrain DS3 solutions when compared to a more style driven approach. Nevertheless, the Architecture Flow Optimisation (AFO) approach was considered attractive in that it can be used to design DS3 and to provide first principle numerical data, such as energy (power), for sizing distributed naval ship systems. Still, the optimisation setup in the Architecture Flow Optimisation was not considered applicable to submarine design. This is because it would not be possible to be assured that any such DS3 design was truly 'optimal', since there are many conflicting visions that must be compromised in the submarine designer's eventual design solution, and to effectively sub optimise a third level system is highly questionable for such a highly interactive system of systems as a submarine (Andrews, 2021). This suggests further investigation would be necessary to devise a less constrained network approach in the submarine DS3 Concept Design process (i.e., inside-out driven and responsive to submarine design balance).

2.5 Research Aim

Following the State-of-the-Art review in this chapter, the following research aim has been defined:

To develop an integrated approach to the synthesis of distributed ship service systems (DS3) that facilitates the consideration of DS3 aspects early in ESSD for a new submarine design option, as part of Requirement Elucidation.

2.6 Research Objectives

The justified research aim stated in Section 2.5, was further broken down to include several (sub) objectives as the key performance indicators of the research. The first objective was focused on the development of the approach in terms of the overall submarine design. The next objective is to underline the criteria to be met in the proposed DS3 synthesis approach. These objectives are summarised in Table 2.3.

Table 2.3: Research objectives

Objective	Description
1	Submarine Design for Distributed Systems
1.1	The proposed approach should assist the designer to get a feel for the contribution to ship weight and space demands of the selected DS3 in a manner that improves on the traditional numerical approach.
1.2	The approach should allow the designer to consider the impact of different DS3 style choices on the whole submarine design for a more effective Requirement Elucidation dialogue with design stakeholders in ESSD.
1.3	Given the approach is not black box based, the designer should be able to develop submarine design <i>ab initio</i> and subsequently select or develop relevant design algorithms (rather than being hardcoded).
1.4	The approach should have a degree of flexibility and scalability to allow innovative options to be explored in ESSD.
2	Submarine Systems Design
2.1	The proposed approach should capture the complexity and interrelations of DS3 and aid design stakeholders' understanding of systems choices. This then would contribute to Requirement Elucidation for the whole design.
2.2	The proposed approach should consider multiple DS3 to be developed and the development of DS3 logical and physical architectures should be both simultaneous and as seamless as possible. This would allow the exploration of DS3 choices in submarine ESD.
2.3	The network application in the proposed approach should be a less constrained approach than using existing methods. Thus, the mathematical model in the network theory should reflect the distinct physics of the submarine's DS3 problem without excessive detail, commensurate with the exploratory nature of submarine ESD.

The first objective, Objective 1.1, reinforces the main problem of the current research, which underlines that various submarine DS3 have traditionally been poorly addressed in submarine ESD. Such a traditional approach assumes implicit configurations and thus has been inhibiting the exploration of DS3 configurations. The proposed approach should enable the designer to depart

from this issue and thus better inform the whole submarine synthesis. This makes a difference to something as weight sensitive as submarine design.

Most of the applications of the network theory to surface ship distributed systems design imply an outside-in philosophy that, as already discussed, limit the DS3 solutions to be produced at the concept. Therefore, this leads to Objective 1.2, which indicates that the new approach should enable the impact of potentially differing DS3 styles to the overall submarine design, to inform the early design process (within a practical timeframe), as part of the Requirement Elucidation.

Submarine as one of the most complex engineering products should not be designed using black box approaches. Different submarine designs with different style choices should employ different design algorithms and assumptions, as part of the decision making to be made to progress the design. Accordingly, as stated in Objective 1.3, the new approach should not hardcode any design algorithms to minimise black box tendency, i.e., to make the resultant submarine design interrogable. This would allow the designer to employ different design algorithms that could give more accurate sizing as designs progress.

Given its glass box nature, Objective 1.4 states that the new approach should be adaptable or responsive to technology changes. If, for example, any updates on components data are required, the approach should allow the designer to easily input the data without changing the main code of the tool. Similarly, to reduce dependency on the database at ESSD, a notional DS3 could still be developed but the proposed approach should be able for the design to include margins as one of the designer's style decisions. This would allow the proposed approach to model DS3 at scalable levels of design detail by allowing the information attached to the network to be altered.

As stated in Objective 2.1, the proposed approach should be able to capture the complexity of DS3 without excessively detailed design, as would be commensurate with ESSD. The use of a network to directly represent the

various DS3 configurations could potentially aid the designer to explore DS3 style decisions, as part of Requirement Elucidation in submarine ESD.

The applications of the network theory to surface ship distributed systems design by current ONR funded research groups have simplified the representation of DS3 physical architecture into 2 or 2.5D representations, where the advancement of modern computers technology should be exploited to enable the advantages of 3D based DS3 synthesis at the concept, such as for 3D physical routing check. Therefore, the proposed approach was intended to fill in this gap and thus was considered to be achievable through a simultaneous process of physical architecture and logical architecture based synthesis, i.e., the designer would be able to go back and forth in viewing and manipulating the various DS3 in different architectures (physical architecture and logical architecture) to allow the exploration of DS3 options in submarine ESD. This is stipulated in Objective 2.2.

The applications of network theory to surface ship distributed systems design have allowed ever greater DS3 analyses of a given system's design at the earliest stages of the ship design. However, as stated in Objective 2.3, the proposed approach was intended to employ network analysis as little as possible, commensurate with the needs of Requirement Elucidation. Thus, the energy balance was considered as a sensible approach to be analysed to give insights on DS3 sizing input, early in the design process.

Chapter 3

Development of the Approach

This chapter outlines the initial investigation into implementing different setups of a network based approach to design distributed systems for submarines. As shown in Figure 3.1, it is divided into three parts. Section 3.1 describes the fundamental theory on how a network problem could be solved and used as a basis for sizing distributed systems. This is followed by Section 3.2, which outlines a proposed network based approach and its application to an initial numerical sizing process. Section 3.3 expands this application to a submarine design case study, which considers the physical, logical, and operational architectures of the submarine DS3.

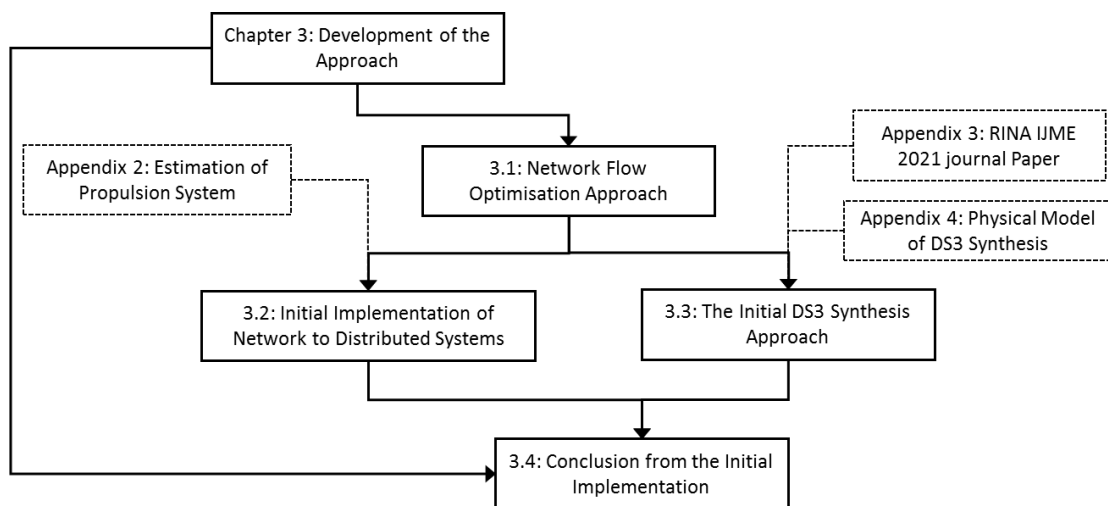


Figure 3.1: Schematic of Chapter 3

3.1 Network Flow Optimisation Approach

As discussed in Subsection 2.3.4, Trapp (2015) has proposed different variations of the Network Flow Optimisation (NFO) approach. His work has been subsequently extended by researchers at Virginia Tech to be the Architecture Flow Optimisation (AFO) (Robinson, 2018). Since then, the AFO has been significantly enhanced and developed for a more specific surface ship survivability application, such as the Dynamic AFO (DAFO) and Vulnerability AFO (VAFO) (Parsons et al., 2020a). However, the AFO process, including its

variants, has been constrained to a specific optimisation setup, which is to minimise the cost, and devised to work well specific to the Virginia Tech's Ship Synthesis Model. This was considered incompatible with the submarine design, which requires a more hands-on DBB-like approach for the physical arrangement architecture. Therefore, to investigate the implementation of the network based sizing for submarine's DS3 design, it is sensible to revisit the earlier version of the AFO, which is the Network Flow Optimisation (NFO) by Trapp (2015). Due to the fundamental importance of the NFO to the research presented here, it is covered below.

Subsection 3.1.1 introduces and provides basic terms used in the current research. Subsection 3.1.2 describes a proposed framework to solve a Network Flow Optimisation (NFO) problem. This then was further applied to a specific NFO problem, which is presented in Subsection 3.1.3. Subsection 3.1.4 summarises the initial findings, which became the basis of the network based approach for sizing submarine DS3.

3.1.1 Mathematical Description of the Network

A network can be defined using an adjacency list or mathematically defined using an adjacency matrix (Newman, 2010). The shape of an adjacency matrix is square, and its size is given by the number of nodes in the network (see Figure 3.2).

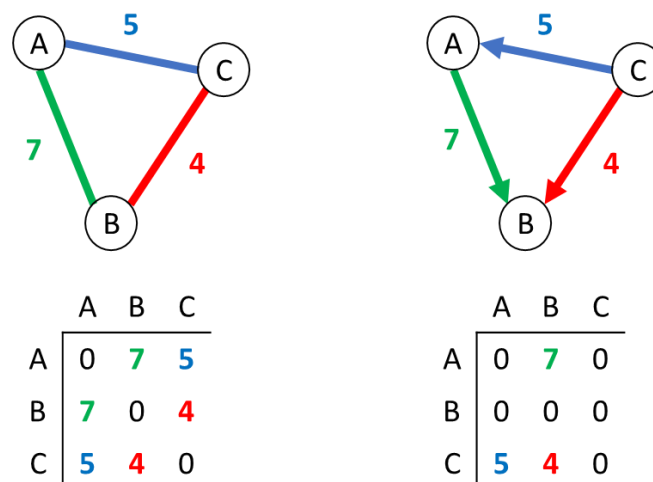


Figure 3.2: Examples of undirected and directed -weighted networks with their adjacency matrices, left and right, respectively

Figure 3.2 shows the element in an adjacency matrix can be zero or non-zero. Zero indicates there is no edge between a pair of nodes and non-zero otherwise. Non-zero numbers in the adjacency matrix (see Figure 3.2 (bottom)), can be used to attach numerical data, such as 7, 5, and 4, forming what is called a weighted network. In an unweighted network, all non-zero numbers are unity in the adjacency matrix (see Figure 2.7 on page 59).

As shown in Figure 3.2, a network can also be directed or undirected. A directed network (see Figure 3.2 (right)) can be used to provide information as to where the arc is connected from node to node while an undirected network (see Figure 3.2 (left)) only gives information that a pair of nodes are connected but without specific information about arc's direction. This means a directed network contains more information than an undirected network.

Therefore, as given in Figure 3.2 (bottom), the adjacency matrix is nonsymmetric for the directed network and symmetric for the undirected network. The number of arcs connected at a node in an undirected network gives the 'degree' level. In a directed network, arcs entering and leaving a node are called in-degree and out-degree, respectively. Hence, the 'degree' can be used to measure how many edges are connected to a node. As the example of a directed network in Figure 3.2 (right), each node has: node A (1 in-degree and 1 out-degree); node B (2 in-degree and 0 out-degree); and node C (0 in-degree and 2 out-degree).

3.1.2 Operational Matrix for the Network Flow Optimisation

In the Network Flow Optimisation (NFO) approach, nodes and arcs are used to store a set of mathematical variables describing the optimisation formulation for linear programming to be undertaken. Linear programming formulation mainly consists of constraints that define the physics of the problem and the objective function to focus the solver to maximise or minimise the solution of the problem (Trapp, 2015). Trapp (2015) has provided different setups with constraints and objective functions from basic to the most complex variations using NFO. The solver used by Trapp (2015) for the NSMCF problem was CPLEX (IBM, 2014). However, in this research, the CPLEX toolbox in MATLAB (2019) was used

instead of using the IBM ILOG CPLEX (2014). This difference might seem trivial, but this streamlined the network analysis to be done fully in MATLAB without the need to build a specific MATLAB code for the CPLEX programming language and vice versa.

Furthermore, the use of the CPLEX toolbox in MATLAB allowed the use of matrices for defining network properties to be read sequentially and visualised instantaneously in MATLAB. This was essential to reduce the risk of error, such as the flow capacity not matching the correct arc as designed or sketched. This would be significant when dealing with a very large network and the development of the DS3 physical architecture, concurrent with the DS3 logical architecture (see Subsection 2.1.1) such as is explored later in the aimed thesis.

Most importantly, the use of the CPLEX toolbox in MATLAB enabled user intervention in the network formulation code for CPLEX using MATLAB programming language, i.e., matrix based computation. This, in turn, could minimise any black-box tendencies of linear programming formulation, by revealing the interaction between the objective function, constraints, and bounds in the form of several matrices constituting a single large matrix. Such a large matrix is referred as to the Operational Matrix framework in the current research. This framework was proposed to assist the designer in formulating linear programming, which should reflect the temporal relationship i.e., the operational architecture of submarine DS3 (Subsection 2.1.1).

To show the applicability of the proposed Operational Matrix framework and explain the NFO approach, it was used to revisit one of the complex variations of the NFO, which is called the Non-Simultaneous Multi Commodity Flow (NSMCF) problem presented by Trapp (2015). This specific problem is referred as to the 'basic' NSMCF problem or example in this section. By revisiting the basic NSMCF example, the application of the NFO for submarine application can then be investigated. The basic NSMCF problem is given in Figure 3.3. The adjacency matrix of that network problem is provided in Table 3.1 with binary values (0-1), indicating connections between nodes. As discussed in

Subsection 3.1.1, to model an undirected network in Figure 3.3, the adjacency matrix must be symmetric (see Table 3.1). The description of the basic NSMCF example by Trapp (2015) and colour codes are described further after Table 3.1.

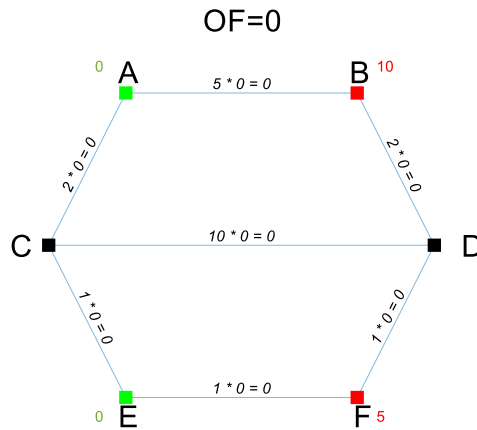


Figure 3.3: The basic NSMCF network problem (Trapp, 2015) coloured and revisited by the candidate using the proposed Operational Matrix framework

Table 3.1: The adjacency matrix, showing how to build the network in Figure 3.3 (Trapp, 2015) using an adjacency matrix

Node	A	B	C	D	E	F
A	0	1	1	0	0	0
B	1	0	0	1	0	0
C	1	0	0	1	1	0
D	0	1	1	0	0	1
E	0	0	1	0	0	1
F	0	0	0	1	1	0

The description of the basic NSMCF example by Trapp (2015) (see Figure 3.3) is explained as follows:

- There are three types of nodes, in a set of nodes n : source nodes (A and E in green); hub or intermediate nodes (C and D in black); and user nodes (B and F in red). The user nodes, B and F, require a (positive) specific amount of commodity b_i , which can be supplied by supplier nodes A and/or E. Such a specific amount of commodity b_i could be derived from the operational architecture of DS3 (Subsection 2.1.1). Node C and D are intermediate or hub nodes that ensure a continuous flow in the network. In this problem, the value for $b_C = 0$ and $b_D = 0$ (i.e., they do not demand any commodity b_i).

- To make this basic NSMCF example relatable to a DS3 example, the following assumptions were made. If the commodity transported in this network is the electric power, nodes A and E could be generator sets, nodes C and D could be switchboards, and nodes B and F could be any electrical components that demand power, such as computer consoles and pumps. The properties of these nodes are summarised in Table 3.2.

Table 3.2: Node properties of the NSCMF network problem in Figure 3.3 so derived from Trapp (2015) node labelling, node type, data type, DS3 example, and sign conventions were added by the candidate

Node	Type	Data	DS3 example	Notation	b_i value	Convention
A	Supply	Output	Generator Set	b_A	≥ 0	(-)
B	Demand	Input	Pump	b_B	10	(+)
C	Hub	Input	Switchboard	b_C	0	(+)
D	Hub	Input	Switchboard	b_D	0	(+)
E	Supply	Output	Generator Set	b_E	≥ 0	(-)
F	Demand	Input	Pump	b_F	5	(+)

- An arc connects node i to node j , hence all arcs in the set of arcs a make all nodes connected, forming the structure of the network. Arcs can be used to model cabling, delivering the power service from node to node. Each arc has an assigned coefficient of the objective function $\mu_{i,j}$ and flow capacity $U_{i,j}$ in a form of $\mu_{i,j} * U_{i,j} = OF_{i,j}$. Thus, as shown in Figure 3.3, the value of $U_{i,j}$ at each arc is zero before the solver is used. The objective function coefficients $\mu_{i,j}$ of these arcs are summarised in Table 3.3.

Table 3.3: Arc properties of the NSCMF network problem in Figure 3.3 connecting node i to node j outlined in Table 3.2 so derived from Trapp (2015)

Arc (i, j)	Notation $\mu_{i,j}$	Coefficient $\mu_{i,j}$ Value
(A,B)	$\mu_{A,B}$	5
(A,C)	$\mu_{A,C}$	2
(B,D)	$\mu_{B,D}$	2
(C,D)	$\mu_{C,D}$	10
(C,E)	$\mu_{C,E}$	1
(D,F)	$\mu_{D,F}$	1
(E,F)	$\mu_{E,F}$	1

- Before the optimisation begins, the value of $U_{i,j}$ at each arc as well as the total objective function 'OF' value at the top part of Figure 3.3 are zero. The objective function of this linear programming was set to minimise the total value of the multiplication between the objective function coefficient $\mu_{i,j}$ and arc flow capacity $U_{i,j}$. Therefore, this formulation constrains the possible flow path in the solution network, i.e., how the commodity would flow from the source nodes to the user nodes. The objective function coefficient $\mu_{i,j}$ can be used to represent the physical distance between DS3 components on a vessel so that selecting a certain arc can indicate a more "costly" routing than alternatives.
- The flow capacity $U_{i,j}$ is the decision variable in this optimisation (i.e., the variable to be minimised or maximised). Since the optimisation was set for a minimisation problem, the flow capacity $U_{i,j}$ must be positive to allow bidirectional flows (i.e., can change direction). To make the value of the flow capacity $U_{i,j}$ always positive, the flow variable $x_{i,j}$ was used, which is known as the 'capacity roll-up' (Trapp, 2015). The flow capacity $U_{i,j}$ could also be used to limit the possible maximum flow capacity at each arc.
- The use of the flow variable $x_{i,j}$ enabled the consideration of flow direction in the network, which was important to ensure continuity in the network, i.e., the flow will not stop at any hub nodes in the network. As introduced in Subsection 3.1.1, if the direction of the flow is in-degree (incoming to a node), the flow is positive and is negative for 'out-degree (outcoming) flow. Therefore, for example, at node C, there is one positive flow variable $x_{A,C}$ and two negative flow variables: $x_{C,E}$ and $x_{C,D}$. While at node A, there are two out-degree flows and no in-degree flow, because node A is a supplier.
- In this example, there was only one flow condition, which means the set of constraints only represent a particular scenario. In this case, all arcs in the network are functional, i.e., no casualties (Trapp, 2015). This is discussed in the following subsection.
- The mathematical notation of the linear programming formulation that is described above is summarised in Table 3.4.

Table 3.4: Linear programming formulation and realisation of the basic NSMCF example (Trapp, 2015) are presented in a table form with colour added by the candidate for the application of the proposed Operational Matrix framework

Linear Programming Formulation	Mathematical Notation	Realisation		
Objective Function Subject To:	$\min. \sum_{(i,j) \in E} \mu_{i,j} U_{i,j}$	$\mu_{A,B} U_{A,B} + \mu_{A,C} U_{A,C} + \mu_{B,D} U_{B,D} + \mu_{C,D} U_{C,D} + \mu_{C,E} U_{C,E} + \mu_{D,F} U_{D,F} + \mu_{E,F} U_{E,F}$		
Continuity	$\sum_{(i,j) \in E} x_{i,j} - \sum_{(i,j) \in E} x_{j,i} - b_i = 0$	$\begin{aligned} -1x_{A,B} - 1x_{A,C} &= -1b_A \\ 1x_{C,D} + 1x_{B,D} - 1x_{E,F} &= 1b_D \end{aligned}$	$\begin{aligned} -1x_{A,B} - 1x_{B,D} &= 1b_B \\ 1x_{C,E} - 1x_{E,F} &= -1b_E \end{aligned}$	$\begin{aligned} 1x_{A,C} - 1x_{C,E} - 1x_{C,D} &= 1b_C \\ 1x_{D,F} + 1x_{E,F} &= 1b_F \end{aligned}$
Capacity Rollup	$ x_{i,j} \leq U_{i,j}$	$ x_{A,B} \leq U_{A,B}$	$ x_{A,C} \leq U_{A,C}$	$ x_{B,D} \leq U_{B,D}$
		$ x_{C,D} \leq U_{C,D}$	$ x_{C,E} \leq U_{C,E}$	$ x_{D,F} \leq U_{D,F}$
Bounds	$ x_{i,j} \leq U_{i,j}$	$ x_{E,F} \leq U_{E,F}$		
		$-\infty \leq x_{A,B} \leq \infty$	$-\infty \leq x_{A,C} \leq \infty$	$-\infty \leq x_{B,D} \leq \infty$
		$-\infty \leq x_{C,D} \leq \infty$	$-\infty \leq x_{C,E} \leq \infty$	$-\infty \leq x_{D,F} \leq \infty$
Operating Scenario	b_i	$b_A \geq 0$	$b_B = 10$	$b_C = 0$
		$b_D = 0$	$b_E \geq 0$	$b_F = 5$
Indices	$(i, j) \in a$	$(A, B) \in a \dots (E, F) \in a$		
	$i \in n$	$A, \dots, F \in n$		

The linear programming formulation in Table 3.4 is then presented as a $[23 \times 21]$ Operational Matrix and outlined in Table 3.5. Since the Operational Matrix in Table 3.5 already includes the network solution in brackets, this could also be used to understand the relationship between the objective function and the constraints of the linear programming formulation. The layout description of such a matrix is outlined as follows:

- The network solution, which consists of values in brackets in the matrix, was obtained using the solver CPLEX toolbox in MATLAB. These values were divided into three groups based on the number of columns in the table. The first seven columns (black) give the flow capacity $U_{i,j}$ values whereas the second seven columns (blue) give the flow variable $x_{i,j}$ values. The remainder values, which are in columns 15 to 20 (green or red), give the amount of supply or demand of the commodity b_i . The supply values (green) are part of the output where the demand values are part of the predefined input as shown in Table 3.2.
- The first row of the matrix in Table 3.5 gives the objective function. The values that are not in the bracket in the first seven columns in this row provide coefficients $\mu_{i,j}$ for the objective function, and the remaining columns (8 to 20) were set to zero because the flow capacity $U_{i,j}$ (black) was the variable that was minimised, not the flow variable $x_{i,j}$ (blue), nor the commodity b_i (green and red).
- Values at rows 2 to 7 and the first seven columns are zero because these rows were dedicated for continuity. The continuity is given by the equality constraints matrix, which consists of rows 2 to 7 and columns 8 to 21 to model six continuity constraints in Table 3.4. Values +1 and -1 in purple represent coefficients of continuity constraints.
- The realisation of 'capacity roll-up' (Trapp, 2015) that connects the flow variable $x_{i,j}$ (blue) and the flow capacity $U_{i,j}$ was applied in the inequality constraints matrix located at rows 8 to 23 and columns 1 to 14 and 21. Values -1 (dark orange) in this region indicate coefficients for the capacity roll-up (Trapp, 2015). As this formulation was applied to arcs instead of

nodes, the remainder values for the inequality constraints matrix situated at rows 8 to 21 and columns 15 to 21 were zero.

- Rows 22 to 23 and columns 1 to 14 show the lower bounds and the upper bounds for the flow capacity $U_{i,j}$ (black) and the flow variable $x_{i,j}$ (blue), respectively. The flow capacity $U_{i,j}$ could be used to limit the possible maximum flow capacity at each arc. However, such a formulation was not used and thus the flow capacity $U_{i,j}$ could be any positive values. Lower bounds and upper bounds that define the supply or demand amount of commodity b_i is located at the same row but in different columns, which are 15 to 20.
- Arrows were added to reveal the relationship between various values and coefficients of the linear programming formulation in the matrix. Although all elements (without bracket) in the Operational Matrix are the input of the linear programming formulation, bounds (situated at rows 22 to 23 and columns 15 to 20) are key inputs in this formulation. Therefore, the arrows are originated from this input, which directly constrains the commodity b_i , the flow variable $x_{i,j}$, and then the flow capacity $U_{i,j}$ solutions. The flow capacity $U_{i,j}$ and the flow variable $x_{i,j}$ solutions are also constrained by bounds located at rows 22 to 23 and columns 1 to 14.

Table 3.5: The Operational Matrix of the basic NSCMF example, showing the basic NSMCF example (Trapp, 2015) (see Figure 3.3 on page 74 and Table 3.4 on page 77) is presented using the proposed Operational Matrix framework with arrows showing relationships of constraints (see six bullet points on pages 78 and 79)

NO	1	2	3	4	5	6	7	8	9	10	11	12	13	14	15	16	17	18	19	20	21		
Objective Function	5 (0) 2 (0) 2 (10) 10 (0) 1 (0) 1 (10) 1 (15)							0 0 0 0 0 0 0							0 0 0 0 0 0 0								
	Arcs							Arcs							Nodes								
	$\mu_{A,B}U_{A,B}$	$\mu_{A,C}U_{A,C}$	$\mu_{B,D}U_{B,D}$	$\mu_{C,D}U_{C,D}$	$\mu_{C,E}U_{C,E}$	$\mu_{D,F}U_{D,F}$	$\mu_{E,F}U_{E,F}$	$x_{A,B}$	$x_{A,C}$	$x_{B,D}$	$x_{C,D}$	$x_{C,E}$	$x_{D,F}$	$x_{E,F}$	b_A	b_B	b_C	b_D	b_E	b_F			
	$\sum_{(i,j) \in E} \mu_{i,j}U_{i,j}$							$\sum_{(i,j) \in E} x_{i,j} - \sum_{(i,j) \in E} x_{j,i}$							$-b_i$							=	0
Equality constraints matrix for continuity	2	0	0	0	0	0	0	-1 (0)	-1 (0)	0	0	0	0	0	1 (0)	0	0	0	0	0	0		
	3	0	0	0	0	0	0	1 (0)	0	-1 (-10)	0	0	0	0	0	-1 (10)	0	0	0	0	0		
	4	0	0	0	0	0	0	0	1 (0)	0	-1 (0)	-1 (0)	0	0	0	0	0	0	0	0	0		
	5	0	0	0	0	0	0	0	0	1 (-10)	1 (0)	0	0	-1 (-10)	0	0	0	0	0	0	0		
	6	0	0	0	0	0	0	0	0	0	0	-1 (0)	0	0	-1 (15)	0	0	0	0	1 (15)	0		
	7	0	0	0	0	0	0	0	0	0	0	0	0	1 (-10)	1 (15)	0	0	0	0	0	-1 (5)	0	
Inequality constraints matrix for bidirectionality	8	-1 (0)	0	0	0	0	0	-1 (0)	0	0	0	0	0	0	0	0	0	0	0	0	0		
	9	0	-1 (0)	0	0	0	0	0	-1 (0)	0	0	0	0	0	0	0	0	0	0	0	0		
	10	0	0	-1 (10)	0	0	0	0	0	-1 (-10)	0	0	0	0	0	0	0	0	0	0	0		
	11	0	0	0	-1 (0)	0	0	0	0	0	-1 (0)	0	0	0	0	0	0	0	0	0	0		
	12	0	0	0	0	-1 (0)	0	0	0	0	0	-1 (0)	0	0	0	0	0	0	0	0	0		
	13	0	0	0	0	0	-1 (10)	0	0	0	0	0	0	-1 (-10)	0	0	0	0	0	0	0		
	14	0	0	0	0	0	0	-1 (15)	0	0	0	0	0	0	-1 (15)	0	0	0	0	0	0		
	15	-1 (0)	0	0	0	0	0	0	1 (0)	0	0	0	0	0	0	0	0	0	0	0	0		
	16	0	-1 (0)	0	0	0	0	0	0	1 (0)	0	0	0	0	0	0	0	0	0	0	0		
	17	0	0	-1 (10)	0	0	0	0	0	0	1 (-10)	0	0	0	0	0	0	0	0	0	0		
	18	0	0	0	-1 (0)	0	0	0	0	0	0	1 (0)	0	0	0	0	0	0	0	0	0		
19	0	0	0	0	-1 (0)	0	0	0	0	0	0	1 (0)	0	0	0	0	0	0	0	0			
20	0	0	0	0	0	-1 (10)	0	0	0	0	0	0	1 (-10)	0	0	0	0	0	0	0			
21	0	0	0	0	0	0	-1 (15)	0	0	0	0	0	0	1 (15)	0	0	0	0	0	0			
Lower bounds matrix	22	0	0	0	0	0	0	$-\infty$	$-\infty$	$-\infty$	$-\infty$	$-\infty$	$-\infty$	$-\infty$	0	10	0	0	0	0	5		
Upper bounds matrix	23	∞	∞	∞	∞	∞	∞	∞	∞	∞	∞	∞	∞	∞	∞	10	0	0	∞	5			
		$U_{i,j} \geq 0$							$-\infty \leq x_{i,j} \leq \infty$							Investigated operating scenario (Table 3.4)							

The NMSCF flow capacity $U_{i,j}$ solution from the Operational Matrix is attached back to the network and is presented in Figure 3.4. Figure 3.4 shows the multiplication between the coefficient $\mu_{i,j}$ and the flow capacity $U_{i,j}$ solution as the label of each arc. Hence, as indicated at the top part of Figure 3.4, the total objective function (OF) value is 45 (i.e., $15+10+20=45$). Figure 3.4 also indicates some arcs have zero flow capacity $U_{i,j}$ solutions, which means those edges or DS3 connections are unnecessary (Trapp, 2015). This, in turn, suggests that the optimisation scheme, i.e., the linear programming formulation plays an important role in constraining DS3 network flow solution, which can then be converted to space and weight input for the relevant DS3 provided that the power to weight and power to volume ratios are known or assumed. Figure 3.4 also shows that the flow path in the Network Flow Optimisation (NFO) can be used for a steady state simulation, i.e., how a DS3 network would respond in a specific set of flow directions to various static loads in an operational scenario. Examples of static loads in this basic NSMCF were nodes B and F.

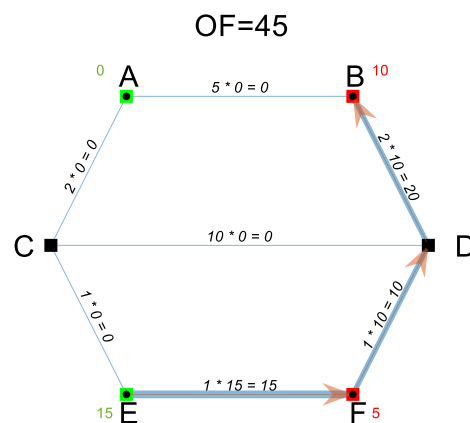


Figure 3.4: A network flow solution of the NSCMF network problem in Figure 3.3 from Trapp (2015), revisited by the candidate using the proposed Operational Matrix framework

The NFO has been introduced and reviewed by revisiting an NSMCF problem from Trapp (2015) using the proposed Operational Matrix framework. The use of the proposed framework reveals the relationship between objective functions, constraints, bounds, and solutions of that linear programming formulation. The next subsection discusses a further application of the proposed Operational Matrix framework to another NFO problem proposed by Trapp (2015).

3.1.3 Edge Loss Scenario in the Network Flow Optimisation

Another key feature in the NSMCF approach is the minus one (M-1) survivability, which guarantees the specified demands in the network can be met with a minimum 'cost' flow although an edge is assumed to be lost (i.e., flow variable $x_{i,j} = 0$) in a given loss scenario (Trapp, 2015). This was used by Trapp to quantify the survivability of an Integrated Engineering Plant of a typical naval combatant (Trapp, 2015). Thus, if there are seven arcs, as in Figure 3.3, there are seven edge loss scenarios. The 'aggregate' solution, which is a term introduced by Robinson (2018), then captures maximum capacity flows in those loss scenarios i.e., an arc from the aggregate solution is sized to accommodate all possible arc flow capacities ($U_{i,j}$) in those loss scenarios.

To simulate edge loss scenarios for the basic NSMCF example, the formulation becomes multicommodity or multiflow conditions (not one flow condition as in Table 3.4). Thus, more than one set of constraints could be considered where each set of constraints represents an edge loss scenario and would be incorporated in a 'global' objective function (Trapp, 2015) (see Table A 1 in Appendix 1). This means the implementation of multiflow conditions would result in a large numbers of constraints for CPLEX to solve. Thus, if the Operational Matrix framework (Table 3.5) is used, the size of the matrix (rows 7 to 23 and columns 8 to 21) will expand seven fold. Since this expansion depends on the number of arcs a and number of nodes n in a network problem, theoretically, it can be mathematically described as a $[a^2 \times (a + n)^2]$ matrix. Hence, the scalability of the Operational Matrix for a network with (say) 100 arcs and 50 nodes would be about 10,000 rows and 22,000 columns, and thus increase both the designer's workload and the CPLEX computational resources if applying the NFO to an ESSD submarine DS3 synthesis. This suggested an alternative approach was necessary for solving the multiflow Network Flow Optimisation (NFO) using the proposed Operational Matrix framework.

Rather than expanding the Operational Matrix in Table 3.5, the basic NSMCF example (Trapp, 2015) with M-1 survivability was revisited and the optimisation was solved individually in each flow situation, using a loop in MATLAB, which

was referred to by the candidate as the ‘single flow formulation’. This, in turn, reduced the effort of defining multicommodity formulation in the proposed Operational Matrix framework. Furthermore, the single flow formulation was likely to result in a less demanding computation as the number of variables and constraints were less than the multicommodity formulation.

The results of using the single flow formulation in the proposed Operational Matrix are presented in Table 3.6 (left) and are compared with the results of multicommodity formulation from Trapp (2015), which is given in Table 3.6 (right). In this comparison, some differences were found, more specifically, the flow path of scenarios (a), (c), (e), and (f), which are marked with an asterisk (*) in Table 3.6. These flow path discrepancies reveal that in those edge loss scenarios, the single flow formulation always gives a local minimum, i.e., the multicommodity formulation in some cases results in a higher OF value than the single flow formulation.

Despite the difference in terms of the local minima, the single flow formulation gives the same aggregate result as the multicommodity formulation (see the aggregate solution at the bottom part of Table 3.6). This confirms that the same aggregate solution in this specific NSMCF example can be obtained more efficiently with fewer constraints without the need to include all edge loss scenarios in the global objective function. Therefore, the current research suggests that the input required for the NFO could potentially be reduced for DS3 sizing focused investigations and is commensurate with the early-stage submarine design application.

3.1.4 Conclusion from the Network Flow Optimisation Approach

In this subsection, the Network Flow Optimisation (NFO) approach is not just reviewed but also revisited with a different solver and formulation, which was fully undertaken in the MATLAB environment. This allowed the proposed Operational Matrix framework to be developed in the current research. There are three key points from this work: (1) the NFO with an appropriate linear programming formulation can be used to perform a steady state simulation of power flow in a DS3 network; (2) the Operational Matrix framework could be

used to manipulate the linear programming formulation; (3) the number of constraints could also be reduced for DS3 synthesis focused and a more style driven approach by excluding the edge loss scenario in the global objective function, without producing a different aggregate network solution. This could also reduce both the designer's workload and computational resources when applying the network flow synthesis for submarine ESD DS3 synthesis.

However, the single flow formulation could potentially lead to a significant discrepancy regarding the individual flow path results when applied to a much larger network problem than this NSMCF example. Such problems may involve hundreds of nodes and arcs, better reflecting the actual DS3 components on the vessel. Nevertheless, the interest of DS3 sizing in this NSMCF example is at the aggregate solution level, not at the individual flow path response (see Table 3.6 (a) to (h)). The next section investigates whether it is sensible to use a network flow based synthesis for submarine ESD without the M-1 survivability (Trapp, 2015). Thus, differences in local minima when applying the M-1 formulation (Trapp, 2015) were likely seen to be trivial for the DS3 synthesis when that is not optimisation driven, i.e., a more style driven approach.

As reviewed in Subsection 2.3.4, the research team at Virginia Tech has expanded the NSMCF approach (Trapp, 2015) to be the Non-Simultaneous Multi Constraints Parallel Commodity Flow (NSMCPCF) that they call Architecture Flow Optimisation (AFO) and have incorporated it into the Virginia Tech's ship design process (Parsons et al., 2020a). One of the distinctive mathematical features in the AFO formulation that was used in this research was the use of coefficients for representing a fraction of a commodity entering and leaving a node (Robinson, 2018). This also assumes a steady-state condition for various DS3 loads and thus has a sufficient level of detail for DS3 component sizing in ESSD (Parsons et al., 2020a). Such coefficients were added to the continuity constraints, which cause a set of elements in the Operational Matrix in Table 3.5 (rows 2 to 7 and columns 8 to 20) to be an integer number instead of +1 or -1. This is discussed further in the following section, which presents the first implementation of the network theory to a submarine's DS3 problem.

Table 3.6: Results comparison of an NSCMF network problem (in Figure 3.3) between single flow formulation and multicommodity formulation, the results due to single flow formulation in the proposed Operational Matrix framework are given in the left part of each cell, while the multicommodity solution from Trapp (2015) is presented in the right part of each cell with the OF value added by the candidate at the top part of each cell (nodes A, B, C, D, E, F are equivalent to nodes 1, 2, 3, 4, 5, 6)

(a) No loss*		(b) Loss of arc A,B	
<p>OF=45</p>	<p>OF=90</p> <p>(Trapp, 2015)</p>	<p>OF=45</p>	<p>OF=45</p> <p>(Trapp, 2015)</p>
(c) Loss of arc A,C*		(d) Loss of arc B,D	
<p>OF=45</p>	<p>OF=90</p> <p>(Trapp, 2015)</p>	<p>OF=55</p>	<p>OF=55</p> <p>(Trapp, 2015)</p>
(e) Loss of arc C,D*		(f) Loss of arc C,E*	
<p>OF=45</p>	<p>OF=55</p> <p>(Trapp, 2015)</p>	<p>OF=45</p>	<p>OF=90</p> <p>(Trapp, 2015)</p>
(g) Loss of arc D,F		(h) Loss of arc E,F	
<p>OF=55</p>	<p>OF=55</p> <p>(Trapp, 2015)</p>	<p>OF=90</p>	<p>OF=90</p> <p>(Trapp, 2015)</p>
Aggregate solution			
<p>OF=120</p>		<p>OF=120</p> <p>(Trapp, 2015)</p>	

3.2 Initial Implementation of Network to Distributed Systems

In this section, two types of network theory were applied to initially synthesising a selected DS3 example for a submarine: semantic network and a new Network Flow Optimisation (NFO) formulation, which is called by the candidate as the Submarine Flow (SUBFLOW) simulation. These selections, as discussed in Subsection 2.2.1, are part of selecting the synthesis model type in the decision making process for complex vessels (Figure 2.3 on page 43). Nonetheless, in this initial implementation, it was kept simple and thus not a “full” vessel synthesis. The size of the vessel was simply derived from the payload data. The main goal of this implementation was to show the SUBFLOW compared to the semantic network and how it could be used, together with the traditional numerical sizing procedure (Subsection 2.2.2) for a specific DS3 choice.

Therefore, this section is divided into six parts. Subsection 3.2.1 outlines the decision making process of the case study. This is followed by Subsection 3.2.2, which outlines a proposed framework used for defining various design style decisions in the current research. Subsection 3.2.3 explains the traditional numerical synthesis procedure as well as the nature of the case study. Subsection 3.2.4 discusses the implementation of semantic network to the case study while Subsection 3.2.5 gives the application of the SUBFLOW to the case study. Subsection 3.2.6 provides an initial conclusion of the case study.

3.2.1 Case Study 3.2.1 Setup

The first instance of sizing a submarine power system was chosen. This exercise became the basis for a much larger DS3 network case study (Chapter 5). Therefore, the broad specification for a submarine, using the UCL submarine Databook (UCL-NAME, 2014), was drawn up to provide performance requirements and an appropriate payload equipment listing. The summary of the decision making necessary to progress this initial network implementation, which is referred as to Case Study 3.2.1, was kept simple and is provided in Table 3.7. The detailed calculation of this case study is provided in Appendix 2.

Table 3.7: The realisation for Case Study 3.2.1, following the decision making sequence for complex vessels outlined in detail in Figure 4 and Appendix of (Andrews, 2018c) in a similar manner to the example in Figure 4 of (Andrews, 2021)

Process Step	Selection Decision / Realisation for Case Study 3.2.1	
Perceived need	Implementation of the network theory for DS3 power sizing	
Outline of initial requirements	Initial submarine key parameters desired (capabilities)	
	Payload equipment (Table 3.8)	
Selection of style of emerging ship design	Style Level	Choice
	Macro Level	Non nuclear (SSK)
	Main Level	Diesel-electric power plant
		Medium size ocean-going submarine
		Single hull with casing
Micro Level	DC distribution	
Selection of major equipment and operational sub-systems	Diesel-electric systems Lead/acid battery	
Selection of whole ship performance characteristics	General Level	Value
	Submerged speed	5 knots (17 hrs)
	Snort speed	7 knots (5 hrs)
	Specific Performance	Value
	Indiscretion ratio (Burcher and Rydill, 1994)	< 25 %
	Margin for energy	20 %
	Margin for charging	5 %
	Efficiency for electrical losses	97 %
	Efficiency converter AC to DC	98 %
Selection of synthesis model type	Numerical design algorithms (Burcher and Rydill, 1994; UCL-NAME, 2012, 2014) Semantic network (Sowa, 1983) SUBFLOW simulation (expanded from (Trapp, 2015; Robinson, 2018))	

Table 3.8: Baseline submarine payload equipment based on the broad specifications of a typical submarine (UCL-NAME, 2014)

Payload Equipment	Description	Unit/Set
600 mm tubes (OD)	Torpedo tubes to eject the torpedo from the submarine	6
Spearfish-UK	Torpedo reloads as the anti-ship or anti-submarine weapon	18
Air turbines	Air turbine pump torpedo discharge system	2
Bandfish-UK	Countermeasures to distract, decoy or destroy incoming torpedoes	2
SPA4 RFOM-81	Sonar systems (1 cylindrical Bow Passive Sonar (BPS), 6 Passive Ranging Sonar (PRS), and 2 Flank Array Sonar (FAS))	1
R3 RFOM-100	Radar mast non-penetrating telescopic	1
EW4 RFOM-72	Submarine Electronic Warfare	1
C5 RFOM-53	Communications fit, which operates across the frequency spectrum	1
CMS7 RFOM-85	Combat Management Systems	1

3.2.2 Proposed Style Framework

As shown in Table 3.7 multiple style decisions need to be made at ESSD including style for DS3. Therefore, a framework for style decisions was proposed to cover four different levels of style decisions. The first four levels of style choice were categorised in order, leading from high level decisions to low level decisions (see Figure 3.5). The highest level was the mega style, which was the government selection (Subsection 2.1.2) while the example of high level style decisions at the *Macro Level* included nuclear or non nuclear. Moving to the mid level, there were *Main/Meso Level* style choices, which included decisions for technology adopted in the design, such as various AIP types. A more detailed style, seen at *Micro Level*, was appropriate to DS3 or other specific style choices.

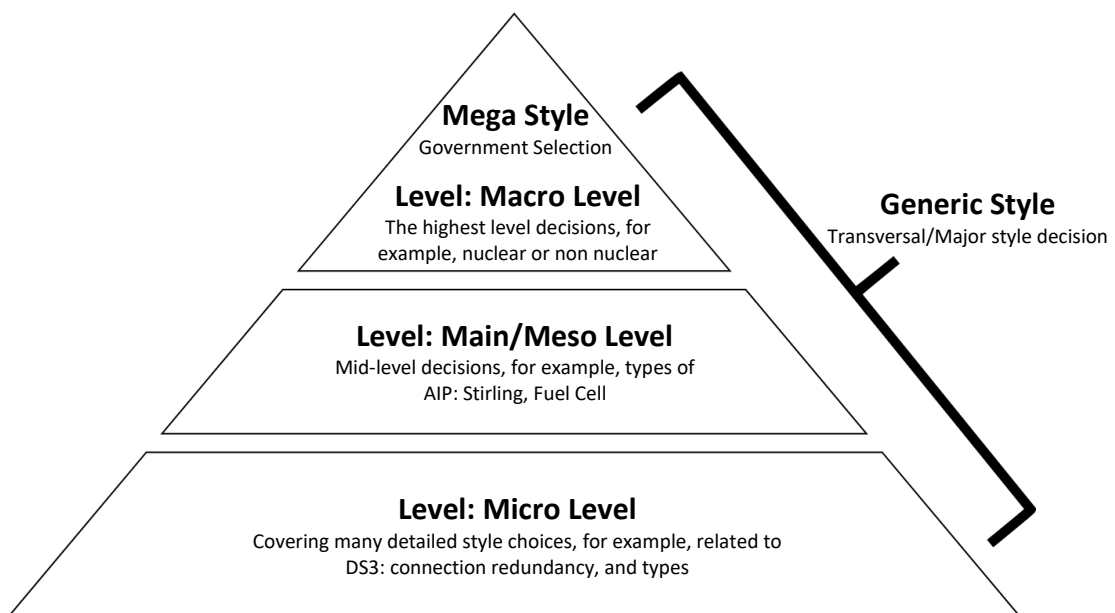


Figure 3.5: Proposed style framework

On top of those four levels, there were generic styles that could be used to host the transversal style decisions (Subsection 2.1.2) or qualitatively cover styles as listed in Table 2.1 on page 41. This generic level of style will influence either directly or indirectly other levels of style choice. Therefore, for example, if a generic style choice, such as robustness, was to be selected, the realisation of that robustness style choice at micro level style could be a ring main DS3 configuration, which would give a high level of redundancy (port and starboard,

forward and aft connections) and thus robustness to the DS3 design. Andrews (2018c) considers these decisions need to be acknowledged by the designer and documented as a mark of good design practice in the decision making process for complex vessels.

3.2.3 Traditional Numerical Synthesis of the Case Study

The case study was commenced by using initial requirements in Table 3.7, to derive payload information, such as volume, weight, and power load, which was taken from open-source data (UCL-NAME, 2014), eliminating any issues of security classification. A specific style decision, that is a diesel electric SSK, was chosen in Case Study 3.2.1. Thus, using the payload volume fraction of an SSK (Burcher and Rydill, 1994), the first shot at pressure hull volume was estimated (2000 m³). By making more assumptions to hull geometry, such as external Main Ballast Tank (MBT), forward and aft end volumes, fin volume, casing volume, and hydroplanes volumes, an initial submarine submerged volume was obtained. The domain knowledge required for this process was visualised in a semantic network (Collins et al., 2015). This initial hull geometry gave key design variables for estimating other design features, such as the estimation of the propulsion system, as spelt out in the procedure by Burcher & Rydill (1994).

Once the procedure entered propulsion system estimation, the relevant design algorithms for this step needed to be determined. To do this, the physics of the case study are discussed. As specified in Table 3.7, the SSK style decision led directly to selecting the major equipment and sub-systems, namely, diesel-electric propulsion with a lead/acid battery. The performance of a modern SSK style is quantified by the visual discretion or indiscretion ratio (IR), which is the proportion of time for battery charging to battery discharge defined by Burcher and Rydill (1994). To calculate IR, some assumptions at sub level were required on top of the general level ship performance characteristics (see Table 3.7). Therefore, the IR was not only an important performance measure but also a driver in the SSK propulsion system sizing (see Appendix 2), part of the DS3 operational architecture of the SSK (Subsection 2.1.1).

A depiction of battery charging and discharging in a typical operational mode for an SSK is described in Figure A.4, Appendix 1. The energy on an SSK is an energy transfer between the fuel, the battery, the power loads, and the environment. Therefore, to calculate power estimation of such a distinct SSK operational architecture (diesel power P_{DIES}), a mathematical relationship for diesel power sizing was used, which is given in Equation (3.1) (Burcher and Rydill, 1994). This algorithm expresses that the power output that a diesel engine fit must be able to satisfy the electric service demand for charging batteries, propulsion load, and hotel load, as well as the likely inefficiencies and margins required to accomplish snorting operations.

$$P_{DIES} = \left[(1 + m)(I_{max} \times 2.4 \text{ Volts} \times N_c) + \frac{P'_s}{\eta_{el}} + H_{snort} \right] \frac{1}{\eta_{conv}} \quad (3.1)$$

The description of Equation (3.1) is broken down as follows:

- Equation (3.1) first shows a margin m is applied to battery charging demand ($I_{max} \times 2.4 \times N_c$). As discussed in Subsection 2.1.2, the selection of margins is part of the design style issues.
- The battery charging demand is described as a physical-law relationship, which is calculated from the multiplication of several variables: the maximum current I_{max} ; maximum charging voltage of 2.4 Volts for lead/acid battery (Burcher and Rydill, 1994); and the number of battery cells N_c . Both the maximum charging current I_{max} and the maximum charging voltage 2.4 Volts are dependent on the type of battery used. As already specified in Table 3.7, the lead/acid battery type was chosen.
- Initial propulsion load in the snorting condition P'_s was obtained using Burcher & Rydill's algorithms in their Appendix 5 and is accounted with an assumed electrical efficiency η_{el} , more specifically, efficiency due to the energy transfer from the diesel prime movers to propulsion motor.
- The hotel load snort H_{snort} covers the power required for both the payload equipment H_{pay} and other DS3 equipment in the snorting condition. The hotel load in the snorting condition is expected to be lower than in the submerged condition H_{sub} due to access to the atmosphere for ventilation

(Burcher and Rydill, 1994). Since Burcher & Rydill (1994) did not quantitatively specify the difference of the hotel load between snorting and submerged operation, the snorting hotel load H_{snort} was assumed to be 80% of submerged hotel load H_{sub} . Burcher and Rydill assumed the hotel load in the submerged condition to be linear to the volume of the pressure hull. Therefore, since this algorithm depends on the submarine size, it implies a parametric approach (Subsection 2.3.1).

- Finally, all loads were multiplied by an efficiency due to electrical conversion η_{conv} . This conversion could be between the alternate current (AC) diesel generators to direct current (DC) power distribution, part of the micro style choice in Table 3.7.

Tables 3.9 and 3.10 give the necessary variables and associated algorithms that were used to solve the power sizing algorithm in Equation (3.1). Some variables in Table 3.9 were obtained from UCL submarine data (UCL-NAME, 2014), such as the physical properties of the lead/acid battery. However, the hotel payload H_{pay} , the volume of the pressure hull PH_{vol} , as well as the propulsion power (P'_s and P''_s) to meet different speed requirements were calculated using Burcher & Rydill's algorithms (1994). Some variables had then to be calculated, as shown in Table 3.10, before Equation (3.1) was solved. By using the values provided by Tables 3.9 and 3.10, the power of diesel calculated was found to be 2.7 MW (see Appendix 2 for detailed calculations).

Table 3.9: Summary of calculated prerequisite variables for diesel sizing, due to the decision making given in Table 3.7 detailed calculations and assumptions are given in Appendix 2

Variable	Description	Value
T_{chmin}	Minimum time to recharge lead/acid battery	5 hr
k_{BAT}	Battery constant/energy density lead/acid battery	15.92 kW
n	Empirical value lead/acid battery	0.08
I_{max}	Maximum current lead/acid battery	1900 A
H_{pay}	Hotel load for payload equipment	83 kW
PH_{vol}	Volume of pressure hull	2000 m ³
P'_s	Propulsion power at snort speed	160.8 kW
P''_s	Propulsion power at submerged speed	72.3 kW

Table 3.10: Summary of variables and algorithms for diesel sizing, detailed calculations and assumptions are given in Appendix 2

Variable	Description	Value	Algorithm (Burcher and Rydill, 1994) (UCL-NAME, 2012)
T_{sub}	Time submerged	17.7 hr	$T_{sub} = \frac{T_{chmin}}{IR} - T_{chmin}$
T_{DIS}	Discharge time	22 hr	$T_{DIS} = \frac{T_{sub}}{1-x}$
E	Energy available of each battery cell	20.4 kW hr	$E = k_{BAT} T_{DIS}^n$
N_c	Number of cells	480	$N_c = \frac{D \left(\frac{T_{sub}}{1-x} \right)}{E(1-x)}$
H_{sub}	Hotel load submerged	280 kW	$H_{sub} = 0.75H_{pay} + 0.075PH_{vol}$
D	Battery drain	354.5 kW	$D = \frac{P''_s}{\eta_{el}} + H_{sub}$
H_{snort}	Hotel load snorting	224 kW	$H_{snort} = 80\% H_{sub}$

3.2.4 Semantic Network Applied to the Case Study

A semantic network (Subsection 2.3.4) was applied to identify the domain knowledge behind all variables required for the power sizing process shown in Tables 3.9 and 3.10 and thus is shown in Figure 3.6. The network is directed (Subsection 3.1.1) and nodes in this network have been arranged to reveal the order of variables needed for the calculation.

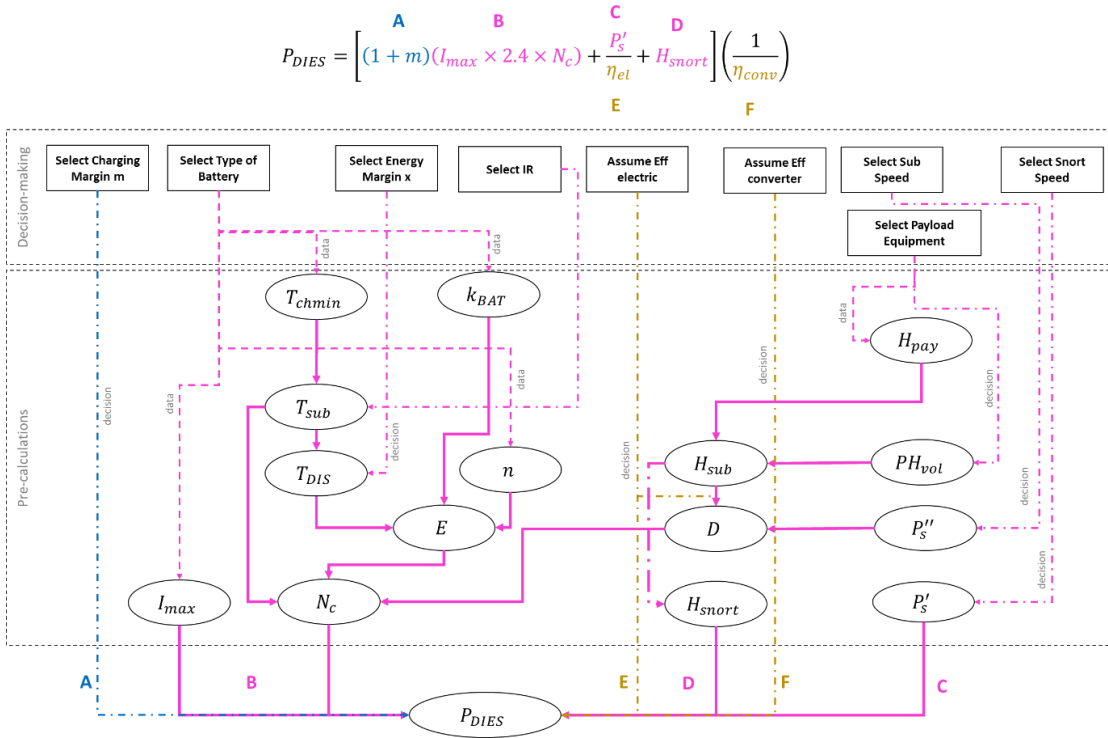


Figure 3.6: Semantic network of diesel powering sizing algorithm for a SSK based on Burcher and Rydill’s (1994) formula (Equation (3.1)) and the UCL submarine design procedure (UCL-NAME, 2012) calculation (see Tables 3.9 and 3.10)

The description of Figure 3.6 is outlined as follows:

- The top part of Figure 3.6 shows Equation (3.1), which is divided into several groups: group A (blue) is for margin m ; groups B, C, D (magenta) are for the battery charging demand $(I_{max} \times 2.4 \times N_c)$, the propulsion load in the snorting condition P'_s , and the hotel load in the snorting condition H_{snort} ; groups E and F (yellow) are for efficiencies due to electrical η_{el} and converter η_{conv} respectively. Arcs are coloured based on these groups.
- The upper dotted box in Figure 3.6 shows variable nodes in a rectangular shape due to decision making (listed in Table 3.7) while the lower dotted

box contains variable nodes identified in Tables 3.9 and 3.10 as ellipsoid shapes.

- The dashed-dotted and dashed arcs infer the first relationship between ‘parent’ nodes (variable nodes inside the decision making dotted box) to the ‘child’ nodes. There are only two types of contextual data attached to each of these arcs: ‘decision’ (dashed-dotted arcs) represents a relationship that can be influenced by the designer through assumptions, rule of thumbs, or engineering judgement while ‘data’ (dashed arcs) delineates a relationship based on a physical law that already determined in the decision making process, listed in Table 3.7.
- Multiple solid line arcs were used to model node relationships that were based on an unchanged physical law.

Figure 3.6 reveals a total of 25 nodes is connected by 28 arcs, where 36% of total nodes are the parent nodes and 64% child nodes, which are dependent on the decision making (Table 3.7). This means, on top of the algorithm used, there are only eight variable nodes that can be used by the designer for directly manipulating the resultant value of the installed diesel power. Some of the parent nodes were directly connected to terms in the main algorithm (Equation (3.1)), such as A, E and F. Other parent nodes are connected to data-driven variable nodes, such as minimum time to recharge lead/acid battery T_{chmin} , (dashed arcs). The rest of the parent nodes are connected to prerequisite variable nodes calculated by terms B, C, and D. Since arcs containing ‘data’ are subject to Requirement Elucidation, any changes in the decision making process such as the use of nuclear instead of non nuclear, would significantly change the semantic network model.

Although the semantic network in Figure 3.6 could reveal the domain knowledge for power sizing, the network structure is bounded to Burcher and Rydill’s algorithm for an SSK power sizing (as selected in the decision making process (Table 3.7)) and thus still requires further step to determine the configuration of DS3. Since the semantic network was not used to model physical models of DS3, it cannot capture the style choices for the DS3, such as decisions on applying redundancy to DS3 connections, or other detailed

micro level styles on specific DS3 components (Subsection 3.2.2). Most importantly, it could not sufficiently aid the designer understanding of this specific system and the power sizing calculation was performed separately from the network model. Therefore, another type of network, which is the Network Flow Optimisation (NFO) (Section 3.1) with a specific network formulation called SUBFLOW, was investigated.

3.2.5 SUBFLOW Applied to the Case Study

Trapp's NSMCF (Trapp, 2015) and Virginia Tech's AFO (Robinson, 2018) formulations were expanded to the submarine's DS3 application, which is referred to by the candidate as the SUBFLOW simulation. The SUBFLOW in this case study was devised and could be applied as soon as the design calculation entered the power estimation step, using Burcher & Rydill's procedure, and undertaken before hull design and hull parameters were fixed for the baseline design. The aim of the SUBFLOW was not to optimise DS3 nor submarine design but for seeking submarine energy balance and subsequently submarine's DS3 sizing through one commodity (power) as the single flow in the network (see Section 3.3). Therefore, the SUBFLOW is not multicommodity as in the NSMCF (see multiflow conditions in Subsection 3.1.3) nor parallel commodity as in the NSMCPCF (AFO) approach. This is discussed further in Chapter 7.

The implementation of the SUBFLOW simulation was commenced by first developing a sketch of the network for the DS3 of interest, i.e., the power system (as specified in Table 3.7). As shown in Figure 3.7, developing the sketch could have been based on a traditional marine engineering line diagram (as a template (Chalfant and Chrysostomidis, 2017)) or could have been evolved from scratch. Unlike the previously shown semantic network (Figure 3.6), the dotted box in Figure 3.7 shows that the structure of the DS3 network was influenced directly by the micro level DS3 styles (Subsection 3.2.2), listed in the decision making for complex vessels (Table 3.7). After sketching, the development of SUBFLOW began by defining the properties of the elements of the network, producing a mathematical model, and then creating an adjacency matrix and an Operational Matrix (Subsection 3.1.2). The process was iterative

until the network model sufficiently reflected the chosen DS3 style and the physics of the submarine.

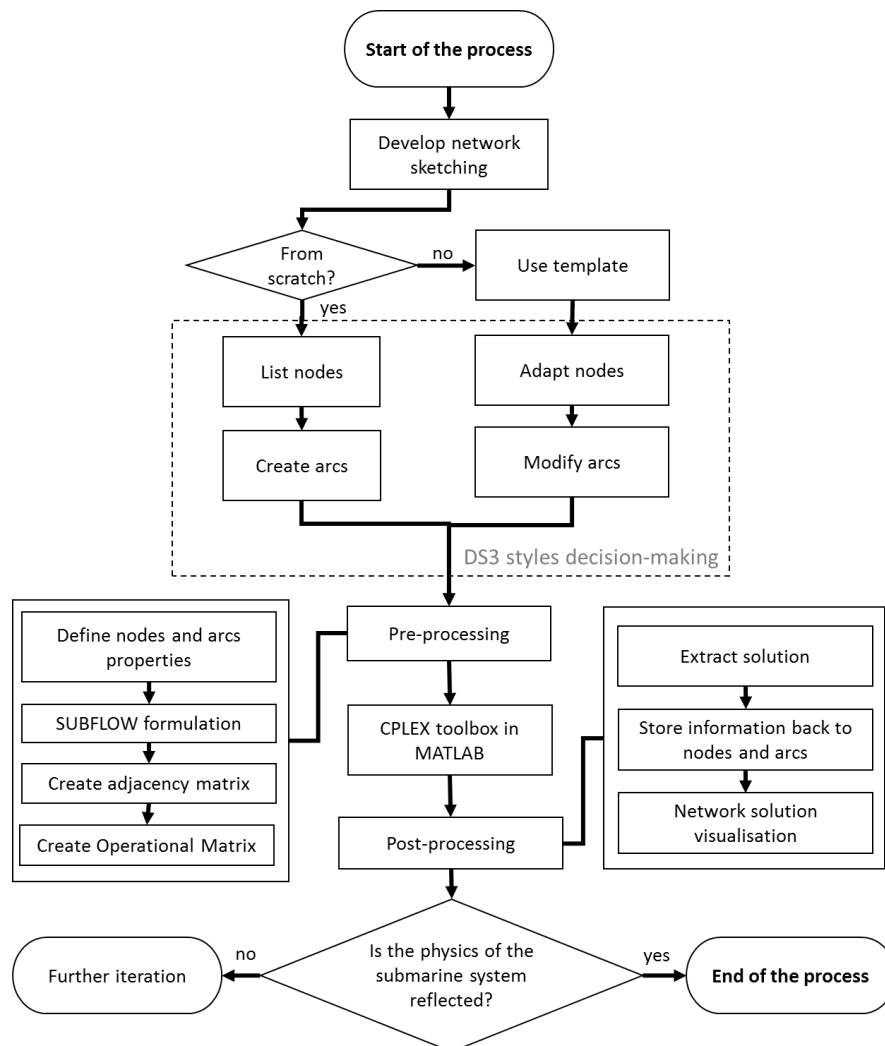


Figure 3.7: Development of the SUBFLOW process

The resultant network sketch (see Figure 3.8) reflects the Macro style SSK choices and did not follow the submarine architectural arrangement, but rather reveals the hierarchal sources and sinks of the SSK power system. Compared to Figure 3.6, the top part of Figure 3.8 also shows Equation (3.1) which was grouped into terms A to F. Nonetheless, in this network, nodes are used to model components in the SSK power system and thus some variables previously shown in the semantic network (Figure 3.6) are attached to relevant nodes in Figure 3.8, such as P_{DIES} to the diesel generator node. Figure 3.8 consists of several nodes starting from the fuel (oil) tankage node as the source of energy followed by the diesel generator node (quantified by P_{DIES}), which

converts the fuel chemical energy (brown) to electric energy. The electrical energy was then converted and distributed by a power converter node to the three main electric loads coloured in magenta: the energy storage or battery charging for fully submerged operation (B); the hotel load in the snorting operation (D); and the propulsion load in the snorting operation (C). Further nodes were modelled to represent conscious design decisions and assumptions. These are the margins (coloured in blue) for battery charging (A) and submerged energy (B) as well as efficiencies (F and E) coloured in yellow, which contributed to energy waste or power loss. The detailed heat due to battery charging and hotel load in the snorting operation was not considered in this model.

$$P_{DIES} = \left[(1 + m) (I_{max} \times 2.4 \times N_c) + \frac{P'_s}{\eta_{el}} + H_{snort} \right] \left(\frac{1}{\eta_{conv}} \right)$$

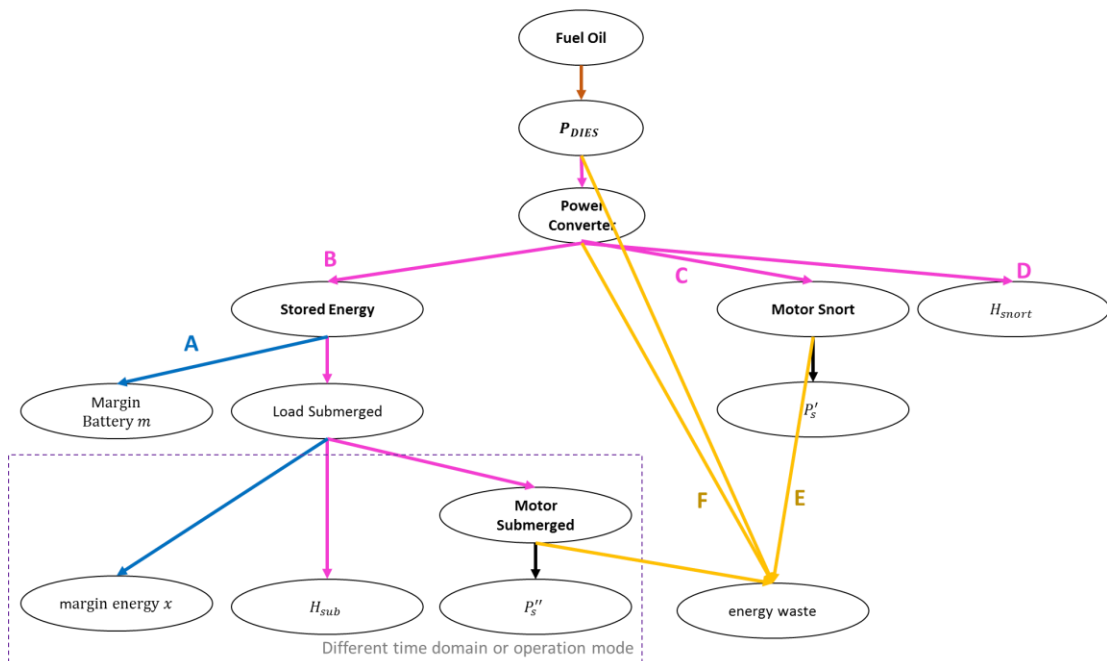


Figure 3.8: Network sketch of an SSK power system and its relationship to the power sizing algorithm of Burcher & Rydill (1994) Equation (3.1)

In the SUBFLOW simulation, a framework was developed to categorise nodes into two broad types of nodes: terminal nodes and hub nodes. Terminal nodes were used to model sources or sinks at the extremities of the flow. The extremities in the network were identified by the number of in-degree and out-

degree flows. If the terminal node has only one or multiple out-degree flows (diverging), that node was taken to be a source. Conversely, if the flow(s) were converging and there were no out-degree flow(s), that node would have been considered as a sink. Therefore, the direction of the flow was important and would have been part of the input to the SUBFLOW network.

The properties of nodes in Figure 3.8 are given in Table 3.11, which shows that each node is assigned a node identification and an appropriate symbol derived from Tables 3.9 and 3.10 on page 92. As listed in Table 3.11, the example of the source node in this study was the Fuel Oil (FO) node, while the rest of the terminal nodes were sinks. Between terminal nodes, there were hub nodes. Unlike terminal nodes, hub nodes must have at least one in-degree and one out-degree flow. Hub nodes, as shown in Table 3.11, are the Diesel Generator (DG), the Power Converter (PC), etc. Compared to the AFO, each arc in the SUBFLOW network also focuses on one commodity, which is energy (chemical, electrics, mechanical, and heat loss). However, in the AFO approach, there could be a non-energy flow, such as data flow (carrying binary 0 and 1 numerical data), as the 'parallel' commodity in the AFO formulation (Robinson, 2018). Reducing the number of commodities within the candidate's SUBFLOW simulation helped to reduce the number of inputs and reduce the complication in the network formulation, making the SUBFLOW more appropriate to be applied early in the design process, as in this implementation. The energy storage was also explicitly modelled as the Load Submerged (LS) node in this network.

Table 3.11: Nodes properties for an SSK power system network in Figure 3.8 and variables (symbols) outlined in Tables 3.9 and 3.10, detailed calculations are provided in Appendix 2

Node Name	Relevant Variable	Node Identification	SUBFLOW Setup	Node Type	Data
Fuel Oil	P_{Fuel}	FO	$P_{FO} \geq 0$	Terminal	(Output)
Diesel Generator	P_{Dies}	DG	$P_{DG} \geq 0$	Hub	(Output)
Power Converter	P_{Conv}	PC	$P_{PC} \geq 0$	Hub	(Output)
Stored Energy	P_{Batt}	SE	$P_{SE} \geq 0$	Hub	(Output)
Margin Battery	m	MM	$P_{MM} \geq 0$	Hub	(Output)
Load Submerged	-	LS	$P_{LS} \geq 0$	Hub	(Output)
Margin Energy	x	MX	$P_{MX} \geq 0$	Terminal	(Output)
Hotel Submerged	H_{sub}	HS	$P_{HS} = H_{sub}$	Terminal	280 kW
Motor Submerged	P''_{Motor}	MS	$P_{MS} \geq 0$	Hub	(Output)
Velocity Submerged	P'_s	VS	$P_{VS} = P'_s$	Terminal	68 kW
Motor Snort	P'_{Motor}	MT	$P_{MT} \geq 0$	Hub	(Output)
Velocity Snort	P'_s	VT	$P_{VT} = P'_s$	Terminal	(Output)
Hotel Snort	H_{snort}	HT	$P_{HT} = H_{snort}$	Terminal	224 kW
Heat Loss	-	HE	$P_{HE} \geq 0$	Terminal	(Output)

At hub nodes, a formulation used in the AFO approach (Robinson, 2018) was applied to define how much energy could come in and out of that node, denoted as energy coefficient e in this SUBFLOW simulation. For example, at the Diesel Generator (DG) node, 100% of the incoming energy flow from the Fuel Oil (FO) node would be converted to the PC node as the electric energy (48%) and the Heat Loss (HE) node (52%) as the heat loss energy. This fraction could be said to be similar to the Sankey diagram that can be used to breaking down energy inputs and outputs (Kennedy and Sankey, 1898). Such an energy breakdown at each node is one of the key inputs of the AFO approach (Robinson, 2018) as adopted in the SUBFLOW formulation. Thus, all hub node's energy coefficients in the SUBFLOW network need to be known either based on available equipment data or assumed. Since the UCL submarine Databook (UCL-NAME, 2014) does not provide this information, some energy coefficients were assumed or drawn from available sources (e.g., Burcher and Rydill (1994), Robinson (2018)) and are summarised in Table 3.12.

Table 3.12: Arcs properties for an SSK power system network in Figure 3.8, see Table 3.11 for node names

Arc (<i>i, j</i>)	Energy	Colour Code	SUBFLOW Setup
(FO,DG)	Chemical	Brown	$P_{FO,DG} = P_{FO}$
(DG,PC)	Electrical	Magenta	$P_{DG,PC} = 48\% P_{DG}$
(DG,HE)	Heat	Yellow	$P_{DG,HE} = 52\% P_{DG}$
(PC,SE)	Electrical	Magenta	$P_{PC,SE} = 98\% P_{PC} - P_{PC,MT} - P_{PC,HT}$
(PC,MT)	Electrical	Magenta	$P_{PC,MT} = 98\% P_{PC} - P_{PC,SE} - P_{PC,HT}$
(PC,HT)	Electrical	Magenta	$P_{PC,HT} = 98\% P_{PC} - P_{PC,SE} - P_{PC,MT}$
(PC,HE)	Heat	Yellow	$P_{PC,HE} = 2\% P_{DG}$
(SE,MM)	Electrical	Blue	$P_{SE,MM} = 4.8\% P_{SE}$
(SE,LS)	Electrical	Magenta	$P_{SE,LS} = 95.2\% P_{SE}$
(MT,HE)	Heat	Yellow	$P_{MT,HE} = 3\% P_{MT}$
(MT,VT)	Mechanical	Black	$P_{MT,VT} = 97\% P_{MT}$
(LS,MS)	Electrical	Magenta	$P_{LS,MS} = 64\% P_{LS} - P_{LS,HS}$
(LS,HS)	Electrical	Magenta	$P_{LS,HS} = 64\% P_{LS} - P_{LS,MS}$
(LS,MX)	Electrical	Blue	$P_{LS,MX} = 36\% P_{LS}$
(MS,HE)	Heat	Yellow	$P_{MS,HE} = 3\% P_{MS}$
(MS,VS)	Mechanical	Black	$P_{MS,VS} = 97\% P_{MS}$

The SUBFLOW could have been solved through push or pull. As opposed to pull, push means the commodity demands at sinks are not constrained. Thus, the size of demand nodes could have been made dependent on the total available commodity defined from all available sources. In this candidate derived SUBFLOW simulation, pull was used through some terminal nodes. The pull nodes in the network must be known and thus, as shown in Table 3.11, they are the Hotel Submerged (HS), the Velocity Submerged (VS), the Velocity Snort (VT), and the Hotel Snort (HT) nodes. On top of Table 3.12, the numerical data attached to pull nodes were minimum inputs for the SUBFLOW simulation to solve and was obtained from design calculations as in Tables 3.9 and 3.10.

Once the sketch of the DS3 had been completed with nodes and arcs properties, the adjacency matrix was built (see Table 3.13). This adjacency matrix defined the structure of the network that was read by MATLAB. In this network, it was found that 28% of all nodes were input nodes (see Table 3.11), so 72% of nodes as well as all arc flows were unknown and needed to be solved

using the SUBFLOW. But before the solver (CPLEX, see Subsection 3.1.2) was used, key distinctive issues in the SUBFLOW application to the SSK problem need to be explained.

Table 3.13: The adjacency matrix of an SSK power system, consisting of nodes and arcs listed in Tables 3.11 and 3.12, respectively

	FO	DG	PC	SE	MM	LS	MX	HS	MS	VS	MT	VT	HT	HE
FO	0	1	0	0	0	0	0	0	0	0	0	0	0	0
DG	0	0	1	0	0	0	0	1	0	0	0	0	0	0
PC	0	0	0	1	0	1	1	1	0	0	0	0	0	0
SE	0	0	0	0	1	0	0	0	0	1	0	0	0	0
MM	0	0	0	0	0	0	0	0	0	0	0	0	0	0
LS	0	0	0	0	0	0	0	1	1	0	0	0	0	0
MX	0	0	0	0	0	0	0	0	0	0	0	0	0	0
HS	0	0	0	0	0	0	0	0	0	0	0	0	0	0
MS	0	0	0	0	0	0	0	0	0	0	0	0	0	0
VS	0	0	0	0	0	0	0	0	0	0	1	0	1	1
MT	0	0	0	0	0	0	0	1	0	0	0	1	0	0
VT	0	0	0	0	0	0	0	0	0	0	0	0	0	0
HT	0	0	0	0	0	0	0	0	0	0	0	0	0	0
HE	0	0	0	0	0	0	0	0	0	0	0	0	0	0

Essentially, to obtain how much energy the power system in Figure 3.8 would consume, the power P at each node n within the set of nodes N (listed in Tables 3.9 and 3.10) need to be multiplied by a time variable, denoted as T_{ops} in Equation (3.2). The time variable T_{ops} in Equation (3.2) is dependent on the operational mode of the vessel, part of the operational architecture (Subsection 2.1.1). The T_{ops} for a naval surface ship, in a specific operational mode (e.g., battle, cruise, or transit), can be considered homogenous (assuming a steady state condition) throughout the system network and this could also be the case with the nuclear submarine. However, unlike other types of naval vessels, the operational nature of the SSK style (Figure A.4, Appendix 1) introduces a distinctive problem when formulating the SUBFLOW.

$$\sum_{n \in N} E_n = \sum_{n \in N} P_n \times T_{ops} \tag{3.2}$$

For a conventional powered submarine design, at least two distinct time dependent variables must be considered: T_{sub} and T_{snort} . The dotted box in Figure 3.8 shows the Margin Energy x (MX), the Hotel Submerged H_{sub} (HS), and the Velocity Submerged (VS) nodes were for the submerged mode and thus the energy of these nodes cannot be determined using a homogenous T_{ops} as in Equation (3.2).

Therefore, to enable two different time domains in the same network structure, a further mathematical formulation was required. All power demands (the 'pulls') while the SSK is fully submerged, such as the Hotel Submerged power P_{HS} (HS) (see the bold text in Table 3.11 with the value given in Table 3.10), had to be multiplied by the time coefficient defined by Equation (3.3).

$$\frac{T_{sub}}{T_{snort}} \quad (3.3)$$

However, it was found that using that time fraction was insufficient. This was because the battery energy per cell when charging and discharging also required different time domains and thus needed to be considered. Therefore, an additional feature was introduced, see Equation (3.4).

$$\frac{T_{sub}}{T_{snort}} \times \frac{E_{chpercell}}{E} \quad (3.4)$$

Where the energy available per cell E is given in Table 3.10 and the energy charging per battery cell $E_{chpercell}$ (for lead/acid battery) is defined as follows (Burcher and Rydill, 1994).

$$E_{chpercell} = I_{max} \times 2.4 \text{ Volts} \times T_{ch} \quad (3.5)$$

These formulations were part of the iterative process by the candidate in developing a DS3 network as indicated in Figure 3.7.

In addition, the coefficients of the objective function (see Subsection 3.1.2) in this SUBFLOW investigation were set to zero because the aim of this optimisation investigation was not to cost the DS3 configuration, as in the case

of Trapp's (2015) NSMCF investigation or Robinson's (2018) AFO study (including its variants (Parsons et al., 2020a)). In this study, SUBFLOW was used to solve the energy balance, through a linear programming, systems of equations. This ensured that the total energy demand on the submarine would be equal to the total energy available, indicating systems design balance. Thus, in this SUBFLOW example, the DS3 network styles were proposed on the basis of prior expert knowledge (see the dotted box in Figure 3.7 on page 96) and were deliberately not validated by analysis in ESSD. Nonetheless, the SUBFLOW network created could have been a suitable basis for further analyses in subsequent design phases, if required. This is discussed further in Chapter 7.

Therefore, the pre-processing step in Figure 3.7 is commenced with MATLAB to read the adjacency matrix, attach appropriate numerical data to nodes and arcs, and then read the Operational Matrix (Subsection 3.1.2) of the SUBFLOW simulation, which is outlined in Table 3.14. If bidirectionality had had to be considered, the size of the Operational Matrix would have become quite large (i.e., a $[61 \times 47]$ matrix). Nonetheless, in this case, bidirectionality was not necessary as there had to be no backward flow from sink to source and thus the size of the resultant Operational Matrix shown in Table 3.14 has only 29 rows and 31 columns. The layout description of Table 3.14 follows the pattern provided in Table 3.5 on page 80. However, compared to the Operational Matrix for the basic NSMCF problem (Trapp, 2015) in Table 3.5, the Operational Matrix in Table 3.14 includes the energy coefficient from the AFO approach (Parsons et al., 2020a), which is reflected as the coefficient e_i for the continuity constraints (rows 2 to 27 and columns 17 to 30).

Table 3.14: The Operational Matrix of an SSK power system, which is developed based on the coefficients and values given in Table 3.11 and Table 3.12 (see Table 3.5 on page 80 for a simple example of the proposed Operational Matrix application)

No	1	2	3	4	5	6	7	8	9	10	11	12	13	14	15	16	17	18	19	20	21	22	23	24	25	26	27	28	29	30	31		
Objective Function	1	0	0	0	0	0	0	0	0	0	0	0	0	0	0	0	0	0	0	0	0	0	0	0	0	0	0	0	0	0	0		
		Arcs															Nodes																
		$\sum_{(i,j) \in E} P_{i,j}$															$-e_i P_i$															=	0
		$P_{FO,DG}$	$P_{DG,PC}$	$P_{DG,HE}$	$P_{PC,SE}$	$P_{PC,MT}$	$P_{PC,HT}$	$P_{PC,HE}$	$P_{SE,MM}$	$P_{SE,LS}$	$P_{MT,HE}$	$P_{MT,VT}$	$P_{LS,MS}$	$P_{LS,HS}$	$P_{LS,MX}$	$P_{MS,HE}$	$P_{MS,VS}$	P_{FO}	P_{DG}	P_{PC}	P_{SE}	P_{MM}	P_{MT}	P_{HT}	P_{HE}	P_{VT}	P_{LS}	P_{MS}	P_{VS}	P_{HS}	P_{MX}		
Equality constraints matrix for continuity	2	1	0	0	0	0	0	0	0	0	0	0	0	0	0	0	-1	0	0	0	0	0	0	0	0	0	0	0	0	0	0		
	3	1	0	0	0	0	0	0	0	0	0	0	0	0	0	0	0	-1	0	0	0	0	0	0	0	0	0	0	0	0	0		
	4	0	1	0	0	0	0	0	0	0	0	0	0	0	0	0	0	-0.48	0	0	0	0	0	0	0	0	0	0	0	0	0		
	5	0	0	1	0	0	0	0	0	0	0	0	0	0	0	0	0	-0.52	0	0	0	0	0	0	0	0	0	0	0	0	0		
	6	0	1	0	0	0	0	0	0	0	0	0	0	0	0	0	0	0	-1	0	0	0	0	0	0	0	0	0	0	0	0		
	7	0	0	0	1	1	1	0	0	0	0	0	0	0	0	0	0	0	-0.98	0	0	0	0	0	0	0	0	0	0	0	0		
	8	0	0	0	0	0	0	1	0	0	0	0	0	0	0	0	0	0	-0.02	0	0	0	0	0	0	0	0	0	0	0	0		
	9	0	0	0	1	0	0	0	0	0	0	0	0	0	0	0	0	0	0	-1	0	0	0	0	0	0	0	0	0	0	0		
	10	0	0	0	0	0	0	0	0	1	0	0	0	0	0	0	0	0	0	-0.952	0	0	0	0	0	0	0	0	0	0	0		
	11	0	0	0	0	0	0	0	1	0	0	0	0	0	0	0	0	0	0	-0.048	0	0	0	0	0	0	0	0	0	0	0		
	12	0	0	0	0	0	0	0	1	0	0	0	0	0	0	0	0	0	0	0	-1	0	0	0	0	0	0	0	0	0	0		
	13	0	0	0	0	0	0	0	0	1	0	0	0	0	0	0	0	0	0	0	0	0	0	0	0	-1	0	0	0	0	0		
	14	0	0	0	0	0	0	0	0	0	0	1	1	0	0	0	0	0	0	0	0	0	0	0	0	-0.64	0	0	0	0	0		
	15	0	0	0	0	0	0	0	0	0	0	0	0	1	0	0	0	0	0	0	0	0	0	0	0	-0.36	0	0	0	0	0		
	16	0	0	0	0	0	0	0	0	0	0	0	0	0	1	0	0	0	0	0	0	0	0	0	0	0	0	0	0	-1	0		
	17	0	0	0	0	0	0	0	0	0	0	0	1	0	0	0	0	0	0	0	0	0	0	0	0	0	0	0	0	-1	0		
	18	0	0	0	0	0	0	0	0	0	0	0	1	0	0	0	0	0	0	0	0	0	0	0	0	0	0	-1	0	0	0		
	19	0	0	0	0	0	0	0	0	0	0	0	0	0	0	1	0	0	0	0	0	0	0	0	0	0	0	-0.970	0	0	0		
	20	0	0	0	0	0	0	0	0	0	0	0	0	0	0	0	1	0	0	0	0	0	0	0	0	0	0	-0.030	0	0	0		
	21	0	0	0	0	0	0	0	0	0	0	0	0	0	0	0	0	1	0	0	0	0	0	0	0	0	0	0	-1	0	0		
	22	0	0	0	0	1	0	0	0	0	0	0	0	0	0	0	0	0	0	0	-1	0	0	0	0	0	0	0	0	0	0		
	23	0	0	0	0	0	0	0	0	0	1	0	0	0	0	0	0	0	0	0	-0.970	0	0	0	0	0	0	0	0	0	0		
	24	0	0	0	0	0	0	0	0	0	0	1	0	0	0	0	0	0	0	0	-0.030	0	0	0	0	0	0	0	0	0	0		
	25	0	0	0	0	0	0	0	0	0	0	0	1	0	0	0	0	0	0	0	0	0	0	-1	0	0	0	0	0	0	0		
	26	0	0	0	0	0	1	0	0	0	0	0	0	0	0	0	0	0	0	0	0	0	-1	0	0	0	0	0	0	0	0		
	27	0	0	1	0	0	0	1	0	0	1	0	0	0	0	1	0	0	0	0	0	0	0	0	-1	0	0	0	0	0	0		
Lower bounds matrix	28	0	0	0	0	0	0	0	0	0	0	0	0	0	0	0	0	0	0	0	0	0	0	224	0	160	0	0	285	1107	0		
Upper bounds matrix	29	Inf	Inf	Inf	Inf	Inf	Inf	Inf	Inf	Inf	Inf	Inf	Inf	Inf	Inf	Inf	Inf	Inf	Inf	Inf	Inf	Inf	Inf	224	Inf	160	Inf	Inf	285	1107	Inf		

$0 \leq P_{i,j} \leq \infty$

Investigated operating condition as shown in Table 3.11 on page 99

The power commodity calculated using the SUBFLOW resulted in Figure 3.9. These could be used to calculate the power system's weight and space attributes provided that power to weight or power to volume ratios are known. Such ratios could be derived from the UCL submarine data (UCL-NAME, 2014). Other equipment ratios could be obtained from equipment data from manufacturers or estimated if systems are novel and still under development.

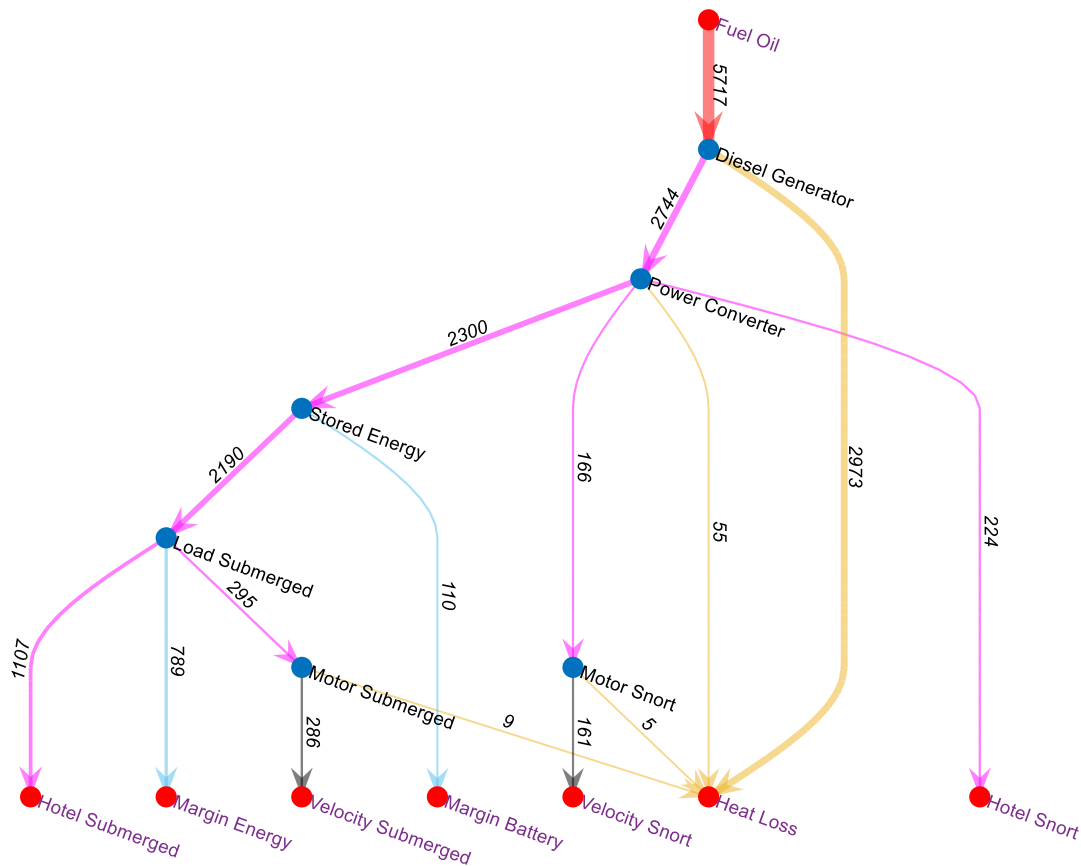


Figure 3.9: SUBFLOW solution for an SSK power system

However, in the SUBFLOW exercise presented here, the sizing was at this point yet to be done for the following reasons. Firstly, as stated at the beginning of this section, this exercise was not a full vessel synthesis and thus the DS3 components had not at this stage been arranged physically on the submarine. This meant all arcs could not yet be sized since the distance between nodes was not able to be measured. Secondly, the largest operational scenario, the sprint scenario had yet to be taken into account when producing the network model. The sprint scenario dictated many power system components, such as the propulsion motor. Thirdly, although the network reflected a diesel-electric

style configuration, detailed style was yet to be specified in this network. Capturing a more detailed set of DS3 style decisions in the network could have been done by duplicating nodes or arcs to show explicit decisions on redundancy style. Such detailed style choices would require a more extensive power system synthesis than one just based on a numerical synthesis.

Furthermore, not all nodes shown in Table 3.15 have geometry, such as hotel nodes or margin nodes. These nodes are termed as the 'numerical' node in this research. A numerical node only provides numerical data for power, i.e., no numerical geometry data, to complete the architecture and the energy flow in the network and thus it is comparable to the variable node as in semantic networks (Subsection 3.2.4). This also was the case for arcs in Table 3.16. If one of the nodes connected by an arc is numerical (power), that arc does not have geometry data or any physical connection. As introduced in Chapter 1, the DS3 physical connection could have been defined by one of three groups based on shipbuilding practice, cabling, piping and trunking. In this SSK power network (Figure 3.9), only piping and cabling could be drawn from the network as is specified in Table 3.16.

Table 3.15: Properties of nodes of the SUBFLOW solution

Node	Node Name	Result (kW)	Geometry	Notation
FO	Fuel Oil	5717	Yes	$P_{Fuel} = P_{FO}$
DG	Diesel Generator	5717	Yes	$P_{Dies} = 48\% P_{DG}$
PC	Power Converter	2744	Yes	$P_{Conv} = P_{PC}$
SE	Stored Energy	2299	Yes	$P_{Batt} = P_{SE}$
MM	Margin Battery	109	No	$m = P_{MM}$
MT	Motor Snort	166	Yes	$P'_{Motor} = P_{MT}$
HT	Hotel Snort	(input)	No	$H_{snort} = P_{HT}$
HE	Heat Loss	3041	No	-
VT	Velocity Snort	(input)	No	$P'_s = P_{VT}$
LS	Load Submerged	2190	No	-
MS	Motor Submerged	295	Yes	$P''_{Motor} = P_{MS}$
VS	Velocity Submerged	(input)	No	$P''_s = P_{VS}$
HS	Hotel Submerged	(input)	No	$H_{sub} = P_{HS}$
MX	Margin Energy	778	No	$x = P_{MX}$

Table 3.16: Properties of arcs of the SUBFLOW solution

Arc (i, j)	Variable	Result (kW)	Physical Connection	DS3 Technology
(FO,DG)	$P_{FO,DG}$	5717	Yes	Piping
(DG,PC)	$P_{DG,PC}$	2744	Yes	Cabling
(DG,HE)	$P_{DG,HE}$	2973	No	-
(PC,SE)	$P_{PC,SE}$	2300	Yes	Cabling
(PC,MT)	$P_{PC,MT}$	166	Yes	Cabling
(PC,HT)	$P_{PC,HT}$	224	No	-
(PC,HE)	$P_{PC,HE}$	55	No	-
(SE,MM)	$P_{SE,MM}$	110	No	-
(SE,LS)	$P_{SE,LS}$	2190	No	-
(MT,HE)	$P_{MT,HE}$	5	No	-
(MT,VT)	$P_{MT,VT}$	161	No	-
(LS,MS)	$P_{LS,MS}$	295	No	-
(LS,HS)	$P_{LS,HS}$	1107	No	-
(LS,MX)	$P_{LS,MX}$	789	No	-
(MS,HE)	$P_{MS,HE}$	9	No	-
(MS,VS)	$P_{MS,VS}$	286	No	-

3.2.6 Conclusion from the Case Study

Section 3.2 presents three different approaches to SSK power system sizing, revealing the advantages and disadvantages of each approach. A numerical sizing was quick, found to be convenient for the designer, and could be readily automated by hardcoding the algorithms to CAD programs. The semantic network showed the relationships between variables, coefficients, and constants in the traditional Burcher and Rydill's (1994) algorithm. However, both approaches did not enable (micro) style choices to be made and provide understating regarding different styles impacts on systems weight and space estimation.

The SUBFLOW in contrast required more engineering and inputs than the other approaches, such as requiring DS3 configurations, also specifying some DS3 properties, and creating mathematical models for the energy balance analysis. However, the SUBFLOW allowed the DS3 style to be captured and aided the designer understanding as to how the systems worked. Most importantly, when combined with the whole ship UCL Design Building Block approach (Andrews et al., 1996) (addressed in the following section), it was found to enable a better DS3 sizing than parametric approach, yet not as detailed as collaborative analysis tools more appropriate to detailed DS3 design.

Finally, this study showed that SUBFLOW without the M-1 survivability formulation (Trapp, 2015) (see Subsection 3.1.4) could be used to undertake an early stage energy balance analysis. The application of SUBFLOW with the M-1 survivability (Trapp, 2015) to a submarine design case study was nonetheless investigated and is discussed further in the next section.

3.3 The Initial DS3 Synthesis Approach

This section is intended to cover two objectives. The first objective is to investigate the application of the M-1 survivability (Trapp, 2015) (see Subsection 3.1.4), to a submarine design case study. The second one is to investigate the implementation of the UCL DBB approach (Andrews and Dicks, 1997) to consider the physical architecture of DS3 (Subsection 2.1.1) together with the SUBFLOW simulation (Subsection 3.2.5). These objectives led to an early version of the proposed DS3 synthesis approach. Much of this had already been presented at ICCAS 2019 (Mukti et al., 2019) and published in the RINA IJME journal (Mukti et al., 2021) in Appendix 3.

Subsection 3.3.1 describes the case study used in the implementation. Subsection 3.3.2 presents the proposed DS3 synthesis approach. This is followed by Subsections 3.3.3 to 3.3.7 which describe each step in the proposed DS3 synthesis approach. Subsection 3.3.8 not only discusses the last step of the proposed approach but also gives the summary of this section.

3.3.1 Case Study 3.3.1 Setup

The decision making process for this case study is given in Table 3.17 was extended from a previous study (Section 3.2) to incorporate the UCL DBB synthesis (Andrews and Dicks, 1997), including specific style decisions relevant to a selected DS3. The main goal of the case study was to test how the DBB approach can be used together with the SUBFLOW and the M-1 survivability (Trapp, 2015) in sizing an example DS3 input. It also captures more detailed DS3 styles decisions associated with system redundancy. As an expansion of Case Study 3.2.1, the typical ocean-going, medium size SSK, was selected in the case study and the actual details were extracted from the database that is provided from the annual UCL submarine design exercise (UCL-NAME, 2014), removing any issues of security classification.

Table 3.17: The realisation for Case Study 3.3.1, following the decision making sequence for complex vessels outlined in detail in Figure 4 and Appendix of (Andrews, 2018c) in a similar manner to the example in Figure 4 of (Andrews, 2021)

Process Step	Selection Decision / Realisation for Case Study 3.3.1	
Perceived need	A test case for initial proposed DS3 synthesis approach	
Outline of initial requirements	Initial SSK key parameters desired (capabilities)	
	Complement/ accommodation	46 personnel
	Operational environment density range	1-1.025 te/m ³
	Design diving depth	250 m
	Patrol length	49 days
	Payload Equipment	As Case Study 3.2.1
Style Level		
Macro Level		
Main Level		
Selection of style of emerging ship design	Micro Level	DS3 style (see following subsections)
	Selection of major equipment and operational sub-systems	
Four diesel electric power plant Two propulsion motors (concentric shaft) Lead/acid battery type		
Selection of whole ship performance characteristics	General Level	Value
	Indiscretion ratio (Burcher and Rydill, 1994)	< 25 %
	Sprint speed	17 knots (7 hrs)
	Submerged speed	7 knots (21 hrs)
	Snort speed	6 knots (5 hrs)
	Specific Performance	As Case Study 3.2.1
Selection of synthesis model type	The DS3 Synthesis approach (Mukti et al., 2021) Numerical design algorithms (Burcher and Rydill, 1994; UCL-NAME, 2012, 2014) The UCL Design Building Block approach (Andrews et al., 1996) The SUBFLOW (Subsection 3.2.5) with M-1 survivability (Trapp, 2015)	

3.3.2 The Initial DS3 Synthesis Approach

Figure 3.10 gives an early version of the proposed DS3 synthesis approach where encompass several items in the decision making Table 3.17, more specifically, the ‘Defining the Problem’ step in Figure 3.10, such as the selection of DS3 baseline. The selection of DS3 baseline is a step to specify the type of DS3 from many different types of distributed systems on a submarine. The selected type of DS3 is then referred as to a candidate architecture that will be synthesised with the selection of DS3 objective. The DS3 objective is not the objective function as in the SUBFLOW formulation but is to define a set of aims to be achieved from the DS3 synthesis. Style features appropriate to the DS3 baseline were then selected (micro level) as already listed in Table 3.17.

Therefore, in this initial investigation, it was a system-by-system synthesis instead of a total ship system synthesis.

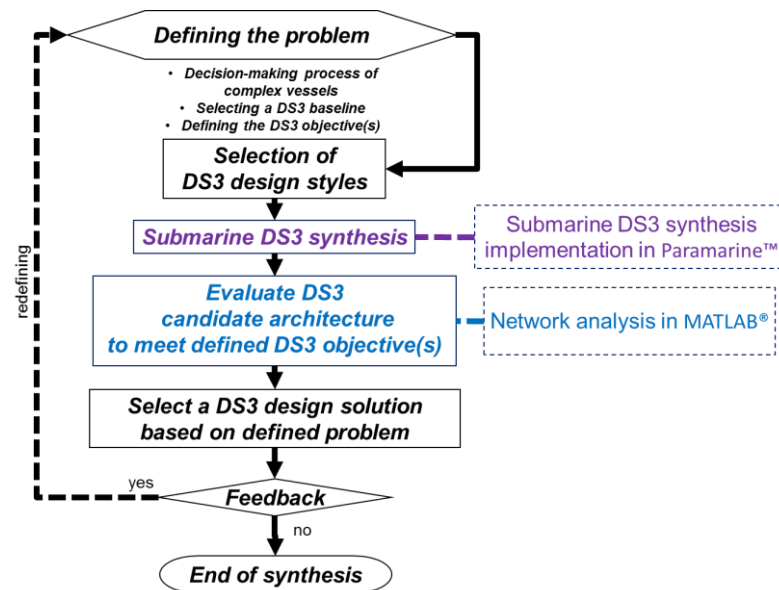


Figure 3.10: An overview of an early version of the DS3 synthesis approach (Mukti et al., 2021) (see Appendix 3)

Once the major decision making has been made, the synthesis of both submarine and initial DS3 configurations can begin using the selected synthesis models, which is the UCL DBB approach in Paramarine as specified in Table 3.17. After this, different flow path (Subsection 3.1.2) for routing possibilities in the DS3 baseline candidate architecture was evaluated using the SUBFLOW with the M-1 survivability (Trapp, 2015) in MATLAB. However, in this case study, the objective function of the SUBFLOW (see Subsections 3.1.2 and 3.2.5) was modified to give direct input to DS3 sizing. The M-1 survivability (Trapp, 2015) was used to give insight on evaluating the candidate DS3 architecture to produce several possible flow path solutions.

Subsequently, the aggregate flow (Subsection 3.1.3) of the candidate architecture was captured and utilised to inform that element of the DS3 input to submarine sizing. This process required redefining the problem that could have emerged from the Requirement Elucidation dialogue and thus any ‘feedback’ would have been conducted towards the end of the proposed synthesis approach. The following subsections take the five main steps in Figure 3.10 in turn.

3.3.3 Defining the Problem

In extending the previous SUBFLOW implementation (see Section 3.2), The Power and Propulsion System (PPS) was selected as the DS3 baseline for this study, as already spelt out in the major decision making of Table 3.17 on page 110. The PPS is one of the key critical systems on a submarine and should be addressed more explicitly than just the traditional numerical algorithm (see Subsection 2.3.1). In this case study, the attention in obtaining the PPS synthesis was the application of M-1 survivability (Trapp, 2015) and submarine space allocation so that the PPS uses the least amount of cabling and takes up the least amount of space, but still have an extent of the level of redundancy, which is to improve safety.

The term safety is a broad concept that can have different meanings in different applications. One of the generic definitions of safety is a condition or a level achieved when the chance that someone (or something) will be adversely affected by a potential harmful intrinsic property of an entity has been reduced to an acceptably low level (Coverdale et al., 2008). As a submarine is as safety critical as an aeroplane, a high level of DS3 redundancy demanding sufficient resources ought to be desirable, even if space is at a premium (Andrews, 2017a). DS3 redundancy can be achieved by the number of components (sources and sinks) or the number of physical connections with similar functionality in a DS3 at the same or lesser level of performance. Hence, to increase a submarine's safety, system redundancy, beyond minimum space while achieving essential weight balance (vertically and longitudinally) had to be addressed simultaneously with safety in the submarine synthesis process.

Robustness could be seen to be ambiguous when reflecting the ability of the DS3 of naval vessels to withstand (a certain magnitude of) perturbations during operation (de Vos and Stapersma, 2018). There are several practical ways to improve DS3 robustness: increasing the extent of redundant components; splitting any centralised DS3 to provide additional stand-alone DS3 for emergency operations; and increasing the extent of redundancy of system's connection to allow additional supply lines from vital source(s) to multiple users (de Vos and Stapersma, 2018). Another practice is to employ diversity, which

varies differently sourced supplies to support a system such as AC or DC powered components (Wrobel, 1984). Perturbations in the context of naval vessels were seen to be closely related to the concept of survivability.

Survivability on a submarine underpins the importance of ensuring electrical systems are maintained or rapid restoration of service supply after a non-hull lethal underwater explosion (UNDEX) shock event (Doerry, 2007). The probability of survival could also be used as a basis to quantify submarine safety (McVoy, 1968). However, performing survivability evaluation in ESSD for submarines can be difficult while still pursuing Requirement Elucidation. Furthermore, performing survivability evaluation in submarine ESD is not just due to a lack of detail, but also the fact that the concept is rapidly evolving. This suggests adopting a basic survivability metric, such as M-1 by Trapp (2015) was seen to be sensible and so, as already discussed at the beginning of this section, its application was investigated in this PPS case study.

In the next subsection, the style decisions for DS3 were more detailed than the SUBFLOW network implementation in Section 3.2. It was not just the need to describe a diesel-electric PPS style but also having to specify more detailed (micro) style decisions. These concurrently included the type of DS3 distribution, DS3 configuration, and the level of redundancy for the DS3.

3.3.4 Selection of DS3 Styles

The options for PPS distribution style range from Medium Voltage DC (MVDC) to AC-DC distribution. In an MVDC architecture, the AC from the power generator is rectified to DC and distributed throughout the vessel, ranging from 50 to 150 MW (Vargas et al., 2011). It is also possible to have a combination of AC and DC distributions, with AC buses dedicated to all AC loads and DC buses for all DC loads (Chalfant et al., 2010).

For this PPS case study, the distribution style choice was drawn from a typical DC distribution for a medium speed SSK, as stated in Table 3.17 on page 110. Figure 3.11 shows the electrical power from multiple AC power generators was rectified to DC and distributed throughout the submarine using the main DC

bus. Many electrical and mechanical consumers constituting the hotel load for the SSK are shown in the dashed box in Figure 3.11. The hotel load was assumed to include control for pumps, transmission, and switches; hotel load (domestic equipment, lighting, heating and ventilation); navigation and communications; weapons and sensors; and emergency functions (power supplies, processing and analysis of signal traffic, and cooling) (see Burcher and Rydill (1994) and Table 3.18) and could be fed using either DC or AC bus with different voltages marked up with different cabling colours.

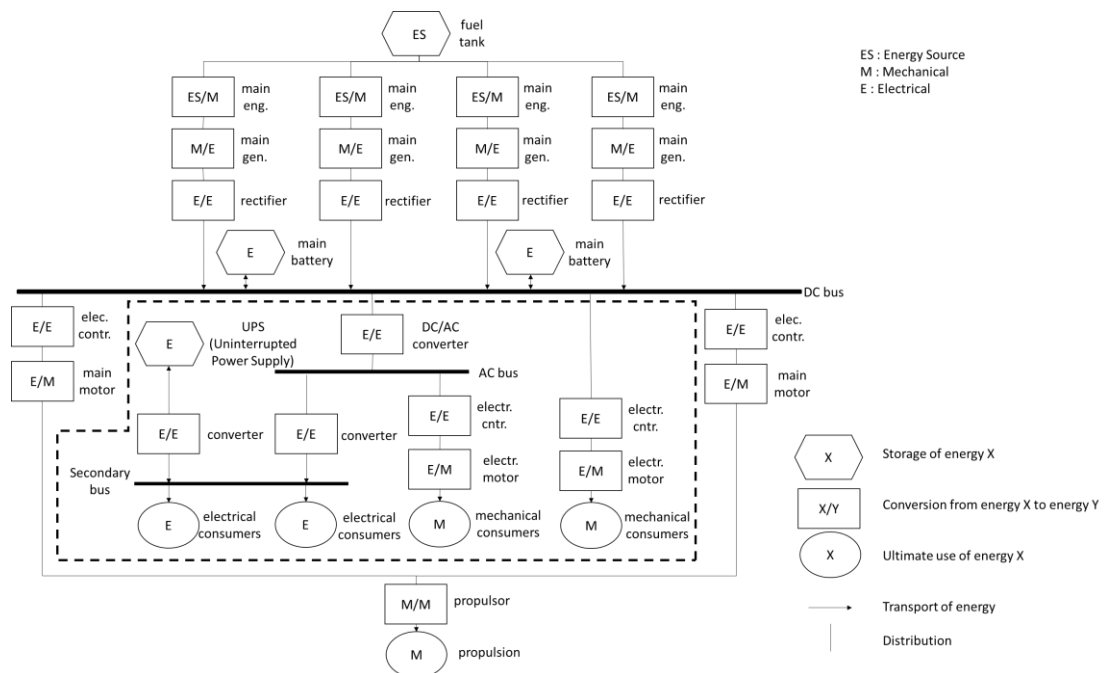


Figure 3.11: Energy flow diagram of a typical DC electric drive for submarines, redrawn from (Woud and Stapersma, 2002)

Table 3.18: An example of power types for various service loads on a submarine (Thornton, 1994)

Power Type	Typical Loads
120 VAC, 60 cycle	Bilge pumps, lighting, atmosphere monitoring equipment, appliances
450 VAC, 60 cycle	Ventilation fans, hydraulic pumps, air compressors, galley equipment
120 VAC, 400 cycle	Precision electronic equipment (gyro compass, weapons control, etc.)
High voltage DC (direct from battery bus)	Trim pumps, lube oil pumps, lighting
Low voltage DC	Ship control, sonar equipment power

Figure 3.11 already shows the type of DS3 distribution but does not at present include much detailed configuration. Therefore, the options that were considered for the physical configuration of PPS architecture included a single bus, dual bus, or a ring system as illustrated in Figure 3.12. The components in Figure 3.12 consist of a power conversion module (PCM), a propulsion motor module (PMM), a power generation module (PGM), a power distribution module (PDM), and zonal loads segregated by dotted lines (Chalfant and Chryssostomidis, 2017). Single-bus and dual-bus options could result in fewer components compared to adopting a ring-bus distribution. However, to achieve sufficient submarine safety (Subsection 3.3.3), a ring main configuration was selected as this provides redundancy through routing cabling both port and starboard as well as forward and aft.

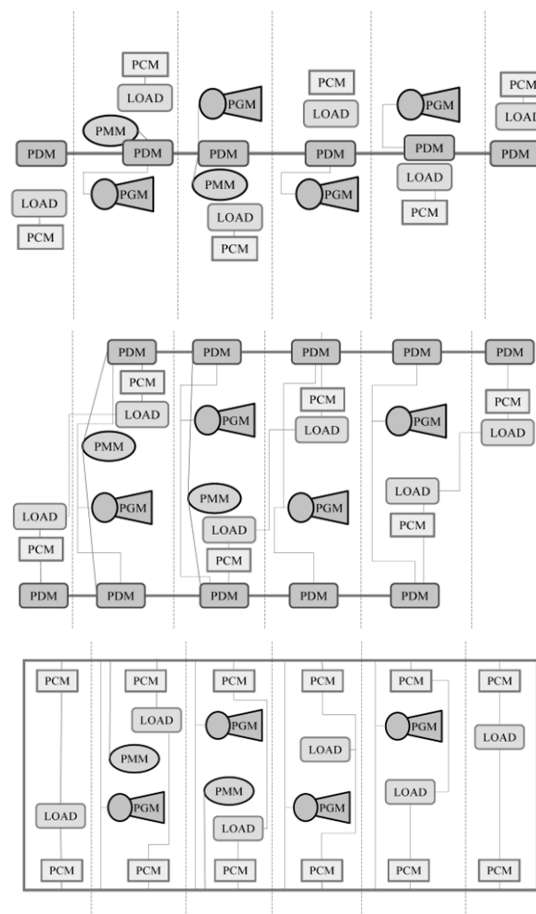


Figure 3.12: Illustration of different distribution styles for electrical systems: single-bus (top), dual-bus (middle), ring-bus (bottom) (Chalfant and Chryssostomidis, 2017)

On top of providing redundancy for PPS cabling, redundancy could have been provided by duplicating the number of sources and sinks by the number of

physical connections. In this case, duplicating power generators and the propulsion motor, together with adopting a ring main for the system's connections were chosen, as outlined in the decision making of Table 3.17 on page 87.

Based on such detailed DS3 style decisions, the PPS architecture adopted is shown in Figure 3.13 and consisted of two Propulsion Motors (PMs), four Power Generations (PGs), and two electrical Stored Energy Devices (SEDs) plus a ring-main distribution. Unlike the previous SUBFLOW implementation in Subsection 3.2.5, the PPS architecture in Figure 3.13 does not indicate numerical nodes. The AC power produced by generators was assumed to be immediately rectified to DC and included in the model of the PGs. In addition, a numerical value for the hotel load was assumed to be contained in the energy storage components, the Stored Energy Device (SED) forward and aft.

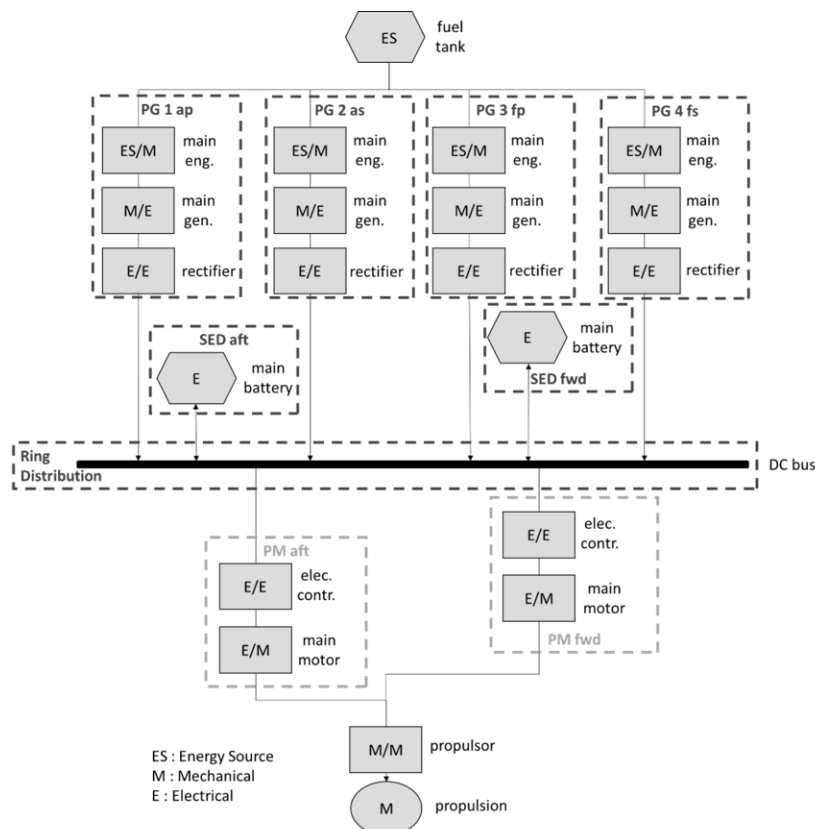


Figure 3.13: Energy flow diagram of the PPS study with a ring distribution is added and the components are a simplified version of Figure 3.11, derived from Woud and Stapersma (2002), the development of this diagram is consistent with the 'Develop Network Sketch' step outlined in Figure 3.7 on page 96

The space and weight of these PPS components were selected from discrete equipment data provided by the UCL Submarine Databook (UCL-NAME, 2014) without needing to undertake SUBFLOW. This meant an initial balanced submarine design was able to be achieved. However, the PPS cabling was only estimated using traditional numerical synthesis, which implied a DS3 style choice and definition. Given cabling sizing was the main object of interest in this PPS study, it was still possible to consider whether a traditional numerical synthesis could be replaced by the SUBFLOW sizing approach.

Once the PPS diagram had been devised, an initial balanced submarine design layout was then concurrently developed with the synthesis of the selected PPS. This aimed to ensure the chosen DS3 design style was feasible within the chosen and synthesised submarine design.

3.3.5 Submarine DS3 Synthesis

Given Paramarine with SURFCON (DBB) module is highly flexible, there are several ways in which an SSK design can be synthesised (see Appendix 4). However, as discussed in Subsection 2.2.3, the implementation of the UCL Design Building Block approach (Andrews and Pawling, 2003) with a focus on generating distributed systems (components and connections) using Paramarine had yet to be undertaken. Therefore, Figure 3.14 attempts to capture the complexity of the Gulfs of Execution and Evaluation (Figure 2.6 on page 51) for a typical SSK requirement and style, together with DS3 (an example PPS synthesis) using the SURFCON module in Paramarine. The output of such a procedure is summarised in Figure 3.15, which illustrates the progression of the submarine DS3 synthesis.

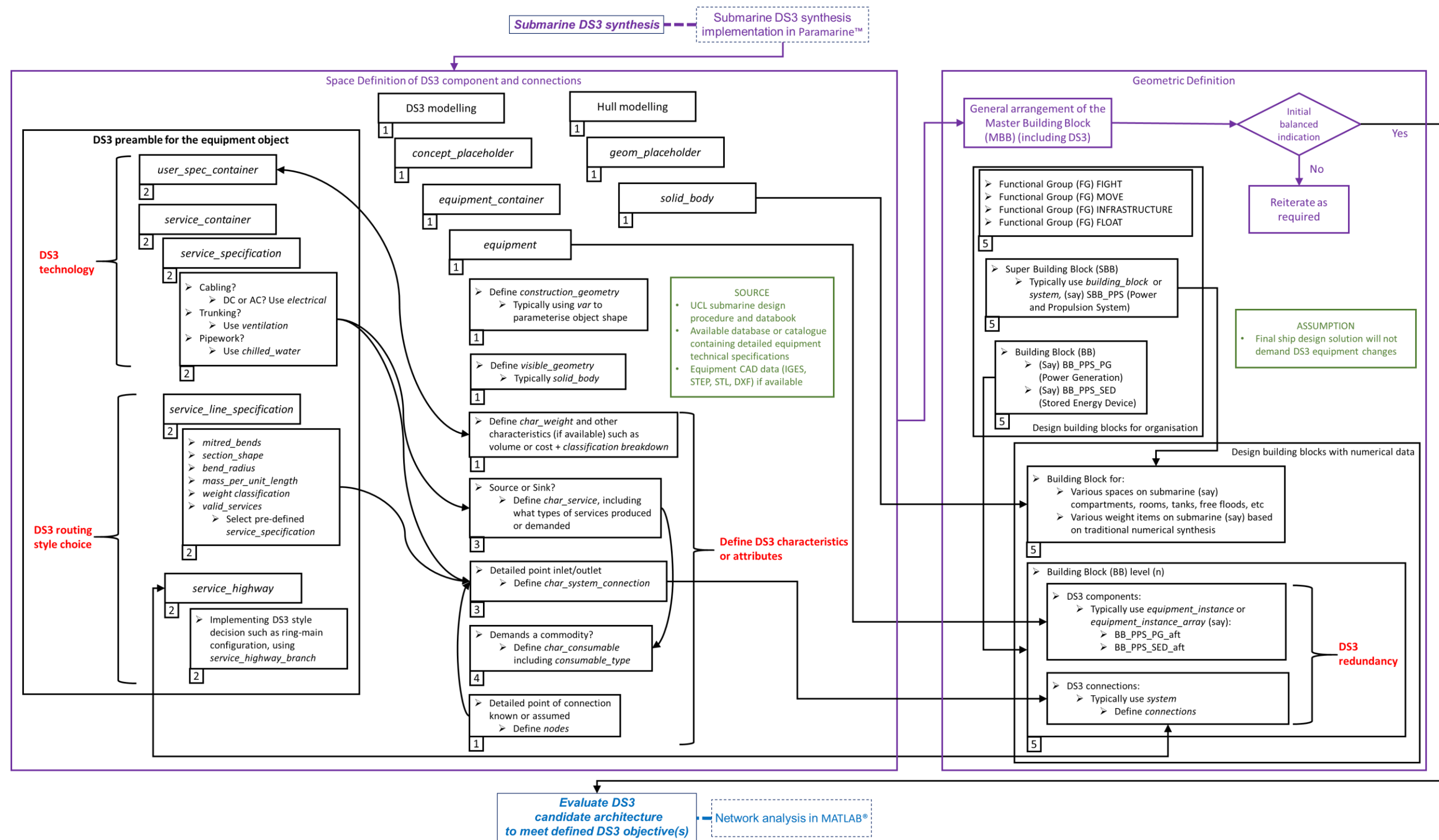


Figure 3.14: Submarine DS3 synthesis implementation in Paramarine showing different colours (purple for main tasks, red for DS3 modelling, green for assumptions, and blue for the network analysis task), part of the procedure outlined in Figure 3.10 on page 111, which consists of five detailed steps (see the left-bottom of each box): **step 1** is to create objects for modelling the hull and DS3 components in Paramarine, shown in *italics*, such as “geom_placeholder” and “equipment_container” (Qinetiq, 2019). The DS3 equipment physical size includes creating objects to host the possible connection point (x, y, z) of equipment; **step 2** is to set up the DS3 connection(s) of a DS3 component adding more objects in Paramarine, such as “user_spec_container”, and “service_container” (Qinetiq, 2019); **step 3** is to provide input for DS3 component as a source or sink and define what relevant DS3 connections could be connected to the DS3 component in terms of DS3 technology; **step 4** is to define the numerical commodity demand of the equipment (if applicable); **step 5** is to perform DS3 modelling using SURFCON module in Paramarine, which consists of creating Design Building Block (DBB) objects that is descriptive (or for ‘organisation’ (Pawling, 2007)) and DBB objects with numerical data, not only for defining space and weight on the submarine but also for the DS3 components and connections (see Appendix 4)

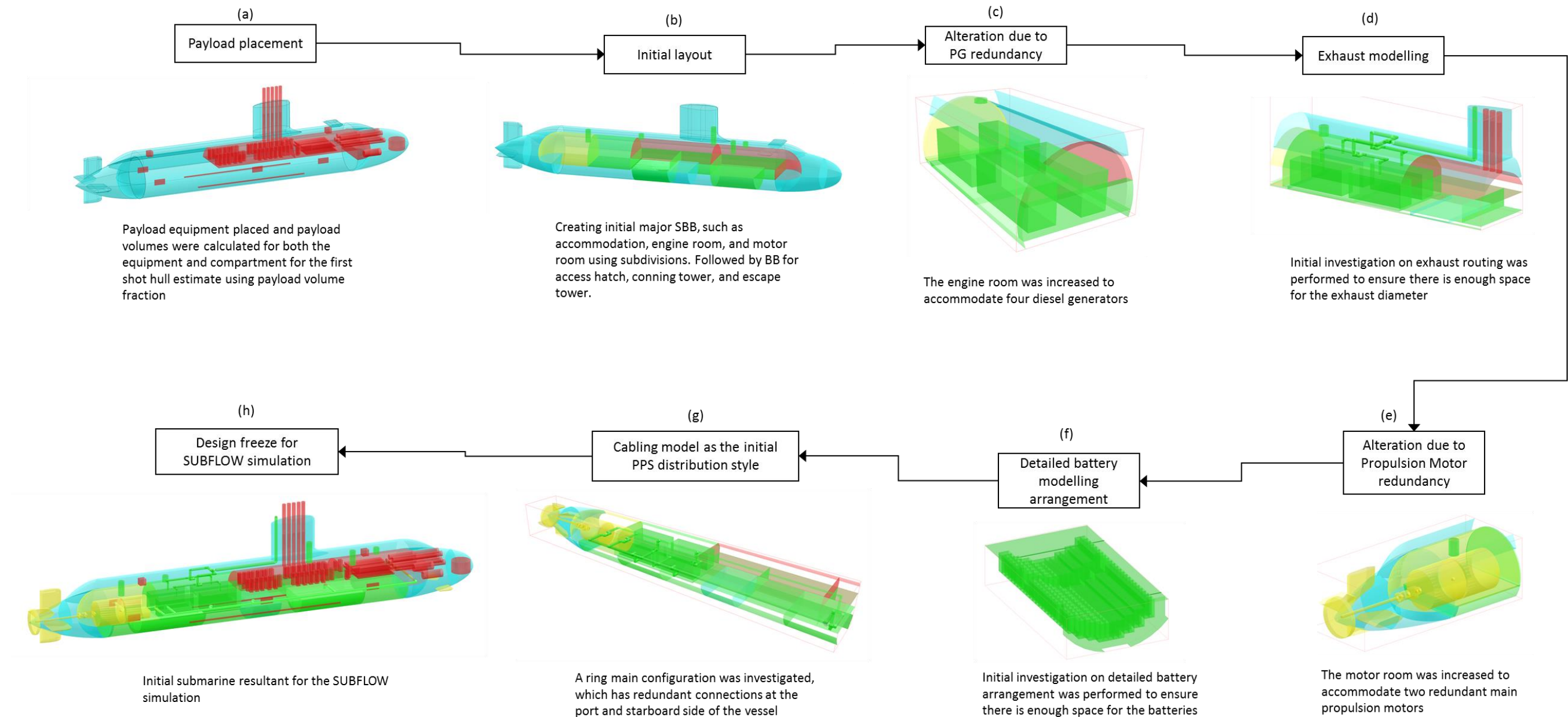


Figure 3.15: Case Study 3.3.1 design progression diagram

Purple boxes in Figure 3.14, represent the main tasks within the ‘Submarine DS3 Synthesis’ step. This is followed by the next step, as shown at the bottom of Figure 3.14, which is the evaluation using a SUBFLOW network step once an initial balanced was achieved. The main tasks include ‘Space Definition’ and ‘Geometric Definition’ boxes that involve five detailed steps outlined in the caption of Figure 3.14. Texts in red in Figure 3.14 indicate tasks specific to DS3 modelling. The submarine DS3 synthesis requires relevant equipment databases and assumes the ship design solution will not demand D3 equipment changes as is shown in green boxes in Figure 3.14. Figure 3.14 also shows that there are many specific Design Building Block (DBB) object terminologies in Paramarine (see the documentation file in the Paramarine software (Qinetiq, 2019)). These are indicated by bold texts and are discussed in bullet points below.

The implementation of the UCL Design Building Block approach in Paramarine-SURFCON allows a 3D based synthesis concurrent with the traditional numerical synthesis (Subsection 2.3.1). Such a numerical synthesis can also be treated as a pre-DBB task, which means a low level numerical balance (space and weight balance) can be achieved without performing the architecturally centred synthesis. Unlike the previous SUBFLOW implementation outlined in Section 3.2.5, this study was not limited to a numerical balance as Burcher and Rydill’s process shows. In this study, the numerical balance was followed by steps 1 to 5 (in Figure 3.14) to synthesise the geometry of both submarine and the selected DS3 using the UCL submarine design procedure (UCL-NAME, 2012) and the UCL Submarine Databook (UCL-NAME, 2014). The development of the proposed SSK design with the selected DS3 styles in Paramarine was therefore investigated as part of this study. The main parts were seen to be:

- The first stage was to prepare the design space, obtaining payload equipment data and creating empty objects in Paramarine as is shown in step 1 of Figure 3.14; This modelling commenced by creating “**concept_placeholder**” object, inserting “**equipment_container**” and

“equipment” objects (Qinetiq, 2019), and then adding numerical data to those equipment objects as is shown in step 1 (left) of Figure 3.14.

- Concurrently, an initial pressure hull was modelled along with external spaces and appendages to assist the placement of the payload equipment. This was done using the **“geom_placeholder”** and **“solid_body”** objects in Paramarine (Qinetiq, 2019) as shown in step 1 (right) of Figure 3.14.
- After the concept setup, **“building_block”** objects (Qinetiq, 2019) or Design Building Block (DBB) objects were populated. DBB objects could be split into two types: DBB objects for organisation (that are descriptive); and DBB objects with numerical data (Pawling, 2007). Hence, both the **“solid_body”** objects and the **“equipment”** objects were inserted to functional **“building_block”** objects, namely Float and Fight, under an organisational **“building_block”** object called Master Building Block (MBB). Such an MBB defines the overall vessel characteristics (see step 5 of Figure 3.14).
- Unlike a previous DBB submarine implementation in Paramarine (Pawling and Andrews, 2011; Purton, 2016), the modelling of DS3 connections required higher Gulfs of Execution and Evaluation (Figure 2.6 on page 51). This includes adding numerical data to **“char_service”**, **“char_system_connection”**, **“char_consumable”**, and **“define_nodes”** objects (Qinetiq, 2019), which require prerequisite objects such as **“user_spec_container”**, **“service_container”**, **“service_specification”**, **“service_line_specification”**, and **“service_highway”** (Qinetiq, 2019) as is shown in step 2 to 4 Figure 3.14. Therefore, as shown in step 5 of Figure 3.14, a DS3 connection can also be inserted under an organisational **“building_block”** object.
- Step 5 in Figure 3.14 indicates the arrangement was manipulated until an initially balanced design was achieved while conducting DBB design breakdown, starting from Super Building Block (SBB) to the BB equipment level (using **“equipment_instance”** object (Qinetiq, 2019) where DS3 equipment or components and connections were allocated. Therefore, the SBB can be volumes or compartments, which have numerical data. If equipment is placed in that SBB, that means such an SBB needs to be

broken down to a BB level to accommodate two objects: the compartment and the equipment. Such a breakdown process is described as follows.

- The “**equipment_instance**” object for the payload equipment in each “**building_block**” object could then be arranged in the design space as illustrated in Figure 3.15 (a). This allows the payload volume to be audited and subsequently be used to have the first shot on the submarine pressure hull using an assumed Payload Volume Fraction (PVF) as in the procedure by Burcher & Rydill (1994).
 - Payload volume Required = 503 m³;
 - PVF assumed = 20%;
 - Pressure hull volume estimated = 2518 m³.
- By making more assumptions on the shape of the submarine hull, as outlined in the UCL submarine design procedure (UCL-NAME, 2012), the form volume and major dimensions were obtained:
 - Number of decks assumed = 2;
 - Pressure hull diameter = 7.6 m;
 - Pressure hull length = 46.5 m;
 - Submarine overall length = 72 m.
- Part of step 5 of Figure 3.14. the initial layout of the design was then developed by broadly modelling major Super Building Block (SBB) volumes for other compartments, such as motor room, engine room, accommodation, messes, and initial volumes for batteries as shown in Figure 3.15 (b). The space requirement for other compartments was derived using scaling algorithms and ‘packing density’ information from the UCL Submarine Databook (UCL-NAME, 2014) and thus could replace the initial PVF assumption. This was done by inserting the numerical data, such as weight and space, under “**characteristics**” placeholder in a “**building_block**” object (Qinetiq, 2019).
- The style of the PPS design was now developed by adding the components from Figure 3.13, such as the two PMs, four PGs, and two SEDs into the functional MBB hierarchy. The PGs and SEDs were seen as DS3 components with a function, namely, to provide (and store) power as a commodity and distributed power to multiple loads, not only for Move

function, but also for Fight, Float, and Infrastructure functions (see Subsection 2.2.3 for the FMFI breakdown). Therefore, two alternatives were considered:

- Place them in the Infrastructure group
- Create a new DS3 functional group
- For this PPS study, the PGs and SEDs were placed in the Infrastructure group. Figure 3.16 shows the philosophy of the Infrastructure group providing power service (originally from fuel energy) to other functional groups in the SSK case study.

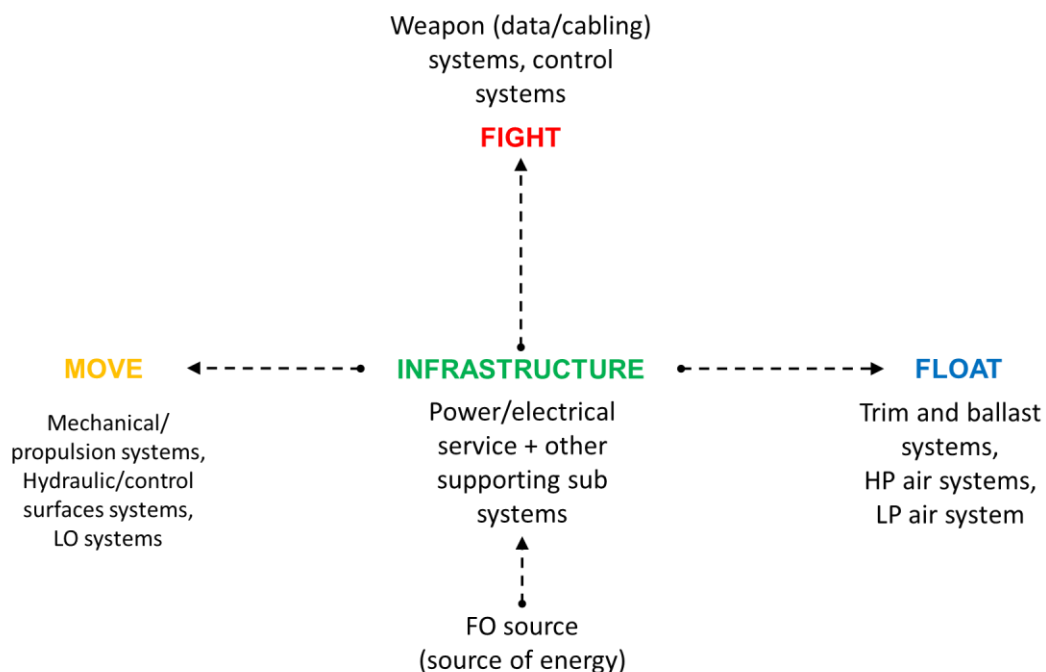


Figure 3.16: A functional group philosophy, showing the PGs and SEDs at the centre of power source, part of the Infrastructure functional group

- The SBB for the engine room was broken down to include the models for four Power Generators (PGs), as depicted in Figure 3.15 (c). Each PG supplies 1.6 MW at the Nominal Continuous Rating (NCR), which was assumed to be 75% of the Maximum Continuous Rating (MCR). This reveals that the size of the engine room needed to be increased to implement the chosen four PGs as recorded in Table 3.17.
- One of the uncertainties in incorporating four PGs was investigated, which was the space required for the exhaust system using the procedure to model

DS3 connections (steps 2 to 4 in Figure 3.14). The sectional area of the exhaust pipe diameter was estimated using an algorithm from the UCL Submarine Databook (UCL-NAME, 2014) and illustrated in Figure 3.15 (d).

- Figure 3.15 (e) shows that the SBB for the motor room was lengthened to incorporate two PMs as decided in Table 3.17. This is followed by Figure 3.15 (f), which shows the detailed battery arrangement or the SEDs.
- Thus, the size of the hull needed to be adjusted to meet the first pass numerical balanced condition where Volume Available = Volume Required and Deep Submerged Weight = Submerged Buoyancy. This could have been achieved with the PPS cabling sized using the traditional whole vessel based numerical algorithms, i.e., scaled from the UCL data (UCL-NAME, 2014). This would have then required a numerical balancing sequence once the cable sizing was replaced by the results from the SUBFLOW sizing approach.
- After the first balancing process, the detailed PPS distribution style was modelled. This was done by graphically investigating the adoption of ring-main routing locations to connect these PPS components, using an object in Paramarine (see steps 2 to 4 in Figure 3.14). This early routing determined possible locations of the PPS physical ring connections, onboard the currently defined submarine design.
- The distance between the pressure hull outer diameter and the PPS ring was obtained by assuming some variables based on fictitious submarine data (UCL-NAME, 2014): the thickness of the pressure hull; the depth of the pressure hull ring stiffeners; an initial width estimation of the cableway; a margin was added for uncertainty; and cable bend angle was assumed to be 90 degrees. These assumptions could be refined during the pressure hull scantling, as the design progressed. The total offset of the centre of PPS cabling to outer pressure hull diameter in this case study was assumed to be about 500 mm.
- The modelling for the PPS cabling is shown in Figure 3.15 (g), which was commenced by creating a “**systems**” object within the MBB hierarchy under the Infrastructure group. The procedure of this modelling is part of step 5 in

Figure 3.14. Detailed modelling issues when using Paramarine-SURFCON are described in Appendix 4, Section A 4.3.

- Hence, an initially balanced submarine concept design and the DS3 synthesis were obtained for initial SSK resultant characteristics (see Figure 3.15 (h) and Figure 3.17). At this point, there were 32 SBBs, which contained various numerical weight and geometric data.
 - Surfaced displacement = 3585 te;
 - Submerged displacement = 4031 te;
 - Overall length = 85 m;
 - Pressure hull diameter = 9.5 m;
 - Solid ballast fraction = 4.8%

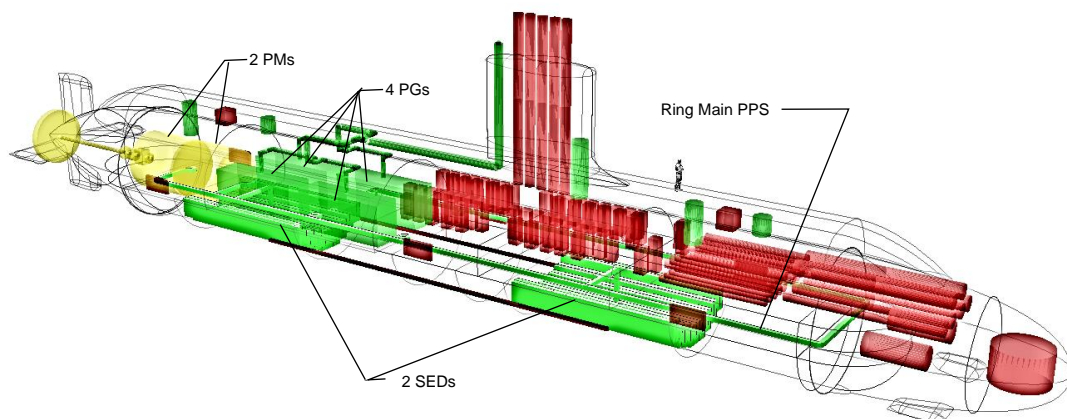


Figure 3.17: Initial SSK design of Case Study 3.3.1 showing PPS elements

3.3.6 Evaluation of the DS3 Candidate Architecture

With the level of granularity adopted for the outlined SSK case study, the SUBFLOW could have been applied not only for sizing the PPS connections but also to evaluate the PPS candidate architecture to meet the defined DS3 objectives. This step could have been taken similar to the previous SUBFLOW process (Section 3.2.5), but this time the definition of nodes and arcs departed from physical based synthesis, not just the network sketch (see Figure 3.7 on page 96). Therefore, the evaluation step consisted of several stages: pre-processing to create the PPS network; the formulation of the SUBFLOW; and post-processing the resultant SUBFLOW solution.

The pre-processing stage was done by first extracting component and connection data manually from Paramarine and inserting it in MATLAB. Component data had unique (centroid) x, y, z locations of PPS components as well as their size as listed in Table 3.19. This information was used to remodel the PPS components in MATLAB as depicted in Figure 3.18.

Table 3.19: The physical architecture properties of PPS for Case Study 3.3.1

System Component	Centroid Location (m)			Dimension (m)			Node (Figure 3.19)
	X	Y	Z	L	B	H	
PM aft	-23.6	0	0	3.7	3.7	3.7	9
PM fwd	-18	0	0	3.7	3.7	3.7	11
PG 1 ap	-11.5	3	0	6.3	1.8	2.6	15
PG 2 as	-11.5	-3	0	6.3	1.8	2.6	21
PG 3 fp	-4.5	3	0	6.3	1.8	2.6	17
PG 4 fs	-4.5	-3	0	6.3 <td 1.8	2.6	23	
SED aft	-15.5	0	-3.7	6.3	5.9	2.2	13
SED fwd	15.3	0	-3.7	6.3	5.9	2.2	19

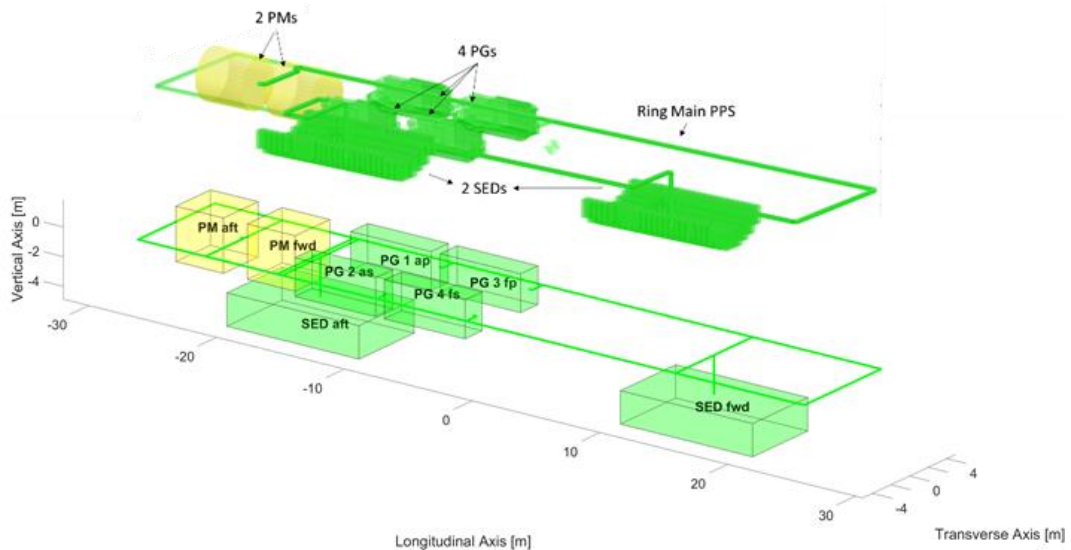


Figure 3.18: PPS architecture displayed in Paramarine (top) translated into MATLAB for the evaluation step (bottom) on the SSK Case Study

The PPS network was then developed to match the physical model depicted in Figure 3.18 for the SUBFLOW simulation. This was done by first labelling each node in the PPS network. Figure 3.19 shows the PPS network consists of 32 nodes and 36 arcs and is defined by a square 32×32 adjacency matrix (see

Table 3.20). As explained in Subsection 3.1.1, when an arc exists between two nodes in Table 3.20, that element is unity and zero otherwise. Since no node is connected to itself in the PPS network in Figure 3.19, the diagonal of the adjacency matrix in Table 3.20 consists of zeros. Likewise, the adjacency matrix is symmetrical as the PPS network was set to be undirected (Subsection 3.1.1) in this pre-processing stage.

Once the pre-processing stage was done, the formulation of the SUBFLOW simulation began. Compared to SUBFLOW simulation produced in Subsection 3.2.5, in this PPS study, some differences were:

- The energy coefficient from the AFO approach (Robinson, 2018) was not used to allow a simpler SUBFLOW formulation.
- The SED nodes were associated with the submerged scenario rather than given explicit numerical nodes and arcs.
- The cable junctions were treated as numerical nodes, which means, as introduced in Subsection 3.2.5, they do not possess geometry data.
- The objective function coefficient was used (not zero) to evaluate the PPS candidate architecture so that it uses the least amount of cabling and takes up the least amount of space.
- The constraints of the PPS components were devised to reflect a selected operating condition of the case study.

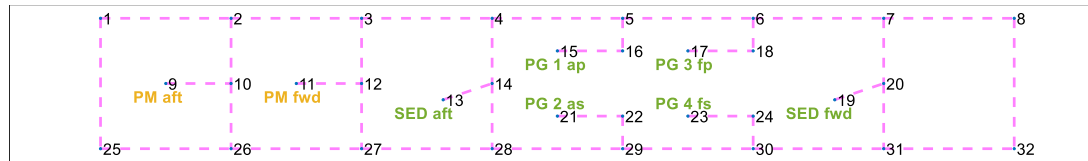


Figure 3.19: Nodes labelling to the PPS architecture in MATLAB (not to scale)

Table 3.20: The adjacency matrix of the PPS study

ID	1	2	3	4	5	6	7	8	9	10	11	12	13	14	15	16	17	18	19	20	21	22	23	24	25	26	27	28	29	30	31	32
1	0	1	0	0	0	0	0	0	0	0	0	0	0	0	0	0	0	0	0	0	0	0	0	0	1	0	0	0	0	0	0	0
2	1	0	1	0	0	0	0	0	0	1	0	0	0	0	0	0	0	0	0	0	0	0	0	0	0	0	0	0	0	0	0	0
3	0	1	0	1	0	0	0	0	0	0	0	1	0	0	0	0	0	0	0	0	0	0	0	0	0	0	0	0	0	0	0	0
4	0	0	1	0	1	0	0	0	0	0	0	0	0	1	0	0	0	0	0	0	0	0	0	0	0	0	0	0	0	0	0	0
5	0	0	0	1	0	1	0	0	0	0	0	0	0	0	0	1	0	0	0	0	0	0	0	0	0	0	0	0	0	0	0	0
6	0	0	0	0	1	0	1	0	0	0	0	0	0	0	0	0	0	1	0	0	0	0	0	0	0	0	0	0	0	0	0	0
7	0	0	0	0	0	1	0	1	0	0	0	0	0	0	0	0	0	0	0	1	0	0	0	0	0	0	0	0	0	0	0	0
8	0	0	0	0	0	0	1	0	0	0	0	0	0	0	0	0	0	0	0	0	1	0	0	0	0	0	0	0	0	0	0	1
9	0	0	0	0	0	0	0	0	1	0	0	0	0	0	0	0	0	0	0	0	0	0	0	0	0	0	0	0	0	0	0	0
10	0	1	0	0	0	0	0	0	1	0	0	0	0	0	0	0	0	0	0	0	0	0	0	0	0	1	0	0	0	0	0	0
11	0	0	0	0	0	0	0	0	0	0	1	0	0	0	0	0	0	0	0	0	0	0	0	0	0	0	0	0	0	0	0	0
12	0	0	1	0	0	0	0	0	0	0	1	0	0	0	0	0	0	0	0	0	0	0	0	0	0	0	1	0	0	0	0	0
13	0	0	0	0	0	0	0	0	0	0	0	0	1	0	0	0	0	0	0	0	0	0	0	0	0	0	0	0	0	0	0	0
14	0	0	0	1	0	0	0	0	0	0	0	0	1	0	0	0	0	0	0	0	0	0	0	0	0	0	0	1	0	0	0	0
15	0	0	0	0	0	0	0	0	0	0	0	0	0	0	1	0	0	0	0	0	0	0	0	0	0	0	0	0	0	0	0	0
16	0	0	0	0	1	0	0	0	0	0	0	0	0	0	1	0	0	0	0	0	0	0	0	0	0	0	0	0	0	0	0	0
17	0	0	0	0	0	0	0	0	0	0	0	0	0	0	0	0	1	0	0	0	0	0	0	0	0	0	0	0	0	0	0	0
18	0	0	0	0	0	1	0	0	0	0	0	0	0	0	0	0	1	0	0	0	0	0	0	0	0	0	0	0	0	0	0	0
19	0	0	0	0	0	0	0	0	0	0	0	0	0	0	0	0	0	0	1	0	0	0	0	0	0	0	0	0	0	0	0	0
20	0	0	0	0	0	0	1	0	0	0	0	0	0	0	0	0	0	0	1	0	0	0	0	0	0	0	0	0	0	0	1	0
21	0	0	0	0	0	0	0	0	0	0	0	0	0	0	0	0	0	0	0	0	1	0	0	0	0	0	0	0	0	0	0	0
22	0	0	0	0	0	0	0	0	0	0	0	0	0	0	0	0	0	0	0	0	1	0	0	0	0	0	0	0	1	0	0	0
23	0	0	0	0	0	0	0	0	0	0	0	0	0	0	0	0	0	0	0	0	0	0	1	0	0	0	0	0	0	0	0	0
24	0	0	0	0	0	0	0	0	0	0	0	0	0	0	0	0	0	0	0	0	0	0	0	1	0	0	0	0	1	0	0	0
25	1	0	0	0	0	0	0	0	0	0	0	0	0	0	0	0	0	0	0	0	0	0	0	0	0	1	0	0	0	0	0	0
26	0	0	0	0	0	0	0	0	0	1	0	0	0	0	0	0	0	0	0	0	0	0	0	0	1	0	1	0	0	0	0	0
27	0	0	0	0	0	0	0	0	0	0	1	0	0	0	0	0	0	0	0	0	0	0	0	0	0	1	0	1	0	0	0	0
28	0	0	0	0	0	0	0	0	0	0	0	0	1	0	0	0	0	0	0	0	0	0	0	0	0	0	1	0	1	0	0	0
29	0	0	0	0	0	0	0	0	0	0	0	0	0	0	0	0	0	0	0	0	0	1	0	0	0	0	0	1	0	1	0	0
30	0	0	0	0	0	0	0	0	0	0	0	0	0	0	0	0	0	0	0	0	0	0	0	1	0	1	0	1	0	1	0	0
31	0	0	0	0	0	0	0	0	0	0	0	0	0	0	0	0	0	0	0	1	0	0	0	0	0	0	0	0	1	0	1	0
32	0	0	0	0	0	0	1	0	0	0	0	0	0	0	0	0	0	0	0	0	0	0	0	0	0	0	0	0	0	0	1	0

As discussed in Section 3.3.3, the SUBFLOW with the M-1 survivability (Trapp, 2015) was applied here using a single flow formulation (see Subsection 3.1.3) and a 144×176 Operational Matrix (see Subsection 3.1.2), as shown in Table 3.21. Equations in Table 3.21 are now described in turn. The objective function for the PPS study, which is given in Equation (3.6), is in the first row and columns 1 to 108 in the Operational Matrix (Table 3.21).

$$\sum_{(i,j) \in E} (\alpha \delta_{i,j} + \beta \delta_{i,j} + \lambda_{i,j} P_{i,j}) \quad (3.6)$$

The objective function in this study evaluates the PPS candidate architecture using two cable sizing methods. The first one was termed as the ‘binary variables’ method that minimised the space taken by PPS connections using coefficients α and β . These coefficients categorised arcs in the PPS network to a certain standard edge component via binary decisions $\delta_{i,j}$. The second one was the ‘integer variables’ method, which also minimised the value of multiplication between the power to volume ratio $\lambda_{i,j}$ and the power $P_{i,j}$. The power to volume ratio $\lambda_{i,j}$ quantifies the power $P_{i,j}$ for each set of arcs connecting a node i and a node j into a discrete volume. To derive the power to volume ratio $\lambda_{i,j}$, the distance between nodes $L(i,j)$ was calculated. Since there were unique x, y, z locations for each node from the DBB synthesis (Table 3.19 on page 126), the L between nodes i and j could be calculated in MATLAB.

Table 3.21: The Operational Matrix of the PPS study, which is developed based on Equations (3.6) to (3.19) on pages 129 to 136 (see Table 3.5 on page 80 and Table 3.14 on page 104 for previous examples of the proposed Operational Matrix applications)

		Formulation for arcs			Formulation for nodes		
No	36 1-36	36 37-72	36 72-108	36 109-144	32 145-176	177	
Objective Function	1	$\alpha \delta_{i,j}$	$\beta \delta_{i,j}$	$\lambda_{i,j} P_{i,j}$	$\sum_{(i,j) \in E} x_{i,n} - \sum_{(i,j) \in E} x_{n,j}$	$-\gamma_n$	= 0
Equality constraints matrix for continuity	2	0	0	0	+1	+1	0
	.	0	0	0	or	or	
	.	0	0	0	-1	-1	
	
33	
34	Equation (3.17)						
Inequality constraints matrix for bidirectionality and binary variables	35	0	0	-1	$-P_{i,j} \pm x_{i,j}$ -1	0	\leq 0
	.	0	0	-1	-1	0	0
	.	0	0	-1	-1	0	
	
	70	
	71	0	0	-1	+1	0	
.	0	0	-1	+1	0		
.	0	0	-1	+1	0		
.	
106	
		$\alpha \delta_{i,j}$	$\alpha \delta_{i,j}$	$P_{i,j}$			\leq 0
107	$-\alpha$	$-\beta$	1	0	0	0	
.	$-\alpha$	$-\beta$	1	0	0		
.	$-\alpha$	$-\beta$	1	0	0		
142		
Lower bounds matrix	143	... 0 0 0 -inf ...	Equations (3.12), (3.13), (3.17), (3.18)	
Upper bounds matrix	144	... 1 1 inf inf ...		
		$\delta(i,j) \in \{0,1\}$		$P_{i,j}^k \geq 0$	$ x_{ij}^k \leq P_{ij}^k$		

Next, the arrangement of PPS cabling in a cableway or a system highway (consisting of multiple longitudinal system (cable) runs) was assumed to give the total cross-sectional area of a cableway. Therefore, a sketch of a cableway, as shown in Figure 3.20 was used to estimate the height (H) and width (W) of the system highway, driven by the number of cables inside the cableway. Figure 3.20 shows the cableway support, typically a threaded steel stud is installed between pressure hull frames, welded to the inner pressure hull, and penetrating hull insulation (U.S. Department of Defense, 2009).

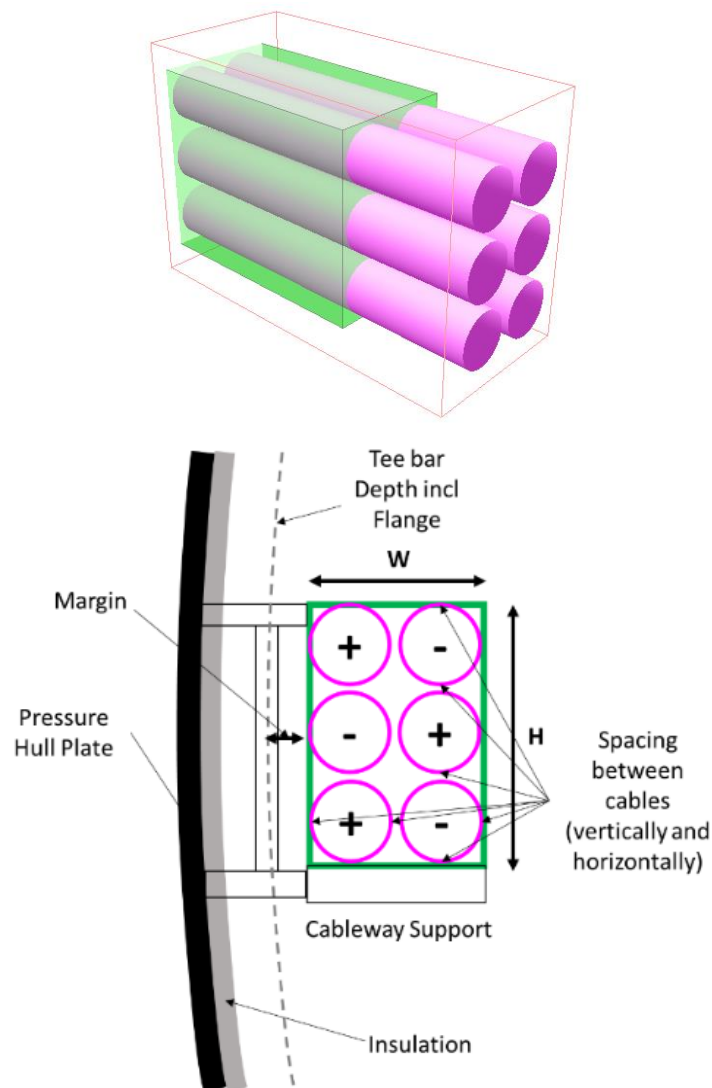


Figure 3.20: A 3D model and a sketch of the PPS cableway arrangement (top and bottom, respectively), where green shows the cable highway as part of the Infrastructure group (see Figure 3.17 on page 125) while magenta shows the individual cables as part of the PPS network evaluated using SUBFLOW

The study assumed the initial maximum capacity flow between nodes P_{wire} of 4.8 MW, while each of the three rows N_{wire} in Figure 3.20 consists of a positive and negative DC cable. If the highest possible voltage V_{wire} was assumed to be 1000 VDC, this gave 1.6 kA current flow I_{wire} per cable. The US DoD cable comparison military handbook (U.S. Department of Defense, 1989) gave an estimation of the diameter required for accommodating such current. A 1.63 kA ampacity cable with a diameter of 56 mm was selected for this case study. By assuming the spacing allowance between cables was 25 mm, the W (188 mm) and H (270 mm) could then be calculated. Therefore, the derivation of power to volume ratio $\lambda_{i,j}$ was given:

$$P_{wire} = I_{wire} \times V_{wire} \times N_{wire} \quad (3.7)$$

$$\lambda_{i,j} = \frac{A_{ij}}{P_{ij}} L_{ij} \quad (3.8)$$

$$= \frac{1.043 \times 10^{-5} m^2}{kW} L_{ij} \quad (3.9)$$

To define variables α and β in Table 3.21 (located in the first row and the first 72 columns) there were two assumed ‘standard’ edge components. The first one was a cable with 0.467 kA ampacity, the second one had 1.63 kA ampacity. Based on the cableway arrangement, the first category α could accommodate a maximum 1.4 MW power capacity and the second category a maximum β of 4.89 MW power capacity. As indicated in rows 143 to 144 and columns 1 to 72 in the Operational Matrix (Table 3.21), the variable $\delta(i,j)$ must be either 0 or 1.

In this case study, SUBFLOW did not just seek the minimum space for PPS cabling but also satisfied several constraints. These constraints were developed to show the distinctive SSK PPS operating conditions. In these constraints, k is an indexed scenario within a set of operating conditions K to represent various operating conditions, such as snorting and submerged conditions. The first constraint (see Equation (3.10)) is the basic continuity formulation (Subsection 3.1.2) that ensures the flow variable or flow path x entering and leaving a node n from a node i or j within a set of nodes N is equal to the amount of commodity γ at that node n and is preserved throughout the

edges E , except at relevant sources and sinks. This equation is indicated in rows 2 to 33 and columns 109 to 176 in the Operational Matrix (Table 3.21).

$$\sum_{(i,j) \in E}^k x_{i,n}^k - \sum_{(i,j) \in E}^k x_{n,j}^k = \gamma_n^k \quad (3.10)$$

To allow a power flow steady state simulation, which can change direction in different scenarios, a formulation from the NSMCF (Trapp, 2015) was used (see Equation (3.11)). This allowed a bidirectional flow path $x_{i,j}$ to be ‘rolled up’ and converted to power capacity flow $P_{i,j}$ as the decision variables in SUBFLOW (see Subsection 3.1.2). This formulation is located in two parts in the Operational Matrix (Table 3.21): rows 35 to 106 and columns 72 to 144; rows 143 to 144 and columns 109 to 144.

$$|x_{ij}^k| \leq P_{ij}^k \quad (3.11)$$

Equation (3.12) defines the lower bound and the upper bound of the amount of power capacity Y of the source nodes s within the set of nodes N to be equal or greater than the power flow produced by the source nodes γ_s . The source nodes in the PPS study were the PGs, i.e., nodes 15, 17, 21, and 23 (see Table 3.19). This equation is assigned at rows 143 to 144 and columns 145 to 176 in the Operational Matrix framework (Table 3.21).

$$\sum_{(s) \in N}^k \gamma_s^k \leq \sum_{(s) \in N}^k Y_s^k \quad (3.12)$$

Equation (3.13) allows modelling of path nodes p , where the commodity γ at a path node p within the set of nodes N is bounded to the source capacity Y_s . The examples of path nodes in the PPS study were nodes 1, 2, 3, etc (see Table 3.19 on page 126). This equation is assigned at rows 143 to 144 and columns 145 to 176 in the Operational Matrix (Table 3.21).

$$\sum_{(p) \in N}^k \gamma_p^k \leq \sum_{(s) \in N}^k Y_s^k \quad (3.13)$$

Equation (3.14) confirms that the required power P_{ij} , as the decision variables in the SUBFLOW formulation, is always positive. This is reflected in Table 3.21 at rows 143 to 144 columns 72 to 108.

$$P_{i,j}^k \geq 0 \quad (3.14)$$

Equation (3.15) is based on the M-1 survivability by Trapp (2015) (see Section 3.4), which is a scenario to find out a set of flow variables x when an edge in the DS3 is assumed to be lost. Thus, each operating condition k is associated with an edge loss scenario m within a set of damaged scenarios M . This equation was applied by setting the upper bound of a power capacity flow $P_{i,j}$ to zero in the Operational Matrix (Table 3.21), which is located at row 144 and columns 72 to 108.

$$P_{i,j}^{k,m} = 0 \quad (3.15)$$

The δ in Equation (3.16) serves as the binary decision to classify a capacity of an edge i to j to achieve certain standards for an edge component (type α and β , see Equation (3.6) on page 129). This equation is assigned at rows 143 to 144 and columns 1 to 72 in the Operational Matrix (Table 3.21).

$$\delta(i,j) \in \{0,1\} \quad (3.16)$$

For evaluating the redundancy of system components, Equations (3.17) and (3.18) were needed to state the system requirement capacity of the sink Y_t in an operating condition k . Equation (3.17) applied to PMs due to the style choice on the propulsion motor (PM). The redundant PMs were set as sinks, but the solver could only select one PM to be online in an operating condition k . Equation (3.18) was the hard constraint for the batteries (SED) charging demand. Therefore, in the PPS study, the sink nodes t were PMs and SEDs (nodes 9, 11, 13 and 19 in Table 3.19 on page 126). These equations are shown in rows 34 and 143 to 144 and columns 145 to 176 in the Operational Matrix (Table 3.21).

$$\sum_{(t) \in N}^k \gamma_t^k = Y_t^k \quad (3.17)$$

$$\gamma_t^k = Y_t^k \quad (3.18)$$

In this PPS study, only the snorting condition was considered, where the SEDs become the highest load in the PPS network, letting operating condition $k = 1$. The submerged load including power and energy margins were allocated directly to the battery nodes (SEDs) as a hard constraint, to maintain the desirable indiscretion ratio, which was calculated based on the procedure explained in the SUBFLOW example in Subsection 3.2.3. Unlike the SUBFLOW example in Subsection 3.2.5, the power sources for the PPS case study were capped at 1.6 MW and that figure was the assumed maximum supply capacity of each Power Generators (PG) as already selected and incorporated in the design (see Figure 3.15 (c) on page 119). The M-1 approach survivability (Trapp, 2015), shown in Equation (3.15), was applied to this SUBFLOW formulation by setting the upper bound of an arc to zero, located in row 144 and one of columns 72 to 108 in the Operational Matrix Table 3.21. This setup forced the solver to be unable to use that arc and then search for an alternative flow path in the network. The commodity required from the source Y_s^k and sink Y_t^k in Equations (3.12), (3.13), (3.17), and (3.18) had to be defined from design requirements, i.e., the demanded power was based on the baseline SSK design, as outlined in Table 3.22.

Table 3.22: The summary of the power commodity in snorting and transit

System Component	Supply Y_s (kW)	Demand Y_t (kW)	Node (Figure 3.19)
PM aft	-	346	9
PM fwd	-		11
PG 1 ap	1600 (max)	-	15
PG 2 as	1600 (max)	-	21
PG 3 fp	1600 (max)	-	17
PG 4 fs	1600 (max)	-	23
SED aft	-	2930	13
SED fwd	-	2930	19

The flow path solutions from the solver (see Subsection 3.1.2), which consisted of numerical data in a matrix, were then extracted and assigned back to the network as part of the post-processing step. This process is comparable to the results shown in Table 3.5 and Figure 3.4. Once the flow path solutions were attached to appropriate arcs, the network could be visualised with this information, showing different line thicknesses and explicit labels, indicating the quantity of power flow of each arc. Comparable to the results presented in Table 3.6, the individual SUBFLOW simulation due to the incorporation of the M-1 survivability (Trapp, 2015) were presented and discussed in detail in Appendix 3. The DS3 sizing was derived from the aggregate solution, not the individual solutions (see Table 3.6 (bottom)). The aggregate solution used in the AFO (Parsons et al., 2020a) is expressed in Equation (3.19).

$$P_{i,j} = \max_{(k,m) \in K,M} (P_{i,j}^{k,m}) \quad (3.19)$$

Therefore, as explained in Subsection 3.1.3, the aggregate solution was compiled by selecting the highest power flow $P_{i,j}$ of each arc in all investigated scenarios K, M . This resulted in the flow solution shown in Figure 3.21.

3.3.7 Selecting A DS3 Solution

Without performing SUBFLOW, the PPS arcs can be sized at the maximum capacity, which can be based on the maximum power available from the four PGs. This is referred to as the conservative solution and is shown in Figure 3.21 (top). However, as shown in Figure 3.21 (middle and bottom), the use of SUBFLOW provides insights for sizing the PPS cabling. The aggregate solutions from the SUBFLOW shown in Figure 3.21 (middle and bottom) reveal the outer arcs become zero, but arcs in Figure 3.21 (middle) have a series of different flow solutions ranging from 300 kW to 3 MW while arcs in Figure 3.21 (bottom) have a flow of either 1.4 MW or 4.8 MW. This was because the binary formulation in the SUBFLOW provided an alternative sizing option by classifying power flow either to arc categories α (1.4 MW) or β (4.8 MW), which was quite different to the integer formulation given in Section 3.3.6. Conversely, the top diagram in Figure 3.21 shows a conservative solution that preserved an

all-ring configuration style, where the power $P_{i,j}$ of all arcs was homogenous at 6 MW, given by the maximum power available from the four PGs. These various flow solutions gave insights to the designer and can be used to obtain the volume of the PPS connections using the power to volume ratio, as outlined in Subsection 3.2.5.

3.3.8 Feedback and Conclusion from the Initial DS3 Synthesis

Although it was recognised that the aft part of the PPS network would have required further operating scenarios k to be considered beyond snorting as discussed in Subsection 3.2.5, a summary of three different sizing methods is given in Subsection 3.3.7. Since there were found to be three possible methods, the designer was able to choose between a smaller space solution (3 m³ and 5 m³) or the conservative solution (10 m³) for the PPS arcs input sizing (see Table 3.23). Unfortunately, there was no readily available real-world submarine data to validate these results. However, it is noteworthy that this type of information was previously unavailable using traditional numerical algorithms. Further application of the SUBFLOW to this case study was not carried out, but the Gulfs of Execution and Evaluation (Figure 2.6 on page 51) to model the physical architecture for other DS3 using Paramarine-SURFCON was investigated and is given in Appendix 4.

It is also the case the M-1 survivability alone could not capture the contribution of forward outer ring component of the specific DS3 to PPS survivability. Recognising the need to reduce designer workload, formulating all possible survivability scenarios for this PPS network was seen to be difficult while still maintaining the fundamental objective of ESSD, that of Requirement Elucidation. Thus, the next chapter outlines the refined SUBFLOW formulation that is less demanding for a DS3 synthesis focused intent and a more style driven approach.

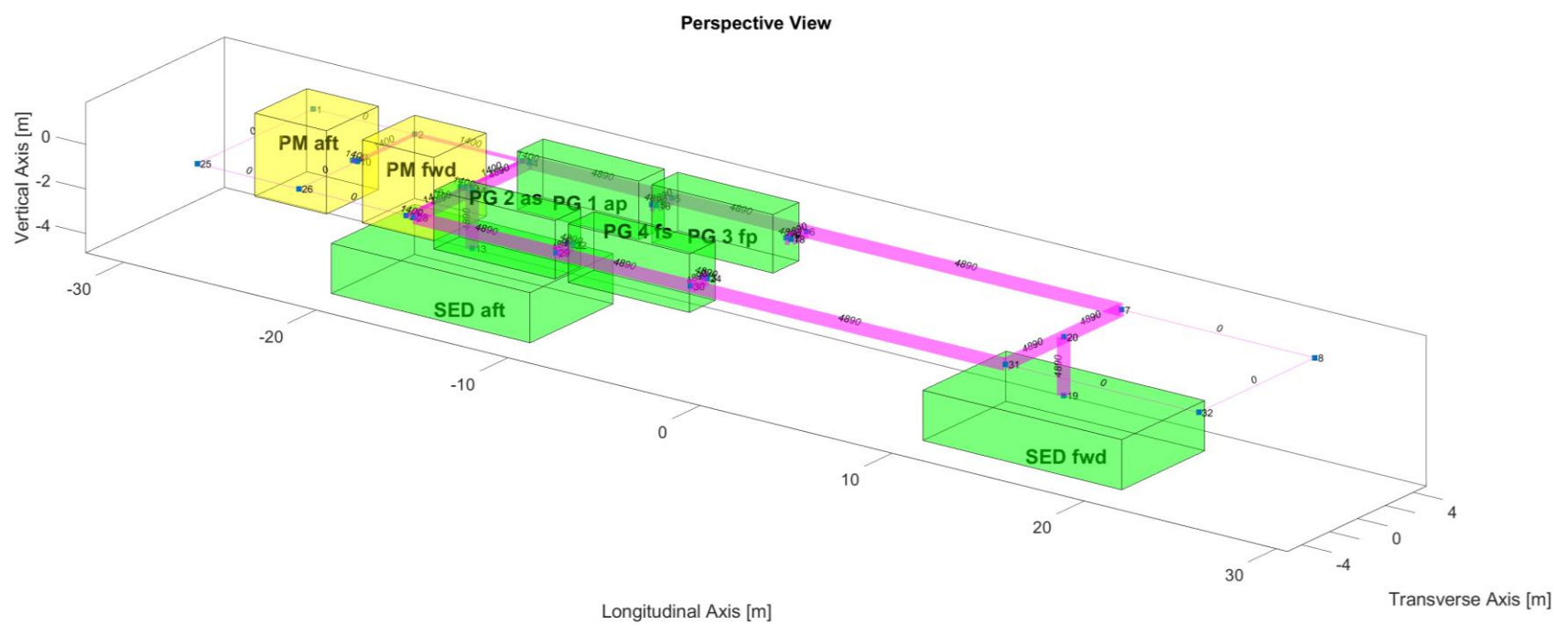
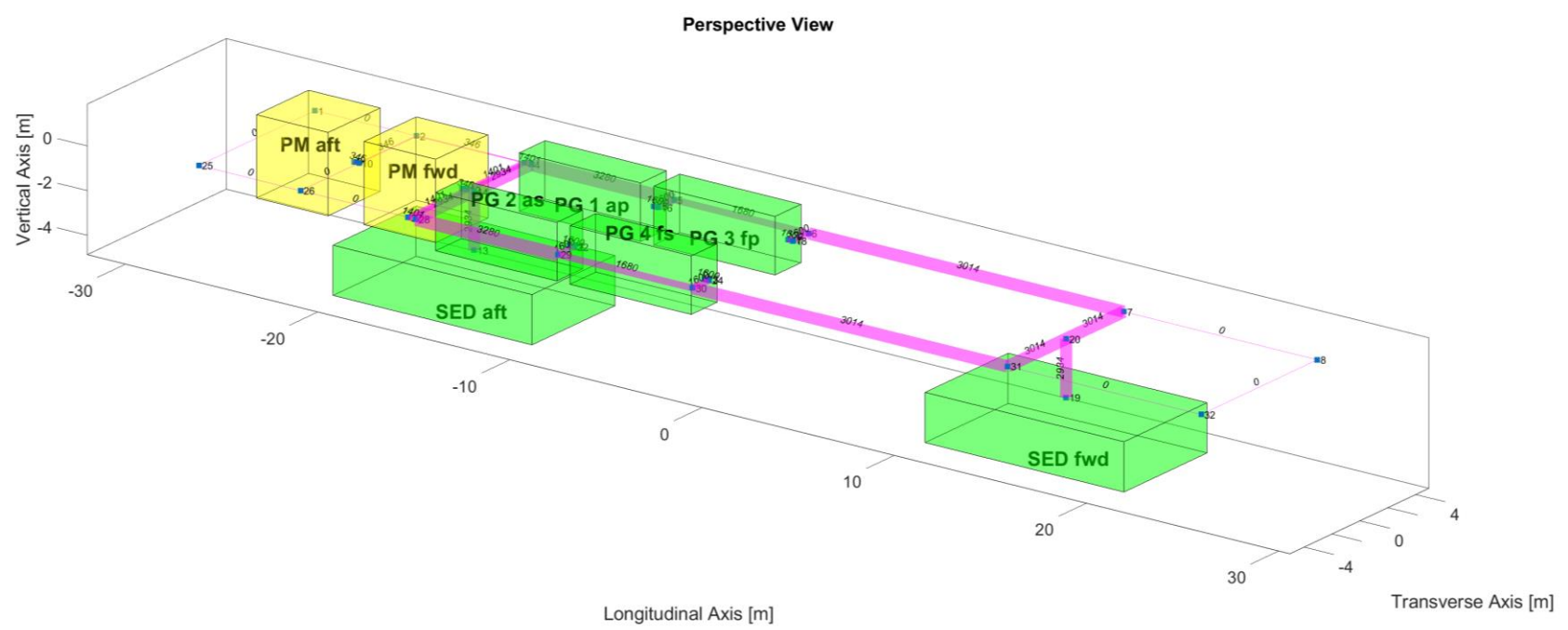
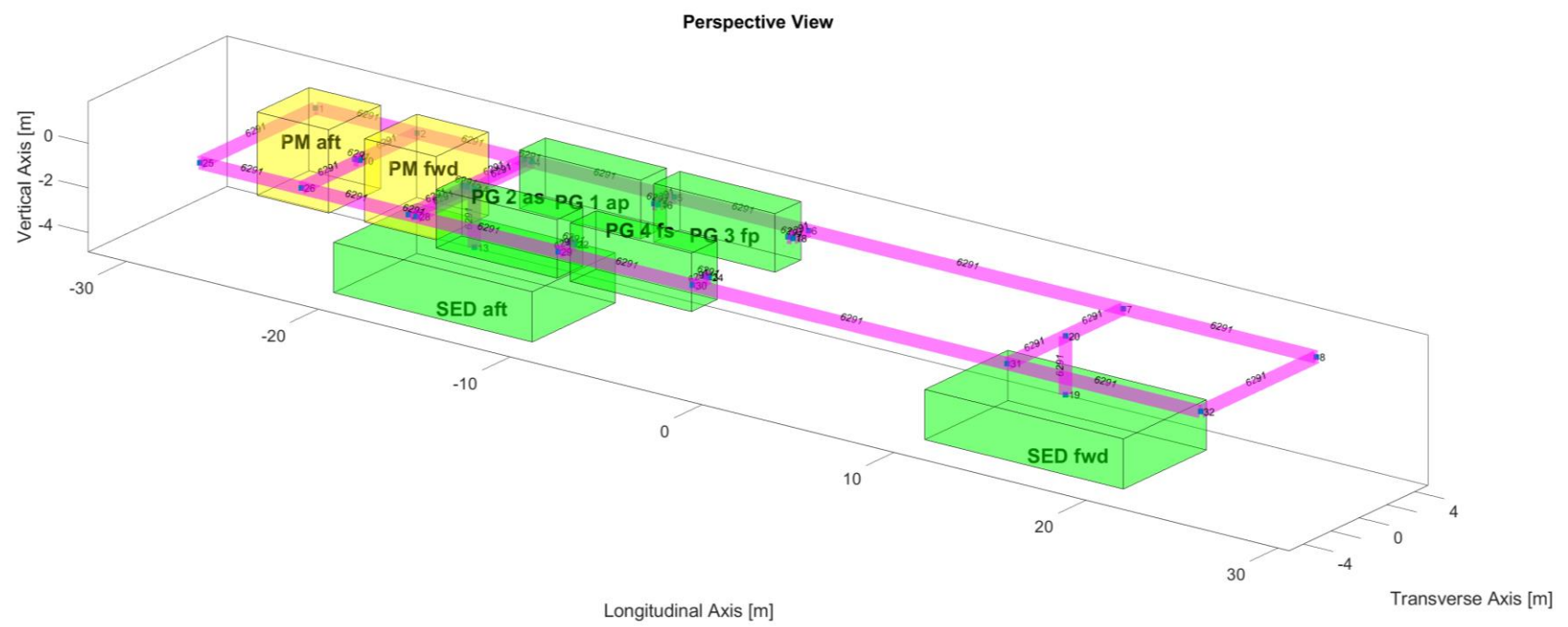


Figure 3.21: Visualisation of the PPS arcs sizing results (magenta), showing the conservative method (top), the integer variables method (middle), and the binary variables method (bottom) (see Subsection 3.3.7) for the SSK Case Study 3.3.1

Table 3.23: Sizing results of the PPS study for the SSK Case Study 3.3.1

Arc No	Node		Power to volume ratio $\lambda_{i,j}$ (m ³ /kW)	Conservative Method		Integer Variables Method		Binary Variables Method			
	<i>i</i>	<i>j</i>		Power $P_{i,j}$	Volume $V_{i,j}$	Power $P_{i,j}$	Volume $V_{i,j}$	Alpha α	Beta β	Power $P_{i,j}$	Volume $V_{i,j}$
				(kW)	(m ³)	(kW)	(m ³)			(kW)	(m ³)
1	1	2	5.52E-05	6291	0.347	0	0.000	-	-	0	0.000
2	1	25	8.68E-05	6291	0.546	0	0.000	-	-	0	0.000
3	2	3	5.84E-05	6291	0.367	346	0.020	yes	-	1400	0.082
4	2	10	4.31E-05	6291	0.271	346	0.015	yes	-	1400	0.060
5	3	4	4.02E-06	6291	0.025	1401	0.006	yes	-	1400	0.006
6	3	12	4.31E-05	6291	0.271	1401	0.060	yes	-	1400	0.060
7	4	5	7.72E-05	6291	0.486	3280	0.253	-	yes	4890	0.378
8	4	14	4.31E-05	6291	0.271	2934	0.127	-	yes	4890	0.211
9	5	6	7.30E-05	6291	0.459	1680	0.123	-	yes	4890	0.357
10	5	16	1.18E-05	6291	0.074	1600	0.019	-	yes	4890	0.058
11	6	7	1.71E-04	6291	1.076	3014	0.515	-	yes	4890	0.836
12	6	18	1.18E-05	6291	0.074	1600	0.019	-	yes	4890	0.058
13	7	8	1.05E-04	6291	0.660	0	0.000	-	-	0	0.147
14	7	20	4.31E-05	6291	0.271	3014	0.130	-	yes	4890	0.211
15	8	32	8.68E-05	6291	0.546	0	0.000	-	-	0	0.121
16	9	10	2.61E-06	6291	0.016	346	0.001	yes	-	1400	0.004
17	10	26	4.36E-05	6291	0.275	0	0.000	-	-	0	0.000
18	11	12	2.61E-06	6291	0.016	346	0.001	yes	-	1400	0.004
19	12	27	4.36E-05	6291	0.275	1401	0.061	yes	-	1400	0.061
20	13	14	2.74E-05	6291	0.172	2934	0.080	-	yes	4890	0.134
21	14	28	4.36E-05	6291	0.275	2934	0.128	-	yes	4890	0.213
22	15	16	2.61E-06	6291	0.016	1600	0.004	-	yes	4890	0.013
23	17	18	2.61E-06	6291	0.016	1600	0.004	-	yes	4890	0.013
24	19	20	2.74E-05	6291	0.172	2934	0.080	-	yes	4890	0.134
25	20	31	4.36E-05	6291	0.275	3014	0.132	-	yes	4890	0.213
26	21	22	2.61E-06	6291	0.016	1600	0.004	-	yes	4890	0.013
27	22	29	1.24E-05	6291	0.078	1600	0.020	-	yes	4890	0.060
28	23	24	2.61E-06	6291	0.016	1600	0.004	-	yes	4890	0.013
29	24	30	1.24E-05	6291	0.078	1600	0.020	-	yes	4890	0.060
30	25	26	5.52E-05	6291	0.347	0	0.000	-	-	0	0.000
31	26	27	5.84E-05	6291	0.367	0	0.000	-	-	0	0.000
32	27	28	4.02E-06	6291	0.025	1401	0.006	yes	-	1400	0.006
33	28	29	7.72E-05	6291	0.486	3280	0.253	-	yes	4890	0.378
34	29	30	7.30E-05	6291	0.459	1680	0.123	-	yes	4890	0.357
35	30	31	1.71E-04	6291	1.076	3014	0.515	-	yes	4890	0.836
36	31	32	1.05E-04	6291	0.660	0	0.000	-	-	0	0.147
Total Volume					10.865		2.723				5.243

3.4 Conclusion from the Initial Implementation

These research experiments revealed the advantages and disadvantages of each implementation against the objective of the research, which is to explore DS3 options as part of a more effective Requirements Elucidation for submarines. Some key points are:

- The application of SUBFLOW has provided not only a more realistic sizing but also aided designer understanding of the distributed systems via power flow simulation than could a traditional numerical based approach. However, formulating SUBFLOW and the process to create the adjacency matrix and Operational Matrix framework were undertaken manually and were laborious, introducing significant Gulfs of Execution and Evaluation (Figure 2.6 on page 51) in the submarine design process. This was seen to be a disadvantage when exploring DS3 options at ESSD using SUBFLOW.
- When SUBFLOW was combined with the UCL Design Building Block (DBB) approach, it enabled a more holistic DS3 synthesis, which was considered to enhance physical and logical descriptions and to show how the DS3 and the design space interacted. Nevertheless, given the proposed DS3 synthesis approach was a discrete process, it took data from the Paramarine definition and manually processed it into MATLAB and then fed the data back to Paramarine for further manually driven design iterations. Within Paramarine itself the effort to generate the design to a sufficient level of granularity for DS3 was substantial, and manually processing the data for SUBFLOW in MATLAB compounded the complexity of the process. This did not include undertaking other design changes and thus this approach was considered overly demanding.

It was therefore considered that to implement SUBFLOW with the UCL Design Building Block approach to explore a range of DS3 options in ESSD, it required a large overhead development to produce a set of new tools to mitigate the drawbacks outlined above and an effort to retain the advantages of both approaches into a new approach for a more integrated and holistic DS3 synthesis.

Chapter 4

The Network Block Approach

Chapter 3 presented an early version of the SUBFLOW simulation for DS3 combined with the UCL Design Building Block approach. That implementation revealed the technical issues when integrating the network based sizing approach with the submarine design process using Paramarine-SURFCON. Significant Gulfs of Execution and Evaluation were required using both approaches (see Figure 2.6 on page 51), which could inhibit exploring DS3 options in ESSD. This chapter presents a new approach that addressed these issues (see Figure 4.1).

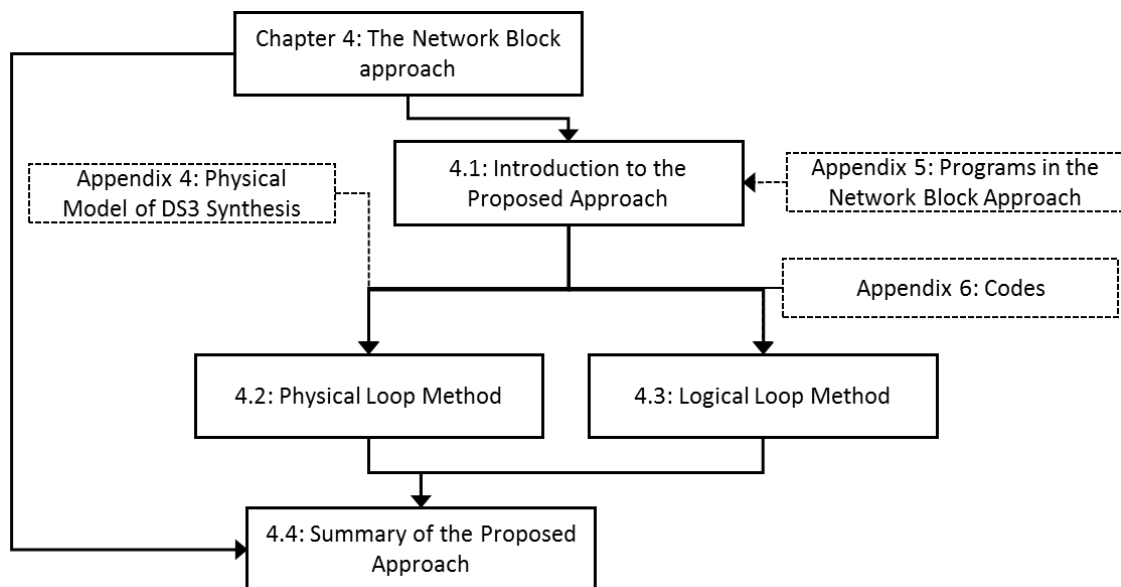


Figure 4.1: Schematic of Chapter 4

Section 4.1 presents a background setting of the development of the new approach by first discussing the nature of Computer-Aided Ship Design (CASD) and subsequently outlines the architecture as well as the description of the new approach. Sections 4.2 and 4.3 expand the description of the detailed framework used by the new approach. Finally, Section 4.4 summarises the key points of the proposed approach.

4.1 Introduction to the Proposed Approach

The implementation of the UCL Design Building Block (DBB) approach in Paramarine with its SURFCON (DBB) module is highly flexible and therefore specifically useful for DS3 synthesis (see Section 3.3 and Appendix 4). The algorithms and assumptions were part of the input and thus the implementation of the UCL DBB approach in Paramarine is not a black-box process. However, such a 'glass box' approach is demanding in the expenditure of time for developing a new design.

Therefore, an approach termed the Network Block Approach (NBA) was proposed. The NBA consisted of frameworks, methods, and design tools that employed a strategy to 'intercept' data flow, before being inputted to Paramarine, and utilised a set of spreadsheet Excel inputs (Microsoft, 2021a). The main objective of the development of the NBA was to create an integrated design procedure that incorporated SUBFLOW and the UCL DBB approach.

On one hand, SUBFLOW required design data at a specific level of design granularity. On the other hand, the UCL DBB approach facilitated the development of a new design *ab initio* at a level of design granularity required for DS3 synthesis (see Section 3.3 and Appendix 4). Therefore, the architecture of the NBA must consider the two distinct design philosophies. To merge the advantages of both approaches, the NBA was developed based on DevOps software practice which is a blend of two different activities, 'Development' and 'Operations' (Hüttermann, 2012). In this case, the 'Development' represents the implementation of the UCL DBB approach in Paramarine and the 'Operations' represents the DS3 synthesis using SUBFLOW in MATLAB. This leads to an infinity loop diagram presented in Figure 4.2, which represents the iterative nature and can be terminated once the design is considered naval architecturally balanced.

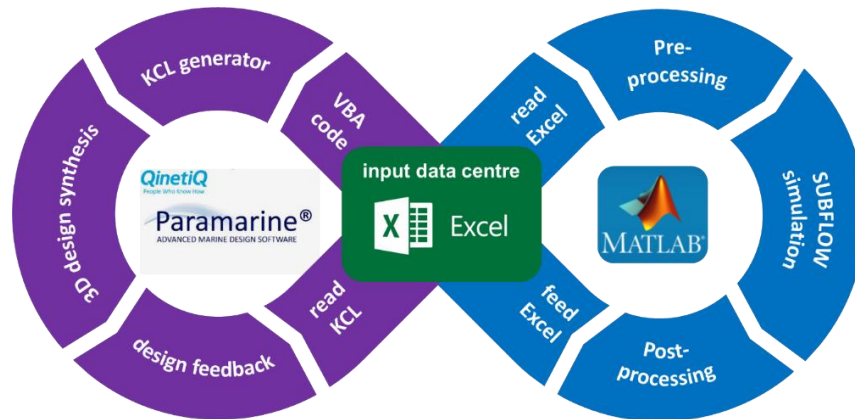


Figure 4.2: The logic of the proposed Network Block Approach showing a high level process of Physical Loop method in purple and Logical Loop method in blue

Figure 4.2 shows centrally the Excel spreadsheet (Microsoft, 2021a), where the design data can be stored and is termed the 'input data centre'. The design data dealt with the design concerns appropriate to ESSD, such as space and numerically defined gross weight, as well as creating DS3 components and connections, including their attributes required for the SUBFLOW network analysis. The NBA consisted of what was termed as the 'Physical Loop' method in purple in Figure 4.2 (left) and the 'Logical Loop' method shown in blue in Figure 4.2 (right). The Physical Loop method focused on the task to synthesise the submarine design and the DS3 in terms of the physical architecture (Subsection 2.1.1), which was done through the interaction between a set of spreadsheets and Paramarine using Visual Basic Applications (VBA) based programming language (Microsoft, 2021b). The Logical Loop method made use of MATLAB codes to perform the development of a DS3 network by pre-processing, analysis, and post-processing through SUBFLOW to enable DS3 energy flow simulation in logical architecture representation and energy based DS3 sizing.

In the Network Block Approach, the VBA based code read the design data from the input data centre spreadsheet at different levels of design granularities and translated the data into Kernel Command Language (KCL) code (Boscarol and Aiello, 1988) for Paramarine to read. Once the design data was in Paramarine, the design could be architecturally manipulated by the designer in the 3D graphical environment until the designer was satisfied. This design data could

then be exported back in KCL codes and read by Excel using a VBA script to fill a set of specific cells in a spreadsheet layout. Concurrently, the designer could develop the architecture of DS3 in the same input data centre spreadsheet, which could be directly read by MATLAB. This enabled the creation of an adjacency matrix and an Operational Matrix automatically, unlike the manual laborious process as in the first implementation (see Chapter 3). The result from the network analysis could then be written back from the MATLAB to the input data centre and thus the designer could manually select the size of DS3. Finally, this sizing input was read by Paramarine for further ship design assessment to achieve a naval architecturally balanced submarine design and the impact of a certain DS3 style choice on the whole ship design made by the designer.

The input data centre consisted of several programs, summarised in Figure 4.3. Each program was developed as a worksheet, which could be read both by Paramarine for rapid modelling of objects and by MATLAB for automatically generating adjacency matrix and Operational Matrix. With this approach, the designer could focus and readily manipulate the architecture of the vessel and perform SUBFLOW simulation without needing to address the Gulf of Execution (Figure 2.6 on page 51) in Paramarine and MATLAB.

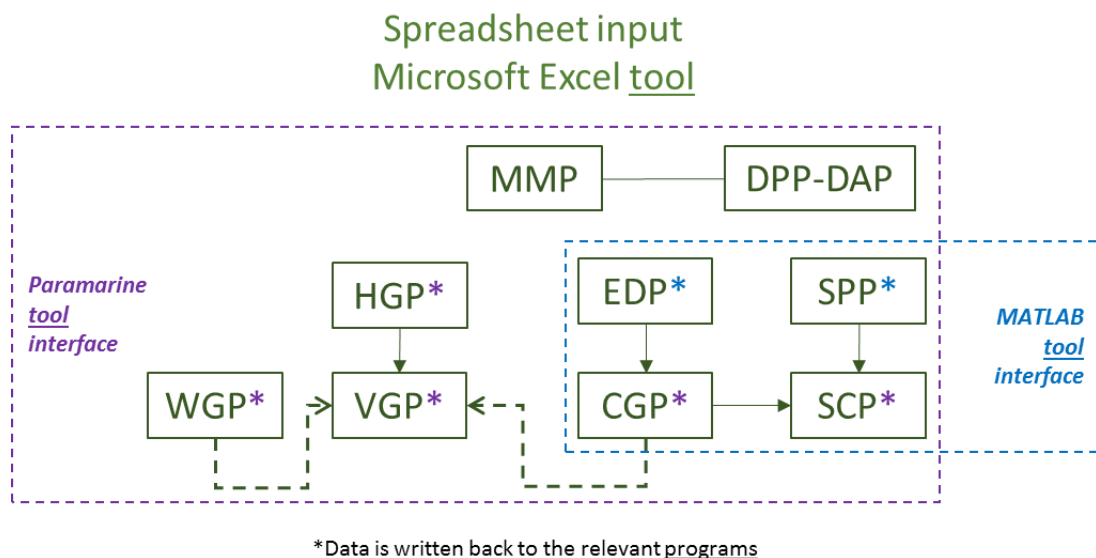


Figure 4.3: The detailed breakdown of the input data centre, showing multiple programs in green, Paramarine interface in purple and MATLAB interface in blue

The top part of Figure 4.3 shows the Main Menu Program (MMP), which is a menu to execute all the programs listed in Table 4.1 through a single 'click'. MMP was also connected to the Design Preamble Program (DPP) and the Design Analysis Program (DAP). The DPP and the DAP are hardcoded KCL scripts for automatically setting up the analytical capability available in the Paramarine system, including the audit function. As shown in the purple dashed box in Figure 4.3, all programs work with Paramarine but only four programs in the blue dashed box work with MATLAB. The application of the programs in Table 4.1 within the Physical Loop and Logical Loop methods is next discussed in Sections 4.2 and 4.3.

Table 4.1: Summary of programs in the Network Block Approach

Program	Description	Function	Reference in Appendix 5
MMP	Main Menu Program	Execution menu to compile all programs	A 5.2.1
DPP	Design Preamble Program	Hardcoded design setup	
DAP	Design Analysis Program	Hardcoded analysis setup	
HGP	Hull Granularity Program	Input for hull size	A 5.2.2
VGP	Volume Granularity Program	Input for spaces	A 5.2.3
WGP	Weight Granularity Program	Input for weight	A 5.2.4
EDP	Equipment Database Program	Input for equipment data	A 5.2.5
CGP	Component Granularity Program	Input for DS3 components for arrangement and SUBFLOW	A 5.2.6
SPP	System Preamble Program	Input for DS3 connections	A 5.2.7
SCP	System Connection Program	Input for DS3 connection and SUBFLOW	A 5.2.8

4.2 Physical Loop Method

As shown in Figure 4.2, the Physical Loop method dealt with the physical design of the submarine, such as the hull geometry and the internal arrangement, including modelling DS3 physical components and connections. With this method, the designer could focus and readily manipulate the architecture of the vessel without needing to address the Gulf of Execution (Figure 2.6 on page 51), i.e., the high number of routine modelling tasks in Paramarine.

The Physical Loop method worked based on multiple frameworks with specific Design Building Block (DBB) object terminologies in Paramarine that are already discussed in Subsection 3.3.5 and Figure 3.14 on page 118. The proposed framework related to different design granularities and design fidelities is outlined in Subsection 4.2.1. Different types of DBB objects for design synthesis are presented in Subsection 4.2.3. A new DBB hierarchical breakdown is proposed in Subsection 4.2.4. This is followed by systems routing approaches, which are described in Subsection 4.2.5. Finally, Subsection 4.2.6 outlines how different DBB types, hull models, and DS3 components were identified so the design data in the design research experiment could be managed.

4.2.1 The Structure of Physical Loop Method

Fundamentally, the structure of the Physical Loop method consisted of two major stages: a coarse stage and a fine stage. In the coarse stage, the design could be developed *ab initio* to define the weight and space models for the architecturally centred submarine synthesis using three programs: the Hull Geometry Program (HGP); the Volume Granularity Program (VGP); and the Weight Granularity Program (WGP). The coarse stage produced a design with a level of granularity that was normally considered sufficient for the submarine concept (see Subsection 2.2.3). However, as this research explored greater detail necessary for DS3, the design needed to be developed to the fine stage in the Physical Loop Method.

Therefore, in the fine stage, four programs: the Equipment Database Program (EDP); the Component Granularity Program (CGP); the System Preamble Program (SPP); and the System Connection Program (SCP), were produced to develop the submarine design to a sufficient level of design detail necessary for DS3 synthesis. The logic of these two major stages is depicted in Figure 4.4 while the detailed pseudocode of each program is provided in Appendix 6. Thus, Figure 4.4 (top left) shows the main outputs of the Physical Loop method in Paramarine:

- The preamble for design synthesis, the Design Preamble Program Output (DPPO) object;
- The object setup for DS3, the System Preamble Program Output (SPPO) object;
- The equipment database setup, the Equipment Database Program Output (EDPO) object;
- The hull setup, the Hull Granularity Program Output (HGPO) object;
- The design synthesis, the Main Menu Program Output (MMPO) object;
- The analysis setup, the Design Analysis Program Output (DAPO) object;

The following subsections describe various frameworks required to support the structure of the Physical Loop method in Figure 4.4.

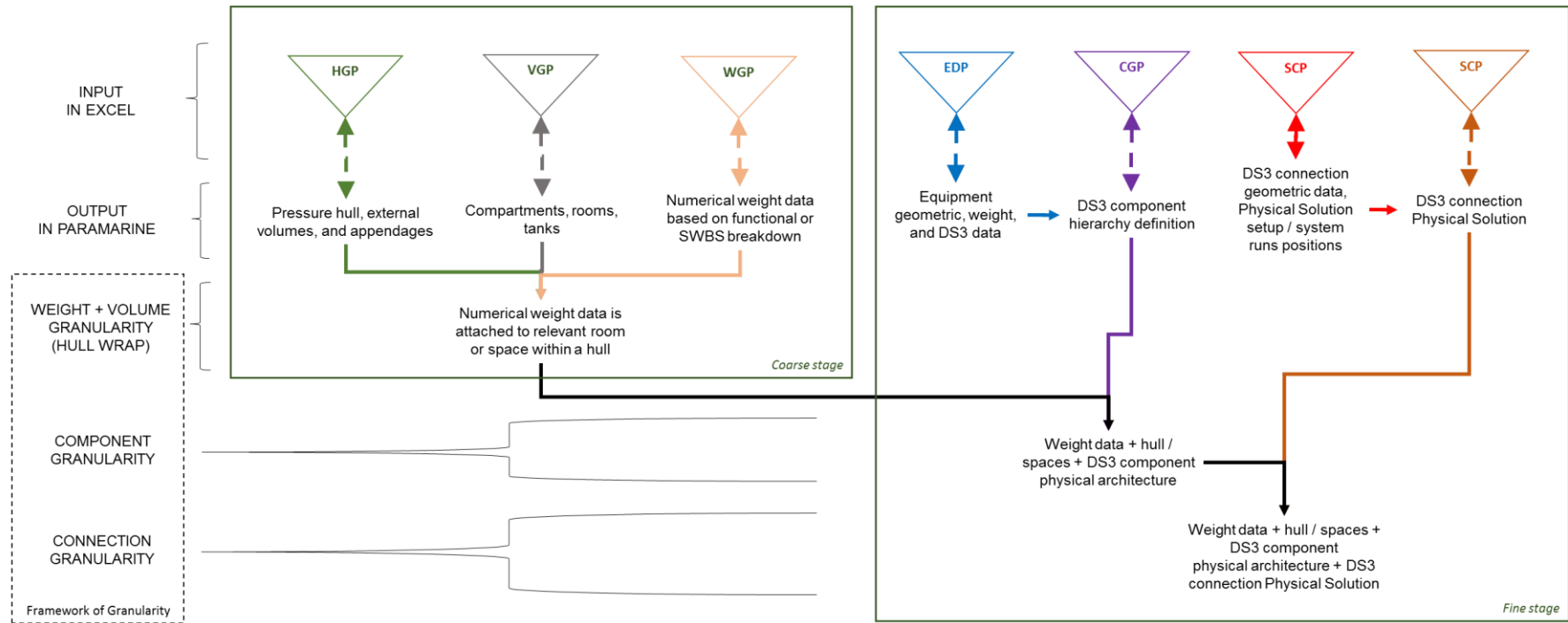
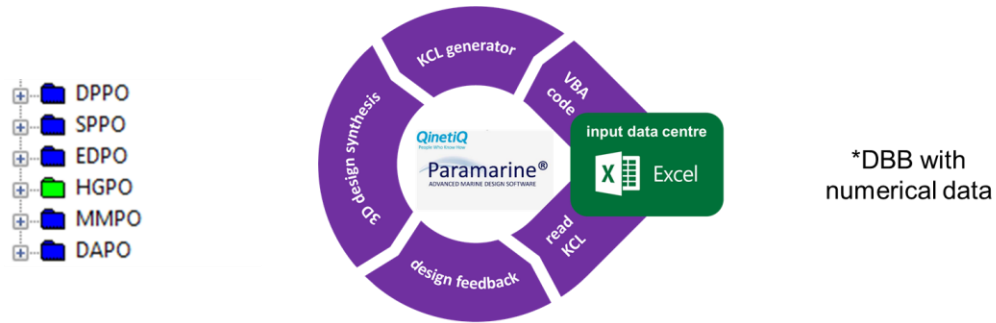


Figure 4.4: The structure of the Physical Loop method with various frameworks described in Subsections 4.2.2 to 4.2.6

4.2.2 Design Granularity and Design Fidelity

To make the Physical Loop method possible, the definitions for different design granularities needed to be clear. A framework was proposed to aid the designer to understand what level of detail was considered necessary for DS3 synthesis. The proposed framework shown in Figure 4.5 distinguishes design granularity and design fidelity. These are illustrated as the two main axes in Figure 4.5. A design can progress from simply weight and space definition to include DS3 components and connections. Thus, the X-axis represents the design granularity as the X-axis. Concurrently, the design can also be more detailed, decomposing models to a more detailed definition, quantified by the design fidelity given in the Y-axis. The highly flexible UCL Design Building Block (DBB) phases aim to explore both axes until a sufficient level of detail is achieved to inform the Requirement Elucidation. Thus, such high flexibility was adopted in this framework.

In this research, design granularity was categorised into several levels ranging from coarse to fine level granularity, see Figure 4.5 (top) from left to right. The first level of granularity is termed weight granularity, which was used to define individual weight sizing without spatial geometry. Such individual weight sizing inputs could be based on the UCL submarine Weight Group or Ship Work Breakdown System (SWBS) (UCL-NAME, 2012). This level of granularity was the input for the Weight Granularity Program (WGP) as outlined in Subsection A 5.2.4, Appendix 5. Using this program, the designer could select relevant design algorithms for each weight sizing, starting from a clean sheet. The Weight Granularity Program (WGP) could then translate the weight data into 'weight' DBB objects in Paramarine by a single 'click'. When the weight granularity was attached and part of attributes of spatial geometry, this became the second level of granularity, which was termed the space or volume granularity.

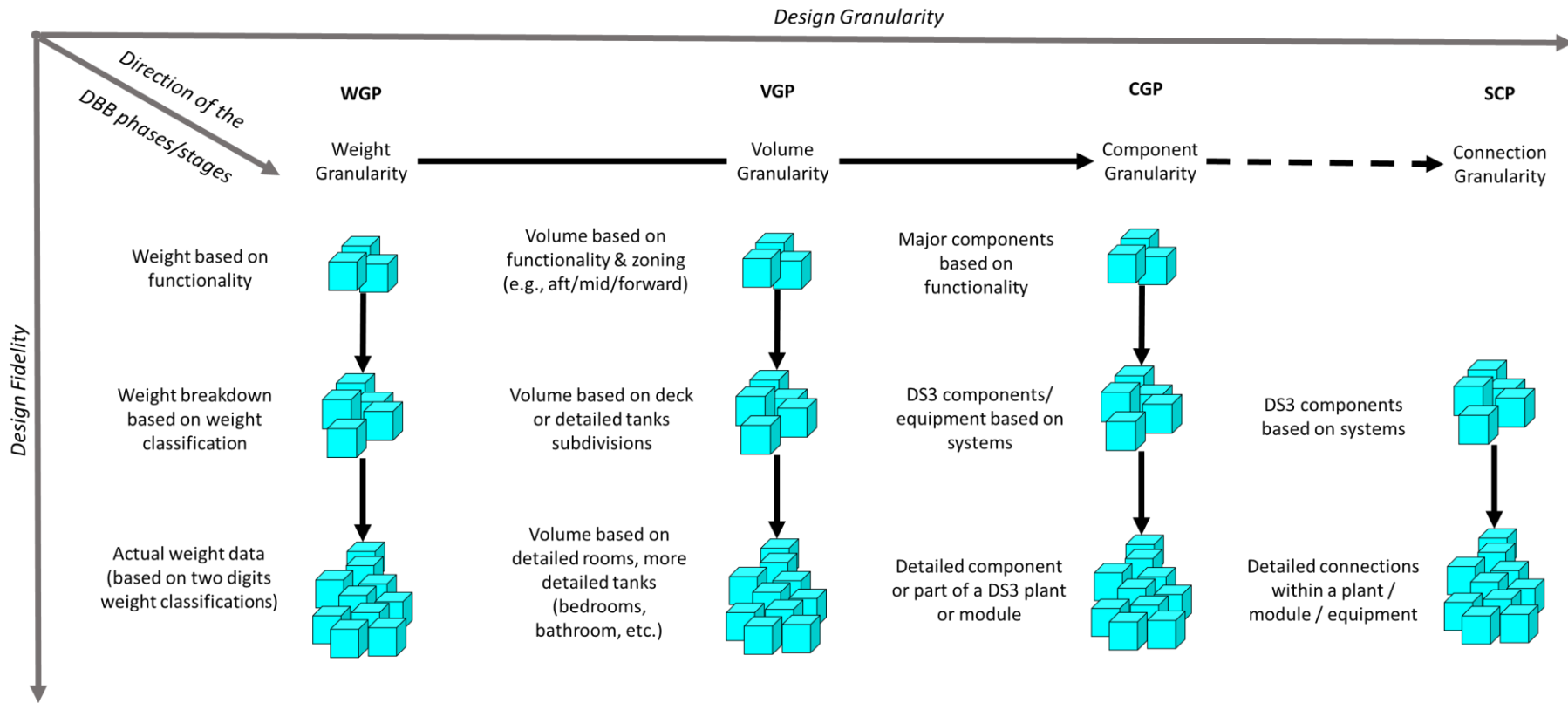


Figure 4.5: Framework of design granularity and fidelity with a horizontal solid arrow and then followed by a dashed arrow, showing a distinct granularity level for DS3 synthesis, which includes systems routings

The volume granularity is related to spaces within the vessel, such as compartments, rooms, or tanks. This level of granularity could be modelled using the Volume Granularity Program (VGP) as given in Subsection A 5.2.3 in Appendix 5. The VGP translated the input into 'volume' Design Building Block (DBB) objects in Paramarine, which could then be 'wrapped' up within the hull geometry, reflecting the inside-out approach to boat synthesis. The hull geometry was defined using the Hull Geometry Program (HGP) (see Subsection A 5.2.2 in Appendix 5), which consisted of several hull parameters, such as dimensions for pressure hull, external forms, and appendages. These parameters controlled the size of a scalable hull model in Paramarine with a specific style. Concurrently, the weight data in the Weight Granularity Program (WGP) could be assigned to VGP to define their x, y, z locations (to the usual X, Y, Z -axes) on the vessel. Therefore, the design at the second level of granularity is comprised of volume DBB objects with numerical data, such as weight data, 'attached' to them as attributes. When the spaces within the vessel were broken down into more detailed design definitions, such as modelling DS3 components and beyond (including systems routing), this became the third level of granularity, which was termed component granularity.

The component granularity model contained DBB objects at the equipment level that required the physical properties of each piece of equipment as their input. This input could have been defined using the Equipment Database Program (EDP) and Component Granularity Program (CGP). The equipment DBB objects were then connected using the System Preamble Program (SPP) and the System Connection Program (SCP). In the System Connection Program, a DS3 connection was defined as a DBB object-to-object connection. The physical properties of this connection were set using the System Preamble Program (SPP) that defined the cross-sectional shape (e.g., rectangle or round, width or diameter) of the DS3 connections and how they were routed on the vessel. The detailed description of the EDP, CGP, SPP, and SCP is provided in Subsections A 5.2.5 to A 5.2.8 in Appendix 5.

As demonstrated in Section 3.3, in considering the DS3 aspects, the study indicated that the design needed to be developed to at least the third level of





granularity, which was the component granularity. To implement this in the Physical Loop method, different types of Design Building Block (DBB) objects needed to be classified.

4.2.3 Types of Design Building Block Objects

As shown in the first implementation (Case Study 3.3), the use of Design Building Block (DBB) objects in Paramarine was highly flexible and there were many different types of DBB objects required to define a design. This could be split into two types: a DBB object for organisation (that is descriptive); and a DBB object with numerical data (Pawling, 2007). The descriptive DBB objects were based on the functionality or zonal (spatial) definition. An example of DBB functionality was the UCL DBB functional grouping (i.e., Fight, Move, Float, and Infrastructure). Examples of a DBB zonal used in submarine design could be a watertight compartment zone (part of dry spaces), an external MBT (part of wet spaces) or a free flood space (part of hull appendages).

Table 4.2 shows that the numerical data for DBB objects in this research can be weight data; volume data; equipment data (length, beam, height, and weight); or connection data (length, diameter (for cross sectional area), and weight). Using different numerical data, the DBB objects could be organised based on various design granularities, starting at the first level, and going to the third level of granularity as explained earlier. Thus, DBB objects with numerical data were divided into those giving individual weight data, those with geometric volume data, those describing DS3 components, and those identifying DS3 connections. These DBB objects were defined using the Volume Granularity Program (VGP), the Weight Granularity Program (WGP), the Component Granularity Program (SGP), and the System Connection Program (SCP).

Table 4.2: Example of numerical data for different types of DBB objects in the Network Block Approach (see Figure 4.5 on page 150)

Type of Design Building Block Objects		Numerical Data
Design Building Block (DBB) objects or "building_block" objects in Paramarine	 Weight	Permanent weight
		Spatial (x, y, z coordinates)
		SWBS group classification
	 Volume/ Space	Geometric data
		Spatial (x, y, z coordinates)
		Buoyant/ tankage / space characteristic
	 Equipment/ Component	Geometric data
		Spatial (x, y, z coordinates)
		Node (x, y, z coordinates)
		Node quantities
		Weight
	 Connection	Inlet/outlet direction
		Length
Area		
Weight		

Having distinguished different types of DBB objects with numerical data, the next subsection discusses how they were integrated with the descriptive (organisational) DBB object under the same "Master Building Block" hierarchy.

4.2.4 Design Building Block Hierarchical Breakdown

Although the development of the DBB model in the Paramarine was intuitive, as discussed in Section 3.3, it was limited to a single view of hierarchy. Hence, to organise DBB objects based on both functionality and spatial definition would have required many descriptive DBB objects, as is illustrated in Figure 4.6. This did not include more detailed DBB objects that could reach the fifth level (see Case Study 3.3.1). Thus, should the designer wish to display all functional groups in the forward zone of a three-zone submarine, the designer had to manually expand the functional-parent DBB object first and then expand the forward zone-daughter DBB object four times. To avoid this, while using the DBB hierarchy, an alternative hierarchy was developed as shown in Figure 4.7.

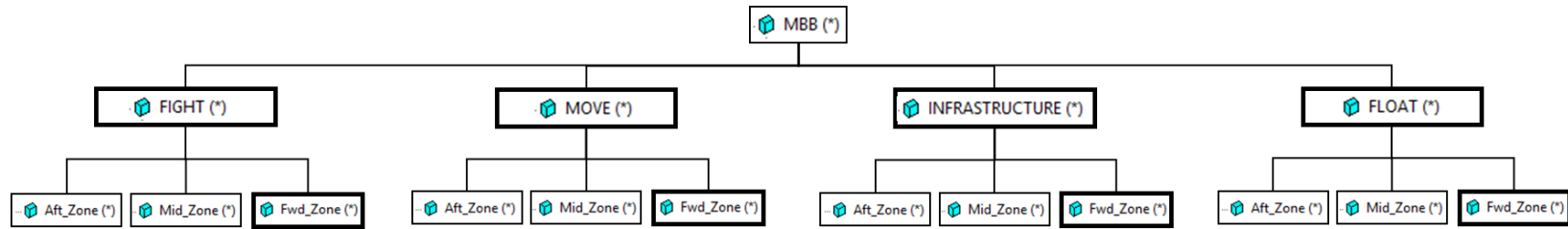


Figure 4.6: A traditional Design Building Block (DBB) hierarchy for descriptive DBBs (*) with functional and spatial classifications

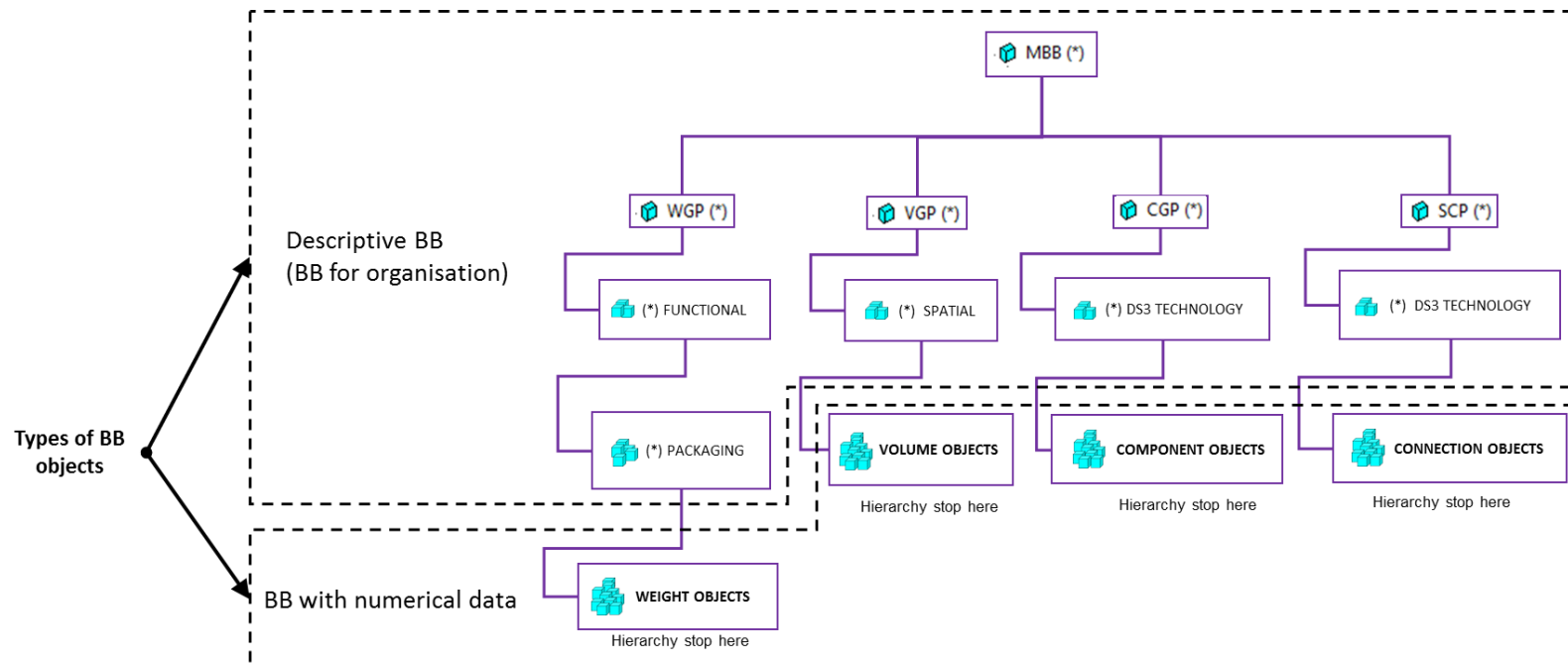


Figure 4.7: A proposed Design Building Block (DBB) hierarchy adopted in the Network Block Approach, showing descriptive DBBs (*) and shapes in purple as part of the Physical Loop method

Figure 4.7 shows that the hierarchy in this research still retained functional, packaging, and spatial or zonal information but it was categorised based on the types of Design Building Block (DBB) objects as discussed in Subsection 4.2.3, which was weight data, volume data, DS3 components data and DS3 connections data. Therefore, the proposed approach did not mix different types of numerical DBB objects under the same parent organisational DBB objects, except the Master Building Block (MBB), which is essentially the whole submarine characteristics (Andrews and Pawling, 2003). With this approach, commonality with those DBB objects with numerical data could be achieved. This enabled the designer to manage the design data more effectively, especially in a design where there were hundreds of DBB objects with numerical data.

Another advantage was that this approach provided consistent depth in the DBB hierarchy (see Figure 4.7). With a consistent depth in the DBB hierarchy, the visualisation of the various DBB objects was considered more efficient because the designer could use a feature called ‘Open to level...’ in Paramarine (Qinetiq, 2019) (see Figure 4.8). Such a feature can automatically expand a DBB hierarchy at a specified DBB hierarchy depth level. This was helpful in terms of the Gulf of Evaluation (Figure 2.6 on page 51), i.e., to avoid the tedious process of chasing and revisiting a particular DBB object with numerical data when there were hundreds of descriptive DBB objects with different depths of hierarchy in the design. The visualisation of the DBB objects also reflected the evolution of design granularities, ranging from weight, volume, component, to connection granularity (see Section 4.2.1).

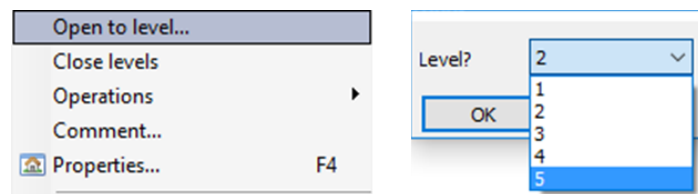


Figure 4.8: A feature to expand a design building block object in Paramarine (Qinetiq, 2019), showing an object can be opened (left) to a specific level of depth, up to a fifth level (right)

Within the programs in the Network Block Approach, the designer could also quickly search and modify the data for the DBB object in a tabular menu format, allowing existing capabilities in the Excel spreadsheet to be exploited. For example, changing the shape of 200 components was as easy as copying a cell throughout the component list in the relevant program, while normally (in Paramarine), it would require each DBB object to be modified (i.e., chase the object, expand the object, click the shape) 200 times. However, when applying the hierarchy based on the weight, volumes and DS3 objects, particular care had to be taken to avoid double-counting between types of DBB objects, for example, if DBB objects for weight data, at the first level of granularity in the Weight Granularity Program (WGP), were being replaced by DS3 component DBB object data, at the third level of granularity in the Component Granularity Program (CGP), as the design progressed.

Initially, DS3 components and connections were modelled as daughter objects under the same parent “**system**” object in Paramarine (see Section A 4.3 in Appendix 4). However, this was found to be inefficient. As mentioned in Subsection 4.2.4, the use of the automatic expansion feature in Paramarine (see Figure 4.8) could show both DS3 components and connections by making a few clicks and thus manipulating the many DS3 component objects each with their connections revealed in Paramarine could be excessive. With a further separated hierarchy, all DS3 connections in the model could be easily hidden and then be rerouted, based on the new locations of the DS3 components. Another consideration was that some components may not be connected or tethered, such as modelling escape towers, ladders, doors or, even, underwater vehicle payloads. This suggested that the Physical Loop method be employed for such areas of concern or further applications.

Once this new approach to managing various DBB objects had been devised, the next subsection focuses on modelling DS3 using the Physical Loop method.

4.2.5 Distributed Systems Routing Model

Paramarine can be used to model systems routing or connections that were not exploitable in the previous UCL DBB research at a PhD level (Pawling, 2007;

Purton, 2016). In this research, the issue with the DS3 modelling, more specifically, DS3 routing in Paramarine has been investigated in Subsection 3.3.5 and Appendix 4, which led to two different systems routing frameworks. The first framework employed automatic routing in Paramarine that was termed as the 'point to point' framework in the current research. However, if, for instance, the designer needed to model a more detailed routing, a framework termed 'highway' framework could be used, combining automatic routing and the use of highways, consisting of multiple longitudinal system runs (see Subsection 3.3.5). Detailed examples of both frameworks are given in Section A 4.3 in Appendix 4.

The input procedure for the point-to-point framework can commence by developing the design to the third level of granularity (i.e., component granularity). Hence, two Design Building Block (DBB) objects (at the component level) could be defined as a connection. This was found to provide a quick routing approach commensurate with early-stage design but would have made the routings of the system overlap each other as the DS3 components had yet to be arranged in unique x, y, and z coordinates. This is demonstrated in the next chapter.

The procedure for the highway framework was akin to the point-to-point framework. However, this procedure requires the selection of a system highway, which hosts multiple system runs, as an additional input and thus the automatic 'point to point' DS3 routing can be guided by the selected highway. The highway framework consisted of some pre-defined longitudinal lines from forward to aft of the vessel and could be modelled using "**service_highway**" objects in Paramarine (Section A 4.3 in Appendix 4). In this approach, the designer needed to first define how many highways of a given distributed system there were on the vessel. The system connection could then be assigned to one of the highways available (see Figure 4.9). To define highways, allowances needed to be assumed for the cross-sectional space taken up by pressure hull stiffeners (see Subsection 3.3). This approach allowed the designer to investigate how much space needed to be reserved for systems routing early in the design process and before the layout become too cramped

further downstream in the design phase. The advantages this now provides are discussed in greater detail in Chapter 7.

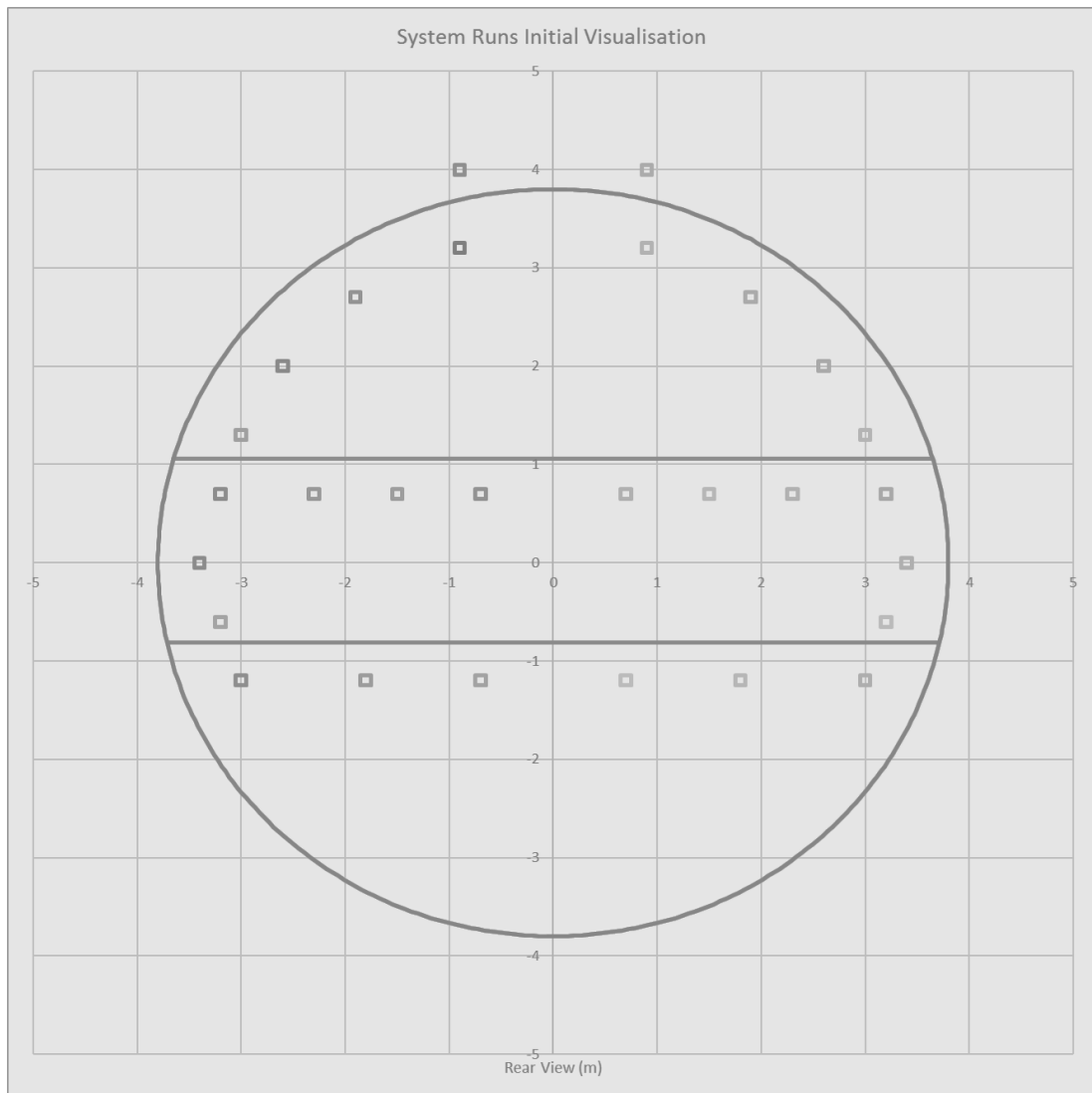


Figure 4.9: Example of initial highways visualisation and setup in the System Preamble Program (SCP) for a typical submarine pressure hull

4.2.6 Naming Convention for Design Building Blocks

As the submarine design needed to be developed to the component granularity level to enable a DS3 synthesis, the number of Design Building Block (DBB) objects with numerical data at the component granularity level escalated to more than 100 objects (see Appendix A 4.4 in Appendix 4). Thus, a naming convention was applied to ease the Gulf of Evaluation (Figure 2.6 on page 51) by making the design data easier to be tracked, revised, and developed using consistent, chronological, and descriptive names (Stanford University, 2021).

The DBB objects with numerical data were identified by an alphabet designation system and separated by some underlines or underscores. Thus, the programs within the Physical Loop method were able to automatically read and write thousands of items of design data back and forth to the Paramarine model.

Generally, each of the naming conventions consisted of several two-digit alphabetic designation systems, giving the information contained in an object's name. The object name started with 'BB' (building block), indicating the object was included in the 'MBB' (master building block) hierarchy. This was followed by the first level of identification system, showing the level of granularity, such as 'NL', which stands for numerical (for the weight granularity), 'VL', which stands for volume (for the space or volume granularity), 'DB', which stands for database (for the DS3 equipment or component granularity). In this research, an 'NL' object was meant to describe a Design Building Block (DBB) object without any physical entity, which can be weight data or power data. If the building block contained a physical entity, it was 'VL' or 'DB'. This framework is summarised in Table 4.3.

Table 4.3: Naming convention framework as design granularity identifier

Granularity Identifier	Physical Entity	Numerical Data	Application
'NL' Numerical	No	Parametric 'gross' weight or Power service (input or output)	Used in weight or component granularity
'VL' Volume	Yes	Length, beam, height (L, B, H) of a volume DBB object, Locations (x, y, z) of a volume DBB object, Volume of a volume object, Weight of fluid (for tanks)	Used in volume granularity
'DB' Database		Length, beam, height (L, B, H) of a piece of equipment, Volume of a piece of equipment, Weight of a piece of equipment	Used in component granularity

As shown in Table 4.3, the 'NL' object could also be used in the component granularity for two functions. Firstly, to model numerical energy that does not have spatial geometry. Secondly, to allow the designer to model a network component at the high level of granularity that has spatial geometry, but the data for which may not be available at ESSD. This could be used to model detailed valves, junctions, and other small components in a DS3 network.

However, if, for example, the ‘NL’ object was used, the connection from and to this object does not have physical information. This type of object is also discussed in Subsection 4.3.1 and Chapter 5.

In the weight granularity, there were only two main levels of identification. The first indicates the weight granularity using “NL” (see Table 4.4). The second level of identification would be the object’s name, which would not be abbreviated. Therefore, the length of characters for this weight granularity would vary from object to object. This was because most objects in the weight granularity were developed based on the UCL submarine Weight Group classification (UCL-NAME, 2014), similar to the Ship Work Breakdown System (SWBS) (Lamb, 1987). Abbreviation at this level of granularity was not considered worthwhile. This method was used in the Weight Granularity Program (WGP).

Table 4.4: Naming convention for weight granularity

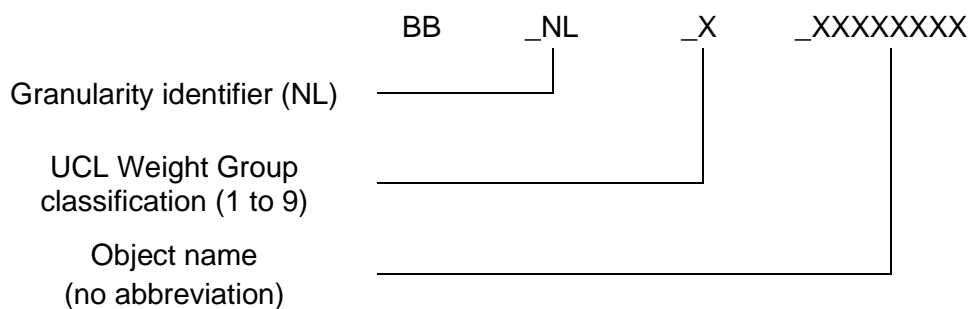
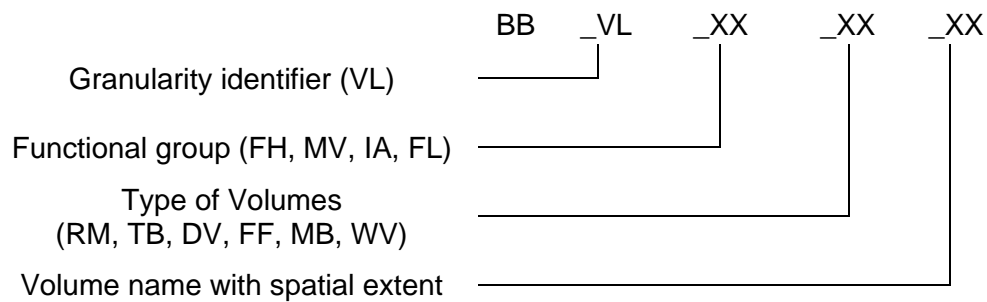


Table 4.5 presents the naming convention for volume objects. Unlike the naming system for weight, this system consisted of four levels of identifications. As mentioned before, the first level was to indicate the level of granularity, which was ‘VL’ (stands for volume). The second level was used for defining the DBB functional groups, such as ‘FH’ for Fight, ‘MV’ for Move, ‘IA’ for Infrastructure, and ‘FL’ for Float. The third level was for determining the type of volumes and the last level was for defining the name of the object.

Table 4.5: Naming convention for volume granularity

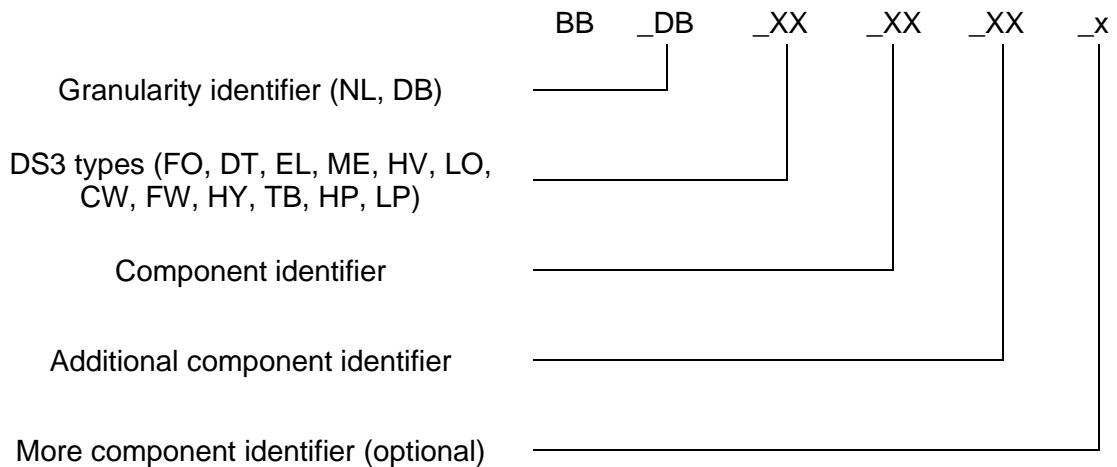


In this research, there were two major sets of spaces defined in Paramarine: internal and external. Internal spaces were located within the pressure hull and could be considered part of the pressure hull buoyancy. Conversely, external spaces could still provide the buoyancy based on the individual assumed permeability coefficient. Major variations within internal and external spaces are described as follows.

- Internal spaces.
 - ‘RM’ stands for room and was used for compartment spaces.
 - ‘TB’ stands for trim ballast, which was used to model trim ballast tanks inside the pressure hull.
 - ‘DV’ stands for dry variable and compensated tank and was used for tanks containing special fluid, such as diesel oil or lubricant oil but could be compensated with other fluid, such as seawater. This could be used to model fuel tanks that were arranged internally within the pressure hull.
- External spaces
 - ‘FF’ stands for free flood, which was used for free flood spaces. As mentioned earlier, this type of volume object could still provide buoyancy in addition to the pressure hull based on the assumed permeability coefficient.
 - ‘MB’ stands for main ballast, which was used to model Main Ballast Tanks. This space provides buoyancy and weight of the fluid based on the floodability coefficient.
 - ‘WV’ stands for wet variable and could be used to model a compensating tank that has a similar characteristic as the ‘DV’ object but is dedicated to defining external fuel tanks.

In the component granularity, five levels of identifications were used, as shown in Table 4.6. The first identifier starts with either database 'DB' or numerical 'NL'. The next level was allocated to individual DS3 types. The types of DS3 were developed based on different service commodities. In this research, there were fuel oil 'FO', information data 'DT', electrics 'EL', mechanical 'ME', HVAC 'HV', lubricant oil 'LO', chilled water 'CW', freshwater 'FW', hydraulic 'HY', trim and ballast 'TB', high-pressure air 'HP', and low-pressure air 'LP'. Beyond this level of identification, there were three levels of identification available for object name and component level identifiers that could be based on the spatial definition or specific DS3 terms (see Chapter 5 for the application).

Table 4.6: Naming convention for component granularity



The object-oriented - UCL Design Building Block philosophy was incorporated in the Physical Loop method. The following section discusses how design building block objects could share some commonalities with nodes in the network theory, and so this became the basis of the development of the proposed Logical Loop method for designing submarine DS3 *ab initio*.

4.3 Logical Loop Method

The Logical Loop method covers the SUBFLOW process that provides a network based sizing for various types of DS3. Generally, any type of DS3 could be sized directly using the SUBFLOW network with a derived length to weight ratio or a derived length to volume ratio for various types of DS3. The SUBFLOW network with flow response simulation adds an early steady-state flow response simulation to submarine ESD, which could then be used to size a set of DS3 that is network flow dependent, such as for the heat removal system. This means some DS3 could be sized directly using the SUBFLOW network without the need to perform the energy flow simulation (see Table 4.7). The more detailed the DS3 network definition, the lesser the design margin is required.

Table 4.7: Two possible ways of using SUBFLOW, as part of the Logical Loop method

Stage	DS3 Sizing	Notes
SUBFLOW Network	Length to weight and volume ratios	Less effort but not sensitive for sizing DS3, which is network flow dependent, for example, the heat removal system
SUBFLOW Network + Energy Flow Simulation	Power to weight and volume ratios	Energy balance and the heat removal system can be calculated but require more engineering and inputs

However, the first implementation of the approach in Chapter 3 suggested that generating a SUBFLOW network also required a considerable number of routine tasks, such as developing an adjacency matrix every time a new DS3 design was developed. This does not include producing a network formulation (using an Operational Matrix, see Subsection 3.1.2) for performing SUBFLOW simulation. Such demanding effort was seen to inhibit the application of the network approach to explore DS3 options as part of requirements elucidation in ESSD. Thus, the objective of the Logical Loop method was to make the application of the network based synthesis for exploring DS3 plausible in the early stages of submarine design.

To understand this method, the following subsections outline key features of the Logical Loop method. Subsection 4.3.1 presents the overall framework of the Logical Loop method. Subsection 4.3.2 outlines the type of nodes employed

in the Logical Loop method. Subsection 4.3.3 highlights the Operational Matrix framework for the Logical Loop Method. Finally, Subsection 4.3.4 outlines different options for visualising the DS3 network.

4.3.1 The Structure of Logical Loop Method

In a nutshell, the Logical Loop method consisted of three general tasks that could be treated as a loop for a given operating condition as shown in Figure 4.10.

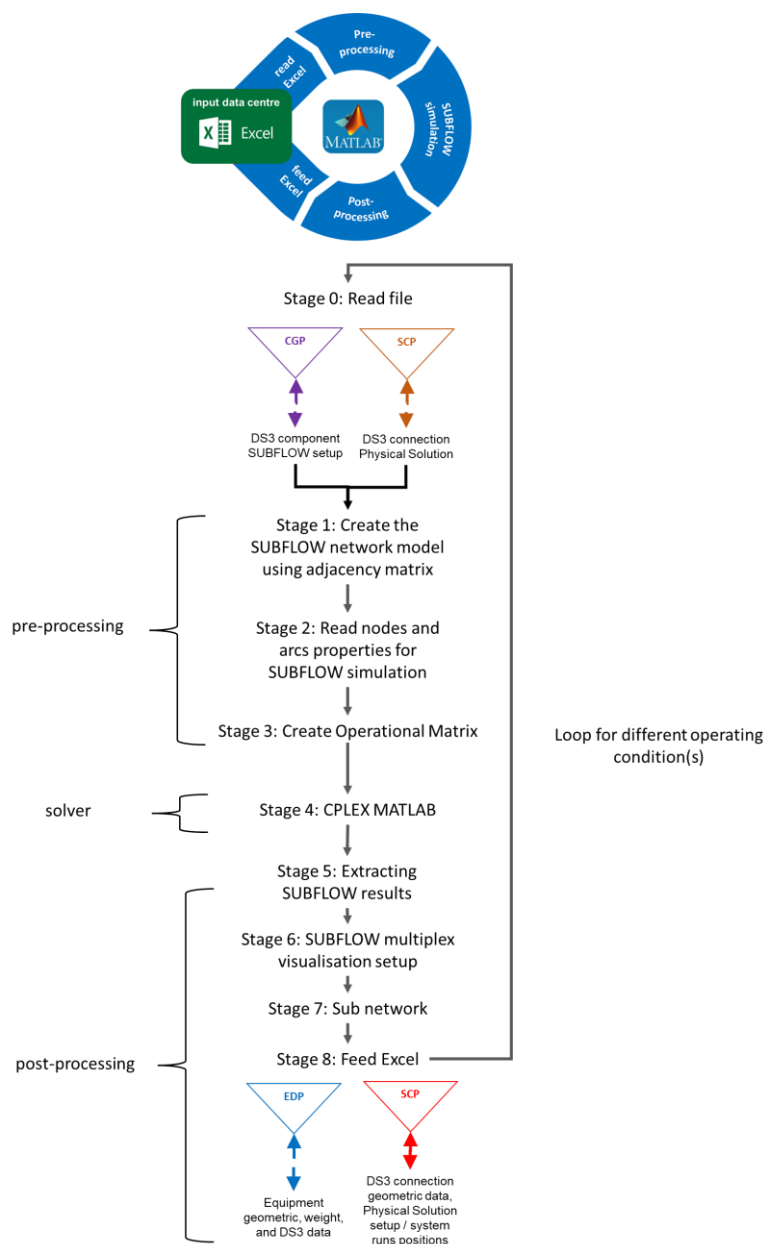


Figure 4.10: The high level tasks performed in the Logical Loop method to DS3 synthesis (see Table 4.1 on page 145 for acronyms and Section A 6.2 in Appendix 6 for codes)

The objective of the general tasks was to automate the routine tasks in the Logical Loop method and thus the designer could go back to work on the Physical Loop method simultaneously. The general tasks consist of pre-processing, the use of the solver, and the post-processing task. The pre-processing task read the input the designer defined in the Component Granularity Program (CGP) and the System Connection Program (SCP), while the post-processing task wrote the results back to two programs (Equipment Database Program (EDP) and the System Preamble Program (SPP)). Once the results were in the spreadsheet, the designer could individually justify the size of each arc dependent on the different types of DS3 technologies. The next subsections expand the input required in modelling the DS3 network for SUBFLOW simulation.

4.3.2 SUBFLOW Network Model

The type of nodes selected for SUBFLOW was simplified for the early-stage design application. There were only two types of nodes, a terminal or a hub node. These were the input required to be defined using the Component Granularity Program (CGP). Another input in the same program was the node type, defined in terms of physical definition. Hence, Figure 4.11 (top) shows in terms of granularity, a node can be either numerical 'NL' or physical 'DB' while in terms of SUBFLOW a node can be a terminal or a hub node. Meanwhile, Figure 4.11 (bottom) shows an arc can be numerical or physical in terms of granularity, but in terms of SUBFLOW, the arc is organised due to their technology, i.e., the type of commodity carried by that DS3 physical connection.

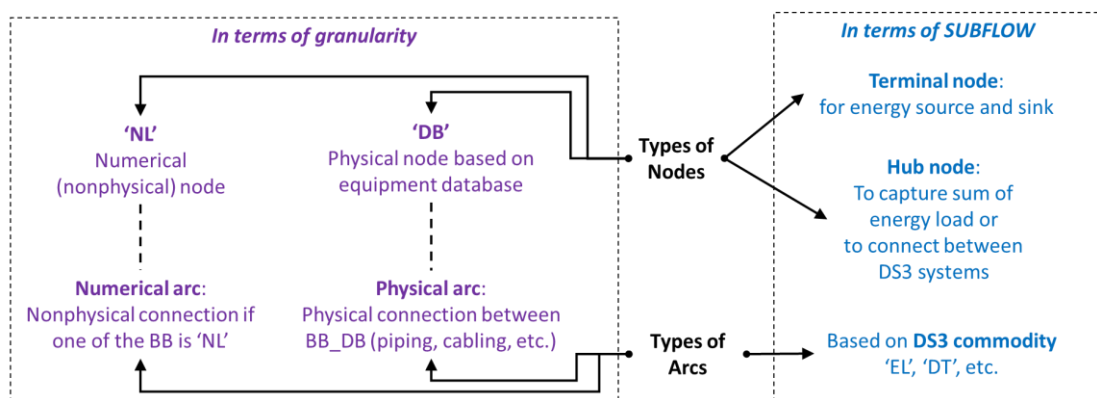


Figure 4.11: Types of nodes and arcs in the Network Block Approach in terms of granularity framework (purple) and SUBFLOW simulation (blue)

Initially, volume objects were considered as a part of the DS3 network, such as nodes for compartments when part of the heat removal system. However, in a similar issue with the FMFI functional breakdown, such models made the entire volume object exclusively belong to a specific type of the DS3 where, within a volume object, other DS3 with different functionality and technology also existed. Therefore, numerical nodes were meant to aid the designer to complete the overall architecture of the DS3 network without using volume objects. Similarly, to reduce the reliance on extensive use of the equipment database, numerical nodes could also be used to handle DS3 components that lacked sufficient detail in ESSD.

Consequently, the type of arcs employed depended on the types of nodes to which they were connected. As discussed in Subsection 4.2.6, if one of the nodes was numerical, then that arc would not have physical geometry associated with it. In the Logical Loop method, the direction of the flow was also the input within the System Connection Program (SCP). This information aided the designer in understanding how the systems would respond in a scenario.

4.3.3 SUBFLOW Operational Matrix

As demonstrated in Subsection 3.1.2, the use of the CPLEX toolbox in MATLAB enabled user intervention in the network formulation code for CPLEX using MATLAB programming language, i.e., a matrix based computation. This, in turn, allowed the Operational Matrix to be used to assist the designer in formulating the SUBFLOW, which should reflect the temporal relationship i.e., the operational architecture of submarine DS3 (see previous applications of the proposed Operational Matrix: Table 3.5 on page 80; and Table 3.14 on page 104; and Table 3.21 on page 130).

The mathematical model for SUBFLOW was not hardcoded to the tool (except for the basic continuity, see Subsection 3.1.2) and could be defined in the Component Granularity Program (CGP) and the System Connection Program (SCP). The formulation process was iterative and substantial to achieve a feasible network solution. The Operational Matrix can now be generated automatically in the Logical Loop method. The pseudo-Operational Matrix is

given in Table 4.8. The number of columns of the Operational Matrix depends on the number of arcs in the SUBFLOW network. This matrix is divided into several groups of boxes in rows. The first box of the matrix in Table 4.8 gives the objective function coefficients (Subsection 3.1.2), which is set to zero for finding the energy balance (Subsection 3.2.5). The second box was dedicated to continuity (Subsection 3.1.2) as well as the energy coefficient e for each node (see Table 3.11 on page 99), which can be positive or negative (see Subsection A 5.2.6 in Appendix 5). The third box was for the inequality constraints (Subsection 3.1.2) and the last two boxes were for the lower bounds and the upper bounds (Subsection 3.1.2). This is where the 'operational' aspect is defined, i.e., the supply or demand of a commodity of a node in each operating condition. Therefore, a different operating condition (e.g., snort and sprint submerged) requires a different Operational Matrix, which can be treated as loops in MATLAB.

Compared to previous Operational Matrices in Chapter 3, the matrix in Table 4.8, is scalable and simpler. This was to make the application of SUBFLOW analysis as little as possible, commensurate with ESSD, which aims to solve the energy balance through the linear programming systems of equations. This would ensure that the total energy demand on the submarine would be equal to the total energy available, indicating systems design balance, which was considered preferable to a numerical crude service load summary. The SUBFLOW can also be used to perform a steady state simulation of power flow in a DS3 network. This would aid the designer's understanding of the temporal behaviour of the DS3 in an operational scenario. Eventually, SUBFLOW aimed to give the DS3 space and weight input early as well as to explore DS3 options for Requirement Elucidation. Once the SUBFLOW analysis was solved using the CPLEX in MATLAB, a distinct network layout could be visualised as part of the post processing step in the Logical Loop method. This is discussed in the following section.

Table 4.8: The pseudo-Operational Matrix of SUBFLOW

	1, 2, ... number of arcs	1, 2, ... number of arcs	1, 2, ... number of arcs	1
Objective Function	0 ...	0 ...	0 ...	0
Equality constraints matrix for continuity	0 0 ... 0 . . .	+e or -e 	+e or -e 	0
Inequality constraints matrix for bidirectionality	-1 -1 ... -1 . . . -1 ... -1 	-1 -1 ... -1 . . . +1 ... +1 	0 0 ... 0 . . . 0 ... 0 	0
Lower bounds matrix	... 0 -inf ...	Based on input provided in the Component Granularity Program (CGP) and the System Connection Program (SCP)	
Upper bounds matrix	... inf inf ...		

4.3.4 SUBFLOW Multiplex Visualisation

The appearance of DS3 architecture depended on how the DS3 components were arranged in the physical and the logical definition. In the physical definition, the DS3 architecture was subject to spatial definitions, such as forward and aft or upper and lower parts of the vessel. Meanwhile, in the logical definition, the DS3 arrangement could be manipulated using different automatic graphical layout algorithms provided by MATLAB, such as a circular layout, force-directed layout (Fruchterman and Reingold, 1991) and layered layout (Barth et al., 2004; Brandes and Köpf, 2002; Gansner et al., 1993) (see Subsection A 5.1.2 in Appendix 5).

Initially, the layered layout of the DS3 example was used to reveal the energy flow of DS3 from the 'super' source at the top of the hierarchy to the 'super' sink at the bottom of the hierarchy, as already demonstrated in Subsection 3.2.5. The use of an automatic layered layout also aided the designer in avoiding additional inputs and routine tasks to determine the unique location for each node in the logical definition. However, such a model could not capture a ring main configuration and could overwhelm the designer when developing the whole ship DS3 network *ab initio*.

Therefore, as discussed in Chapter 2, a 3D multiplex network (Mucha et al., 2010) that allowed the DS3 to be stored as several 2D layers in a 3D network was investigated as a potential means to resolve this limitation. The SUBFLOW multiplex network clustered various DS3 technologies like the 3D multiplex network but nodes were manipulated in the Z-axis so they would not overlap in the X-Y view. The SUBFLOW DS3 network was inspired by the London underground tube map, which shows the tube network not to scale (see Figure 4.12) but has a sense of direction (east-west, north-south, etc). Therefore, the SUBFLOW DS3 logical network was devised to maintain the spatial aspect of the vessel (e.g., forward-aft, upper-lower, port-starboard) but also adopted a node shape differentiation as well as colour coding, which represented different types of DS3 technologies.



Figure 4.12: Partial London tube network taken from Elliot (2007)

Consequently, an additional design effort was required to arrange DS3 components manually, both in the physical and logical definition. In the physical definition, the DS3 components could be allocated at the centre of volume objects but could be further arranged graphically in Paramarine if preferred. In the logical definition, the DS3 nodes needed to be arranged in unique x, y, and z coordinates within the 3D SUBFLOW multiplex network.

4.4 Summary of the Proposed Approach

The proposed approach, summarised in Figure 4.13, supports the 3D based submarine DS3 synthesis both in terms of physical and logical architectures. In the physical architecture, the proposed Physical Loop method in purple in Figure 4.13, allows a designer to develop the DS3 design at different levels of granularities, ranging from modelling individual DS3 components to various DS3 routings using pre-defined highways. The logical architecture using the proposed Logical Loop method in blue in Figure 4.13, allows the designer to solve the energy balance of the set of distributed systems and to visualise the complexity of the DS3 set in a 3D SUBFLOW multiplex network configuration. This has greatly improved the process of communicating submarine DS3 design to others, be it in design reviews with the supervisor or other members of the project team.

Although the Network Block Approach (NBA) required a large investment in developing nine programs and thousands of lines of MATLAB code, without this, the process of synthesising DS3 using the network approach would have discrete and disconnected as demonstrated in the initial process in Section 3.3. The new approach was not only devised to retain the benefit of sophisticated 3D design in Paramarine but also to employ DS3 network analysis as little as possible. This was done to determine DS3 load balance, which is commensurate with the needs of Requirement Elucidation at ESSD. To demonstrate the applicability of the NBA, this new approach was applied to a generic submarine design and the results compared to a notional submarine weight data design study, based on the UCL Submarine Databook (UCL-NAME, 2014) in Chapter 5.

The Network Block Approach

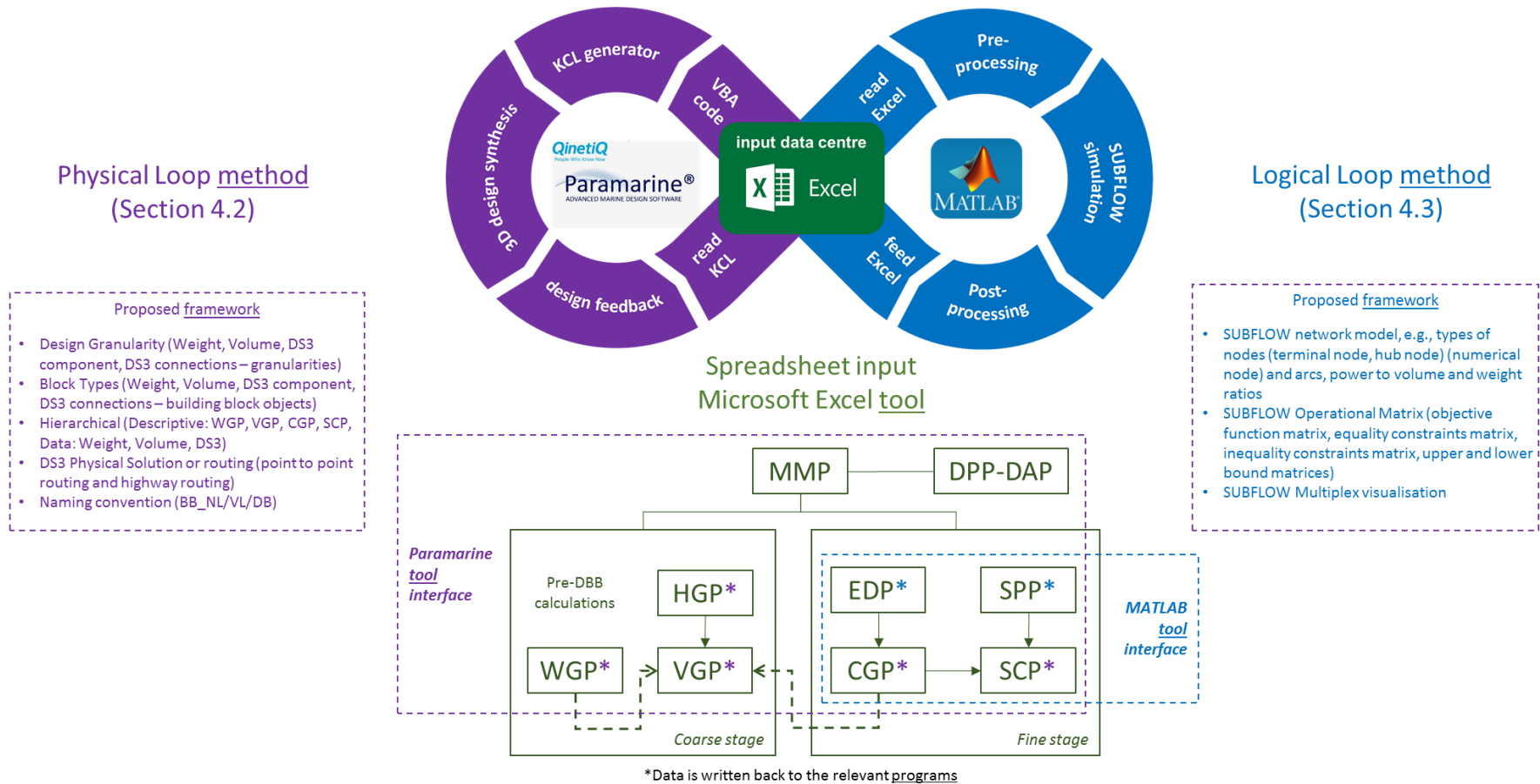


Figure 4.13: Summary of the proposed Network Block Approach (NBA) consisting of proposed methods (Physical Loop method in purple, various inputs in green – see Table 4.1 for acronyms, and Logical Loop method in blue) thus, the frameworks, tools, and programs are identified as subsets of the proposed approach

Chapter 5

The Approach Applied to a Submarine Study

The main objective of this chapter is to show that the new Network Block Approach (NBA) not only could provide more accurate or better-budgeted allowances for the weight and space of DS3, but also inform Requirement Elucidation regarding the chosen DS3 style in the design. Thus, this chapter consists of nine sections (see Figure 5.1).

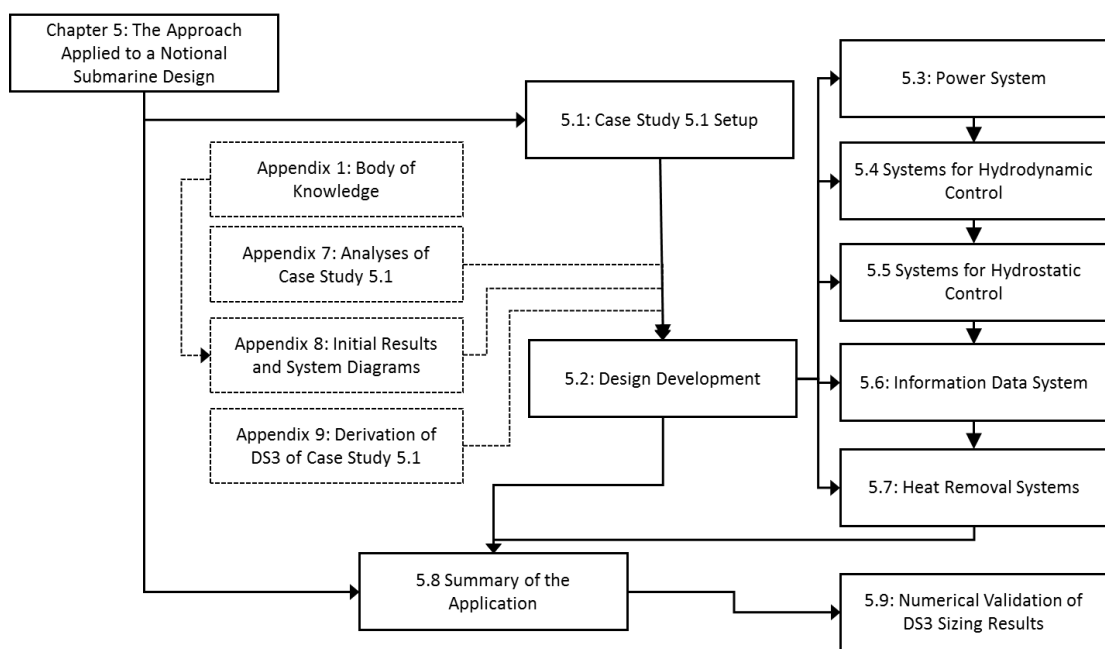


Figure 5.1: Schematic of Chapter 5

Section 5.1 presents the setup of the submarine design case study and the logic behind the choices made. This is followed by the application of the Physical Loop and the Logical Loop methods to the case study in Section 5.2. Sections 5.3 to 5.7 discuss the development of various DS3 incorporated in the design case study, which involved simultaneous use of the Logical and Physical Loop methods. This includes the formulation of the SUBFLOW simulation for DS3 sizing. Section 5.8 presents the network solution of overall DS3, which was used as the basis to provide DS3 space and weight inputs to the case study. This input was then validated with the notional submarine data and thus is outlined in Section 5.9.

5.1 Case Study 5.1 Setup

To test whether the new approach could capture the style choices of DS3 at a component granularity level and could be validated with available data, a case study was developed with the payload and style choices akin to the ocean-going 2500 tonne generic submarine. This design was extracted from the database used in the annual UCL submarine design exercise (UCL-NAME, 2014) and is summarised in Table 5.1.

The next section describes the development of the case study *ab initio*, which includes the application of Physical Loop and Logical Loop methods.

Table 5.1: The realisation for Case Study 5.1, following the decision making sequence for complex vessels outlined in Figure 4 and Appendix of (Andrews, 2018c) in a similar manner to the submarine example in Figure 4 of (Andrews, 2021)

Process Step	Selection Decision / Realisation for Case Study 5.1	
Perceived need	Demonstrate the application of the Network Block Approach (NBA)	
Outline of initial requirements	Initial SSK key parameters desired (capabilities)	
	Payload equipment in Table 3.8 on page 87	
	Initial Performance	Value
	Complement/ accommodation	46 personnel
	Operational environment density range	1-1.025 te/m ³
	Deep Diving Depth	250 m
Selection of style of emerging ship design	Style Level	Choice
	Macro Level	Non nuclear (SSK)
	Main Level	Diesel-electric power plant
		Medium size ocean-going submarine
		Single hull with casing
	Micro Level	Detailed DS3 styles (Subsections 5.3 to 5.7)
Selection of major equipment and operational sub-systems	DS3 configurations (see Subsections 5.3 to 5.7)	
Selection of whole ship performance characteristics	General Performance	Value
	Sprint speed	20 knots (2 hrs)
	Submerged speed	5 knots (17 hrs)
	Snort speed	6.5 knots (5 hrs)
	IR (Burcher and Rydill, 1994)	22 %
	Sub Level	Value
For DS3	Subsections 5.3 to 5.7	
Selection of synthesis model type	The Network Block Approach (NBA) (Chapter 4) Physical Loop method (Section 4.2) and Logical Loop method (Section 4.3)	

5.2 Design Development

Although major design decisions are listed in Table 5.1, there were many detailed decisions made for the submarine design to progress physical and logical DS3 synthesis much earlier in the design process than traditionally. These decisions were dependent on the nature of different DS3 technologies, many of which are discussed later in this chapter. Thus, for Case Study 5.1, the following different DS3 were considered to test the applicability of the new approach: fuel oil (FO) system; electrical (EL) system; mechanical (ME) system, as part of the propulsion system; heat removal (HV) systems; water distribution or trim and ballast (TB) systems; high-pressure air (HP) system; low-pressure (LP) air system; hydraulic (HY) systems, and important data (DT) systems.

Figure 5.2 shows the logic of the approach for Case Study 5.1, which consists of several steps and is iterative. This used various programs that are listed in Table 4.1 on page 145. There were two possible ways to commence the first step of the Physical Loop method. The first way was a concurrent synthesis, which was in a similar manner to Figure 3.15 on page 119 but made use of the Component Granularity Program (CGP) to calculate the payload and then initially size the whole vessel. In addition, the spaces within the submarine were allocated using the Volume Granularity Program (VGP) while the weight sizing used the Weight Granularity Program (WGP).

The second way to commence the submarine synthesis was to conduct the traditional numerical synthesis using a simple synthesis spreadsheet, estimating the initial crude weight and space balance of the design in the manner of a pre-DBB synthesis. The traditional numerical synthesis would then help the designer to size the submarine *ab initio*. Subsequently, the Weight Granularity Program (WGP) and the Volume Granularity Program (VGP) could have been used to architecturally manipulate the arrangement of the submarine at the coarse stage (Subsection 4.2.1). As the design was developed, the Component Granularity Program (CGP) could also have been used to model escape towers, torpedo tubes, and other significant components, as necessary.

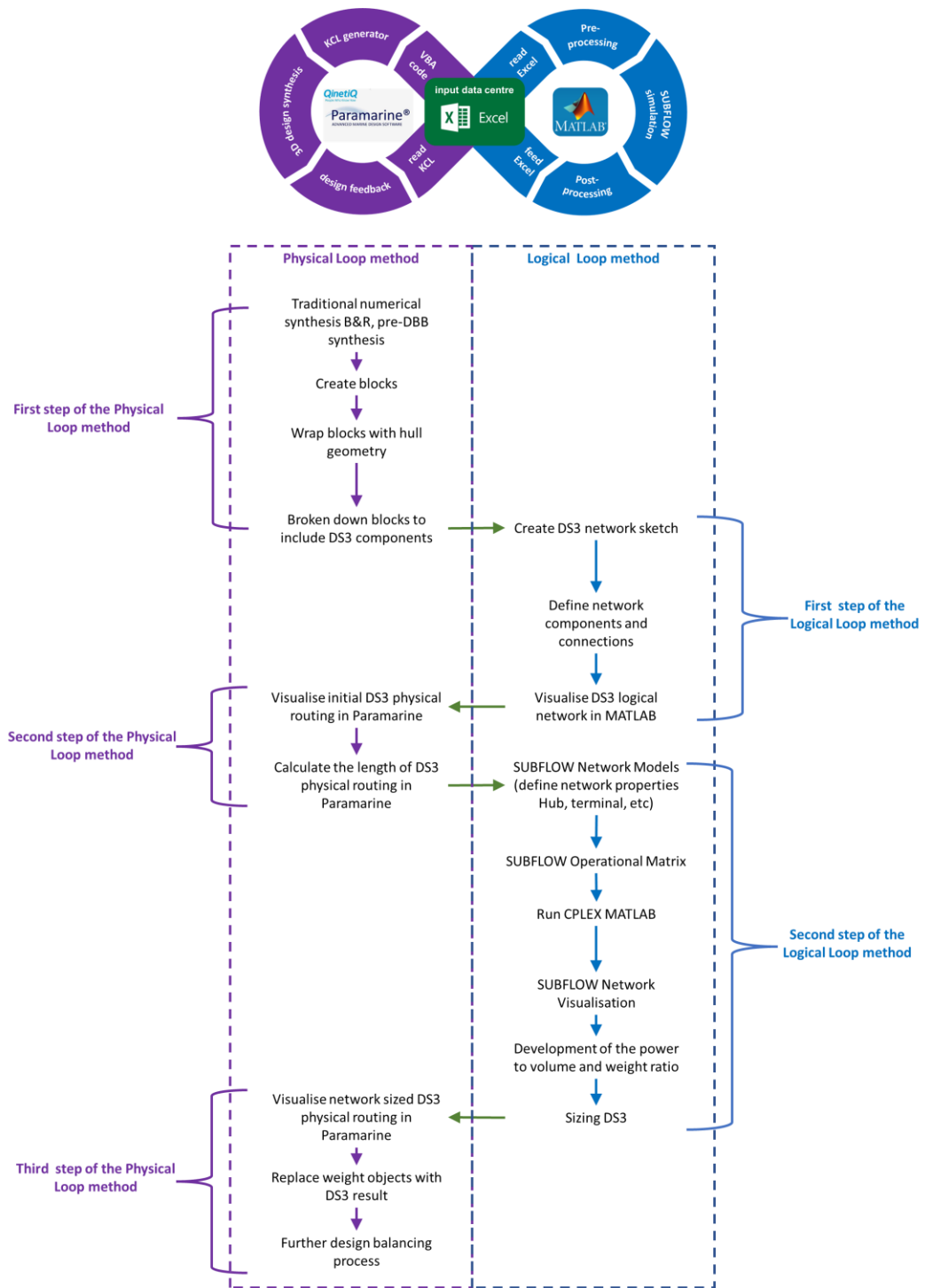


Figure 5.2: The logic of the proposed Network Block Approach (NBA) to DS3 synthesis for submarine design ESD, see Subsection 3.1.2 for CPLEX MATLAB

Although both ways were possible with the Physical Loop method, the first way required a back-and-forth process between the relevant programs (WGP, VGP, and CGP in Table 4.1) and Paramarine, while the second way seemed to be quicker, as a numerical synthesis was possible without resorting to the 3D

model. At this point, the design would have had implicit DS3 styles, since it would have been sized using the gross weight displacement based algorithms.

The second way began by inputting the numerical synthesis data into the Volume Granularity Program (VGP) and the Weight Granularity Program (WGP). Using the two programs, the designer created volume objects (see Figure 5.3 (top) and Table 5.2). These 21 volume objects not only represented spaces within the submarine but also 181 items of weight data, which were attached to the volume objects as attributes (see Table A 3 in Appendix 7). At this coarse stage, some weights that were distributed throughout the submarine, such as DS3, were allocated at the longitudinal centre of the pressure hull with assumed z coordinates, based on the previous submarine data (UCL-NAME, 2014).

The volume objects were then be included within the hull using the Hull Geometry Program (HGP) to obtain an initial indication of longitudinal balance. This then resulted in a more refined volume due to additional data being estimated, as well as obtaining the weight of the total fluids in the tanks, as is shown in Figure 5.3 (middle). Some of the major equipment components, such as the diesel engines, propulsion motor, escape towers, and torpedo tubes could also be modelled at this point to aid sizing volume objects when using the Component Granularity Program (CGP) (see Figure 5.3 (bottom)). This is the first step of the Physical Loop method as shown in Figure 5.2.

The level of design granularity shown in Figure 5.3 (middle) or even in Figure 5.3 (bottom) was considered sufficient for typical submarine concept level design. However, since this research concerned DS3 synthesis, it was decided that the design had to be developed beyond this level of granularity. Some DS3 style choices subject to spatial definition, such as zoning for electrical systems, could only be investigated once the design progressed to this level of design granularity. Therefore, the procedure to develop various DS3 technologies is discussed after Section 5.2 to cover the second step of the Logical Loop method as well as the third step of the Physical Loop method (see Figure 5.2).

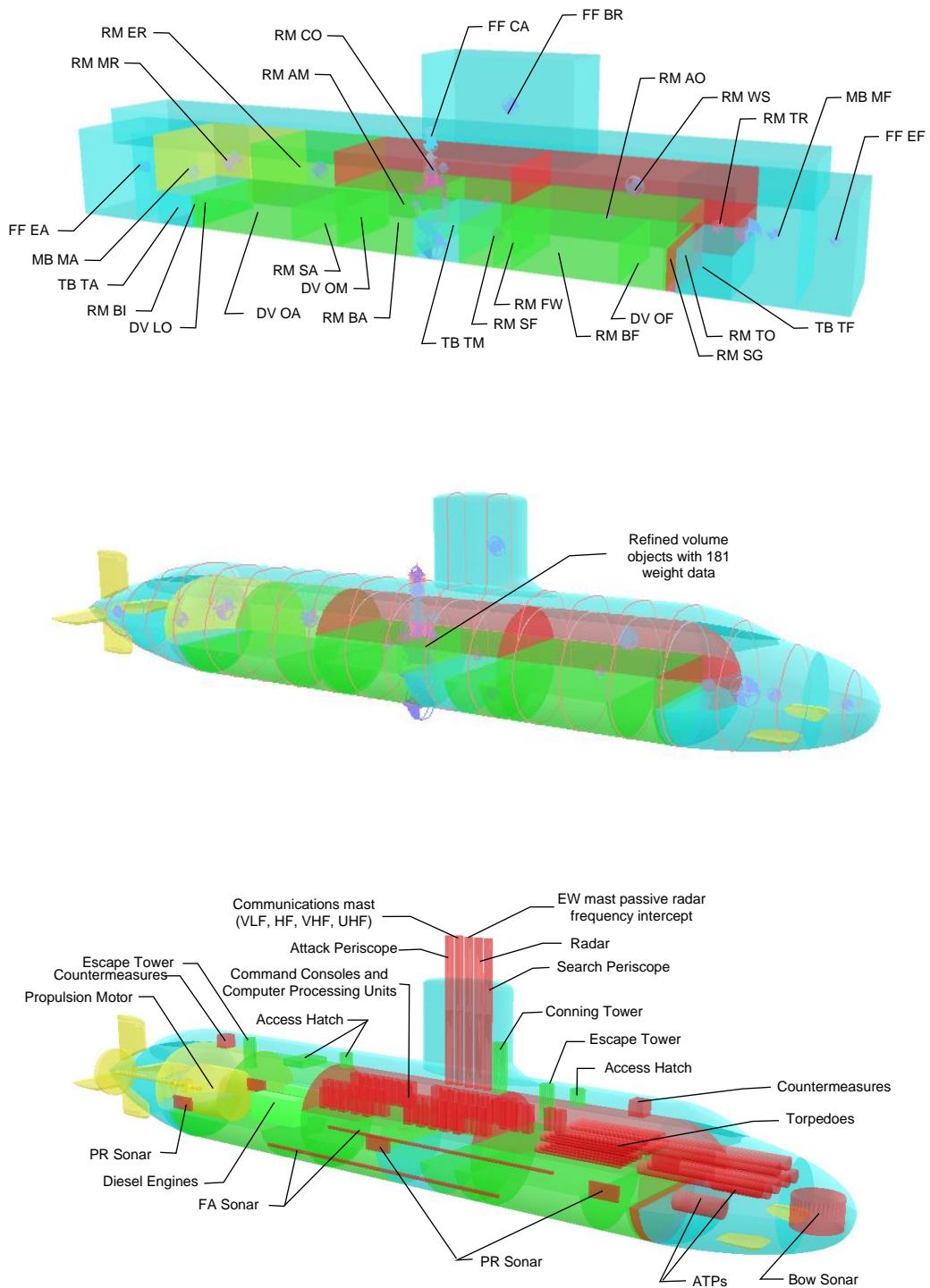


Figure 5.3: Design progress of Case Study 5.1, showing (top) volume objects and weight data are defined in Appendix 7 for the details of the 181 items of weight data, (middle) and included in the hull, (bottom) concurrent with placement of major components (see acronyms for payload items in Table 3.8)

Items named in top diagram by four letters are individually identified in Table 5.2

Table 5.2: List of volume objects of Case Study 5.1 defined in the Volume Granularity Program (VGP) (see Table A 4 in Appendix 7 for detailed calculations)

Zones	Volume Objects	Description
External Spaces	BB_VL_FL_FF_EA	Free flood volume aft occupied by equipment
	BB_VL_FL_MB_MA	External Main Ballast Tank volume aft
	BB_VL_FL_MB_MF	External Main Ballast Tank volume forward
	BB_VL_FL_FF_EF	Free flood volume forward occupied by equipment
	BB_VL_FL_FF_BR	Bridge fin volume
	BB_VL_FL_FF_CA	Casing volume
Aft Zone	BB_VL_MV_RM_MR	Motor room
	BB_VL_IA_RM_ER	Engine room
	BB_VL_FL_TB_TA	Trim tank aft
	BB_VL_FL_RM_BI	Bilge tank
	BB_VL_IA_DV_LO	Lubricant oil tank
	BB_VL_IA_DV_OA	Fuel tank aft
	BB_VL_IA_RM_SA	Storage aft
Mid Zone	BB_VL_FH_RM_CO	Control room
	BB_VL_IA_RM_AM	Auxiliary Machinery Space (AMS)
	BB_VL_IA_RM_MS	Messes, etc.
	BB_VL_IA_DV_OM	Fuel tank mid
	BB_VL_IA_RM_BA	Battery aft
	BB_VL_FL_TB_TM	Trim and Compensating tank
	BB_VL_IA_RM_SF	Storage forward (food store)
	BB_VL_IA_RM_FW	Fresh water tank
Forward Zone	BB_VL_FH_RM_WS	Weapon stowage compartment
	BB_VL_IA_RM_AO	Accommodation
	BB_VL_FH_RM_TR	Space for ATP and WRT
	BB_VL_IA_RM_BF	Battery forward
	BB_VL_IA_DV_OF	Fuel tank forward
	BB_VL_IA_RM_SG	Sewage tank
	BB_VL_FH_RM_TO	Torpedo Operating Tank (TOT)
	BB_VL_FL_TB_TF	Trim tank forward

The development of each DS3 network required an understanding of the individual DS3 technologies and how the physics drove a different formulation for the network models. The architecture of each DS3 was also dependent on detailed system types, technology changes and styles of redundancy at the component or connection level.

As shown in the first step of the Logical Loop method of Figure 5.2, the procedure began by decomposing the volume granularity to component granularity level using the sketch of the DS3 network (Subsection 3.2.5), itself based on the style decisions appropriate to each type of DS3. When developing the network sketch, spatial aspects, such as zoning, port-starboard, forward-aft locations needed to be considered. Although these may have needed to be explicitly neglected in the logical layout of the DS3 network, the spatial order was retained, along with each node's identification. Using the network sketch the number of DS3 components and connections was identifiable. Thus, relevant equipment data needed to be researched and defined in the Component Granularity Program (CGP). Meanwhile, the connections between the DS3 components were defined using the System Preamble Program (SPP) and the System Connection Program (SCP). The DS3 network could then be logically visualised in MATLAB and was checked as to whether the network sketch had been accurately modelled.

As the development of the DS3 network was not intended to 'bottom out the preferred design', i.e., it required openness to revision, simplifying assumptions were made for each DS3 technology. This kept the network simple for the ESSD application while avoiding the loss of sufficient DS3 complexity. Therefore, although each DS3 network was developed based on the relevant system line diagram in Appendix 1, some nodes were modelled as 'DB' but without yet having geometric data. They were produced to complete the network structure and to aid the DS3 routing decisions. Furthermore, the detailed components, which were not explicitly modelled in this network, were accommodated using typical design margins. This input could be manually adjusted using the System Connection Program (SCP) and the Component Granularity Program (CGP) (Table 4.1).

In this case study, different DS3 technologies, ranging from cables to piping for transporting either gas or liquid were developed and are discussed further in Sections 5.3 to 5.7. Figure 5.4 indicates the overall DS3 network developed in the first step of the Logical Loop method, while Figure 5.5 shows the DS3 network as multiplex, with the fuel 'FO' as the source of energy being transferred to various DS3 demands, ranging across data 'DT', electrical 'EL', mechanical 'ME', heat removal 'HE', hydraulics 'HY', trim and ballast 'TB', high-pressure, and low-pressure air systems 'HP' & 'LP'.

Nodes shown in Figure 5.4 and Figure 5.5 adopted the naming convention outlined in Subsection 4.2.6. All connections in the network were modelled as dashed-dotted lines before the SUBFLOW simulation except cable data, which was modelled as dashed lines. There were 231 nodes and 468 arcs. The shape and colour coding for the network nodes are given in Table 5.3, while Table 5.4 provides the colour coding for network arcs for the various DS3 technologies. Each of the 14 DS3 in this case study will be considered in turn (Sections 5.3 to 5.7) so their contribution to Figure 5.4 and Figure 5.5 can then be appreciated.

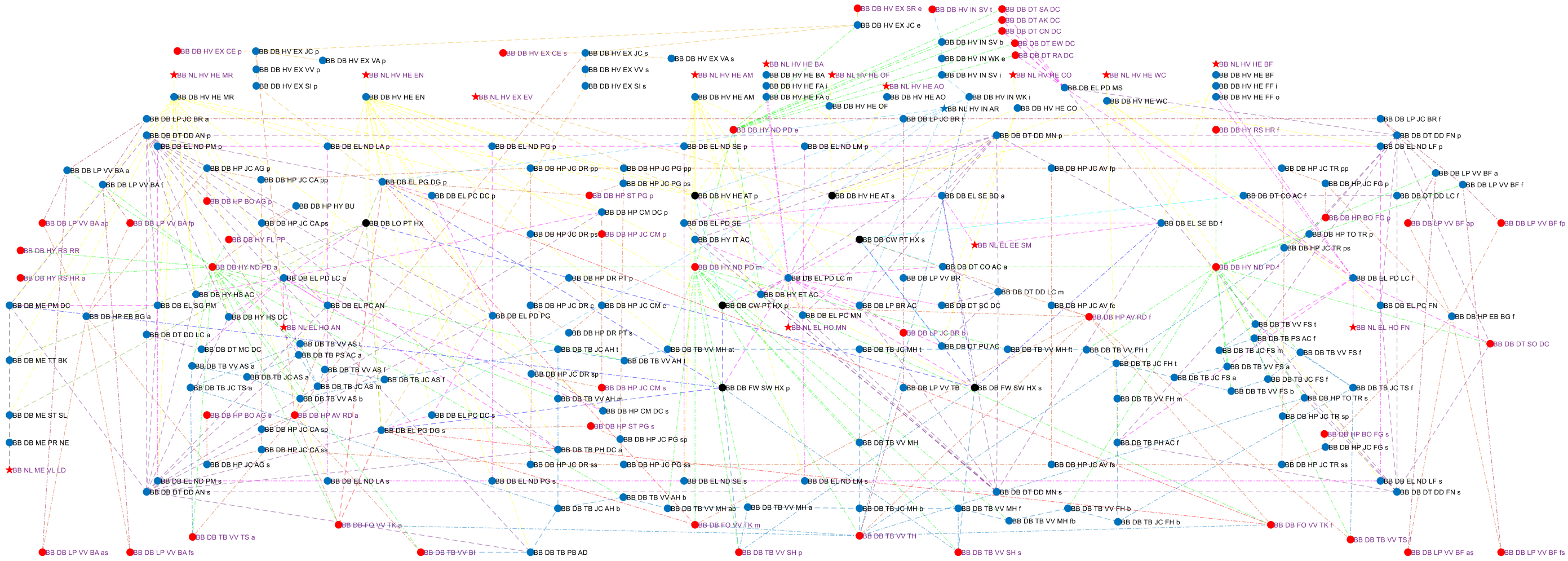


Figure 5.4: Overall DS3 network logic for Case Study 5.1, see Table 5.3 and Table 5.4 for the description of the shape and colour coding used for different types of nodes and arcs for various DS3 technologies

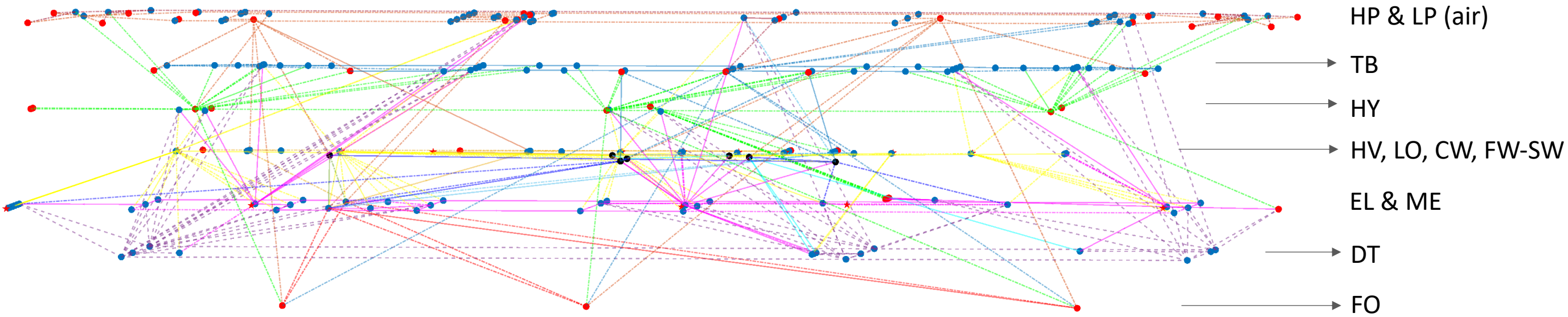


Figure 5.5: Multiplex 3D network of the overall DS3 for Case Study 5.1 showing each layer for a specific type of DS3, see Table 5.3 and Table 5.4 for the description of the shape and colour coding used for different types of nodes and arcs for various DS3 technologies

Table 5.3: Shape and colour coding for different types of nodes



















No	Type of Nodes	Granularity	Shape Coding	Colour Coding
1	Terminal	Numerical (NL)	Star	
		Component (DB)	Circle	
2	Hub	Numerical (NL)	Star	
		Component (DB)	Circle	
		Component (DB) for Heat exchanger	Circle	

Table 5.4: Colour coding and description of arcs for various DS3 technology

No	Service Commodity	DS3 Name	Colour Coding	Description
1	Fuel oil	FO		Subsection 5.3.1
2	Electrics	EL		Subsection 5.3.2
3	Data	DT		Section 5.6
4	Mechanical	ME		Subsection 5.4.1
5	Trim and ballast	SW		Subsection 5.5.3
	SW (cooling)	TB		Section 5.7
6	High-pressure air	HP		Subsection 5.5.1
7	Low-pressure air	LP		Subsection 5.5.2
8	Hydraulics	HY		Section 5.4
9	Air intake	HVIN		Section 5.7
10	Air heat	HVHE		Section 5.7
11	Air exhaust	HVEX		Section 5.7
12	Chilled water	CW		Section 5.7
13	Lubricant oil	LO		Section 5.7
14	Freshwater (cooling)	FW		Section 5.7

Once the DS3 logical network was firm, the indication of the overall DS3 network logic in Figure 5.4 could also be translated into physical definition rapidly by the new programs (Table 4.1) as part of the second step of the Physical Loop method (Figure 5.2). This was done by first assigning the DS3 components to the volume objects listed in Table 5.2. As this step occurred before the network based sizing, some simplifications in the inputs for the Component Granularity Program (CGP) and the System Connection Program (SCP) were made just for the visualisation, enabling the designer to simultaneously develop the DS3 design both physically and logically. Firstly, the program was set to employ point to point connection (Subsection 4.2.5), which meant the 468 connections overlapped each other. Secondly, the size of all connections was adjusted so they can be reasonably visible in the 3D model. Thirdly, the 231 DS3 components were assigned at the centroid of each object's

volume, which are modelled as simple spheres. These simplifications resulted in a visualisation of all 14 DS3 routings are given in Figure 5.6.

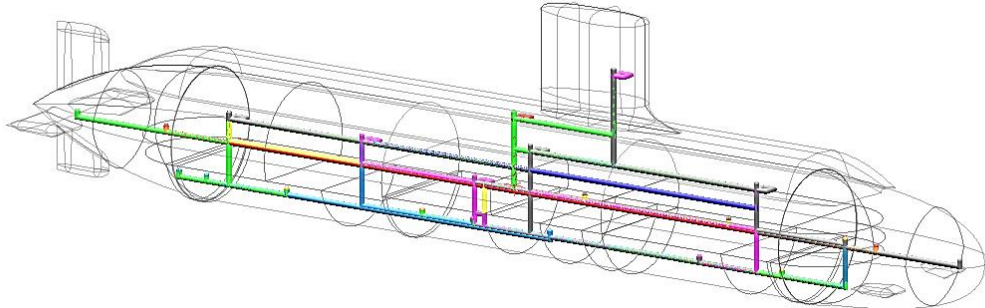


Figure 5.6: Initial routing in the second step of the Physical Loop method (Figure 5.2 on page 176), showing DS3 connections (see Table 5.4 for the colour description) and components situated at the centre of each volume space, which had been defined using the Component Granularity Program (CGP), the System Preamble Program (SPP), and the System Connection Program (SCP) (Table 4.1 on page 145)

This demonstrates that the new programs within the Network Block Approach (NBA) could rapidly translate 230 nodes to 230 Design Building Block (DBB) objects at the component granularity and 468 arcs to 468 DBB objects at the connection granularity from MATLAB to Paramarine. Hence, at this point, there were 698 DBB objects with numerical data only for DS3 (excluding other types of DBB objects, such as weight objects and volume objects as outlined in Subsection 4.2.3). This was sufficient to estimate the initial DS3 routing length for commencing the SUBFLOW simulation, part of the second step of the Logical Loop method in Figure 5.2. Appendix 8 provides individual DS3 visualisations including their system line diagrams using Paramarine. This however was found to be limited in capturing the overall set of DS3 logical architectures (compared to the DS3 network in Figure 5.4 and Figure 5.5 using MATLAB).

Beyond the second step of the Physical Loop method of Figure 5.2, the mathematical models for the SUBFLOW could be defined in the Component Granularity Program (CGP). This consisted of three categories of input: the type of nodes; the (Sankey) energy coefficient input of each DS3 component (see Table 3.11 on page 99); and the calculation of power demand of user

components. Therefore, if there were 230 components as in Case Study 5.1, this meant a total of 690 additional inputs for the SUBFLOW on top of the (181) weight data to be defined in the second step of the Logical Loop method. The resultant Operational Matrix in Case Study 5.1 has 1971 rows and 1640 columns. SUBFLOW simulation only took around 40-90 seconds for each operating condition.

Before the power information from SUBFLOW could be translated into DS3 space and weight input for ESSD, the power to volume and weight ratios of each node needed to be derived. The derivation of these ratios also requires an understanding of what information the nodes represented in the design (see Appendix 9). As discussed in Subsection 4.3.2, only nodes that were marked as 'DB' could be translated into space and weight input. However, some 'DB' nodes were modelled to aid the DS3 routing and thus may not have sufficiently consequential spatial geometry, such as DB nodes representing valves in the air intake or exhaust system.

In the third step of the Physical Loop method of Figure 5.2 on page 176, a more refined Paramarine model was produced to demonstrate the applicability of the novel DS3 routing framework outlined in Subsection 4.2.5. As shown in Figure 5.7, this was done using the graphical interface in Paramarine by arranging each DS3 component, compartment by compartment. Thus, 230 unique x, y, z locations for the DS3 components could be identified and stored in the Component Granularity Program (CGP). Furthermore, the appropriate system highways (Subsection 4.2.5) could be added as additional inputs to the existing 698 items of DS3 data in the System Connection Program (SCP), as illustrated in Figure 5.8.

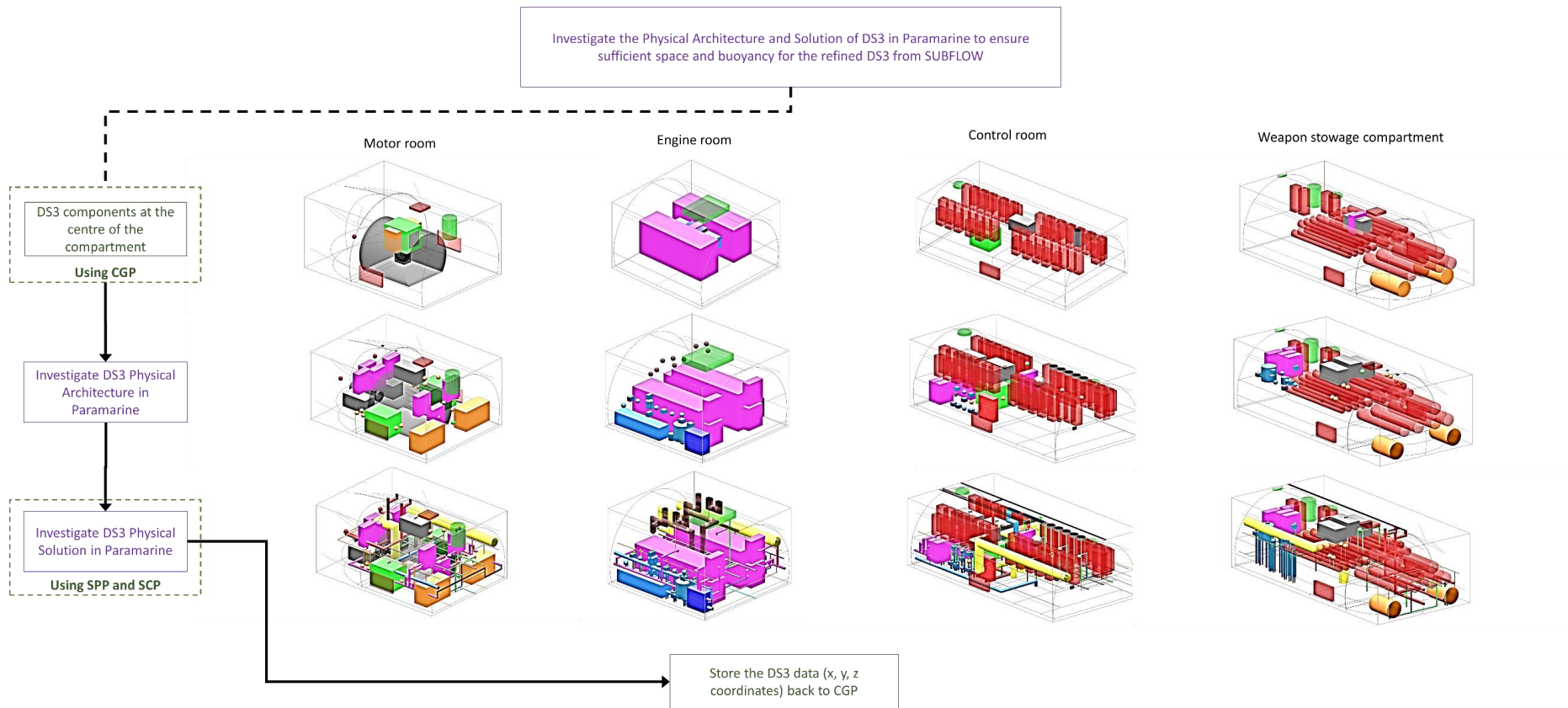


Figure 5.7: The schematic of performing 3D layout arrangement of DS3 at ESSD fine stage (see Table 5.4 on page 184 for DS3 identifiers) while purple and green texts and boxes, showing gradual step by step arrangement of procedure compartment by compartment using the Component Granularity Program (CGP), the System Preamble Program (SPP), and the System Connection Program (SCP) (Table 4.1 on page 145)

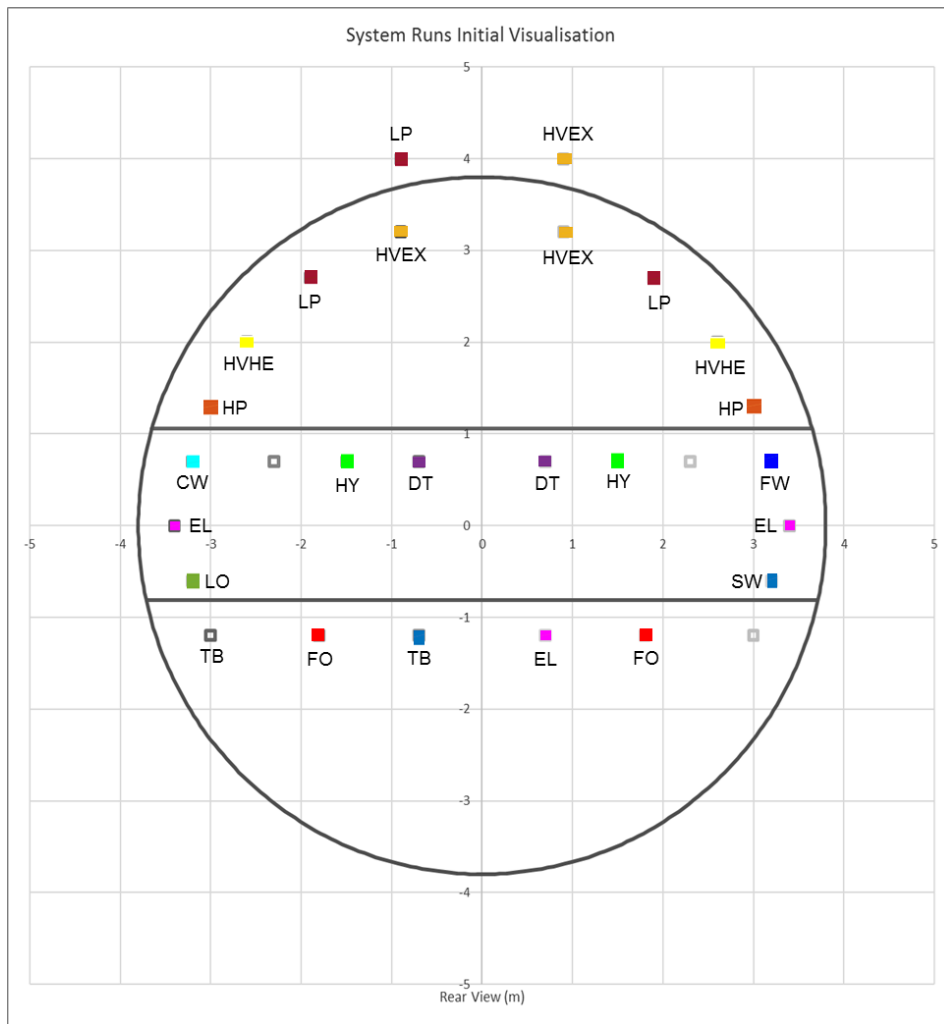


Figure 5.8: Initial highways of Case Study 5.1 defined using the System Preamble Program (SPP) part of the Network Block Approach (NBA) (see Table 5.4 on page 184 for DS3 identifiers)

The refined overall submarine model is given in Figure 5.9, showing gradual steps in manipulating DS3 components in the 3D layout. Starting from major components based on the FMFI breakdown as in Figure 5.9 (top), followed by the electrical ‘EL’, mechanical ‘ME’, and data ‘DT’ systems in Figure 5.9 (middle), and finally, the rest of the systems listed in Table 5.4 were arranged, as shown in Figure 5.9 (bottom). Each DS3 technology of Case Study 5.1 discussed individually in the following sections covers three main areas: the sketch of the SUBFLOW network; SUBFLOW formulation; SUBFLOW simulation result; and refined 3D model produced using the Physical Loop method. Following the DS3 descriptions, Section 5.8 expands the process beyond the third step of the Physical Loop method (Figure 5.2 on page 176).

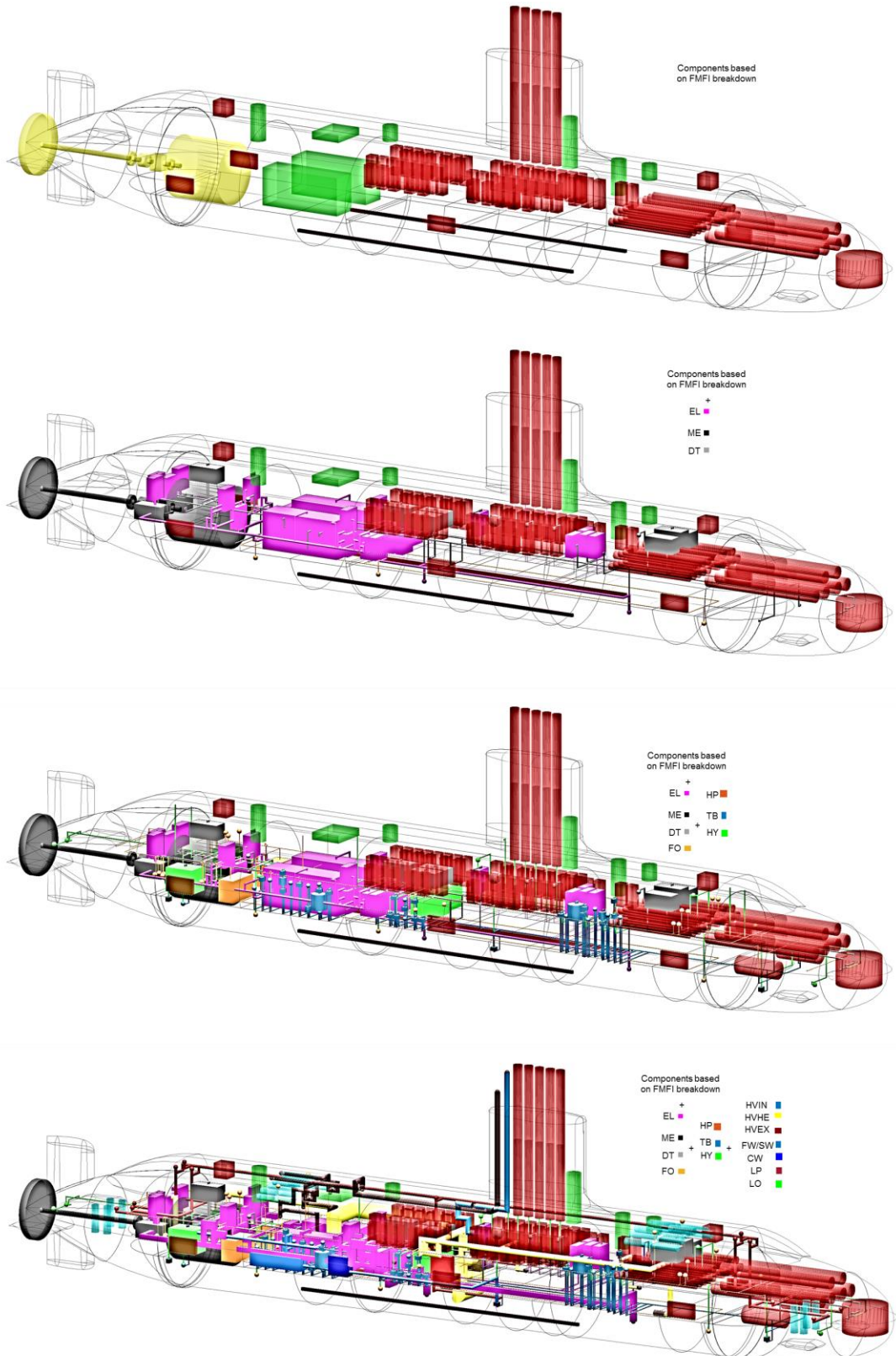


Figure 5.9: Refined DS3 model in the third step of the Physical Loop method (Figure 5.2 on page 176) showing the progress of placing DS3 system by system in the 3D layout. There were 365 DBB objects at the component granularity and 472 DBB objects at the connection granularity level. The latter shows 14 DS3 top level routings

5.3 Power System

The objective of the power system was to provide power for the submarine to 'Fight', 'Move', 'Float', and 'Support' the personnel who operate the submarine. Therefore, it might seem logical that this system was sized to meet the demands of those functions. Before the system could be sized, the Macro style of each system needed to be selected, given the power system options ranged from diesel-electric, diesel with AIP, to nuclear-powered configuration. The decision on these options would drive the approach in designing the architecture of the system, as well as selecting relevant design algorithms necessary for system synthesis. As listed in Table 5.1 on page 174, the power system adopted for Case Study 5.1 was that for a conventional ocean-going SSK.

As discussed in Section 3.2, the DS3 sizing for the SSK style was driven by two operating conditions. In the snorting condition, the diesel engines produce high power for charging batteries, which can be a driver for sizing the power system. Meanwhile, the high power from the battery in the sprint submerged condition drives the size of the propulsion system. Mathematically, these two operating conditions can be defined as indexed *snort* and *sub* notations. The network based sizing also worked based on two fundamental types of nodes, which is the source node and sink node. Unlike AFO and its variants (Parsons et al., 2020a), all the source nodes in this research were not capped and subject to revision, reflecting the inside-out approach (Andrews, 2018c) where the design is still fluid as for ESSD application. The size of the source nodes was driven by the power demand of the sink nodes.

To estimate the power demands of the chosen SSK submarine, the equation provided by Burcher and Rydill (1994) was used in a similar manner to that already discussed in Subsection 3.2.3. The initial calculation of the total diesel power was 2.7 MW. The selected style choice configuration was to incorporate two diesel engines with each supplying 1.4 MW at the Nominal Continuous Rating (NCR), which was assumed to be 75% of the Maximum Continuous Rating (MCR). This was because most diesels are advertised with their surface

ratings, whereas in a submarine environment their performance will be severely hampered. Furthermore, although the second diesel engine implies redundancy, the output of both engines is necessary for the full power requirement to meet the power demands in the snorting operating condition.

As discussed in Subsection 3.2.3. the power demands mainly consisted of the battery charging load, the propulsion load, and the hotel load in the snorting operation or condition. However, the 'gross' hotel load estimation in Subsection 3.2.3 needed to be broken down for power system synthesis. In this case study, the diesel-electric configuration was modelled as a network that includes fuel, diesel engines, converters, switchboards, distributions, and many power consumers on the vessel, including the propulsion demand. Two 'sub-systems' are now outlined.

5.3.1 Fuel System

Three internal fuel source nodes (VV TK) were chosen as the micro style choice in this case study (see Table 5.5). They are cross-connected and can independently supply the fuel oil to the two diesel power generator nodes (PG DG) (see Figure 5.10). The fuel nodes (VV TK) were also used to attach numerical data for fuel energy, quantifying the size of the fuel storage tanks. To keep this network simple for ESSD application, other detailed FO components, such as pumps, valves and expansion tanks were estimated using margins applied either to the FO arcs or nodes. As these three fuel storage tanks were arranged internally within the pressure hull, they could be set with dry compensating tanks, as opposed to external (wet) compensating tanks (see Subsection 4.2.6), although this decision may result in a larger pressure hull size for the same operational range requirement. In short, there are three nodes and six arcs for the fuel 'FO' system.

Table 5.5: List of nodes for the fuel oil (FO) system of Case Study 5.1

Node		Description
BB_DB_FO_VV_TK	_(a/m/f)	Fuel tanks (connected to valves) (aft/mid/forward)
BB_DB_EL_PG_DG	_(p/s)	Power generation diesel generator (port/starboard)

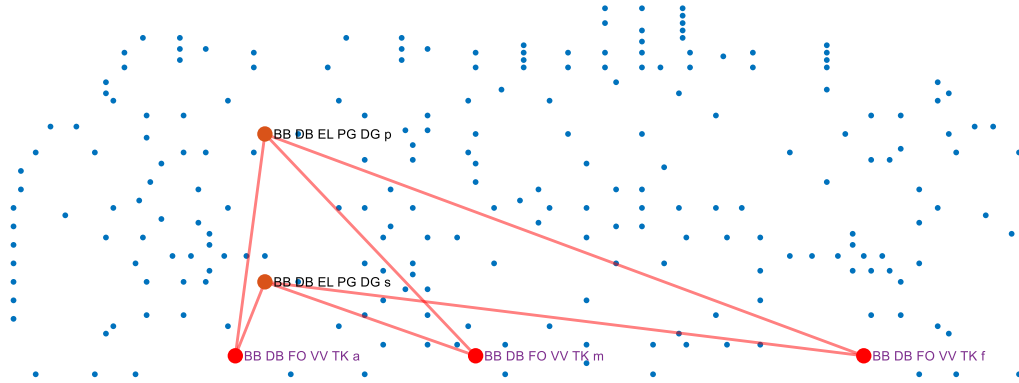


Figure 5.10: Network visualisation of the fuel oil 'FO' system (red lines) and the adjacent 'EL' system components where blue dots represent the overall DS3 nodes in Case Study 5.1 (Figure 5.4 on page 182)

In the snorting condition, there are only two source nodes, which were fuel nodes and an air intake node, part of the air intake 'HVIN' system (Table 5.4). The power at the fuel nodes in the snorting condition $P_{VV_TK}^{snort}$ was driven directly by the diesel nodes (PG DG) and thus it should be any positive values as shown in Equation (5.1).

$$P_{VV_TK}^{snort} \geq 0 \tag{5.1}$$

These fuel nodes (VV TK) became inactive or closed as the submarine is in the sprint submerged operating condition. Therefore, Equation (5.2) reflect the physics of such an operating condition.

$$P_{VV_TK}^{sprint} = 0 \tag{5.2}$$

The SUBFLOW result is given in Figure 5.11, which shows that the 2 x 1.8 MW of fuel energy is required to perform the snorting operation. This was taken from the aft tank, which can then be transformed to weight and space input for the fuel estimation. Meanwhile, the rest of the fuel pipelines was sized at 1.8 MW

as this reflected the maximum power of the total diesel generator nodes (PG DG).

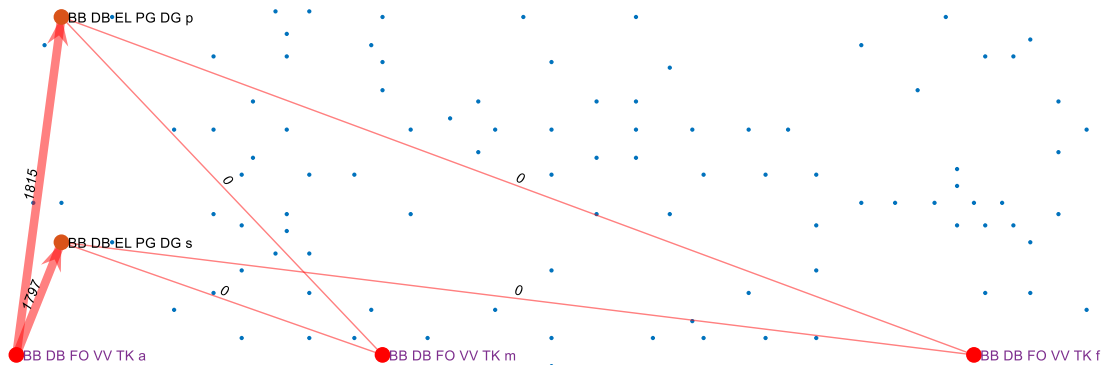


Figure 5.11: SUBFLOW solution of the fuel oil 'FO' system in the snorting operating condition (red lines) and the adjacent 'EL' system components where blue dots represent other DS3 nodes in Case Study 5.1 (Figure 5.4 on page 182)

To check the physical routing of the fuel system, the fuel oil 'FO' system nodes were first assigned to the fuel oil tanks (objects) (see Table 5.2) using the Component Granularity Program (CGP) and then assigning the fuel lines to the system highways defined in Figure 5.8 on page 188. The total length of the FO system connection was 107 m. Thus, as shown in Figure 5.12, the FO system is routed at the port and starboard sides of the vessel. The diesel power generators (PG DG) were also modelled and is shown in magenta in Figure 5.12, now part of the electrical 'EL' system instead of the Infrastructure functional group (increased in terms of design fidelity, see Figure 4.5 on page 150). This is discussed in the following subsection.

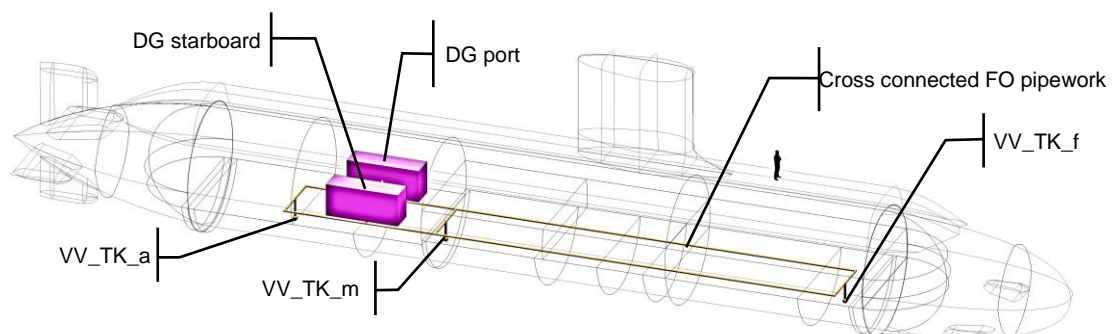


Figure 5.12: The initial model of the fuel oil 'FO' system of Case Study 5.1 (dark yellow lines) showing the placement of FO distribution in the overall 3D layout

5.3.2 Electrical System

The electric 'EL' system converts the chemical energy from the fuel 'FO' system to electrical energy and subsequently distributes it throughout the vessel. In this case study, the style choice for the type of diesel engines was AC, as an AC diesel takes up less space and has less weight than its DC equivalent (Burcher and Rydill, 1994). The AC power is directly converted to DC using two power converters and is forwarded to a diesel switchboard or generator breaker that was modelled as a power distribution node. The power distribution node then distributes the DC power service via a DC ring main configuration to three different zones (based on the number of watertight bulkheads, part of the main style choice listed in Table 5.1). Initially, a numerical hotel load was modelled for each zone. As the design progresses, the demand at the zonal hotel node can be broken down into more detail, including the utilisation of a power converter node to convert the DC distribution to a more detailed level by a variation of AC and DC voltages. This distribution would involve many hub nodes and terminal nodes (users) as is shown in Table 5.6 and Figure 5.13.

The diesel generator nodes (PG DG) (see the green circles (dashed) in Figure 5.13) are first directly converted to DC output using converter nodes (PC DC) and then transferred to a generator breaker node (PD PG) before being distributed to various load demands throughout the vessel. As a ring style was adopted, the generator breaker node (PD PG) was connected to the port and starboard bus nodes (ND PG). From these nodes, the power could travel either to the forward, or aft part of the vessel. The propulsion switchboard node (PD PM) and aft zone load nodes (ND LA) covered the demands from the equipment situated at the motor room and engine room in the aft part of the vessel. Moving on to the forward part of the vessel, there were mid zone load nodes (ND LM), and forward zone load nodes (ND LF). The mid zone load nodes (ND LM) included demands from the equipment located in the mid zone, such as control room and Auxiliary Machinery Space (AMS), while the forward zone load mainly covered the demands from Fight or information data 'DT' system components, such as masts, and bow sonar.

Table 5.6: List of nodes for the electrical system of Case Study 5.1

Node				Description
BB_DB_EL (building block database electrics)	_PG	_DG	_(p/s)	Power generation diesel generator (port/starboard)
	_PC	_DC	_(p/s)	Power converter DC (port/starboard)
		_AN		Power converter aft node
		_MN		Power converter mid node
		_FN		Power converter forward node
	_ND	_PG	_(p/s)	Bus node for power generation (port/starboard)
		_SE	_(p/s)	Bus node for power stored energy (port/starboard)
		_PM	_(p/s)	Bus node for propulsion motor (port/starboard)
		_LA	_(p/s)	Bus node load aft (zone) (port/starboard)
		_LM	_(p/s)	Bus node load mid (zone) (port/starboard)
		_LF	_(p/s)	Bus node load forward (zone) (port/starboard)
	_SE	_BD	_(a/f)	Stored energy battery device (aft/forward)
	_SG	_PM		Switchgear Propulsion Motor
	_PD	_PG		Power distribution power generation (generator breaker)
		_SE		Power distribution stored energy (battery breaker)
		_PM		Power distribution propulsion motor (propulsion switchboard)
		_MS		Power distribution mast
		_LC	_(a/m/f)	Power distribution load centre (aft/mid/forward)
BB_DB_DT (building block database data)	Payload demand node (or Fight components)			
	_SA	_DC		Search periscope (assumed DC)
	_AK			Attack periscope (assumed DC)
	_CN			Communication (assumed DC)
	_EW			Electronic warfare (assumed DC)
	_RA			Radar (assumed DC)
	_SO			Sonar (assumed DC)
BB_NL_EL (building block numerical electrics)	_HO		_AN	
		_MN		Hotel mid node (zone)
		_FN		Hotel forward node (zone)
	_EE	_SM		Energy submerged

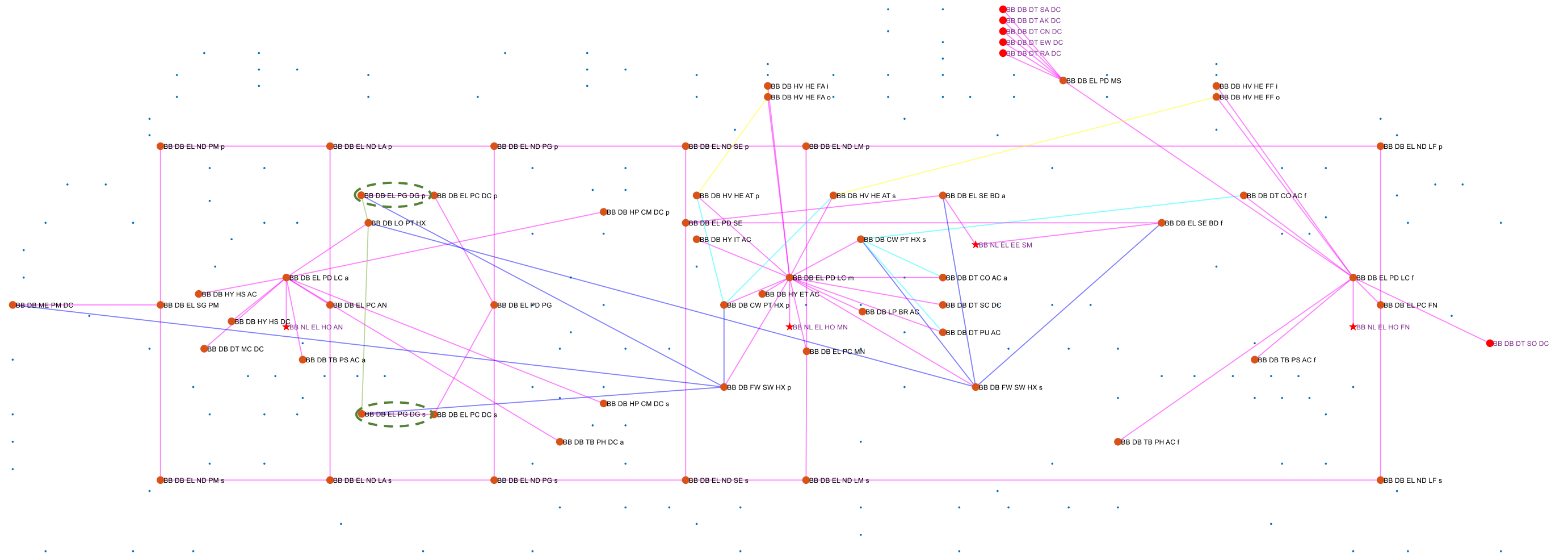


Figure 5.13: Network visualisation of the electrical 'EL' system (magenta lines) and the adjacent (HE, LO, CW, FW) system (Table 5.4) where blue dots represent the overall DS3 nodes for Case Study 5.1 (see Figure 5.4 on page 182) while the green circles (dashed) highlight the diesels

One of the major user nodes in the snorting condition was battery charging. The power required to charge the energy storage or battery in the snorting condition $P_{EE_SM}^{snort}$ is given in Equation (5.3). Equation (5.3) estimates the power demands for charging batteries of the chosen SSK submarine in a similar manner to that already discussed in Subsection 3.2.5. This includes the power margin in charging the battery m_{ch} , power margin when battery discharge x , the battery drain D , and some coefficients. These coefficients cover submerged time T_{sub} , charging time T_{ch} , energy charging per battery cell $E_{chpercell}$ and energy available per cell E .

$$P_{EE_SM}^{snort} = (1 + m_{ch}) \cdot \frac{D}{(1 - x)^2} \cdot \frac{T_{sub}}{T_{ch}} \cdot \frac{E_{chpercell}}{E} \quad (5.3)$$

Meanwhile, in the sprint submerged condition, the major user node was the propulsion node (PM DC) and thus energy node of the battery was changed from the user node as in Equation (5.3) to the source node, which is defined in Equation (5.4).

$$P_{EE_SM}^{sprint} \geq 0 \quad (5.4)$$

Unlike previous SUBFLOW implementations in Chapter 3, the hotel load was broken down in more detail to include the demands from payload nodes. Therefore, Equations (5.5) to (5.9) state the power required for the hotel payload load in the snorting condition. This requires associated load factor LF , as they are assumed to be not operating at 100% capacity.

$$P_{SA_DC}^{snort} = P_{search_periscope}^{snort} \cdot LF_{SA_DC}^{snort} \quad (5.5)$$

$$P_{AK_DC}^{snort} = P_{attack_periscope}^{snort} \cdot LF_{AK_DC}^{snort} \quad (5.6)$$

$$P_{CN_DC}^{snort} = P_{comms_mast}^{snort} \cdot LF_{CN_DC}^{snort} \quad (5.7)$$

$$P_{EW_DC}^{snort} = P_{EW_mast}^{snort} \cdot LF_{EW_DC}^{snort} \quad (5.8)$$

$$P_{RA_DC}^{snort} = P_{radar_mast}^{snort} \cdot LF_{RA_DC}^{snort} \quad (5.9)$$

There were also power demand nodes that need to be considered regardless of the operating conditions. These nodes consisted of payload equipment and

DS3 equipment. As given in Equations (5.10) to (5.13), the power demands of the payload equipment, such as the total power demand of CCs or CPUs in a room $\sum_{CC \in RM} P_{CC/CPU}$, were derived from the UCL submarine data (UCL-NAME, 2014) based on the decision making (see Table 5.1 on page 174). These power demands also require an assumed load factor LF , consistent with the payload equipment load in the snorting condition.

$$P_{CO_AC_a}^{snort/sprint} = \sum_{CC \in RM_CO} P_{CC} \cdot LF_{CO_AC_a}^{snort/sprint} \quad (5.10)$$

$$P_{CO_AC_f}^{snort/sprint} = \sum_{CC \in RM_WS} P_{CC} \cdot LF_{CO_AC_f}^{snort/sprint} \quad (5.11)$$

$$P_{PU_AC}^{snort/sprint} = \sum_{CPU \in RM_CO} P_{CPU} \cdot LF_{PU_AC}^{snort/sprint} \quad (5.12)$$

$$P_{SO_DC}^{snort/sprint} = P_{sonar}^{snort/sub} \cdot LF_{SO_DC}^{snort/sprint} \quad (5.13)$$

However, decomposing the hotel load P_{HO} to further nodes, without a complete database was considered prohibitive at the Concept Phase. As a resolution, the ‘gross’ equipment load equation provided by Burcher and Rydill (1994) was still used to cover the power demands that are not explicitly modelled in the network but with assumed load factors LF and was subtracted by the total hotel load for each zone $\sum P_{zone}$. This, in turn, is expressed by Equations (5.14) to (5.17).

$$P_{HO_AN}^{snort/sprint} = H_{equip}^{snort/sprint} \cdot LF_{aft_zone}^{snort/sprint} - \sum P_{aft_zone}^{snort/sprint} \quad (5.14)$$

$$P_{HO_MN}^{snort/sprint} = H_{equip}^{snort/sprint} \cdot LF_{mid_zone}^{snort/sprint} - \sum P_{mid_zone}^{snort/sprint} \quad (5.15)$$

$$P_{HO_FN}^{snort/sprint} = H_{equip}^{snort/sprint} \cdot LF_{forward_zone}^{snort/sprint} - \sum P_{forward_zone}^{snort/sprint} \quad (5.16)$$

$$LF_{aft_zone}^{snort/sprint} + LF_{mid_zone}^{snort/sprint} + LF_{forward_zone}^{snort/sprint} = 1 \quad (5.17)$$

The diesel engine nodes (PG DG) could be capped after several iterations to reflect that the two nodes need to operate to meet the power demands on the vessel. The power simulation flow results for the snorting and the sprint submerged are given in Figure 5.14 and Figure 5.15, respectively.

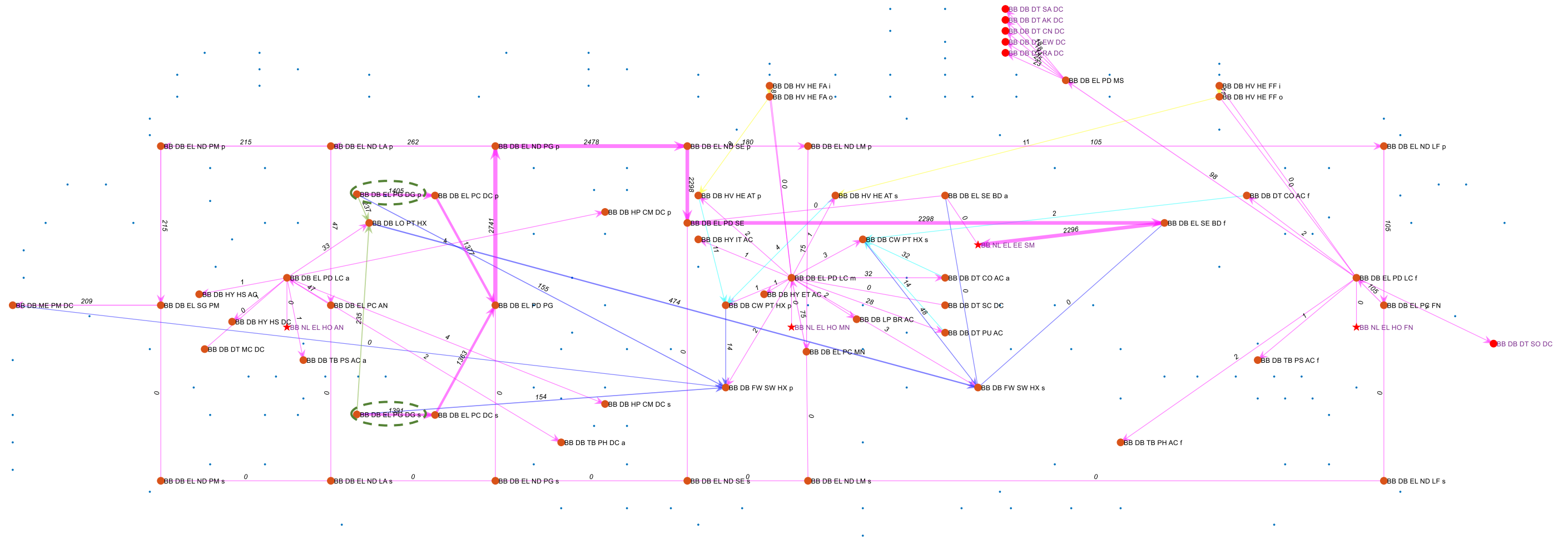


Figure 5.14: SUBFLOW solution of the electrical 'EL' system in the snort condition (magenta lines) showing blue dots represent the overall DS3 nodes in Case Study 5.1 (Figure 5.4 on page 182) while the green circles (dashed) highlight the energy source in the system

As expected, in the snorting condition, the power comes from the diesel nodes (PG DG) (see the green circles (dashed) in Figure 5.14). Conversely, in the sprint submerged condition, the power comes from the battery nodes (SE BD) (see the green circle dashed in Figure 5.15). In both scenarios, the power flow was then distributed throughout the vessel for various demands. This revealed that the major power demand in the snorting condition was the battery charging node while in the sprint submerged condition was the propulsion node. Moving on to the third step of the Physical Loop, the numerical data at each arc in Figure 5.14 and Figure 5.15 was used to size the EL system as is shown in Figure 5.16.

Figure 5.16 shows that the cabling of the electrical system is distributed throughout the volume objects of the vessel. The aft bus nodes (ND LA) were situated in the motor room together with the propulsion switchboard (PD PM) and its buses (ND PM). The generator breaker (PD PG) and its bus nodes (ND PG) were assigned to the engine room. The mid bus nodes (ND LM) were arranged in the AMS while the forward bus nodes (ND LF) were placed in the weapon stowage compartment. These buses were arranged so that they do not clash with other components from other systems. The total length of the EL system connection was 846 m.

Following the electrical 'EL' system, the next section discusses a set of systems that is one of the major consumers of the electrical system.

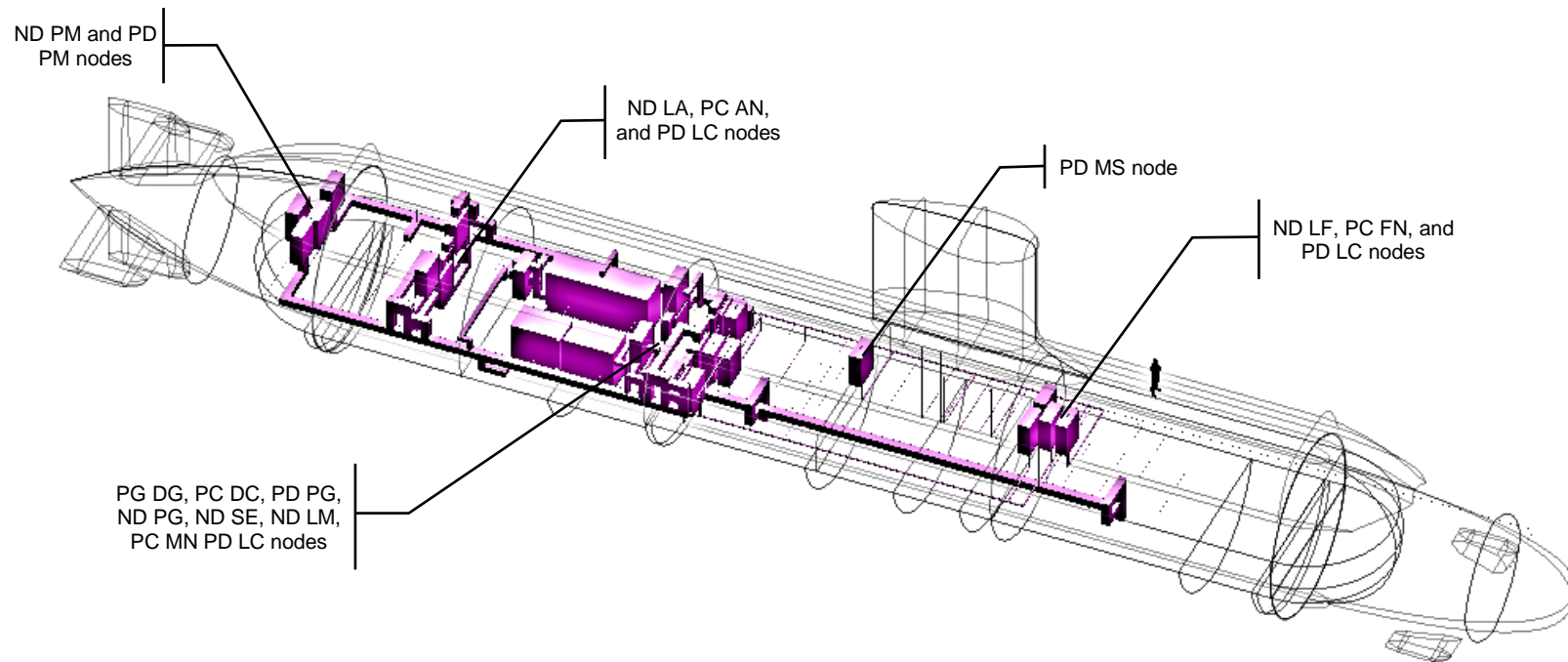


Figure 5.16: The initial model of the electrical 'EL' system (magenta) of Case Study 5.1 showing the EL equipment and ring distribution

5.4 Systems for Hydrodynamic Control

As opposed to other types of DS3, the propulsion system is typically not distributed throughout the ship. However, this system is one of the major power loads on the vessel and being electric hard to disconnect from consideration of DS3. When submerged, the submarine moves in a 3D environment using this system and is controlled by the forward and aft hydroplanes including rudders. Thus, the DS3 powering and controlling this function are considered vital systems on the submarine. These vital systems are now outlined in turn.

5.4.1 Propulsion System

The propulsion system aims to 'Move' the boat by delivering the energy from a propulsion motor node to a numerical propulsion load node via mechanical or kinetic energy. One of the important aspects of designing the propulsion system is to manage the acoustic signature risk of the propeller design (Hamson, 2016). The configuration of this system was driven by the macro (hull) and main (diesel-electric) style choices (see Table 5.1 on page 174). Hence, the micro style choices for propulsion systems varied from the adoption of a (single or twin) screw propeller configuration to a pump jet. Another alternative style choice in the propulsion system would be the more radical shaftless rim driven configuration (i.e., akin to pump jet, but without shafting (Collins et al., 2015)).

Regardless of the style choice made, the network of the system needs to be developed. In this case study, a single screw propeller configuration was chosen, consistent with the single hull style. This system consisted of a series of five nodes connected by arcs listed in Table 5.7, representing line shafts as shown in Figure 5.17. Although the system is depicted in the logical definition, Figure 5.17 also shows that the propulsion system is localised at the aft end of the submarine relative to the overall DS3 network in Figure 5.4 on page 182.

Table 5.7: List of nodes for the mechanical system of the case study 5.1

Node		Description
BB_DB_ME (building block database mechanical)	_PM _DC	Propulsion motor DC
	_TT _BK	Thrust block
	_ST _SL	Stern seal
	_PR _NE	Propeller and cone
BB_NL_ME (building block numerical mechanical)	_VL _LD	Velocity load based on different operating conditions

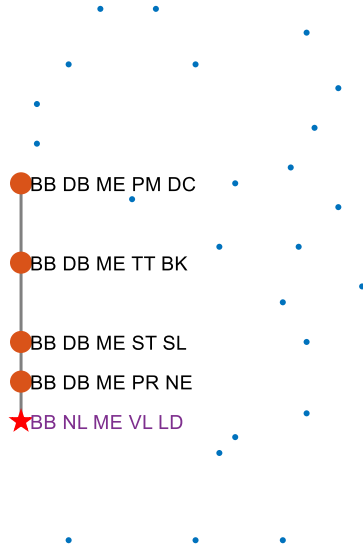


Figure 5.17: Network visualisation of the mechanical 'ME' system (black line) where blue dots are other DS3 nodes in Case Study 5.1 (Figure 5.4 on page 182)

In the snorting condition, the propulsion demand at the velocity load node $P_{VL_LD}^{snort}$ is expressed in Equation (5.18). The propulsion demand in the snorting scenario P'_s was obtained using the algorithm provided by Burcher and Rydill (1994) as already discussed in Subsection 3.2.3. However, the difference was that the efficiency of the mechanical system η_{ME} covering a series of nodes (PM DC to PR NE) needed to be accounted for as the power load was located at the end part of the mechanical system.

$$P_{VL_LD}^{snort} = P'_s \cdot \eta_{ME} \tag{5.18}$$

Meanwhile, in the sprint submerged operating condition, the propulsion node $P_{VL_LD}^{sprint}$ was one of the major pulls in the DS3 network, as it contained numerical data for the propulsion demand in the sprint submerged scenario P''_{SS} . This is

quantified in Equation (5.19) that also needs to be multiplied by the total efficiency of the mechanical 'ME' system nodes η_{ME} .

$$P_{VL_LD}^{sprint} = P_{SS}'' \cdot \eta_{ME} \quad (5.19)$$

Since the sprint submerged operating condition is the largest propulsion demand, the SUBFLOW simulation result for the ME system is given in Figure 5.18.

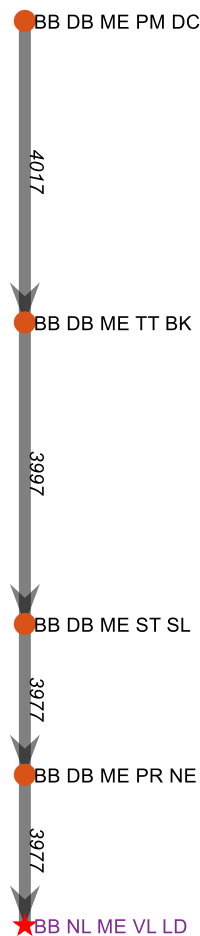


Figure 5.18: SUBFLOW solution of the electrical 'ME' system (black line) of Case Study 5.1 in the sprint submerged condition

Figure 5.18 reveals that to perform the sprint submerged scenario, the numerical node (VL LD) requires 3.9 MW. However, as each node was not 100% efficient to reflect the physics of the propulsion system, the power at the propulsion motor node (PM DC) was slightly higher, at 4 MW. Using these power numerical data, the individual baseline ME system components and the

connection (shaft) could be adjusted (scale up or down) accordingly. This resulted in an arrangement as shown in Figure 5.19 (top). Figure 5.19 (bottom) gives the approximate length of the shaft from the propulsion motor node (PM DC) in the motor room and to the propeller node (PR NE) at the aft part of the vessel. The total length of the shaft was 8 m.

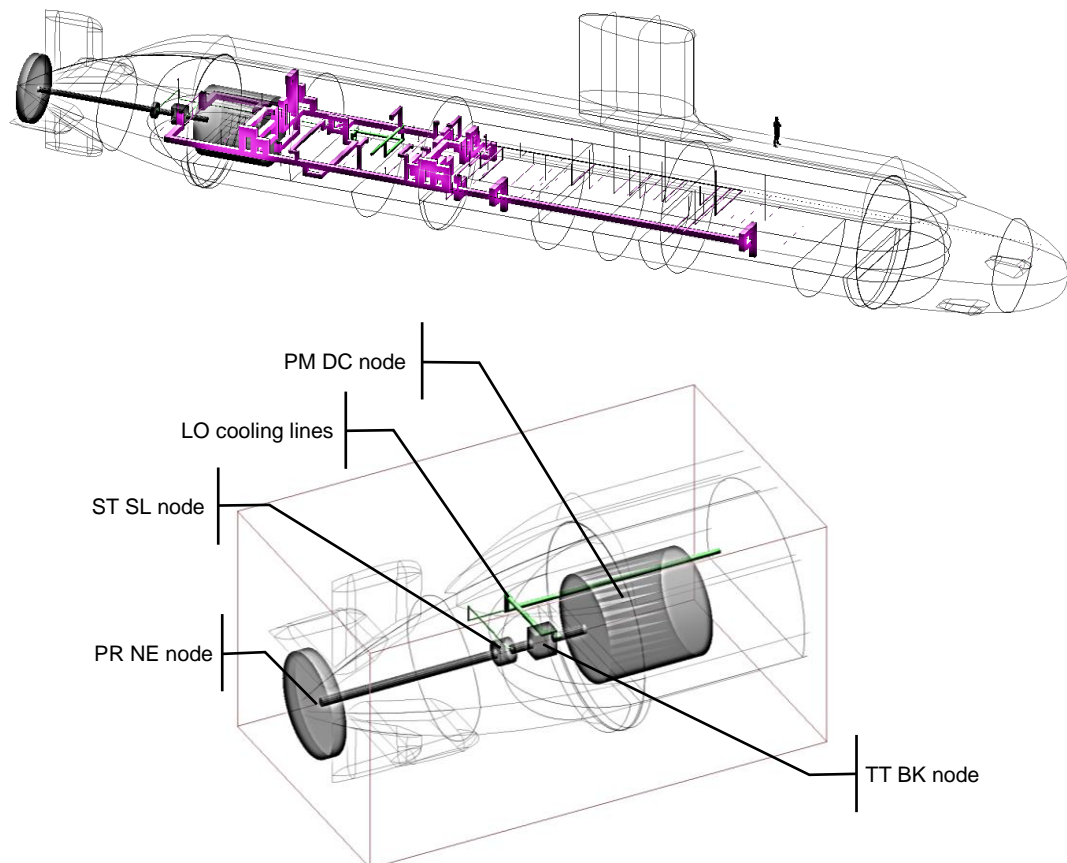


Figure 5.19: The initial model of the mechanical 'ME' system of Case Study 5.1, showing ME components in black located at the aft part of the vessel (top) with EL (magenta) and LO (green) systems and the close-up view of propulsion motor (PM DC), thrust block (TT BK), stern seal (ST SL) to propeller component (PR NE) connected by a line shaft and cooled by the LO system in green (bottom)

Unlike surface vessels, a modern submarine is designed to mainly operate underwater. To do this, submarine relies on hydrodynamic and hydrostatic control systems to control its depth or depth-keeping below sea surface level. The propulsion system works closely with the hydrodynamic control system to "Move" the submarine in a 3D environment like aeroplanes. This is discussed in the following section.

5.4.2 Hydraulic System

As a large piece of equipment, with estimated maximum lift forces around 100 to 200 MN (Appendix 9), a set of hydroplanes are typically actuated by the hydraulic system, though it may be replaced by the electric based actuator in the future. The hydraulic based actuator however provides a more compact actuator than its motor equivalent (Thornton, 1994). The adoption of a hydraulic based actuator also allows the use of a hand pump mechanism as a fall-back system. Besides actuating hydroplanes (Move function), the hydraulic system also provides vital power to many actuators on board the submarine, such as raising and lowering periscopes (Fight function), opening, and closing valves (Float function) subject to Design/Deep Diving Systems Test Pressure (DDSTP) (Burcher and Rydill, 1994). Submarine operational depth can be divided into three types: Deep Diving Depth (DDD); test depth (or DDSTP or Maximum Excursion Depth (MED) (Renilson, 2015)); and crush depth (or Minimum Collapse Depth (MCD) (Burcher and Rydill, 1994)). The test depth is typically slightly deeper than the DDD (typically 20% below DDD), while the MCD is a theoretical depth where the pressure hull is expected to fail.

Generally, there are two types of hydraulic system, as Burcher and Rydill (1994) outlined. The first type was known as the 'Telemotor System', which provides hydraulic power on demand. Powered by the electric motors in the telemotor system, this system needs to operate frequently, pumping the hydraulic fluid to the various actuators and thus creates undesirable noise emissions. Conversely, the second type of hydraulic system can be seen as advantageous in resulting in less impact on the level of acoustic signature. This is because the second type can provide constant hydraulic pressure using backed pressure accumulators, all in one package of the hydraulic plant. If the hydraulic liquid inside the accumulators drops below the standard operating condition, pumps within the system can be actuated to top up the hydraulic pressure in the accumulators. Whereas, to maintain the working hydraulic pressure in the accumulators, nitrogen gas is used, which is stored in air bottles and are part of the high-pressure air 'HP' system.

In this research, the configurational arrangement chosen for the hydraulic system consisted of four hydraulic plants: two for hydroplanes; one for internal demands; and one for external demands. Redundancy and diversity were achieved by two plants for the aft hydroplanes and rudders (AC and DC powered, respectively) and a plant each for internal (main) and external hydraulic demands. These plants and the users in the hydraulics were connected by hydraulic pipework. The highways of the hydraulic system could have been either port or starboard sides of the vessel. Without running a series of routing options for the hydraulic system, the usual high level of redundancy on existing submarines (typically triple redundancy on the vital hydraulic systems) was selected. Therefore, the connection between any two nodes in the hydraulic system was only modelled as a single arc but represent three pipelines. This model is the same as that used to quantify the size of the cableway, in the electrical power system discussed in Section 3.3.

However, unlike the case of sizing the cableway technology, the sizing of hydraulic pipework was based on the volume flow rate of the hydraulic fluid flow and the type of hydraulic fluid inside the pipework (see Appendix 9). In this case study, the volume flow rate of the hydraulic system was assumed to be 95 litres/min with the standard fluid, Renolin OX-30 (UCL-NAME, 2014).

There was a total of 13 nodes in the hydraulic system, which are listed in Table 5.8. Since the hydraulic system was adopted to provide power for many actuators on the submarine, Figure 5.20 shows the hydraulic system is connected to the Trim and Ballast 'TB' in blue and mast nodes in Figure 5.20 (top), part of the data 'DT' system or Fight functional group. The rest of the actuation demand on the vessel was modelled by a zoning approach via three distribution nodes (ND PD): forward; mid; and aft zones. As shown in Figure 5.20 (left), there are 15 demand nodes connected to the aft zone hydraulic node. The manual hand pump node was provided and connected to the aft zone node on top of the two redundant hydraulic plants for hydroplanes (HS DC/AC). Meanwhile, there are 14 demand nodes each connected to the mid and forward zone nodes. The internal (IT AC) and external (ET AC) hydraulic

plants are connected to the mid zone node. In summary, 12 nodes and 55 edges were modelled for the hydraulic system in this case study.

Table 5.8: List of nodes for the hydraulic system of Case Study 5.1

Node Identification				Description
BB_DB_HY (building block database hydraulic)	_HS	_DC		Hydroplanes and steering (plant) DC powered
		_AC		Hydroplanes and steering (plant) AC powered
	_IT	_AC		Internal (plant) AC powered
	_ET	_AC		External (plant) AC powered
	_ND	_PD	_(a/m/f) _(e)	Node power distribution (aft/mid/forward) (external)
	_RS	_RR		Ram servo rudder
		_HR	_(a/f)	Ram servo hydroplanes (aft/fwd)
	_FL	_PP		Fallback (hand) pump

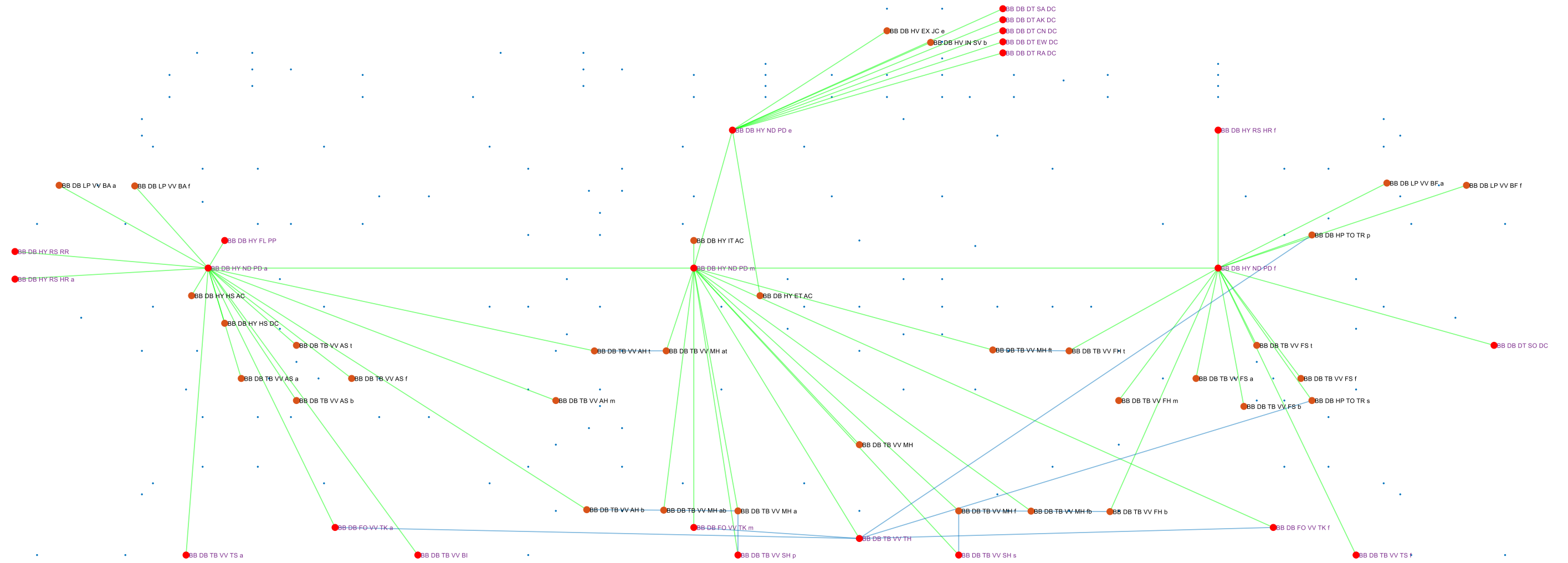


Figure 5.20: Network visualisation of the hydraulic 'HY' system (green lines) and the adjacent systems (trim and ballast systems in blue lines, see Subsection 5.5.3) where blue dots represent the overall DS3 nodes in Case Study 5.1 (Figure 5.4 on page 182)

As discussed previously, the hydraulic ‘HY’ system requires power from the ‘EL’ system to maintain its working pressure. The load of the hydraulic plant node $P_{HY_PT}^{snort/sprint}$ (HS, IT, and ET AC/DC) in the snorting and the sprint submerged operating conditions could be derived from the flow rate requirement as expressed in Equation (5.20). The required hydraulic capacity \dot{V}_{PT} on the vessel was estimated (90 litres/min) using an algorithm provided by the UCL submarine data (UCL-NAME, 2014) while the typical hydraulic working pressure p_{HY} is assumed to be 207 bar (Burcher and Rydill, 1994). Finally, an assumed load factor LF at each operating condition was necessary since the hydraulic plant nodes (HS, IT, and ET AC/DC) will not operate all the time.

$$P_{HY_PT}^{snort/sprint} = \dot{V}_{PT} \cdot p_{HY} \cdot LF_{HY_PT}^{snort/sprint} \quad (5.20)$$

The early visualisation of the hydraulic system routing is shown in Figure 5.21. This early visualisation shows that the routing is distributed throughout the submarine. The hydraulic pipeline is routed at the port side of the submarine, as already defined in Figure 5.8 on page 188. Figure 5.21 (top) shows the two redundant hydraulic plants for the diving planes (HS DC/AC) are situated in the engine room while the internal and external hydraulic plants (IT and ET AC) are arranged in the AMS. The total length of the HY system connection was 746 m.

Having considered the hydraulic system, the next section outlines another special system on the submarine that required a different formulation to what would be the case for any surface vessel application.

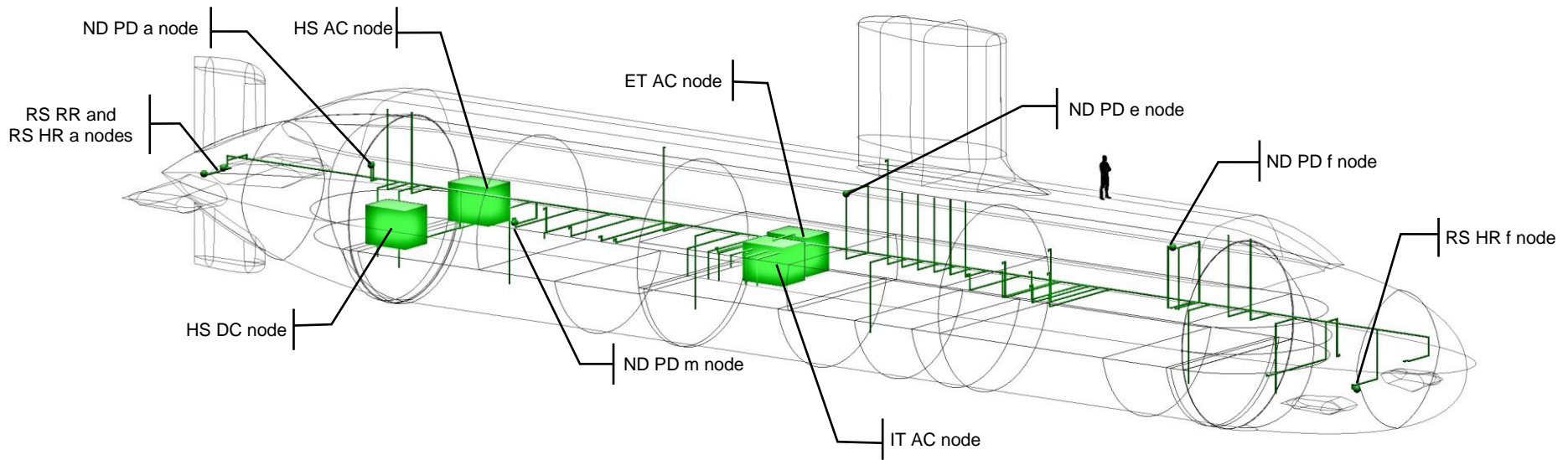


Figure 5.21: The initial model of the hydraulic 'HY' system of Case Study 5.1, showing the main HY system distribution in green

5.5 Systems for Hydrostatic Control

Unlike surface vessels, the submarine must have the ability to manipulate the buoyancy from positive (surface condition) to neutral (submerged condition) and vice versa as well as to maintain neutral buoyancy when submerged, for depth control. These abilities can be achieved using the high-pressure air 'HP' system, the low-pressure air 'LP' system, and the trim and ballast 'TB' system. Given the importance of these systems, the decision making related to these systems is substantial for ensuring safety of the submarine. Some submarine DS3 are designed to cope with unforgiving hydrostatic pressure due to various operational depths, more specifically the DDSTP. Thus, the capability to better estimate the provisions for vital DS3 is necessary for submarine ESD.

The HP system provides the ability to bring the submarine to the surface from the submerged condition. Another important role of the HP system is for the backup system. If the electrical 'EL' and hydraulic 'HY' systems for hydrodynamic control fail in an emergency during submerged, the HP system can be used to provide buoyancy for an emergency blow. This is because the HP system works based on pneumatic energy stored in high-pressure bottles, which can be operated independently of other systems. Therefore, as a backup system, the piping integrity of this system is important to ensure submarine safety. Considering the importance of the pneumatic energy stored in the HP bottles, the HP air is premium. Thus, the low-pressure air 'LP' system is usually used to conserve the HP air when blowing the Main Ballast Tanks (MBTs) at the periscope depth.

When submerged, the low-pressure trim and hard ballast 'TB' system is used to maintain hydrostatic balance. It was also decided to connect the TB system to the hard and low-pressure bilge system to discharge bilge water from any compartment to the sea. The configuration of the ballast and trim system depended on the arrangement of the trim tanks. In this case study, a three-tank arrangement was adopted as already been modelled in the volume objects (see Table 5.2), which was sized using an early stage estimation algorithm and could be refined by producing a trim polygon as the design progresses to cover the

full set of seawater densities and operating conditions (Burcher and Rydill, 1994).

5.5.1 High-Pressure Air System

In changing a submarine's state from submerged condition to surface condition, the high-pressure air 'HP' system and the low-pressure air 'LP' system are used. The HP system is used to partially discharge seawater from Main Ballast Tanks (MBTs). This gives positive buoyancy to the boat and once the boat is at the periscope depth, the LP system could be used to complete the discharging process of the MBTs to conserve the high-pressure air reserves. The HP system is also used to provide pneumatic service for mechanical actuation of equipment, such as starting the diesel generators or releasing high-pressure valves of the emergency or direct blow bottles, which are typically sited in the MBTs. This means in the event of the electrical power 'EL' system being lost throughout the boat, the emergency blow system could still be operated.

For Case Study 5.1 there was a total of 44 nodes in the high-pressure air 'HP' system (see Table 5.9). The high-pressure air is stored in the bottle group nodes (BO AG/FG) and is typically topped up by the high-pressure compressor nodes (CM DC) when the submarine has access to the atmosphere as in snorting or fully surfaced conditions. The high-pressure air produced by the compressors flows through the dryer node (DR PT) and is distributed using a ring main configuration as reflected in the DS3 network in Figure 5.22. Some bottles are usually filled with nitrogen to top up the accumulators for the hydraulic HY system. The reducing station node (AV RD) was also modelled to provide various pneumatic services, i.e., the auxiliary vent and blow systems at various pressures. However, the detailed nodes were modelled without geometric data for the ESSD application. As shown in Figure 5.22, the HP air system network in orange is connected to adjacent systems: hydraulic system in green as a fall-back system (especially for hydroplanes) and to provide top up for the hydraulic accumulators; exhaust system to blow exhaust pipe for snorting operation; trim and ballast systems in blue; and auxiliary vent and blow systems. The HP system could also be connected to breathing apparatus charging panels: Internal Compressed Air Breathing Apparatus (ICABA) and

Diving System Self Contained Compressed Air (DSSCA) (UCL-NAME, 2014), which were not modelled in this network.

The sizing of the high-pressure system was not subject to energy flow in the network. The piping connection can be sized directly with derived length to space and weight ratios (Appendix 9). The number of bottles was obtained numerically subject to several design parameters, such as the size of the MBT and the DDSTP. For a given size of the MBT, the deeper DDSTP increases the number of bottles required to perform a direct blow. To conserve the space due to the number of bottles, the capacity (in pressure) of the bottle matters. The range of capacity of each HP air bottle used for a military submarine is between 276 bar (Wrobel, 1984) to 300 bar (Thornton, 1994). The submarine's HP Air Compressor (HPAC) could then be selected based on desirable capacity (in m^3/hr), which is driven by: the number of the bottles to be charged; assumed working pressure (200-300 bar); and the charging time (in the snorting operation) (UCL-NAME, 2014). This implies the longer snorting time would reduce the required size or capacity of the HPAC for charging the bottles but is not desirable in terms of indiscretion ratio.

In this case study, the bottles were arranged into two main groups: forward and aft direct/emergency blow groups (each group has 4 bottles) and forward and aft bottle groups (each group has 13 bottles). Although the forward and aft groups include bottles for hydraulic top-up and Built-in Breathing System (BIBS), the BIBS requires its separated piping network with the Emergency Breathing Systems (EBS), which was sized parametrically in this case study since their size was very small (less than one tonne).

Table 5.9: List of nodes for the high-pressure air system of Case Study 5.1

Node				Description
BB_DB_HP (building block database high- pressure air)	_CM	_DC	_(p/s)	Compressor DC (assumed with DC motor) (port/starboard)
	_DR	_PT	_(p/s)	Dryer plant (port/starboard)
	_JC	_CM	_(p/c/s)	Junction adjacent to compressor (port/centre/starboard)
		_DR	_(c) _(pp/ps) _(sp/ss)	Junction adjacent to dryer (centre) (port-port/port-starboard) (starboard-port/starboard-starboard)
		_CA	_(pp/ps) _(sp/ss)	Junction adjacent to connection aft (port-port/port-starboard) (starboard-port/starboard-starboard)
		_AG	_(p/s)	Junction at aft group (port/starboard)
		_FG	_(p/s)	Junction at front group (port/starboard)
		_AV	(fp/fc/fs)	Junction adjacent to auxiliary vent (forward- port/centre/starboard)
		_PG	_(pp/ps) _(sp/ss)	Junction adjacent to starter for power generator (port-port/port-starboard) (starboard-port/starboard-starboard)
		_TR	_(pp/ps) _(sp/sp)	Junction adjacent to torpedo tubes (port-port/port-starboard) (starboard-port/starboard-starboard)
	_BO	_AG	_(p/s)	Bottle aft group (port/starboard)
		_FG	_(p/s)	Bottle forward group (port/starboard)
	_AV	_RD	_(a/f)	Auxiliary vent reducing station (aft/forward)
	_EB	_BG	_(a/f)	Emergency blow bottle group (aft/forward)
	_ST	_PG	_(p/s)	Starter power generator (port/starboard)
	_TO	_TR	_(p/s)	Torpedo tube Air Turbine Pump (ATP) demand (port/starboard)
_HY	_TU		Hydraulic top up (connection node)	
BB_DB_FF	_SS	_WC		Fire fighting

The only pull in the high-pressure air 'HP' system is the demand for the compressors as is expressed in Equation (5.21). The power required for the high-pressure air compressor in the snorting condition $P_{HP_CM}^{snort}$ could be based on the equipment manufacturer data with an assumed load factor LF .

$$P_{HP_CM}^{snort} = P_{HP_compressor}^{snort} \cdot LF_{CM}^{snort} \quad (5.21)$$

Although the components in the system were not sized by energy flow, the size of the high-pressure air connections was obtained using the network. The network approach aided the designer to capture the distribution style of the system, as well as the initial length estimation for the high-pressure air pipework on the vessel using the Logical and Physical Loop methods simultaneously.

Figure 5.23 shows the main components of the HP system in orange. Initially, the compressors (CM DC) were assigned to the engine room. However, it was found that the size of the compressor was quite big when physically modelled in Paramarine-SURFCON, and the engine room is already crowded with other DS3 components (see Figure 5.7 on page 187). As a resolution, it was decided to place the compressors (CM DC) in the motor room by first reassigning these components to the motor room and then graphically arranged in Paramarine-SURFCON.

The ring main distribution style of the high-pressure air system is routed at the port and starboard sides of the pressure hull (see Figure 5.23). The Air Turbine Pump (ATP) can be considered part of the HP system (as a user) or Fight functional group. There are 8 bottles dedicated for emergency blow and stored in the MBT while the rest of the bottles are divided evenly to the forward and aft of the vessel to maintain longitudinal balance. The HP bottles can be considered part of the HP system if modelled specifically in the HP system network or be kept as part of the Float functional group. The total length of the HP system connection was 708 m.

There are several practices where bottles are arranged on the vessel. As shown in Figure 5.23, the main bottles are situated under the casing, external to the

pressure hull, and thus create additional buoyancy. This, in turn, pushed the Centre of Buoyancy (CoB) of the vessel to a higher position, which was found to be about 2% higher compared to placing bottles internally in the pressure hull. Additionally, when bottles are located under the casing, it would provide easy access to replenish nitrogen bottles when in the base. Conversely, placing bottles internally in the pressure hull lowered the Centre of Gravity (CoG) of the vessel by around 1% compared to placing bottles under the casing. Placing bottles internally in the pressure hull would also lessen the number of hull penetrations required for the HP air piping system.

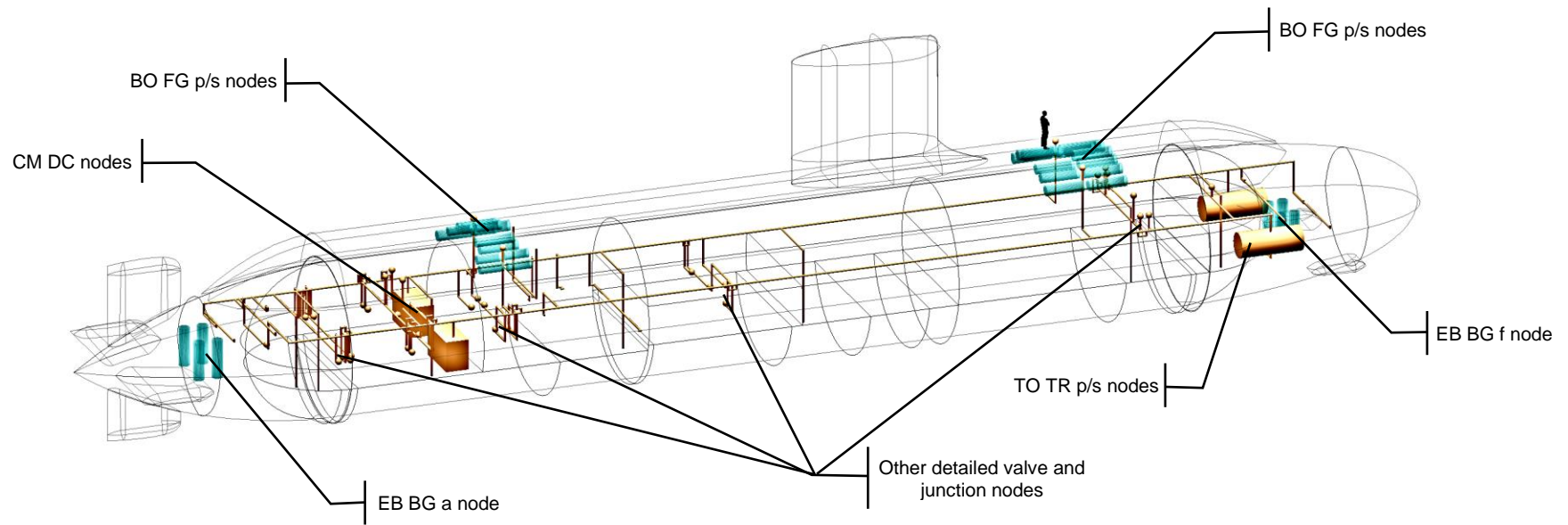


Figure 5.23: The initial model of the high-pressure air 'HP' system of Case Study 5.1, showing the HP system and ATPs in orange and HP air bottles part of the Float function

5.5.2 Low-Pressure Air System

To save the high-pressure air in the HP bottles from being used to fully blow the MBTs, the low-pressure air system would be normally employed. Another function of the low-pressure air system is to replenish the air inside the pressure hull when snorting. In this study, the low-pressure system consisted of a blower node and valves (total of 19 nodes) (see Table 5.10).

Table 5.10: List of nodes for the low-pressure air system of Case Study 5.1

Node				Description
BB_DB_LP (building block database low- pressure air)	_BR	_AC		Blower AC powered
	_JC	_BR	_(b/t) _(a/f)	Junction adjacent to blower (bottom/top) (aft/forward)
	_VV	_BR		Valve adjacent to blower
		_BA	_(a/f) _(ap/as) _(fp/fs)	Valve ballast aft (aft/forward) (aft-port/aft-starboard) (forward-port/forward-starboard)
		_TB		Valve trim ballast
		_BF	_(a/f) _(ap/as) _(fp/fs)	Valve ballast forward (aft/forward) (aft-port/aft-starboard) (forward-port/forward-starboard)

As shown in the middle part of Figure 5.24, the system takes the air inside the pressure hull via a blower node (BR AC) and is not connected physically to the snort valve part of the intake air system. The system could also be used to blow the trim tank at periscope depth or on the surface and thus it is connected to a valve node (VV TB), part of the trim and ballast 'TB' system.

In the snorting operating condition, the power demand $P_{LP_BR}^{snort}$ at the LP blower node (BR AC) is one of the pulls in the DS3 network and is expressed in Equation (5.22) with an assumed load factor LF . Like other DS3 components, this could be based on the equipment manufacturer data provided that the flow rate requirement can be derived or assumed.

$$P_{LP_BR}^{snort} = P_{LP_blower}^{snort} \cdot LF_{BR}^{snort} \quad (5.22)$$

Although the blower node (BR AC) was one of the demands of the electrical 'EL' system, the size of the low-pressure air 'LP' system was not driven by the energy flow in the network (Appendix 9). The blower was able to be sized based on the air change requirement or the flow rate required to displace seawater from MBT for surfacing. In this case study, this requirement was assumed to be 43m³/min at 1 bar (UCL-NAME, 2014). Meanwhile, the size of the low-pressure air pipework was calculated using the Physical and Logical Loop methods. Figure 5.25 (top) shows the LP blower (BR AC), situated in the Auxiliary Machinery Space (AMS), which distributes low-pressure air service using a pipeline that runs to the forward and aft Main Ballast Tanks (MBTs) under the casing, outside of the pressure hull. Figure 5.25 (bottom) shows that the LP system is not connected physically to the snort valve part of the intake air system shown in blue. The total length of the LP system connection was 161 m.

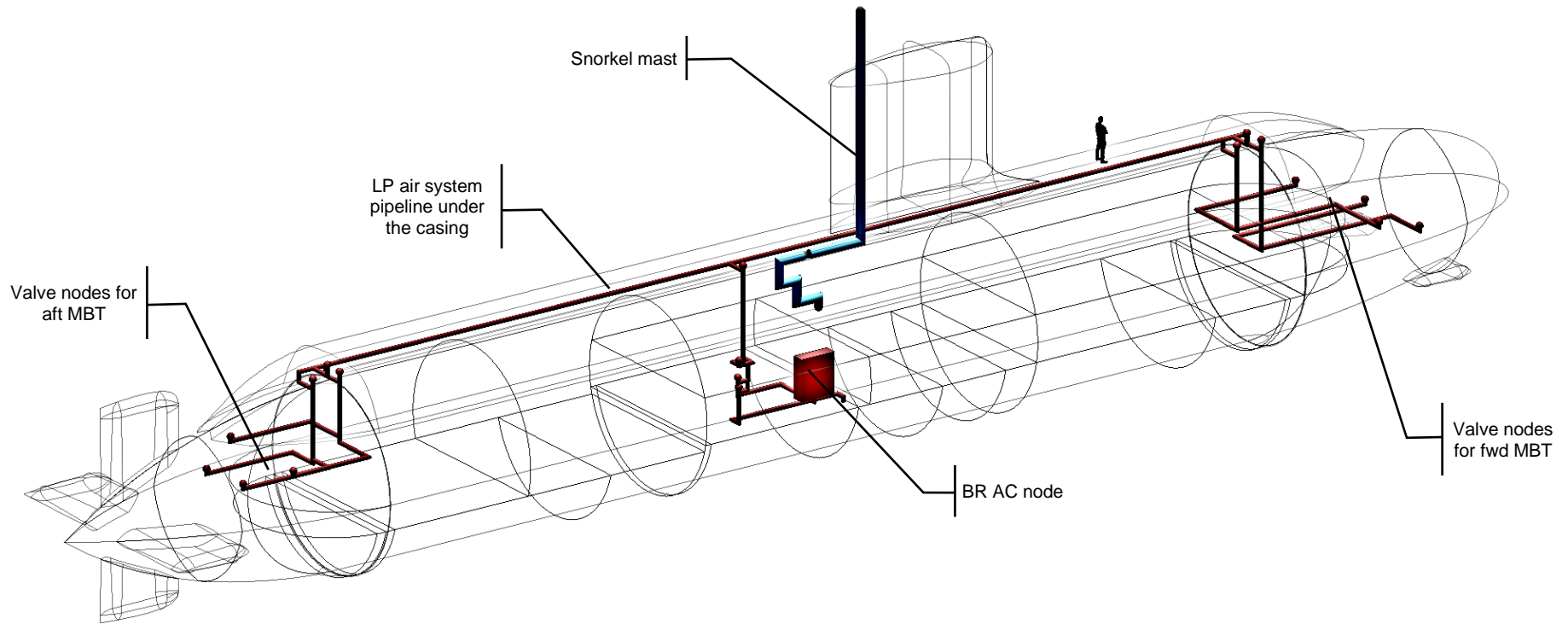


Figure 5.25: The initial model of the low-pressure air 'LP' system of Case Study 5.1, showing the LP system in red and the snorkel mast in blue

5.5.3 Trim and Ballast System

The components and piping connections in the trim and ballast 'TB' system would require more margins to cover allowance for corrosion as this system is in direct contact with seawater. Furthermore, since the 'hard' ballast and bilge systems are subject to Design/Deep Diving Systems Test Pressure (DDSTP), the size of the pumps, valves, and the piping of this system would be relatively larger than (internal) 'soft' (low-pressure) trim and bilge systems. Unlike other DS3 connections, DDSTP pipework should not be designed in the straight system runs to allow for sufficient flexibility when hull compression and contraction occurs (Burcher and Rydill, 1994). Although such a complex routing is unlikely to be resolved in ESSD, multiple highways could be dedicated or reserved for DDSTP pipework using the System Preamble Program (SPP), as already reflected in Figure 5.8 on page 188.

The options for DDSTP pumps are screw positive displacement (vertical) pumps or centrifugal pumps. One of the advantages of using vertical pumps is that it uses less pipework compared to centrifugal pumps given vertical pumps are bidirectional. However, vertical pumps require more space than centrifugal pumps producing the same output levels (Stewart, 2018). For that reason, centrifugal pumps were used for this case study. The further selected style choice for connection was the redundant distribution to mirror each pump capability. Nodes in the trim and ballast 'TB' system are listed in Table 5.11.

The TB system network given in Figure 5.26 shows the Logical Loop method allows detailed TB configuration consisting of 47 nodes and 59 arcs to be modelled at ESSD. The trim and ballast 'TB' system was connected to the bilge system via a bilge valve node (VV BI). The TB system was also connected to various systems via the mid fuel valve node (VV TK) to provide the ability to manipulate water distribution on the vessel, such as the fuel oil 'FO' system and intake air system. Meanwhile, the forward trim tank valve node (VV AS f) was connected to various junctions and valve nodes from the forward junction node (JC TS f) to the aft junction node (JC TS a) and subsequently to the aft trim tank valve node (VV AS a). Due to the importance of the 'hard' pump, it was decided

to diversify the selection of the pump, e.g., DC powered pump at the aft (PH DC) and AC powered pump at the forward (PH AC).

Table 5.11: List of nodes for the trim and ballast 'TB' system for Case Study 5.1

Node			Description
BB_DB_TB (building block database trim and ballast)	_VV	_BI	Valve bilge
		_AS	Valve aft soft (bottom/top) (aft/forward)
		_TS	Valve trim soft (aft/forward)
		_FS	Valve forward soft (bottom/top) (aft/forward)
		_AH	Valve aft hard (mid bottom/top)
		_MH	Valve mid hard (aft bottom/top) (bottom/top) (aft/forward) (forward bottom/top)
		_FH	Valve forward hard (aft/mid/top)
		_TH	Valve trim hard
		_SH	Valve sea chest hard (port/starboard)
	_JC	_AS	Junction aft soft (aft/mid/forward)
		_FS	Junction forward soft (aft/mid/forward)
		_AH	Junction aft hard (bottom/top)
		_FH	Junction forward hard (bottom/top)
		_TS	Junction trim soft (aft/forward)
	_PB	_AD	Pump bilge AC & DC
	_PS	_AC	Pump soft AC powered (aft/forward)
	_PH	_DC	Pump hard DC powered (aft)
		_AC	Pump hard AC powered (forward)

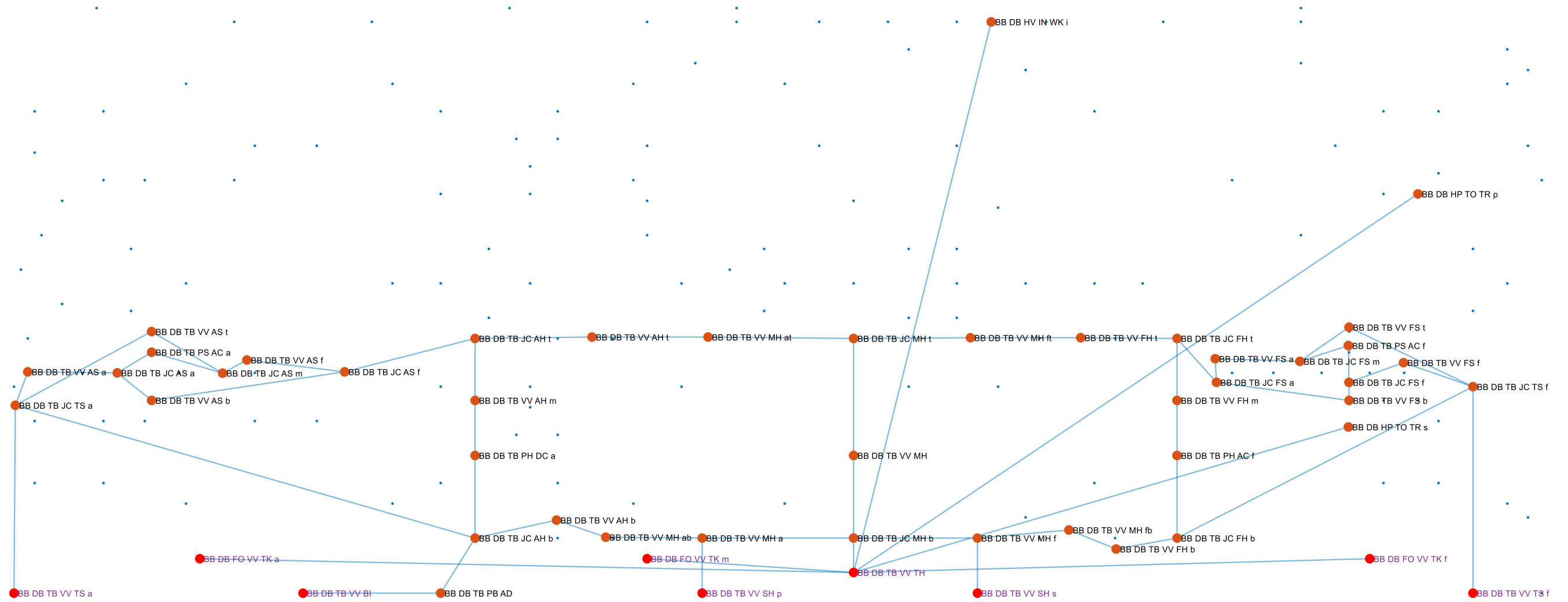


Figure 5.26: Network visualisation of the trim ballast and bilge 'TB' system (blue lines) and the adjacent systems where blue dots represent the overall DS3 nodes in Case Study 5.1 (Figure 5.4 on page 182)

As part of the hotel load, the power pull due to the pump nodes (TB PP) is expressed in Equation (5.23). The power required for such pump nodes (TB PP) was assumed to be online to maintain the trim of the submarine during both surfaced and submerged modes. It was found that the frictional loss for a 100-meter length of a pipeline is comparable to a 2 m pressure head or hydrostatic pressure at one meter depth. Therefore, the power pump $P_{TB_PP}^{snort/sprint}$ was largely governed by the DDSTP, i.e., the hydrostatic pressure p_{DDSTP} , rather than the loss of pressure due to the pipe friction p_{loss} . Still, the use of margin m_{PP} was necessary to cover uncertainty. In this case study, the volume flow rate requirement \dot{V}_{PP} was assumed to be 22 m³/min (UCL-NAME, 2014).

$$P_{TB_PP}^{snort/sprint} = \dot{V}_{PP} \cdot (p_{DDSTP} + p_{loss}) \cdot (1 + m_{PP}) \quad (5.23)$$

The size of the TB system was also not driven by the energy flow in the network (Appendix 9). The sizing of the TB nodes was subject to the volume flow rate requirement \dot{V}_{PP} . Therefore, the initial physical routing check of the ballast and trim system is given in Figure 5.27. As previously depicted in Figure 5.26, two internal ‘soft’ and high-pressure ‘hard’ pumps are situated at the forward and aft part of the pressure hull. Some valves and junctions are assigned to the AMS. As expected, the pumps that are subject to DDSTP look bigger than the internal ‘soft’ pumps. However, both pumps were able to be fitted in the relevant compartment objects, showing the system was initially feasible within the 3D layout. The total length of the TB system connection was 772 m.

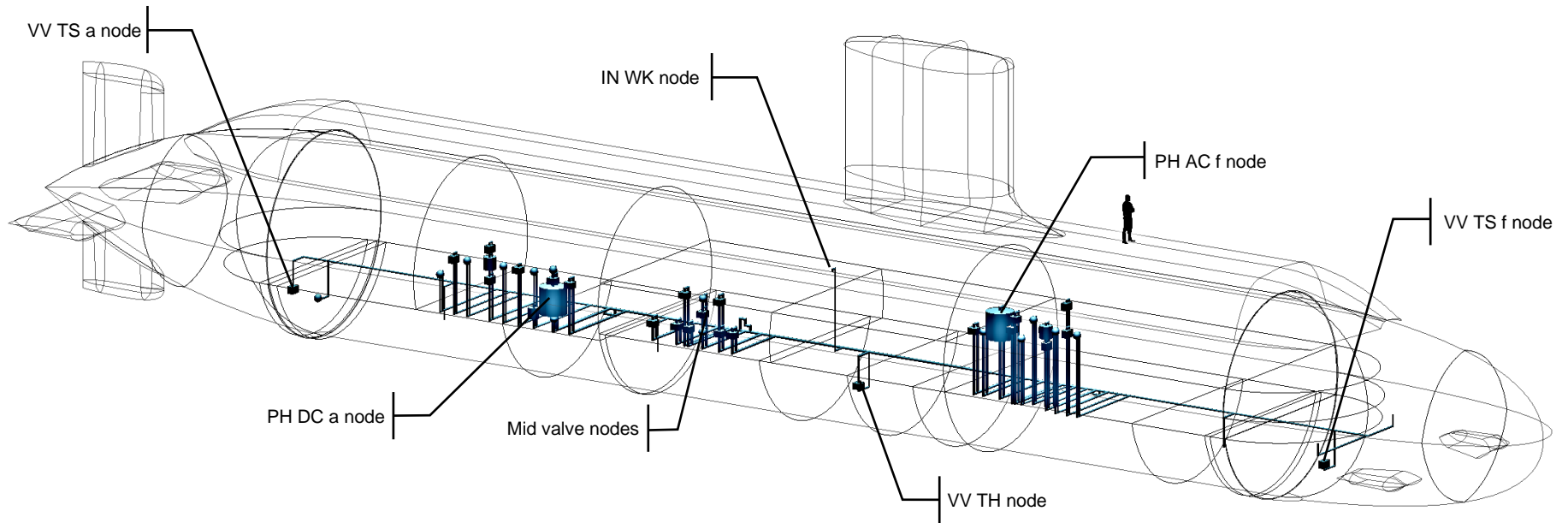


Figure 5.27: The initial model of the trim and ballast 'TB' system of Case Study 5.1 in blue

5.6 Information Data System

The data system not only provides surveillance to the components onboard the submarine but also controls the submarine functioning via information or data service, which covers complex Command Management System (CMS) as well as navigation. As one of the vital systems on the submarine, a manual fall-back capability is also needed to anticipate if the data system fails. Due to the advancement of computer technology, the data system could be considered as one of the most disruptive systems on the vessel. The choice of data cables, for example, can vary from conventional copper to fibre optics. However, in this case study, the data system was developed based on the available data on the UCL Submarine Databook (UCL-NAME, 2014) (see Figure A.20 in Appendix 1) and the surface ship data (Stinson, 2019). The configuration includes combat systems (CPUs and Consoles), ship control systems (Ship Control Console), and propulsion systems (Machinery Control Console). There was a total of 14 nodes in the data system network as given in Table 5.12. Those 14 nodes are connected by 63 arcs as shown in Figure 5.28.

Table 5.12: List of nodes of the data system of Case study 5.1

Node				Description
BB_DB_DT (building block database data)	_CO	_AC	_(a/f)	Command console (AC powered) (aft/forward)
	_PU	_AC		Central Processing Unit (CPU) (AC powered)
	_SC	_DC		Ship Control Console (SCC) (DC powered)
	_MC	_DC		Machinery Control Console (MCC) (DC powered)
	_DD	_LC	_(a/m/f)	Data distribution load centre node (aft/mid/forward)
		_AN	_(p/s)	Data distribution aft node (port/starboard)
		_MN	_(p/s)	Data distribution mid node (port/starboard)
		_FN	_(p/s)	Data distribution forward node (port/starboard)

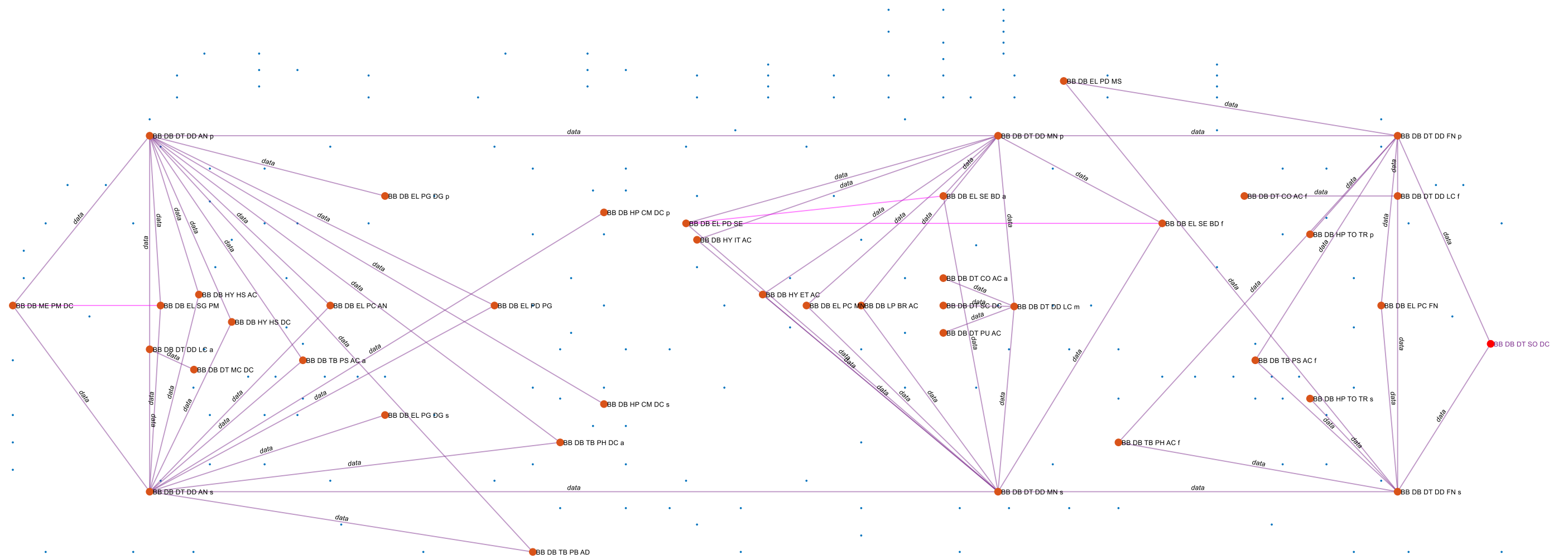


Figure 5.28: Network visualisation of the data 'DT' system (purple lines) and the adjacent 'EL' and mechanical 'ME' systems where blue dots represent the overall DS3 nodes in Case Study 5.1 (Figure 5.4 on page 182)

The development of the network for the data system was defined as a node-to-node connection using the System Connection Program (SCP) (Table 4.1 on page 145). However, compared to other energy based systems, arcs that connect data nodes are simultaneous (two ways) and they were modelled to carry string data instead of numerical (energy or even binary) data. Therefore, the size of each arc could be developed using length to weight and space ratios (see Appendix 9). This approach not only could reduce the computational time in the Logical Loop method (due to a simpler network formulation), but also makes it arguably suitable for early-stage design applications. Most of the user components in the data 'DT' system are already formulated in Subsection 5.3.2. Figure 5.28 shows that the DT system uses ring distribution, adopting zones: aft, mid, and forward. Each zone employs a pair of bus nodes and a CMS node or a distribution node (DD LC). The size of these nodes was adopted from open source surface ship data (Stinson, 2019).

The logical network was then translated to the physical routing of the data system as shown in Figure 5.29. The bus nodes for the aft, mid, and forward zones were located in the motor room, control room, torpedo room objects, respectively. Figure 5.29 shows that the bus and data distribution nodes were arranged such they can be placed in the same compartment. The DT system was routed around the centre of the boat but split to the port and starboard sides of the vessel to represent the ring distribution style (as defined in Figure 5.8). Figure 5.29 also shows the DT system with some Fight components. Some of these Fight components, such as the bow sonar and masts, were included in the DT system since these were already modelled in the network. The total cabling length of the DT system was 711 m.

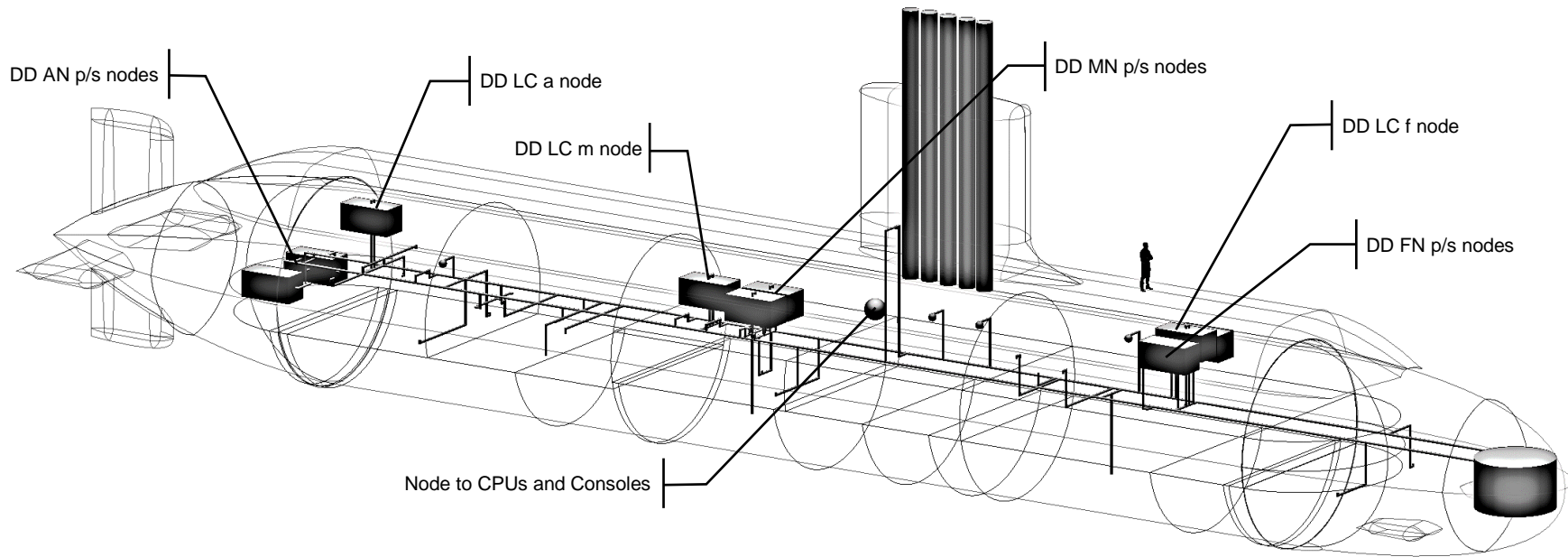


Figure 5.29: The initial model of the information data 'DT' system of Case Study 5.1 in dark grey

5.7 Heat Removal System

Every hub and user node in the overall DS3 network is not 100% efficient in converting electrical energy to work. This means some of the energy output is transformed to heat waste. Some of this can be dissipated directly to the environment via the pressure hull. However, the rest of the heat waste needs to be removed from the vessel using the heat removal system, which is part of the Heating Ventilation and Air Conditioning (HVAC) DS3. As with other DS3, the main SSK style choice influences the architecture of the HVAC system. For an SSK, the HVAC system is also important to replenish the atmosphere on the vessel from the contaminants, such as hydrogen from the battery during charging as well as to provide breathable air for the personnel (Burcher and Rydill, 1994). In this case study, the DS3 style chosen for HVAC was to adopt several separate systems as the cooling medium: air 'HV'; chilled water 'CW'; freshwater and seawater 'FW SW'; and lubricant oil 'LO'. The seawater SW system is subject to operational depth as this system aims to discharge heat through seawater.

Figure 5.30 depicts the high level network for the SSK's style example. This covers the heat removal subsystems and other systems that produce waste heat, such as electrical 'EL', mechanical 'ME', and data 'DT'. The electrical system, such as diesel prime mover requires air (see light blue lines in Figure 5.30) to convert fuel to electrical energy (see purple lines in Figure 5.30). As discussed in Subsection 5.3, this electrical energy is the power source on the vessel for various functions. Some of the energy is transformed to heat loss (see yellow lines in Figure 5.30) and then dissipated to the environment via exhaust air and the pressure hull. This is shown in the numerical node/box (NL EV) in Figure 5.30. For submarines operating in a low seawater temperature like in northern Europe, they likely get a less demanding load for the heat removal system because of the 'free cooling' effect through hull heat transfer (Hemsley, 2015). As demonstrated in Subsection 3.2.5, the cooling demands in the SUBFLOW were calculated based on the assumed efficiency at each user node. This was initially found to be larger than the cooling load of the baseline design. The use of such a numerical node (NL EV) improved the result

and thus the cooling demands calculated using SUBFLOW were more relatable to the baseline design. The rest of the waste energy (see yellow lines in Figure 5.30) is removed via air (Air Treatment/ Handling Unit (ATU)), chilled water 'CW', lubricant oil 'LO', freshwater and seawater 'FW SW' heat exchangers (HX). Each heat exchanger (HX) has a 'Coefficient of Performance' (CoP) which defines how much electrical energy would be needed to remove the total heat energy coming into that system. Each CoP is the main input to determine the size of each cooling plant.

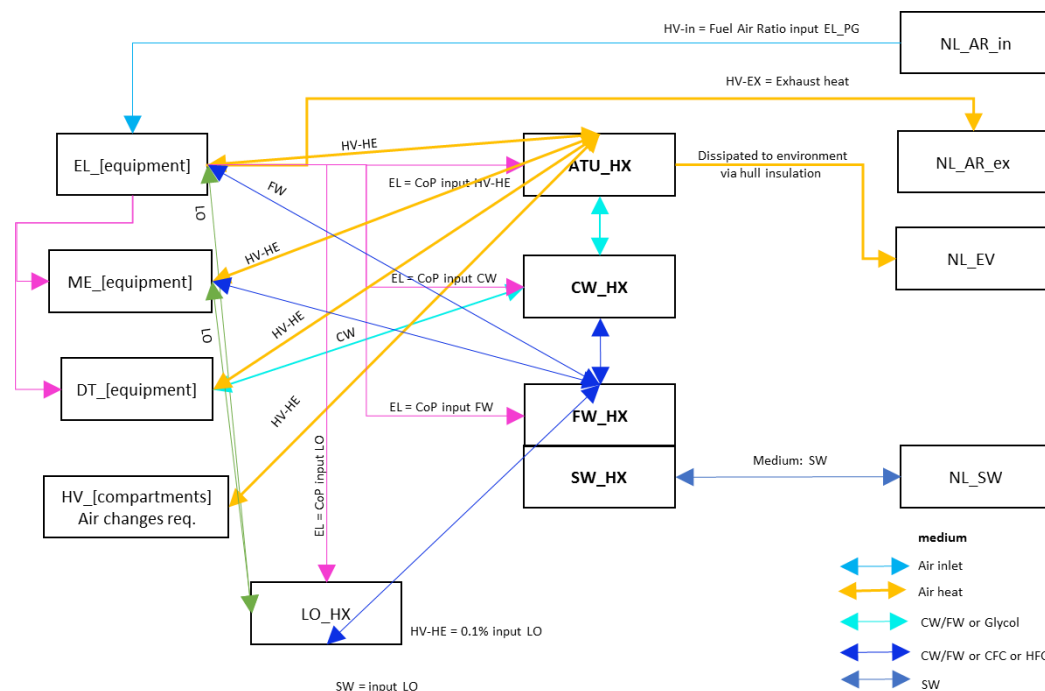


Figure 5.30: High level relationship between various cooling mediums in the heat removal system of Case Study 5.1

Figure 5.30 shows that arcs related to heat exchangers have two arrows reflecting the supply and return in the cooling systems. The fluid captures the heat energy (via supply line) and releases it (via return line) from systems to systems until it leaves the vessel via the submarine's seawater system. Unlike the AFO modelling of the heat removal system (Parsons, 2019), each loop in SUBFLOW was modelled as a single arc rather than two explicit supply and return arcs. This aided the designer to focus on how much energy was being removed by each plant without excessive marine engineering details, which suited the ESSD application. This also meant that the trace flow formulation

adopted by the AFO (Robinson, 2018) is no longer needed, leading to fewer computations for the SUBFLOW used. The provision of these supply and return lines could be adjusted directly in the System Preamble Program (SPP). Nodes for the heat removal system are given in Table 5.13.

Table 5.13: List of nodes for the heat removal system of Case Study 5.1

Node				Description
BB_DB/NL_HV (building block database/ numerical heating ventilation air conditioning)	_IN	_SV	_(b/t) _(i)	Intake air snort valve (bottom/top) (internal)
		_WK	_(i/e)	Intake air water trap tank (internal/external)
		_AR		Air intake
	_HE	_EN		Heat in engine room (database/numerical)
		_MR		Heat in motor room (database/numerical)
		_AM		Heat in AMS (database/numerical)
		_OF		Heat in messes, etc. (database/numerical)
		_AO		Heat in accommodation (database/numerical)
		_CO		Heat in control room (database/numerical)
		_WC		Heat in WSC (database/numerical)
		_BA		Heat in battery aft (database/numerical)
		_BF		Heat in battery forward (database/numerical)
		_FA	_(i/o)	(battery) fan aft (in/out)
		_FF	_(i/o)	(battery) fan forward (in/out)
	_AT	_(p/s)	Air treatment unit / air handling unit (port/starboard)	
	_EX	_EV		Exhaust/exit air environment
		_SI	_(p/s)	Exhaust air silencer (port/starboard)
		_VV	_(p/s)	Exhaust air valve (port/starboard)
		_VA	_(p/s)	Exhaust air valve (Kingston valve) (port/starboard)
		_JC	_(p/s) _(e)	Exhaust air junction (port/starboard/external)
		_SR	_(e)	Exhaust air snort mast (external)
_CE		_(p/s)	Casing exhaust (port/starboard)	
BB_DB_LO	_PT	_HX	Lubricant oil heat exchanger plant	
BB_DB_CW	_PT	_HX	_(p/s)	Chilled water heat exchanger plant (port/starboard)
BB_DB_FW	_SW	_HX	_(p/s)	Freshwater seawater heat exchanger plant (port/starboard)

Nodes listed in Table 5.13 are visualised in Figure 5.31, showing 48 nodes and 118 arcs in the heat removal system.

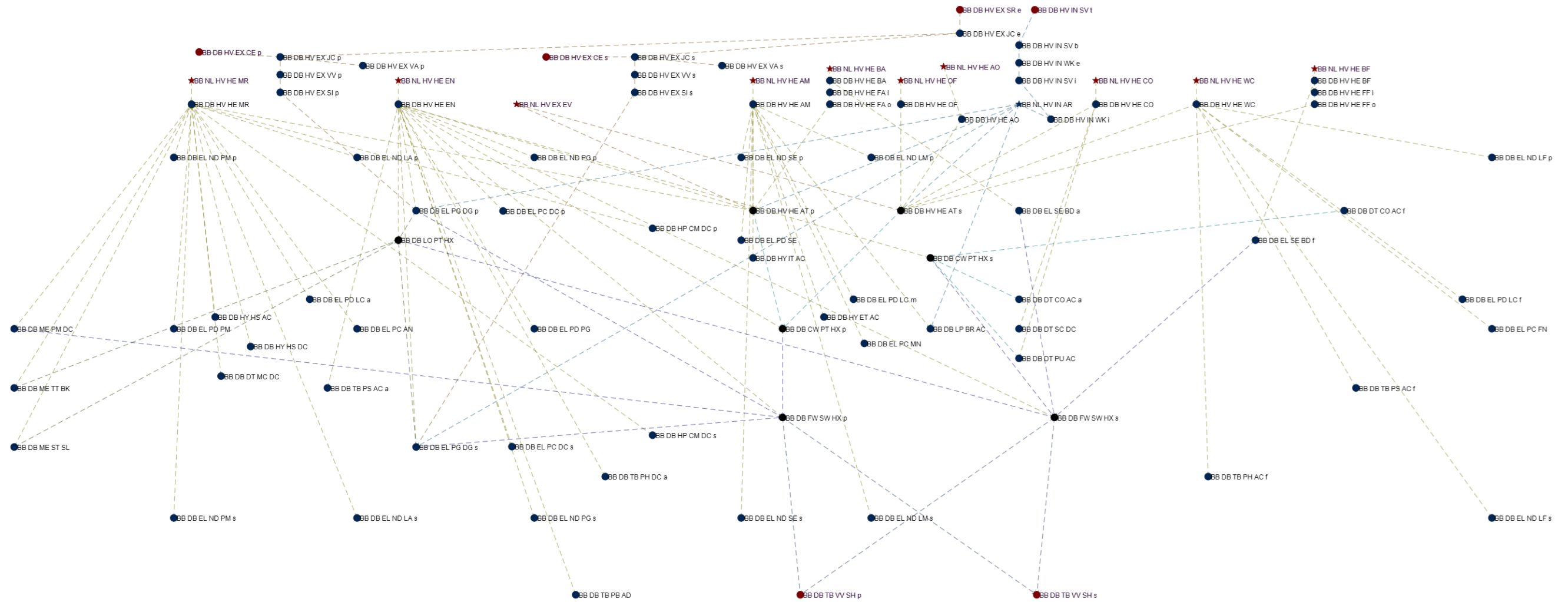


Figure 5.31: Network visualisation of the heat removal system (see Figure 5.30 for colour description) where the blue dots represent the overall DS3 nodes in Case Study 5.1 (Figure 5.4 on page 182) are hidden for clarity

As shown in Figure 5.31, the ventilation systems are categorised into three different stages. The first stage, HVIN, was the intake of fresh air through the snort mast (coloured bright blue). The second stage, HVHE, was the hot air radiated from equipment (coloured yellow). In the submerged operation, the HVHE system also worked as the atmosphere control system of the submarine, to ensure the controlled quality of the air, which include the use of the CO₂ scrubber and oxygen candles or LOX tank from the AIP system, could be distributed through various operational spaces on the submarine. The last stage, HVEX, is the hot air leaves the vessel through the exhaust (coloured dark yellow) where silencers are used to manage the acoustic signature of a submarine (Howard, 2010). Figure 5.31 shows some systems remove the heat from their adjacent systems. These systems were the lubricant oil 'LO' system (coloured green), the chilled water 'CW' system (coloured cyan), the freshwater 'FW' system (coloured dark blue) and the seawater 'SW' system (coloured blue). As shown in Figure 5.31, several physical nodes at each major compartment, such as the motor room (HE MR) and the engine room (HE EN), are used to capture the heat emanated from all hub nodes. Unlike the AFO (Parsons et al., 2020a), the heat flows from hub nodes were explicitly modelled as yellow arcs but they did not possess geometric data.

The overall heat removal system was part of the hotel load and one of the major demands in the vessel. To calculate this load, the heat load of each compartment on the submarine must be known. In detailed calculation, such a load could be estimated using a psychometric chart (ASHRAE, 2017) by first assuming many design parameters in ESSD, such as the dry bulb temperature, specific humidity of various air conditions, and subsequently determining the temperature in each compartment (Hemsley, 2015). The SUBFLOW provided an alternative approach to calculating the heat load, as already illustrated in Figure 3.9 on page 105. Similar to the AFO (Parsons et al., 2020a), SUBFLOW could also accurately estimate the total cooling demand in each compartment if the heat emanated from all hub nodes within that compartment is known. Nonetheless, such information is unlikely to be available at concept sizing without the use of an extensive equipment database. As an alternative, a rule of thumb air change per hour (ACH) data from the UCL Submarine Databook

(UCL-NAME, 2014) was used to estimate the total heat of some compartments. However, this also would reduce the sensitivity of the SUBFLOW in terms of capturing heat from different style decisions, e.g., the use of more redundant bus nodes will likely produce more cooling demands, which will not be captured by the previous air change requirement data.

Thus, the heat load at the compartment (room) is given in Equation (5.24) that consists of the volume of the compartment or room V_{RM} , the air change requirement ACH_{RM} , the specific heat of air cp_{air} , and the normal temperature difference between hot and cold sides ΔT_{air} . The ΔT_{air} was assumed to be 10°C . Using the UCL Submarine Databook (UCL-NAME, 2014), the calculated cooling demand can be visualised (see Figure 5.32).

$$P_{HV_HE_RM}^{snort/sprint} = V_{RM} \cdot ACH_{RM} \cdot cp_{air} \cdot \Delta T_{air} \quad (5.24)$$

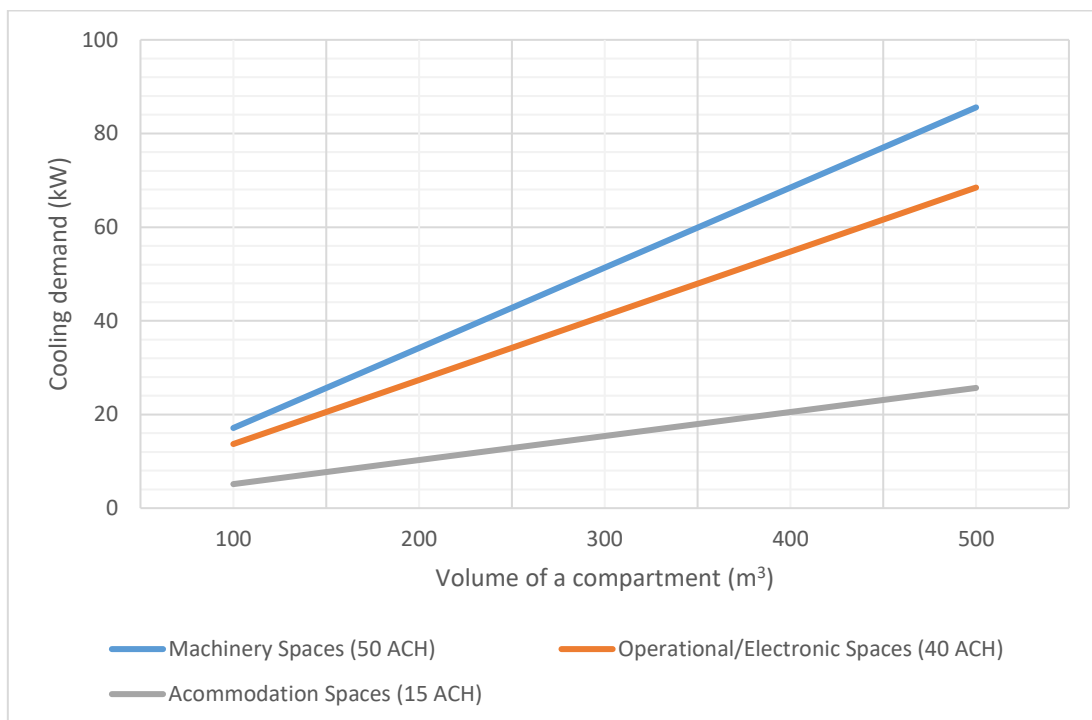


Figure 5.32: Parametric cooling demand and volume with an assumed ΔT_{air} at 10°C based on the air change requirement ACH_{RM} from UCL Submarine Databook (UCL-NAME, 2014)

Once the heat load had been estimated, the hotel load for the heat removal system could be calculated. This could be based on the ratio of the total heat ΣHE removed by the heat exchanger to the work required by the heat

exchanger, i.e., the Coefficient of Performance (CoP). In ESSD, the CoP value could be assumed or be based on the heat exchanger's manufacturer data and thus the power demands for various heat exchangers P_{HX} in the snorting/sprint submerged condition are provided in Equations (5.25) to (5.28).

$$P_{HV_HE_AT_p/s}^{snort/sprint} = \sum HE_{EX_p/s} \cdot CoP_{ATU} \quad (5.25)$$

$$P_{LO_PT_HX}^{snort} = \sum HE_{LO_p/s} \cdot CoP_{LO_HX} \quad (5.26)$$

$$P_{CW_PT_HX_p/s}^{snort/sprint} = \sum HE_{CW_p/s} \cdot CoP_{CW_HX} \quad (5.27)$$

$$P_{FW_SW_HX_p/s}^{snort/sprint} = \sum HE_{FW_p/s} \cdot CoP_{FW_SW_HX} \quad (5.28)$$

In the initial iteration of the Logical Loop method, the air intake system was modelled to quantify airflow for the heat removal system. However, the size of the intake air system for the SSK was found to be largely governed by the need to provide air for the diesel to operate. The internal pressure will drop abruptly and can make all personnel suffocate if the diesel engine operates without the air supplied by the intake air 'HVIN' system. Therefore, to sufficiently size the HVIN system, the fuel-air ratio assumption was used. The fuel-air ratio for diesel is higher than petroleum fuel, which is around 1:25, i.e., 25 kg of air is needed to burn 1 kg of diesel (Harrington, 1992). This resulted in a very large power flow in the HVIN system. Thus, a simplifying assumption was made to simulate the fuel air ratio requirement instead of using the actual fuel air ratio (see Appendix 9). The SUBFLOW result for the intake air system is given in Figure 5.33 reveals 2.2 MW of energy flow through this system. This numerical data can then be used to size the diameter of the air intake 'HV IN' system. In the submerged condition, all arcs in the HVIN system were zero, reflecting the physics of the SSK.

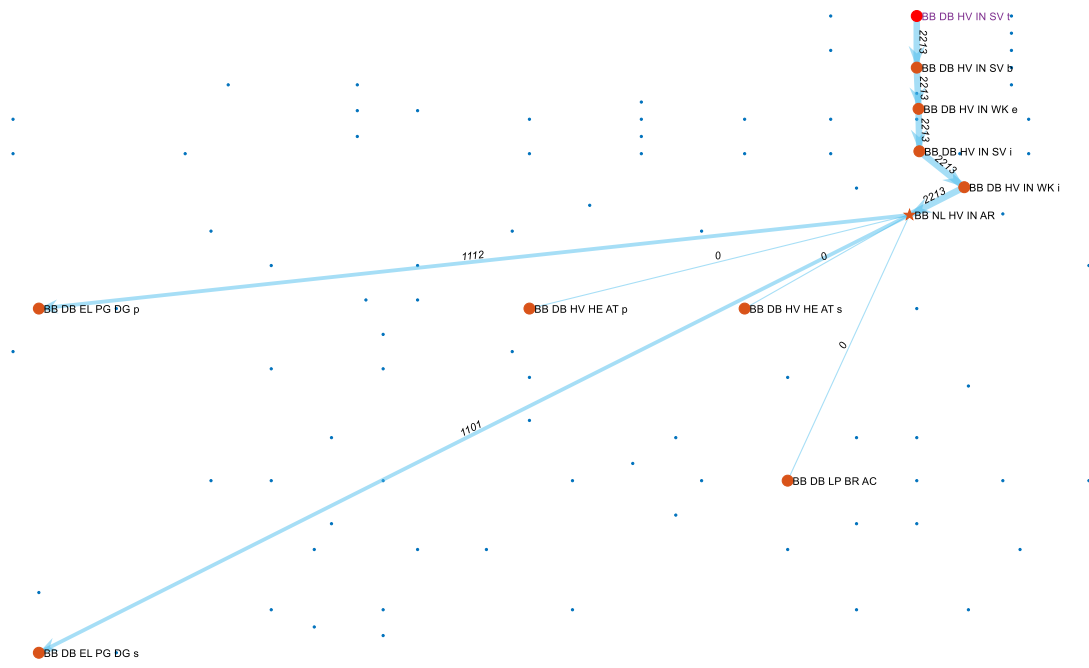


Figure 5.33: SUBFLOW solution of the air intake 'HV IN' system (blue lines) of Case Study 5.1 in the snort condition where the blue dots represent other DS3 nodes in Case Study 5.1 (Figure 5.4 on page 182)

The SUBFLOW result for the exhaust system is given in Figure 5.34. Figure 5.34 (top) shows the result in the snorting operation where the diesel generator nodes (PG DG) at the port and starboard sides of the vessel emanate 1 MW heat flow to the silencer node (EX SI). Passing through several valves and junctions, the heat flow from both sides of the vessel merged at the external junction node (EX JC e) and subsequently leave the submarine through the exhaust mast node (EX SR). The arc between the junction node (EX JC) and casing exhaust head node (EX CE) shows zero in this snorting condition. However, this arc can be sized at 1 MW for surface running operation where the exhaust gas can flow through the exhaust under the casing. Meanwhile, in the sprint submerged condition, Figure 5.34 (bottom) shows the exhaust nodes have zero flow, reflecting no access to the surface atmosphere. However, there were 192 kW and 26 KW heat flows from the ATU nodes (HE AT) at the port and starboard sides, respectively, due to the loss from the DS3 systems in the sprint submerged condition. Such numerical flows were released to the environment to avoid overestimated cooling demands of the heat removal system.

Section 5.7: Heat Removal System

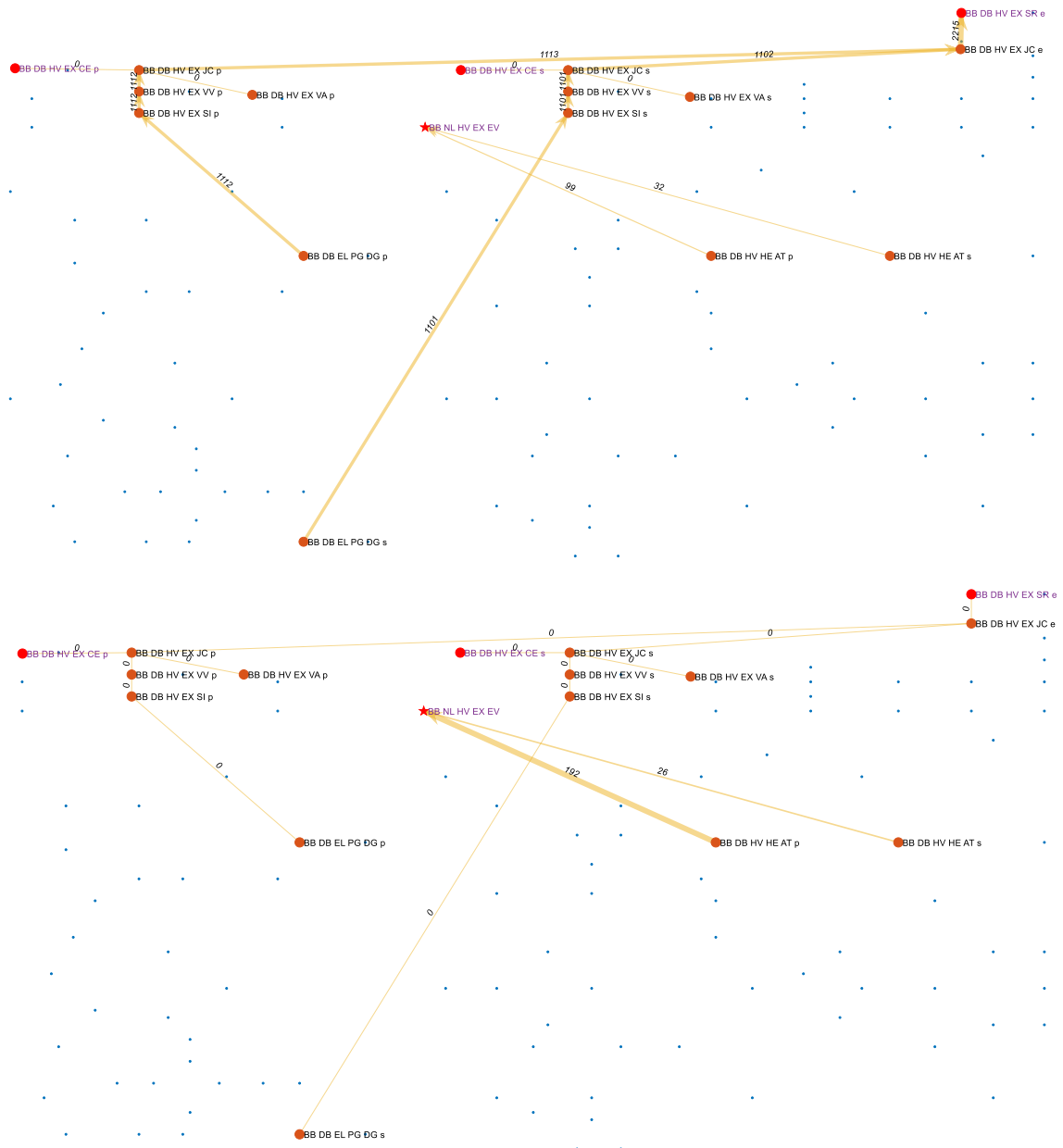


Figure 5.34: SUBFLOW solution of the exhaust 'HV EX' system (yellow lines) of Case Study 5.1 in the snort condition (top) and the sprint submerged condition (bottom) where the blue dots represent other DS3 nodes in Case Study 5.1 (Figure 5.4 on page 182)

The SUBFLOW results for the chilled water 'CW' system in the snorting and sprint submerged conditions are given in Figure 5.34 (top) and (bottom), respectively. As expected, in the snorting condition, the cooling demands for CW were 34% lower than when in the sprint submerged condition. This was because, in the sprint submerged condition, the ATU received more heat losses from other DS3 components, more specifically, the EL and ME components. Similarly, at the starboard side of the vessel, the cooling demand for the CW in the snorting condition was 30% lower than the submerged condition due to assumed load factors applied to the payload equipment, e.g., the CPU (PU AC) and CC (CO AC) nodes. Based on this result, the CW plant nodes at both sides of the vessel could be sized at about 65 kW capacity, which excluded margins for uncertainty.

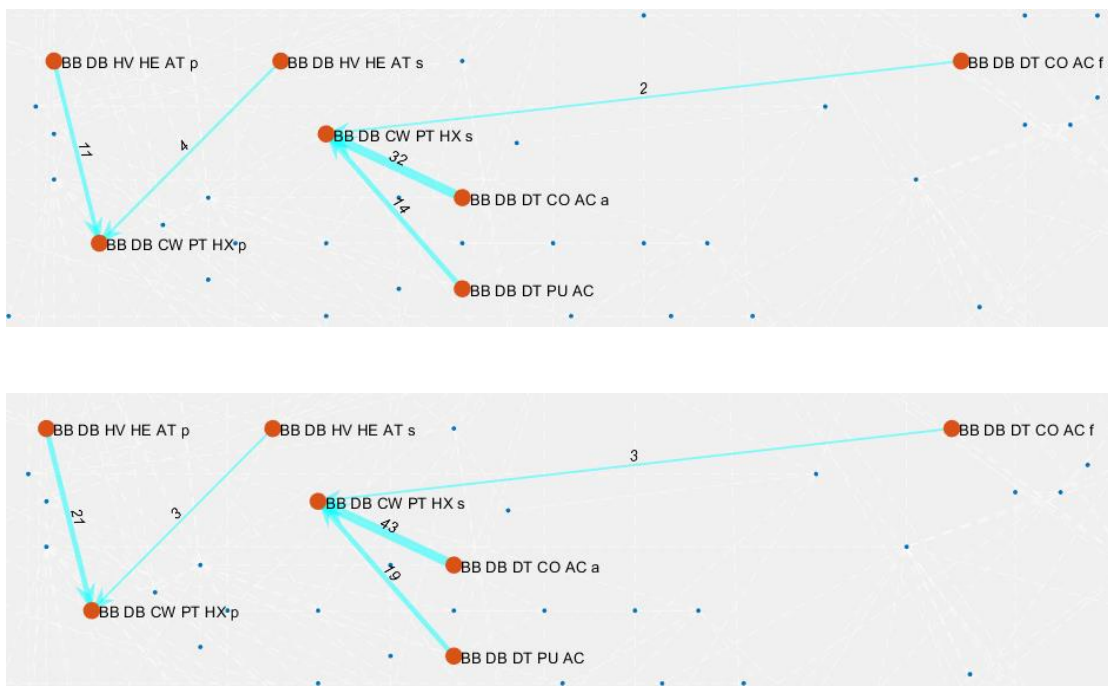


Figure 5.35: SUBFLOW solution of the chilled water 'CW' system (cyan lines) of Case Study 5.1 in the snort condition (top) and the sprint submerged condition (bottom) where the blue dots represent other DS3 nodes in Case Study 5.1 (Figure 5.4 on page 182)

The SUBFLOW result for the freshwater cooling 'FW' and lubricant oil 'LO' systems are given in Figure 5.36. The heat from the diesel generator nodes (PG DG) was assumed to emanate from lubrication, LO system, as well as direct freshwater cooling 'FW' system. Therefore, in the snorting condition, as shown in Figure 5.36 (top), the total cooling demand for the LO system is 474 kW while the cooling load from the generator nodes (PG DG) for the FW system is 309 kW. Figure 5.36 also shows the FW cooling system receive cooling demand from the CW plant nodes (PT HX). The FW cooling system was also connected to the propulsion motor node (PM DC) and battery nodes (SE BD) for emergency cooling and thus arcs are shown zero in both operating scenarios. The SUBFLOW reveals the cooling demand experienced by the FW cooling system in the snorting condition was 147% higher than in the submerged condition. Based on this result, the LO heat exchanger node (PT HX) could be sized at 470 kW while the FW SW heat exchanger node (SW HX) plant nodes at both sides of the vessel could be sized at about 500 kW capacity.

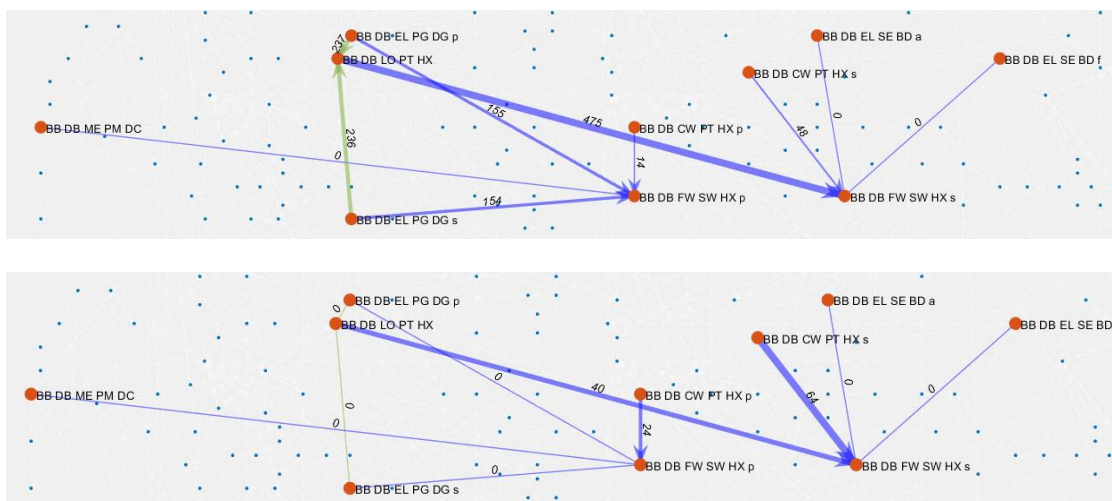


Figure 5.36: SUBFLOW solution for the 'LO' and 'FW' systems (dark blue lines) of Case Study 5.1 in the snort condition (top) and the sprint submerged condition (bottom) where the blue dots represent other DS3 nodes in Case Study 5.1 (Figure 5.4 on page 182)

Finally, the SUBFLOW result for the seawater cooling 'SW' system is given in Figure 5.37. Figure 5.37 shows the FW SW heat exchanger nodes (SW HX) are connected to the 'hard' valve of the TB system (VV SH) for circulating heat to the seawater environment. Based on the SUBFLOW result shown in Figure 5.37, all SW system pipework could be sized at the maximum capacity possible, which is at about 500 kW as they are cross connected for the connection redundancy.

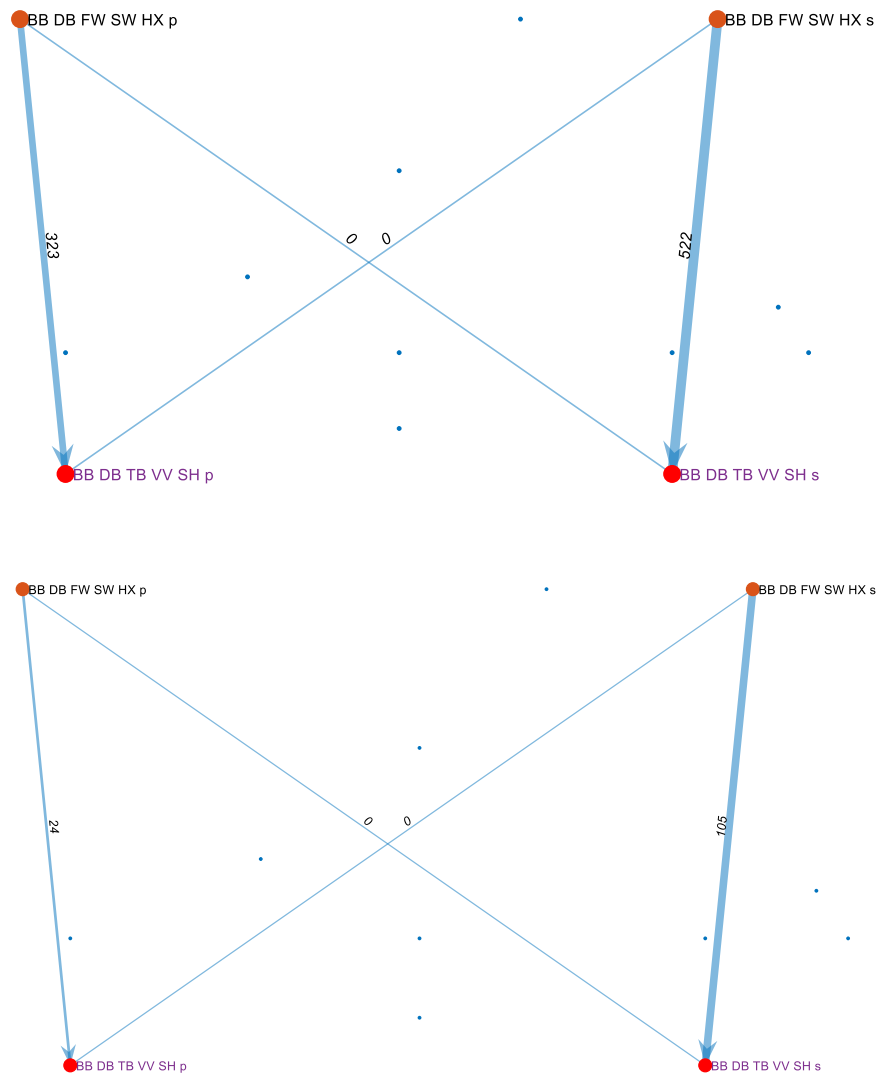


Figure 5.37: SUBFLOW solution for the seawater cooling 'SW' system (blue lines) of Case Study 5.1 in the snort condition (top) and the sprint submerged condition (bottom) where the blue dots represent other DS3 nodes in Case Study 5.1 (Figure 5.4 on page 182)

Without SUBFLOW, the detailed sizing of the trunking HVHE system would have been needed to consider many detailed aspects, such as the pressure loss due to the friction that is influenced by the shape, material, length, and various bends of the trunking including the fittings used in the ventilation system, which is time-consuming to be done in ESSD. Nevertheless, one of the important aspects in deriving the power to volume ratio for sizing the HVHE connection was the trade-off between the space required for HVHE routing and the noise due to the air velocity. This is illustrated in Figure 5.38. The higher velocity of air in the trunking (e.g., 10 m/s) was found to give a small space of trunking but create a higher noise emission to the submarine. Conversely, the lower air velocity (e.g., 2,5 m/s) could give a lower noise emission but double the diameter of the trunking to maintain the same volume rate of air required for a given cooling demand.

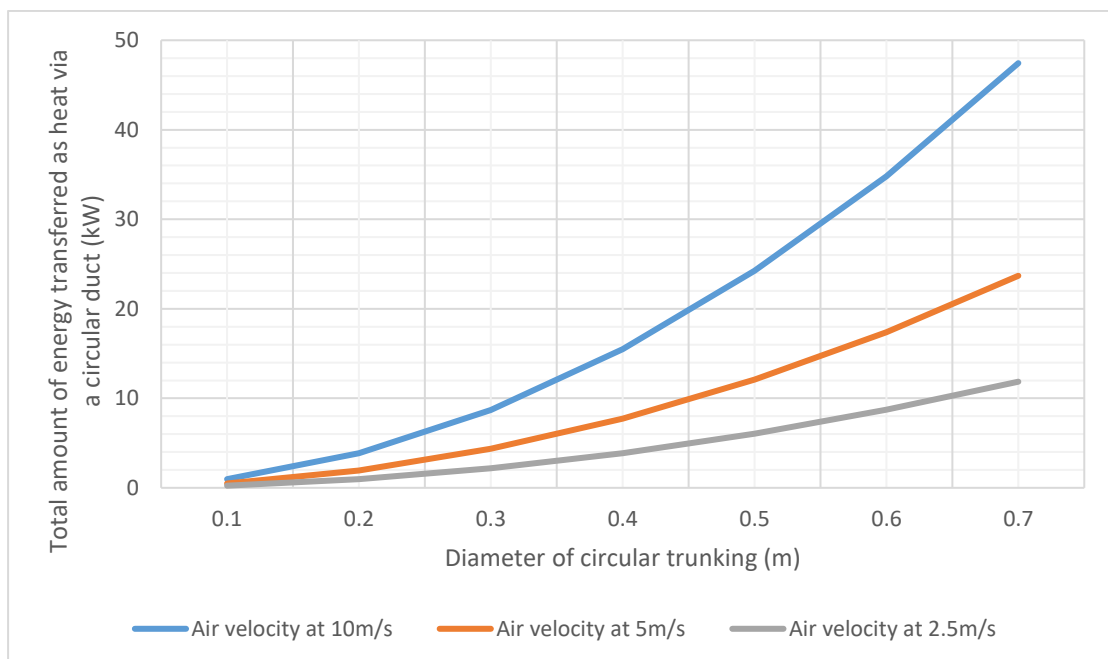


Figure 5.38: HVHE connection size vs air velocity with an assumed ΔT_{air} at 10°C

Having presented the SUBFLOW results for the heat removal system, Figure 5.39 shows the refined model of the systems, part of the third step in the Physical Loop Method (see Figure 5.2 on page 176). The HVIN system (coloured blue) was routed from the bridge fin to the AMS where the ATUs are located. The total length of the HVIN system connection was 16 m. The fresh air from the HVIN system then flowed through various compartments, such as

battery spaces and motor room nodes, via the HVHE system (coloured yellow). The highways for the aft part of the HVHE system were assigned to the port side of the submarine and the starboard side for the forward part of the HVHE system. The total length of the HVHE system connection was 201 m.

Figure 5.39 also shows the CW plants, the LO, and FW-SW heat exchangers are able to be fitted in the engine room, adjacent to the diesel engines. The highways for the CW, FW, and SW systems were located at various locations, consistent with the initial system highways allocations given in Figure 5.8 on page 188. The total connection length of those systems (CW, FW, and SW) were 107 m, 131 m, and 93 m, respectively while for the LO was 18 m. Finally, in the snort scenario, the heat could escape from the submarine to the environment via the HVEX system through the casing exhaust or the exhaust mast (coloured brown). The total connection length of this HVEX system was 68 m.

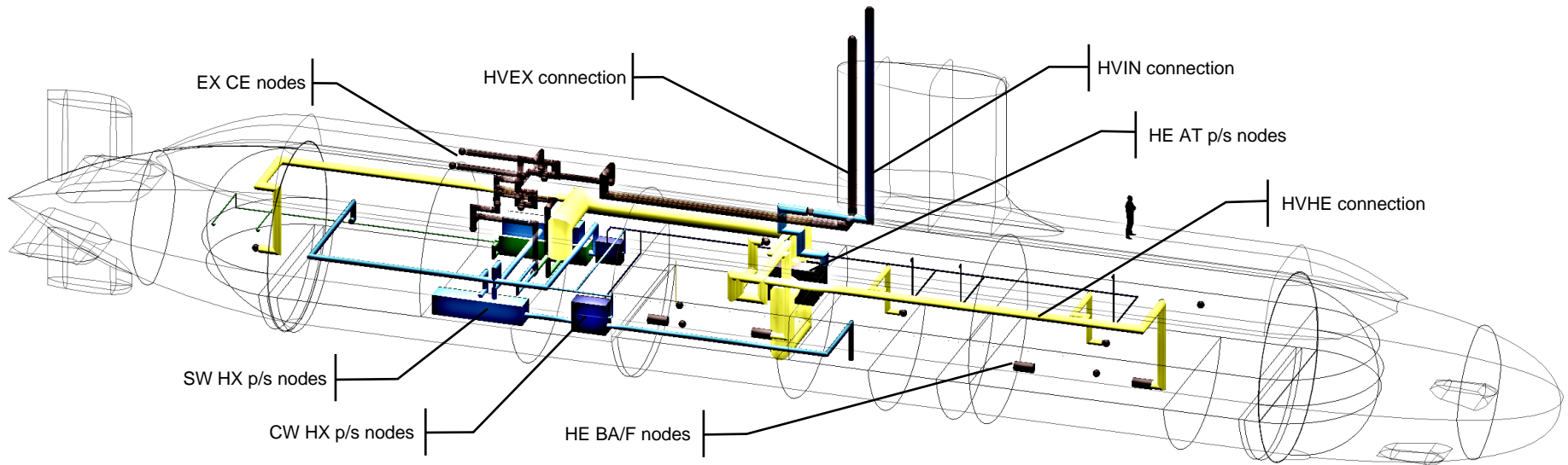


Figure 5.39: The initial model of the heat removal system of Case Study 5.1 showing the air intake 'HVIN' system in blue, air heat 'HVHE' system in yellow, the exhaust 'HVEX' system in brown, the chilled water 'CW system in dark blue, the freshwater cooling 'FW' system in blue, and the seawater cooling 'SW' system in light blue

5.8 Summary of the Application

Besides the power definition at source and sink nodes defined in previous sections, there were hub nodes that also needed to be defined. As discussed in Subsection 3.2.5, the power at hub nodes P_{hub} was driven by the energy coefficient input and thus is defined as in Equation (5.29).

$$P_{hub_node}^{snort/sprint} \geq 0 \quad (5.29)$$

There was a total of 170 hub nodes and 956 equality constraints in Case Study 5.1. Such constraints could be generated automatically in the Logical Loop method to ensure continuity in the SUBFLOW simulation. Thus, the overall DS3 network solution for Case Study 5.1 is summarised in Figure 5.40 for the snorting condition and Figure 5.41 for the sprint submerged condition. These network solutions show the energy balance on the vessel has been achieved with a specific set of flow paths. This set is akin to the energy balance chart, which serves as an insight for the designer to understand how the energy flow comes in and out from the submarine. As arcs between systems in SUBFLOW were explicitly modelled, the energy transfer between systems could be observed visually (see SUBFLOW 3D multilayer networks in Figure 5.42 for the snorting operating condition and Figure 5.43 for the sprint submerged operating condition). This is unlike the previous DS3 research (Subsection 2.3.4).

Furthermore, the NBA allowed the designer to evaluate and manually justify the size of each node and arc in the input data centre (Section 4.1). This means the designer could add, duplicate, or increase the power calculated by the network and this implies that any optimisation technique used in this research would not directly constrain the size of the DS3. For example, as already discussed in Subsection 5.3.1, arcs for the fuel forward are zero because the “optimisation” only chooses the fuel aft node to supply the energy to the diesel nodes. This is not necessarily true because the forward fuel node could be used when there is no available fuel left from the fuel aft tank. However, the power information at the fuel aft arcs represents the maximum power flow when a fuel tank is used. Therefore, the designer could use this information for sizing the fuel aft arcs in the SCP.

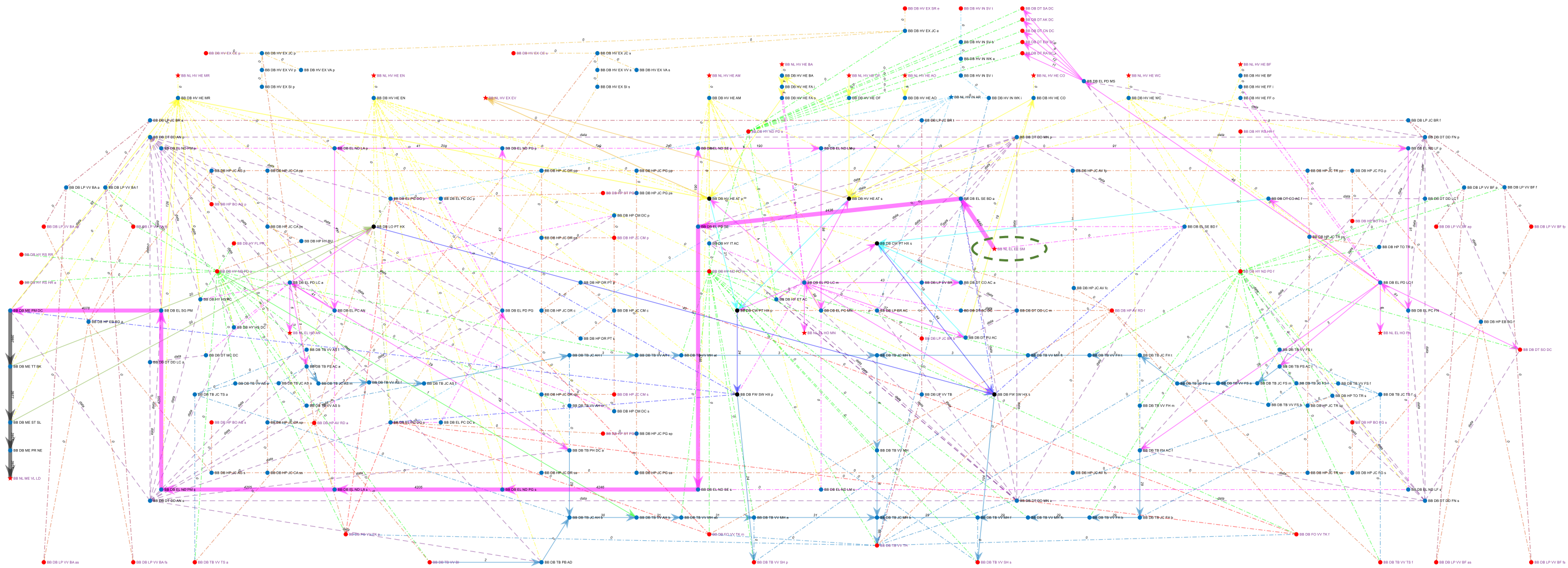


Figure 5.41: DS3 network response in the sprint submerged operating condition of Case Study 5.1

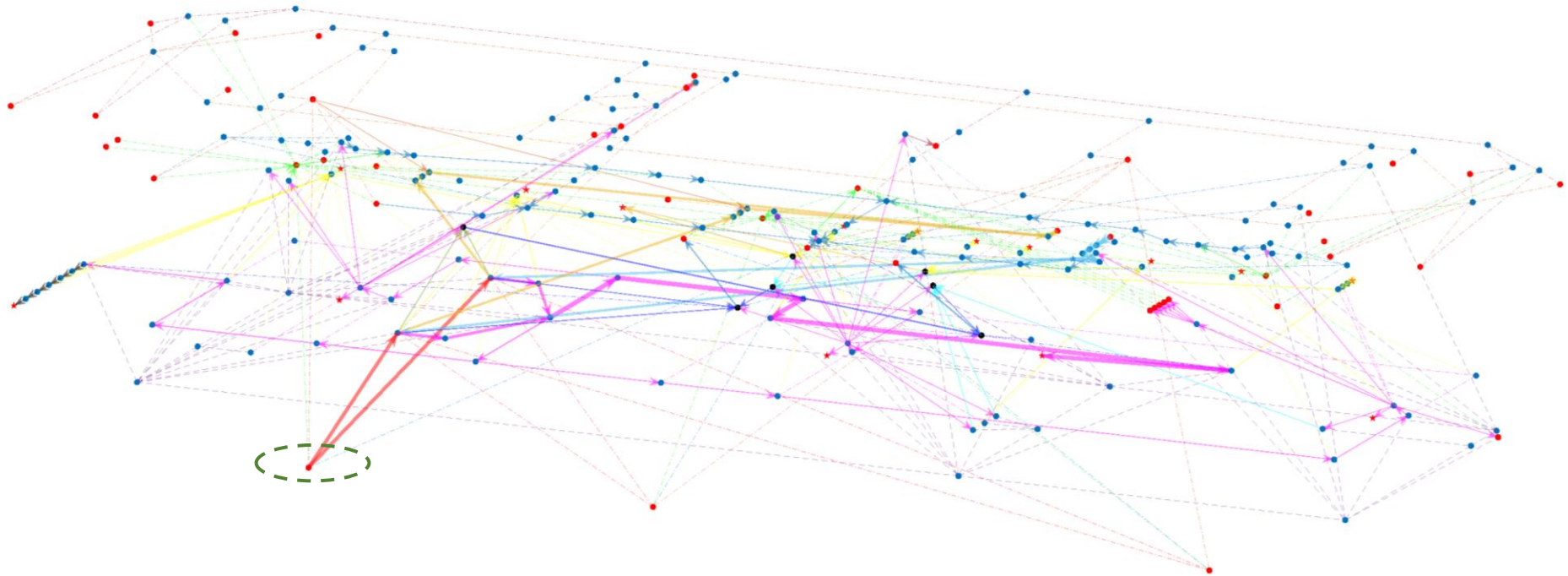


Figure 5.42: Multiplex DS3 network response in the snorting operating condition of Case Study 5.1, node labels are hidden for clarity

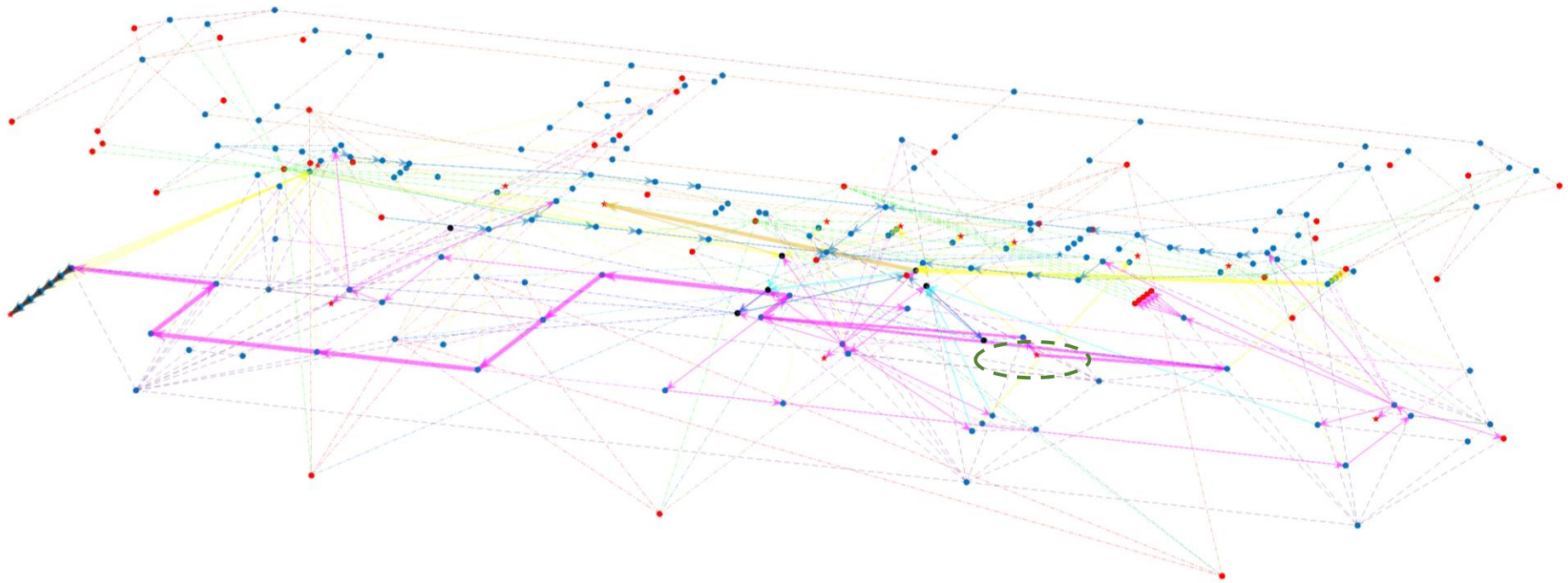


Figure 5.43: Multiplex DS3 network response in the sprint submerged operating condition of Case Study 5.1, node labels are hidden for clarity

The balancing process is a step towards the end of the third step of the Physical Loop method (see Figure 5.2 on page 176). This process is illustrated in Figure 5.44 on page 256, which assumes that the calculation of basic numerical weight and space balance could be achieved using Burcher and Rydill's procedure via simple spreadsheet sizing. However, this is not considered enough to achieve a sufficiently balanced design, and thus it is proposed that this is followed by the preparation stage step for applying an architecturally centred synthesis (Andrews and Pawling, 2003). The preparation stage gathers relevant data and prerequisite knowledge regarding Paramarine (see Figure 3.14 on page 118 for example). For the designer to be able to move from simple numerical synthesis to a configuration based synthesis (e.g., using Paramarine-SURFCON), the calculated weight and spaces need to be transformed into weight and volume (DBB) objects using the Weight Granularity Program (WGP) and the Volume Granularity Program (VGP), respectively (see Table 5.2). Using the Hull Granularity Program (HGP), a selected style of a hull configuration can be rapidly modelled and from the volume location, the weight objects in the pressure hull can then be attached to relevant volume objects to indicate longitudinal moment and vertical stability, before connecting for necessary weight or displacement and stability balance of the whole boat.

The next major step in Figure 5.44 is the transition of the submarine design from the coarse stage to a fine stage for DS3 synthesis, which makes this research significantly different to the previous UCL submarine DBB research (Pawling and Andrews, 2011; Purton, 2016). Previously, the DS3 modelling task was found to be demanding and considered impractical at the Concept Phase given the hundreds of DS3 components and connections. Furthermore, processing data from Paramarine-SURFCON to MATLAB back and forth to accomplish DS3 sizing, using SUBFLOW at the logical architecture abstraction, only became possible having produced the set of programs in the Network Block Approach (NBA) (Table 4.1) such as the Equipment Database Program (EDP), coloured green in Figure 5.44. The activities within the SUBFLOW controlled process are shown in blue to be consistent with Figure 5.4 on page 182.

Once the energy balance is achieved, a more refined sizing of DS3 can be fed back into the weight objects using the Weight Granularity Program (WGP) as shown in Figure 5.44. This is followed by a step to check whether a sufficiently balanced design has been achieved (see Appendix 7). The term ‘a balanced design’ can have many meanings. This can range from basic numerical weight or volume balance to a broader sense of a naval architecturally balanced design. A fully ‘naval architecturally balanced design’ means a submarine design that has been sized sufficiently to accommodate the space and weight required to meet certain agreed requirements. Those requirements should include strength, speed, stability, manoeuvrability, and style as defined generally in the S^5 term by Brown and Andrews (1980) and are specifically addressed in Andrews (2017a) for submarines with style detailed in Andrews (2021). This includes the buoyancy and stability balance that makes this submarine design balance distinct from surface ship design balance. Figure 5.44 shows different types of submarine design balance: weight balance; space balance; longitudinal balance; stability balance; and energy balance. Figure 5.45 on page 257 then takes Figure 4.4 on page 148 and uses Case Study 5.1 for visualising the output of the Physical Loop Method using relevant programs.

Having described the whole process of the proposed approach, the following section discusses the validation of this approach by comparing the weight calculation results from the network sizing to a numerical balance of a fictitious 2500 SSK using UCL data (UCL-NAME, 2014).

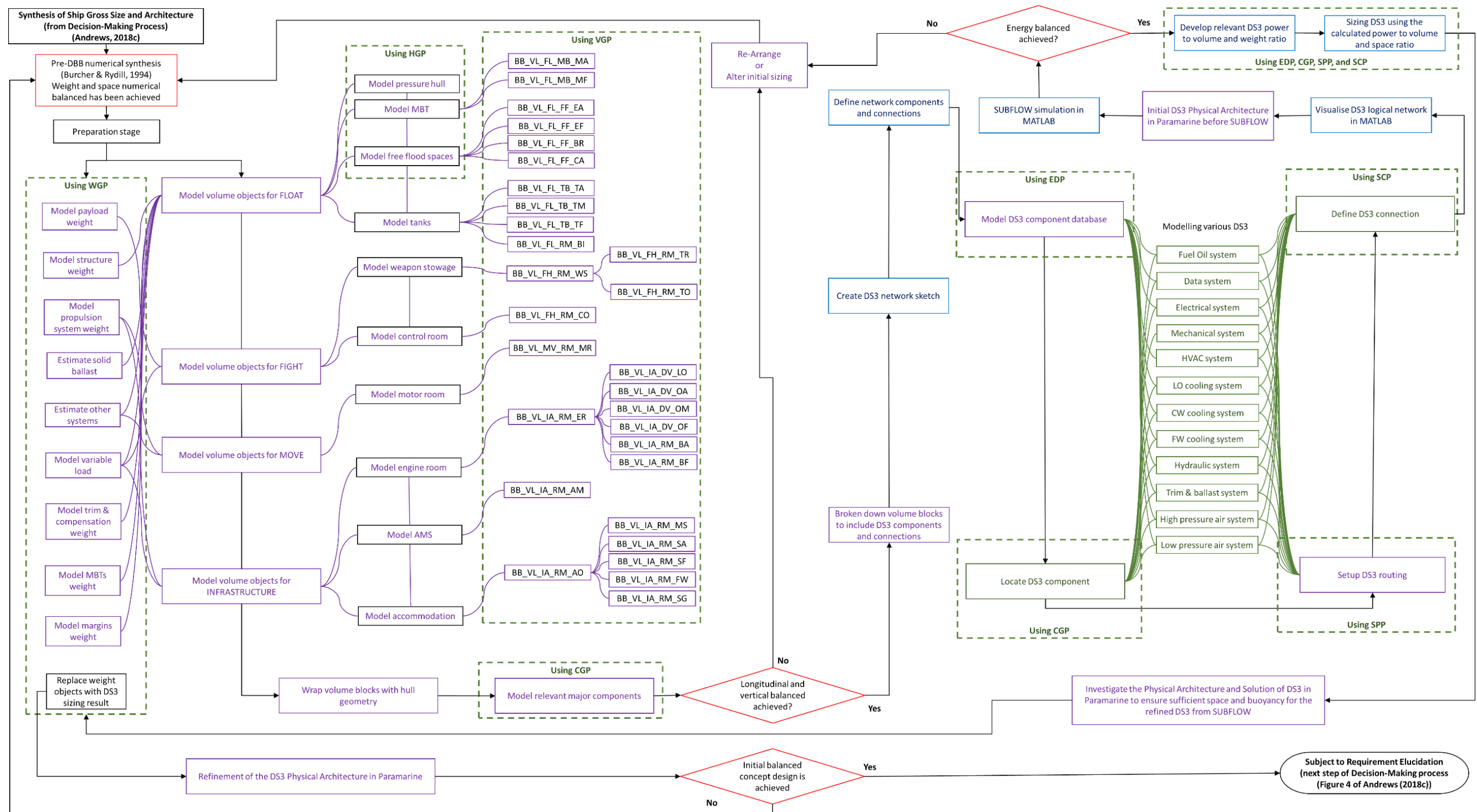


Figure 5.44: Detailed proposed Network Block Approach (NBA) procedure, which consists of balance check gates (red), the Physical Loop method (purple), input data centre (green), and Logical Loop method (blue). Thus, also relates to Figure 3.14 on page 118 for the preparation stage, Figure 5.2 on page 176 for the overall logic of the proposed approach, and Table 5.2 on page 179 for detailed abbreviations of the volume objects

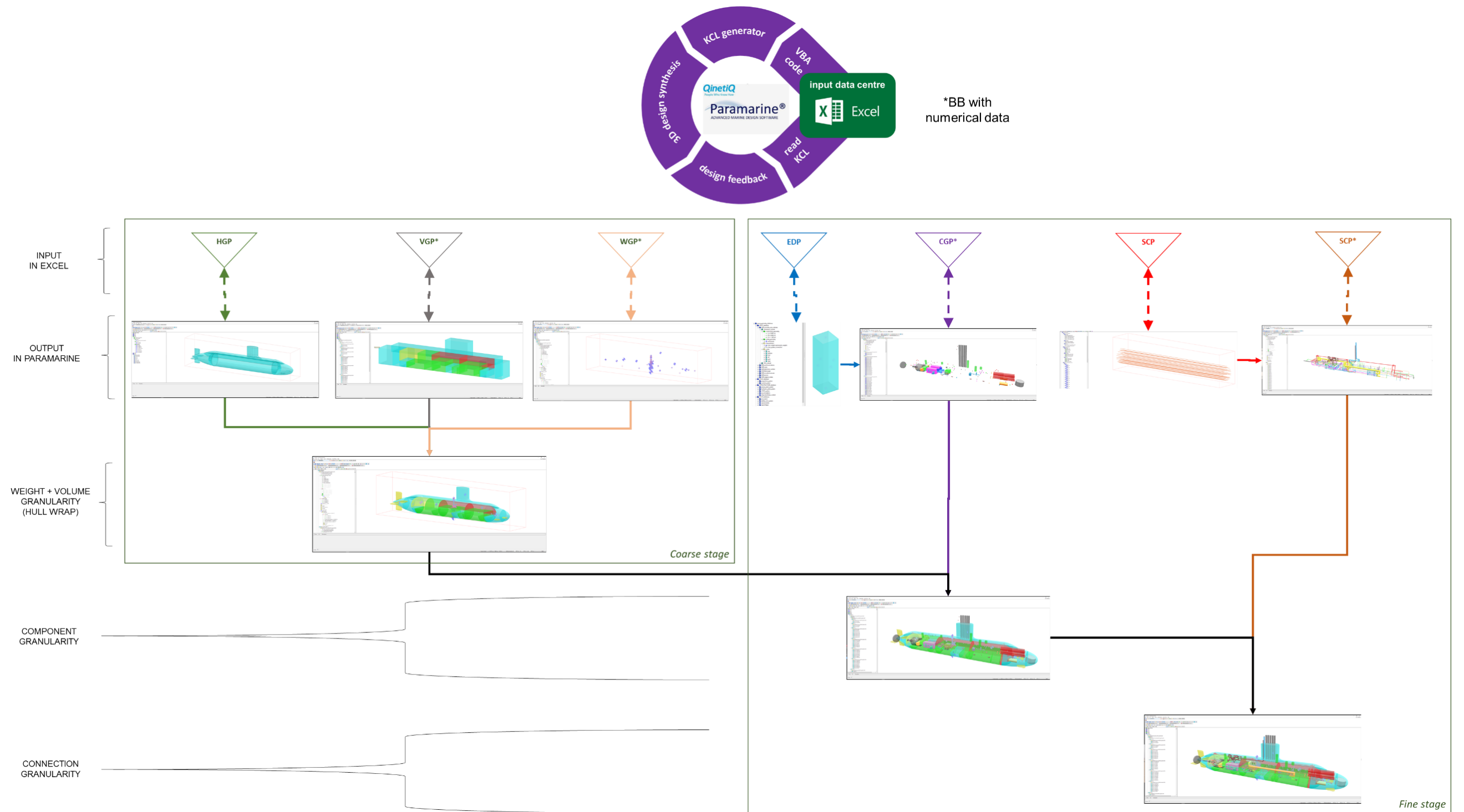


Figure 5.45: Summary of the output in the Physical Loop method using Case Study 5.1

5.9 Numerical Validation of DS3 Sizing Results

The DS3 weight inputs for the Case Study 5.1 calculated using the network approach are compared to the fictitious yet not unrealistic submarine design data in Table 5.14. In summary, the network could be used to give about 50 weight and space inputs to the design. As discussed in Section 3.3, there was no available data to compare individual volume results and thus only weight was compared in the study.

The Weight Group 2 classification system used at UCL-NAME mostly contains the mechanical 'ME' system. Since the power to weight ratio for these components was derived from the UCL submarine data (UCL-NAME, 2014), the difference between the NBA/SUBFLOW sizing and the data should have been small. Initially, there were no significant differences except for the main batteries and the propulsion motor, which were about 5% different from the Weight Group 2 data. The difference in the size of the batteries was due to the energy losses modelled in the overall DS3 network for Case Study 5.1 (see Section 5.7) that then demanded a slightly higher power source to account for these losses. After introducing a numerical node to allow the heat to escape into the environment, the difference was reduced to 0.7%.

Meanwhile, although the electrical 'EL' system in the network used more recent components, such as the Power Converter (PC) or bus nodes (ND), the overall weight of the electrical system in the Weight Group 3 shows a relatively good agreement with the UCL 2500 data in that it only differed by some 4.8%.

For Weight Group 4, the power to weight ratio data for the payload equipment was developed from the UCL submarine design data and thus there was also no significant difference, from that for Weight Group 2 (~3 tonnes). However, in percentage terms, the difference was likely to be higher, at 9.3 %.

Essentially, the majority of DS3 components are in Weight Group 5 where it was found that the result from network sizing was lower than the UCL submarine data by 20.7% or 15 tonnes. This was presumably due in some degree to the fact that the many detailed 'DB' nodes, such as valves and

junctions (summarised in Appendix 1), had not been modelled explicitly in the network case. However, another reason might be the style decision of each DS3 in Case Study 5.1 not exactly matching the style decision made in the fictitious UCL 2500 submarine design. It would have been possible to reduce the difference by increasing the design margins of each DS3 in the relevant programs, where these were initially assumed to be about 20% each.

Although the size of the fuel tanks could be determined by simple numerical calculation, the fuel nodes could be used to refine the size of the fuel tank objects in Table 5.2 on page 179. The derivation of the power to volume ratio of the fuel nodes required more input, such as the specific fuel consumption (SFC) and fuel weight density. A similar reason seemed to arise in the electrical 'EL' system size, where the difference in Weight Group 9 was about 7.1%.

Overall, the difference in the weight between 2500 UCL data (UCL-NAME, 2014) and the network sizing based SSK was only 18 tonnes or less than 1% of overall submerged displacement. As discussed above, the major contributor to such difference was Weight Group 5. Having demonstrated the application of the Network Block Approach (NBA) to a generic and very conventional SSK study, it was necessary to produce sensitivity analyses exploiting the NBA capability. This is covered in the next chapter.

Table 5.14: Weight results for the 2500 data vs Network Block Approach via SUBFLOW

Weight Group	Item	Network Name	2500 Data (te)	NBA/SUBFLOW Sizing (te)
2	Shafting	(SCP)_ME	7.4	7.4
	Thrust block	ME_TT_BK	3.2	3.1
	Stern seal	ME_ST_SL	1.8	1.7
	Propeller, rope guard & cone	ME_PR_NE	7.2	8
	Main motor	ME_PM_DC	83	84.9
	Propulsion switchgear	EL_SG_PM	4.5	6
	Main batteries	EL_SE_BD	269	263
	Machinery Control & Console (MCC)	DT_MC_DC	3.3	3.3
	Total WG 2 Classification			379.4
3	Cabling	(SCP)_EL	19.5	10
		(SCP)_DT		3.7
	140 kW 60 Hz motor generators	EL_PC_(ALL)	10.7	6
	1.4 MW diesel generators	EL_PG_DG	37.9	43.4
	DG lubricant oil system	(SCP)_LO	1.5	0.1
		LO_PT_HX		1.3
	DG fuel oil system	(SCP)_FO	1.1	0.1
	Diesel exhaust system	(SCP)_HVEX	12.6	4
	Main battery breakers	EL_PD_(ALL) EL_ND_(ALL)	3	11
	Distribution equipment 440 V 60 Hz		1.1	
	Distribution equipment 115 V 60 Hz		2.3	
	Distribution equipment 200/115 V 400 Hz		0.1	
	Distribution equipment main DC		1	
	Distribution equipment 24 V DC		1	
Total WG 3 Classification			91.8	
4	Periscopes	DT_SA_DC	4	2.2
		DT_AK_DC		1.9
	Ship Control Console (SCC)	DT_SC_DC	0.8	0.8
	Miscellaneous control & instrumentation	DT_DD_(ALL)	2	1.8
	Wireless mast & hoist	DT_CN_DC	1.5	1.5
	Radar mast and hoist	DT_RA_DC	2.5	2.5
	EW mast and hoist	DT_EW_DC	2.7	2.7
	Main passive sonar dome	DT_SO_DC	3.6	4
	Sonar processing & display	DT_CO_AC	7.5	5.2
	Data handling computer & display	DT_PU_AC	3.5	3
Total WG 4 Classification			28.1	25.6
5	Snort induction system	(SCP)_HVIN	4.2	1.1
	Ventilation trunking	(SCP)_HVHE	3.5	1.6
	Ventilation fans control	HV_HE_(ALL)	1.3	7.9
	Vent valves and filters		1.3	
	Vent heaters		0.1	
	Chilled Water (CW) plants	(SCP)_CW	5.1	0.5
		CW_PT_HX		1.6
	Chilled Water (CW) system	(SCP)_SW	3	11
	Ships Saltwater (SW) cooling system	FW_SW_HX	12.3	2.8
	Trim, bilge & ballast system	(SCP)_TB	8.8	3.7
		TB_VV		4.8
	Trim pumps & starter	TB_P (ALL)	0.4	2.5
	HP bilge pump & starter		1.5	
	LP bilge pump & starter		0.2	
	HP ballast pump & starter		1.5	
	Ships Fresh Water (FW) cooling system	(SCP)_FW	2.9	2.2
	HP air compressors	HP_CM_(ALL)	5	5.4
	HP air system	(SCP)_HP	3.9	0.6
	Direct blow system		2.1	
	Auxiliary vent & blow system		3.6	
	LP blower	LP_BR_(ALL)	1.8	2
	LP blow system	(SCP)_LP	4	3.4
	Main hydraulic system	(SCP)_HY	4.5	4.7
	External hydraulic system		2.3	
	Steering & hydroplane control system		1.4	
	Steering & diving hydraulic plant	HY_(ALL)	2.8	10
	Main hydraulic plant		1.6	
External hydraulic plant	1.5			
Total WG 5 Classification			80.6	65.8

Chapter 6

Design Experiments

As part of the justification of the ability of the Network Block Approach (NBA) to assist in the DS3 synthesis of submarines, it was necessary to test its sensitivity to different design decisions. Thus, the NBA was applied to three case studies (see Figure 6.1).

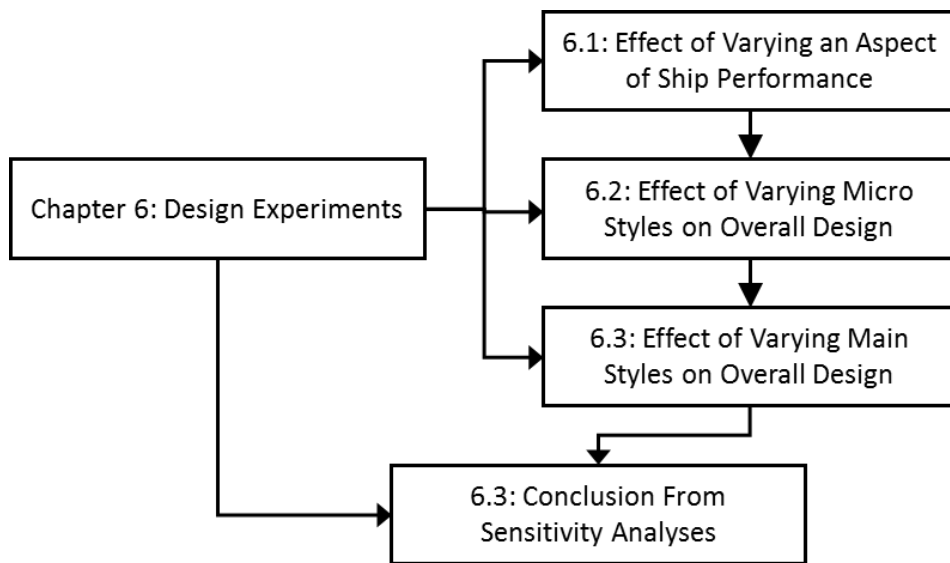


Figure 6.1: Schematic of Chapter 6

The first has been presented in Section 6.1 and focused on the impact of varying selected vehicle characteristics, part of design requirements, on the overall submarine design. The second case varied the micro and main design style based on the style framework proposed in Subsection 3.2.2. The effect of the micro level of style on the overall submarine design is presented in Section 6.2, while the effect of the main level of style is discussed in Section 6.3. The summary of these sensitivity analyses is provided in Section 6.4.

6.1 Effect of Varying an Aspect of Ship Performance

The first demonstration of the NBA in Chapter 5 suggests that the power load can drive the size of DS3 components, more specifically, those for the electrical (EL), the mechanical propulsion (ME), and the heat removal system (HE). Therefore, it was considered sensible to investigate the impact of varying one of the performance characteristics used for DS3 sizing. That chosen was the maximum speed for short periods submerged. The setup for this study is outlined in Subsection 6.1.1 and the results are presented in Subsection 6.1.2.

6.1.1 Case Study 6.1.1 Setup

In this subsection, the case study in Chapter 5 is expanded to include varying the submarine's maximum submerged speed: 20 knots for Variant A, 18 knots for Variant B, and 16 knots for Variant C. The structure of this sensitivity analysis is summarised in Table 6.1.

Table 6.1: Scheme for compiling the sensitivity analysis for Case Study 6.1.1, following the decision making sequence for complex vessels outlined in detail in Figure 4 and Appendix of (Andrews, 2018c) in a similar manner to the submarine example in Figure 4 of (Andrews, 2021)

Process Step	Selection Decision / Realisation for Case Study 6.1.1				Description	
Perceived need	Effect of different maximum speeds on DS3 sizing and overall design				Topic	
Outline of initial requirements	Common initial requirements as in Table 5.1					
	Initial Performance		Value			
	Accommodation		46 personnel			
	Patrol endurance		49 days			
Selection of style of emerging ship design	Common style selections					
	Style Level		Choice			
	Macro Level		Non nuclear (SSK)			
	Main Level		Diesel-electric power plant			
			Medium size ocean-going submarine			
			Single hull with casing			
Micro Level		Three watertight bulkheads				
		Detailed DS3 styles (Subsections 5.3 to 5.7)				
Selection of major equipment and operational sub-systems	Common DS3 configurations as in Subsections 5.3 to 5.7					
	Major equipment		DS3 redundancy			
Selection of whole ship performance characteristics	Common whole ship performance as in Table 5.1					
	General Performance		Value			
	Submerged speed		5 knots (>17 hrs)			
	Snort speed		6.5 knots (<6 hrs)			
	Design Variants		Variant 6.1.1.A	Variant 6.1.1.B	Variant 6.1.1.C	
	Maximum speed (knots)		20	18	16	
	Specific Performance		Value			
Indiscretion ratio		22 %				
DS3 Performance		see Subsections 5.3 to 5.7 and Appendix 9				
Selection of synthesis model type	Approaches as in Table 5.1 and The Network Block Approach (NBA)					
Selection of basis for decision making in initial synthesis	Common basis for decision making in initial synthesis					
	UPC while meeting S ⁴ criteria		Endurance at different speeds, longitudinal and vertical stability, e.g., submerged BG>0.2			
	Energy balance for DS3		energy supply is equal to energy demand			
Synthesis of ship gross size and architecture	Initial submarine resultant characteristic					
	Surfaced displacement (te)					
	Submerged displacement (te)					
	Maximum speed range (nm)					
	Maximum speed endurance (hr)					
	Diesel generators (MW)					
	Total power required for DS3 (kW)					
	Type of DS3		Weight (te)	Space (m³)	Weight (te)	Space (m³)
	Various DS3 - 12 systems					
	Total DS3					
	Weight Group Classifications		Weight (te)	Cost (£ mil)	Weight (te)	Cost (£ mil)
WG 1 to 9						
Total WG						
Exploration of impact of style, major items, and performance characteristics	Effect of varying a performance characteristic, maximum speed for short periods submerged, on overall design				Independent variables	

Table 6.1 shows a set of common initial requirements, design styles, major equipment, and whole ship performance characteristics used in Case Study 6.1.1 such that they were able to be met by all the variant designs in studying the effects of different maximum speeds. Various DS3 were compared in terms of weight and space of the DS3 components and connections, in a similar manner to the demonstration in Section 5.9, and Table 5.14. At the same time, the Weight Group classification and cost were used to compare whole boat effects.

In terms of the design experiment, Table 6.1 has been divided into the topic of the experiment, independent variables, control variables and dependent variables. The topic of the experiment was to study the effect of different maximum speeds on DS3 sizing and overall design. Therefore, the independent variables of this experiment are different maximum submerged speeds of the submarine. The control variables were the common payload assumptions, common design styles, common equipment selections, common whole ship performance characteristics (except the maximum speed) and the common synthesis model. Variables observed as the dependent variables in this investigation were range and endurance in each maximum speed scenario, with appropriately sized diesel engines, and DS3.

6.1.2 Results from the Performance Study

Within this relatively coarse survey of the solution space, the individual designs were assessed for the effects of changing requirements by the development of sub-variants. SUBFLOW was used to find the energy balance of the submarine in a maximum submerged speed operating condition. The network flow simulation results of Case Study 6.1.1 for Variants A, B, and C are given in Figure 6.2, Figure 6.3, and Figure 6.4, respectively, which shows the power flow as the label of each arc indicating the maximum speed affecting these figures. The green circle dashed in each figure indicates that the energy was originated from the batteries. The SUBFLOW simulation revealed the amount of power drawn from the batteries was different between design variants.

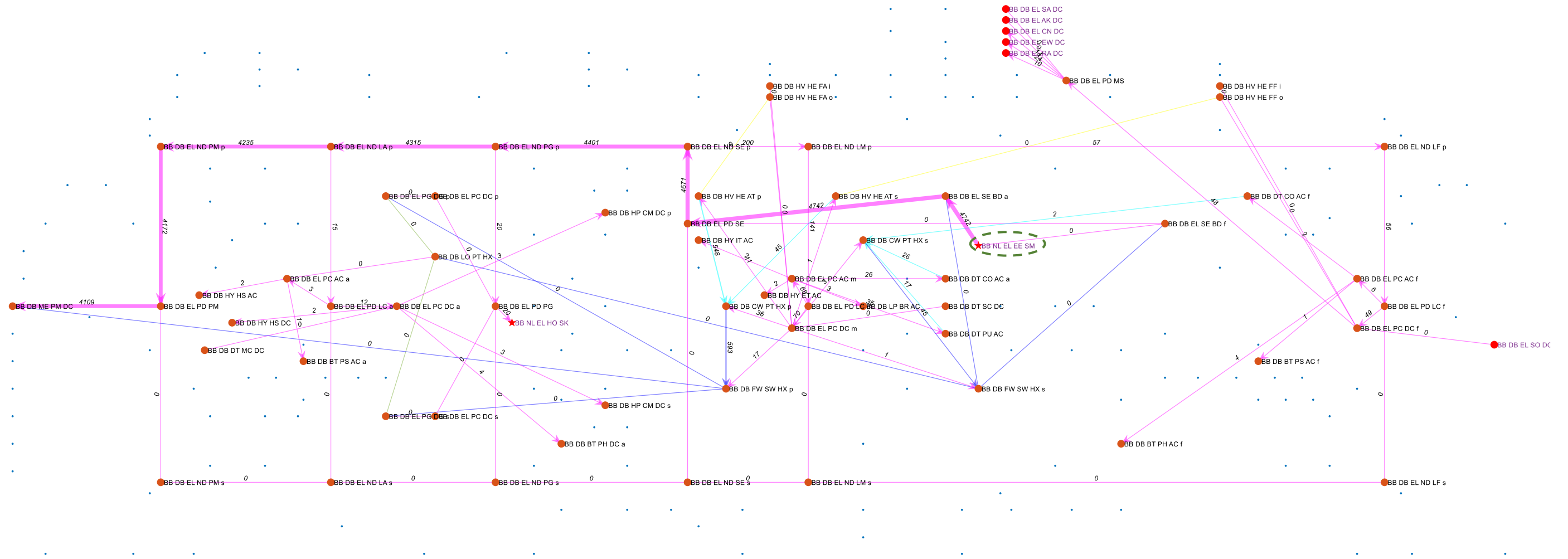


Figure 6.2: SUBFLOW simulation result for design Variant 6.1.1.A, which shows the energy flow of the electrical (EL) system (magenta lines) in a maximum speed (20 knots) operating condition. The adjacent systems are also shown, and the blue dots represent the overall DS3 nodes in Case Study 6.1.1 while the green circle dashed highlights the energy source in the system

In the sprint submerged operating condition, the source of energy came from the batteries (see the green circles (dashed) in Figures 6.2, 6.3, and 6.4), starting from the numerical node (EE SM), which were 4.7 MW, 3.8 MW, and 3 MW, respectively. These were then distributed throughout the ship to satisfy various power (EL) demands, not only for Move function, but also for Fight, Float, and Infrastructure. These demands for these functions could be met by the battery nodes (SE BD), as the energy source of the submarine in a maximum submerged speed operating condition. The flow path result of the SUBFLOW steady-state simulation of this investigation was classified into three zonal loads: forward, mid, and aft.

In the aft zone, the energy was first departed from battery breakers or switchboard (PD SE) to the port side of the electric (EL) system towards the aft part of the boat, which consisted of bus nodes for battery breaker (ND SE), generator breaker (ND PG), aft zonal load (ND LA), and propulsion switchboard (ND PM). For the aft zonal load (ND LA), a small part of the energy (15 kW) was first converted by the converter nodes (PC AC/DC) and then distributed to satisfy the hotel load demands of the aft zone of the boat, through a switchboard or load centre node (PD LC). The aft zone hotel load includes hydraulic plants (HS AC/DC), machinery control console (MC DC), trim pumps (TB PS), and high-pressure ballast pumps (PH DC). These loads were not affected by the variation of propulsion load since the drivers of these loads were set as the control variables. However, the energy for propulsion switchboard nodes (PD PM) was quite different between the three design variants. They were 4.1 MW, 3.3 MW, and 2.6 MW, respectively. The main propulsion motor node (PM DC) captured and converted the relevant electrical energy to the mechanical (ME) nodes for sprint propulsion demand.

Some of the electrical energy went to the mid part of the vessel, starting from the bus node for battery (ND SE), mid zone hotel load (ND LM), and forward zone hotel load (ND LF). At the bus node for mid zone hotel load (ND LM), most of the energy was transported to the mid zonal load centre (PD LC), converted by the relevant power converter nodes (PC AC/DC), and subsequently distributed to the hotel load at the mid zone. The hotel load in the mid zone

included hydraulic plants (IT/AT AC), command consoles (CO AC), CPUs (PU AC) and the heat removal system. The heat removal system consisted of ATUs (HE AT) battery fans (HE FA), CW plants (PT HX), and FW/SW heat exchangers (SW HX). As expected, the load demand for this zone was affected by different maximum speed propulsion demands. This was because higher loss means a higher power demand for the heat removal system to work, which would be mainly located at the mid part of the submarine. The load demands of the mid zone for variants A to C of Case Study 6.1.1 were 141 kW, 128 kW, 118 kW, respectively.

At the bus node mid zonal load (ND LM), a small part of energy was allocated to the bus node forward zonal load (ND LF). From this node, the forward load centre then converted the power to relevant power demands, such as command consoles (CO AC), battery fans (HE FF), trim pumps (PS AC), high-pressure ballast pumps (PH AC). The power at this zone was 57 kW, which was also not affected by the variety of different maximum speed setups.

From the SUBFLOW network simulation, the incorporation of some bus nodes and switchboard nodes with associated efficiency ratios (total of six nodes with each having between 1.5%) increased the energy loss to 9% from that initially assumed as only 2% from the numerical calculation (efficiency electric in Subsection 3.2.3). This loss affected the size of the heat removal system and ultimately the initial sizing of the power generator, as the source of electrical energy on the vessel.

To understand the holistic impact on the initial sizing of the submarine, the energy balance information from the SUBFLOW simulation was then converted to DS3 weight and space input using relevant power to weight and volume ratios. However, as shown in Figures 6.1, 6.2, and 6.3, some arcs have zero flow, this requires the designer's engineering judgement to size the relevant arcs, based on the micro style choices made for the DS3. For example, arcs of the electrical (EL) system on the starboard side (ND PM to ND LF) are shown as zero, but because this was designed to be a ring style redundancy, they

were manually sized by mirroring the power flow from the port side to starboard side connection.

Since the weight and space of DS3 can be refined using the Network Block Approach (NBA), the compartment density assumption from (UCL-NAME, 2014) was used as the basis to resize the relevant compartments, despite the fact that some compartments are area driven rather than volume driven and thus the overall submarine size could be reassessed. The order of the arrangement or layout as the major style decision was the control variable of this investigation and thus remained unchanged in all three speed variants.

The physical architecture of the Baseline Design is shown in Figure 6.5. The initial arrangement of the DS3 components was produced to show the applicability of the tools within the NBA to inform the 'layout'. In Figure 6.5, major components are modelled, such as bow cylindrical sonar and masts (grey-DT system), torpedo tubes (red-Fight), Air Turbine Pumps (ATP), access hatches, conning tower, escape towers (green-Infrastructure), and diesel engines (magenta-EL system). The connections of various DS3 were also shown indicating relevant highway choice, for example, the low-pressure air piping (see the upper red connection in Figure 6.5), running from forward to the aft Main Ballast Tanks under the casing. This pipeline was adjusted so that it did not clash with the components at the crown of the vessel, such as conning tower, masts, and access hatches. Still, many clashes require more detailed arrangement and routing modelling, which are unlikely to be resolved in ESSD. The model shown in Figure 6.5 was considered sufficient to show the extent of the complexity of the physical architecture of DS3 can be undertaken rapidly in ESSD, using the novel tools within the NBA.

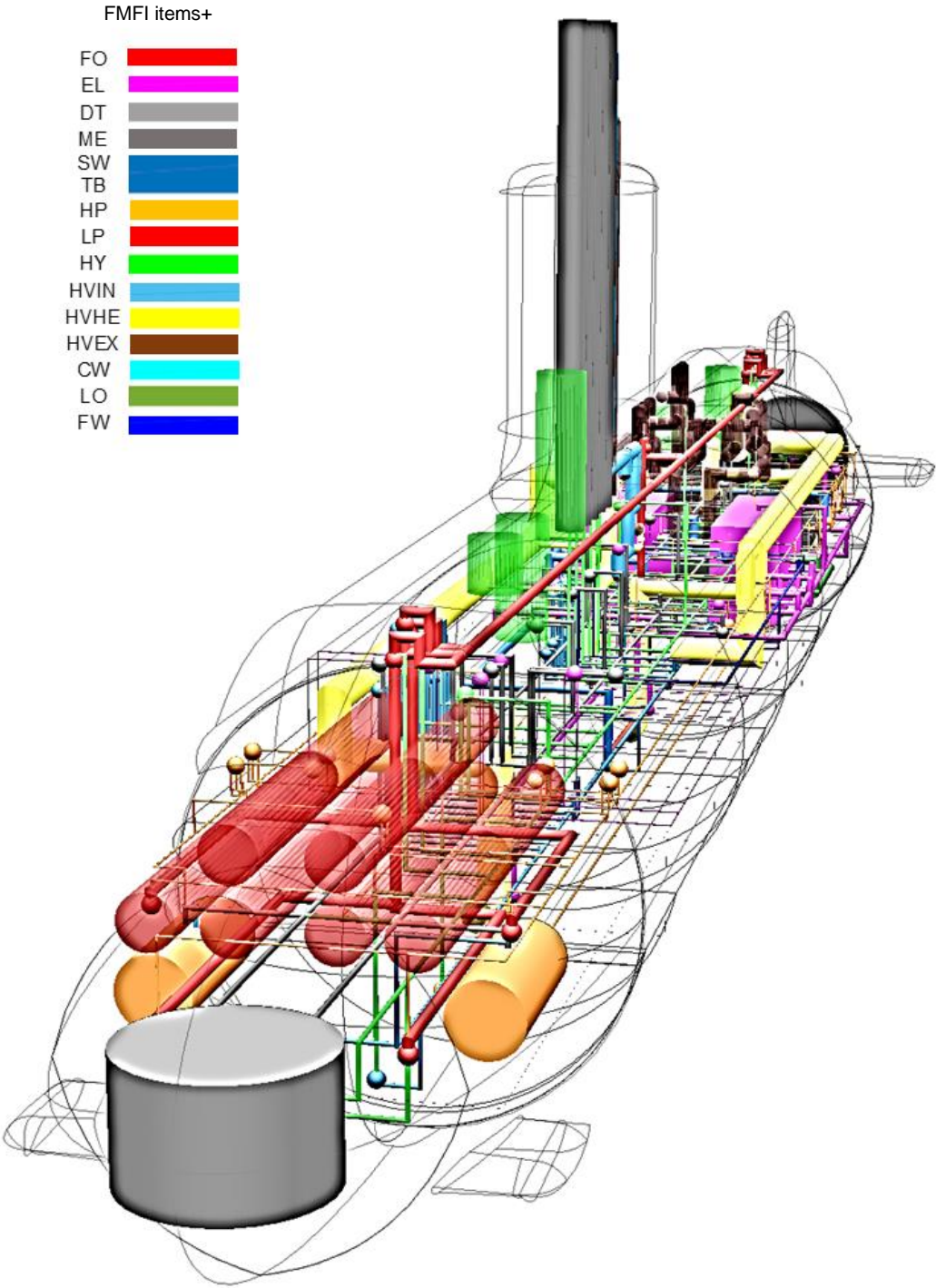


Figure 6.5: Physical Loop method result of design Variant 6.1.1.A, which shows the physical architecture of DS3 components and connections in different colour codes with the pressure hull, hydroplanes, casing, and other external volumes are shown in transparent edges line.

The sizing results from this investigation are summarised in Tables 6.2 and 6.3. Generally, Table 6.2 shows the total weight and space of the DS3 are affected by choices of maximum speed. The lower maximum speed led to lesser weight and space for the DS3. As indicated in Table 6.3, the total space for the DS3 was reduced by 5% and 4%, while the weight was reduced by 6% and 4%, respectively, with each reduction in the maximum speed by 2 knots. Conversely, the range and endurance in a maximum speed operation of design Variants 6.1.1.B (18 knots) and C (16 knots) were increased by 11% and 23% for the range and 25% and 54% for the endurance (relative to design Variant 6.1.1.A). As expected, the size of diesel engines and associated supporting systems (fuel and lubricant oil systems) were not affected since the size of diesel was found to be more sensitive to the snort speed rather than maximum speed (only if the number of battery cells is derivative of indiscretion ratio instead of maximum submerged). Some DS3 components, such as information data and hydraulics were seen to not be dependent on power flow and were thus not directly affected by the maximum speed although more detailed design iterations might show otherwise.

From this study, the variation of maximum speed from 20 knots to 16 knots can affect the weight of the DS3 up to 11% (equivalent to ~53 tonnes). However, the overall impact on the submarine was to alter the total submerged weight by 4%, which was equivalent to 110 tonnes, with a predicted cost impact of maximum speed variation also some 6%. Although these findings were relatively small, the speed investigations demonstrated the Network Block Approach (NBA) is sensitive to the DS3 impact from variation in maximum submerged speed as a key part of the overall design requirements.

Table 6.2: Summary of Results for Case Study 6.1.1, for Variants A, B, and C

Process Step	Selection Decision / Realisation for Case Study 6.1.1				Description		
Perceived need	Effect of different maximum speeds on DS3 sizing and overall design				Topic		
Outline of initial requirements	Common initial requirements as in Table 5.1						
	Initial Performance		Value				
	Accommodation		46 personnel				
	Patrol endurance		49 days				
Selection of style of emerging ship design	Common style selections						
	Style Level		Choice				
	Macro Level		Non nuclear (SSK)				
	Main Level		Diesel-electric power plant				
			Medium size ocean-going submarine				
			Single hull with casing				
Micro Level		Detailed DS3 styles (Subsections 5.3 to 5.7)					
Selection of major equipment and operational sub-systems	Common DS3 configurations as in Subsections 5.3 to 5.7						
	Major equipment		Implementation of micro level style in DS3 redundancy				
Selection of whole ship performance characteristics	Common whole ship performance as in Table 5.1						
	General Performance		Value				
	Submerged speed		5 knots (>17 hrs)				
	Snort speed		6.5 knots (<6 hrs)				
	Design Variant		Variant 6.1.1.A	Variant 6.1.1.B	Variant 6.1.1.C		
	Maximum speed (knots)		20	18	16		
	Specific Performance		Value				
Indiscretion ratio		<23 %					
DS3 Performance		see Subsections 5.3 to 5.7 and Appendix 9					
Selection of synthesis model type	Approaches as in Table 5.1 and The Network Block Approach (NBA)				Control variables		
Selection of basis for decision making in initial synthesis	Common basis for decision making in initial synthesis						
	UPC while meeting S ⁴ criteria		Speed, longitudinal and vertical stability, e.g., submerged BG>0.2				
	Energy balance for DS3		energy supply is equal to energy demand				
Synthesis of ship gross size and architecture	Initial submarine resultant characteristic						
	Surfaced displacement (te)	2250	2140	2059			
	Submerged displacement (te)	2603	2551	2493			
	Maximum speed range (nm)	48.4	53.9	59.7			
	Maximum speed endurance (hr)	2.4	3	3.7			
	Diesel generators (MW)	2.8	2.8	2.8			
	Total power required for DS3 (kW)	140.3	131.5	124.5			
	Type of DS3	Weight (te)	Space (m ³)	Weight (te)	Space (m ³)	Weight (te)	Space (m ³)
	Data (DT) system	17.2	22.8	17.2	22.8	17.2	22.8
	Fuel oil (FO) system	222	261	222	261	222	261
	Electric (EL) system	67	83.4	64	80	61	77.2
	Mechanical (ME) system	110.5	77.2	88.4	61.7	70.2	49
	Ventilation (HV) system	22.3	73.4	20.3	64.6	18.5	57.3
	Lubricant oil (LO) system	1.6	2.7	1.6	2.7	1.6	2.7
	Chilled water (CW) system	7.7	14.7	6.4	12.3	5.3	10.2
	FW/SW heat systems	13.6	9.3	13.5	9.3	13.5	9.3
	Hydraulic (HY) system	15.1	21.6	15.1	21.6	15.1	21.6
	Trim ballast (TB) system	12	8.9	12	8.9	12	8.9
	High-pressure air (HP) system	6	8.4	6	8.4	6	8.4
	Low-pressure air (LP) system	5.5	12.9	5.5	12.9	5.5	12.9
	Total DS3	501.44	596.7	472.3	566.4	448.2	541.4
	Weight Group Classifications	Weight (te)	Cost (£ mil)	Weight (te)	Cost (£ mil)	Weight (te)	Cost (£ mil)
	WG 1 structure	905	81	889	80	871	78
	WG 2 main propulsion	397	71	373	67	353	63
	WG 3 electrical services	105	25	101	24	98	23
	WG 4 control and communications	50	10	50	10	50	10
	WG 5 ship services	156	62	152	61	149	59
	WG 6 outfit	67	38	67	37	66	37
WG 7 payload	87	16	87	16	87	16	
WG 8 fixed ballast	164	-	168	-	163	-	
WG 9 variable load	668	10	660	9	653	9	
Total WG	2603	316	2551	307	2493	299	
Exploration of impact of style, major items, and performance characteristics	Effect of varying a performance characteristic, maximum speed for short periods submerged, on overall design				Independent variables		

Table 6.3: Normalised results for Case Study 6.1.1, figures are given as a percentage of the characteristics for Variant A

Process Step	Selection Decision / Realisation for Case Study 6.1.1				Description		
Perceived need	Effect of different maximum speeds on DS3 sizing and overall design				Topic		
Outline of initial requirements	Common initial requirements as in Table 5.1				Control variables		
	Initial Performance	Value					
	Accommodation	46 personnel					
Patrol endurance	49 days						
Selection of style of emerging ship design	Common style selections						
	Style Level	Choice					
	Macro Level	Non nuclear (SSK)					
	Main Level	Diesel-electric power plant					
		Medium size ocean-going submarine					
		Single hull with casing					
Micro Level	Three watertight bulkheads						
Selection of major equipment and operational sub-systems	Common DS3 configurations as in Subsections 5.3 to 5.7						
	Major equipment	Implementation of micro level style in DS3 redundancy					
Selection of whole ship performance characteristics	Common whole ship performance as in Table 5.1				Independent variables		
	General Performance	Value					
	Submerged speed	5 knots (>17 hrs)					
	Snort speed	6.5 knots (<6 hrs)					
	Design Variant	Variant 6.1.1.A	Variant 6.1.1.B	Variant 6.1.1.C			
	Maximum speed (knots)	20	18	16			
	Specific Performance	Value					
Indiscretion ratio	<23 %						
DS3 Performance	see Subsections 5.3 to 5.7 and Appendix 9						
Selection of synthesis model type	Approaches as in Table 5.1 and The Network Block Approach (NBA)				Control variables		
Selection of basis for decision making in initial synthesis	Common basis for decision making in initial synthesis						
	UPC while meeting S ⁴ criteria	Speed, longitudinal and vertical stability, e.g., submerged BG>0.2					
	Energy balance for DS3	energy supply is equal to energy demand					
Synthesis of ship gross size and architecture	Initial submarine resultant characteristic						
	Surfaced displacement	100%	95%	91%	96%	96%	
	Submerged displacement	100%	98%	111%	123%	154%	
	Maximum speed range	100%	125%	-	-	-	
	Maximum speed endurance	100%	-	-	-	-	
	Diesel generators	-	-	-	-	-	
	Total power required for DS3	100%	93%	88%	-	-	
	Type of DS3	Weight (te)	Space (m³)	Weight (te)	Space (m³)	Weight (te)	Space (m³)
	Data (DT) system	-	-	-	-	-	-
	Fuel oil (FO) system	-	-	-	-	-	-
	Electric (EL) system	100%	100%	95%	96%	91%	92%
	Mechanical (ME) system	100%	100%	80%	80%	63%	63%
	Ventilation (HV) system	100%	100%	91%	88%	83%	78%
	Lubricant oil (LO) system	-	-	-	-	-	-
	Chilled water (CW) system	100%	100%	83%	84%	68%	69%
	FW/SW heat systems	100%	100%	99%	100%	99%	100%
	Hydraulic (HY) system	-	-	-	-	-	-
	Trim ballast (TB) system	-	-	-	-	-	-
	High-pressure air (HP) system	-	-	-	-	-	-
	Low-pressure air (LP) system	-	-	-	-	-	-
	Total DS3	100%	100%	94%	95%	89%	91%
	Weight Group Classification	Weight (te)	Cost (£ mil)	Weight (te)	Cost (£ mil)	Weight (te)	Cost (£ mil)
	WG 1 structure	100%	100%	98%	99%	96%	96%
	WG 2 main propulsion	100%	100%	94%	94%	88%	88%
	WG 3 electrical services	100%	100%	96%	96%	93%	92%
	WG 4 control and communications	-	-	-	-	-	-
	WG 5 ship services	100%	100%	97%	98%	95%	95%
WG 6 outfit	100%	100%	100%	97%	98%	97%	
WG 7 payload	-	-	-	-	-	-	
WG 8 fixed ballast	100%	-	98%	-	99%	-	
WG 9 variable load	100%	100%	99%	89%	98%	89%	
Total WG	100%	100%	98%	97%	96%	94%	
Exploration of impact of style, major items, and performance characteristics	Effect of varying a performance characteristic, maximum speed for short periods submerged, on overall design				Independent variables		

6.2 Effect of Varying Micro Styles on Overall Design

In the previous section, that investigation shows the relatively small impact on DS3 and the whole boat sizing of varying one of the major demands of the submarine. In this study, the Network Block Approach (NBA) was tested to see whether the approach could capture the overall design impact of different style decisions at the micro level of an individual DS3. The selected micro style for this study was the variations of electric (EL) system configuration. This is described in Subsection 6.2.1 while Subsection 6.2.1 discusses the results of the study.

6.2.1 Case Study 6.2.1 Setup

In this subsection, the case study in Chapter 5 is expanded to include varying the electrical (EL) system style. In the case study in Chapter 5, a ring EL system was adopted, which includes the use of four redundant bus nodes at the port and starboard sides of the vessel. This was used as the baseline design, which is Variant A. Meanwhile, Variant B employs a single bus line that significantly reduces the number of redundant bus nodes and directly connects switchboard to switchboard between zones. The formulation of this sensitivity analysis is summarised in Table 6.4.

The comparison between the two configurations is given in Figure 6.6 on page 277. Figure 6.6 (top) shows the ring main configuration that is also adopted in Case Study 6.1.1. The ring configuration incorporates several redundant bus nodes (e.g., ND PM, ND LA, ND PG, ND SE, ND LM, and ND LF) at the port and starboard sides of the vessel. In contrast, the single bus configuration, shown in Figure 6.6 (bottom) eliminate the use of these nodes so that the generator breaker node (PD PG) was directly connected to the aft zonal load centre node (PD LC) and battery breaker node (PD SE). This configuration resulted in less weight, as it had fewer electrical (EL) components and connections than the ring bus configuration.

Table 6.4: Scheme for compiling the sensitivity analysis for Case Study 6.2.1, following the decision making sequence for complex vessels outlined in detail in Figure 4 and Appendix of (Andrews, 2018c) in a similar manner to the submarine example in Figure 4 of (Andrews, 2021)

Process Step	Selection Decision / Realisation for Case Study 6.2.1				Description	
Perceived need	Effect of different maximum speeds on DS3 sizing and overall design				Topic	
Outline of initial requirements	Common initial requirements as in Table 5.1				Control variables	
	Initial Performance	Value				
	Accommodation	46 personnel				
	Patrol endurance	49 days				
Selection of style of emerging ship design	Common style selections				Control variables	
	Style Level	Choice				
	Macro Level	Non nuclear (SSK)				
	Main Level	Diesel-electric power plant				
		Medium size ocean-going submarine				
		Single hull with casing				
	Micro level	Detailed DS3 styles (Subsections 5.3 to 5.7)				
Design Variants	Variant 6.2.1.A	Variant 6.2.1.B		Independent variables		
Micro Style for EL System	Ring bus configuration	Single bus configuration				
Selection of major equipment and operational sub-systems	Common DS3 configurations as in Subsections 5.3 to 5.7				Control variables	
	Major equipment	DS3 redundancy				
Selection of whole ship performance characteristics	Common whole ship performance as in Table 5.1					
	Sprint speed	20 knots (>2 hrs)				
	Submerged speed	5 knots (>17 hrs)				
	Snort speed	6.5 knots (<6 hrs)				
	Specific Performance	Value				
	Indiscretion ratio	22 %				
	DS3 Performance	see Subsections 5.3 to 5.7 and Appendix 9				
Selection of synthesis model type	Approaches as in Table 5.1 and The Network Block Approach (NBA)				Control variables	
Selection of basis for decision making in initial synthesis	Common basis for decision making in initial synthesis					
	UPC while meeting S ⁴ criteria	Endurance at different speeds, longitudinal and vertical stability, e.g., submerged BG>0.2				
	Energy balance for DS3	energy supply is equal to energy demand				
Synthesis of ship gross size and architecture	Initial submarine resultant characteristic				Dependent variables	
	Surfaced displacement (te)					
	Submerged displacement (te)					
	Maximum speed range (nm)					
	Maximum speed endurance (hr)					
	Diesel generators (MW)					
	Total power required for DS3 (kW)					
	Type of DS3	Weight (te)	Space (m³)	Weight (te)		Space (m³)
	Various DS3 - 12 systems					
	Total DS3					
	Weight Group Classifications	Weight (te)	Cost (£ mil)	Weight (te)		Cost (£ mil)
WG 1 to 9						
Total WG						
Exploration of impact of style, major items, and performance characteristics	Effect of varying micro level styles, a DS3 routing choice, on overall design				Independent variables	

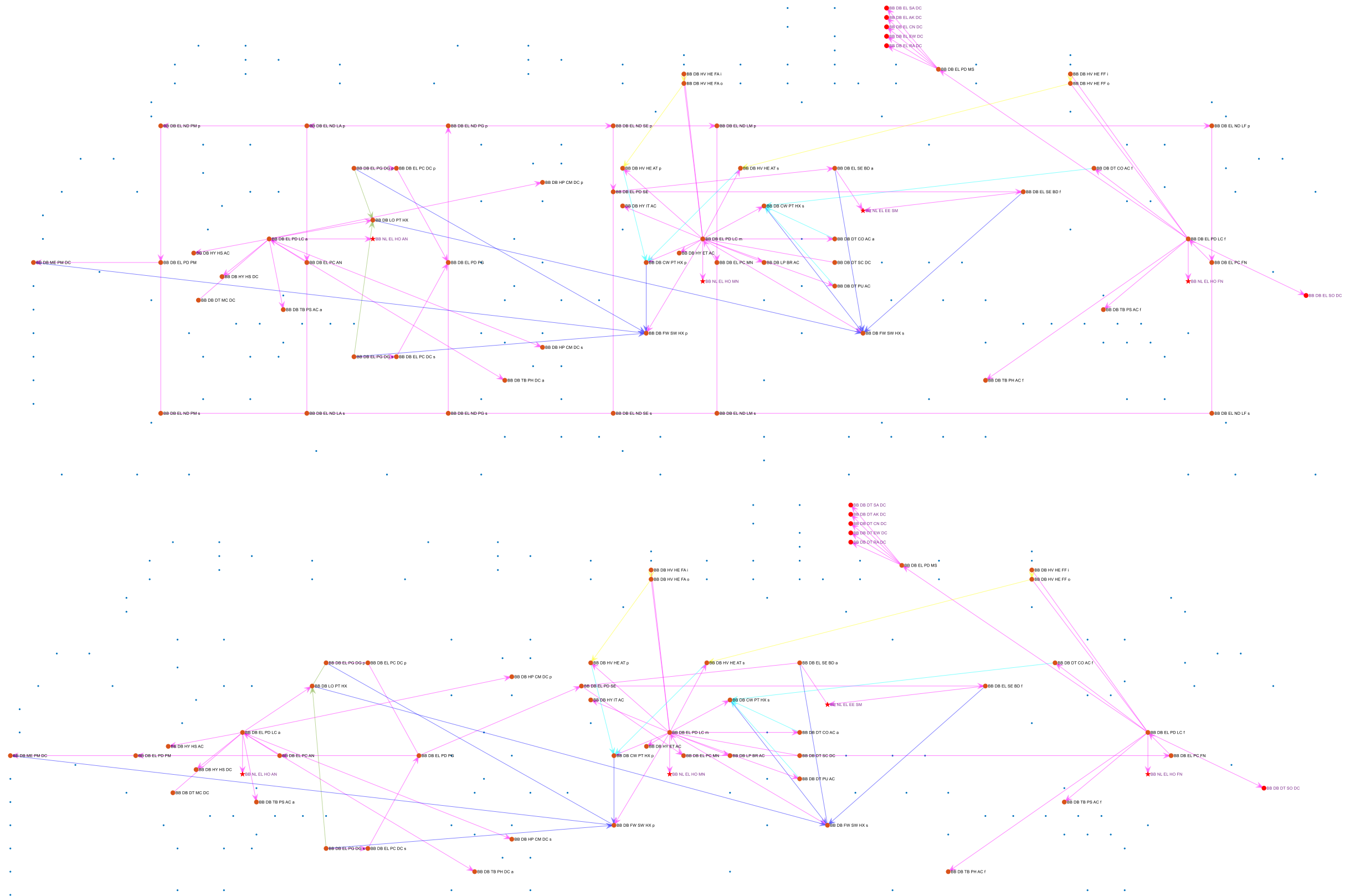


Figure 6.6: Network comparison of Case Study 6.2.1, which shows electrical (EL) system (magenta lines) of Variant A (top) and Variant B (bottom) before the SUBFLOW simulation. The adjacent systems are also shown, and the blue dots represent the overall DS3 nodes in Case Study 6.2.1

6.2.2 Results from the Micro Style Study

Since the SUBFLOW simulation result for Variant 6.2.1.A of this investigation is the same as the SUBFLOW result shown in Figure 6.2 on page 265, the result for Variant 6.2.1.B (single bus) in both snort and sprint submerged scenarios is given in Figure 6.7 on page 280 and Figure 6.8 on page 281, respectively. These figures show the energy flow in the DS3 network. In the snorting condition, the 2.8 MW of electrical energy came from the running diesel node (PG DG), moved to the power converter node (PC DC), and finally to the generator breaker node (PD PG) before being distributed throughout the ship (see the green circle dashed in Figure 6.7). At the generator breaker node (PD PG), the energy flow was reduced to 2.7 MW due to energy losses. Some of these losses, such as 309 kW, were directly removed by the FW and SW cooling system (SW HX) and subsequently ejected to the sea via trim and ballast pumps (TB).

The losses due to electrical components, such as the power converter node (PC DC), were first captured by the heat (HE) nodes and then removed by the ATU nodes (HE AT), CW nodes (PT HX) and FW SW cooling system (SW HX). Beyond the generator breaker node (PD PG), 2.4 MW of power in Figure 6.7 were distributed to the forward part of the ship for battery charging and the forward zone hotel load, while 264 kW was distributed to the aft part of the vessel. This took the demand for 47 kW aft zone hotel load as well as 216 kW propulsion load, in the snorting condition. At the forward part of the submarine, 2.4 MW of power was first received by the battery breaker node (PD SE), for charging battery nodes (SE BD) at 2.3 MW, while 182 kW of power was used for the forward zone hotel load. These figures included the energy losses due to electrical components and the power load to run the pumps within the heat removal system.

In comparison, in the sprint submerged condition, 4.7 MW of power came from the numerical submerged energy node (EE SM) and was then transported to the battery nodes (ND SE) (see the green circle dashed in Figure 6.8). The battery breaker node (PD SE) captured 4.4 MW of energy and divided it into two parts: 4.3 MW for the aft part of the ship, which was demanded by the high

load for maximum speed operation; and 188 kW for the forward part of the vessel, which was mainly for the forward zone hotel load.

The numerical data for each arc (see Figures 6.6 and 6.7) was then evaluated for DS3 sizing. The maximum energy flow first needed to be selected, given unlike Variant 6.2.1.A (ring bus), there was no zero-energy flow for design Variant 6.2.1.B (single bus). In the snort operating condition, the source of energy of design Variant 6.2.1.B came from the diesel engine (PG DG) (see the green circle dashed in Figure 6.7). Meanwhile, in the sprint submerged scenario, the main electric (EL) distribution 'line' of design Variant 6.2.1.B was identified as consisting of several nodes, from forward to the aft part of the vessel (see the green circle dashed in Figure 6.8): forward power converter node (PC FN); mid power converter node (PC MN); battery breaker node (PD SE); generator breaker node (PD PG); aft power converter node (PC AN); and propulsion switchboard (PD PM).

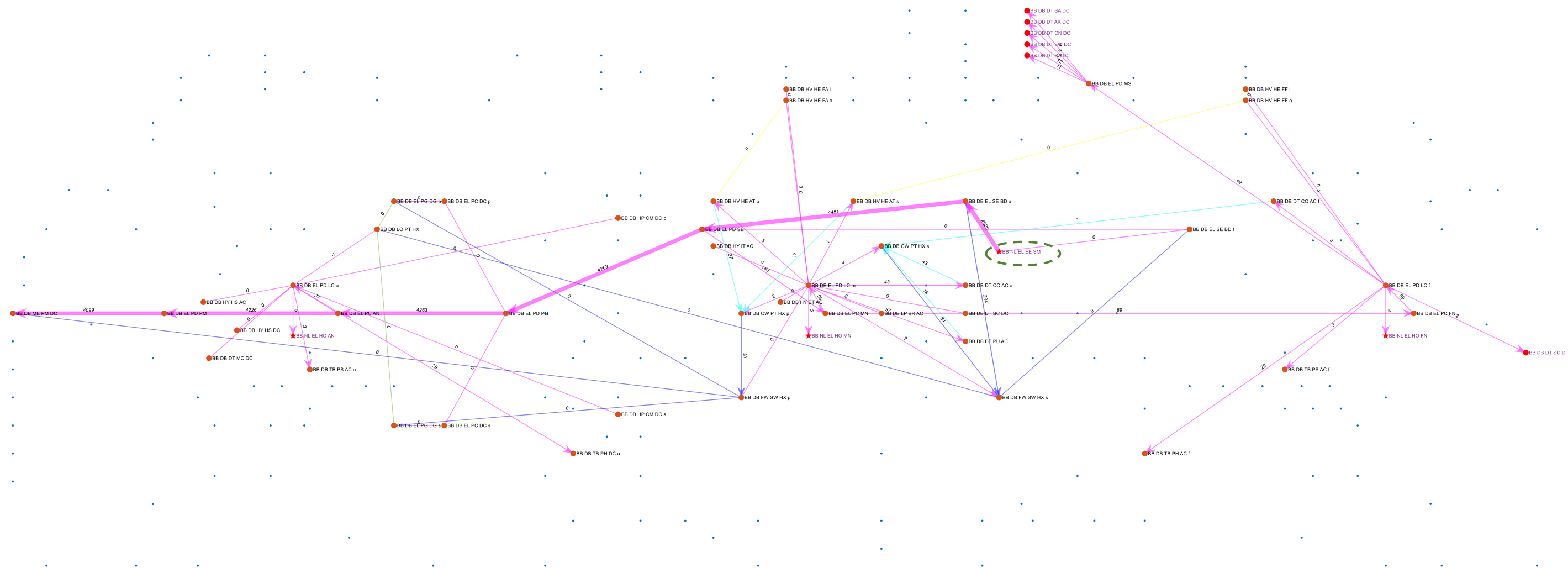


Figure 6.8: SUBFLOW simulation result for design Variant 6.2.1.B submerged, which shows the energy flow of the electrical (EL) system (magenta lines) in the sprint submerged operating condition. The adjacent systems are also shown, and the blue dots represent the overall DS3 nodes in Case Study 6.2.1 while the green circle dashed highlights the energy source in the system

The physical architecture comparison of the two design variants is shown in Figure 6.9. Figure 6.9 (top) depicts Variant 6.2.1.A with cabling routed both port and starboard sides, while Figure 6.9 (bottom) indicates how the main electrical (EL) distribution line or cabling of the design Variant 6.2.1.B was only routed to the port side of the submarine. Figure 6.9 reveals that the redundancy of DS3 connections can be applied in two different ways. The spatial highway redundancy, which is shown in Figure 6.9 (top), with port and starboard sides redundancy while the system run level of redundancy (e.g., the single line of cabling) could have been doubled or even tripled but would have still been located on one side of the submarine. Spatial highway redundancy was seen to have an advantage over the system run redundancy as should there be an incident or need for maintenance to occur locally on one side of the submarine, the connection on the other side of the submarine can be used as a fallback.

The extent of cable penetration (e.g., Figure 10 in Chapter VI of (Allmendinger, 1990)) can also be identified from Figure 6.9, especially for the power connection to masts and bow cylindrical sonar. The novel tools in the Network Block Approach (NBA) provided such information early in the design process. Furthermore, although only diesel generators were modelled to give their actual size in Figure 6.9, detailed DS3 arrangement (done by hand) could have been provided using the tools, once detailed component ratio size (e.g., the length, the beam, and the height of relevant DS3 components data on the submarine) could have been obtained for the tools facilitated by the NBA.

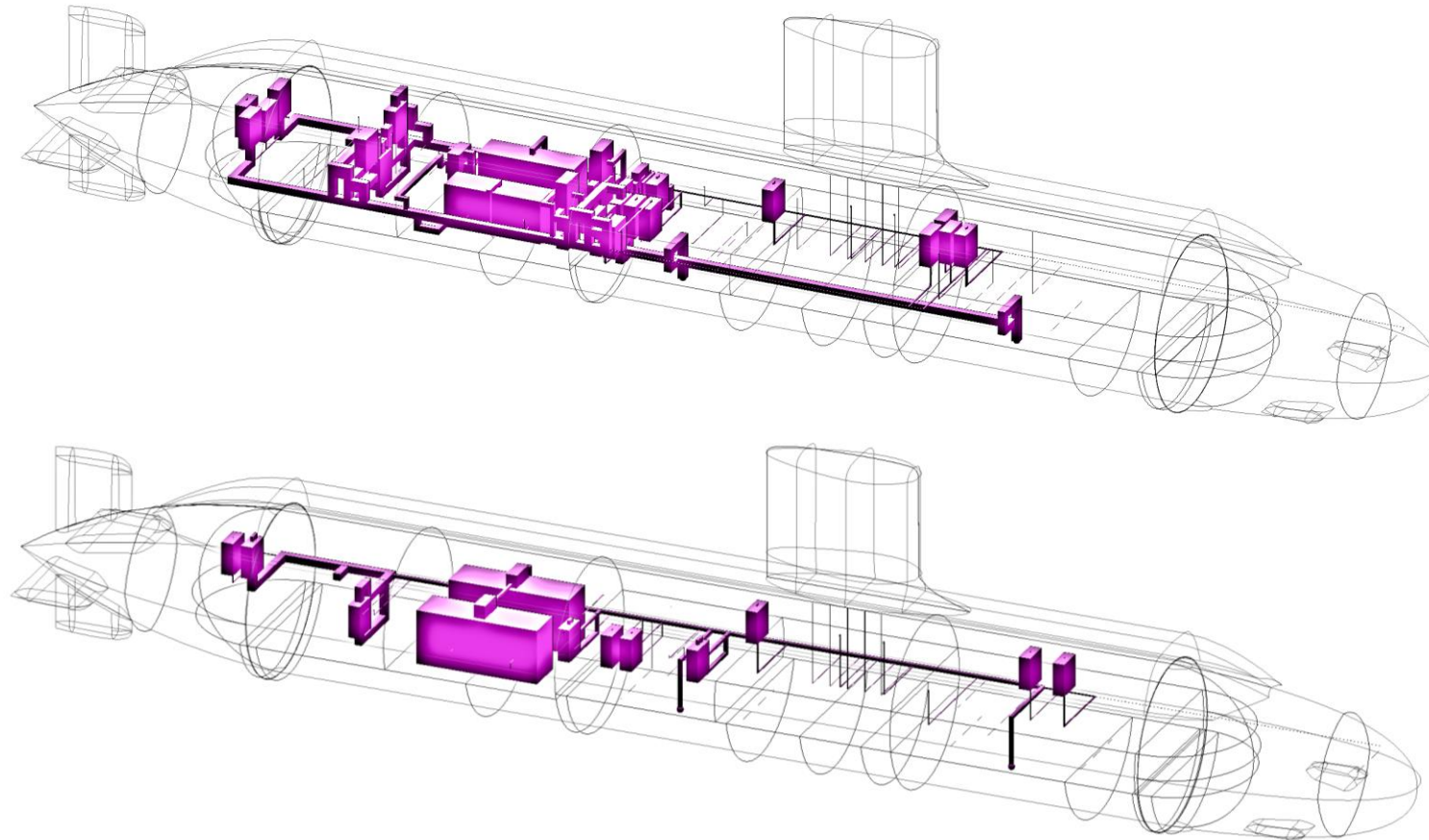


Figure 6.9: The physical architecture of Case Study 6.2.1, which shows a 3D perspective of the electrical (EL) system (in magenta) routing style of Variant A, adopting the ring routing configuration at the port and starboard part of the vessel (top) and Variant B, adopting single configuration routing at the port side of the vessel only (bottom). The hull is shown as transparent edge lines for reference. Unlike Figure 6.5, the other ~200 components are hidden for clarity

Since the variants were essentially at a micro style level of the baseline SSK study, the overall design impacts were commensurately quite marginal. As shown in Tables 6.5 and 6.6, the overall submarine submerged displacement remained unchanged in altering from a ring bus to a single line for power distribution. However, the maximum submerged speed performance was slightly hampered due to the power loss difference between the two network configurations. Consequently, this led to a decrease in the maximum submerged speed performance of 5% relative to the baseline design.

As shown in Table 6.6, there are very small differences (higher or lower) in some of the DS3 between the two design variants. This was because the resultant hull size was not altered, nor some DS3 connection lengths, which was calculated via the proposed routing framework as part of the Physical Loop method (see Subsection 4.2.5). This includes the information data (DT) system, the low-pressure air (LP) system. Table 6.6 shows the design Variant 6.2.1.B increased the weight of some heat removal DS3 (HV and LO), which is 30-80% due to the power loss difference between the two design variants. As expected, the electrical (EL) system of design Variant 6.2.1.B was less (4.8%) than design Variant 6.2.1.A through adopting single bus line.

Table 6.5: Summary of results for Case Study 6.2.1 Variants A and B

Process Step	Selection Decision / Realisation for Case Study 6.2.1				Description	
Perceived need	Effect of different maximum speeds on DS3 sizing and overall design				Topic	
Outline of initial requirements	Common initial requirements as in Table 5.1				Control variables	
	Initial Performance	Value				
	Accommodation	46 personnel				
	Patrol endurance	49 days				
Selection of style of emerging ship design	Common style selections				Control variables	
	Style Level	Choice				
	Macro Level	Non nuclear (SSK)				
	Main Level	Diesel-electric power plant				
		Medium size ocean-going submarine				
		Single hull with casing				
	Micro Level	Three watertight bulkheads				
	Detailed DS3 styles (Subsections 5.3 to 5.7)					
	Design Variant	Variant 6.2.1.A	Variant 6.2.1.B		Independent variables	
	Micro Style for EL System	Ring bus configuration	Single bus configuration			
Selection of major equipment and operational sub-systems	Common DS3 configurations as in Subsections 5.3 to 5.7				Control variables	
	Major equipment	DS3 redundancy				
Selection of whole ship performance characteristics	Common whole ship performance as in Table 5.1				Control variables	
	General Performance	Value				
	Sprint speed	20 knots (>2 hrs)				
	Submerged speed	5 knots (>17 hrs)				
	Snort speed	6.5 knots (<6 hrs)				
	Specific Performance	Value				
	Indiscretion ratio	22 %				
	DS3 Performance see Subsections 5.3 to 5.7 and Appendix 9					
Selection of synthesis model type	Approaches as in Table 5.1 and The Network Block Approach (NBA)					
Selection of basis for decision making in initial synthesis	Common basis for decision making in initial synthesis				Control variables	
	UPC while meeting S ⁴ criteria	Endurance at different speeds, longitudinal and vertical stability, e.g., submerged BG>0.2				
	Energy balance for DS3	energy supply is equal to energy demand				
Synthesis of ship gross size and architecture	Initial submarine resultant characteristic				Dependent variables	
	Submerged displacement (te)	2498	2498			
	Maximum speed range (nm)	52.6	49.9			
	Maximum speed endurance (hr)	2.6	2.4			
	Solid ballast fraction (%)	6	7			
	Item	Weight (te)	Space (m³)	Weight (te)		Space (m³)
	Data (DT) system	38.3	44.0	38.4		44.1
	Fuel oil (FO) system	216.6	255.5	216.8		254.3
	Electric (EL) system	346.6	206.6	330.0		174.8
	Mechanical (ME) system	105.1	76.4	101.1		138.5
	Ventilation (HV) system	13.9	50.3	18.4		46.7
	Lubricant oil (LO) system	3.0	3.3	5.3		4.3
	Chilled water (CW) system	1.7	2.4	1.5		2.7
	FW/SW heat systems	19.8	6.9	18.5		7.6
	Hydraulic (HY) system	18.3	23.1	18.1		23.0
	Trim ballast (TB) system	22.2	14.9	22.2		14.9
	High-pressure air (HP) system	6.6	8.9	6.5		8.8
	Low-pressure air (LP) system	3.6	6.5	3.5		6.3
	Total DS3	795.7	698.7	780.5		725.9
	Weight Group Classifications	Weight (te)	Cost (£ mil)	Weight (te)		Cost (£ mil)
	WG 1 structure	871	78.4	871		78.4
	WG 2 main propulsion	388	69.9	384		69.1
	WG 3 electrical services	110	26.2	99		23.5
	WG 4 control and communications	48	10.4	48		10.4
	WG 5 ship services	163	65.3	163		65.1
	WG 6 outfit	67	37.6	67		37.6
	WG 7 payload	87	16.5	87		16.5
WG 8 fixed ballast	173	-	173	-		
WG 9 variable load	615	9.2	615	9.2		
Total WG	2522	313.5	2506	309.9		
Exploration of impact of style, major items, and performance characteristics	Effect of varying micro level styles, a DS3 routing choice, on overall design				Independent variables	

Table 6.6: Normalised results for Case Study 6.2.1, figures are given as a percentage of the characteristics for Variant A

Process Step	Selection Decision / Realisation for Case Study 6.2.1				Description	
Perceived need	Effect of different maximum speeds on DS3 sizing and overall design				Topic	
Outline of initial requirements	Common initial requirements as in Table 5.1				Control variables	
	Initial Performance	Value				
	Accommodation	46 personnel				
	Patrol endurance	49 days				
Selection of style of emerging ship design	Common style selections				Control variables	
	Style Level	Choice				
	Macro Level	Non nuclear (SSK)				
	Main Level	Diesel-electric power plant				
		Medium size ocean-going submarine				
		Single hull with casing				
	Micro Level	Three watertight bulkheads				
	Micro Level	Detailed DS3 styles as in Subsections 5.3 to 5.7				
	Design variant	Variant 6.2.1.A	Variant 6.2.1.B		Independent variables	
	Micro Style for EL system	Ring bus configuration	Single bus configuration			
Selection of major equipment and operational sub-systems	Common DS3 configurations as in Subsections 5.3 to 5.7				Control variables	
	Major equipment	DS3 redundancy				
Selection of whole ship performance characteristics	Common whole ship performance as in Table 5.1				Control variables	
	General Performance	Value				
	Sprint speed	20 knots (>2 hrs)				
	Submerged speed	5 knots (>17 hrs)				
	Snort speed	6.5 knots (<6 hrs)				
	Specific Performance	Value				
	Indiscretion ratio	22 %				
	DS3 Performance	see Subsections 5.3 to 5.7 and Appendix 9				
Selection of synthesis model type	Approaches as in Table 5.1 and The Network Block Approach (NBA)					
Selection of basis for decision making in initial synthesis	Common basis for decision making in initial synthesis				Control variables	
	UPC while meeting S ⁴ criteria	Endurance at different speeds, longitudinal and vertical stability, e.g., submerged BG>0.2				
	Energy balance for DS3	Energy supply is equal to energy demand				
Synthesis of ship gross size and architecture	Initial submarine resultant characteristic				Dependent variables	
	Submerged displacement (te)	100%		100%		
	Maximum speed range (nm)	100%		95%		
	Maximum speed endurance (hr)	100%		95%		
	Solid ballast fraction (%)	100%		110.2%		
	Item	Weight	Space	Weight		Space
	Data (DT) system	100%	100%	100.3%		100.1%
	Fuel oil (FO) system	100%	100%	100.1%		99.5%
	Electric (EL) system	100%	100%	95.2%		84.6%
	Mechanical (ME) system	100%	100%	96.2%		180.4%
	Ventilation (HV) system	100%	100%	131.7%		92.5%
	Lubricant oil (LO) system	100%	100%	180.4%		131.5%
	Chilled water (CW) system	100%	100%	88.6%		110.7%
	FW/SW heat systems	100%	100%	93.5%		110.6%
	Hydraulic (HY) system	100%	100%	99.2%		99.7%
	Trim ballast (TB) system	100%	100%	100.1%		99.8%
	High-pressure air (HP) system	100%	100%	98.8%		99.2%
	Low-pressure air (LP) system	100%	100%	98.6%		97.4%
	Total DS3	100%	100%	98.1%		103.7%
	Weight Group Classifications	Weight	Cost	Weight		Cost
	WG 1 structure	-	-	-		-
	WG 2 main propulsion	100%	100%	98.9%		98.9%
	WG 3 electrical services	100%	100%	89.8%		89.8%
	WG 4 control and communications	-	-	-		-
	WG 5 ship services	100%	100%	99.7%		99.7%
	WG 6 outfit	-	-	-		-
	WG 7 payload	-	-	-		-
WG 8 fixed ballast	-	-	-	-		
WG 9 variable load	-	-	-	-		
Total WG	100%	100%	99.4%	98.8%		
Exploration of impact of style, major items, and performance characteristics	Effect of varying micro level styles, a DS3 routing choice, on overall design				Independent variables	

6.3 Effect of Varying Main Styles on Overall Design

As discussed in Chapter 3, the longer a submarine can operate underwater without the need to snort, the better. Unlike a nuclear powered SSN, which has what could be considered the ultimate Atmosphere or Air Independent Propulsion (AIP) system, the performance of an SSK is limited underwater, i.e., indiscretion ratio. To improve this ratio, different AIP systems for SSK were investigated to show the applicability of the Network Block Approach (NBA) in assessing a main level style choice.

6.3.1 Case Study 6.3.1 Setup

In this investigation, the baseline design presented in Chapter 5 was modified to include an AIP powering system using SUBFLOW simulation. Only two types of proven AIP systems were considered, the Stirling AIP power system (Kagawa, 1991) and the Proton Exchange Membrane Fuel Cell (PEMFC) (Psoma and Sattler, 2002). Figure 6.10 shows the high level schematic of the Stirling AIP system, which was used as the basis for modelling an additional AIP node to the DS3 logical architecture network previously used for the baseline design.

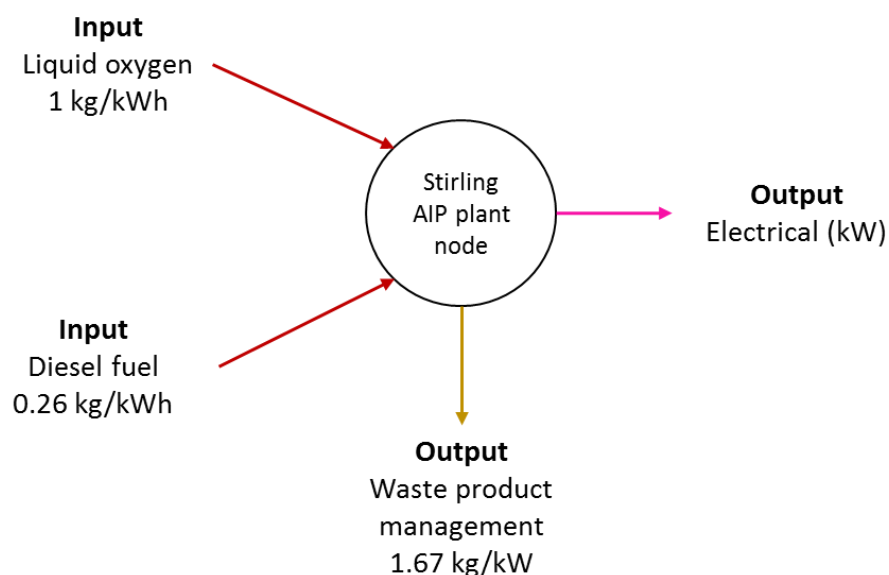


Figure 6.10: Node modelling of the Stirling AIP system with associated power and energy to weight ratio data suggested by Thornton (1994). The node consists of fuel lines in brown, waste product in yellow and electrical output in magenta

Figure 6.10 shows that the Stirling AIP system uses liquid oxygen and diesel fuel as the energy sources for the plant. The Stirling engine plant then converts these into electric power with an energy loss, which becomes the waste product (Nilsson, 1988). This waste product requires special equipment to mitigate the additional signature implications of the Stirling plant for the boat as a major concern in submarine design (Thornton, 1994).

Similarly, the PEMFC AIP system, shown in Figure 6.11, converts the fuel energy into net electrical output and waste product. The fuel for the PEMFC system is essentially an oxidant and hydrogen that are stored in different forms or reformed from other sources (Krummrich and Llabrés, 2015). Methanol was selected in this investigation because it gives a high hydrogen density compared to other forms of hydrogen storage, although methanol requires special arrangement as it is miscible in water if stored outside of the pressure hull (Thornton, 1994). The Hull Granularity Program (HGP) (Table 4.1 on page 145) was easily modified to account for such a special arrangement. Unlike the Stirling AIP, the waste product of a PEMFC AIP is pure water, which can be used as potable water consumption or discharged overboard through the trim and ballast (TB) system.

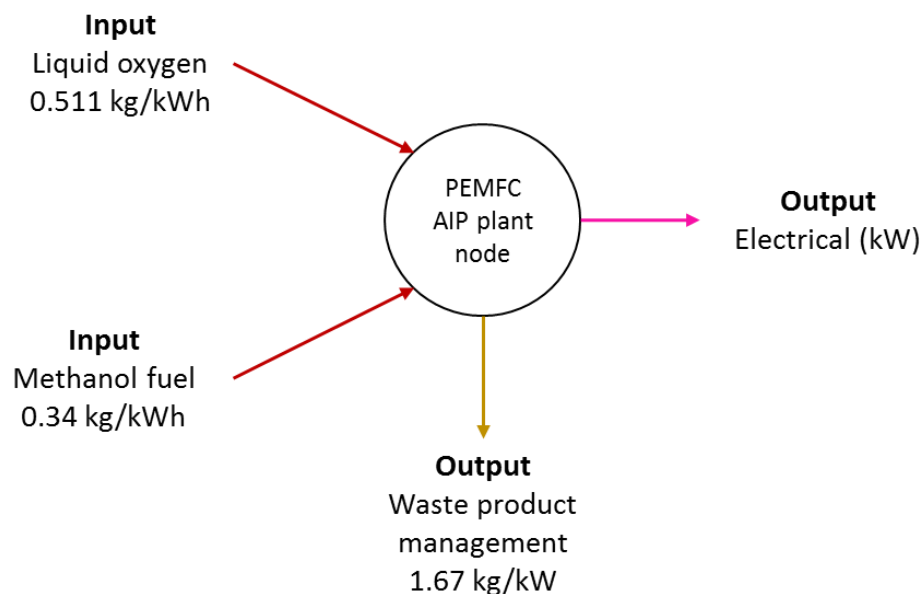


Figure 6.11: Node modelling of the PEMFC AIP system with associated power and energy to weight ratio data suggested by Thornton (1994). The node consists of fuel lines in brown, waste product in yellow and electrical output in magenta

The structure of this sensitivity analysis is summarised in Table 6.7, which shows that the Stirling AIP system and the PEMFC were compared to a non-AIP SSK baseline design. In this study, a very small 140 kW power output demand was selected as the control variable of both AIP systems. The impact of adding such a power to the non-AIP baseline design was investigated not only in terms of the impact on the overall submarine size but also the performance of the vessel, more specifically, the effect on the indiscretion ratio of the submarine.

Table 6.7: Scheme for compiling the sensitivity analysis for Case Study 6.3.1, following the decision making sequence for complex vessels outlined in detail in Figure 4 and Appendix of (Andrews, 2018c) in a similar manner to the submarine example in Figure 4 of (Andrews, 2021)

Process Step	Selection Decision / Realisation for Case Study 6.3.1							Description
Perceived need	Effect of different maximum speeds on DS3 sizing and overall design							Topic
Outline of initial requirements	Common initial requirements as in Table 5.1							Control variables
	Initial Performance	Value						
	Accommodation	46 personnel						
Patrol endurance	49 days							
Selection of style of emerging ship design	Common style selections							
	Style Level	Choice						
	Macro Level	Non nuclear (SSK)						
	Main Level	AIP power plant						
		Medium size ocean-going submarine						
		Single hull with casing						
	Micro Level	Three watertight bulkheads						
	Detailed DS3 styles as in Subsections 5.3 to 5.7							
Selection of major equipment and operational sub-systems	Design Variant	Variant 6.3.1.A	Variant 6.3.1.B	Variant 6.3.1.C			Independent variables	
	Main Style for AIP	No AIP	Stirling AIP	PEM-FC AIP				
	AIP Configuration	Baseline no AIP	Diesel fuel with liquid oxygen	Methanol with liquid oxygen				
Selection of whole ship performance characteristics	Common DS3 configurations as in Subsections 5.3 to 5.7							Control variables
	AIP power output	2x70 kW						
	Major equipment	DS3 redundancy						
	Common whole ship performance as in Table 5.1							
Selection of synthesis model type	General Performance	Value						
	Sprint speed	20 knots (>2 hrs)						
	Submerged speed	5 knots (>17 hrs)						
	Snort speed	6.5 knots (<6 hrs)						
	Specific Performance	Value						
	Indiscretion ratio	<23 %						
Selection of basis for decision making in initial synthesis	DS3 Performance	see Subsections 5.3 to 5.7 and Appendix 9						
	Approaches as in Table 5.1 and The Network Block Approach (NBA)							
	Common basis for decision making in initial synthesis							
Synthesis of ship gross size and architecture	UPC while meeting S ⁴ criteria	Endurance at different speeds, longitudinal and vertical stability, e.g., submerged BG>0.2						Dependent variables
	Energy balance for DS3	energy supply is equal to energy demand						
	Initial submarine resultant characteristic							
	Surfaced displacement (te)							
	Submerged displacement (te)							
	AIP indiscretion ratio (%)							
	Maximum speed range (nm)							
	Maximum speed endurance (hr)							
	Diesel generators (MW)							
	Type of DS3	Weight (te)	Space (m³)	Weight (te)	Space (m³)	Weight (te)	Space (m³)	
	Various DS3 - 12 systems							
	Total DS3							
	Weight Group classifications	Weight (te)	Cost (£ mil)	Weight (te)	Cost (£ mil)	Weight (te)	Cost (£ mil)	
	WG 1 to 9							
Total WG								
Exploration of impact of style, major items, and performance characteristics	Effect of varying Main styles on overall design							Independent variables

6.3.2 Results from the Main Style Study

The first procedure in this investigation was to calculate the extension to the submerged period given by the additional 140 kW in the submerged operating condition, i.e., the AIP endurance. Once the AIP period was known, the total energy required for the AIP was calculated. This gave the estimation of the size of the oxygen storage tank (LOX tank). The provision to use the oxygen for breathing during AIP endurance was also considered in sizing the LOX tank, which replaced the use of oxygen candles, defined in the Weight Granularity Program (WGP) (Table 4.1). Therefore, an initial layout investigation was undertaken using the Physical Loop method (see Section 4.2), with the relevant configuration given in Figure 6.12.

Figure 6.12 (top) shows that the AIP module is inserted as a new pressure hull section between the Engine Room and the Control Room. This lengthened the submarine by 16% compared to design Variant 6.3.1.A. To achieve longitudinal stability, the mid trim and compensation tank was moved next to the AIP section. Another major decision was to accommodate two 3.6 m diameter LOX tanks, which led to the pressure hull diameter being increased by 11% relative to design Variant 6.3.1.A. Figure 6.12 (top) also illustrates that some DS3 connections needed to be lengthened due to additional AIP section: trunking (HV) system in yellow; electrical (EL) system in magenta; pressured air and water distribution systems with different colour codes given in Table 5.4 on page 184. As shown in Figure 6.12 (top), the tools within the Network Block Approach (NBA) enabled the realisation of the crowded DS3 routing in the submarine much earlier than would normally occur in the design.

Figure 6.12 (bottom) shows the major components of the Stirling AIP system that drove the sizing of the AIP section. Two LOX tanks were placed in the lower part of the hull, port and starboard sides, while the Stirling plant was located above these tanks. The weight factor and volume packing density assumptions suggested by Thornton (1994) were used to numerically estimate the Stirling system auxiliaries, which included helium and nitrogen gas tanks, a generator control cabinet and a power distribution panel.

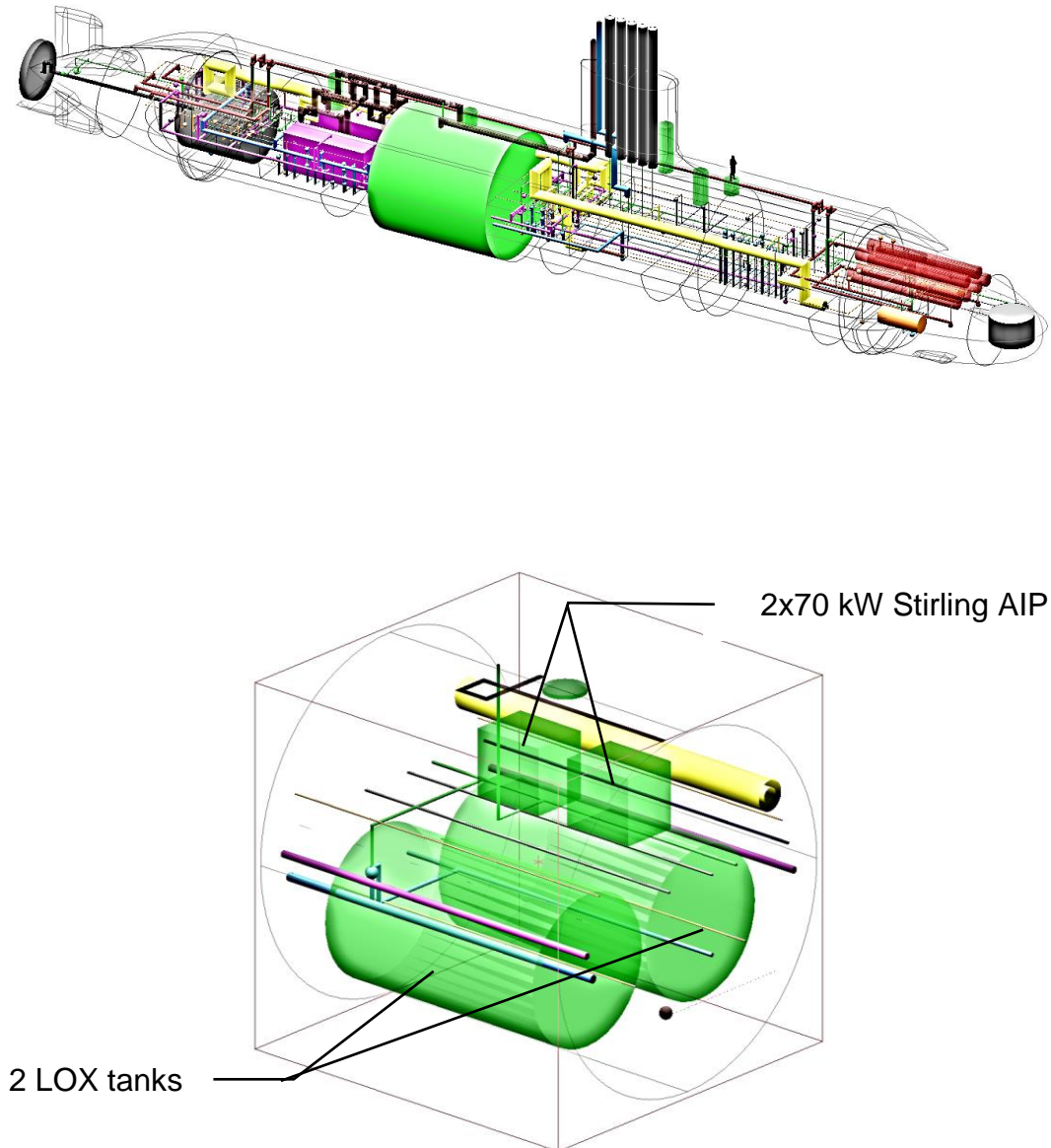


Figure 6.12: The physical architecture of design Variant 6.3.1.B, which shows a 3D perspective of the Stirling AIP module in the overall submarine 3D layout (top) and major components of the AIP module (bottom). The DS3 routing complexity is also shown with the colour code presented in Table 5.4 on page 184 with certain Fight components shown in red and Infrastructure components shown in green

Figure 6.13 shows the initial layout of the PEMFC AIP system in the overall vessel layout. Unlike the Stirling AIP section, the PEMFC AIP only incorporated one large LOX tank (see Figure 6.13 (bottom)) while the other important fuel source for the PEMFC system, the methanol, was stored externally to the pressure hull, in the keel is shown in Figure 6.13 (top). A set of dabblers or flexible plastic bags could then be used in such a storage space to prevent the methanol from mixing with seawater. There were 36 bags in total, each took 0.9 m³ of space.

A major decision made in the initial arrangement of the PEMFC investigation was to lengthen the initial submarine size by 16% compared to design Variant 6.3.1.A but because of the mass flow rate difference, the space for the oxidant for the PEMFC AIP (see Figure 6.10) is at least 40% lower than for the Stirling AIP (see Figure 6.11) and thus only one LOX tank was needed. This means the pressure hull diameter was kept the same as the pressure hull diameter of design Variant 6.3.1.A. As with the Stirling AIP system, the weight factor and volume packing density assumptions suggested by Thornton (1994) were used to numerically estimate the PEMFC AIP system auxiliaries necessary to produce the required additional 140 kW of electricity.

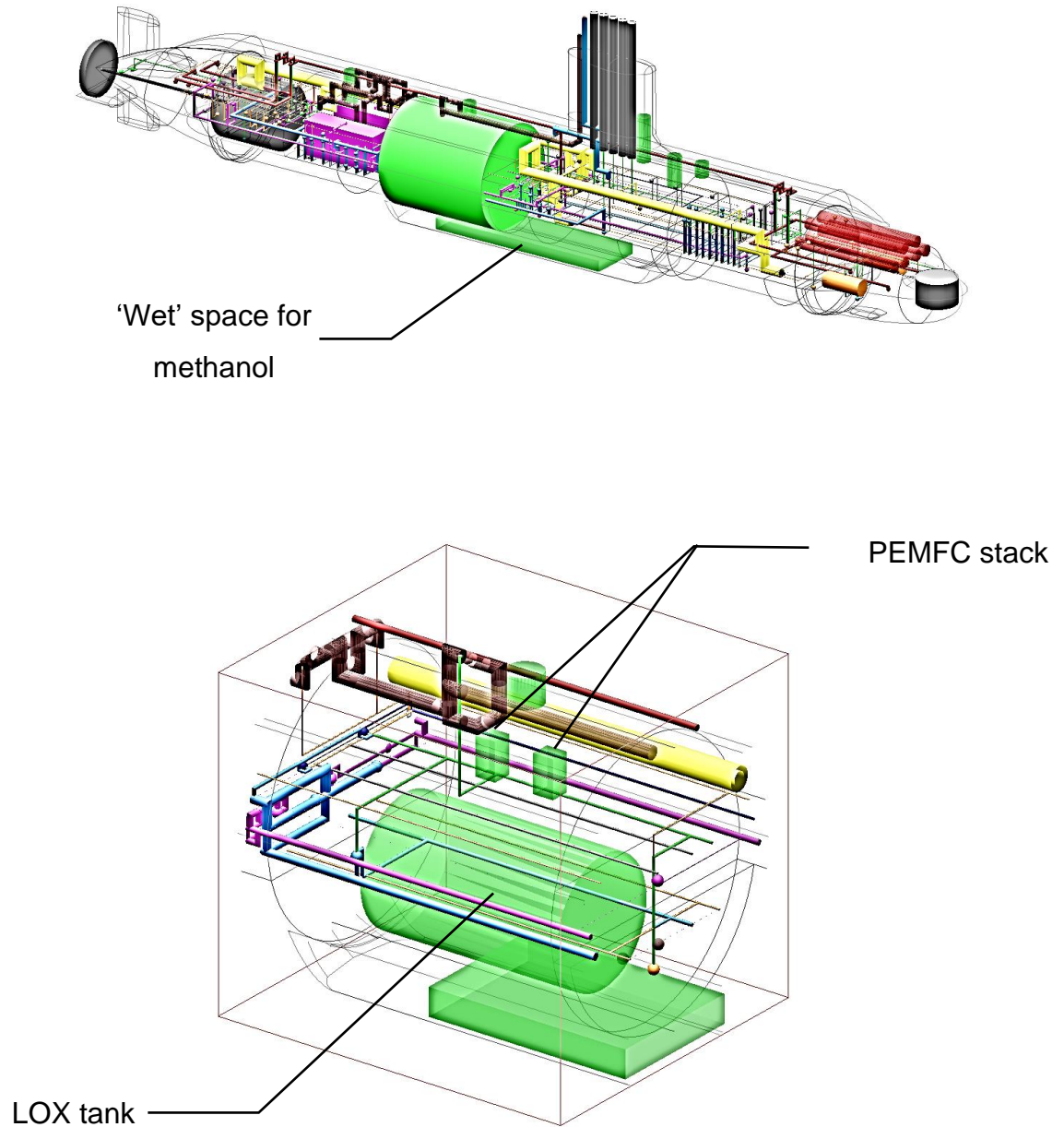


Figure 6.13: The physical architecture of design Variant 6.3.1.C, which shows a 3D perspective of the PEMFC AIP module in the overall submarine 3D layout (top) and major components of the AIP module (bottom). The DS3 routing complexity is also shown with the colour code presented in Table 5.4 on page 184 with certain Fight components shown in red and Infrastructure components shown in green

The SUBFLOW simulation results of this third sensitivity investigation were organised around the operating condition. The incorporation of AIP in the design requires at least three operating conditions to be addressed: snort, sprint, and submerged using AIP. Due to the insertion of the AIP module to the submarine design, the individual power flow was changed.

Generally, the energy flow of Case Study 6.3.1.B in the snorting scenario was raised due to the increased size of the pressure hull (see Figure 6.14 on page 267). In this scenario, 3.5 MW of power was delivered from the diesel generator node (PG DG) to the converter node (PC DC) and to the generator breaker node (PD PG) before being distributed throughout the vessel for various assumed steady-state load demands (see the green circle dashed in Figure 6.14). SUBFLOW analysis suggested 3 MW of power needed to be distributed to the starboard side of the vessel, while 378 kW to the port side of the vessel giving a total of 3.4 MW. Since DS3 sizing via SUBFLOW is not optimisation driven, the cable sizing for the connections PD PG and ND PG port/starboard was sized to full capacity 3 MW + 378 kW. This also took account of those arcs that showed zero flow. Therefore, the energy required for the mid and forward part of the vessel was 105 kW + 3 MW, which covered the hotel load and the energy for charging batteries in a short period to meet the desired indiscretion ratio. Meanwhile, 273 kW + 55 kW was transferred to the hotel load aft and the propulsion load in the snorting evolutions.

In the sprint scenario, only the battery node (SE BD) was used to meet the high propulsion demand and necessary hotel load (see the green circle dashed in Figure 6.15 on page 298). This was as high as 5.8 MW from a numerical submerged energy node (EE SM). Only 89 kW was transferred for the forward zone hotel load and 106 kW for the mid zone hotel load, to cover the heat removal system. The rest of the energy, 5.3 MW was transferred to the aft zone hotel load and sprint propulsion load demand. This SUBFLOW simulation revealed that such high demand (5 MW) would not be available from the low power 140 kW AIP system, and even from the high power 500 kW AIP system and thus the use of battery remained necessary to meet the high-power demand for sprint submerged scenario.

The Stirling AIP contribution gave 140 kW to partially satisfy the load requirement in the submerged operating condition (see the green circle dashed in Figure 6.16 on page 299). Interestingly, the SUBFLOW suggests that the generator breaker node (PD PG) distributed 115 kW (116 rounded-up) of power to the port side and 25 kW to the starboard side of the submarine. This meant that to size the cabling between bus node (ND LA) and bus node (ND PG), 140 kW was selected for both port and starboard sides of the submarine instead of individual values of 115 kW and 25 kW, provided that 140 kW was the largest flow in the operational architecture consideration (i.e., snort, sprint, and submerged AIP) in that the case study. On the port side of the submarine, more specifically at the bus node (ND PG port), no energy was required to be transferred to the forward part of the submarine. Meanwhile, on the starboard side, 25 kW of power from the Stirling AIP was intended for the aft hotel load demand. However, this was insufficient and thus 46 kW was required from the battery node (SE BD). Therefore 116 kW could be solely dedicated to the submerged speed propulsion demand.

Furthermore, the forward power load demand, which consists of mid and forward hotel load, was also fulfilled by the battery node (SE BD) (see Figure 6.16). At the battery breaker node (PD SE), the power was split 94 kW to the port and 171 kW to the starboard side of the submarine. At the port side of the submarine, the bus node (ND SE) received 94 kW of electrical energy, and it was forwarded for the forward zone hotel load. Meanwhile, at the starboard side of the submarine, the 171 kW energy was first received by the bus node for battery (ND SE) and subsequently used for the mid zone hotel load. Therefore, the SUBFLOW steady-state simulation reveals there was no contribution from the Stirling AIP to the forward power load demand.

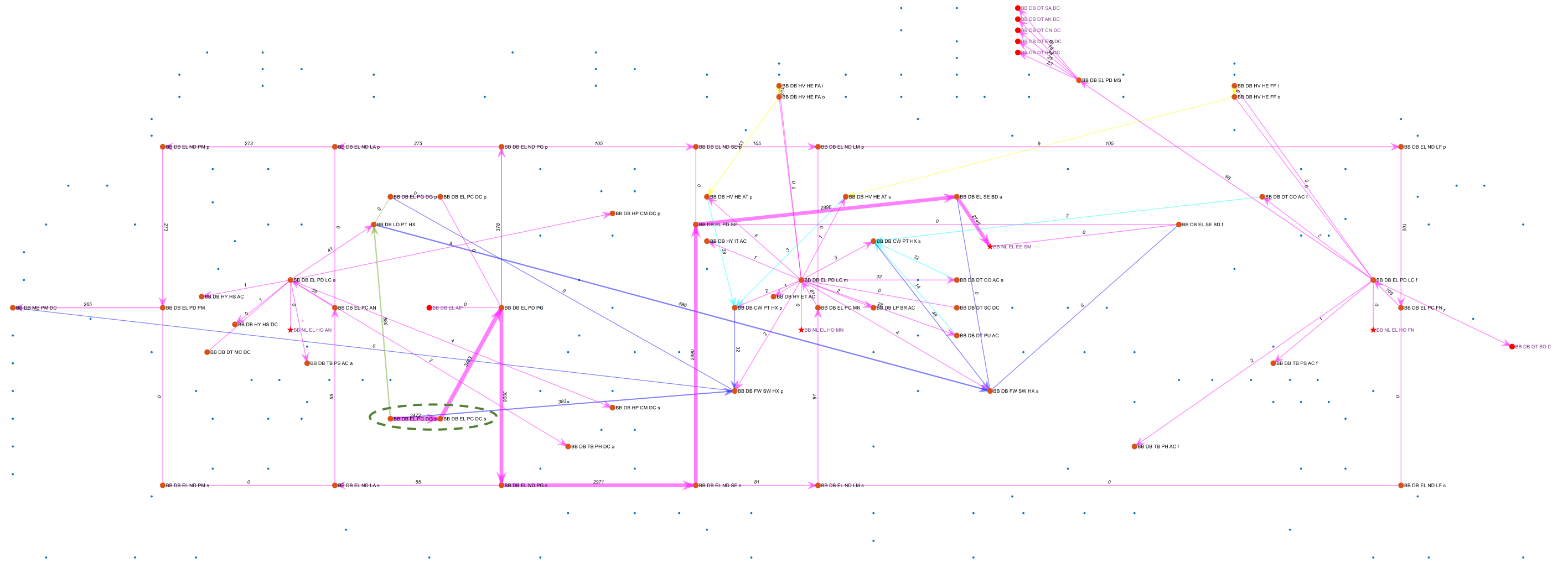


Figure 6.14: SUBFLOW simulation result for design Variant 6.3.1.B snort, which shows the energy flow of the electrical (EL) system in the snorting condition. The adjacent systems are also shown, and the blue dots represent the overall DS3 nodes in design Variant 6.3.1.B while the green circle dashed highlights the energy source in the system

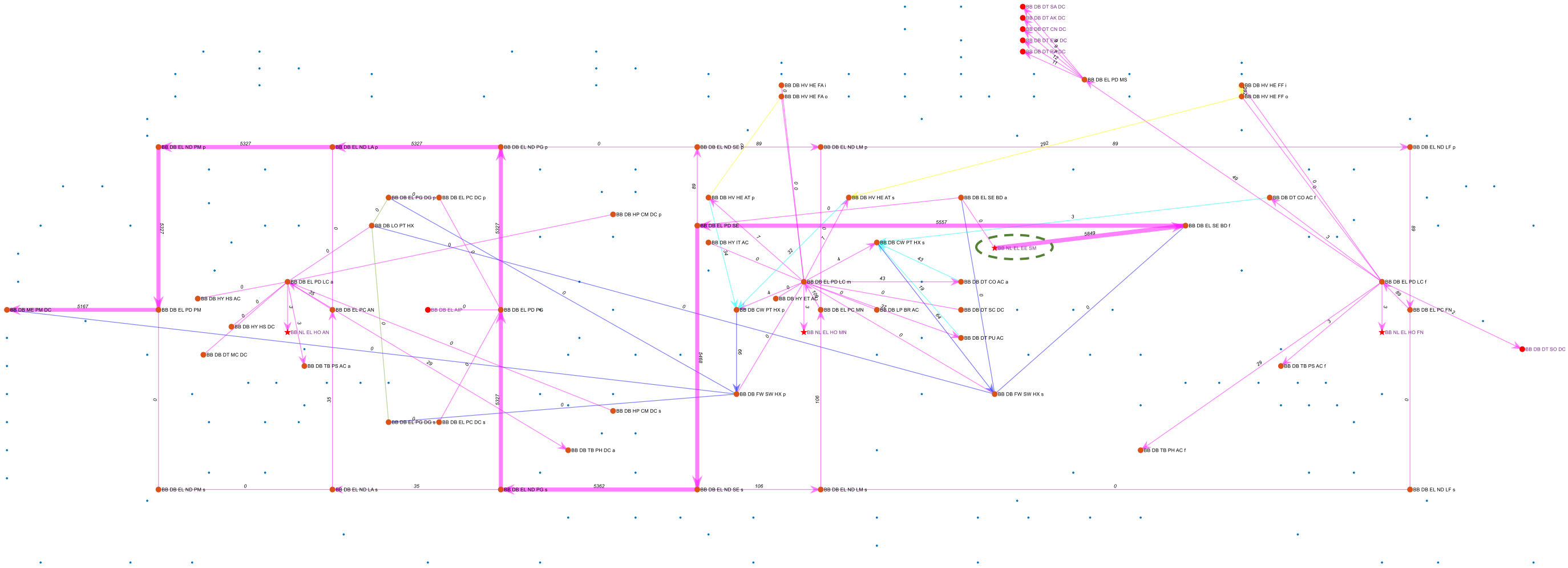


Figure 6.15: SUBFLOW simulation result for design Variant 6.3.1.B sprint, which shows the energy flow of the electrical (EL) system in the sprint submerged condition. The adjacent systems are also shown, and the blue dots represent the overall DS3 nodes in design Variant 6.3.1.B while the green circle dashed highlights the energy source in the system

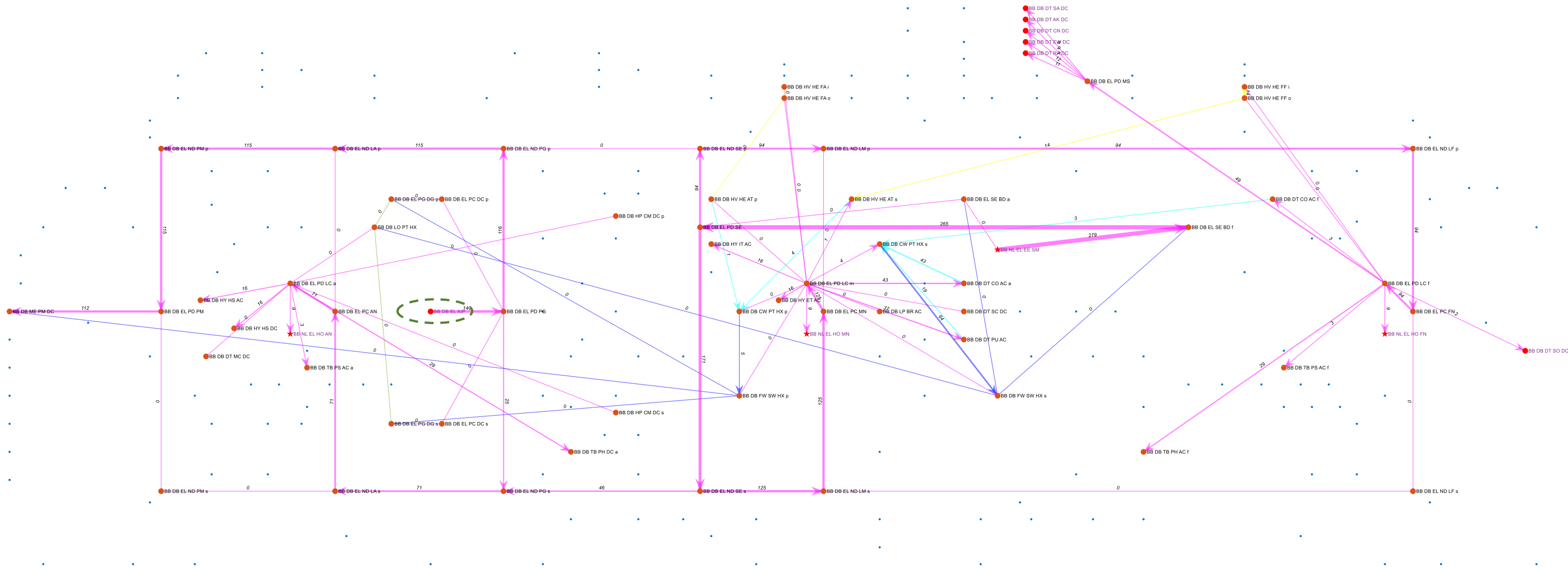


Figure 6.16: SUBFLOW simulation result for design Variant 6.3.1.B submerged, which shows the energy flow of the electrical (EL) system in the submerged condition. The adjacent systems are also shown, and the blue dots represent the overall DS3 nodes in design Variant 6.3.1.B while the green circle dashed highlights the AIP node

The steady-state SUBFLOW simulations for the design Variant 6.3.1.C for snort, sprint, and submerged scenarios are given in Figures 6.16, 6.17, and 6.18, respectively. In the snorting condition, 2.8 MW of power was produced by the diesel nodes (PG DG), converted by the converter nodes (PC DC), and then the generator breaker (PD PG) splits the 2.7 MW flow into 341 kW to the port side of the submarine and 2.4 MW to the starboard side of the submarine (see the green circle dashed in Figure 6.17 on page 302). At the port side of the submarine, more specifically, at the bus node (ND PG), 235 kW was transferred to the aft part of the submarine for the propulsion load at snort speed and 106 kW to the forward part of the submarine for the forward zonal hotel load. At the starboard side of the submarine, 47 kW was used for aft hotel load, while 2.3 MW was transferred to the forward part of the submarine. This energy was then used for battery charging at 2.2 MW, while 79 kW was used for mid hotel zonal load.

In the sprint scenario, 5 MW of energy was needed to meet the propulsion demand at maximum submerged speed and the necessary hotel load (aft, mid, and forward) (see the green circle dashed in Figure 6.18 on page 303). The SUBFLOW simulation revealed that at the battery breaker node (PD SE), 90 kW was used for the forward zonal hotel load and 4.7 MW was used for the propulsion load as well as the aft and mid zonal load. The 90 kW flow for the forward zonal hotel load was first received by the bus node (ND SE) and then went through several nodes, such as the bus node (ND LM) and eventually was received by the forward load centre node (PD LC) for the local load nodes at the forward part of the vessel. In this simulation, SUBFLOW suggested one direction of the major power flow, which was deducted in steps to several loads. This started from the bus node (ND SE) that deducted 104 kW for the mid hotel zonal load, leaving 4.6 MW towards the aft part of the submarine. At the next bus node (ND PG), a very small portion of the 4.6 MW (36 kW) was taken for the aft zonal load where the rest of the power was carried through several nodes towards the propulsion load node (PM DC).

In the sprint submerged scenario, the PEMFC AIP was used to produce 140 kW (see the green circle dashed in Figure 6.19 on page 304). When compared

to the Stirling AIP SUBFLOW simulation, the power produced by the PEMFC was also used for the propulsion load at sprint submerged speed, consisting of 78 kW with an aft hotel load of 63 kW (see the battery breaker node (PD PG)). That 63 kW power from the AIP node was still not enough to meet the aft zone hotel load requirement for the submerged scenario and thus 9 kW of power was used to meet this deficiency. The 9 kW power came from the 134 kW power of the battery breaker node (PD SE), which was originated from the battery nodes (SE BD). Therefore, 125 kW from the 134 kW of power was solely used for the mid zone hotel load. As in the PEMFC AIP SUBFLOW simulation, 94 kW was first transported from the battery breaker node (PD SE) to the port side of the submarine for the forward zone hotel load. This was because the payload power load was unchanged, being part of the control variable in this case study.

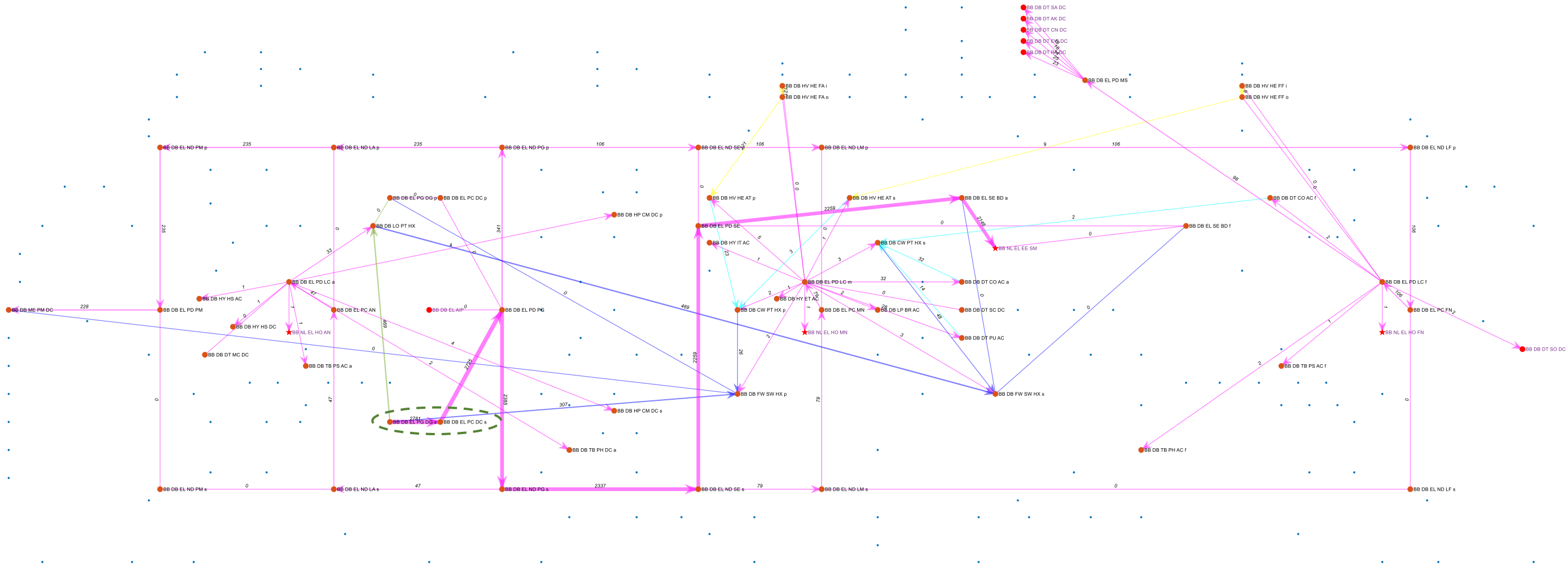


Figure 6.17: SUBFLOW simulation result for design Variant 6.3.1.C snort, which shows the energy flow of the electrical (EL) system in the snorting condition. The adjacent systems are also shown, and the blue dots represent the overall DS3 nodes in design Variant 6.3.1.C while the green circle dashed highlights the energy source in the system

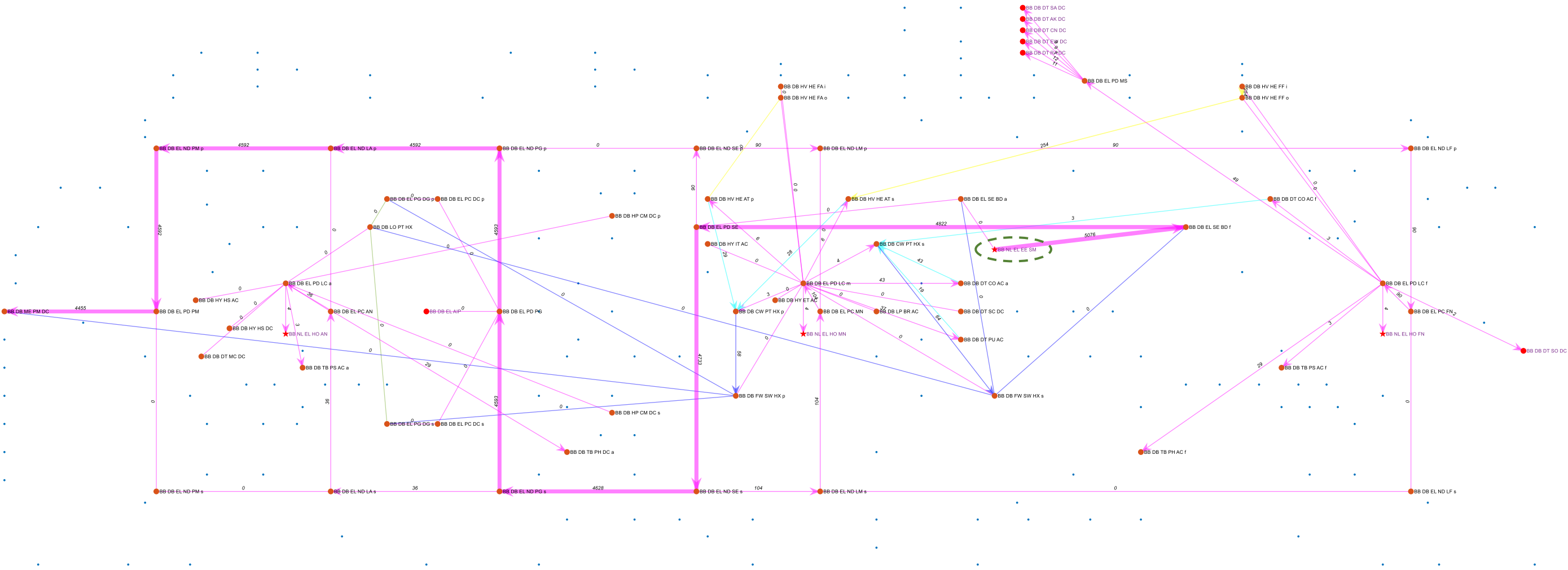


Figure 6.18: SUBFLOW simulation result for design Variant 6.3.1.C sprint, which shows the energy flow of the electrical (EL) system in the sprint submerged operating condition. The adjacent systems are also shown, and the blue dots represent the overall DS3 nodes in design Variant 6.3.1.C while the green circle dashed highlights the energy source in the system

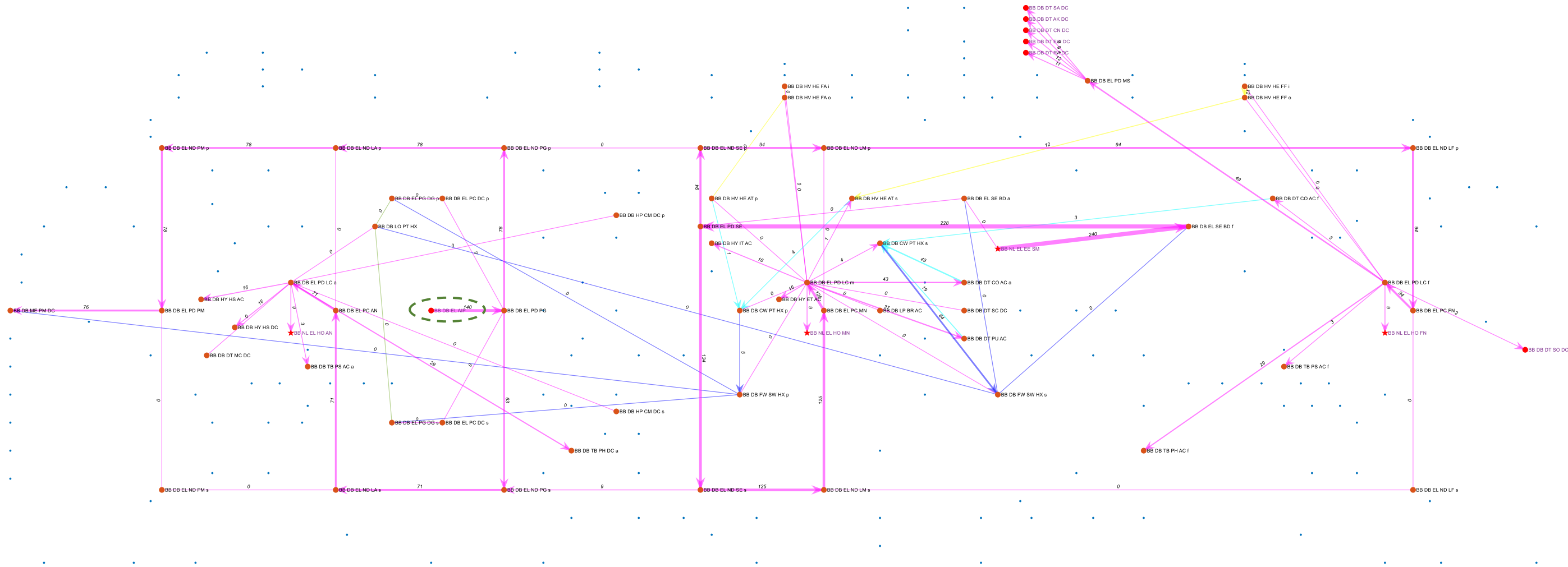


Figure 6.19: SUBFLOW simulation result for design Variant 6.3.1.C submerged, which shows the energy flow of the electrical (EL) system in the submerged operating condition. The adjacent systems are also shown, and the blue dots represent the overall DS3 nodes in design Variant 6.3.1.C while the green circle dashed highlights the AIP node

Having discussed the results of the AIP case study in terms of the physical architecture and logical architecture, the overall sizing impact is presented in Tables 6.8 and 6.9. To accommodate the major components of the Stirling AIP system, the design Variant 6.3.1.B submerged displacement became ~3700 tonnes compared to the baseline design Variant 6.3.1.A of 2500 tonnes. While incorporating the PEMFC AIP system, the increase of the submarine size was not anything like as great, being only 2870 tonne or 15% more than design Variant 6.3.1.A. Moreover, in contrast, the indiscretion ratio provided by the PEMFC AIP system in this study was 3% lower than the Stirling AIP system.

Although the indiscretion ratio was improved, Tables 6.8 and 6.9 show that the increase of the hull volume due to the incorporation of AIP also required a bigger diesel and battery size to maintain the two different speed requirements, being as the control variable in this study. Therefore, for the Stirling study, the diesel weight was increased by 21% compared to the design Variant 6.3.1.A, while for the PEMFC study the diesel weight was increased by 7%. Similarly, the battery for design Variants 6.3.1.B and C rose 25% and 8%, respectively.

The sizing impact in terms of the DS3, as shown in Tables 6.8 and 6.9, were affected and the changes could be seen to be generally proportional to the changes in the size of the resultant submarine. Similarly, in terms of the Weight Group (WG) or SWBS breakdown system, WG 2 for the design Variant 6.3.1.B was doubled over the design Variant 6.3.1.A. This was because of a bigger propulsion motor being required, as well as the 25% increase in the number of battery cells. In terms of cost, the incorporation of the Stirling AIP and PEMFC AIP systems led to a 45% and a 17% increase over the design Variant 6.3.1.A, respectively. These cost estimates specifically excluded the procurement costs of the two AIP systems.

Table 6.8: Summary of results for Case Study 6.3.1 Variants A, B, and C

Process Step	Selection Decision / Realisation for Case Study 6.3.1				Description		
Perceived need	Effect of different maximum speeds on DS3 sizing and overall design				Topic		
Outline of initial requirements	Common initial requirements as in Table 5.1						
	Initial Performance		Value				
	Accommodation		46 personnel				
	Patrol endurance		49 days				
Selection of style of emerging ship design	Common style selections						
	Style Level		Choice				
	Macro Level		Non nuclear (SSK)				
	Main Level		AIP power plant				
			Medium size ocean-going submarine				
			Single hull with casing				
	Micro Level		Three watertight bulkheads				
		Detailed DS3 styles as in Subsections 5.3 to 5.7					
Selection of major equipment and operational sub-systems	Design Variant		Variant 6.3.1.A	Variant 6.3.1.B	Variant 6.3.1.C		
	Main Style for AIP		No AIP	Stirling AIP	PEM-FC AIP		
	AIP Configuration		Baseline no AIP	Diesel fuel with liquid oxygen	Methanol with liquid oxygen		
Selection of whole ship performance characteristics	Common whole ship performance as in Table 5.1						
	General Performance		Value				
	Sprint speed		20 knots (>2 hrs)				
	Submerged speed		5 knots (>17 hrs)				
	Snort speed		6.5 knots (<6 hrs)				
	Specific Performance		Value				
	Indiscretion ratio		<23 %				
	DS3 Performance		see Subsections 5.3 to 5.7 and Appendix 9				
Selection of synthesis model type	Approaches as in Table 5.1 and The Network Block Approach (NBA)						
Selection of basis for decision making in initial synthesis	Common basis for decision making in initial synthesis						
	UPC while meeting S ⁴ criteria		Endurance at different speed				
	Energy balance for DS3		Longitudinal and vertical stability, e.g., submerged BG>0.2 energy supply is equal to energy demand				
Synthesis of ship gross size and architecture	Initial submarine resultant characteristic						
	Surfaced displacement (te)	2250	3327	2586			
	Submerged displacement (te)	2498	3694	2870			
	AIP indiscretion ratio (%)	22	9.8	9.2			
	Diesel generators (MW)	2.8	3.4	3			
	Battery cells (lead acid)	480	600	522			
	Item	Weight (te)	Space (m ³)	Weight (te)	Space (m ³)	Weight (te)	Space (m ³)
	Data (DT) system	38.46	38.46	66.85	41.04	67.97	41.18
	Fuel oil (FO) system	216.73	216.73	268.50	314.98	234.75	275.12
	Electric (EL) system	341.89	341.89	437.17	238.77	381.82	209.18
	Mechanical (ME) system	105.68	105.68	134.09	179.92	114.86	155.03
	Ventilation (HV) system	20.60	20.60	24.67	68.58	24.20	72.36
	Lubricant oil (LO) system	5.34	5.34	6.64	5.34	5.78	4.66
	Chilled water (CW) system	1.45	1.45	1.60	3.03	1.71	2.97
	FW/SW heat systems	17.98	7.31	22.20	9.37	24.05	8.18
	Hydraulic (HY) system	18.11	18.11	18.14	23.05	18.14	23.05
	Trim ballast (TB) system	22.12	22.12	22.05	14.83	22.70	15.06
	High-pressure air (HP) system	6.54	6.54	6.52	8.77	6.60	8.84
	Low-pressure air (LP) system	3.50	3.50	3.45	6.10	3.81	7.28
	Total DS3	798.39	787.73	1011.89	913.78	906.39	822.88
	Weight Group Classification	Weight (te)	Cost (£ mil)	Weight (te)	Cost (£ mil)	Weight (te)	Cost (£ mil)
	WG 1 structure	871	78.42	1258	113.21	990	89.133
	WG 2 main propulsion	383	68.939	835	150.27*	553	99.467*
WG 3 electrical services	117	27.802	158	37.654	142	33.914	
WG 4 control and communications	48	10.367	49	10.518	49	10.518	
WG 5 ship services	164	65.698	189	75.602	179	71.647	
WG 6 outfit	67	37.633	76	42.697	69	39.209	
WG 7 payload	87	16.549	87	16.549	87	16.549	
WG 8 fixed ballast	173	-	255	-	202	-	
WG 9 variable load	615	9.2242	814	12.216	679	10.179	
Total WG	2525	314.63	3721	458.72	2950	370.62	
Note	*Cost exclude Stirling and PEM-FC AIP equipment						
Exploration of impact of style, major items, and performance characteristics	Effect of varying Main styles on overall design				Independent variables		

Table 6.9: Normalised results for Case Study 6.3.1 figures are given as a percentage of the characteristics for Variant A

Process Step	Selection Decision / Realisation for Case Study 6.3.1				Description		
Perceived need	Effect of different maximum speeds on DS3 sizing and overall design				Topic		
Outline of initial requirements	Common initial requirements as in Table 5.1						
	Initial Performance		Value				
	Accommodation		46 personnel				
	Patrol endurance		49 days				
Selection of style of emerging ship design	Common style selections						
	Style Level		Choice				
	Macro Level		Non nuclear (SSK)				
	Main Level		AIP power plant				
			Medium size ocean-going submarine				
			Single hull with casing				
	Micro Level		Three watertight bulkheads				
		Detailed DS3 styles as in Subsections 5.3 to 5.7					
Selection of major equipment and operational sub-systems	Design Variant		Variant 6.3.1.A	Variant 6.3.1.B	Variant 6.3.1.C		
	Main Style for AIP		No AIP	Stirling AIP	PEM-FC AIP		
	AIP Configuration		Baseline no AIP	Diesel fuel with liquid oxygen	Methanol with liquid oxygen		
Selection of whole ship performance characteristics	Common DS3 configurations as in Subsections 5.3 to 5.7 and Appendix 9						
	AIP power output		Low power 2x70 kW AIP modules				
	Major equipment		2x1.4 MW diesels				
	DS3 equipment		Detailed DS3 equipment as in Table 5.1				
Selection of synthesis model type	Common whole ship performance as in Table 5.1						
	General Performance		Value				
	Sprint speed		20 knots (>2 hrs)				
	Submerged speed		5 knots (>17 hrs)				
	Snort speed		6.5 knots (<6 hrs)				
	Specific Performance		Value				
Selection of basis for decision making in initial synthesis	Indiscretion ratio		<23 %				
	DS3 Performance		see Subsections 5.3 to 5.7 and Appendix 9				
Selection of synthesis model type	Approaches as in Table 5.1 and The Network Block Approach (NBA)						
Selection of basis for decision making in initial synthesis	Common basis for decision making in initial synthesis						
	UPC while meeting S ⁴ criteria		Endurance at different speed				
	Energy balance for DS3		Longitudinal and vertical stability, e.g., submerged BG>0.2 energy supply is equal to energy demand				
Synthesis of ship gross size and architecture	Initial submarine resultant characteristic						
	Surfaced displacement (te)	100%	147.8%	114.9%			
	Submerged displacement (te)	100%	147.8%	114.9%			
	AIP indiscretion ratio (%)	100%	44%	41%			
	Diesel generators (MW)	100%	121%	107%			
	Battery cells (lead acid)	100%	125%	108%			
	Item	Weight (te)	Space (m ³)	Weight (te)	Space (m ³)	Weight (te)	Space (m ³)
	Data (DT) system	100%	100%	173.8%	93.1%	176.8%	93.4%
	Fuel oil (FO) system	100%	100%	123.9%	123.9%	108.3%	108.2%
	Electric (EL) system	100%	100%	127.8%	130.3%	111.6%	114.1%
	Mechanical (ME) system	100%	100%	126.9%	126.1%	108.7%	108.7%
	Ventilation (HV) system	100%	100%	119.7%	113.9%	117.5%	120.2%
	Lubricant oil (LO) system	100%	100%	124.3%	124.1%	108.3%	108.3%
	Chilled water (CW) system	100%	100%	110.0%	110.8%	117.6%	108.5%
	FW/SW heat systems	100%	100%	123.5%	123.6%	133.8%	107.9%
	Hydraulic (HY) system	100%	100%	100.2%	100.1%	100.2%	100.1%
	Trim ballast (TB) system	100%	100%	99.7%	99.8%	102.6%	101.3%
	High-pressure air (HP) system	100%	100%	99.8%	99.8%	100.9%	100.6%
	Low-pressure air (LP) system	100%	100%	98.5%	97.3%	108.6%	116.0%
	Total DS3	100%	100%	126.7%	121.5%	113.5%	109.4%
	Weight Group Classification	Weight (te)	Cost (£ mil)	Weight (te)	Cost (£ mil)	Weight (te)	Cost (£ mil)
	WG 1 structure	100%	100%	144.4%	144.4%	113.7%	113.7%
	WG 2 main propulsion	100%	100%	218.0%	218.0%	144.3%	144.3%
	WG 3 electrical services	100%	100%	135.2%	135.2%	121.8%	121.8%
	WG 4 control and communications	-	-	101.5%	101.5%	101.5%	101.5%
	WG 5 ship services	100%	100%	115.1%	115.1%	109.1%	109.1%
	WG 6 outfit	100%	100%	113.5%	113.5%	104.2%	104.2%
WG 7 payload	-	-	100.0%	100.0%	100.0%	100.0%	
WG 8 fixed ballast	100%	-	147.7%		116.8%		
WG 9 variable load	100%	100%	132.4%	132.4%	110.4%	110.4%	
Total WG	100%	100%	147.4%	145.8%	116.8%	117.8%	
Exploration of impact of style, major items, and performance characteristics	Effect of varying Main styles on overall design				Independent variables		

6.4 Conclusion from Sensitivity Analyses

The objective of this chapter was to show that the Network Block Approach (NBA) can be used to explore the impact of different design decisions on DS3 sizing as well as the overall impact on submarine design. The studies begin with the exploration of vehicle performance, namely maximum speed when submerged, which was found to affect the size of the electrical (EL) system as well the mechanical (ME) and heat removal system. This was followed by the exploration of design style, which was at the micro and main levels. It was discovered that even at the micro level style decision, the proposed Network Block Approach (NBA) was sensitive. This is because the Network Block Approach (NBA) employs an integrated SUBFLOW with network flow response simulation and the sophisticated 3D based synthesis using Paramarine-SURFCON. The next chapter discusses the overall research in more detail.

Chapter 7

Discussion

This chapter first considers whether the research has met the aim and the several objectives spelt out in Tables 7.1 and 7.2 below. Subsequent sections discuss what the findings mean in relation to the body of knowledge in the field of submarine DS3 design. Each section covers three main areas: the strategic level, considering the wider submarine design implications and linked to the research background in Chapter 2; the tactical level, providing specific points that arose concerning work undertaken to meet the research aim; and finally, at the detailed level, outlining the emergent issues and further emergent work.

7.1 Meeting the Research Aim

Chapter 2 as a State-of-the-Art review proposed that the different submarine DS3 architectures ought to be considered together. It was considered that none of the existing approaches was able to achieve an integrated DS3 synthesis that works well across all three architectures (physical, logical, and operational), and particularly, addressed both the physical and logical architectures.

A sophisticated 3D based synthesis such as the UCL Design Building Block (DBB) approach (Andrews, 2018c), when using the SURFCON module in the Paramarine CASD system, enables the designer to model DS3 physical architecture to whatever level of detail is deemed necessary. This could be well beyond the DS3 concept design level but was found to be limited in capturing the overall set of DS3 logical architectures. In contrast, most of the current network theory applications to surface ship distributed systems, including Architecture Flow Optimisation (AFO) and its variants (Parsons et al., 2020a), are focused on performing optimisation while keeping the DS3 physical architecture as simple as possible. This has been achieved by sacrificing the quality of the definition of the DS3 physical architecture in order to apply sophisticated optimisation driven and network analysis much earlier in the ship design process.

The novel approach to DS3 architecture presented in this thesis is seen to close the gap, by combining the advantages of the 3D physical based synthesis of the UCL DBB ship design approach with the network based AFO type synthesis for DS3, when applied to the complexity of submarine DS3 design where current simplistic DS3 sizing is considered a limitation. This new approach is considered to thus meet the overall aim presented in Section 2.5:

To develop an integrated approach to the synthesis of distributed ship service systems (DS3) that facilitates the consideration of DS3 aspects early in ESSD for a new submarine design option, as part of Requirement Elucidation.

A degree of confidence has been established that this aim has been satisfactorily achieved in largely meeting the research objectives stipulated in Section 2.6. However, further development is considered necessary to comprehensively address all the objectives and thus confirm the extent to which the aim has been met.

The research first investigated the fundamental theory of Network Flow Optimisation (NFO) outlined in Section 3.1. Subsequently, the candidate proposed and developed the SUBFLOW simulation, having an Operational Matrix framework to reduce the black box elements of the extant NFO approach. SUBFLOW was first demonstrated for energy balance in Section 3.2 and then was used to minimise the volume of the Power and Propulsion System (PPS) cabling in Section 3.3. This led to achieving an energy balance rather than a flow optimisation focus and became the basis of the SUBFLOW application in the case study presented in Chapter 5 and sensitivity studies in Chapter 6.

The investigation of DS3 synthesis using the SURFCON module in Paramarine to produce a physical architecture was presented in Section 3.3. This revealed that the effort of modelling DS3 using Paramarine was demanding and could be seen to be both inhibiting and distracting the designer from the advantages of 3D informed insights revealed, for both DS3 and the overall SSK design

when using the Paramarine CASD tool. The high flexibility of the Paramarine ship design toolset, particularly the descriptive ability of the Design Building Block (DBB) objects in storing data at different levels of design granularity, facilitated exploring different levels of design hierarchy (Pawling, 2007). However, excessive flexibility in such a modelling approach ran the risk of hindering the speed at which the data could be rapidly read, as required to run the SUBFLOW simulation (Subsection 4.2.4).

Therefore, a new approach was proposed, which the candidate termed the Network Block Approach (NBA) (see Figure 4.13 on page 172). The NBA enabled synthesising various DS3 in terms of their physical architecture and their logical architecture. Regarding the physical architecture, the proposed Physical Loop method (Section 4.2) allowed a designer to develop the DS3 design at different levels of granularities, ranging from modelling individual DS3 components to various DS3 routings using pre-defined highways. While for the logical architecture, the proposed Logical Loop method (Section 4.3) allowed the designer to solve the energy balance of a set of distributed systems and to visualise the complexity of the DS3 within a 3D multiplex network configuration. Such 3D based physical and logical syntheses have the potential to greatly improve communicating the design of submarine DS3 to others, be they other members of the project team or reviewers of the design.

Besides the Physical Loop and Logical Loop methods, the NBA also required several programs, which were implemented in the spreadsheet environment. Such programs consisted of thousands of lines of VBA based programs (macro) and MATLAB codes to automate those features readily automated. In particular, this consisted of the demanding physical modelling effort as part of using Paramarine-SURFCON. These codes required frameworks outlined in Subsections 4.2.1 to 4.2.6. These include the following frameworks: different levels of design granularities and fidelities; types of DBB objects; a DBB hierarchy based on design granularities; DS3 routings; and a coherent naming convention for various types of DBB objects. The spreadsheet environment also allowed rapid data transfer to the MATLAB format, so that the Operational

Matrix (Subsection 3.1.2) could be generated automatically for the SUBFLOW program to analyse the energy balance of the different DS3 categories.

The summary of the outcome of the work undertaken to meet the various research objectives is discussed in the next two subsections.

7.1.1 Improving the Submarine Concept Design

Table 7.1: First part of the strategic view of meeting the research objectives

Objective	Description	Outcome Satisfactory?
1.1	The proposed approach should assist the designer to get a feel for the contribution to ship weight and space demands of the selected DS3 in a manner that improves on the traditional numerical approach.	Yes. The proposed approach uses energy based sizing, i.e., the power at each DS3 node and connection that can be converted not only into relevant weight group but also space input to the submarine ESD.
1.2	The approach should allow the designer to consider the impact of different DS3 style choices on the whole submarine design for a more effective Requirement Elucidation dialogue with design stakeholders in ESSD.	Mostly. As discussed in Chapter 3, a significant amount of work to develop new design tools was necessary to make the Network Block Approach (NBA) plausible for practical ESSD application. Consequently, not many DS3 style studies were produced in this research in contrast to what might be done using black box tools.
1.3	Given the approach is not black box based, the designer should be able to develop submarine design <i>ab initio</i> and subsequently select or develop relevant design algorithms (rather than being hardcoded).	Yes. The proposed approach involves programs that were designed to be of a glass box nature so they can be initiated from a clean sheet. Thus, no design algorithms are hardcoded into the tools. This eases the task and applicability for any new user in learning the inner structure of the programs.
1.4	The approach should have a degree of flexibility and scalability to allow innovative options to be explored in ESSD.	Mostly. Several case studies were developed with different design granularities to show the proposed approach can have a degree of flexibility and scalability, considered more appropriate for submarine ESD than the gross size based algorithm used currently.

The network based synthesis, SUBFLOW, has been shown in Chapter 5 to meet this objective by aiding the designer to, first, develop each system's line diagram and then convert it into a network, and finally attach the numerical power demand to relevant DS3 nodes. Although some DS3 connections could be directly sized from weight or volume to length assumptions, by using the numerical power demand inputs, SUBFLOW could seek an energy balance and

then produce solutions for the power level at nodes and arcs. The designer could use such solutions as the basis for scaling up or down the size of relevant DS3 using power to weight or power to volume ratios. Still, such a proposed approach is seen to require a significantly larger amount of input data than is usually the case for submarine ESD. For example, the power to volume or weight ratios of each DS3 equipment could be obtained from the energy coefficients 'Sankey Diagram' (see Table 3.11 on page 99) for all DS3 being considered using SUBFLOW. Such insight would not normally be available at ESSD without extensive use of high-quality and detailed equipment databases.

Since the proposed approach was intended to be of a glass box nature, the number of design explorations could not readily match hundreds of apparently (but simplistically and numerically described) balanced design studies that could be readily produced by usual highly automated and black box tools. This is because the latter are based on hardcoded design algorithms, assumptions, and rarely obvious implied design decisions for balancing the design and therefore would overly constrain 'out of the box' design options. It could be considered worthwhile to undertake further case studies beyond the current research to show that the proposed Network Block Approach (NBA) can be used for style exploration at a wider macro and main level of style, such as nuclear power plant and even single skin vs double skin hull configurations. The changes at this level could be more significant, especially in comparison with those that have been addressed in Chapter 6, which were primarily to demonstrate the approach.

The NBA uses a simple spreadsheet environment that allows a designer to develop one or more design options *ab initio*. The designer can select and update the relevant design algorithms into the design sheets at any point as the design progresses. This is different to a black box approach in which hardcoding many design algorithms means it is difficult for a new user to appreciate the implications of the hidden assumptions and if such an investigation is required for their concept, then how they can coherently modify the design data or design algorithms. The programs composing the NBA are intended to automate what could be considered as the Gulfs of Execution and

Evaluation (Figure 2.6 on page 51) and thus enable Paramarine to perform repetitive actions for both DS3 physical modelling and network based energy balancing (see Section 4.1). These NBA programs can be readily modified in any future development. To do so simply requires pre-requisite knowledge of the relevant programming languages (VBA and MATLAB) as well as familiarity with Paramarine-SURFCON.

A set of frameworks which can be used to distinguish different design granularities was proposed in Subsection 4.2.1. This would allow the NBA to be applied at whatever level of detail deemed appropriate to a given DS3 submarine concept design. The case study in Section 3.3 shows a minimum number of DS3 equipment necessary for cable sizing analysis, while the case study in Chapter 5 used many electrical (EL) components to show the approach can also be developed to a greater level of detail than might usually be appropriate. This then showed the capability needed to explore certain DS3 subsets and style alternatives appropriate to a given submarine concept investigation.

Any further development of the DS3 network would only be possible provided that the designer can produce a DS3 line diagram (e.g., Piping Instrumentation Diagram (PID)) and access or produce an equipment database. Thus, further case studies using the proposed NBA ought to be undertaken for a more comprehensive demonstration of this objective. This might require exploring the impact of new technologies to facilitate wider innovation in the submarine design, so fostering “radical ideas”. Candidate technologies include the integration of a ‘rim driven’ propulsion system (Collins and Wrobel, 2014) or an electrically based actuation approach replacing the hydraulic system as part of exploring a possible Integrated Full Electric Propulsion (IFEP) submarine (Section 5.4).

7.1.2 Enabling DS3 Synthesis Approach

Table 7.2: Second part of the strategic view of meeting the research objectives

Objective	Description	Outcome Satisfactory?
2.1	The proposed approach should capture the complexity and interrelations of DS3 and aid design stakeholders' understanding of systems choices. This then would contribute to Requirement Elucidation for the whole design.	Yes. In Chapter 5, the Network Block Approach (NBA), with the Logical Loop method, has been applied to design multiple submarine DS3 using a multilayer, multislice, 3D network (see for ~200 nodes and ~400 connections in Section 5.2). This revealed the dependency of the total ship systems on the various DS3 technologies.
2.2	The proposed approach should consider multiple DS3 to be developed and the development of DS3 logical and physical architectures should be both simultaneous and as seamless as possible. This would allow the exploration of DS3 choices in submarine ESD.	Yes. The new tools, which consist of several Excel based programs and were built using VBA codes, have enabled a two-way synthesis. Thus, as discussed in Chapter 5, the designer can develop DS3 in terms of the physical architecture concurrently with the logical architecture.
2.3	The network application in the proposed approach should be a less constrained approach than using existing methods. Thus, the mathematical model in the network theory should reflect the distinct physics of the submarine's DS3 problem without excessive detail, commensurate with the exploratory nature of submarine ESD.	Yes. The SUBFLOW, part of the Network Block Approach (NBA) was not used to optimise DS3 design nor the overall submarine design. Only continuity constraints were hardcoded into the SUBFLOW process to find energy balance on the submarine and for early stage sizing using power to volume or power to weight ratios. The rest of the constraints could be modified in the programs within the NBA. Thus, the energy flow simulations in the case studies could reflect the physics of snorting and submerged operating conditions for a study of a SSK with/without AIP.

The early stage design of distributed systems could have been developed and facilitated in a UCL DBB implementation using Paramarine-SURFCON but this was considered to be unlikely to enable the development of a necessarily responsive DS3 synthesis approach. In particular, logical and operational architectural considerations could be addressed beyond just physical models, i.e., the physical architecture of DS3 (see Subsection 2.1.1). It was found in using Paramarine that the ability to adequately visualise DS3 line diagrams was limited (see Appendix 8). Thus, it was seen to be sensible to consider approaches specific to designing DS3 and in particular approaches aiding the designer to develop the logical architecture of DS3 in ESSD. In Chapter 5, the

Logical Loop method removes this limitation by employing multilayer 3D DS3 networks in MATLAB. The case study in Chapter 5 is considered to reveal at ESD the recognised total distributed ship systems dependency of the submarine (see Figure 5.4 on page 182). However, the DS3 network in Chapter 5 could be developed to a greater level of detail to model more of the total distributed ship systems of a submarine, especially systems where there are many more pumps and valves than modelled in the case study. Countering this is the question of whether further levels of detail, beyond that presented in Chapter 5, would overwhelm the designer with DS3 information in ESSD and inhibit their ability to control what is displayed. Thus, for some DS3, such as domestic and water systems the use of a simple scaling approach was considered sufficient. This is discussed further in Section 7.5.

As discussed in Chapter 4, the Network Block Approach consists of the Physical Loop and Logical Loop methods modelled using the software tools, Paramarine-SURFCON and MATLAB, respectively. Bridging these methods, a simple spreadsheet tool was produced to store the relevant inputs for submarine DS3 synthesis. This spreadsheet tool, which provides rapid Paramarine modelling and streamlined data flow for the SUBFLOW tool in MATLAB, is composed of ten programs listed in Table 4.1 on page 145. These programs have made possible the development of the full set of DS3 physical and logical architectures, consistent with the UCL inside-out ship design philosophy (Andrews, 2018c) for ESSD.

When developing the various and diverse DS3s in terms of their logical architectures, the current network theory applied to surface ship distributed systems (Brown, 2020) were found to be dependent on optimisation schemes that constrain DS3 solutions when compared to the preferred more style driven approach (Andrews, 2018c). The AFO process, including its variants (VAFO and DAFO, see Subsection 2.3.4), has been constrained to a specific optimisation setup and devised to work well as part of Virginia Tech's Ship Synthesis Model (Brown and Waltham-Sajdak, 2015). This was considered less appropriate for submarine concept design, which requires a more hands-on DBB-like approach for the physical arrangement architecture significant in such

a highly balanced system of systems (Andrews, 2017a). As justified in Chapter 3 and subsequently developed in Chapter 4, the SUBFLOW tool was formulated to solve the DS3 energy balance by linear programming without optimising the DS3 design and even less inappropriately to the overall submarine concept design.

Although further improvements would enhance the proposed approach, it has been shown to be capable of combining the UCL DBB approach (Andrews, 2018c) and the Network based approach to DS3 sizing (Parsons et al., 2020a) through a new and more integrated Network Block Approach (NBA). The new programs within the NBA were developed not just to improve the speed of synthesising DS3, but to help the designer by reducing labour-intensive modelling in Paramarine of new design options (see Figure 2.6 on page 51). Thus, the designer can readily explore and manipulate the architecture of the submarine without undertaking tedious repetitive tasks that would be required by solely modelling DS3 in Paramarine-SURFCON,

7.2 DS3 Synthesis in the Initial Submarine Design

One of the major issues in adding DS3 exploration to the concept phase is that it requires extra design effort and time with extra input and detailed information that is unlikely to be available early in the design process. Therefore, simple gross ship size based algorithms adopted in ship design have been traditionally seen as a convenient approach since it gives quick estimates of weight and space but is thus evolutionary with ‘type ship’ assumptions (Andrews, 2018c). So, the question then is, is there a better way to synthesise DS3 that is less complex than detailed DS3 sizing? The initial case studies (Sections 3.1 and 3.2) show a network theory could aid DS3 sizing by initially breaking down the DS3 power flow as early in the synthesis as with a traditional numerical calculation. However, applying a network theory at that numerical level synthesis was still found to have limitations. These suggested the use of network theory still needed architectural modelling to allow a fuller DS3 synthesis for ESSD. Unlike previous DS3 researches (Brownlow et al., 2021), which adopt low detail 2.5D physical architecture (see Table 2.2 on page 58), in this research the use of network theory was expanded to incorporate a sophisticated 3D based synthesis, the UCL DBB approach (Andrews, 2018c).

Case study 3.3.1 has demonstrated the implementation of the UCL DBB approach in Paramarine-SURFCON could greatly improve the application of a network approach to DS3 synthesis. Without a sophisticated 3D based synthesis, it was considered difficult to ensure the identified DS3, with their appropriate style choices, were able to be fitted and integrated into an initial submarine design. By departing from physical architecture, a DS3 network could be modelled and then be used to size DS3 connections, as demonstrated in Case Study 3.3.1. That case study also demonstrates that the length of the pressure hull for that design study and the height of its casing had to be altered (see Figure 3.14 (d) on page 118), to accommodate all four diesel generators (required for redundancy) and their external exhausts, while Paramarine was used to recalculate the design’s hull resistance. This was achieved while keeping the 3D DS3 synthesis loop process in a single software environment, which meant the design features could be linked based on the dimensionality

of the relationships (Pawling, 2007) and thus any change automatically causing changes to cascade through the entire design. Despite the benefits provided by such a sophisticated 3D based synthesis, some researchers have already argued designing layouts according to the DBB approach in 3D Paramarine-SURFCON remains labour intensive (Gillespie, 2012; Rigterink, 2014; Pawling et al., 2015). However, these critiques did not include the example of the DS3 synthesis, as it is demonstrated in Case Study 3.3.1, which was also found to require a significant amount of additional design effort just to model a simple DS3 in Paramarine. So, there were two modelling issues when developing a single design in a 3D based Paramarine synthesis: modelling the 3D submarine design; and then subsequently modelling the 3D DS3. This was seen to inhibit the aim of exploring multiple designs in concept. It is thus worth considering as alternatives to the DBB implementation in Paramarine: both reducing 3D into 2.5D synthesis or the use of automated approaches, as discussed in the following two subsections.

7.2.1 Alternative Design Tools: 2.5D

The first alternative would be to reduce the 3D based synthesis to what is called '2.5D' to allow a simpler architecturally oriented design tool. This has been developed in the UCL Design Research Centre (DRC) specifically for surface ship design research and education and is called the "UCL layout exploration tool", which uses the JavaScript language (Kouriampalis et al., 2021). However, a 2.5D design tool has to sacrifice many advantages from using a 3D based synthesis. This then raised the question as to whether a submarine design approach needs to be 3D based and what might be the advantages identified of using such a 3D based synthesis in concept design?

As demonstrated in Case Study 5.1, more specifically, Figure 5.9 on page 189, submarine DS3 arrangement and physical routing are reasonably complex and thus any 2.5D design tool will be unlikely to be able to capture overlapping DS3 routing due to different highways being on the same deck. Furthermore, the physical interactions of DS3 components are going to be scattered in a 3D space within a compartment and, without a 3D representation, consideration of accessibility to those DS3 in the confines of a crowded compartment would be

hard to address (see the HP air system example in Subsection 5.5.1). The identification of such 3D related issues early in the design process would help ensure the selected DS3 design could be integrated into the submarine design beyond compartment or packing densities assumptions (such as (Purton, 2016)) that need to be based on previous designs. Furthermore, given the advances in computer graphics, not utilising such technology to create a 3D based synthesis was seen to be not taking advantage of CAD developments. The issue is seen rather be how to make the 3D based synthesis execution process as simple as possible so that the designer is able to manipulate the 3D architecture of the vessel and focus on important architecturally driven decision making in ESSD.

The research has therefore focused on countering the drawbacks in implementing Paramarine rather than developing a further separate or standalone design tool, such as the UCL 2.5D surface ship derived design tool (Kouriampalis et al., 2021). Unlike surface ship design, any changes in major DS3 size and locations on a submarine will also notably impact the submarine's Centre of Gravity ($\overline{KG/LCG}$) and hence \overline{BG} and longitudinal balance (Subsection 2.1.1). Thus, in Case Study 3.3.1, the incorporation of redundant major PPS components resulted in the adjustment of the battery and solid ballast location to counter the longitudinal moment and thus ensure the achievement of the submarine's longitudinal balance. This was an example of the submarine design being 'highly tuned' or highly sensitive in comparison to surface ship design (Andrews, 2017a).

7.2.2 Alternative Design Tools: An Automated Approach

The second alternative would be to make use of more automated approaches. As already discussed in Subsection 2.2.3, more automated approaches can produce many design solutions at a certain level of detail and are often optimised to an objective function (Shields et al., 2017). Many design algorithms, assumptions, steps, and decisions required to achieve a result are made by default, which is the opposite of the UCL DBB Paramarine system (Andrews and Pawling, 2003). Although Paramarine has some "hardcoded"

sizing algorithms as objects (e.g., “**generator_sizing**” object (Qinetiq, 2019)), the designer still has the ability to use such objects without resorting to the main codes of the software. What makes modern automation have black box characteristics is not just their inaccessible algorithms or data, but also the difficulty in determining the causal link between input databases or design rules and the resulting options generated.

As demonstrated in Case Study 3.3.1, the implementation of the UCL DBB approach in Paramarine for DS3 was intended to be used to commence a new ship design from a blank sheet. Assuming the development of the tool is prior to starting a given design study, there would seem to be a trade-off between the level of design automation and the transparency of the tool. Figure 7.1 shows that more design steps, choices, or design algorithms hardcoded into the tool means less design effort to generate more design concepts. However, this then reduces the flexibility of the design tool and makes the tool highly opaque as those hardcoded inputs are not revealed easily to the designer using a black box tool. Conversely, the glass box, Paramarine-SURFCON design tool with the intent to be able to explore radical solutions, starts the design *ab initio*, to be highly flexible, without any step-by-step menu (or any dialogue box) for commencing a new submarine design study, which requires more designer inputs, i.e., more design effort than the black box tool. Therefore, the solution space produced by a glass box approach will be less populated than the myriad design solutions produced by a black-box approach, however as Purton (2016) showed each solution may not be practical and the solution space is likely to be much more restricted (Andrews, 2018c).

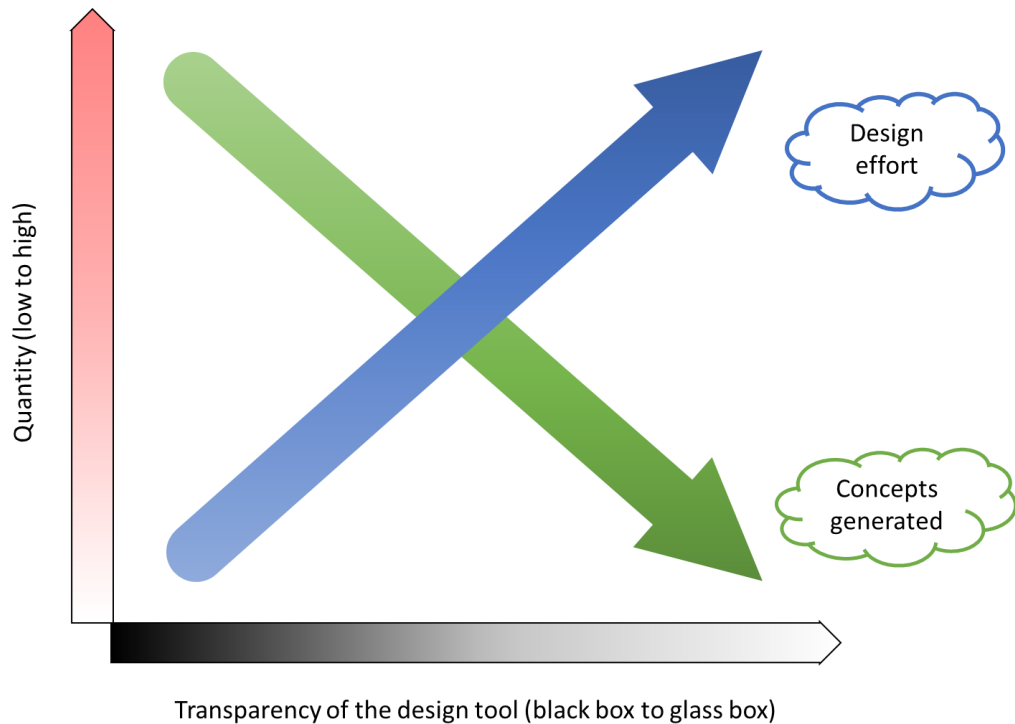


Figure 7.1: A simplified nature of the Computer Aided Ship Design tool, with the X-axis as the indicator of design transparency, i.e., it is getting darker on the left-hand side (for black box approach) and getting brighter on the right-hand side (for glass box approach) while the Y-axis (red) indicates the level of quantities from low to high, which corresponds to the design effort in blue and the number of design solution(s) produced by the tool in green

This then raised questions on what should be automated in a design tool and what should not. Figure 7.2 summarises important decision making, such as design algorithms, which ought to be kept as the designer choice and not hardcoded into design tools. This will reduce constraining the overall ship design solution space size early in the design process and retain design flexibility consistent with the objective in ESSD any design study that the Concept Phase is focused on the Requirement Elucidation dialogue. Thus, in Case Study 3.3.1, the engine room was quickly resized due to the need to fit additional diesel generators for necessary redundancy. The proposed approach appreciated the need for design flexibility and thus only automated routine tasks while design choices and selecting design algorithms remain with the designer.

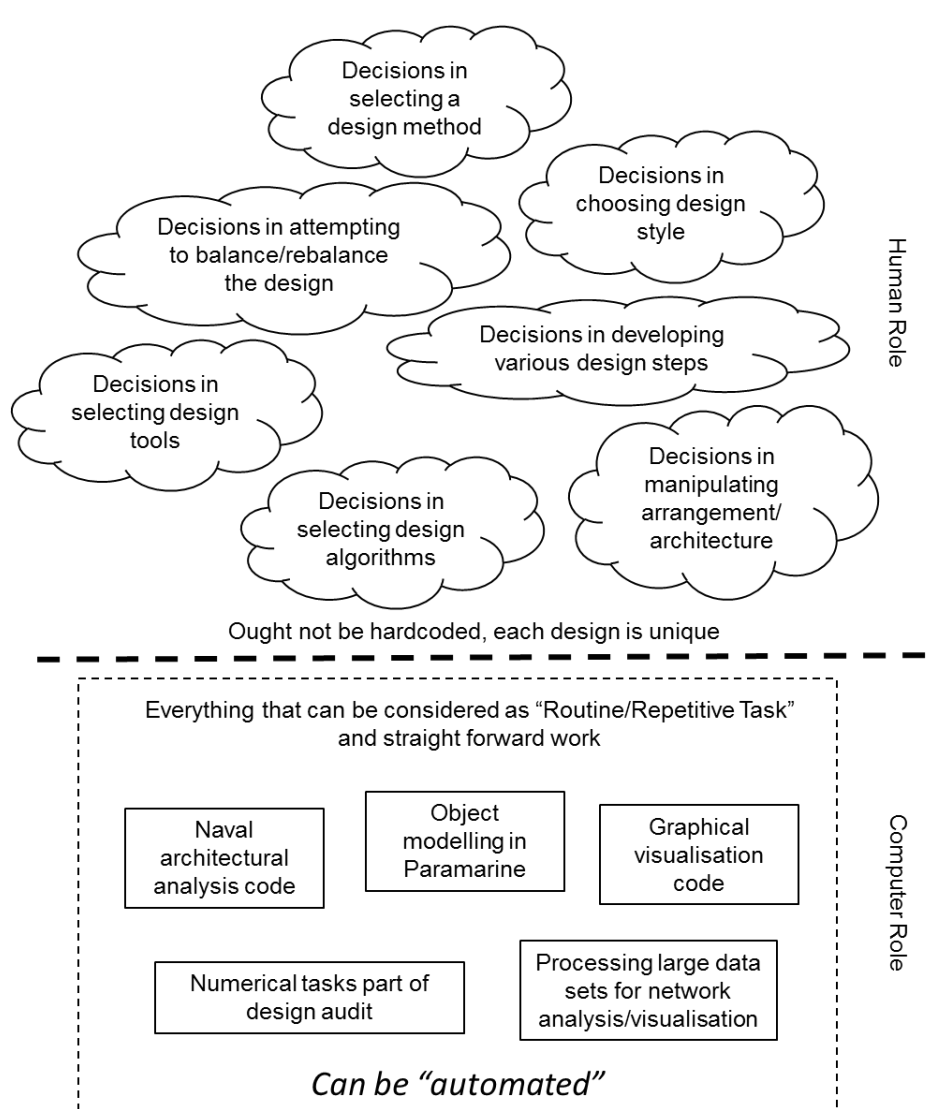


Figure 7.2: Decision making CAD processes vs human designer showing what ought and ought not to be automated

7.2.3 The Strategy of the Proposed Approach

As demonstrated in Section A 4.3, in Appendix 4, the procedure to model a DS3 component as a Design Building Block (DBB) object, including connecting it to another DBB object, required at least 40 clicks. This meant if a design consists of typically 50 pairs of connected DBB objects, the modelling process would require at least 2000 clicks, without including any design changes or alterations to the modelling. Such a laborious process is depicted as the “bottleneck” process in red in Figure 7.3 and considered as the ‘repetitive/routine task’ in the Gulfs of Execution and Evaluation (Figure 2.6 on page 51) in modelling DS3 in ESSD.

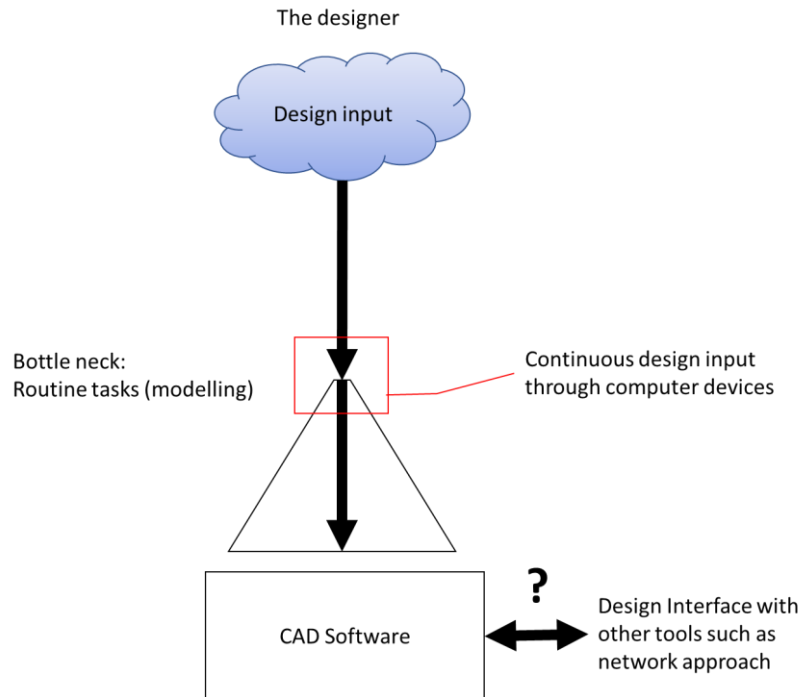


Figure 7.3: A depiction of data flow problem, showing the input in blue and the bottleneck problem in red

It was found in the design studies undertaken in this research that the reliance on the software was increased once the design had been developed into a sufficient level of detail for DS3 synthesis. This is indicated by the question mark in Figure 7.3. For example, the need to extract specific design data to other tools, as demonstrated in Case Study 3.3.1, was found to be time consuming. An example of this in Subsection 3.3.6, was that multiple clicks were required, including tracing the location of the relevant DBB objects in a specific DBB hierarchy with hundreds of DBB objects, or putting the data manually into MATLAB. This reliance may not be an issue if, for example, the analysis is not directly part of the design synthesis process and thus the process is not iterative, i.e., it would not be necessary to feed the data back to the Paramarine ship synthesis process simultaneously. However, in the proposed approach, the SUBFLOW network activity was significant to the DS3 synthesis process, which meant frequent data transfer and so the speed of data flow between design tools mattered. Such rapidity of transfer was seen to be essential to ensure the designer could perform the many iterations required to design DS3 both in terms of each DS3 physical architecture and logical architecture. Thus, the manual process as demonstrated in Section 3.3 was considered

prohibitively long and thus not readily plausible for the design to incorporate sufficient key DS3 components in ESSD without a new approach.

The approach termed the Network Block Approach (NBA) was thus proposed. The NBA consists of frameworks, methods and design tools that employ a strategy to 'intercept' data flow before being inputted to Paramarine and use of Excel spreadsheet input (as shown in green in Figure 7.4). It must be emphasised that although Paramarine already has an interface with Excel as an object, using this Excel object in Paramarine causes the Excel file to be embedded in the Paramarine file. This inhibited MATLAB from reading the design data in such an embedded Excel file for network analysis. Using Excel with Paramarine is also not novel (Fiedel, 2011; Thurkins, 2012; Jurkiewicz et al., 2013) but using Excel to combine the UCL DBB approach with the SUBFLOW simulation for DS3 synthesis has not been done before. Furthermore, the NBA is not just an Excel tool, it comes with extensive frameworks and methods (see Figure 4.13 on page 172) that leverage and sit in the gap between the benefits of the Paramarine 3D based synthesis tool and the SUBFLOW network based DS3 synthesis.

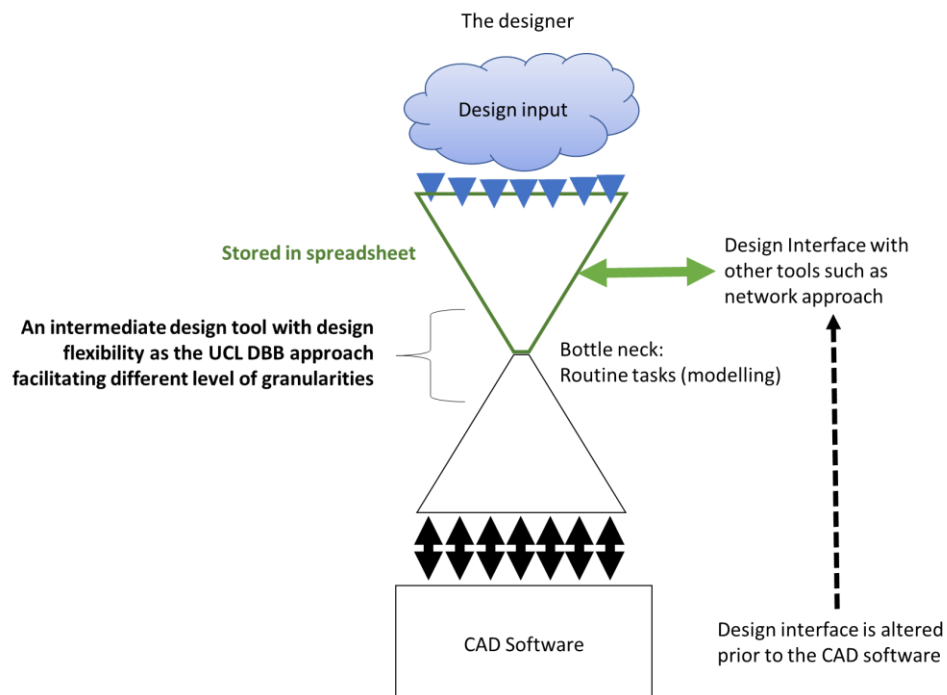


Figure 7.4: A proposed strategy for data flow adopted by the Network Block Approach, showing the bottleneck issue in Figure 7.3 can be mitigated by the spreadsheet tool in green

With the proposed approach, the designer can define design data in the spreadsheet program instead of manually inserting it into Paramarine, as demonstrated in Case Study 5.1. Thus, the necessary data has been converted to thousands (e.g., more than 20,000 lines) of 'Kernel Command Language' (KCL) lines (see Subsection A 5.1.1 in Appendix 5). Paramarine can then automatically produce objects necessary for any DS3 synthesis, based on such KCL lines. This was shown to save days of laborious modelling in Paramarine and unlocked the possibility for employing a new approach, such as the network based DS3 synthesis using MATLAB. This was achieved without losing the benefits of a 3D architecturally centred submarine and DS3 synthesis and the 3D informed dialogue that Paramarine-SURFCON provides. Since the design data was readily available in the spreadsheet environment, this could be transferred to MATLAB with ease, unlike the manual procedure shown in Section 3.3 as in the earlier pre-NBA implementation.

7.2.4 The Design Building Block Object and the Network Theory

This research had shown that a Design Building Block (DBB) object employs a similar philosophy to the network approach in terms of the capability of storing different types of data. As first exploited by Pawling (2007), a DBB object in Paramarine could be used to store almost any type of data, such as numerical, contextual or string data, geometry data, cost data, and even various design algorithms. Thus, as shown in Figure 7.5 (left), the possible type of data that can be stored in a DBB object in Paramarine is essentially limitless. Similarly, a node in Figure 7.5 (right) as part of a network object in MATLAB, could also store any information as to its properties. This revealed both the DBB object and the node object have the same capability in storing any type of data. However, since there are many possibilities that a DBB object and a node can represent, this then raised a question as to what type of DBB object could be modelled as a network and how they would contribute to DS3 synthesis.

A building block object in Paramarine-SURCON



Name	Description
char_buoyant	Declare Block/Equipment as buoyant
char_compressibility	Define compressibility of Block/Equipment
char_consumable	Consumable demand for Block/Equipment
char_freeflooding	Declare Block/Equipment as free flooding
char_personnel	Crew demand/supply for Block/Equipment
char_service	A service demand/supply for Block/Equipment
char_service_conversion	Define a service conversion eg transformer
char_space	Define a space demand for Block/Equipment
char_system_connection	Define a connection point for a block or equipment
char_tankage	Define tankage for Building Block/Equipment
char_tankage_compensated	Define Block as compensated tank
char_user	User-defined demand/supply for Block/Equip
char_weight	Define a weight for Building Block/Equipment
char_weight_from_solid	Define a weight from block solid & density
tag	Add markup information to the design
var	Variable

A set of node objects in a typical graph network in MATLAB



G.Nodes						
	1	2	3	4	5	6
	Name	String Data	Numerical Data 1	String Data 1	String Data 2	Numerical Data
1	'Node A'	"volume"	32.0357	Inf	NaN	0
2	'Node B'	"weight"	0	Inf	NaN	0
3	'Node C'	"volume"	2.4643	Inf	NaN	0
4	'Node D'	"volume"	0	Inf	NaN	0
5	'Node E'	"volume"	27.7500	Inf	NaN	0
6	'Node F'	"weight"	0	Inf	NaN	0
7	'Node G'	"weight"	0	Inf	NaN	0
8	'Node H'	"weight"	0	Inf	NaN	0
9	'Node I'	"weight"	0	Inf	NaN	0
10	'Node J'	"weight"	0	Inf	NaN	0
11	'Node K'	"volume"	0	Inf	NaN	0
12	'Node L'	"volume"	0	Inf	NaN	0
13	'Node M'	"volume"	0	Inf	NaN	0
14	'Node N'	"volume"	0	Inf	NaN	0

Figure 7.5: Illustrative types of data that can be stored in a DBB object in Paramarine-SURFCON (left) and a set of node objects in MATLAB (right)

One of the possibilities found from Case Study 3.3.1 is shown in Figure 7.6 where a set of DBB objects under a Master Building Block (MBB) could be modelled as a network. Therefore, in this network, arcs (Subsection 3.1.1) represent relationships in terms of DBB hierarchy (e.g., FMFI breakdown see Subsection 2.2.3) instead of DS3 connections. Using a layered layout algorithm (Gansner et al., 1993; Brandes and Köpf, 2002; Barth et al., 2004) in MATLAB, this network can reveal various depths of DBB hierarchy under an MBB (overall submarine design characteristics, see Subsection 2.2.3) node in black based on the DBB functional breakdown (FMFI).

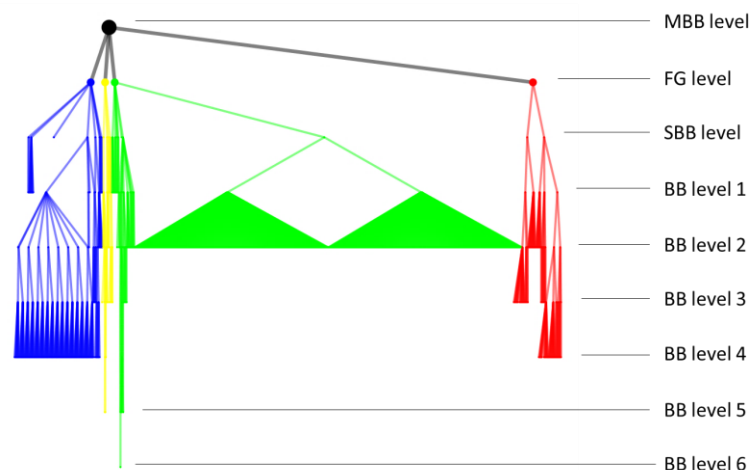


Figure 7.6: Hierarchical network of Case Study 3.3.1, showing nodes could be used to model Design Building Block (DBB) objects based on FMFI breakdown and arcs to model the hierarchical relationship between DBB objects (black for the main BB (the placeholder for overall submarine design characteristics) (MBB), red for Fight, yellow for Move, green for Infrastructure, and blue for Float), it is not considered worthwhile to show the label at each node due to the large number (>1000) of nodes

Figure 7.7 shows the progression of a design that could potentially be tracked using this network model but using a different layout algorithm, i.e., the 3D forced graphical layout (Fruchterman and Reingold, 1991) (Subsection 4.3.4), starting from a few nodes representing a few Super Building Blocks (SBBs) (Subsection 2.2.3) volumes (Figure 7.7 (left)) and as the design progresses, such a network expands, carrying more DBB nodes with different level of depth in the hierarchy (Figure 7.7 (right)), indicating there is more data or the detail is increased as the design definition expands. Hence, for example, Figure 7.7 reveals that some of the green (Infrastructure) nodes changed into two groups of nodes. These groups are the individual battery cells modelled as the DBB objects (see Figure 3.15 on page 119) and are shown as two large collections.

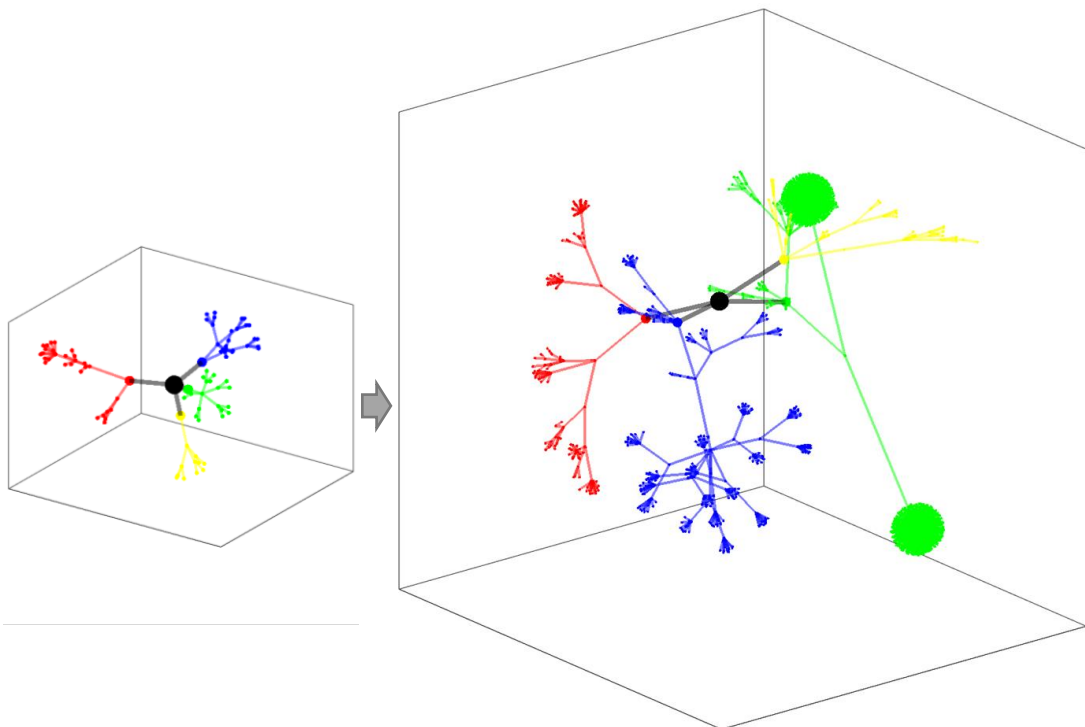


Figure 7.7: Illustrative 3D network hierarchy of Case Study 3.3.1 in capturing design progression and hierarchical complexity, this takes Figure 7.6 and changes the arrangement into a 3D forced graphical network (Fruchterman and Reingold, 1991) (black for MBB, red for Fight, yellow for Move, green for Infrastructure, and blue for Float)

Such a hierarchical network could show hierarchy complexity but was not found to be useful for DS3 synthesis. As already discussed in Section 4.2, retaining flexibility in terms of DBB hierarchy comes with several drawbacks. For example, different depths of DBB hierarchy in Case Study 3.3.1 made it difficult

to trace which DBB contained DS3 component data and thus time consuming as this process is iterative for DS3 synthesis. Hence, a set of frameworks proposed in Subsections 4.2.1 to 4.2.6, standardised various types of DBB with different types of data. This then left two possibilities in modelling DS3 using DBBs that contain geometric data: DBB with volume granularity or component granularity. Modelling a network utilising DBB with volume granularity (Figure 5.3 on page 178) would have created a network representation akin to the 2.5D surface ship application (see Table 2.2 on page 58), which sacrificed the benefit from a 3D informed dialogue in ESSD. Therefore, it was considered that only a specific DBB object, at a certain level of granularity, could contribute to DS3 synthesis, as illustrated in Figure 7.8.

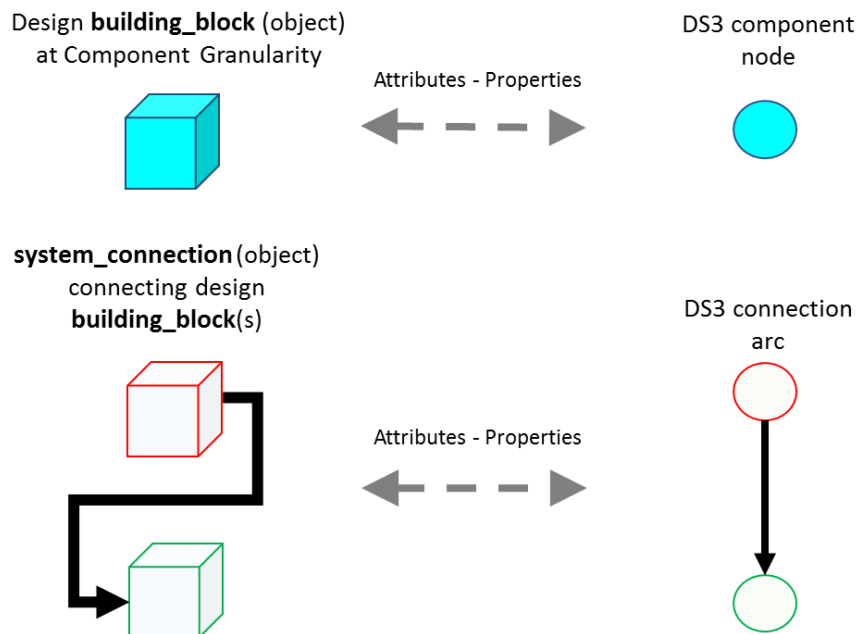


Figure 7.8: Commonalities between DBB objects and network elements node (top) and arc (bottom) in Paramarine-SURFCON (left) and MATLAB (right) respectively

Since the proposed approach utilised an Excel tool as the basis, the use of a semantic network, as already demonstrated in Case Study 3.2.1, could also be applied to represent the overall SSK complexity by modelling the relationship between design variables and constants used in the numerical sizing. For example, Figure 7.9 on page 331 shows that the selection of payload in category **(a)** directly influenced the size of Weight Group (WG) 7. Category **(a)** is connected to category **(b)** and had direct impacts on the WGs 1, 2, 5, 8, and

9. Meanwhile, the number of billets in category **(a)** directly influenced WGs 4, 5, 6, and 9. Another example revealed is that the speed characteristics in category **(a)** were the drivers for WGs 2 and 3 due to the size of the propulsion system. In summary, this network shows that most of the Weight Group items are scaled using submarine displacement based algorithms (see many arcs come from category **(d)**).

However, although the complexity could be revealed, this semantic network was seen to be limited to the realm of design variables and constants. Different design algorithms would alter the structure of the network significantly. Furthermore, as already discussed in Case Study 3.2.1, the use of such a semantic network cannot capture style issues, such as the adoption of DS3 ring distribution, and thus it was considered purely relevant to a traditional numerical relationship, given numerical synthesis is governed by the design algorithms selected in that simple sizing process.

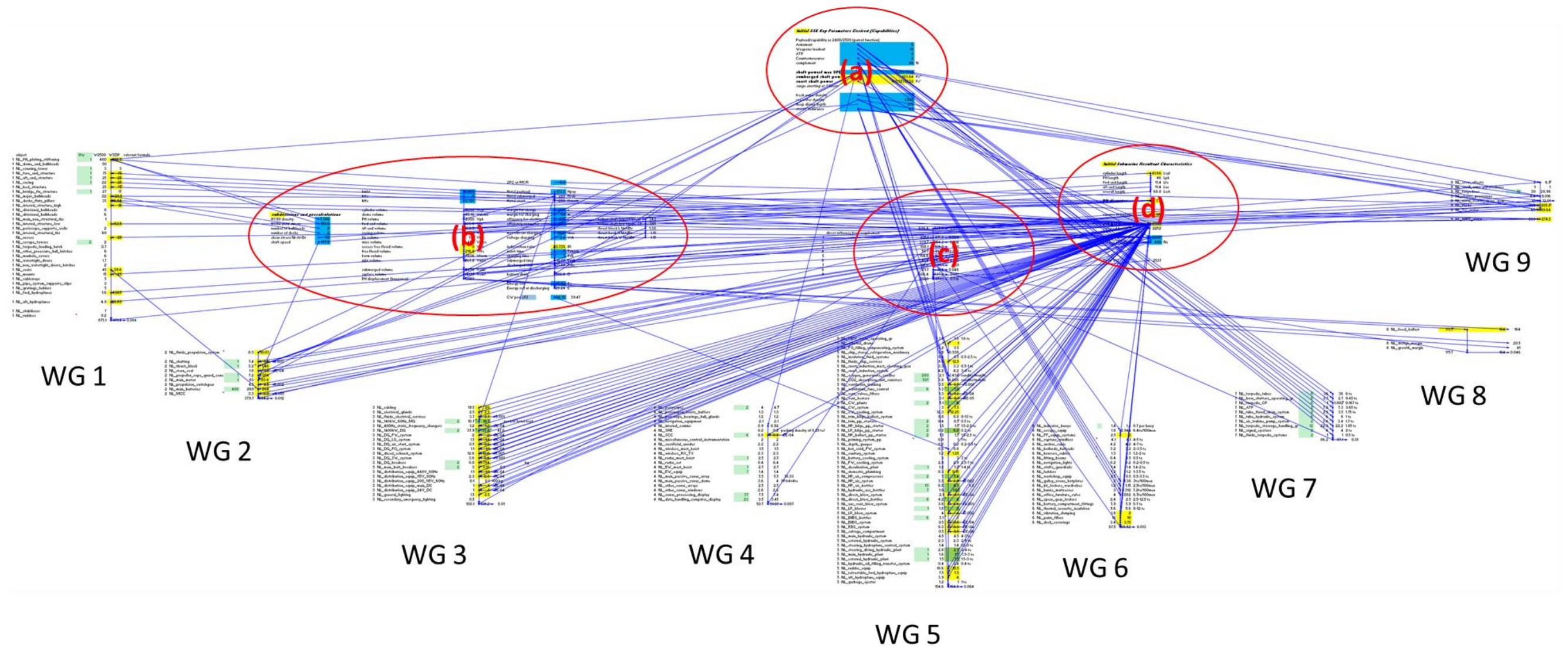


Figure 7.9: Visualisation of numerical sizing relationship for a generic SSK baseline design in a directed network generated using Excel showing more than 250 nodes, such as the vessel characteristic variables: payload, speed performance, complement (category (a)); sub decision variables and constants: steel density, pressure hull dimensions (category (b)), Weight Group audit: SWBS breakdown, a summary of WG1 to WG 9 (UCL-NAME, 2012) (category (c)) see Appendix A 7.1.1; major vessel dimensions: submerged displacement (category (d))

Section 7.2: DS3 Synthesis in the Initial Submarine Design

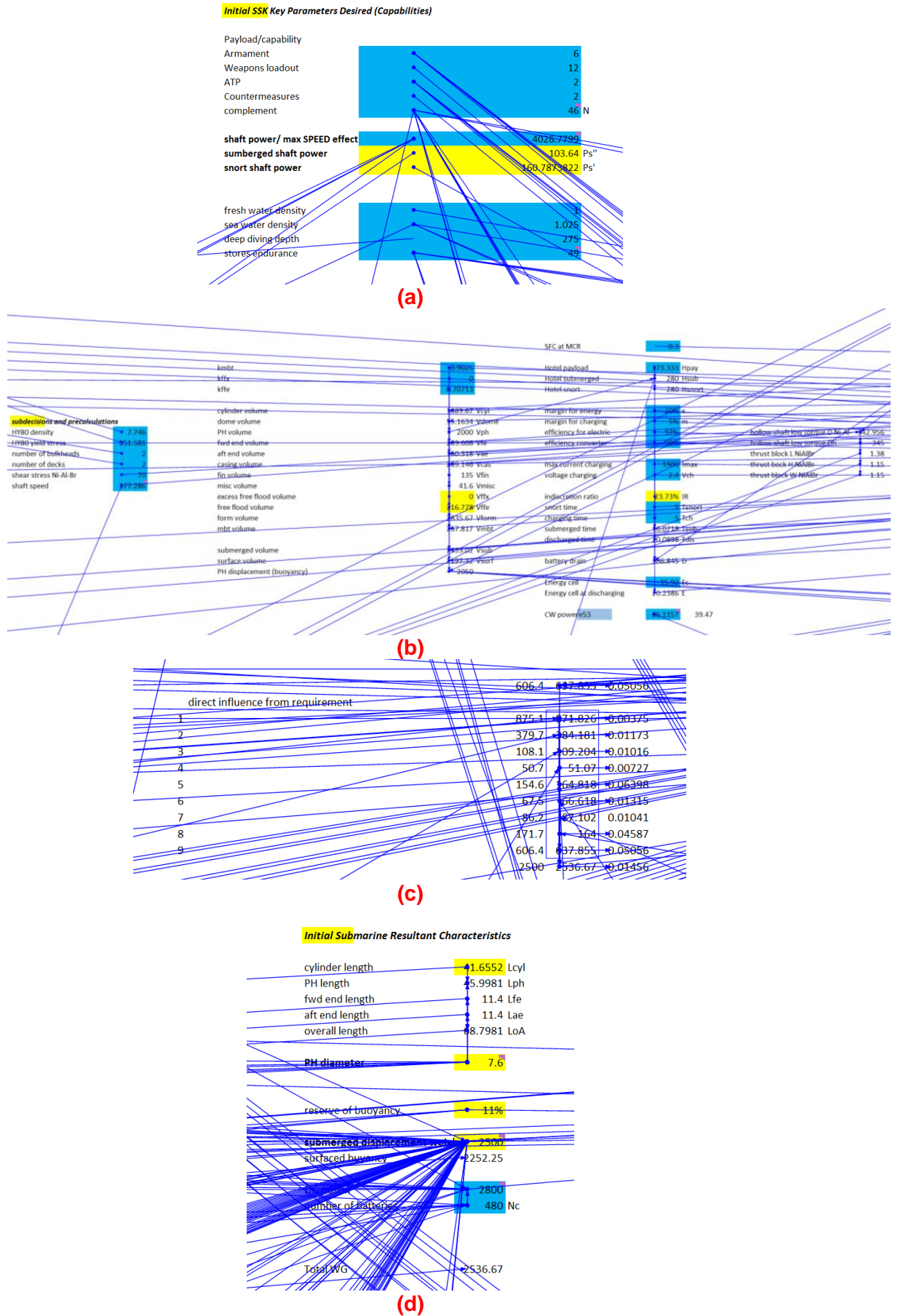


Figure 7.10: Major variables in Figure 7.9

7.3 The Novel Network Block Approach

The proposed Network Block Approach combines two sophisticated approaches for the whole submarine and DS3 synthesis. By properly connecting the philosophy between the UCL Design Building Block (DBB) approach and the network theory, Case Study 5.1 has shown that the DS3 synthesis could be introduced at the start of the design process, allowing the designer not only to manage weight, volume, and energy balance but also reveal the 3D physical and logical DS3 interactions at the beginning of the submarine design process. This expanded on the numerical synthesis design procedure proposed by Burcher and Rydill (1994) (see Figure 2.4) to include the architectural aspect of DS3 and produced a more plausible design (as summarised in Figure 7.11) than the previous research in DS3 (Table 2.2 on page 58), which is important to submarine design given its highly dependent on the DS3.

Although the execution of the modelling task in the proposed approach is automated, this has still required a significantly larger quantity of input data than is the 'usual' case with submarine ESD. However, improving the DS3 synthesis in terms of its 3D physical and logical definitions was considered to unlock many potential benefits with regard to aspects of integrity, maintenance, and supportability, which have not been addressed in this research. This includes the potential of assessing the impact on structure weight, such as the structural supports and seats for various DS3 components and connections, which is also subject to DS3 style choices and the DS3 physical architecture. The proposed approach has provided the foundation to consider such aspects plausible in ESSD.

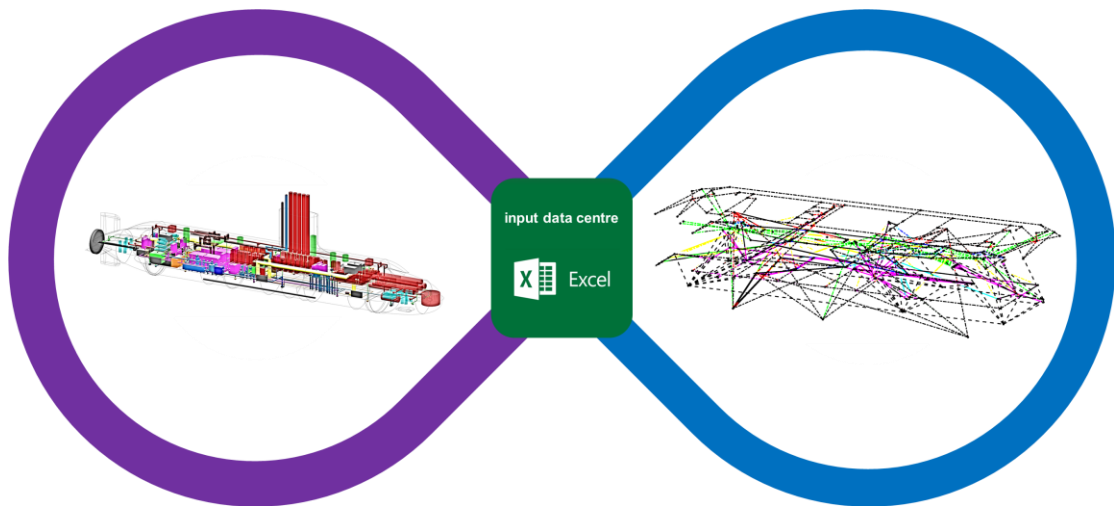


Figure 7.11: Illustrative output of the proposed Network Block Approach combining the advantages of 3D based physical synthesis (purple) and logical DS3 synthesis (blue) with the design information populated in traditional spreadsheet Excel (green) (see Chapter 5), this shows the proposed approach could work well for different architectures

7.3.1 Responsiveness to Design Flexibility

Although the proposed approach has been demonstrated for a quite complex DS3 synthesis, it still maintained design flexibility and thus was not considered to be a rigid approach. For example, in Case Study 3.3, the SUBFLOW could be applied to a DS3 problem with a minimum number of DS3 models, i.e., only a few sources and sinks. Consequently, at that level of detail, SUBFLOW could only provide insights to size the DS3 connections modelled in that case study, whereas the level of detail provided by the SUBFLOW network in Case Study 5.1, provided insight on DS3 configurations beyond a specific DS3 type. This confirmed that the more detailed DS3 are modelled in the SUBFLOW network, the more information can be obtained.

Another flexibility could be seen regarding the ability of the proposed approach to show technology changes. This was shown in Case Study 5.1 where a novel technology, namely a converter module, was used instead of a motor generator. Furthermore, in terms of the scalability of the proposed approach, the SUBFLOW network in Case Study 5.1 was expanded from a simple SSK power network in Figure 3.9 on page 105 to include many DS3 nodes in Figure 5.4 on page 182, while in Case Study 6.3.1, an AIP system technology was incorporated into the design. This was modelled as a single node instead of

detailed nodes. These examples showed the scalability of the proposed approach, which could be scaled up or down as necessary.

The power commodity results calculated using the SUBFLOW could be used to calculate the power system's weight and space attributes provided that power to weight or power to volume ratios are known. Such ratios could be derived from the UCL submarine data (UCL-NAME, 2014). Other equipment ratios could be obtained from equipment data from manufacturers or estimated for novel systems likely to still be under development. The use of power weight/volume ratios for future/unconventional solutions has been adopted in the aerospace industry (Campbell, 2014). This indicates that sizing through this approach would be responsive to technology changes. No matter how far the technology advancement might proceed, provided that the network structure and the power weight/volume ratios could be developed and examined, this sizing approach can provide a better approach than a whole vessel displacement based scaling approach (Subsection 2.3.1).

Another example of design flexibility was the ability of the proposed approach to readily adopt previous design practices. The buoyancy of small DS3 components and connections that are located outside of the hull, required more detailed input by the designer as Paramarine cannot automatically identify whether an object is located inside or outside of the pressure hull. Thus, design practice utilising a permeability equipment assumption, *kmbt* coefficient, was adopted. Furthermore, in Case Study 5.1 when there was a lack of data regarding detailed equipment demands for small equipment, like lighting, a parametric algorithm from Burcher & Rydill (1994) to estimate the power demand could still be used and modelled as a numerical node containing one variable. This demonstrated that the flexibility of the Network Block Approach was not limited to physical DS3 nodes but also encompassed numerically varying nodes.

However, as demonstrated in Chapter 3, the more parametric algorithms were used in the proposed approach, the less sensitive the approach was likely to be in capturing the impact of different DS3 styles at that level where the

parametric approach was appropriate. If the designer would accept such a penalty, then the proposed approach could have been used with an appropriate margin to cover this. Therefore, the use of a parametric approach for DS3 sizing is seen to be relevant for sizing some ‘straight forward’ DS3 with limited style options or those considered to have little impact on the overall size of the submarine, such as sanitary system and domestic plumbing.

To investigate the overall impact of certain DS3 configurations, the sizing of DS3 was investigated using the Physical Loop method. Initially, it was thought it would be difficult to arrange these DS3 components individually as there a great number of DS3 components needed to be considered in such a case study, by individually arranging some 200 components in a 3D coordinate system for a single design, which was seen to be a substantial task to be performed in ESSD. However, the programs in the Network Block Approach automated the modelling tasks for those components, so the arrangement process was found to be readily undertaken with the existing “drag and drop” approach in 3D provided by Paramarine-SURFCON, see Figure 7.12.

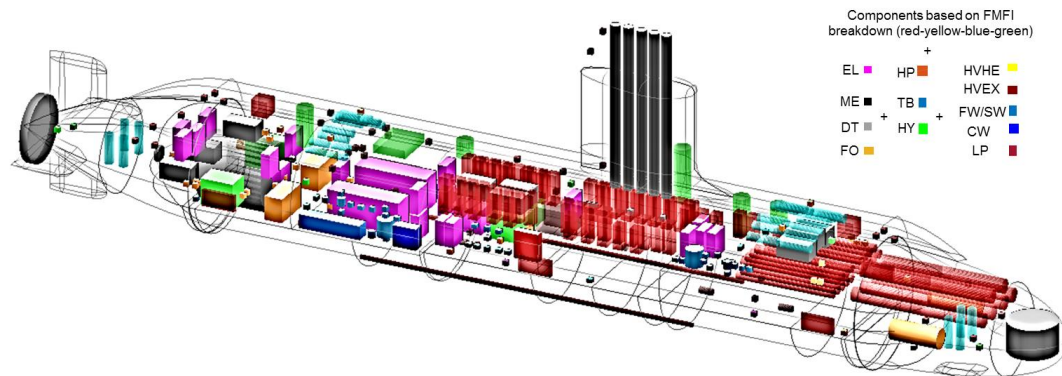


Figure 7.12: DS3 components arrangement in the 3D layout conducted using a “drag and drop” approach in Paramarine-SURFCON (see Case Study 5.1 and Figure 5.7 on page 187), as part of the Physical Loop method (Section 4.2)

Alternatively, the use of a packing density approach could be used by the designer to numerically assess whether a specific DBB object at the volume granularity needed to be resized, which would affect the overall submarine size by the subsequent necessary rebalancing. However, a packing density approach would be inherently insensitive to the 3D layout that is key to early

stage submarine design. Furthermore, if compartment density were used and the design progress was stopped at a level of detail such as that given in Figure 5.6 on page 185, this then raised the question as to whether a more automated approach would be suitable for this level of detailed arrangement of DS3 components. As already argued in Subsection 7.2.2 and shown by Figure 7.2, this level of detail is likely to be performed manually by the design organisation downstream in the subsequent design phases. This would be in preference to using an automated arrangement approach for arranging such DS3 components in ESSD, such as Van Oers (2012) and Purton (2016) employed. As a complex vessel, many of the stakeholders in submarine design, including specialist engineers, are likely to have conflicting visions that must be resolved in the eventual design solution (see Figure 1.2 on page 29) and thus detailed arrangement should not be made by default or determined by a black box toolset.

The proposed Network Block Approach also offered design flexibility in terms of DS3 modelling, more specifically, when it comes to the 3D architecture. As demonstrated in Case Study 6.3.1, when an AIP section was added to the design, there was no need to manually rearrange the more than 200 DS3 components in their individual DS3 location. This was possible because the spatial data of the DS3 components were held in the program and connected to the centroid of a volume object in the Component Granularity Program (CGP). This means when the position of a DBB object at the volume granularity was altered, the DS3 components inside it were also automatically changed without the need to graphically display and select those components in Paramarine-SURFCON. Thus, although the candidate had to arrange the positions of many DS3 components in a baseline design, this did not reduce the flexibility to manipulate the overall architecture of the vessel, which would be highly desirable given the exploratory nature of ESSD.

7.3.2 Space Reservation for DS3 Routing

The proposed approach has demonstrated that the initial DS3 routing is amenable to automation or preferably a semi-automatic approach such that the designer could still have the ability to define where the highways are located

(see Figure 7.13). This gives estimates of 1.5 km of cabling, 280 m of trunking, and 2.8 km of piping are required to build such a submarine DS3. However, Case Study 5.1 revealed a realistic routing (as shown in Figure 1.3 on page 30) remained difficult to achieve in the Concept Phase. This was due to requiring input data (beyond the overall DS3 network in Figure 5.4 on page 182) and design work (to model complex shapes, such as ‘structure duct’ routing (Appendix 4), and many small cables or pipework), which was considered unlikely to be available or seen to be necessary for ESSD. This further suggested that such modelling refinement is then likely to require design margins, which would need to be addressable in the relevant programs within the Network Block Approach. Furthermore, since it was found that the automatic routing provided by Paramarine did not detect the presence of other DS3 physical models (see Appendix 4), a more robust automatic routing would allow further DS3 routing density assessment to investigate whether there might be greater impact on space utilisation in submarine ESD.

However, the quality of 3D based semi-automatic DS3 routing produced using the Network Block Approach in the Paramarine-SURFCON could be said to be more plausible than the current 2.5D routing approaches on the surface ship application (see Table 2.2 on page 58). Furthermore, another potential advantage of an initial definition of the DS3 element shown by the case study presented in Chapter 5, was to reveal whether there was adequate space for various DS3 connections and the lessening of potential routing clashes when it came to allocating detailed DS3 components within relevant compartments. This would benefit downstream design development.

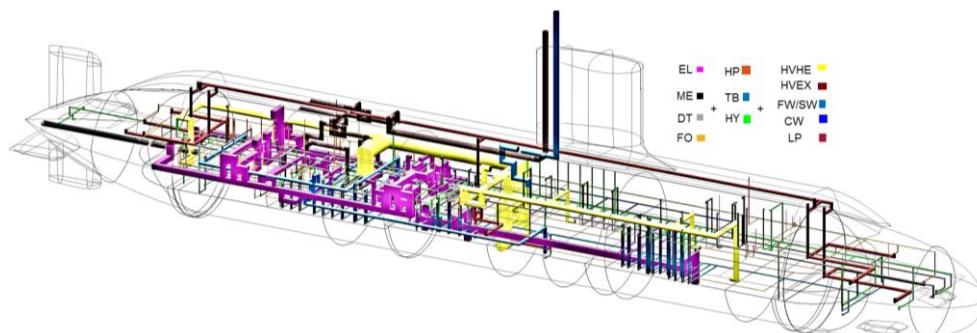


Figure 7.13: DS3 connections in the 3D layout based on the proposed DS3 routing framework in Subsection 4.2.5 (see Case Study 5.1 in Figure 5.7 and Figure 5.8 on page 187) using Paramarine-SURFCON

Given an assembly of connected individual components can be considered as a network or graph, this then raises questions as to whether the Network Block Approach (NBA) could also be used to model access passageways in typical submarine design studies by considering them to be like distributed systems routings. Thus, doors or hatches could be modelled as nodes and arcs used to model the access runs. However, the routing for a passageway will likely require more design (routing) input than currently adopted in the proposed DS3 focused approach.

Another potential application is when exploiting Virtual Reality in ESSD (Pawling et al., 2017). Since the use of the NBA makes the 3D based synthesis plausible in ESSD given its rapid modelling capability, this then would allow the designer to use recent technologies, such as Virtual Reality, much earlier in the design process. If such a technology was to be connected to the NBA's input data centre, the designer could potentially adjust the DS3 physical architecture using a set of Virtual Reality devices. This would enhance the process of manipulating the architecture of the submarine. However, this needs further investigation which might reveal whether incorporating such technology would improve the Requirement Elucidation need or might inhibit the exploratory design element of ESSD.

7.3.3 The Inside-Out Early Submarine Design

Since the Network Block Approach (NBA) was developed to incorporate the UCL DBB approach (Andrews and Pawling, 2003), in that the physical architecture has not been constrained when it comes to DS3 style decisions. This can be seen in contrast to the physical architecture example shown in the surface ship distributed systems framework approach (see Figure 2.2 on page 37). In the NBA case, the DS3 components were able to be fitted and integrated, although this resulted in the need to resize the hull to ensure the relevant compartment could accommodate the DS3 components and the connections in it (e.g., see Case Study 5.1 on page 218 which evaluates compartment density and Case Study 6.1 on page 269 able to better predict power demands). This would not be readily achieved with the traditional outside-in design sequence adopted by Brefort et al (2018), where the hull was

arguably, fixed too soon and possible DS3 options were likely to be limited by the resultant hull form constraints.

The case study in Chapter 5 also suggested that adopting newer technology, such as an electrical system component (e.g., converter), could give a lower weight solution when compared to the weight estimate based on whole vessel scaling. This could potentially give a smaller overall size of the submarine. However, in the outside-in approach, any potential reduction of hull size would not directly be taken advantage of as the hull size would have been essentially fixed before DS3 design consideration.

7.3.4 Findings from the Sensitivity Analyses

The sensitivity analyses conducted as part of this research were based on a baseline single hull SSK style design with various levels of design decisions, ranging from ship performance characteristics to the gamut of main and even micro style choices. Other types of submarines (e.g., nuclear submarine, see Figure A.22 in Appendix 2), major style aspects (e.g., the double hull and multihull submarine or combination of both) and radical technologies (e.g., dive by wire, IFEP) were not investigated. In addition, the baseline submarine design and the sensitivity studies were developed based on public available data and able to be obtained without recourse to classified defence sources. By using the UCL submarine design procedure and database, the data was derived from UK MoD submarines and declassified data based on UK MoD practices and data. The database and submarine design procedures used by other countries and navies are likely to be different, as reflected in published sources such as Arentzen and Mandel (1960), Jackson (1992), and Kormilitsin and Khalizev (2001).

Despite such limitations, Case Study 6.1 showed that the size of the vessel could be affected by the variation of maximum submerged speed. Meanwhile, Case Study 6.2 showed that the proposed approach was sensitive, down to a micro level of style decision. Case Study 6.2 suggests that without an architecturally oriented, 3D based synthesis, it would be difficult to investigate the impact of varying micro style decisions that could lead to reductions in the

overall submarine weight but not necessarily reduction in internal space requirement. This then raises questions as to whether pursuing specific design explorations in ESSD at a micro level of style would be worthwhile. This should be dependent on a case-by-case basis. For example, for an experienced designer, such a micro level of style exploration might be covered by the designer's engineering judgement in assigning appropriate weight and space margins. However, for an inexperienced designer, going to such a level of detail using the proposed approach would increase the confidence in the design and provide a learning experience.

Furthermore, Case Study 6.3 revealed that the insertion of typical AIP technology into an existing design was possible, as an example of the sort of Requirement Elucidation exploration, but the example revealed no significant contribution to the indiscretion ratio. This was because although the AIP power generator module to produce a large 500 kW output is relatively small, the required AIP fuel, more specifically, the LOX, to perform a 25-day submerged performance was found to demand significant space on the vessel beyond that available in the AIP section. Therefore, this suggested further investigation would be required of employing large capacity AIP to achieve extended submerged performance.

7.3.5 Various DS3 Based on Functional Group

The proposed approach adopted the functionality classification from the UCL DBB approach, more specifically, the FMFI breakdown (Fight, Move, Float, and Infrastructure). This was introduced (Andrews et al., 1996) to encourage the designer to focus on the purpose or functionality of the design, clustering or identifying various service demands on the vessel. Thereby not necessarily adopting past practice which meant departing from the traditional SWBS breakdown. In Case Study 3.3.1, it was found that, since the power produced by this system was mainly used to "move" the ship as the largest demand on the vessel, the power generator system has been traditionally considered as part of the propulsion system and classified as the 'Move' group. For merchant vessels, this would make sense as the main purpose of the vessel is to "Move" goods from place to place and thus the rest of the power demands were seen

as “parasitic” to the ship, which could be deducted from the propulsion system. Nevertheless, this then raised questions as to whether the submarine as a complex and multirole vessel could also be seen only as a transport vehicle. Modern submarines and even future mothersub carrying UUVs may mainly operate in a ‘hover’ condition and this would have any implications for other functional groups, such as Fight and Float. Thus, seeing the power system as part of the Move group, with the integrated nature of electrical power, was considered questionable.

Classifying the power system as part of the Infrastructure group significantly reduced the Move group and increase the Infrastructure group. However, the latter functional group also contained components to support life and provide comfort for the personnel on the vessel, such as accommodation, stores, and air conditioning (Andrews and Dicks, 1997). This then raised the issue as to whether the components for the personnel should be allocated in a separated functional group, such as proposed by the functional clustering of various DS3, illustrated in Figure 7.14. Figure 7.14 shows that based on Case Study 5.1, the fuel (with air) could be seen as the only source of energy on the vessel, which could then be converted to electrical energy, stored in batteries, and distributed by the ‘EL’ system (under the Infrastructure group) to various types of DS3 under four main functions: Fight; Move; Float; and ‘Support’ the vessel.

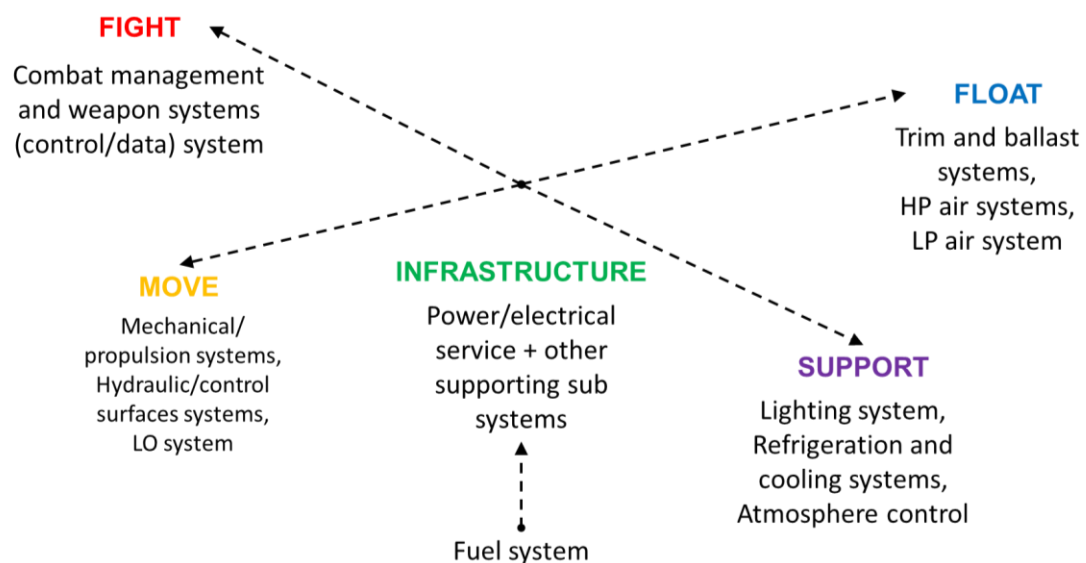


Figure 7.14: Illustrative energy flow of various DS3 based on functionality on the SSK example showing Fight in red, Move in yellow, Float in blue, Infrastructure in green, and Support in purple with the energy direction indicated by dashed lines and arrows

Figure 7.14 raises two points: the first point is whether the Support group would shrink in the future due to automation, i.e., a more advanced autopilot technology would reduce the number of required personnel to operate the submarine, leading to a smaller size of accommodation and its supporting systems. This would mean a future complex UUV could be seen as a vehicle that has all functional groups except (or with minimal) the (personnel) Support group. The second point is whether a type of DS3 that has multifunctionality, like the hydraulic system, could also be categorised in the Infrastructure group since such multifunctional DS3s provide actuation to various functional demands, not only for hydroplanes in the Move group but also periscopes in the Fight group as well as DDSTP capable valves in the Float group. Similarly, a HP air system is not just used to bring the submarine to the surface (Float function) but also be connected: (a) to a hydraulic system as a fallback (Move function); or (b) to the weapon system to discharge torpedoes (Fight function). Despite this, it was considered that the interpretation of the FMFI breakdown for various DS3 should remain flexible as it was intended to aid the designer to construct a complete set of systems for the submarine from a functional basis, rather than confusing the designer as to which functional group a particular DS3 should belong.

7.3.6 Basic Taxonomy of Design Detail in the Proposed Approach

The case study presented in Chapter 3 suggested that the capability provided by the UCL DBB synthesis approach using Paramarine is highly flexible in terms of modelling the submarine design to any degree of granularity. This could range from coarse numerical objects to detailed physical DS3 components and connections. Thus, the location of DS3 components could be manipulated to assist in achieving the initial longitudinal balance of the submarine. This scalability advantage was maintained in the Network Block Approach where its programs could be used to model space for detailed DS3 connections.

The case study in Chapter 5 is considered to reveal at ESD the recognised total distributed ship systems dependency of submarines. The DS3 network in Chapter 5 could still be developed to a greater level of detail to model more of

the total distributed ship systems of a submarine, such as degaussing system or salvage blow system, which would introduce many more pumps and valves than in the case study modelled. This raises the issue as to whether the greater detail, beyond that presented in Chapter 5, might not be seen to overwhelm the designer with DS3 information in ESSD. However, some DS3, such as plumbing and water system, were not seen to present this issue as they do not need to be modelled to further levels of design granularity, and so the use of a simple scaling approach for these systems was considered sufficient.

The use of an architecturally centred philosophy as part of the proposed approach also allowed the definition of a basic taxonomy for different types of Design Building Block (DBB) objects for different design entities when identifying the level of design detail sufficient for ESSD. The effort required to model a single design study could then be quantified, based on the design inputs provided in the programs in the proposed approach. Figure 7.15 shows the number of DBB objects based on Case Study 5.1, which are seen to provide a definition of various levels of design detail appropriate to the proposed Network Block Approach. This suggests a design can have an increase in design granularity but not necessarily mean a resultant increase in design fidelity, (i.e., information).

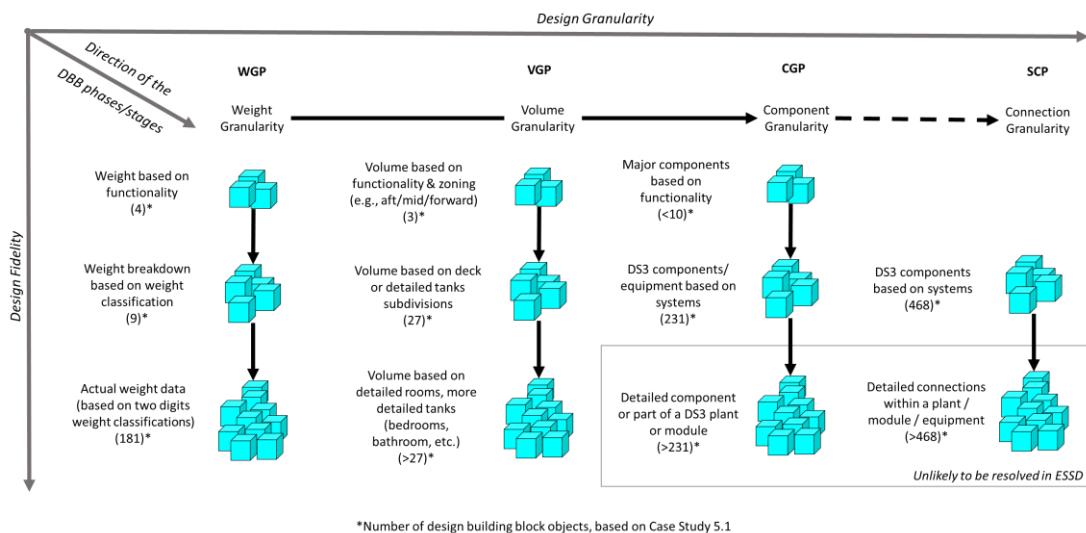


Figure 7.15: Taxonomy of design granularity and design fidelity (see Subsection 4.2.2) in the proposed approach using design data of Case Study 5.1

7.4 Emergent Issues in the Proposed Network Block Approach

The design tools within the Network Block Approach automated a considerable part of the modelling process but the design algorithms and the 3D based synthesis UCL DBB approach logic were still retained as the input of the process. This mitigated against the consideration that synthesising 3D based models for DS3 was “too long to make” (Rigterink, 2014). The programs have been shown to reduce the design labour intensive Paramarine process without creating a further separate or standalone design tool. However, some emergent issues were identified.

Since the design data was saved as an Excel file format instead of within Paramarine-SURFCON, it was not possible to keep the DS3 synthesis loop in a single software environment. Thus, deleting a DS3 node in Excel was not automatically reflected in Paramarine, so communication between software needed to be manually triggered using a macro link. Such a manual execution is amenable to additional automation using other commercial software, such as ModelCenter, which can automate the execution of multiple computer tools (Phoenix Integration, 2021). However, this type of tool has been mainly used to automate the optimisation workflows (Stevens, 2016), which is a different process to that of the Network Block Approach. Furthermore, the manually facilitated macro approach in Excel was seen to give distinct advantages. Firstly, the macro approach gave more control to the designer when updating the model or the calculation, rather than requiring continuous updating that would be computationally expensive. Secondly, the proposed approach could operate with a standard Microsoft Excel 365 office environment (Microsoft, 2021a) using the VBA programming language (Microsoft, 2021b), which is in widespread use by engineers, and thus new users should be able to alter the programs should the need arise.

Initially, it took 3-5 minutes to display and analyse the network presented in Chapter 5 on a standard PC machine used by the candidate. After the code in MATLAB was enhanced, the simulation time was improved to under a minute. Similar improvements were made to the proposed programs for performing the

modelling task in Paramarine. The proposed programs could convert within a minute the input data provided in Case Study 5.1, which consisted of some volume objects, more than 150 numerical weight objects, 200 component objects, and 400 connection objects, to 20,000 lines of KCLs. Therefore, the execution time of the programs, both for sending macros to Paramarine and performing SUBFLOW simulation in MATLAB, was driven by the quality of the code and there remains scope for this to be further improved.

The programs within the Network Block Approach did not limit the range of possible styles to be incorporated in the submarine and DS3 designs, except for very (Macro) extensive style configurations. The degree of effort to model a complex submarine hull shape or architecture would require a new version of the Hull Granularity Program (HGP) (Table 4.1 on page 145). This includes the potential application to other complex vessels, such as surface warships or offshore oil and gas service vessels (FPSO ships) although the issues of DS3 sizing on surface vessel design are unlikely to be as demanding as in the highly tuned submarine design. The current version of HGP was devised to model a scalable single pressure hull submarine configuration. This allowed the designer to focus on the complexity of interrelated DS3 configuration without being distracted by the modelling issues in Paramarine and thus enabled assessment of the overall impact of the DS3 on the most common submarine configuration.

The programs were also devised to facilitate the input required for the physical and logical DS3 definition. Therefore, although the DS3 components could have been directly defined as Design Building Block (DBB) objects in the Component Granularity Program (CGP) without the need of using the Equipment Database Program (EDP) (Table 4.1 on page 145), the use of EDP was found to simplify or reduce overcrowded data input in the CGP. This, in turn, meant the CGP could facilitate the designer constructing the input required for DS3 in terms of physical architecture and logical architecture. Another issue was the approach to defining the connection point of a DS3 component (in and out), since a piece of equipment could have multiple connection points in different directions in 3D (forward-aft and top-bottom). Initially, the EDP was developed using a common

database approach, for example, multiple DBB objects for bus nodes (Subsection 5.3.2) can refer to a specific equipment data cell for a standard specification of a bus node in Paramarine. However, it was found that each DS3 equipment was unique in so far as it could have one connection setup and thus in a ring bus configuration, some bus nodes could be set up with either port connection or starboard connection points. Furthermore, there was found to be a series of setups in Paramarine that required each DS3 equipment to be defined manually for different line specifications (see Appendix 4). Such setups were found to be tedious, given there were more than 400 connections in Case Study 5.1. This was mitigated by the Equipment Database Program (EDP) (Table 4.1 on page 145) and thus, this concern was found not to inhibit the process of modelling DS3 in Paramarine-SURFCON.

As discussed in Subsection 4.3.4, the DS3 arrangement when presented at the logical architecture format could be manipulated using different automatic layout algorithms provided by MATLAB, such as forcing a graphical layout (Fruchterman and Reingold, 1991). However, none of the existing algorithms was suitable to show typical style choices due to the range of possible physical DS3 configurations, such as the ring main configuration for electrical power or for the HP air system. Furthermore, it was found that using an automatic network layout could potentially overwhelm the designer when developing the whole ship DS3 network *ab initio* (see Figure A.41 in Appendix 5). Therefore, it was concluded that the logical architecture of DS3 should be able to reflect some aspects of the physical architecture. For example, a DS3 component node that is located at the forward part of the vessel should also be located at the forward part of the network. Therefore, the overall DS3 network, presented in Figure 5.4 on page 178 could then be presented in the form of multiplex configuration (see Figure 2.7 on page 59) and was readable for the example DS3 studied in this research. Consequently, the candidate had to arrange the DS3 components (more than 200 entities in Case Study 5.1), both in the physical and logical definitions, defined in the Component Granularity Program (CGP). However, this approach could be improved if the DS3 network was to be arranged to use a “drag and drop” approach in MATLAB or an automatic

layout algorithm devised to capture the physical architecture of the submarine. The latter will likely require more spatial inputs being provided by the designer.

Although the initial comparison to the broadly realistic but unclassified submarine design data provided by UCL (UCL-NAME, 2014) has been made in Chapter 5, validating the accuracy of sizing of the various DS3 using SUBFLOW simulation would require further comparison of the SUBFLOW sizing results with several real submarine designs. However, given the lack of such detailed data in the public domain due to military or commercially sensitivity, the level of effort to perform such validation would have been significant, if at all possible, in an academic environment. However, in industry, such validation could be undertaken using weight and space breakdown data from previous real submarine designs available to government or submarine designers and builders.

7.5 The Nature of DS3 Synthesis in Concept Design

Given that the proposed approach could facilitate an improved quality of the 3D based DS3 synthesis, this then raised a question as to whether such detail is needed at the concept. Submarine concept investigations are unlikely to go into such detail every time, but this research has demonstrated the potential advantages and shown that such detail could be done in the Concept Phase using the proposed approach. This would particularly be the case if there is seen to be a need to investigate uncertainty in DS3 synthesis, as with the adoption of new DS3 technology or a significantly different overall submarine DS3 style configuration where simple algorithms based on a small set of submarine parameters would be suspect.

It might be argued that a parametric coefficient for disparate DS3 styles could be sufficient for a quick estimation in ESSD. For example, a ring main electrical system might have a 1.5 factor relative to the existing scaling algorithm (UCL-NAME, 2014). However, as shown in Case Study 6.2, even at the micro level of style decision, the use of such a parametric approach was not able to infer the different impact of adopting a single or ring bus configuration for the 'EL'

system, which appeared to give a lower weight, but not necessarily lower space demand (see Subsection 6.2.2). Thus, it was concluded that a few design parameters (e.g., submerged displacement, hull volume, endurance, personnel size, propulsion power, or a mix of parameters) would not be able to capture the complexity and interrelated interactions between various DS3. This was due to the DS3 style influencing the selection of relevant design algorithms and that various DS3 can be significantly different from submarine type to submarine type. If the designer wants to integrate a potentially different DS3 style into a submarine design or new DS3 technology into the new design, the Network Block Approach is considered to provide a means of assessing the impact of a new style in submarine ESD. It must be emphasised that the Network Block Approach is only a guide to a first estimate of vital DS3, but it is clearly helpful to have a starting point that is more reliable than the current parametric approach. The tailored design guidance for various DS3 using the NBA is summarised in Table 7.3.

Table 7.3: Tailored design guidance of the NBA to ensure the provision of DS3 space and weight within the submarine hull could be addressed in ESSD

SUBFLOW setup (see Table 4.7 on page 163)	Type of system	Level of detail to be modelled	Example of possible DS3 styles/technologies to be explored	Notes
Energy flow dependent	Fuel oil	Fuel oil tanks, fuel oil piping cross connections/redundancy	Internal vs external fuel oil tank locations.	This could affect the size of the pressure hull and thus the overall size of the submarine.
	Power/Electrics	Major components, power sources, hubs, and sinks including sufficient connection redundancy	Various nuclear power system configurations with a more electric architecture (using an electric propulsion motor).	This is doable provided that a sufficient level of detailed system line diagram and the relevant equipment database is declassified/available.
	Information data	Major information data components and connections	The use of fibre optics, "dive by light".	Provided that the relevant data is available.
	Mechanical	Motor room, shaft, thrust block, main gearboxes, propeller	Pump jet configuration or rim driven propulsion systems.	This could potentially alter the arrangement, more specifically the location of the motor room.
	Air intake	Major HVAC components and connections, such as ATUs, heat exchangers, mast intake and exhaust, trunking, and DDSTP piping	Various air intake mast configurations, e.g., folding mast.	This could be important to ensure there is enough space in the bridge fin to accommodate the required pipe diameter for the chosen redundancy of diesel engines. Alternatively, the use of a folding mast could eliminate the bridge fin.
	Air heat		Centralised vs localised air conditioning units per compartment.	The connections for the HVAC trunking are more space driven, local cooling unit per compartment may reduce the required trunking diameter while maintaining the desirable airflow/noise.
	Air exhaust		The presence of silencer components would improve the signature level of the submarine.	This could be important to ensure there is enough space under the casing to accommodate the required pipe diameter for the chosen redundancy of diesel engines.
	Chilled water		Different cooling system configurations and equipment choices could be explored.	This could lead to more energy efficient HVAC systems, less main power requirement, and thus the overall size of the submarine.
	Lubricant oil			
	Freshwater (cooling)			
Seawater (cooling)				
Could be sized directly using SUBFLOW network and the derivation of space/weight to length ratios	Trim and ballast	Trim and compensation tanks, DDSTP valves and pumps	The use of screw positive displacement (vertical) pumps or centrifugal pumps.	The complexity of piping could be identified for routing density checks when adopting vertical pumps.
	High-pressure air	HP air bottles, HP air compressors that could consume a considerable amount of space, connection redundancy vital for DDSTP operations	The location of HP bottles (internal vs external under the casing or even in trim tanks), level of redundancy in terms of components or connections.	The physical models of the compressors could help to identify compartments that are traditionally difficult and have density hotspots, such as machinery room and AMS. These buoyancy manipulator technologies for submarines (so far) could not be replaced by other technologies.
	Low-pressure air	LP air compressor	Level of redundancy of the components or connections. The location of piping runs under the casing.	
	Hydraulics	Major components, hydraulic plants	Towards a more electric architecture using electro-based actuation.	This could replace various hydraulic plants and piping.
Could potentially be explored using SUBFLOW network	Degaussing	Crude weight with little regard for space (using packing density approach)	Different degaussing technologies or the level of redundancy of the components or connections.	The size of these systems could be seen to be not energy flow dependent and quite marginal. Thus, scaling approach may be sufficient. The SUBFLOW network within the NBA nonetheless could be used to address a specific issue within these systems.
	BIBS			
	Fire fighting			
	Domestic plumbing and water			
	Salvage blow			

As there is now a better way to explore different options for DS3 to that based on gross weight displacement driven algorithms, this then raised the question of how to assess which is best. To answer this, several case studies have been undertaken to see if a design variant with a certain DS3 choice could be seen as better than others. For example, Case Studies in Chapter 6 revealed that, although a design variant offered a benefit in a certain design measure, such as weight, it is not necessarily true that there is a corresponding benefit in terms of other design measures or other design aspects that only arise when the design is subsequently worked up. This is because as a complex vessel, the submarine has no absolute measure like the merchant ship (e.g., freight cost measurement) (Andrews, 2018c). A complex vessel must be designed from the keel up responding to different design stakeholders to satisfy (sometimes) conflicting requirements (Andrews, 1998). Many of the stakeholders in submarine design have conflicting visions that must be compromised in the submarine designer's eventual design solution and thus a set of subjective multicriteria at best only provide insights rather than absolute preferences, i.e., selecting the "right" design should emerge from the Requirement Elucidation dialogue (Andrews, 2020). This is consistent with the main aim of the Concept Phase, which is not about producing a design solution but rather working out what is wanted and what can be afforded by making important decisions as part of the decision making process for complex vessels (Andrews, 2018c).

7.6 DS3 Synthesis and Network Optimisation

Given the naval vessel is "engineering's greatest compromise" (Purvis (1974), the SUBFLOW outlined in Chapter 4 was not used to optimise the submarine design, nor the various DS3 designs. As already investigated in Case Studies 3.1 to 3.3, pursuing all possible scenarios applicable to a complex vessel into a set of optimisation setups in ESSD was seen to be prohibitive and highly questionable (Andrews, 2018c). Minimising a set of multicriteria parameters would not be seen as sensible because the impact of many unknowns only arises once designs have been worked up into more detail in subsequent design phases. This is also consistent with Gale's statement from more than 42 years of naval experience: "... ship design has so far proven to be too complex

to be described by a set of equations” (Gale, 2003). Thus, SUBFLOW was used in the Network Block Approach to simulate the energy balance on the submarine with the ‘zero’ objective function (Subsection 4.3.3). This also demonstrated that the proposed approach employed network analysis as little as possible commensurate with the needs of Requirement Elucidation. Further complicated network optimisation analysis was seen as inappropriate to be applied in ESSD.

SUBFLOW read and subsequently wrote the energy balanced results to the Component Granularity Program (CGP) and the System Connection Program (SCP). Therefore, the input layout in the CGP was devised to include necessary input for the SUBFLOW simulation. This included input or output energy of each relevant DS3 component in the following SSK operating conditions: snort; submerged; and sprint scenarios, placed in specific columns (cell location) in the CGP and SCP. Any changes within the CGP sheet layout would have a cascading effect on the rest of the programs, which would require code modification in MATLAB to make the SUBFLOW read the data correctly and be able to produce feasible balanced energy solutions. It has been explained in Appendix 5 that each such modification would take a few hours to incorporate.

Another issue concerning further modifications centred on the SUBFLOW simulation, showing initially the production of a large quantity of heat had to be removed by the CW system. As this heat should be able to escape naturally to the environment, SUBFLOW was relatively easily modified to reflect such physics. This was done by redefining the energy coefficient at the numerical nodes in each compartment using CGP and connecting it to the numerical node ‘internal air’ of the submarine using SCP, which led to a more realistic cooling load for the CW plant (see Section 5.7). This also suggested the Operational Matrix framework and the relevant Excel programs reflect an ‘open architecture’ approach that allows for easy modification of the SUBFLOW formulation should the need arise. This was possible because only continuity constraints were hardcoded into the SUBFLOW formulation while the rest of the SUBFLOW constraints could be modified in the spreadsheet environment without the need to change the main code in MATLAB (see Appendix 5). The SUBFLOW was

devised to comply with the basic thermodynamic law, ensuring that the energy entering into a DS3 component would be equal to the energy coming out of that DS3 component.

As already discussed in Chapter 5, the development of each DS3 required an understanding of the individual DS3 technology and thus it was found that not all submarine DS3 could be sized solely using energy flow. For example, the derivation of power to weight and volume ratios for the part of the heat removal system requiring heat exchangers must include the consideration of DDSTP, as they would have to be tested at such pressure. Similarly, as discussed in Section 5.5, one of the drivers for the emergency blow system part of the 'HP' system and the 'hard' trim and ballast 'TB' systems was the DDSTP requirement. Another example was that the power to weight and volume ratios for hydraulic system connection were derived based on triple redundancy style as well as the required capacity to provide actuation of various DS3 components on the submarine. A further energy flow response at the submarine specific systems level was seen unnecessary to be applied in ESSD, given the aim is to provide an improved sizing in a practical time. Therefore, it was concluded that the energy based sizing was only applicable for components that require power 'EL' to operate and thus other remaining DS3 could be sized directly by deriving relevant weight or volume to length assumptions (see Appendix 9).

Despite the limitation of the energy flow based sizing, the use of a logical network in SUBFLOW was found to assist the designer to facilitate the development of DS3 design *ab initio*. This was demonstrated in Case Study 5.1 where the modelling trim and ballast 'TB' system components directly in Paramarine without the use of the network approach was seen to be questionable, due to the complexity of piping having to incorporate the chosen unidirectional pumps. This meant the DS3 synthesis approach required consideration not solely by physical models or the DS3 physical architecture. SUBFLOW was also found to guide the designer to size DS3 by calculating the weight and space of DS3 components and connections that should be best reflected in the SUBFLOW network. Still, to accommodate any potential

uncertainty, margins could be used in the proposed approach, specifically in the Component Granularity Program (CGP) and the System Connection Program (SCP).

Most importantly, SUBFLOW could be used to aid Requirement Elucidation for synthesising the majority of DS3 architecture. The major differences between the network application, namely SUBFLOW, adopted in this research and the previous Network Flow Optimisation (NFO) approach (Trapp, 2015) and the Architecture Flow Optimisation (AFO), including its variants (Parsons et al., 2020a) were seen to be as follows:

- SUBFLOW could also perform a steady state simulation of power flow in a DS3 network and would aid the designer's understanding of the temporal behaviour of the DS3 in an operational scenario. Nevertheless, the coefficients of the objective function in SUBFLOW were set to zero because the aim of this optimisation was not to cost the DS3 configuration as in the case of Trapp's (2015) NSMCF investigation or Robinson's (2018) AFO study (including its variants (Parsons et al., 2020a)). SUBFLOW was used to solve the energy balance through linear programming systems of equations, which was considered preferable to a simple numerical service load summary. This ensured that the total energy demand on the submarine would be equal to the total energy available, indicating system design balance. Thus, various DS3 styles (e.g., ring mains) could be proposed on the basis of prior expert knowledge and would not be expected to be deliberately validated in ESSD by analysis. The 3D model SUBFLOW networks created using the CGP and the SCP programs can nonetheless provide a suitable basis for modelling (say) survivability concerns in subsequent design phases if required.
- Network based analysis with a specific formulation can be complicated and demanding to be applied in ESSD. As the goal of the network flow programming proposed in the current research was to obtain better size estimates for the DS3 than with the traditional parametric approach, the network formulation was not hardcoded and could be adjusted using the Component Granularity Program (CGP) and the System Connection

Program (SCP) (see Table 4.1 on page 145). Therefore, the objective function coefficient (Section 3.1.2) could be set to zero (Subsection 4.3.3) and this enabled the candidate to manually size each DS3 component, including adding any DS3 design margins, which would not be available in the cost optimisation in existing NFO research by Trapp (2015) and Robinson (2018). As the cost of individual DS3 (engineering, procurement, and installation cost (Trapp, 2015; Brown, 2020)) may well be the reasonable variable for the objective function coefficient in the existing NFO analyses, such a setup could be seen very detailed and may be unsuitable for submarine ESD, especially regarding the cost for incorporating new/radical DS3 technology. Setting up objective coefficient to zero also meant a great reduction in the number of inputs (reduced designer's workload), especially as the size of the DS3 network reached 230 nodes and 468 arcs in Case Study 5.1 in Chapter 5.

- The Operational Matrix could minimise any black-box tendencies of the linear programming formulation, by revealing the interaction between the objective function, constraints, and bounds in the form of several matrices constituting a single large matrix. This framework reflected the temporal relationship (i.e., the operational architecture of submarine DS3 - see Subsection 2.1.1) and was found to facilitate the designer in formulating linear programming and making any modifications, such as the case of the cooling demand for the CW system (see Section 5.7).
- The Network Block Approach used the UCL DBB approach as the basis of an 'inside-out' hull sizing, based on the layout demands. The latter could have been driven by exploring the DS3 style decisions, consistent with the inside-out approach. The vessel design was developed *ab initio*, from the first level of granularity to the third level of granularity where the DS3 was able to be synthesised (Figure 4.5 in Subsection 4.2.2). The DBB objects at the third level of granularity were then modelled as a network for the SUBFLOW simulation.
- Robinson (2018) first proposed the terms implicit and explicit arcs to reduce the complexity of the AFO network. In SUBFLOW, no implicit arcs were used, all arcs in the SUBFLOW DS3 network were explicit, as already

shown in Chapter 5. This aided the designer's understanding as to how the systems would respond within the whole-ship system.

- As there was no implicit arc, the whole DS3 network could be visualised as a multilayer or a multiplex 3D network (see Figure 2.7 on page 59) in terms of its logical architecture. The numerical data (power) attached to arcs were visualised as labels, revealing to the designer how much energy was transferred and converted from node to node. This has been fully demonstrated in Chapter 5.
- The visualisation of DS3 networks also employed node shape differentiation, a naming convention (Subsection 4.2.6), and colour coding for both nodes and arcs. This aided the candidate to visually check, revisit, revise, and develop the whole DS3 network design. The naming convention was also found to greatly reduce the burden of entering data when defining a DS3 connection into the System Connection Program (SCP). Without consistent naming, it would be difficult to locate a DBB object name within hundreds of DS3 components considered in the case studies.
- A type of DS3 that had one or more connection redundancies but were to be in the same highway location (see Figure 4.9 on page 158) was provided with an explicit arc in the network. However, if there were to be an instance of spatial redundancy, such as port and starboard redundancy, then explicit arcs (for port and starboard connections) would have been provided in the network. This simplification was useful for the designer when focusing on the overall ship systems' complexity and avoided being overwhelmed by the excessive detail at the connections level. For instance, supply and return lines of cooling systems were in the same highway (see Figure 4.9 on page 158) located on the port side of the ship, which was then able to be modelled as a single explicit arc (see Subsection 5.4).
- The energy, be it chemical energy, electrical energy, heat energy, or mechanical energy in a steady state condition (Subsection 2.3.4), was also considered in this research for sizing DS3 components and connections, using power to weight and space ratios approach. However, for such instances, the mathematical models had to be quite different, thus the use of the fuel-air ratio for sizing the cross-sectional area of the snort mast as

well as modelling the energy storage. This reflected the nature of a specific style appropriate to an SSK submarine design, the specifics of which is discussed in Chapter 5.

- Physical routing was defined using the 3D automatic routing feature in Paramarine (Qinetiq, 2019) and made use of the ‘highway’ framework (Subsection 4.2.5 and Appendix A 4.3) instead of being constrained by the M-1 survivability metric (Trapp, 2015) or ellipsoid damage metric used with AFO (Parsons, 2021). Therefore, a designer could justify the highway of each system based on the DS3 style driven decisions. This could also provide a more realistic 3D routing than a ‘2.5D’ approach (Table 2.2 on page 58), and so allows a designer to investigate how much space might be needed to be reserved for the detailed systems routing downstream in the design process (Subsection 4.3.1).
- The choice of DS3 technology for which the Network Block Approach could have been applied, via the Component Granularity Program (CGP), was flexible, up to fifteen different types of systems, and was tested on fourteen distinct distributed ship service systems (see Table 5.4 on page 184).

Chapter 8

Conclusions and Recommendations

Traditionally, distributed ship service systems (DS3) have been poorly addressed in Early Stage Submarine Design (ESSD) and thus a significant part of this thesis has been the development of a process model for making the submarine DS3 synthesis plausible in ESSD, by merging capabilities provided by 3D based architecturally centred physical design synthesis and the 3D network steady state flow simulation. Thus, the main aim of this research was: to propose and demonstrate a novel submarine DS3 synthesis approach that facilitates the consideration of DS3 aspects early in ESSD for a new submarine design option as part of Requirement Elucidation. In general, this aim was met, a series of conclusions were recorded and are summarised in this final chapter. Despite meeting the overall aim, several significant issues and limitations emerged during both the development as well as the implementation of the proposed Network Block Approach (NBA). Several of these aspects are considered to require further investigation with the potential to improve the proposed approach.

ESSD is about making a big design decision and this research has demonstrated that the decision making process outlined by Andrews (2018c) enabled the candidate to investigate and document important decisions made in ESSD to meet Requirement Elucidation needs as a mark of good design practice for such complex vessels. Therefore, various DS3 styles (e.g., ring mains) were proposed on the basis of prior expert knowledge without proceeding to further validation by analysis in ESSD. The 3D model SUBFLOW networks created using the open architecture spreadsheet programs within the NBA could nonetheless be a suitable basis for modelling concerns such as survivability in subsequent design phases.

None of the existing approaches was considered able to provide an integrated DS3 synthesis that works well in all three architecture modes (Brefort et al., 2018) with a specific focus on the physical and logical architectures. Previous

DS3 research, which adopt a 2.5D approach, were seen to sacrifice the advantages have been produced using the 3D based synthesis UCL DBB approach within the Paramarine ship design toolset. However, the 3D capability of that has often been considered too time consuming to undertake. In the current research, this feature was compounded by the network theory applications previously applied to surface ship distributed systems. The network approaches were also considered to be too optimisation focused for the submarine applications in that they were seen to minimise a limited, albeit important, set of design parameters. The NBA has been shown to be able to fill this gap by providing a less constraining approach (i.e., a human-centred approach and a preferred more style driven approach (Andrews, 2018c)). It also combines the advantages of the sophisticated 3D based UCL DBB synthesis in Paramarine-SURFCON and the 3D network based DS3 synthesis approach. Thus, with the proposed approach, the demanding 3D based synthesis in Paramarine, has been mitigated (Subsection 7.2.3) with improved flexibility in the DS3 network based synthesis, which was not constrained by demanding optimisation intent. This then allowed more radical ideas to be explored in future submarine concept design as a key element of Requirement Elucidation during ESSD.

In developing the NBA, it was realised that DS3 are architecturally constrained and require physical models beyond that of a 2.5D layout. In dealing with submarine DS3, different DS3 architectures (logical and operational) ought to be considered together and this could be achieved using the programs within the NBA.

The flexibility of the proposed approach, both in terms of physical models, which adopted the UCL DBB approach and the SUBFLOW network model, allowed several case studies with different design granularities to be investigated. Thus, the proposed approach could still permit in the design synthesis the use of existing practice and a parametric approach, such as compartment densities or permeability equipment assumption. This is because the proposed approach was devised to be essentially a glass box, open architecture approach, where there were no hardcoded design algorithms.

Another example was the ability to model DS3 components at different levels of design granularity and fidelity. So, the NBA could be applied to whatever level of detail is deemed necessary at DS3 submarine concept design. This then showed the capability to explore certain DS3 subsets and style alternatives that might be appropriate to a given submarine concept investigation (see Andrews (2018c) for the range of design approaches and Andrews (2021) for choices in submarine concept design). Still, any further development of the DS3 network to facilitate wider innovation in the submarine design, encompassing various DS3 styles and fostering “radical ideas”, would only be possible provided that the designer can produce a DS3 line diagram and access or produce an equipment database.

The benefits of the proposed approach are considered to be: firstly, a more plausible submarine design than 2.5D definition could previously have produced, enabling a 3D informed dialogue and more realistic space reserved for DS3 routing; secondly, highly automated 3D modelling of DS3, while the transparent approach is now possible mitigating the demanding modelling task in implementing the UCL DBB approach in Paramarine-SURFCON; thirdly, the DS3 complexity could be identified and visualised as networks, since the relevant design data can be stored centrally and be readily available in spreadsheet format; fourthly, the approach is responsive to technology changes where any new equipment or technology could be integrated, with relative ease into the design.

Despite the benefits identified above, realistic routing remains difficult in ESSD, as it required more design input effort and tends to bottom out the preferred submarine design (the final submarine design solution will not demand many DS3 components and connections changes). Furthermore, although some alternative approaches have been proposed (such as the use of margins and numerical nodes), still, to accurately size various DS3, with specific style choices, would require the use of an extensive equipment database.

The main areas of future work that were discussed in detail in Chapter 7 are summarised here, in a suggested order of significance:

- Expanding the case studies to facilitate wider innovation in the submarine design, encompassing various DS3 styles and fostering the exploration of “radical ideas” for the future submarine concept design as a key element in Requirement Elucidation during ESSD.
- Improving the process of developing the DS3 logical architecture by providing many DS3 templates as well as adding a “drag and drop” capability when sketching a DS3 network directly on the computer.
- Incorporating a more robust DS3 automatic routing, that currently cannot automatically detect and avoid routing clash. This would allow further DS3 routing density assessment to investigate greater impact on space in submarine ESD.
- Checking whether the existing execution time of the suite of programs produced by the candidate (Appendix 6) could be further improved to ensure a designer could perform the many iterations required to design DS3 both in terms of physical architecture and logical architecture.
- Broadening the application of the proposed approach to other complex vessels, including but not limited to various surface warships or oil and gas service vessels (Floating Production Storage and Offloading (FPSO) ship, drilling ship, etc). This includes expanding the consideration of aspects of integrity, maintenance, and supportability for evaluating various submarine DS3 style choices.
- Validating the sizing results for several real and distinctly different submarine designs and thus a more generic weight per length for cable or pipe supports for various DS3 could be derived.
- Integrating the Network Block Approach (NBA) with Virtual Reality facilities would provide demanding physical models and are readily achievable using the programs within the NBA.

References

- Allmendinger, E.E. (ed.) (1990) *Submersible vehicle systems design*. Jersey City, N.J: Society of Naval Architects and Marine Engineers.
- Andrews, D.J. (1981) Creative Ship Design. *Trans. RINA*, 123. doi:10.3940/rina.trans.1981.23.
- Andrews, D.J. (1984) *Synthesis in Ship Design*. Ph.D. thesis, University College London.
- Andrews, D.J. (1993) The Management of Warship Design: The MOD Warship Project Manager's Perspective. *Trans. RINA*, 135. doi:10.3940/rina.trans.1993.01.
- Andrews, D.J. (1994) Preliminary Warship Design. *Trans. RINA*, 136. doi:10.3940/rina.sbt.1994.a2.
- Andrews, D.J. (1998) A comprehensive methodology for the design of ships (and other complex systems). *Proceedings of the Royal Society A: Mathematical, Physical and Engineering Sciences*, 454 (1968): 187–211. doi:10.1098/rspa.1998.0154.
- Andrews, D.J. (2003) A Creative Approach to Ship Architecture. *International Journal of Maritime Engineering*, 145 (3): 229–252. doi:10.3940/rina.ijme.2003.a3.9031.
- Andrews, D.J. (2011) Marine Requirements Elucidation and the Nature of Preliminary Ship Design. *RINA IJME*, 153. doi:10.3940/rina.ijme.2011.a1.202.
- Andrews, D.J. (2012) Art and science in the design of physically large and complex systems. *Proceedings of the Royal Society A: Mathematical, Physical and Engineering Sciences*, 468 (2139): 891–912. doi:10.1098/rspa.2011.0590.
- Andrews, D.J. (2013) "The True Nature of Ship Concept Design – And What it Means for the Future Development of CASD." *12th International Conference on Computer and IT Applications in the Maritime Industries*. Cortona, Italy, April 2013.
- Andrews, D.J. (2017a) "Submarine Design Is Not Ship Design." *RINA Warship Conference: Naval Submarines & UUV's*. Bath, UK, June 2017. Royal Institution of Naval Architect. p. 16. doi:10.3940/rina.ws.2017.21.
- Andrews, D.J. (2017b) "The Key Ship Design Decision - Choosing the Style of a New Design." *16th Conference on Computer and IT Applications in the Maritime Industries*. Cardiff, UK, May 2017.
- Andrews, D.J. (2018a) Choosing the Style of a New Design - The Key Ship Design Decision. *Trans RINA*, 160 (Part A1). doi:10.3940/rina.ijme.2018.a1.457.

- Andrews, D.J. (2018b) “Is a naval architect an atypical designer—or just a hull engineer?” *Marine design XIII: proceedings of the 13th International Marine Design Conference (IMDC 2018)*. Helsinki, Finland, June 2018.
- Andrews, D.J. (2018c) The Sophistication of Early Stage Design for Complex Vessels. *RINA IJME Special Edition*, 472 Part A. doi:10.3940/rina.ijme.2018.SE.472.
- Andrews, D.J. (2020) Design Errors in Ship Design. *Journal of Marine Science and Engineering*, 9 (1). doi:10.3390/jmse9010034.
- Andrews, D.J. (2021) *Who Says There Are No Real Choices in Submarine Design?* Virtual, June 2021. Royal Institution of Naval Architects.
- Andrews, D.J., Casarosa, L. and Pawling, R. (2009) “Integrating Simulation and Computer Aided Ship Design Software and Processes.” *RINA Int’l Conference on Computer Applications in Shipbuilding in September 2009*. September 2009. Royal Institution of Naval Architect. doi:10.3940/rina.iccas.2009.53.
- Andrews, D.J., Cudmore, A.C., Humble, P., et al. (1996) “SUBCON - A New Approach to Submarine Concept Design.” *RINA Warships Proc. Symp. Naval Submarines 5: The Total Weapons System*. London, UK, June 1996. Royal Institution of Naval Architect. doi:10.3940/rina.warship.1996.13.
- Andrews, D.J. and Dicks, C.A. (1997) “The Building Block Design Methodology Applied to Advanced Naval Ship Design.” *Proc. IMDC*. Newcastle, June 1997. International Marine Design Conference (IMDC).
- Andrews, D.J. and Pawling, R.J. (2003) “SURFCON A 21st Century Ship Design Tool.” *The 8th International Marine Design Conference*. Athens, Greece, May 2003. IMDC.
- Andrews, D.J. and Pawling, R.J. (2008) A Case Study in Preliminary Ship Design. *RINA IJME*. doi:10.3940/rina.ijme.2008.a3.139.
- Arentzen, E.S. and Mandel, P. (1960) Naval Architectural Aspects of Submarine Design. *Trans. SNAME*, 68.
- ASHRAE (2017) *2017 ASHRAE handbook: Fundamentals : SI edition*. Atlanta, GA: ASHRAE, 2017, ©2017.
- Asmara, A. (2013) *Pipe routing framework for detailed ship design*. Ph.D. thesis, Delft University of Technology. Available at: <http://resolver.tudelft.nl/uuid:4da99646-37d7-49e5-9d3b-51de81ba29dd> (Accessed: 3 September 2018).
- Babae, H., Chalfant, J., Chrysostomidis, C., et al. (2015) “System-level analysis of chilled water systems aboard naval ships.” *2015 IEEE Electric Ship Technologies Symposium (ESTS)*. Old Town Alexandria, VA, USA, June 2015. IEEE. pp. 370–375. doi:10.1109/ESTS.2015.7157921.

- Barth, W., Mutzel, P. and Junger, M. (2004) Simple and Efficient Bilayer Cross Counting. *Journal of Graph Algorithms and Applications*, 8 (2).
- Boscarol, M. and Aiello, L.C. (1988) *Foundations of Logic and Functional Programming: Workshop, Trento, Italy, December 15-19, 1986. Proceedings*. Springer Science & Business Media. (Google-Books-ID: ZbHRbvGaanMC).
- Brandes, U. and Köpf, B. (2002) “Fast and Simple Horizontal Coordinate Assignment.” Mutzel, P., Jünger, M. and Leipert, S. (eds.) *Graph Drawing*. Berlin, Heidelberg: Springer Berlin Heidelberg. pp. 31–44. doi:10.1007/3-540-45848-4_3.
- Brefort, D., Shields, C., Habben Jansen, A., et al. (2018) An architectural framework for distributed naval ship systems. *Ocean Engineering*, 147: 375–385. doi:10.1016/j.oceaneng.2017.10.028.
- Brown, A.J. (2020) *Design of Marine Engineering Systems in Ship Concept Design*. SNAME. (to be published). Available at: <https://www.sname.org/marine-engineering>.
- Brown, A.J. and Waltham-Sajdak, J. (2015) Still Reengineering the Naval Ship Concept Design Process. *Naval Engineers Journal*, 127 (1): 49–61.
- Brown, D.K. and Andrews, D.J. (1980) “The Design of Cheap Warships.” *Proc. of International Naval Technology Expo 80*. Rotterdam, Netherlands, 1980.
- Brownlow, L.C., Goodrum, C.J., Sypniewski, M.J., et al. (2021) A multilayer network approach to vulnerability assessment for early-stage naval ship design programs. *Ocean Engineering*, 225: 108731. doi:10.1016/j.oceaneng.2021.108731.
- Budell, R. (2014) “Future Submarine Programmes: Observations Lessons.” *Naval Submarines & UUV's*. Bath, UK, 2014. Royal Institution of Naval Architects.
- Burcher, R. and Rydill, L. (1994) *Concepts in Submarine Design*. Cambridge ocean technology series. Cambridge [England]: Cambridge University Press.
- Campbell, A.M. (2014) *Architecting aircraft power distribution systems via redundancy allocation*. Georgia Institute of Technology. Available at: <https://smartech.gatech.edu/handle/1853/53087> (Accessed: 4 April 2019).
- Chalfant, J.S. (2015) Early-Stage Design for Electric Ship. *Proceedings of the IEEE*, 103 (12): 2252–2266. doi:10.1109/JPROC.2015.2459672.
- Chalfant, J.S. and Chryssostomidis, C. (2011) “Analysis of various all-electric-ship electrical distribution system topologies.” *2011 IEEE Electric Ship Technologies Symposium*. Alexandria, VA, USA, April 2011. IEEE. pp. 72–77. doi:10.1109/ESTS.2011.5770844.
- Chalfant, J.S. and Chryssostomidis, C. (2017) “Application of templates to early-stage ship design.” *2017 IEEE Electric Ship Technologies Symposium*

- (ESTS). Arlington, VA, USA, August 2017. IEEE. pp. 111–117. doi:10.1109/ESTS.2017.8069268.
- Chalfant, J.S., Chryssostomidis, C. and Angle, M.G. (2010) “Study of Parallel AC and DC Electrical Distribution in the All-Electric Ship.” *Grand Challenges in Modeling and Simulation (GCMS10)*. Ottawa, Canada, July 2010.
- Chalfant, J.S., Langland, B., Rigterink, D., et al. (2017) “Smart Ship System Design (S3D) integration with the leading edge architecture for Prototyping Systems (LEAPS).” *2017 IEEE Electric Ship Technologies Symposium (ESTS)*. Arlington, VA, USA, August 2017. IEEE. pp. 104–110. doi:10.1109/ESTS.2017.8069267.
- Cieraad, S., Duchateau, E., Zandstra, R., et al. (2017) “A Packing Approach Model in Support of the Conceptual Design of Naval Submarines.” *16th Conference on Computer and IT Applications in the Maritime Industries*. Cardiff, UK, May 2017. COMPIT.
- Collins, L. and Wrobel, P. (2014) “The Current State of Rim Drive Technology and its Application to Submarine Propulsion.” *Warship 2013: Naval Submarines & UUV's*. Bath, UK, June 2014.
- Collins, L.E., Andrews, D. and Pawling, R.J. (2015) “A New Design Approach for the Incorporation of Radical Technologies: Rim Drive for Large Submarines.” *International Marine Design Conference (IMDC)*. Tokyo, Japan, May 2015.
- Coverdale, A., Roberts, T., Systems, A., et al. (2008) “Assuring Submarine Safety for the Future SSBN.” *Warship 2008: Naval Submarines 9*. Glasgow, UK, June 2008.
- Danilovic, M. and Browning, T.R. (2007) Managing complex product development projects with design structure matrices and domain mapping matrices. *International Journal of Project Management*, 25 (3): 300–314. doi:10.1016/j.ijproman.2006.11.003.
- Deb, K., Pratap, A., Agarwal, S., et al. (2002) A fast and elitist multiobjective genetic algorithm: NSGA-II. *IEEE Transactions on Evolutionary Computation*, 6 (2): 182–197. doi:10.1109/4235.996017.
- Defence Equipment and Support (2007) *Maritime Acquisition Publication No 01-070 Surface Ship and Submarine Margins Guidance*.
- Dennis, P., Hield, P., Wharington, J., et al. (2019) “A Platform-Focused Power and Energy Modelling Capability for Submarines.” *Pacific International Maritime Conference*. Sydney, Australia, 2019.
- Dijkstra, E.W. (1959) A note on two problems in connexion with graphs. *Numerische Mathematik*, 1 (1): 269–271. doi:10.1007/BF01386390.

- Doerry, N. (2007) Designing Electrical Power Systems for Survivability and Quality of Service. *Naval Engineers Journal*, 119 (2): 25–34. doi:10.1111/j.0028-1425.2007.00017.x.
- Donohue, J., Goodrum, C., Sypniewski, M., et al. (2019) “A Method for Generation and Analysis of Feasible General Arrangement and Distributed System Configurations in Early Stage Ship Design.” *18th International Conference on Computer and IT Applications in the Maritime Industries*. Tullamore, March 2019.
- Duchateau, E.A.E. (2016) *Interactive evolutionary concept exploration in preliminary ship design*. Ph.D. thesis, Delft University of Technology. doi:10.4233/uuid:27ff1635-2626-4958-bcdb-8aee282865c8.
- Duchateau, E.A.E., de Vos, P. and van Leeuwen, S. (2018) “Early stage routing of distributed ship service systems for vulnerability reduction.” *Marine design XIII: proceedings of the 13th International Marine Design Conference (IMDC 2018)*. Helsinki, Finland, June 2018.
- Elliott, C. and Deasley, P. (2007) *Creating systems that work: principles of engineering systems for the 21st century*. London: Royal Academy of Engineering. Available at: <https://www.raeng.org.uk/publications/reports/rae-systems-report>.
- Fiedel, E.R. (2011) *Cooling System Early-Stage Design Tool For Naval Applications*. Master's thesis, MIT.
- Friedman, N. (1984) *Submarine Design and Development*. London: Conway Maritime Pr.
- Fruchterman, T.M.J. and Reingold, E.M. (1991) Graph drawing by force-directed placement. *Software: Practice and Experience*, 21 (11): 1129–1164. doi:10.1002/spe.4380211102.
- Gabler, U. (2000) *Submarine Design*. Bonn: Bernard und Graefe.
- Gale, P.A. (2003) The Ship Design Process, Chapter 5 of LAMB, T. (Ed.). *SNAME, Newark, NJ, 1–2*. Available at: <https://app.knovel.com/hotlink/toc/id:kpSDCV0001/ship-design-construction/ship-design-construction>.
- Gansner, E.R., Koutsofios, E., North, S.C., et al. (1993) A technique for drawing directed graphs. *IEEE Transactions on Software Engineering*, 19 (3): 214–230. doi:10.1109/32.221135.
- Gillespie, J.W. (2012) *A Network Science Approach to Understanding and Generating Ship Arrangements in Early-Stage Design*. Ph.D. thesis, University of Michigan.
- Gillespie, J.W. and Singer, D.J. (2013) Identifying drivers of general arrangements through the use of network measures of centrality and hierarchy. *Ocean Engineering*, 57: 230–239. doi:10.1016/j.oceaneng.2012.09.002.

- Gomez, S., Mazzone, F., Baudu, C., et al. (2013) 2796 – Resistant depression in the elderly: effects of treatment on symptomatology, cognitive functioning and functional abilities. *European Psychiatry*, 28: 1. doi:10.1016/S0924-9338(13)77385-1.
- Gongora, R. de (2019) “Practical Use Cases of Artificial Intelligence in the Ship Design Stage.” *ICCAS International Conference on Computer Applications in Shipbuilding*. Rotterdam, Netherlands, September 2019. Royal Institution of Naval Architect.
- Goodrum, C.J., Shields, C.P.F. and Singer, D.J. (2017) “Investigating the Impact of Distributed System Routing Densities on Vessel Operability.” *ICCAS 2017: International Conference on Computer Applications in Shipbuilding*. Singapore, September 2017.
- Gottschalk, S., Lin, M.C. and Manocha, D. (1996) “OBBTree: a hierarchical structure for rapid interference detection.” *Proceedings of the 23rd annual conference on Computer graphics and interactive techniques - SIGGRAPH '96*. Not Known, 1996. ACM Press. pp. 171–180. doi:10.1145/237170.237244.
- Hamson, K.G. (2016) “A New Approach to Managing the Acoustic Signature Risk in Warship Design.” *Warship 2016: advanced technologies in naval design, construction, & operation*. Bath, UK, June 2016. Royal Institution of Naval Architects.
- Harbour, J.P. (2001) *Evaluation and Comparison of Electric Propulsion Motors for Submarines*. Master’s thesis, Massachusetts Institute of Technology.
- Harrington, R.L. (1992) *Marine engineering*. Jersey City, N.J: Society of Naval Architects and Marine Engineers (SNAME).
- Hemsley, R. (2015) “HVAC Considerations for Small SSK Submarine Design.” *Undersea Defence Technology*. Rotterdam, Netherlands, June 2015.
- Howard, C.Q. (2010) “Technologies for the Management of the Acoustic Signature of a Submarine.” *The 5th Biennial SIA Conference*. Fremantle, Australia, November 2010.
- Hu, Y. (2016) *Dimension Prediction of Marine System Equipment Based on First Principles*. Master’s thesis, Delft University of Technology.
- Hüttermann, M. (2012) *DevOps for developers*. The expert’s voice in web development. New York, NY: Apress.
- IBM, C. (2014) *IBM Knowledge Center*. Available at: https://www.ibm.com/support/knowledgecenter/SSSA5P_12.5.0/ilog.odms.cpl ex.help/CPLEX/MATLAB/topics/cplex_matlab_overview.html (Accessed: 29 June 2019).
- Jackson, C.H.A. (1992) Fundamentals of Submarine Concept Design. *SNAME Transactions*, 100: 419–448.

- Jurkiewicz, D.J., Chalfant, J. and Chryssostomidis, C. (2013) "Modular IPS machinery arrangement in early-stage naval ship design." *2013 IEEE Electric Ship Technologies Symposium (ESTS)*. Arlington, VA, April 2013. IEEE. pp. 121–127. doi:10.1109/ESTS.2013.6523722.
- Kagawa, N. (1991) Noise and Vibration Characteristics of a 3 kW-class Stirling Engine. *JSME international journal. Ser. 2, Fluids engineering, heat transfer, power, combustion, thermophysical properties*, 34 (4): 575–582. doi:10.1299/jsmeb1988.34.4_575.
- Kennedy, A.B.W. and Sankey, H.R. (1898) The Thermal Efficiency of Steam Engines. Report of The Committee Appointed to The Council Upon the Subject of The Definition of a Standard or Standards of Thermal Efficiency for Steam Engines: With an Introductory Note. (Including Appendixes and Plate at Back of Volume). *Minutes of the Proceedings of the Institution of Civil Engineers*, 134 (1898): 278–312. doi:10.1680/imotp.1898.19100.
- Koenig, P. (2017) *Lecture XI Design for Production*. Shipbuilding Operations and Technology. MIT 2N Professional Summer Notes. Available at: <https://naval-pro-summer.mit.edu/>.
- Koren, Y. (2005) Drawing graphs by eigenvectors: theory and practice. *Computers & Mathematics with Applications*, 49 (11–12): 1867–1888. doi:10.1016/j.camwa.2004.08.015.
- Kormilitsin, Y.N. and Khalizev, O.A. (2001) *Theory of Submarine Design*. First Edition edition. Bush Hill Park: Riviera Maritime Media.
- Kouriampalis, N. (2019) *Applying Queueing Theory and Architecturally-Oriented Early Stage Ship Design to the Concept of a Vessel Deploying a Fleet of Uninhabited Vehicles*. Ph.D. thesis, University College London.
- Kouriampalis, N., Pawling, R.J. and Andrews, D.J. (2021) Modelling the operational effects of deploying and retrieving a fleet of uninhabited vehicles on the design of dedicated naval surface ships. *Ocean Engineering*, 219: 108274. doi:10.1016/j.oceaneng.2020.108274.
- Krummrich, S. and Llabrés, J. (2015) Methanol reformer – The next milestone for fuel cell powered submarines. *International Journal of Hydrogen Energy*, 40 (15): 5482–5486. doi:10.1016/j.ijhydene.2015.01.179.
- Lamb, T. (1987) Engineering for Ship Production. *Journal of Ship Production*, 3 (04): 274–297. doi:10.5957/jsp.1987.3.4.274.
- Langland, B., Leonard, R., Smart, R., et al. (2015) "Modeling and data exchange in a concurrent and collaborative design environment for electric ships." *2015 IEEE Electric Ship Technologies Symposium (ESTS)*. Old Town Alexandria, VA, USA, June 2015. IEEE. pp. 388–394. doi:10.1109/ESTS.2015.7157924.

- Lee, J.H., Kim, S.H. and Lee, K. (2012) Integration of evolutionary BOMs for design of ship outfitting equipment. *Computer-Aided Design*, 44 (3): 253–273. doi:10.1016/j.cad.2011.07.009.
- Mahonen, C., Spradley, W. and Gerdon, M. (2007) “Automating Early Stage Submarine Design: Development of the Submarine Concept Design (SUBCODE) Program.” *ASNE Day 2007*. Arlington, VA, 2007. American Society of Naval Engineers.
- Mathcad (2021) *Mathcad: Math Software for Engineering Calculations | Mathcad*. Available at: <https://www.mathcad.com> (Accessed: 20 July 2021).
- MATLAB (2019) *MATLAB - MathWorks*. Available at: <https://uk.mathworks.com/products/matlab.html> (Accessed: 8 July 2019).
- McVoy, J.L. (1968) An Analytical Approach to the Evaluation of Submarine Safety. *Naval Engineers Journal*, 80 (2): 213–229. doi:10.1111/j.1559-3584.1968.tb04503.x.
- Microsoft (2021a) *Buy Microsoft Excel Spreadsheet Software or Try Excel, Free*. Available at: <https://www.microsoft.com/en-gb/microsoft-365/excel> (Accessed: 27 June 2021).
- Microsoft (2021b) *Office Visual Basic for Applications (VBA) reference*. Available at: <https://docs.microsoft.com/en-us/office/vba/api/overview/> (Accessed: 27 June 2021).
- Morais, D., Waldie, M. and Larkins, D. (2018) “The Digital Twin Journey.” *17th International Conference on Computer and IT Applications in the Maritime Industries*. Pavone, Italy, May 2018.
- Morris, D. and Spinney, D. (2017) “Designing for Support to meet Challenging Submarine Availability Targets.” *Undersea Defence Technology*. Bremen, Germany, June 2017. Undersea Defence Technology.
- Mucha, P.J., Richardson, T., Macon, K., et al. (2010) Community Structure in Time-Dependent, Multiscale, and Multiplex Networks. *Science*, 328 (5980): 876–878. doi:10.1126/science.1184819.
- Mukti, M.H., Pawling, R.J. and Andrews, D.J. (2021) Distributed Ship Service Systems Architecture in The Early Stages of Designing Physically Large and Complex Vessels: The Submarine Case. *IJME*, 163. doi:<https://doi.org/10.5750/ijme.v163iA2.755>.
- Mukti, M.H., Pawling, R.J., Savage, C., et al. (2019) “Distributed Ship Service Systems Architecture in the Early Stages of Physically Large and Complex Products.” *ICCAS International Conference on Computer Applications in Shipbuilding*. Rotterdam, Netherlands, September 2019. RINA.
- Mukti, M.H. and Randall, R.E. (2017) “Graphic Method for Improved Indonesian Navy Submarine Design Acquisition; the Investigation of Small (Midget) Naval

- Submarine Development.” *RINA Warship: Naval Submarines & UUVs*. Bath, UK, June 2017. doi:10.3940/rina.ws.2017.07.
- NAVSEA (1978) *Military Specification, Tube, Copper Alloy, Seamless and Welded*. MIL-T-16420K NAVSEA. Available at: Downloaded from <http://www.everyspec.com> on 28/06/2019.
- Newman, M. (2010) *Networks: An Introduction*. Oxford University Press. Available at: <http://www.oxfordscholarship.com/view/10.1093/acprof:oso/9780199206650.001.0001/acprof-9780199206650> (Downloaded: 22 November 2018).
- Newman, M.E.J. (2004) Analysis of weighted networks. *Physical Review E*, 70 (5): 056131. doi:10.1103/PhysRevE.70.056131.
- Nilsson, H. (1988) Submarine Power Systems Using the V4-275R Stirling Engine. *Proceedings of the Institution of Mechanical Engineers, Part A: Power and Process Engineering*, 202 (4): 257–267. doi:10.1243/PIME_PROC_1988_202_036_02.
- Norman, D. (2013) *The design of everyday things*. Revised and expanded edition. Cambridge, Massachusetts: MIT Press.
- van Oers, B. (2012) “An integrated approach for the design of resilient ship services systems.” *11th International Naval Engineering Conference and Exhibition INEC*. Edinburgh, UK, May 2012. INEC.
- van Oers, B.J. van (2011) *A packing approach for the early stage design of service vessels*. Ph.D. thesis, Delft University of Technology.
- ONR-ESRDC (2018) *ESRDC | Electric Ship Research and Development Consortium*. Available at: <https://www.esrdc.com/> (Accessed: 25 December 2018).
- Parsons, M.A. (2019) *Network-Based Naval Ship Distributed System Design using Architecture Flow Optimization*. Master’s thesis, Virginia Tech.
- Parsons, M.A. (2021) *Network-Based Naval Ship Distributed System Design and Mission Effectiveness using Dynamic Architecture Flow Optimization*. Ph.D. thesis, Virginia Tech.
- Parsons, M.A., Kara, M.Y., Robinson, K.M., et al. (2020a) Early-Stage Naval Ship Distributed System Design Using Architecture Flow Optimization. *Journal of Ship Production and Design*, 37: 1–19. doi:10.5957/JSPD.10190058.
- Parsons, M.A., Robinson, K.M., Kara, M.Y., et al. (2020b) Application of a Distributed System Architectural Framework to Naval Ship Concept and Requirements Exploration. *Naval Engineers Journal*, 132 (4): 105–124.
- Pawling, R.J. (2007) *The Application of the Design Building Block Approach to Innovative Ship Design*. Ph.D. thesis, University College London.

- Pawling, R.J. and Andrews, D.J. (2011) "A Submarine Concept Design - The Submarine as an UXV Motherhip." *Proc. Warship 2011: Naval Submarines and UUVs*. Bath, UK, June 2011. doi:10.3940/rina.ws.2011.04.
- Pawling, R.J. and Andrews, D.J. (2018) "Seeing Arrangements As Connections: The Use of Networks in Analysing Existing and Historical Ship Designs." *Marine design XIII: proceedings of the 13th International Marine Design Conference (IMDC 2018)*. Helsinki, Finland, June 2018.
- Pawling, R.J., Andrews, D.J., Picks, R., et al. (2013) "An Integrated Approach to Style Definition in Early Stage Design." *12th International Conference on Computer and IT Applications in the Maritime Industries*. Cortona, Italy, April 2013.
- Pawling, R.J., Kouriampalis, N., Esbati, S., et al. (2017) "Expanding the Scope of Early Stage Computer Aided Ship Design." *16th Conference on Computer and IT Applications in the Maritime Industries*. Cardiff, UK, 15 May 2017.
- Pawling, R.J., Piperakis, A. and Andrews, D. (2015) "Developing Architecturally Oriented Concept Ship Design Tools for Research and Education." *12th International Marine Design Conference 2015*. Tokyo, Japan, May 2015.
- Phoenix Integration (2021) *Phoenix Integration's ModelCenter is THE framework for Model Based Engineering, which reduces development costs, improves efficiency and stimulates innovation*. Available at: <https://www.phoenix-int.com/> (Accessed: 17 May 2021).
- Piperakis, A.S. (2013) *An Integrated Approach to Naval Ship Survivability in Preliminary Ship Design*. Ph.D. thesis, University College London.
- Psoma, A. and Sattler, G. (2002) Fuel cell systems for submarines: from the first idea to serial production. *Journal of Power Sources*, 106 (1–2): 381–383. doi:10.1016/S0378-7753(01)01044-8.
- Purton, I.M. (2016) *Concept Exploration for a Novel Submarine Concept Using Innovative Computer-Based Research Approaches and Tools*. Ph.D. thesis, University College London.
- Purton, I.M., Pawling, R.J. and Andrews, D.J. (2015) "The Use of Computer Tools in Early Stage Design Concept Exploration to Explore a Novel Submarine Concept." *International Marine Design Conference (IMDC)*. Tokyo, Japan, May 2015. IMDC.
- Qinetiq (2019) *Paramarine*. Available at: <https://paramarine.qinetiq.com/products/paramarine/index.aspx> (Accessed: 8 July 2019).
- Renilson, M. (2015) *Submarine Hydrodynamics*. SpringerBriefs in Applied Sciences and Technology. Springer International Publishing. Available at: [//www.springer.com/gb/book/9783319161846](http://www.springer.com/gb/book/9783319161846) (Downloaded: 4 October 2018).

- Rigterink, D., Piks, R. and Singer, D.J. (2014) The use of network theory to model disparate ship design information. *International Journal of Naval Architecture and Ocean Engineering*, 6 (2): 484–495. doi:10.2478/IJNAOE-2013-0194.
- Rigterink, D.T. (2014) *Methods for Analyzing Early Stage Naval Distributed Systems Designs, Employing Simplex, Multislice, and Multiplex Networks*. Ph.D. thesis, University of Michigan.
- Robinson, K.M. (2018) *Modeling Distributed Naval Ship Systems Using Architecture Flow Optimization*. Master's thesis, Virginia Tech.
- SAAB (2021) *A submarine in space | Stories | Saab*. Available at: <https://www.saab.com/newsroom/stories/2020/july/a-submarine-in-space> (Accessed: 13 August 2021).
- Shields, C.P.F., Rigterink, D.T. and Singer, D.J. (2017) Investigating physical solutions in the architectural design of distributed ship service systems. *Ocean Engineering*, 135: 236–245. doi:10.1016/j.oceaneng.2017.02.037.
- Shields, C.P.F., Sypniewski, M.J. and Singer, D.J. (2018) Characterizing general arrangements and distributed system configurations in early-stage ship design. *Ocean Engineering*, 163: 107–114. doi:10.1016/j.oceaneng.2018.05.053.
- Shin, J.G. (2017) “New Innovative Shipbuilding Technologies - Shipbuilding in Asia-.” *MIT 2N Professional Summer Notes*. <https://naval-pro-summer.mit.edu/>.
- Smart, R., Chalfant, J., Herbst, J., et al. (2017) “Using S3D to analyze ship system alternatives for a 100 MW 10,000 ton surface combatant.” *2017 IEEE Electric Ship Technologies Symposium (ESTS)*. Arlington, VA, USA, August 2017. IEEE. pp. 96–103. doi:10.1109/ESTS.2017.8069266.
- Sowa, J.F. (1983) *Conceptual structures: Information processing in mind and machine*. Available at: <https://www.osti.gov/biblio/5673179> (Accessed: 5 December 2020).
- Stanford University (2021) *Best practices for file naming*. Available at: <https://library.stanford.edu/research/data-management-services/data-best-practices/best-practices-file-naming> (Accessed: 22 January 2021).
- Stapersma, D. and de Vos, P. (2015) “Dimension prediction models of ship system components based on first principles.” *12th International Marine Design Conference 2015*. Tokyo, Japan, May 2015.
- Stevens, A.P. (2016) *Naval Ship Preliminary Arrangements for Operability and Reduced Vulnerability*. Master's thesis, Virginia Tech. Available at: https://vtechworks.lib.vt.edu/bitstream/handle/10919/82975/Stevens_AP_T_2016.pdf?sequence=1&isAllowed=y.
- Stewart, M. (2018) *Surface production operations: volume iv: pump and compressor*. 1st edition. Cambridge, CA: Elsevier.

- Stinson, N.T. (2019) *Refinement of Surface Combatant Ship Synthesis Model for Network-Based System Design*. Master's thesis, Virginia Tech.
- Thornton, G.B. (1994) *A Design Tool for the Evaluation of Atmosphere Independent Propulsion in Submarines*. Master's thesis, Massachusetts Institute of Technology.
- Thurkins, E.J. (2012) *Development of an early stage ship design tool for rapid modeling in Paramarine*. Master's thesis, Massachusetts Institute of Technology. Available at: <http://dspace.mit.edu/handle/1721.1/74992> (Accessed: 16 January 2019).
- Trapp, A. (2015) *Shipboard Integrated Engineering Plant Survivable Network Optimization*. Ph.D. thesis, Massachusetts Institute of Technology.
- Tupper, E.C. (2013) *Introduction to naval architecture / E.C. Tupper*. 5th ed. Amsterdam ; Boston, Amsterdam ; London: Elsevier, Butterworth Heinemann, Butterworth-Heinemann. Available at: <http://app.knovel.com/hotlink/toc/id:kpINAE0011/introduction-to-naval> (Downloaded: 4 July 2018).
- UCL (2021) *Submarine Design & Acquisition Course*. Available at: <https://www.ucl.ac.uk/mechanical-engineering/study/other-programmes/submarine-design-acquisition-course> (Accessed: 20 January 2022).
- UCL-NAME (2012) *Submarine Design Procedure*. London: UCL Department of Mechanical Engineering, Naval Architecture and Marine Engineering.
- UCL-NAME (2014) *Submarine Data Book*. London: UCL Department of Mechanical Engineering, Naval Architecture and Marine Engineering.
- U.S. Department of Defense (1989) *Military Handbook: Cable Comparison Handbook Data Pertaining To Electric Shipboard Cable*. MIL-HDBK-299(SH) downloaded on 28.06.2019 from everyspec.com. Available at: Downloaded from <http://www.everyspec.com> on 28/06/2019.
- U.S. Department of Defense (2009) *Department of Defense Standard Practice. Electric Plant Installation Standard Methods for Surface Ships and Submarines (Cableways)*. MIL-STD-2003-4A(SH) downloaded on 28.06.2019 from everyspec.com. Available at: Downloaded from <http://www.everyspec.com> on 28/06/2019.
- Vargas, J.V.C., Souza, J.A., Hovsopian, R., et al. (2011) "ESRDC ship notional baseline medium voltage direct current (MVDC) architecture thermal simulation and visualization." *2011 Grand Challenges on Modeling and Simulation Conference*. The Hague, Netherlands, 2011.
- de Vos, P. (2018) *On early-stage design of vital distribution systems on board ships*. Ph.D. thesis, Delft University of technology. doi:10.4233/uuid:eb604971-30b7-4668-ace0-4c4b60cd61bd.

- de Vos, P. and Stapersma, D. (2018) Automatic topology generation for early design of on-board energy distribution systems. *Ocean Engineering*, 170: 55–73. doi:10.1016/j.oceaneng.2018.09.023.
- Wilgenhof, J. and Reijmers, J. (2010) “Ventilation system design and application in a new submarine,.” *UDT 2010: UDT Europe : Undersea Defence Technology*. Hamburg, Germany, June 2010.
- Wolfe, J. and Roa, M.J. (2017) Advanced Methods for Tabulation of Electrical Loads During Special Modes of Marine Vessel Operation. *IEEE Transactions on Industry Applications*, 53 (1): 667–674. doi:10.1109/TIA.2016.2602343.
- Woud, H.K. and Stapersma, D. (2002) *Design of propulsion and electric power generation systems*. London: IMarEST, Institute of Marine Engineering, Science and Technology.
- Wrobel, P.G. (1984) Design of the Type 2400 Patrol Class Submarine. *Trans. RINA*, 01. doi:10.3940/rinq.trans.1985.01.
- Yen, J.Y. (1971) Finding the K Shortest Loopless Paths in a Network. *Management Science*, 17 (11,): 712–716.

Appendix 1

Body of Knowledge

This appendix consists of figures related to literature review, network flow approach, and DS3 diagrams (e.g., Piping Instrumentation Diagram (PID)) taken from various sources.

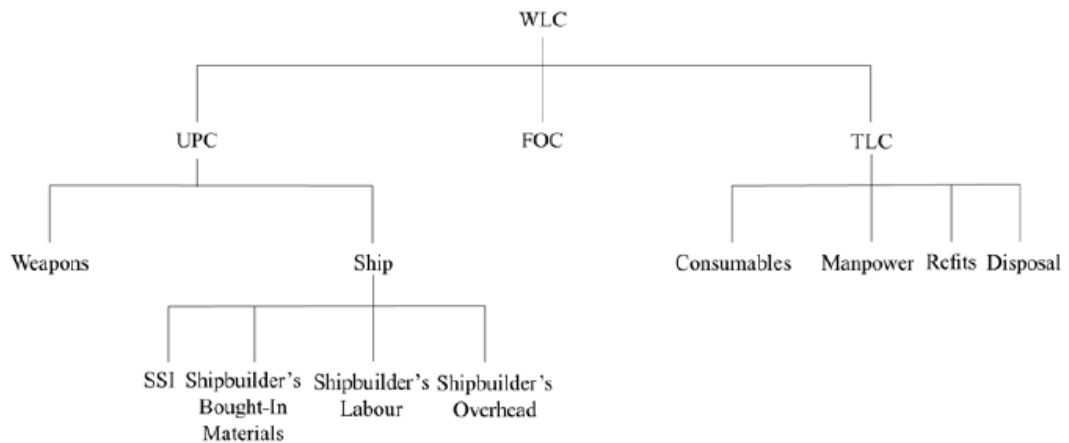


Figure A.1: Breakdown of naval ship cost showing Whole Life Cost (WLC) consisted of Unit Production Cost (UPC), First of Class cost (FOC) (drawing, mockup, etc), Through Life Cost (TLC) (Brown and Andrews, 1980) redrawn by Kouriampalis (2019)

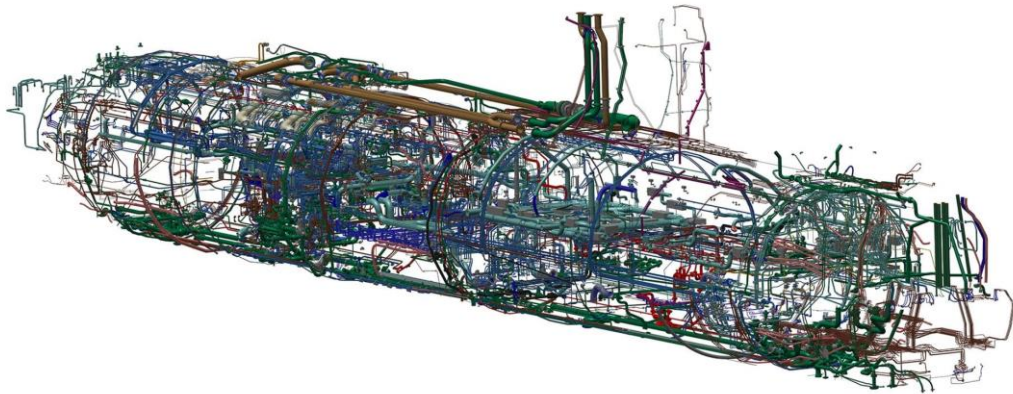


Figure A.2: Example of pipe routing on the project A26 submarine (SAAB, 2021)

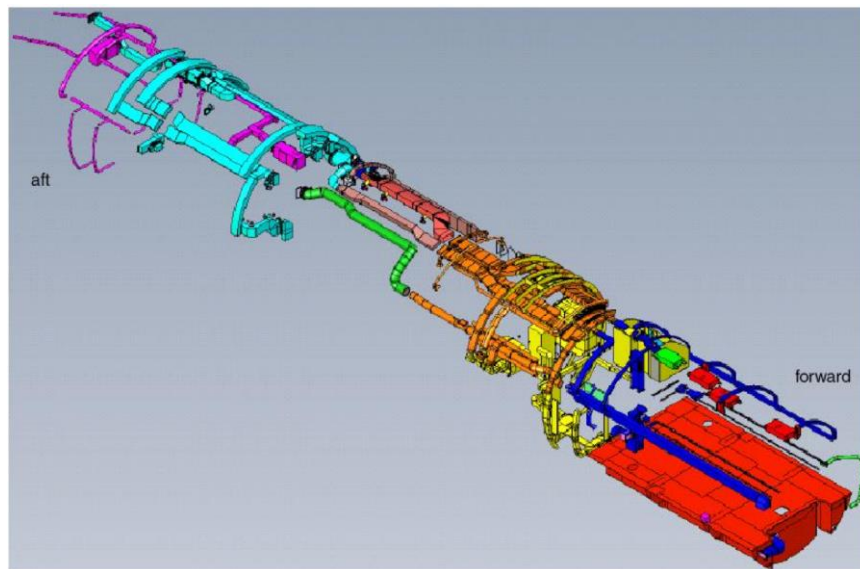


Figure A.3: Example of HVAC duct routing showing structure duct in blue and other unidentified ducts in other colours (Wilgenhof and Reijmers, 2010)

Table A 1: The basic NSMCF formulation with M-1 Survivability (Trapp, 2015) showing superscripts 0 to 7, i.e., 0 for no casualty and 1 to 7 edge loss scenarios, total of 8 scenarios

Linear Programming Formulation	Realisation			
Objective Function Subject To:	$c_{12}U_{12} + c_{13}U_{13} + c_{24}U_{24} + c_{34}U_{34} + c_{35}U_{35} + c_{46}U_{46} + c_{56}U_{56}$			
Continuity	$-x_{12}^0 - x_{13}^0 + b_1^0 = 0$ $x_{34}^0 + x_{24}^0 - x_{46}^0 = 0$ \vdots $-x_{12}^7 - x_{13}^7 + b_1^7 = 0$ $x_{34}^7 + x_{24}^7 - x_{46}^7 = 0$	$x_{12}^0 - x_{24}^0 - b_2^0 = 0$ $x_{35}^0 - x_{56}^0 + b_5^0 = 0$ \vdots $x_{12}^7 - x_{24}^7 - d_1^7 = 0$ $x_{35}^7 - x_{56}^7 + S_2^7 = 0$	$x_{13}^0 - x_{35}^0 - x_{34}^0 - b_3^0 = 0$ $x_{46}^0 + x_{56}^0 - b_6^0 = 0$ \vdots $x_{13}^7 - x_{35}^7 - x_{34}^7 = 0$ $x_{46}^7 + x_{56}^7 - b_6^7 = 0$	
Capacity Rollup	$ x_{12}^0 \leq U_{12}$ $ x_{35}^0 \leq U_{35}$ \vdots $ x_{12}^7 \leq U_{12}$ $ x_{35}^7 \leq U_{35}$	$ x_{13}^0 \leq U_{13}$ $ x_{46}^0 \leq U_{46}$ \vdots $ x_{13}^7 \leq U_{13}$ $ x_{46}^7 \leq U_{46}$	$ x_{24}^0 \leq U_{24}$ $ x_{56}^0 \leq U_{56}$ \vdots $ x_{24}^7 \leq U_{24}$ $ x_{56}^7 \leq U_{56}$	$ x_{34}^0 \leq U_{34}$ \vdots $ x_{34}^7 \leq U_{34}$
Bounds	$-\infty \leq x_{12}^0 \leq \infty$ $-\infty \leq x_{34}^0 \leq \infty$ \vdots $-\infty \leq x_{12}^7 \leq \infty$ $-\infty \leq x_{34}^7 \leq \infty$	$-\infty \leq x_{13}^0 \leq \infty$ $-\infty \leq x_{35}^0 \leq \infty$ $-\infty \leq x_{56}^0 \leq \infty$ \vdots $-\infty \leq x_{13}^7 \leq \infty$ $-\infty \leq x_{35}^7 \leq \infty$ $-\infty \leq x_{56}^7 \leq \infty$	$-\infty \leq x_{24}^0 \leq \infty$ $-\infty \leq x_{46}^0 \leq \infty$ \vdots $-\infty \leq x_{24}^7 \leq \infty$ $-\infty \leq x_{46}^7 \leq \infty$	
Casualty & Operating Conditions	$x_{12}^1 = 0$ $x_{45}^5 = 0$ $b_1^0 \geq 0$ $b_5^0 \geq 0$ \vdots $b_1^7 \geq 0$ $b_5^7 \geq 0$	$x_{13}^2 = 0$ $x_{46}^6 = 0$ $b_2^0 = -10$ $b_6^0 = -5$ \vdots $b_2^7 = -10$ $b_6^7 = -5$	$x_{24}^3 = 0$ $x_{56}^7 = 0$ $b_3^0 = 0$ \vdots $b_3^7 = 0$	$x_{34}^4 = 0$ $b_4^0 = 0$ \vdots $b_4^7 = 0$

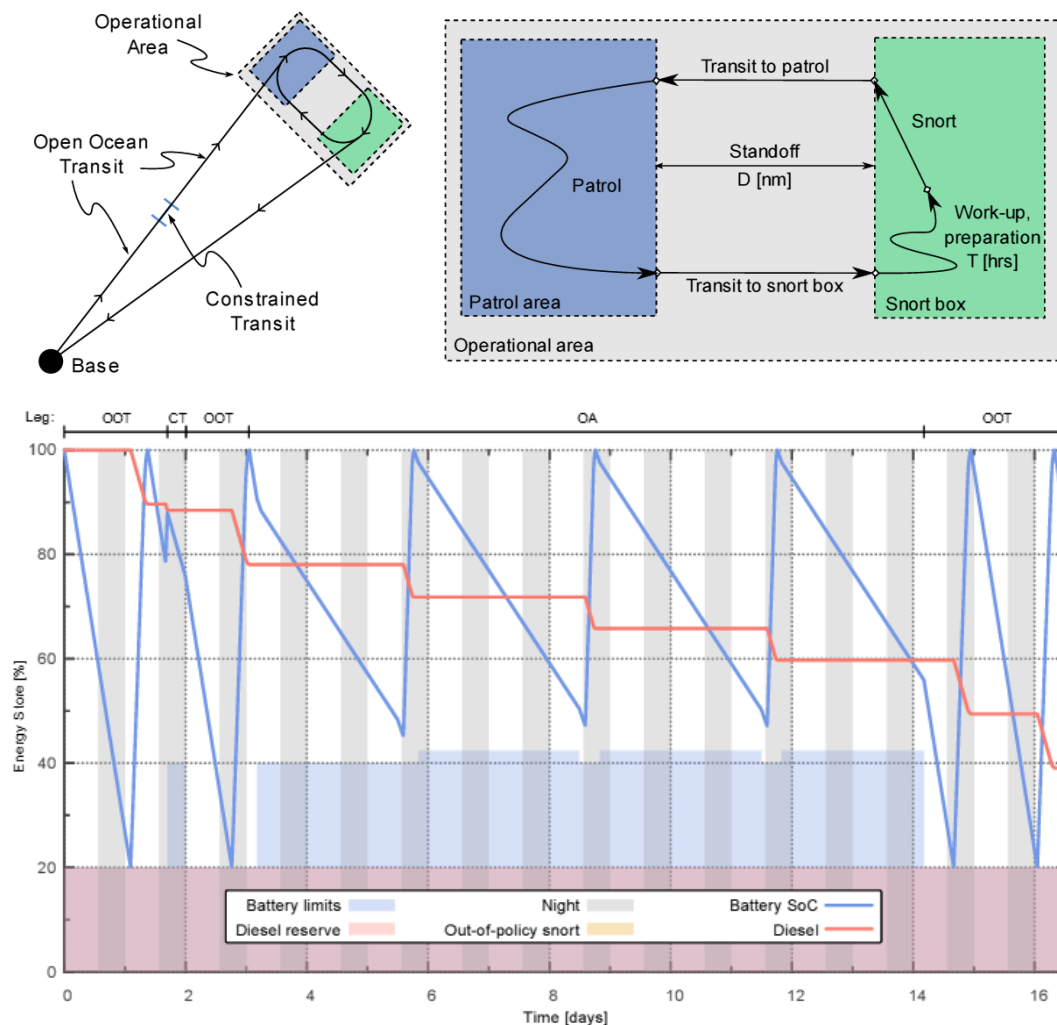


Figure A.4: A fictional operational profile for an SSK (Dennis et al., 2019) showing various operational conditions (top) and battery State of Charge (SoC) simulation (bottom). Although it was recognised that this operation may not be relevant in a war condition, this is simply used to illustrate a generic energy cycle of an SSK in a patrol operation. On leaving its home base for transit, an SSK would have two energy sources, fuel and battery at an assumed 100% level of capacity ready for a patrol mission. Once SSK submerges, it is operating at submerged speed, discharging battery energy to an assumed minimum level of capacity (20%). Then, (typically) during night-time, the diesel fuel is converted to electrical energy for various loads including topping up the battery energy. This takes the battery back to a full capacity while depleting fuel energy. In short, it forms a cycle of charging and discharging during the duration of the patrol or the operational range drawn from the initial requirement. By the end of the patrol, when the SSK returns, the fuel energy is reduced to a certain level of capacity where there should be some margin left in the fuel tanks and the battery was charged to a full capacity for the next patrol operation.

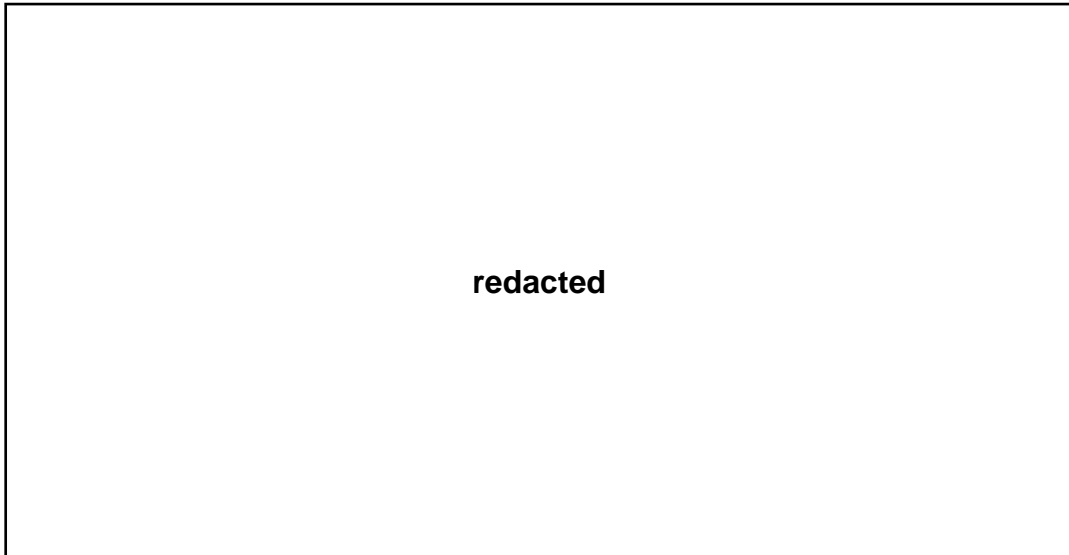


Figure A.5: Fuel system line diagram (Gabler, 2000)

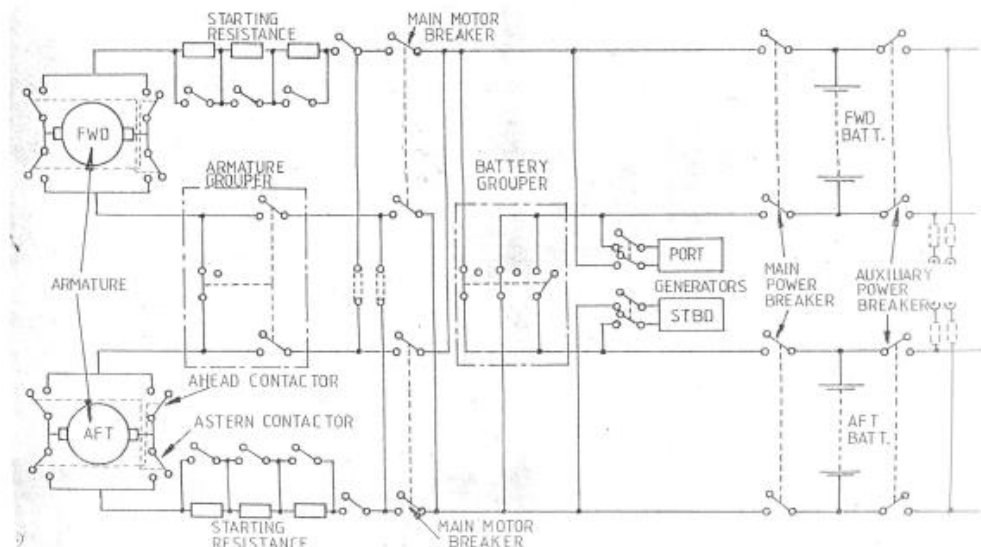


Figure A.6: Line diagram of electrical propulsion system (UCL-NAME, 2014)



Figure A.7: A single shaft system with direct electric drive and separate diesel generators showing: port and starboard diesel engines (1 & 2); port and starboard motor generators (3 & 4); dual drive motor (5); thrust bearing (6); propeller (7); partial batteries (8-10) (Gabler, 2000)

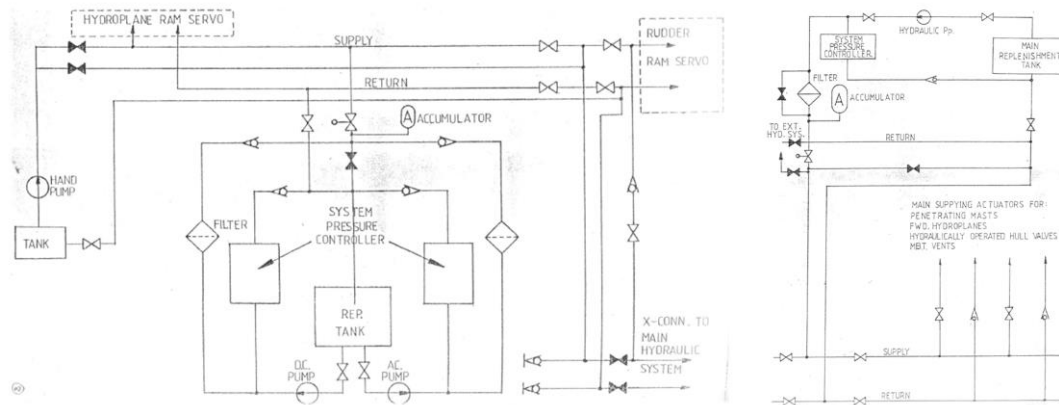


Figure A.8: Line diagram of hydraulic system (UCL-NAME, 2014)

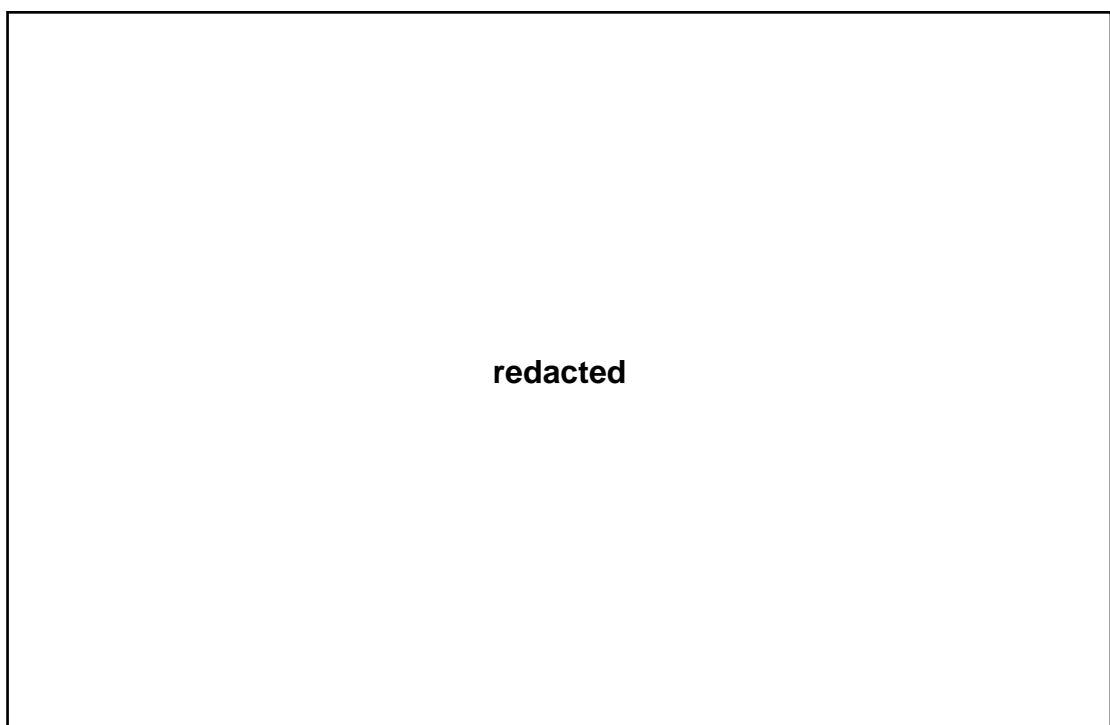


Figure A.9: Central hydraulic plant (Gabler, 2000)

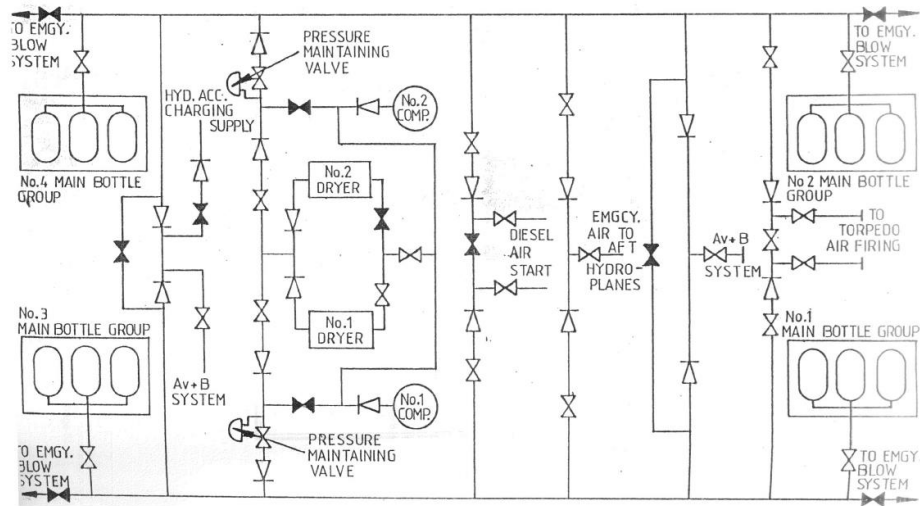


Figure A.10: Line diagram of high-pressure air system (UCL-NAME, 2014)

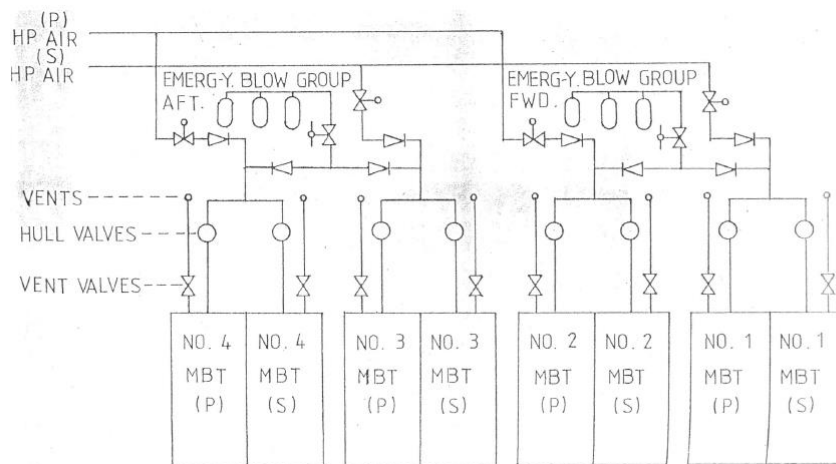


Figure A.11: Line diagram of emergency blow system (UCL-NAME, 2014)

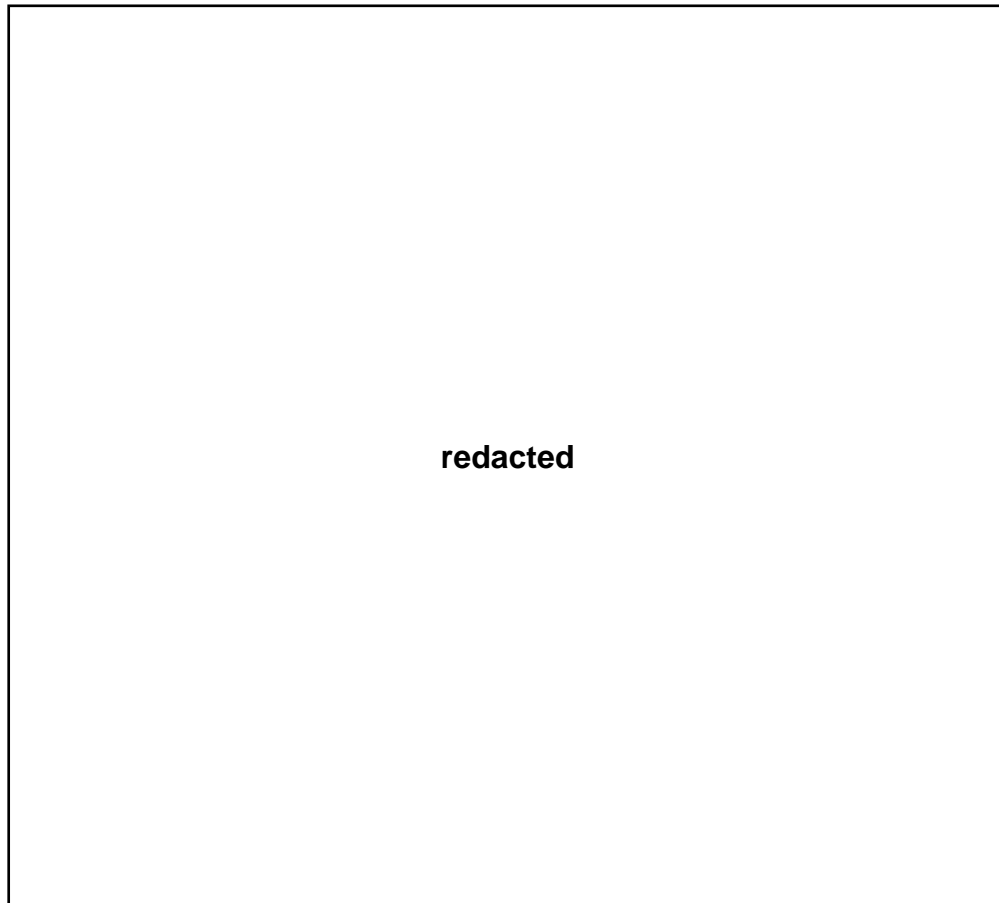


Figure A.12: Compressed air system (Gabler, 2000)

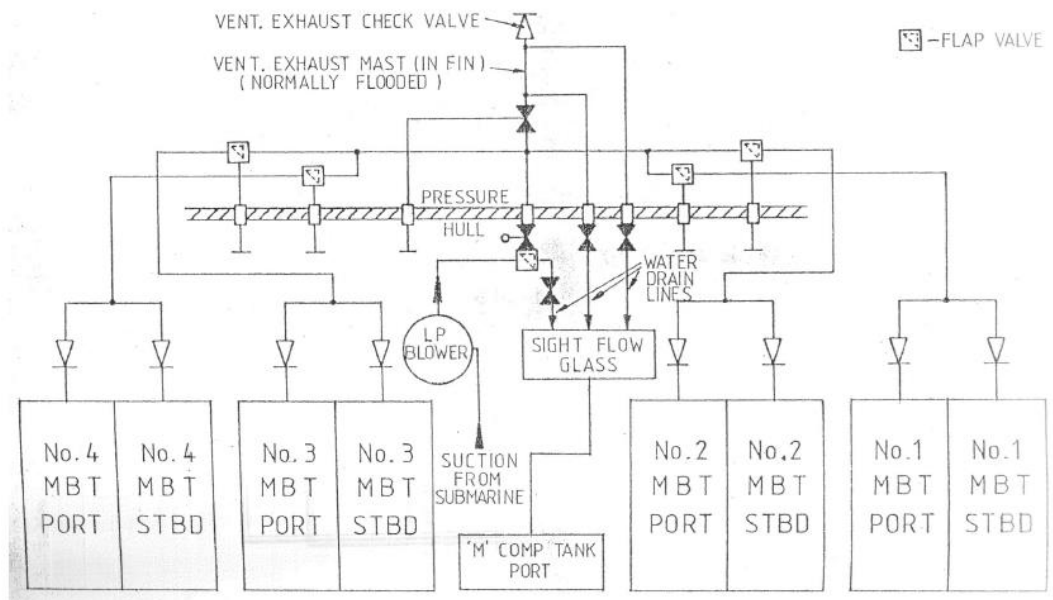


Figure A.13: Line diagram of low-pressure air system (UCL-NAME, 2014)

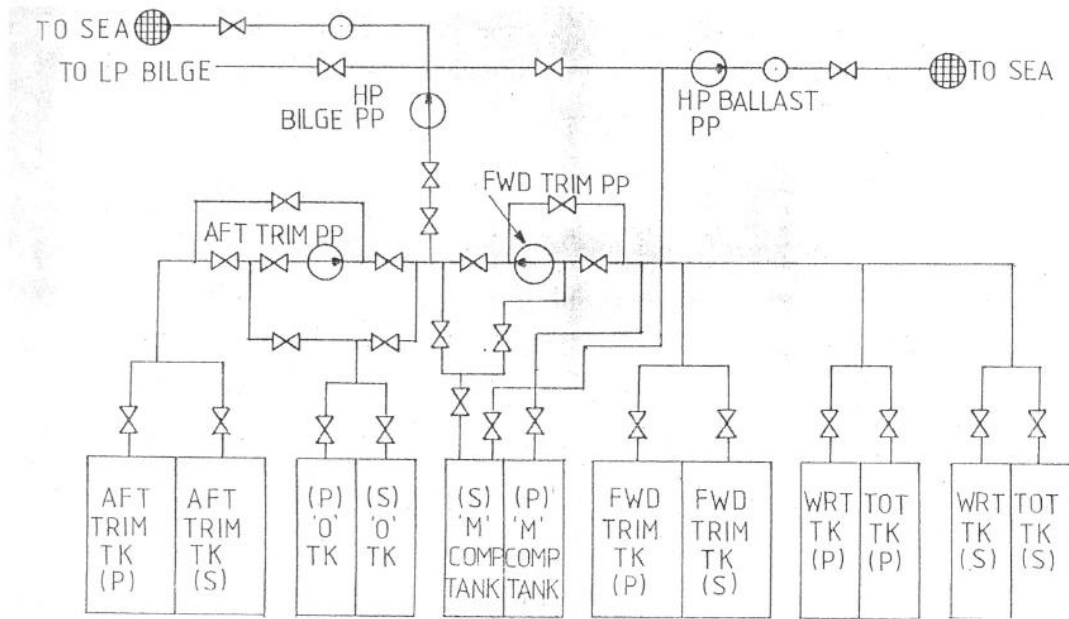


Figure A.14: Line diagram of trim and ballast systems (UCL-NAME, 2014)

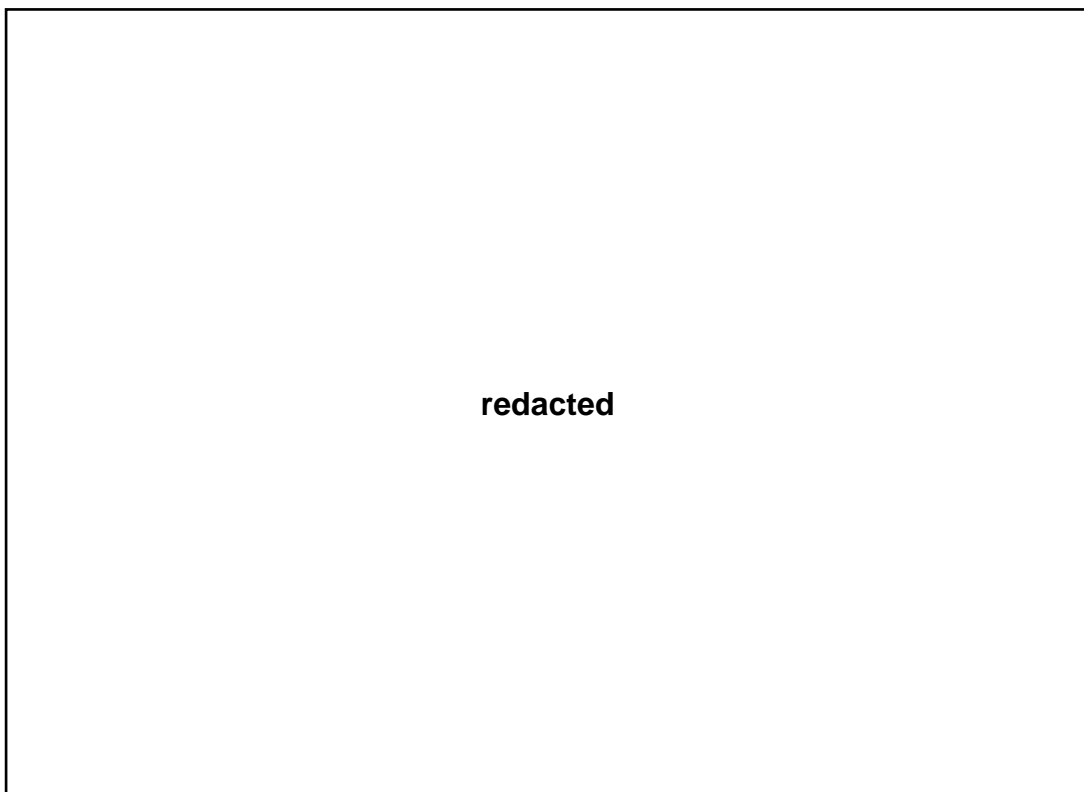


Figure A.15: The drain and flood system (Gabler, 2000)

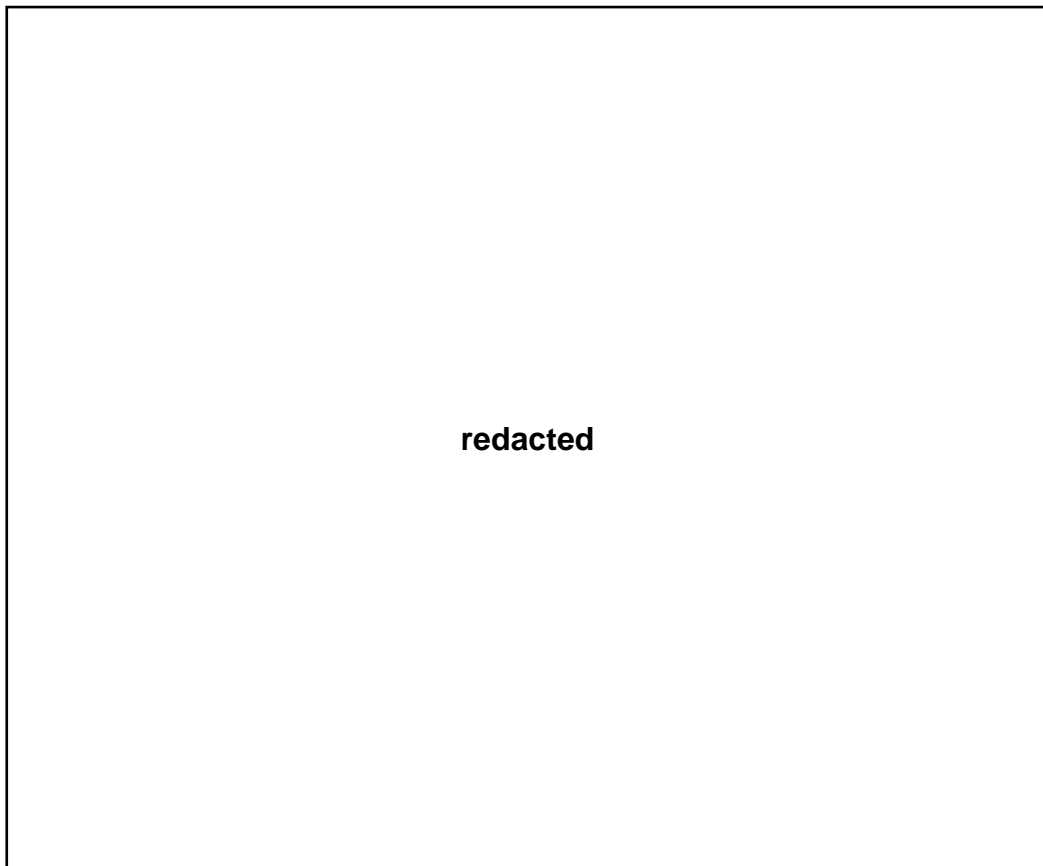


Figure A.16: Connections of electrically controlled and compressed air actuated snorkel head valve (Gabler, 2000)

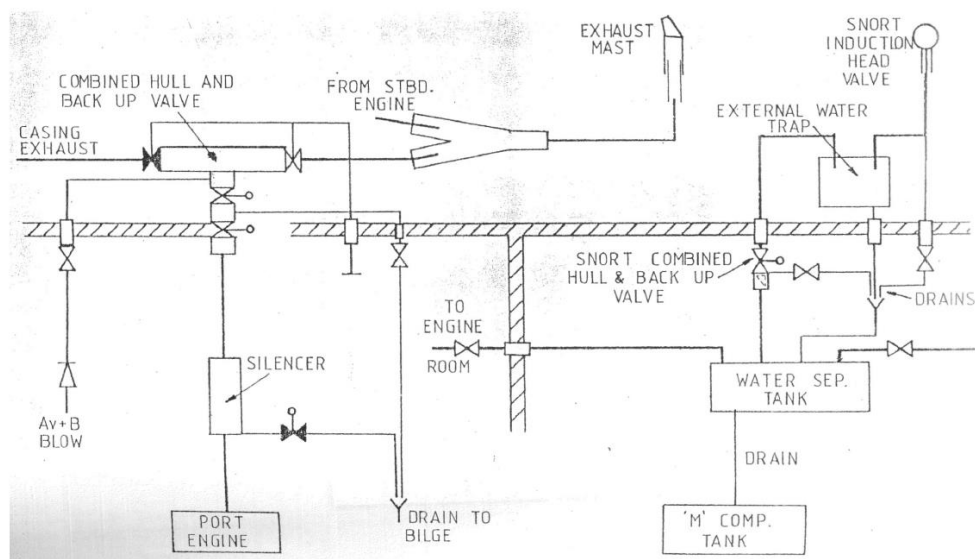


Figure A.17: Snort induction and diesel exhaust systems (UCL-NAME, 2014)

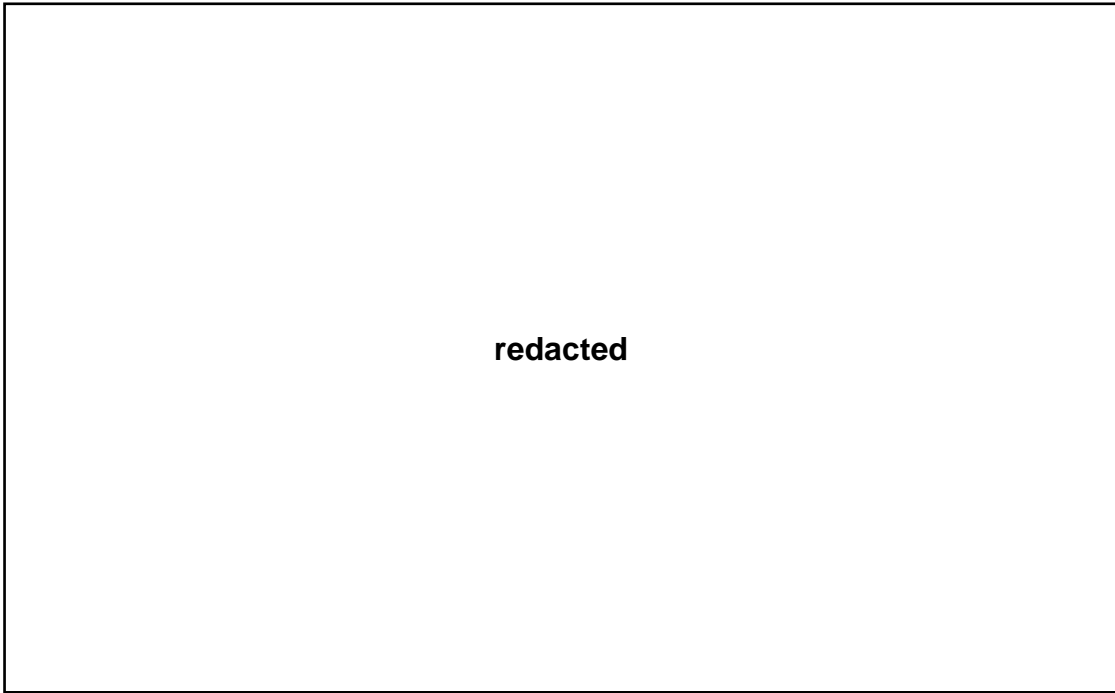


Figure A.18: A ventilating and air purification systems (Gabler, 2000)

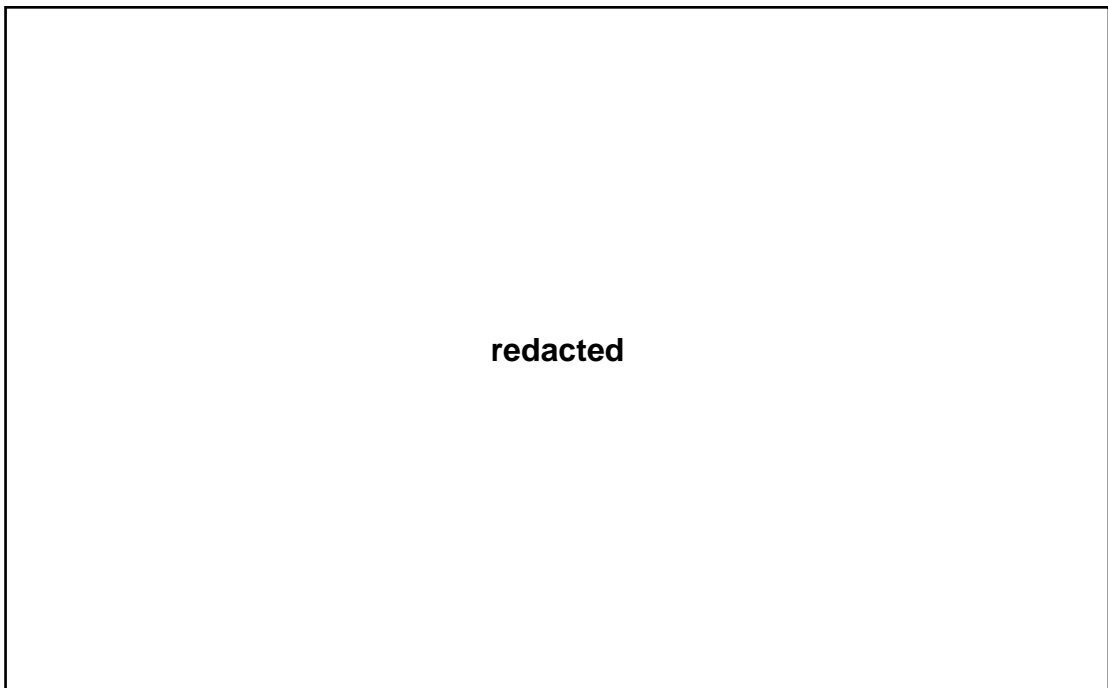


Figure A.19: Air circulations in various operating conditions (Gabler, 2000)

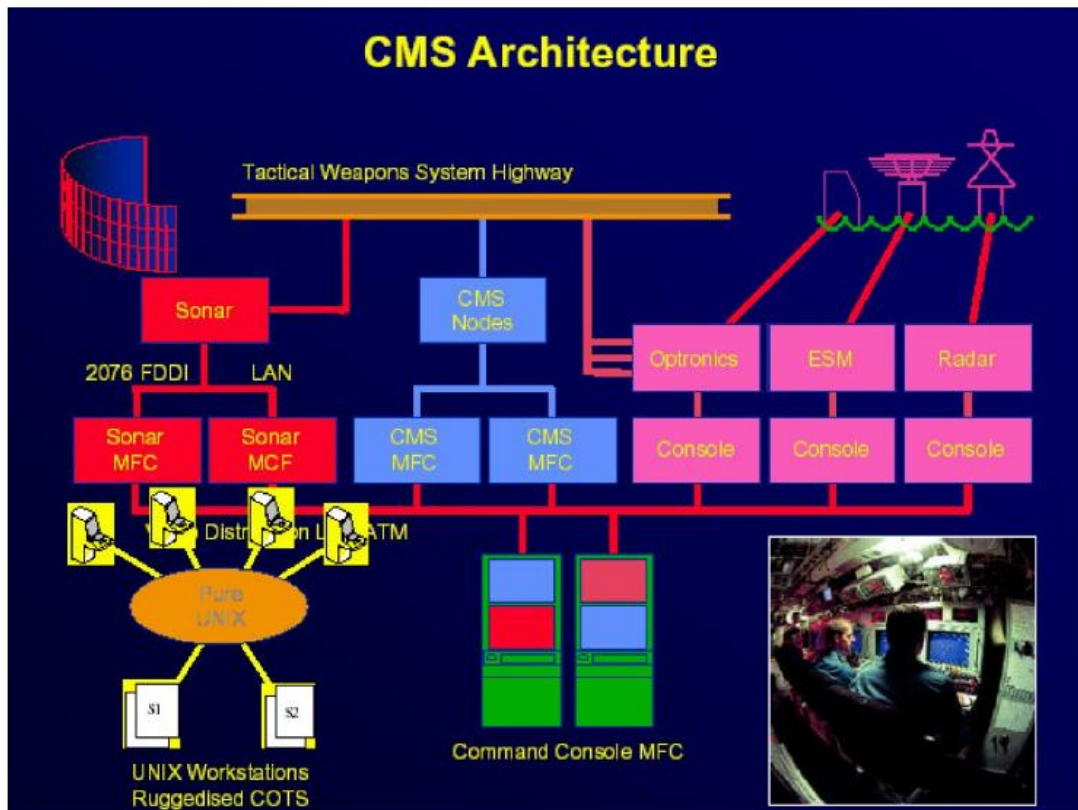


Figure A.20: Command Management System (CMS) architecture (UCL-NAME, 2012)

Appendix 2

Estimation of Propulsion System

The estimation of propulsion system for Case Study 3.2.1 was developed with MATHCAD 4.0 (Mathcad, 2021). The algorithms used in the calculation are self-explanatory and are taken either from the Burcher and Rydill (1994) or the UCL submarine data (UCL-NAME, 2012, 2014). Some external volumes were scaled based on the Type 2400 design (Wrobel, 1984), summarised in Figure A.21. This was done by first reconstructing 2D general arrangement of the Type 2400 design and creating the 3D model in Paramarine-SURFCON. With a consistent scale, the volume of each compartment/room/tank could be calculated. This could also be applied to nuclear submarines using data from the public domain (Friedman, 1984) (see Figure A.22).

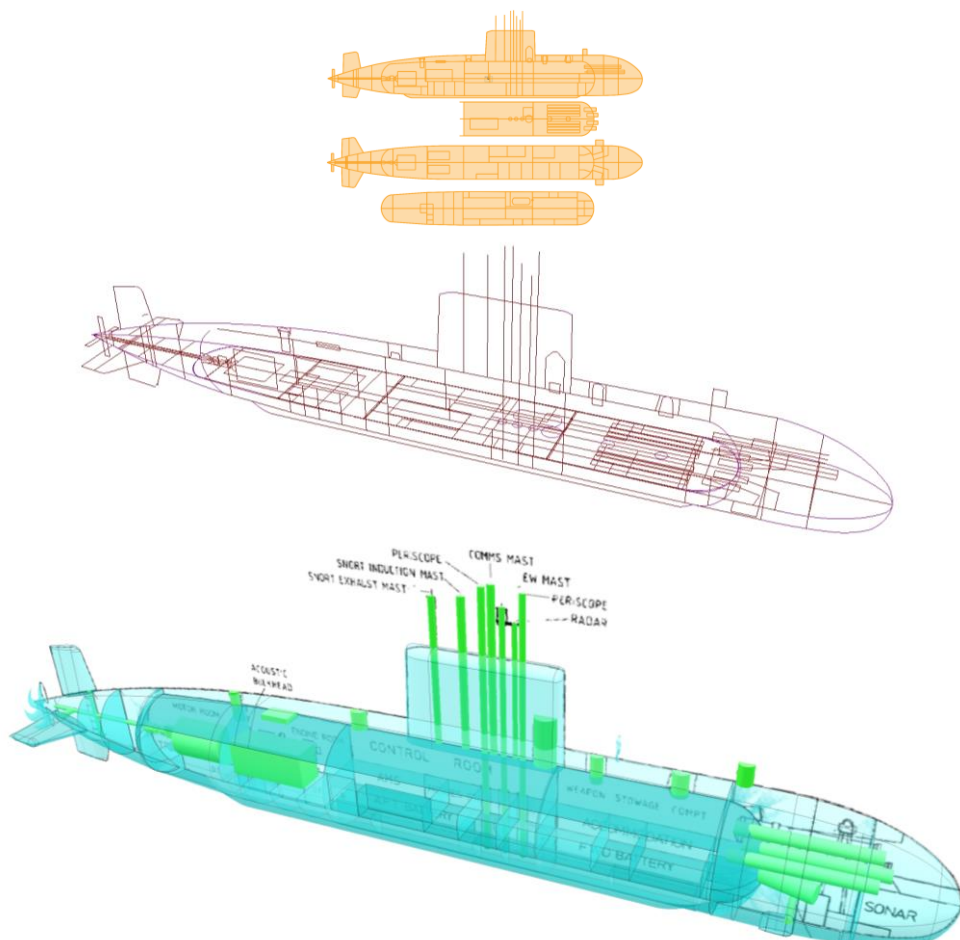


Figure A.21: Reverse engineering Type 2400 design showing the 2D arrangement (Wrobel, 1984) (top and middle) and Paramarine-SURFCON was used to calculate spaces and major components (bottom)

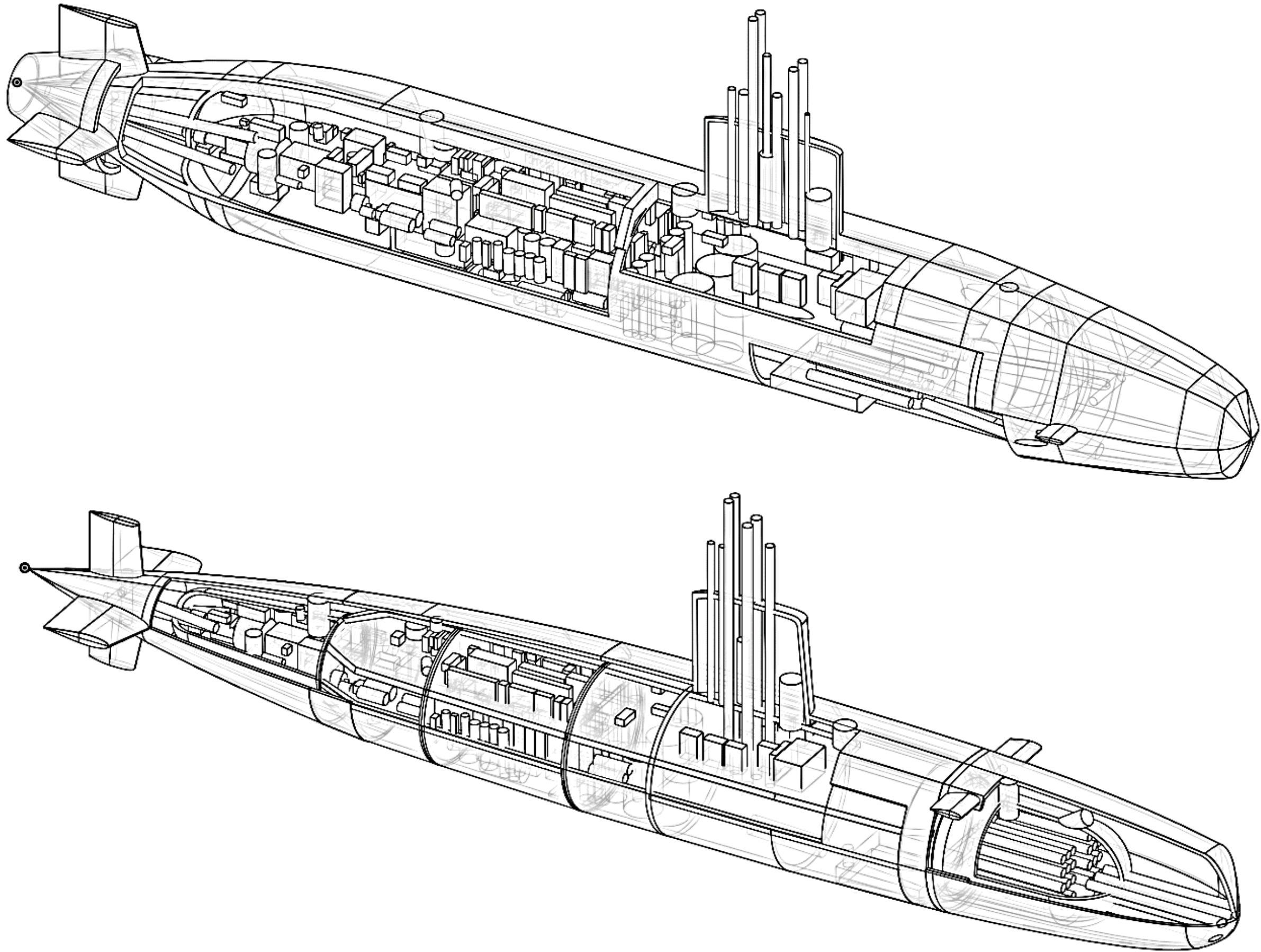


Figure A.22: 3D CAD model for nuclear submarines (SSN) showing the physical architecture of various DS3 components could be identified for future work

Case Study 3.2.1

Calculated payload volume from the UCL Submarine Databook (2014) with an assumed packing density	$V_{pay} := 400 \text{ m}^3$
Assumed payload volume fraction	$pvf := 20\%$
First shot at pressure hull volume	$V_{ph} := \frac{V_{pay}}{pvf} = (2 \cdot 10^3) \text{ m}^3$ $PH_{vol} := V_{ph}$
Rule of thumb diameter to achieve acceptable L/D ratios (UCL submarine design procedure, 2012)	$D_{ph} := 0.6 \cdot V_{ph}^{\frac{1}{3}} = 7.6 \text{ m}$
Length of forward end, assuming ellipsoid shape	$L_{fe} := 1.5 \cdot D_{ph} = 11.3 \text{ m}$
Volume of dome, assuming hemisphere dome	$V_{dome} := 0.04 \cdot \pi \cdot D_{ph}^3 = 54.3 \text{ m}^3$
Volume of forward end	$V_{fe} := \frac{2}{3} \cdot \pi \cdot \left(\frac{D_{ph}}{2}\right)^2 \cdot L_{fe} - V_{dome} = 285 \text{ m}^3$
Length of aft end, assuming a mean conical/parabolic shape	$L_{ae} := 1.5 \cdot D_{ph} = 11.3 \text{ m}$
Volume of aft end	$V_{ae} := \left(\frac{\frac{1}{3} + \frac{1}{2}}{2}\right) \cdot \pi \cdot \left(\frac{D_{ph}}{2}\right)^2 \cdot L_{ae} - V_{dome} = 157.8 \text{ m}^3$
Various initial external volumes assumptions (fin, casing, appendages) based on Type 2400 design (Wrobel, 1984)	$V_{fin} := 6.75\% \cdot V_{ph} = 135 \text{ m}^3$ $V_{cas} := 10.5\% \cdot V_{ph} = 210 \text{ m}^3$ $V_{misc} := 2.5\% \cdot V_{ph} = 50 \text{ m}^3$
Form volume	$V_{form} := (V_{ph} + V_{fe} + V_{ae}) + (V_{fin} + V_{cas} + V_{misc}) = (2.8 \cdot 10^3) \text{ m}^3$
Assumed typical form for submerged performance (pg. 255 Burcher & Rydill (1994))	$K_p := 20$
Snorting speed	$U_{snort} := 7 \text{ knot}$
Thrust power for snorting speed	$P_{eff} := K_p \cdot \left(\frac{V_{form}}{\text{m}^3}\right)^{0.64} \cdot \left(\frac{U_{snort}}{\frac{\text{m}}{\text{s}}}\right)^{2.9} \cdot \frac{1}{1000} \text{ kW} = 133.2 \text{ kW}$

Propulsor efficiencies assumptions
(pg. 255 Burcher & Rydill (1994))

$$\eta_0 := 0.866 \quad \eta_H := 0.866 \quad \eta_s := 0.98$$

Initial estimate propulsion for snorting
speed

$$P_{smort} := \frac{P_{eff}'}{\eta_0 \cdot \eta_H \cdot \eta_s} = 181.3 \text{ kW} \quad P_s' := P_{smort}$$

Margin for charging

$$m_{ch} := 5\%$$

Lead/acid battery parameters (max
current, voltage, min charging time,
and energy density per cell) (UCL
Submarine Databook, 2014)

$$I_{max} := 1900 \text{ A} \quad V_{ch} := 2.4 \text{ V}$$

$$T_{ch} := 5 \text{ hr} \quad k_{batt} := 15.92$$

Submerged speed

$$U_{sub} := 5 \text{ knot}$$

Thrust power for submerged speed

$$P_{eff}'' := K_p \cdot \left(\frac{V_{form}}{m^3} \right)^{0.64} \cdot \left(\frac{U_{sub}}{m/s} \right)^{2.9} \cdot \frac{1}{1000} \text{ kW} = 50.2 \text{ kW}$$

Initial estimate propulsion for
submerged speed

$$P_{sub} := \frac{P_{eff}''}{\eta_0 \cdot \eta_H \cdot \eta_s} = 68.3 \text{ kW} \quad P_s'' := P_{sub}$$

Efficiency electric conversion

$$\eta_{el} := 97\%$$

Assumed hotel payload from the UCL
Submarine Databook (2014) data

$$HL_{pay} := 173.3 \text{ kW}$$

Hotel load during submerged operation

$$HL_{sub} := 0.75 \cdot HL_{pay} + 0.075 \cdot PH_{vol} \cdot \frac{\text{kW}}{m^3} = 280 \text{ kW}$$

Indiscretion ratio

$$IR := 22\%$$

Submerged time

$$T_{sub} := \frac{T_{ch}}{IR} - T_{ch} = 17.7 \text{ hr}$$

Battery drain

$$D := \frac{P_{sub}}{\eta_{el}} + HL_{sub} = 350.4 \text{ kW}$$

Margin for energy

$$x := 20\%$$

Time for total discharge

$$T_{dis} := \frac{T_{sub}}{1-x} = 22.2 \text{ hr}$$

Energy available from each cell battery

$$E := k_{batt} \cdot \left(\frac{T_{dis}}{\text{hr}} \right)^{0.08} \cdot \text{kW} \cdot \text{hr} = 20.4 \text{ kW} \cdot \text{hr}$$

Number of lead/acid battery cells

$$N_c := \text{round} \left(\frac{D \cdot \left(\frac{T_{sub}}{1-x} \right)}{E \cdot (1-x)}, 0 \right) = 476$$

Hotel load during snort operation $HL_{snort} := 80\% HL_{sub} = 224 \text{ kW}$

Efficiency for DG converter $\eta_{conv} := 98\%$

Therefore, diesel power is:

$$P_{DIES} := \left((1 + m_{ch}) (I_{max} \cdot V_{ch} \cdot N_c) + \frac{P_{snort} + HL_{snort}}{\eta_{el}} \right) \cdot \left(\frac{1}{\eta_{conv}} \right) = (2.7 \cdot 10^3) \text{ kW}$$

Various operating conditions $snort := 0$ $sprint := 1$ $sub := 2$

$$P^{(sub)} := P_{sub} \quad HL^{(sub)} := HL_{sub}$$

Power at the Velocity Submerged node

$$P_{VS}^{(sub)} := P^{(sub)} \cdot \frac{T_{sub}}{T_{ch}} \cdot \frac{I_{max} \cdot V_{ch} \cdot T_{ch}}{E} = [270.8] \text{ kW}$$

Power at the Hotel Submerged node

$$P_{HS}^{(sub)} := HL^{(sub)} \cdot \frac{T_{sub}}{T_{ch}} \cdot \frac{I_{max} \cdot V_{ch} \cdot T_{ch}}{E} = [1.1 \cdot 10^3] \text{ kW}$$

Power at the Hotel Snort node

$$P_{SE}^{(snort)} := (1 + m_{ch}) \cdot \frac{D}{(1-x)^2} \cdot \frac{T_{sub}}{T_{ch}} \cdot \frac{I_{max} \cdot V_{ch} \cdot T_{ch}}{E} = [2.3 \cdot 10^3] \text{ kW}$$

Power at the Hotel Submerged node

$$P_{SE_{LS}}^{(sub)} := \left(\frac{P_{VS}^{(sub)}}{\eta_{el}} + P_{HS}^{(sub)} \right) \cdot \frac{1}{(1-x)^2} = [2.2 \cdot 10^3] \text{ kW}$$

Appendix 3

RINA IJME 2021 Journal Paper

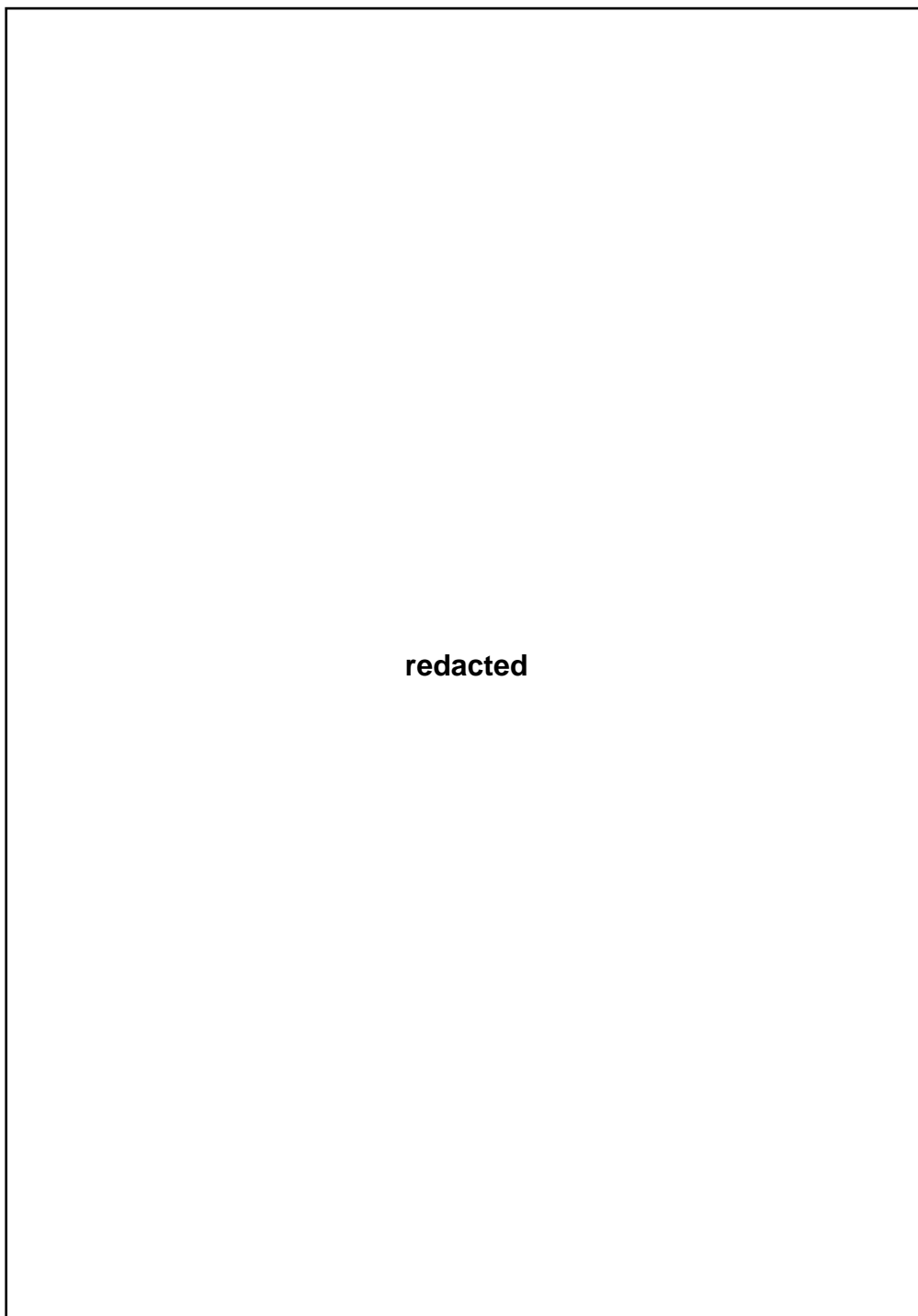
TRANS RINA, Vol 163, PART A2, INTL J MARITIME ENG, APR-JUN 2021

DISTRIBUTED SHIP SERVICE SYSTEMS ARCHITECTURE IN THE EARLY STAGES OF DESIGNING PHYSICALLY LARGE AND COMPLEX VESSELS: THE SUBMARINE CASE

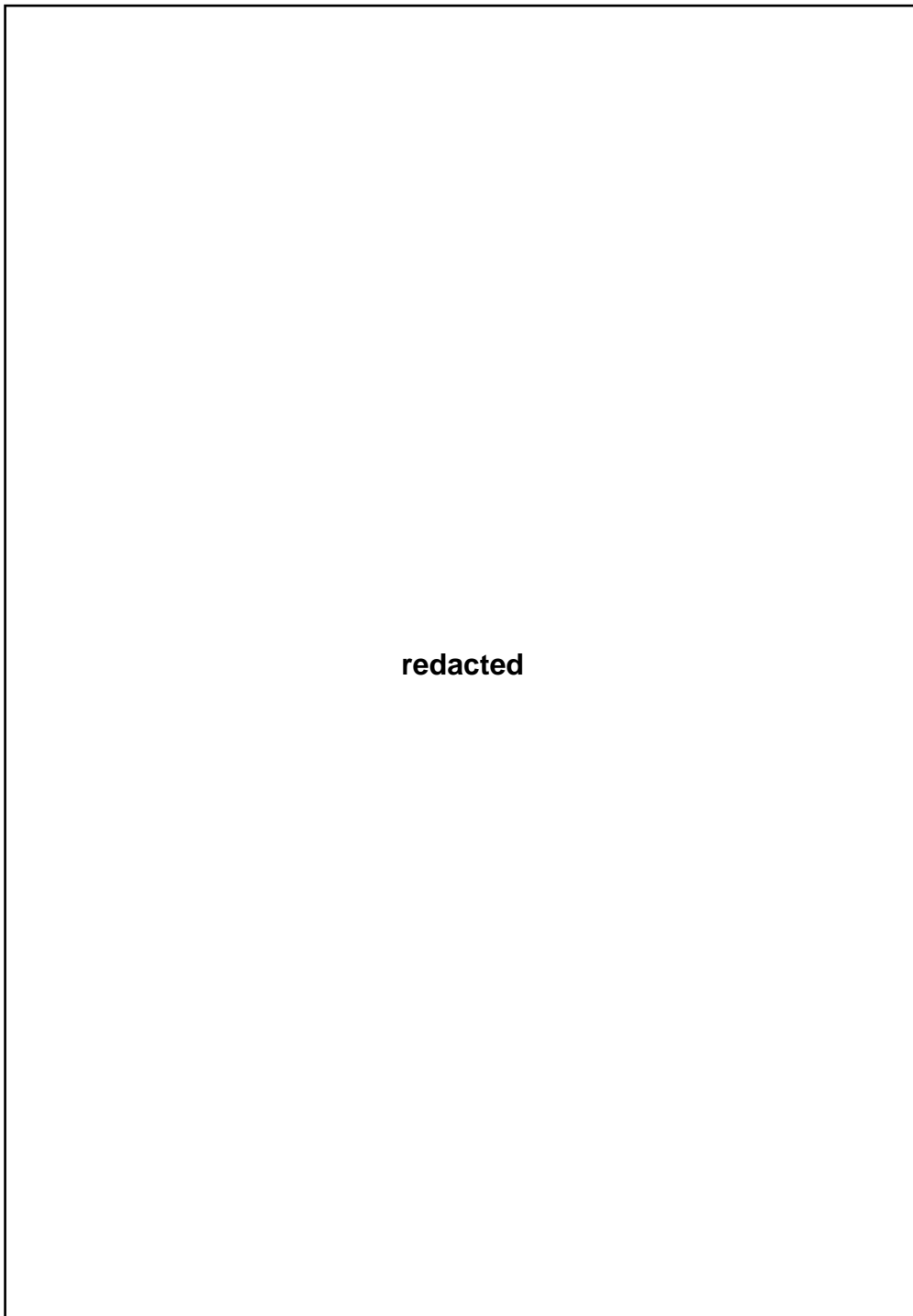
M H Mukti, R J Pawling, and D J Andrews, University College London, UK

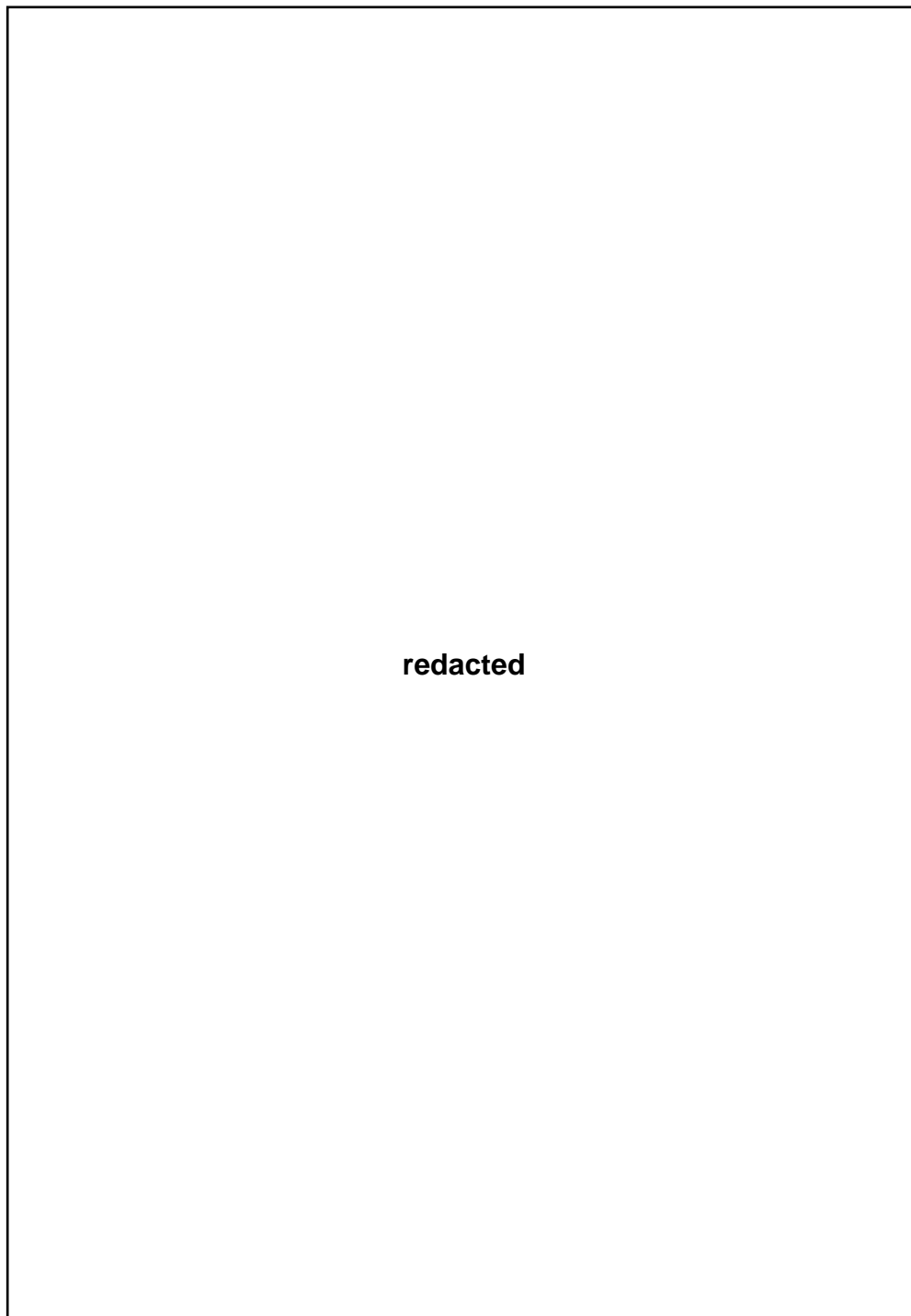
redacted

TRANS RINA, Vol 163, PART A2, INTL J MARITIME ENG, APR-JUN 2021

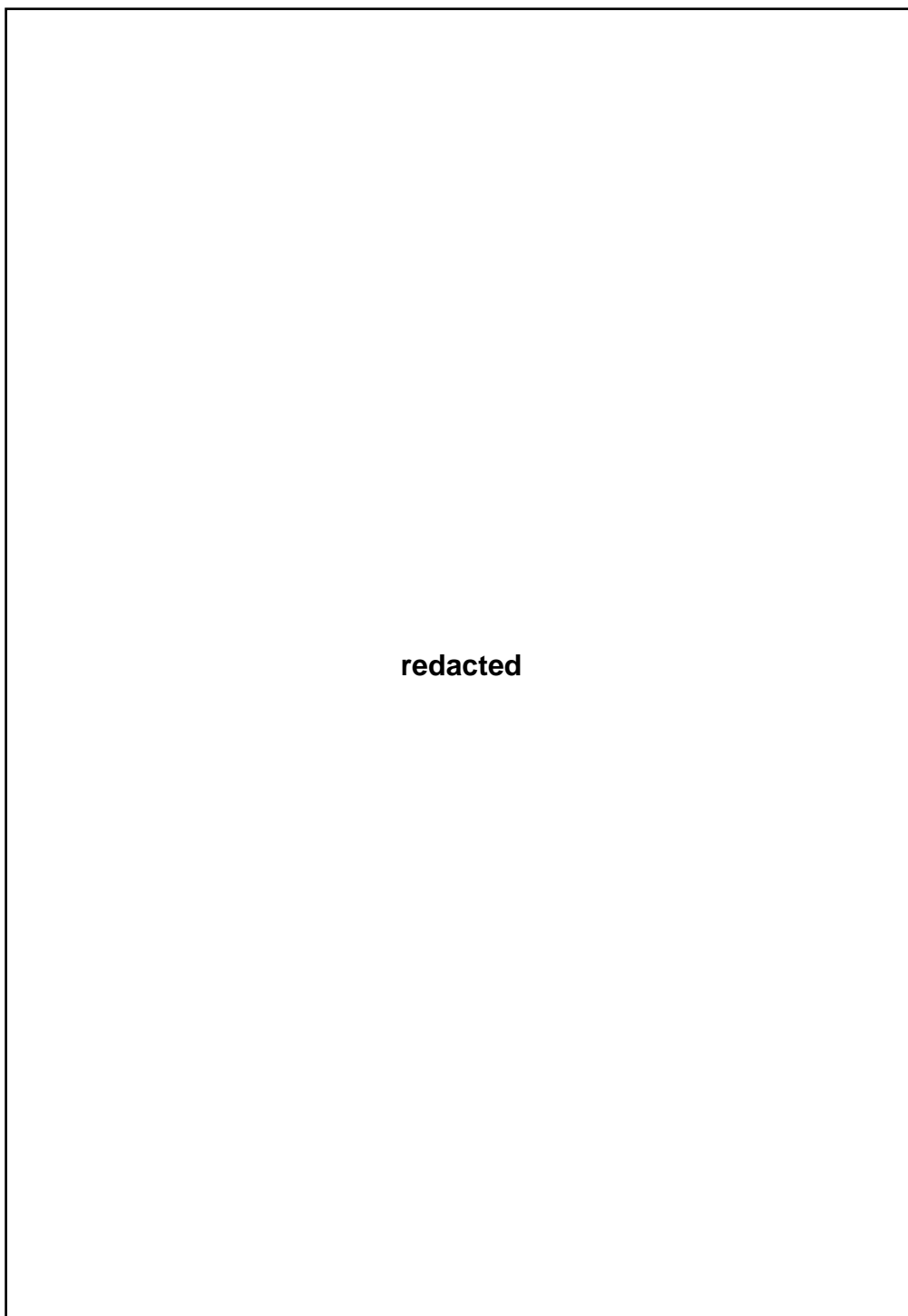


TRANS RINA, Vol 163, PART A2, INTL J MARITIME ENG, APR-JUN 2021

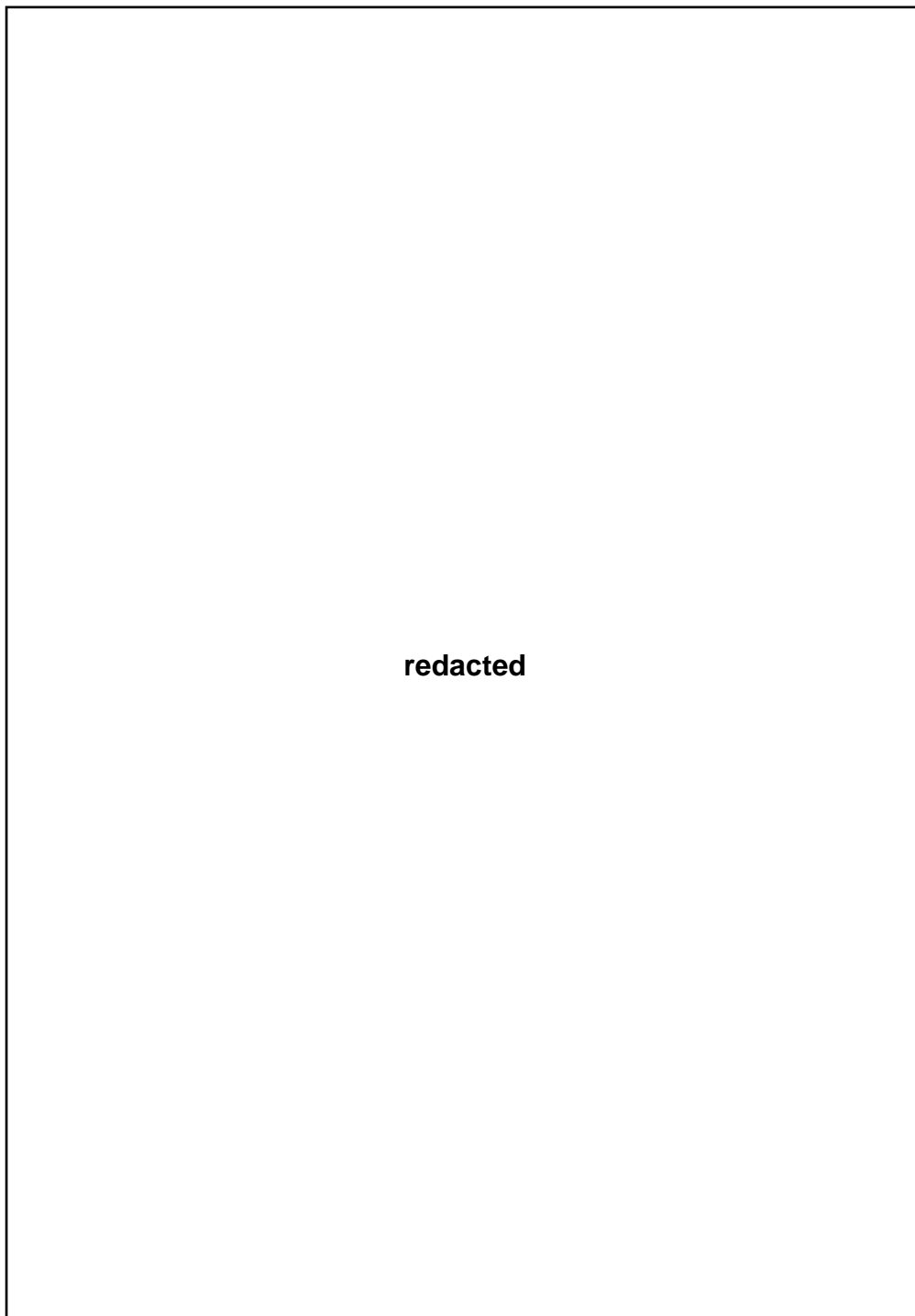




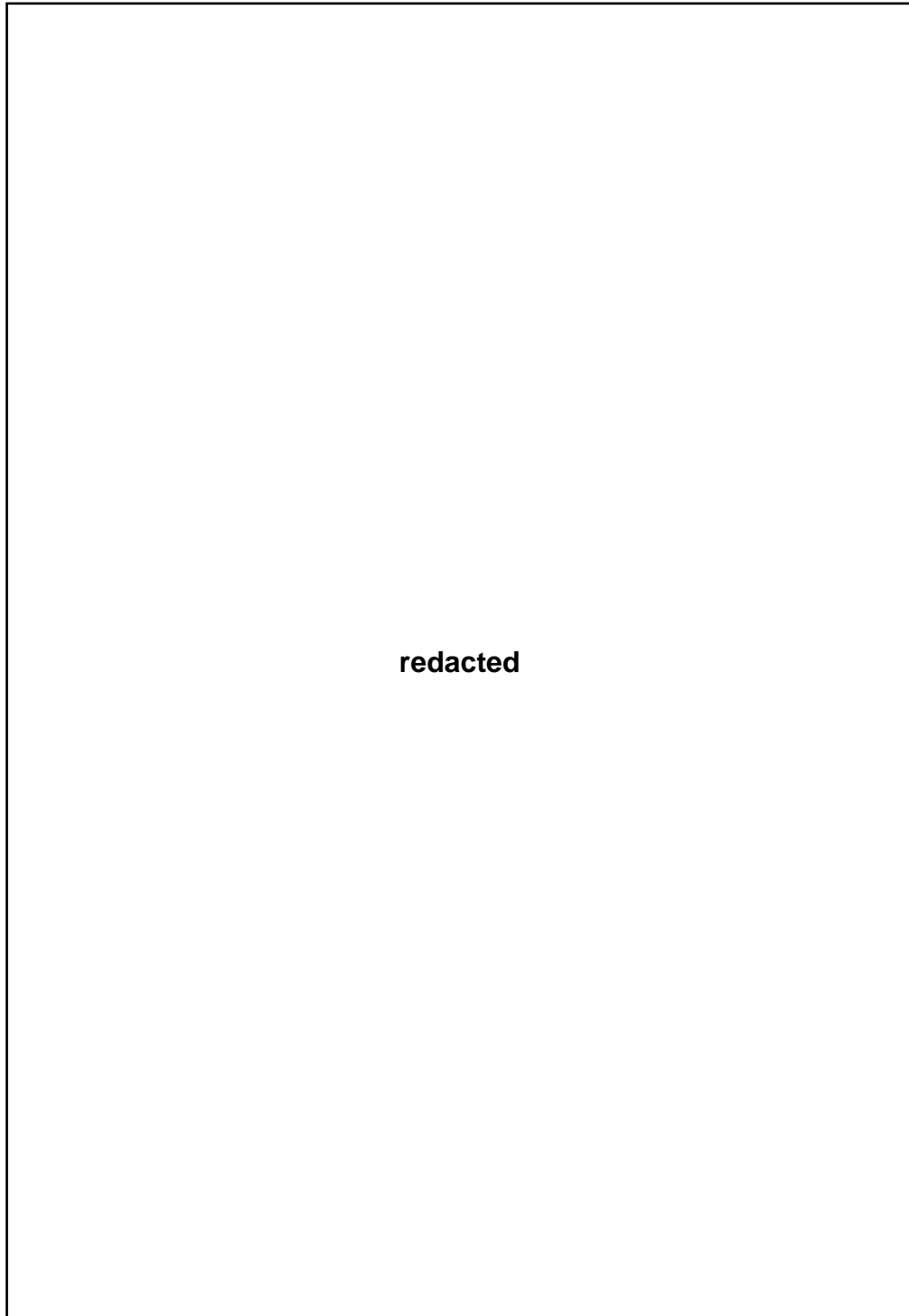
TRANS RINA, Vol 163, PART A2, INTL J MARITIME ENG, APR-JUN 2021



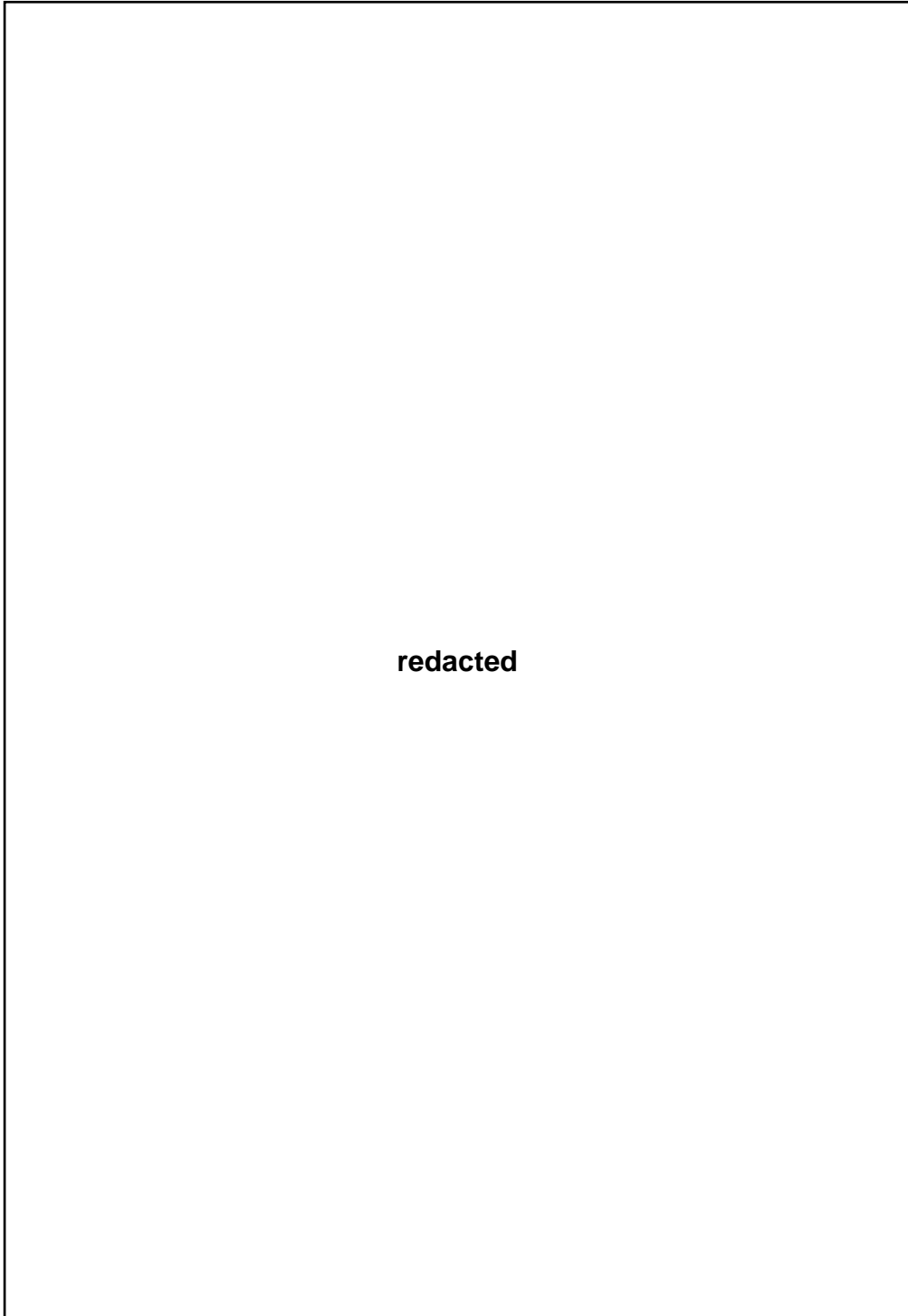
TRANS RINA, Vol 163, PART A2, INTL J MARITIME ENG, APR-JUN 2021



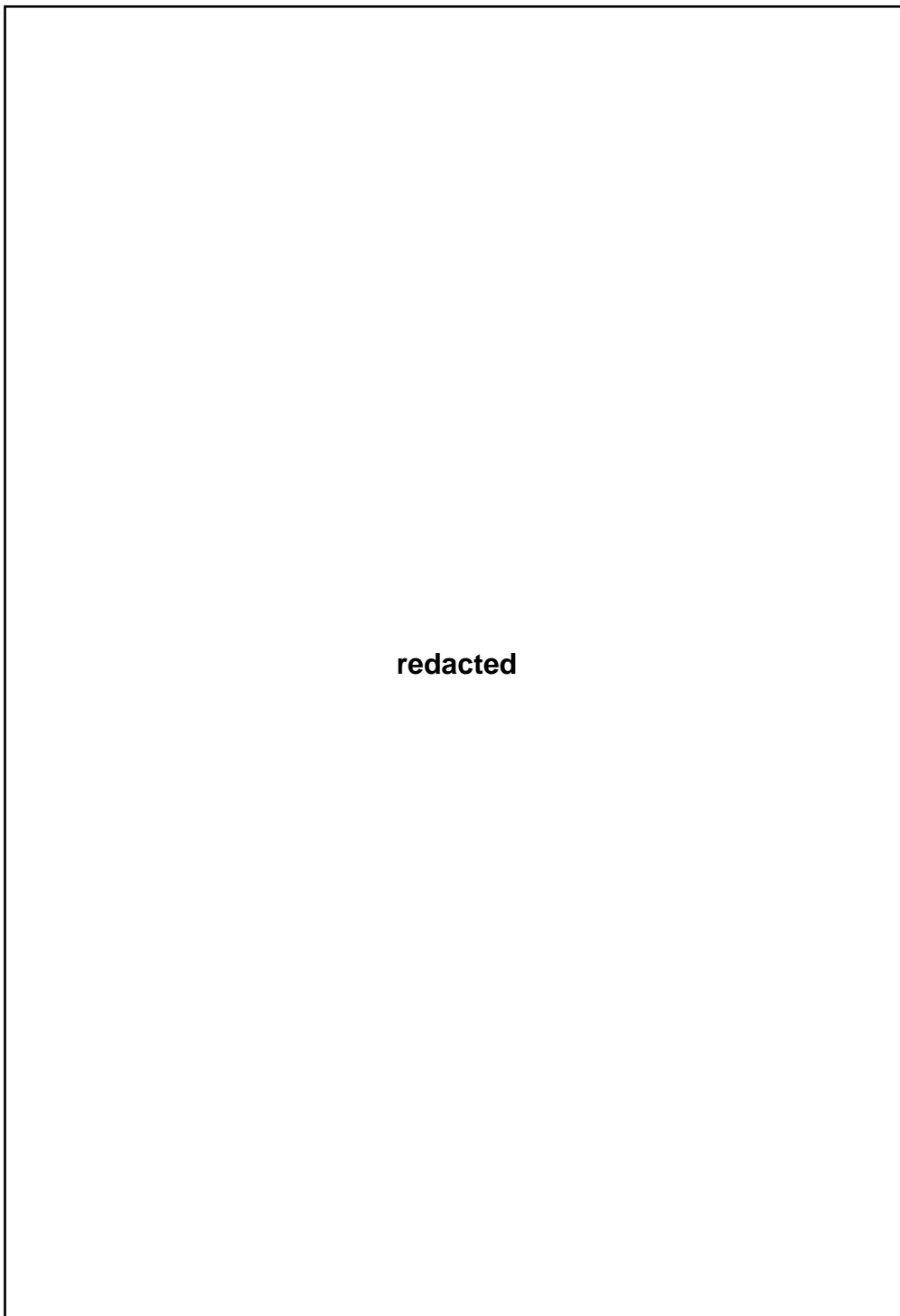
TRANS RINA, Vol 163, PART A2, INTL J MARITIME ENG, APR-JUN 2021



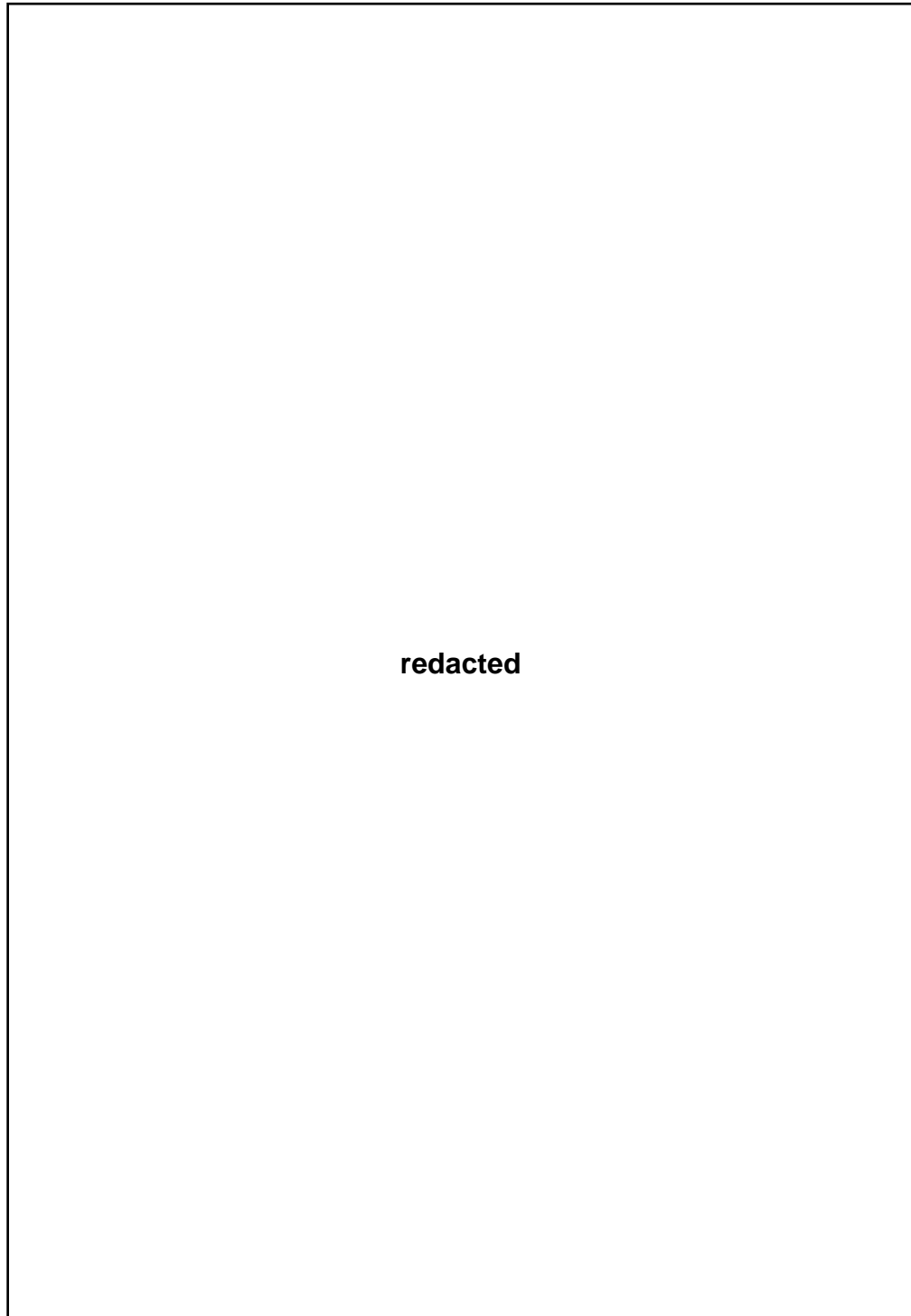
TRANS RINA, Vol 163, PART A2, INTL J MARITIME ENG, APR-JUN 2021



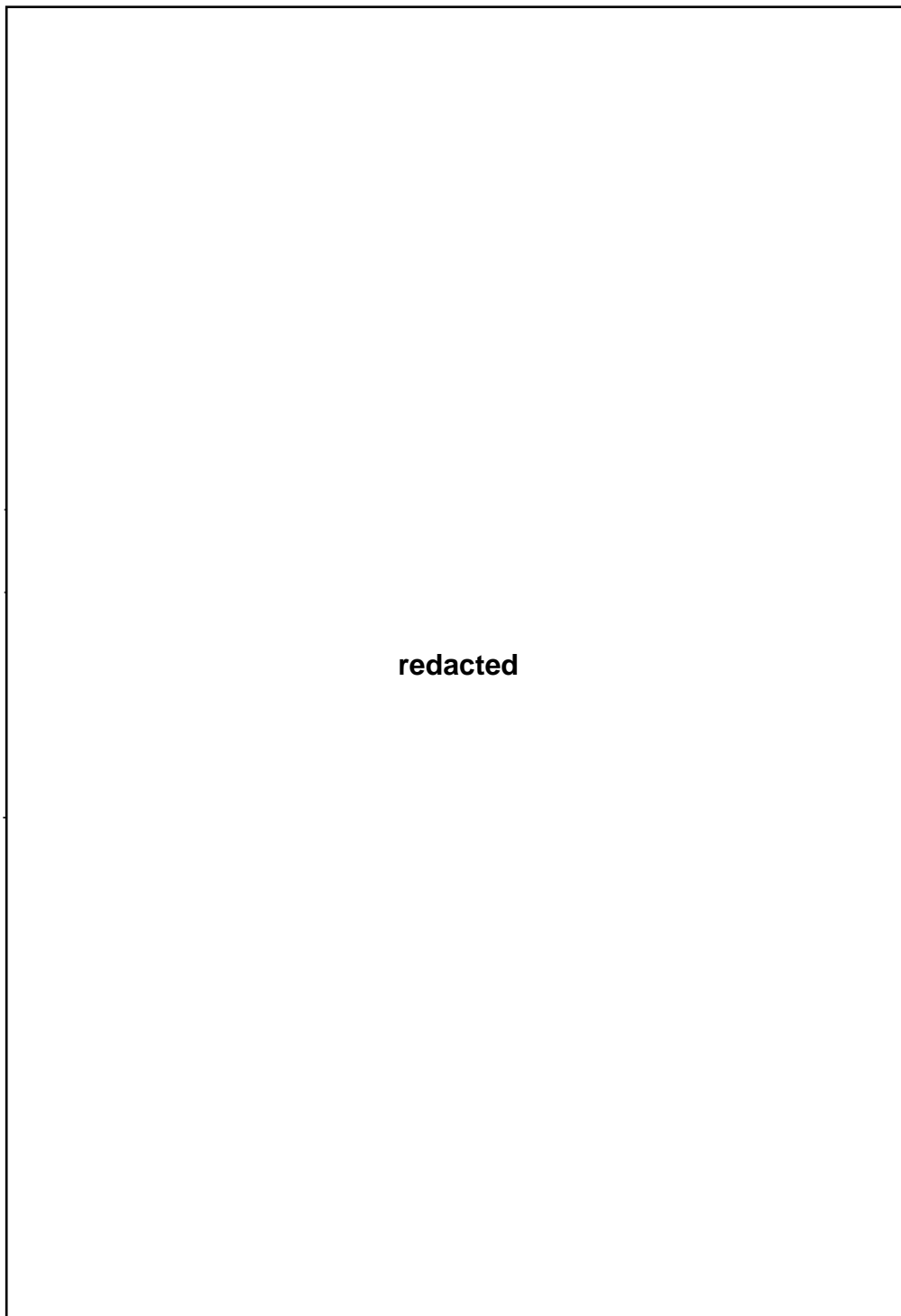
TRANS RINA, Vol 163, PART A2, INTL J MARITIME ENG, APR-JUN 2021



TRANS RINA, Vol 163, PART A2, INTL J MARITIME ENG, APR-JUN 2021

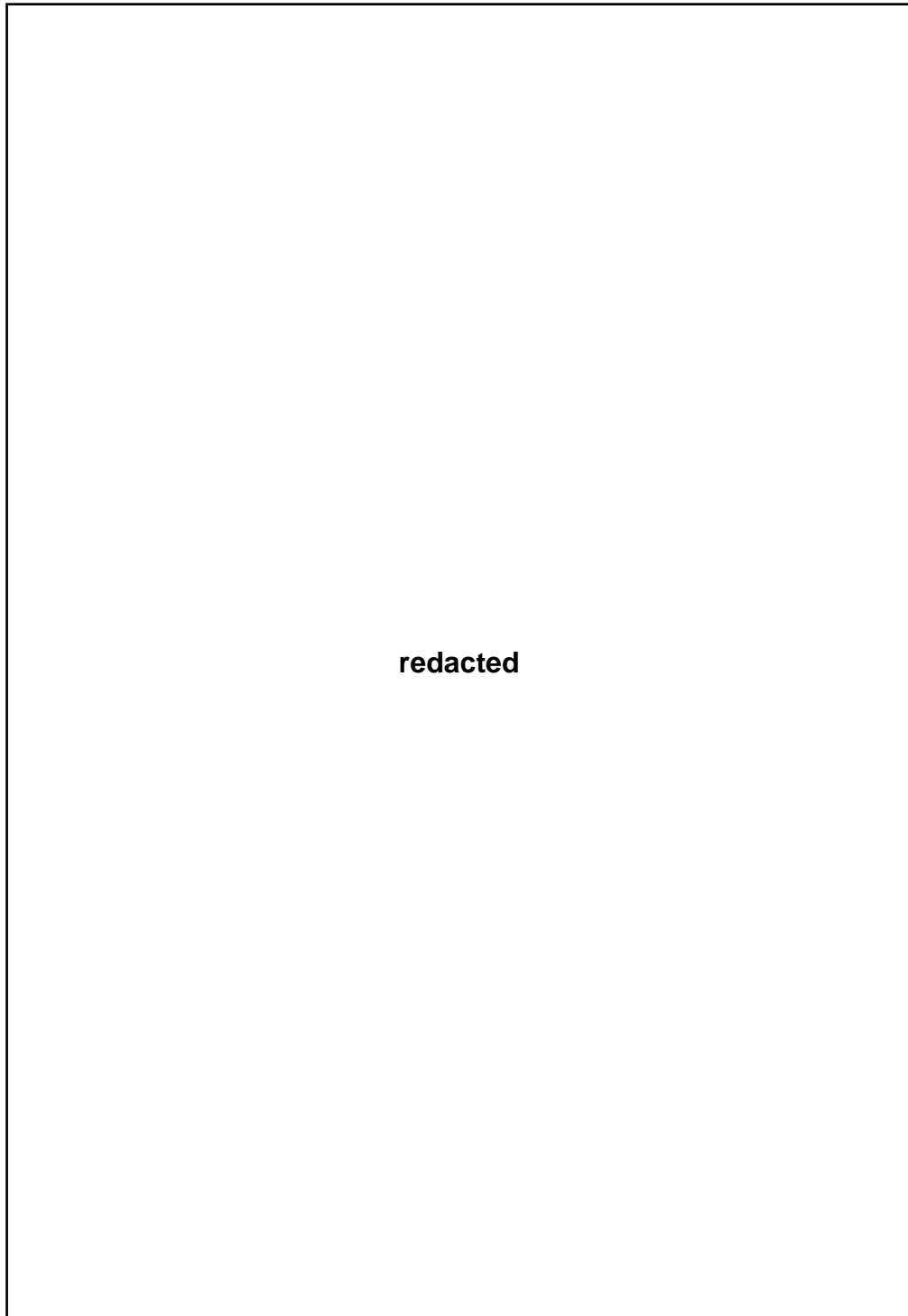


TRANS RINA, Vol 163, PART A2, INTL J MARITIME ENG, APR-JUN 2021



redacted

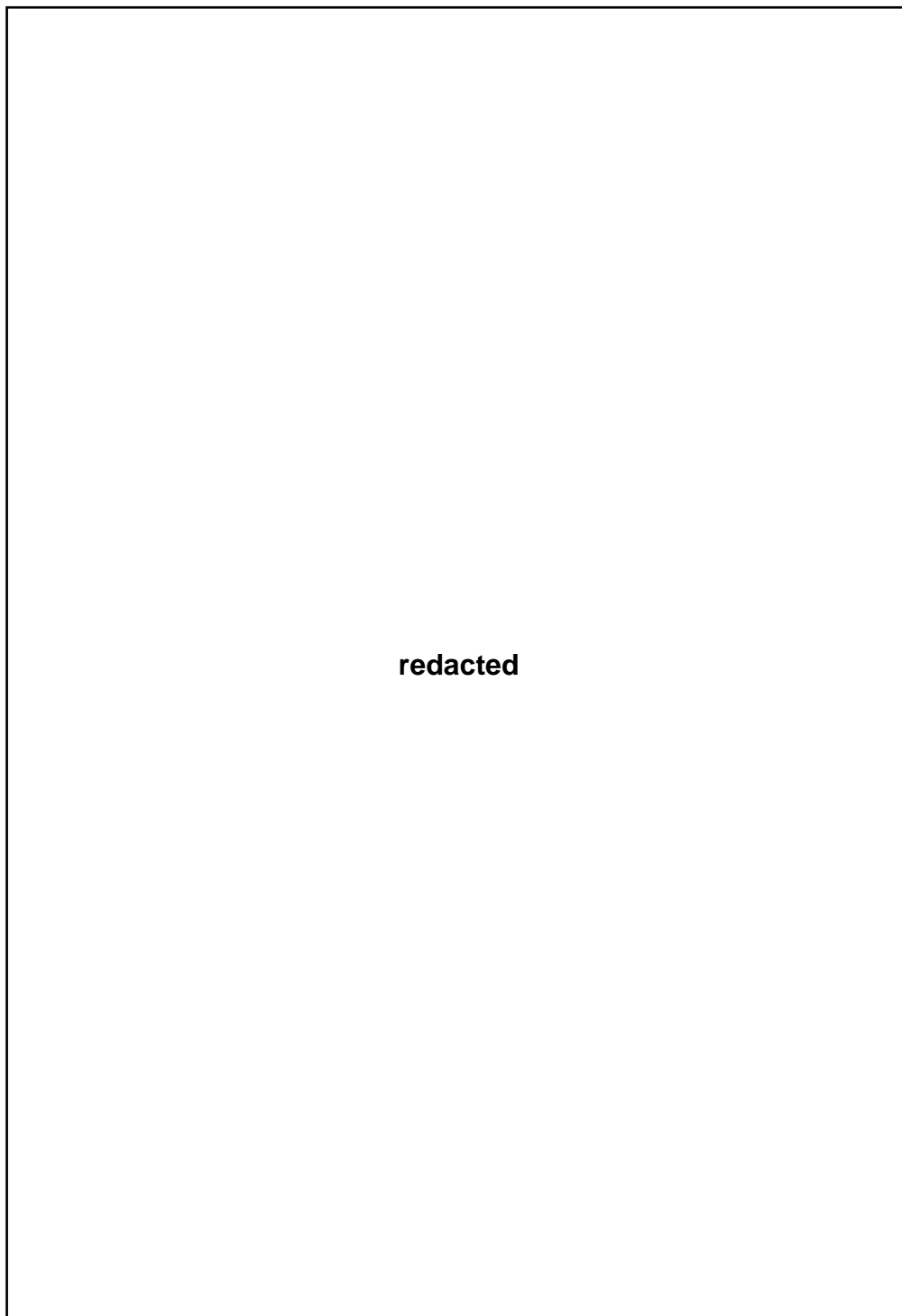
TRANS RINA, Vol 163, PART A2, INTL J MARITIME ENG, APR-JUN 2021



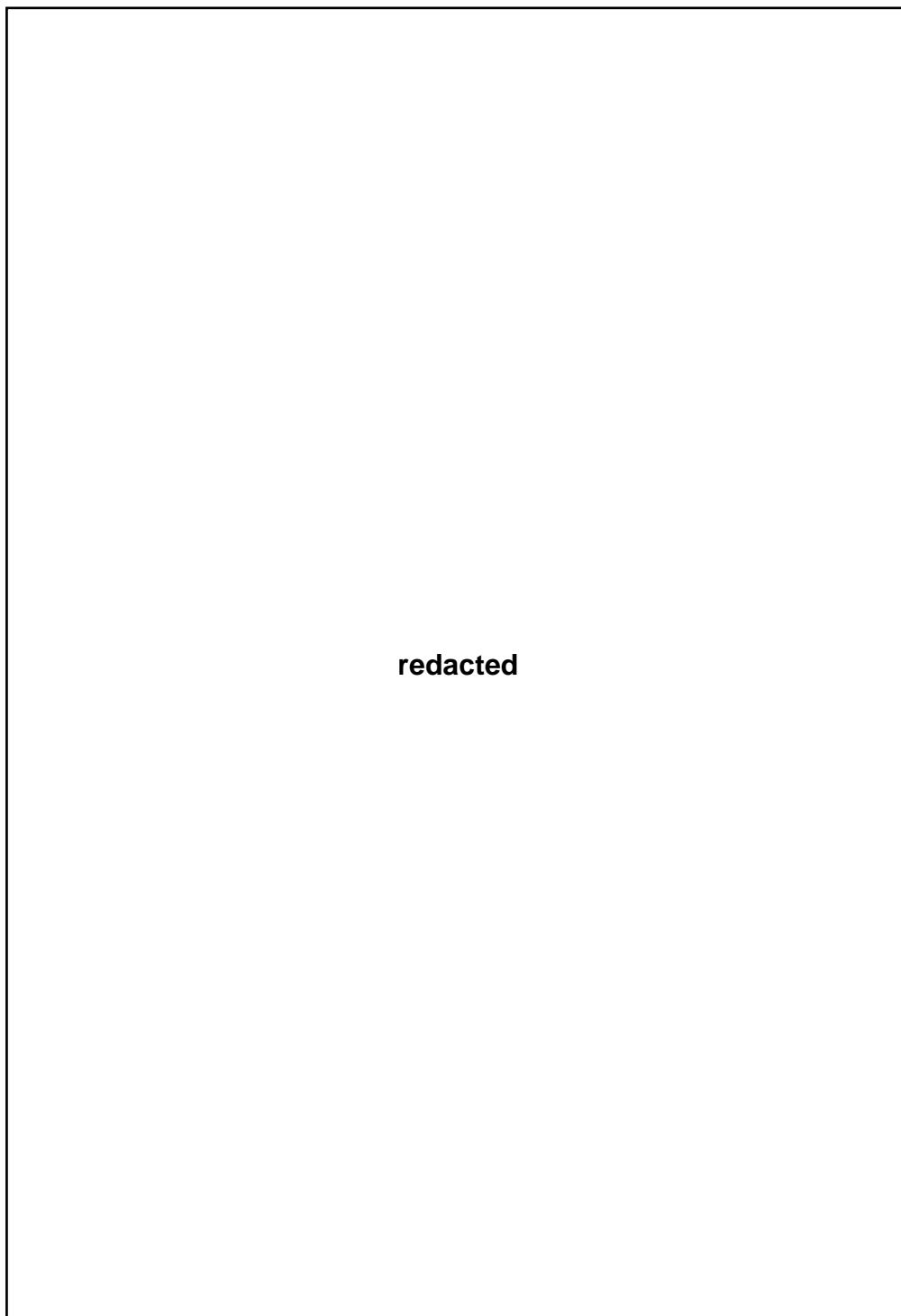
TRANS RINA, Vol 163, PART A2, INTL J MARITIME ENG, APR-JUN 2021

redacted

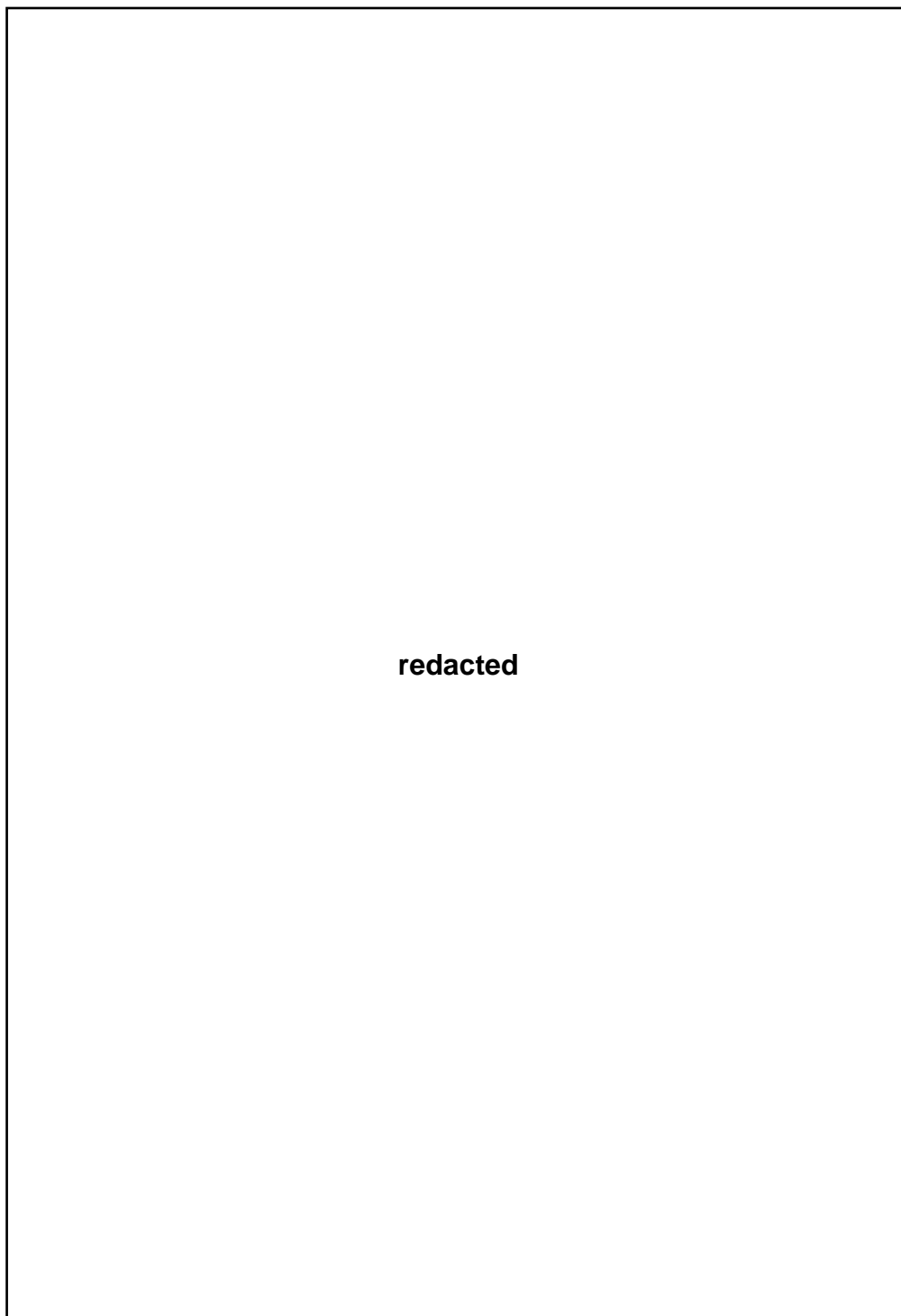
TRANS RINA, Vol 163, PART A2, INTL J MARITIME ENG, APR-JUN 2021



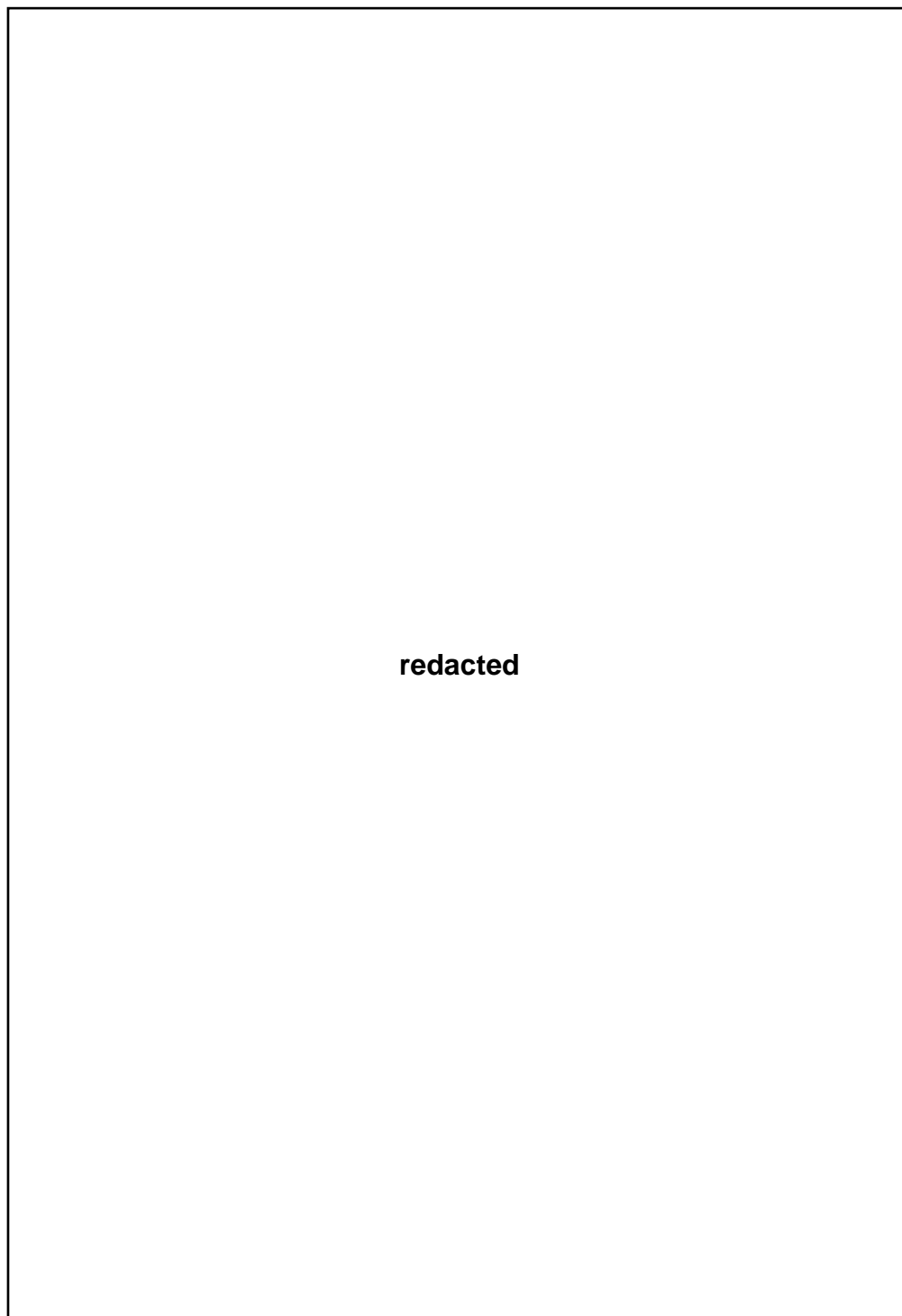
TRANS RINA, Vol 163, PART A2, INTL J MARITIME ENG, APR-JUN 2021



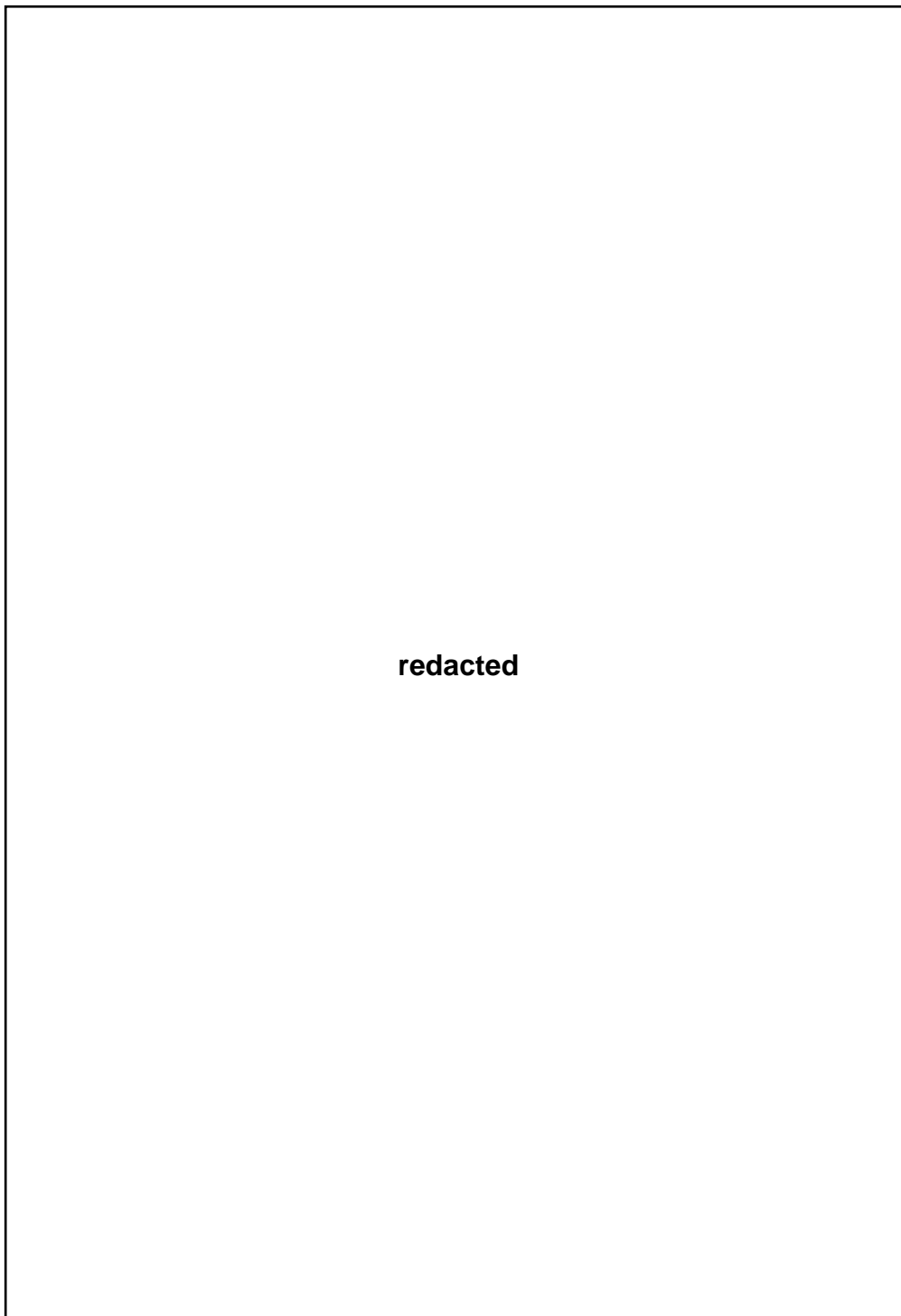
TRANS RINA, Vol 163, PART A2, INTL J MARITIME ENG, APR-JUN 2021

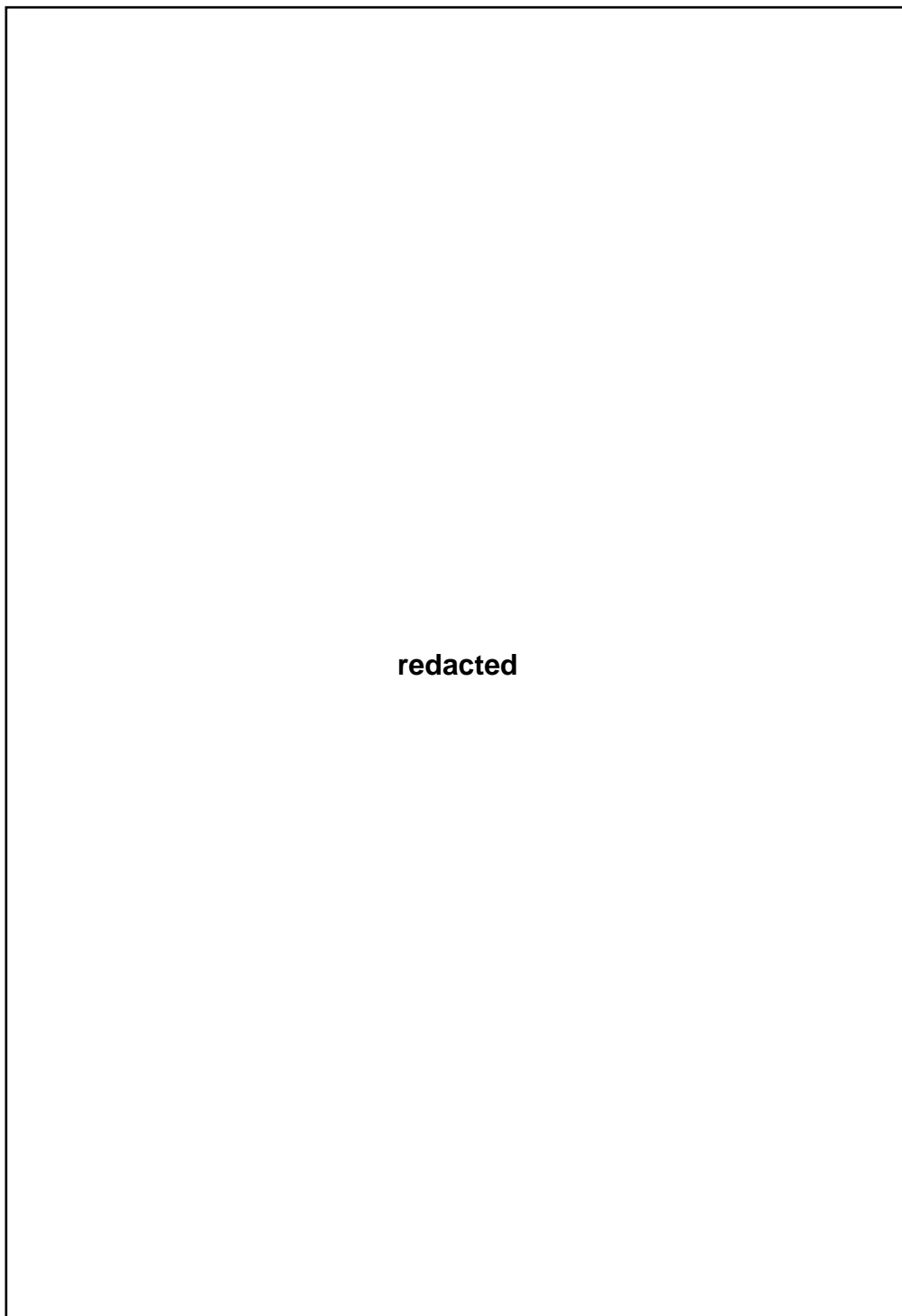


TRANS RINA, Vol 163, PART A2, INTL J MARITIME ENG, APR-JUN 2021

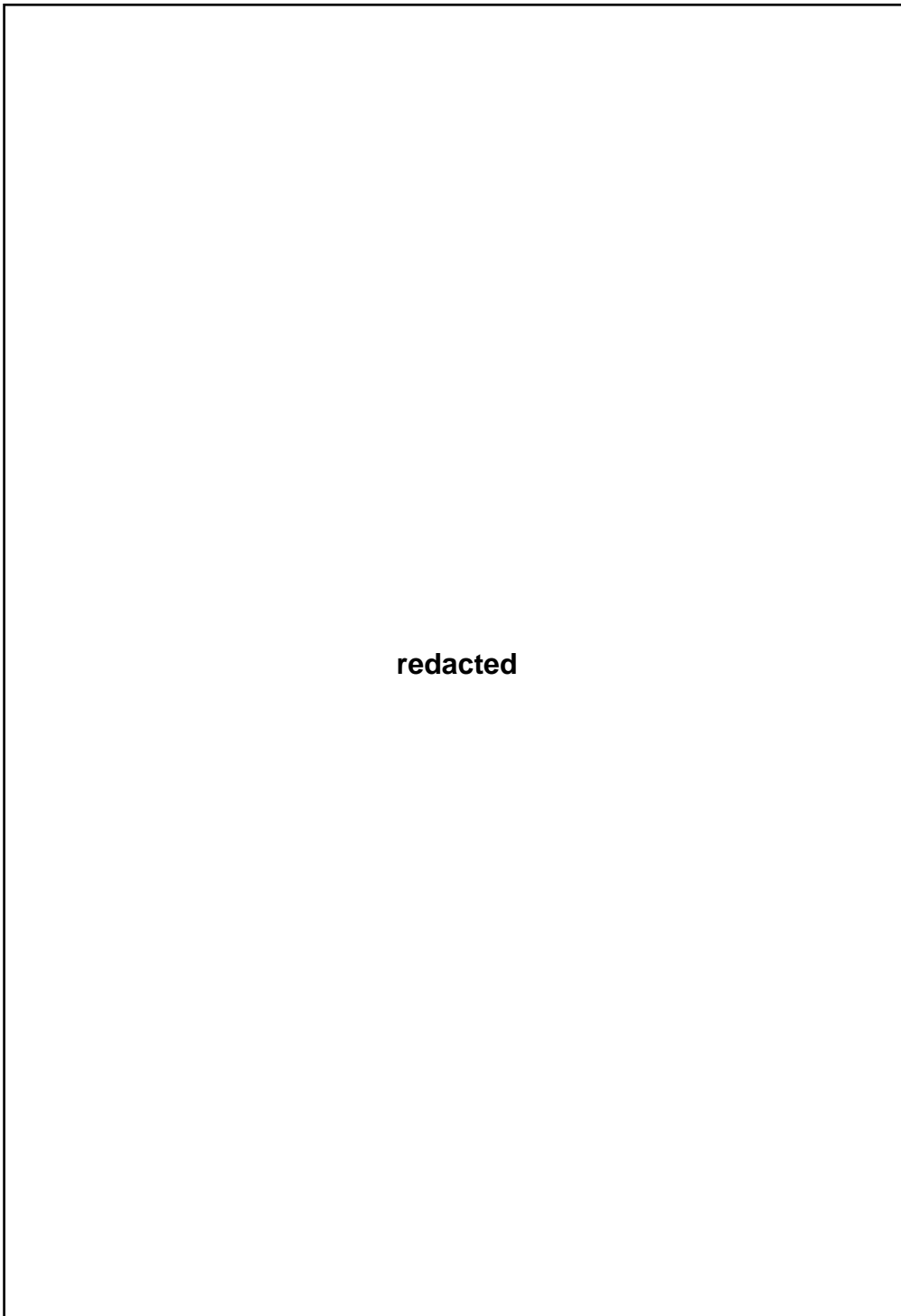


redacted





TRANS RINA, Vol 163, PART A2, INTL J MARITIME ENG, APR-JUN 2021



Appendix 4

Physical Model of DS3 Synthesis

The approach to model a physical entity in Paramarine is highly flexible. This means there are many ways to model various parts of a submarine in Paramarine. This appendix discusses several manners to model different types of physical entities: space; equipment; and connection. To consider the physical architecture of DS3, it is essential to distinguish between space and the equipment within that space.

A 4.1 Space Model

The “**solid_body**” object in Paramarine is typically used to model major parts of the vessel, such as pressure hull, external volumes, and appendages. If the solid body is subdivided using one or more “**plane**” objects, it can be used to model a more spatial definition within the hull, such as compartments, rooms, tanks, and free flood spaces. This process is illustrated in Figure A.23. Subsequently, the “**building_block**” objects (or Design Building Block (DBB) objects) can ‘point’ to these many “**solid_body**” objects. This approach requires more steps, creating many subdivisions planes, and is difficult to manipulate the order location of compartments or tanks around the hull, although the accuracy of the model is good.

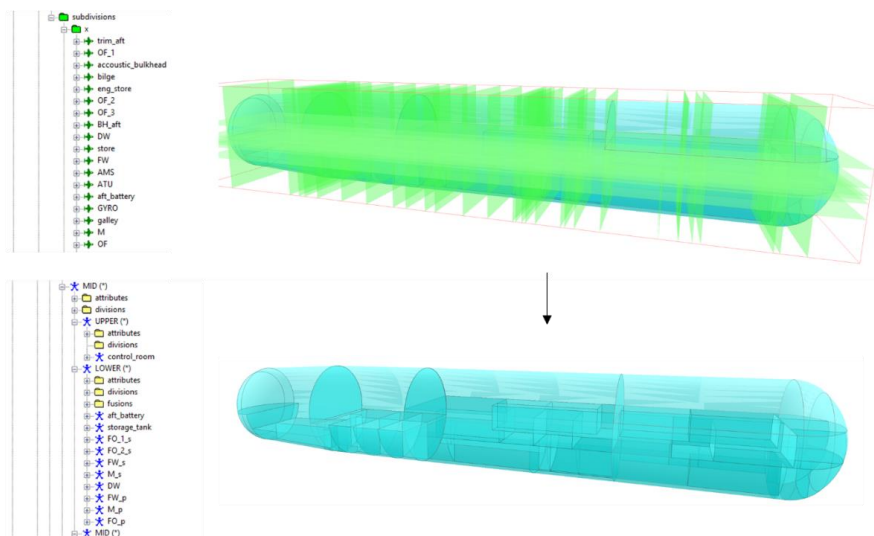


Figure A.23: Subdivision - solid SURFCON model of a pressure hull showing internal subdivision produced using subdivision planes in Paramarine

If the “**solid_body**” object is not subdivided using “**plane**” objects, some “**building_block**” objects can be inserted under a “**concept_placeholder**” to model the DBB objects for compartments. A “**solid_body**” object of the pressure hull was required to perform an “**intersect**” operation as shown in Figure A.24. This modelling approach allows easy manipulation of compartments locations, but it requires careful modelling to ensure there is no gap or design infringement between DBB objects at the volume granularity. A particular drawback with this modelling approach is that an additional effort was required to model the “sheets” of spaces when defining the structural model using Paramarine. Conversely, Paramarine can automatically detect the sheets of spaces when using the subdivision modelling approach.

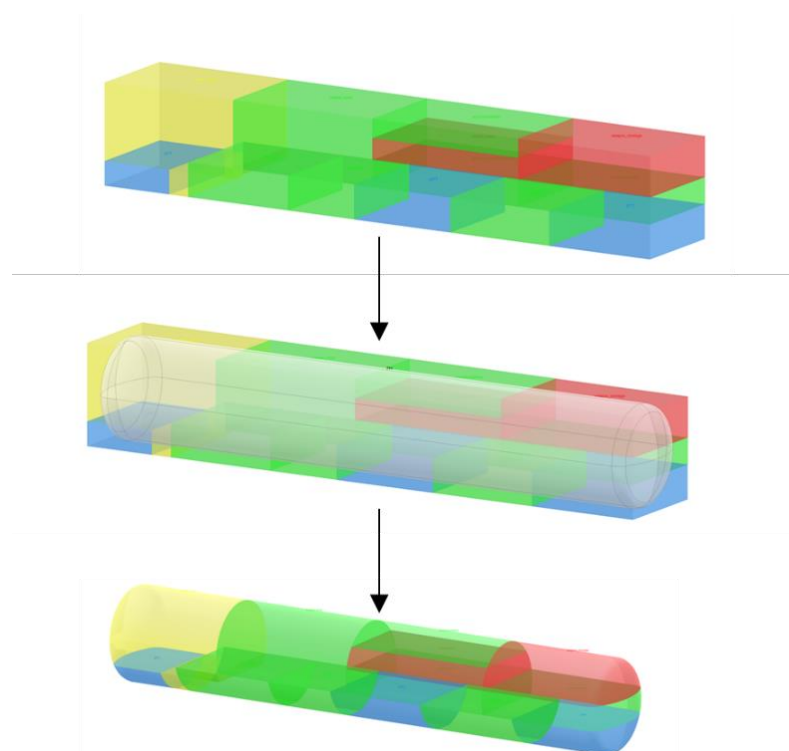


Figure A.24: DBB objects - solid SURFCON model of a pressure hull showing internal subdivision produced using several DBB objects in Paramarine

A 4.2 Equipment Model

Modelling a DS3 component can be achieved using a “**building_block**” object or using “**equipment**” object and then using a ‘drag and drop’ approach to move it under a “**building_block**” object hierarchy as an “**equipment_instance**” object. The second approach allows a reusable equipment database for

multiple entities in the design. This also permits the use of **“equipment_array”** object that automates the creation of multiple equipment objects with several inputs of spacing in X, Y, and Z directions, such as battery cells as illustrated in Figure A.25. This means if, for example, the **“equipment”** object for the battery cell is modified, this would have a cascading effect on the whole battery arrangement in Figure A.25.

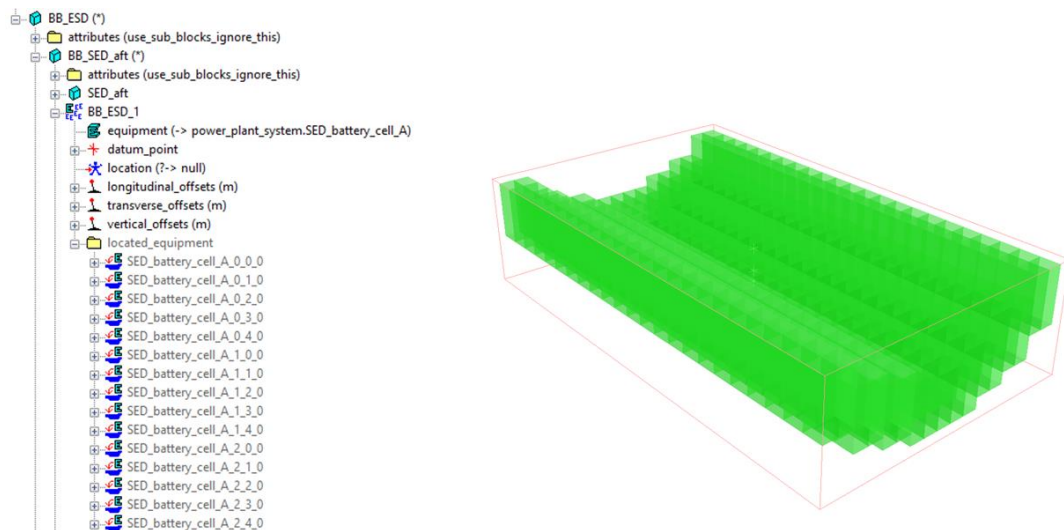


Figure A.25: Equipment model of batteries showing detailed battery arrangement using **“equipment_array”** in Paramarine

As part of distributed ship service systems, an **“equipment”** object can also be inserted under a **“system”** object as depicted in Figure A.26. The use of the **“system”** object allows a mechanism to cluster different types of DS3, which is discussed in the next subsection.

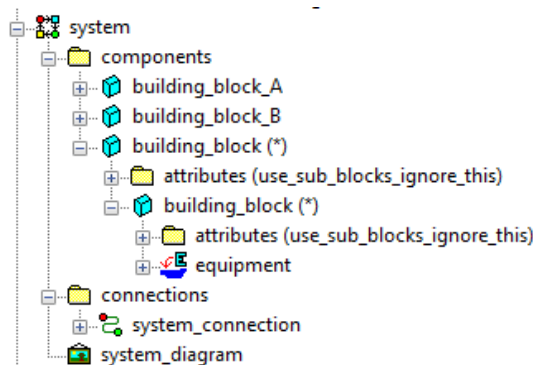


Figure A.26: Equipment model part of a system object

A 4.3 Connection Model

As shown in Figure A.26, a “**system**” object contains a “**system_diagram**” two “**placeholder**” objects, namely components and connections. Some DS3 components could be inserted under the “components” placeholder whereas DS3 connections under the “connections” placeholder. These connections can then be visualised as a simple line diagram using the “**system_diagram**” object. But before a connection can be modelled there was a significant Gulf of Execution (Figure 2.6 on page 51) that needed to be addressed. One of them was to define the connection or line specification using a “**service_line_specification**” object, some detailed connection properties needed to be known or assumed. These were the definition of the cabling shape (e.g., circular or rectangular) and allowable bending radius as shown in Figure A.27.

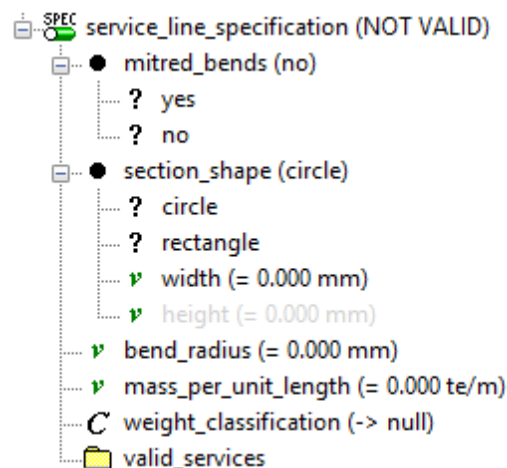


Figure A.27: Service line specification input in Paramarine

When it comes to DS3 specification, the Paramarine™ V8.x and the 2019 update 2 only provide four different specifications, namely electrical AC and DC, chilled water, and ventilation. Hence, these are the only available options to model cabling, piping, and trunking as shown in Figure A.28.

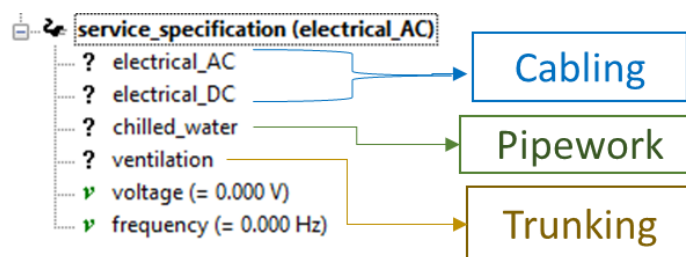


Figure A.28: Service specification input in Paramarine

Paramarine has the capability to perform automatic routing to some extent. This is demonstrated using an example as follows. Let us say there are two DBB objects at the component granularity. These are components A and B, which are situated on different decks in green with unique X, Y, and Z coordinates (see Figure A.29 (top)). Paramarine then can seek the shortest path between these two DBBs and thus, as shown in Figure A.29 (bottom), a DBB object at the connection granularity can be generated.

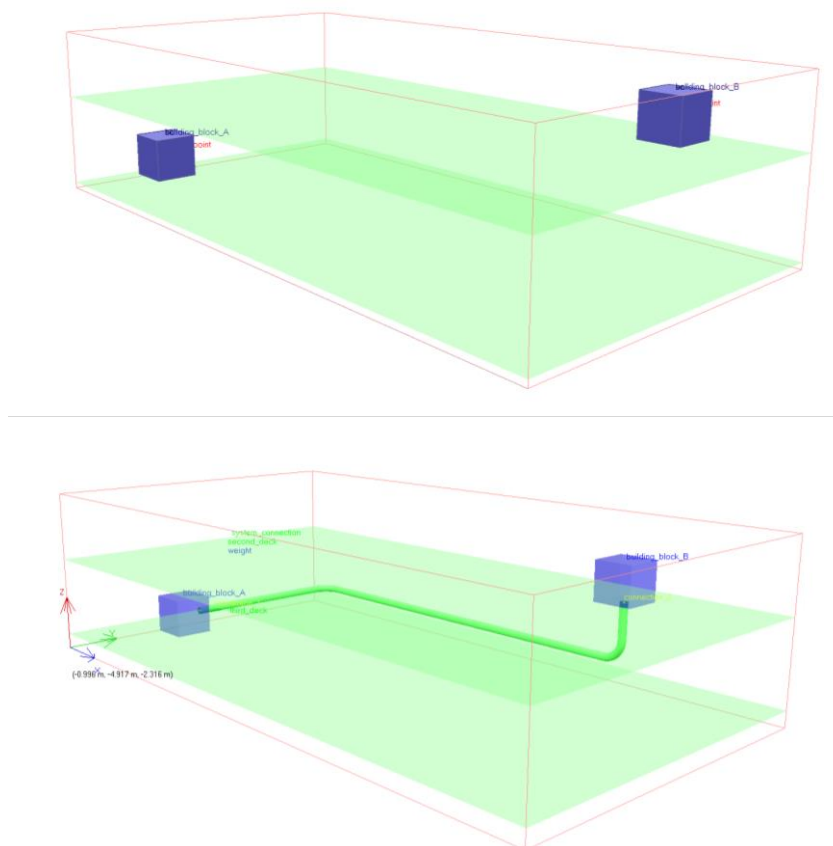


Figure A.29: DS3 models using Paramarine showing two components A and B in purple (top) are connected by a connection in green (bottom), at this point, the number of clicks required was 40 clicks

However, when another DBB C is added into the model, the automated routing does not detect the presence of that DBB object and thus a clash occurs as shown in Figure A.30.

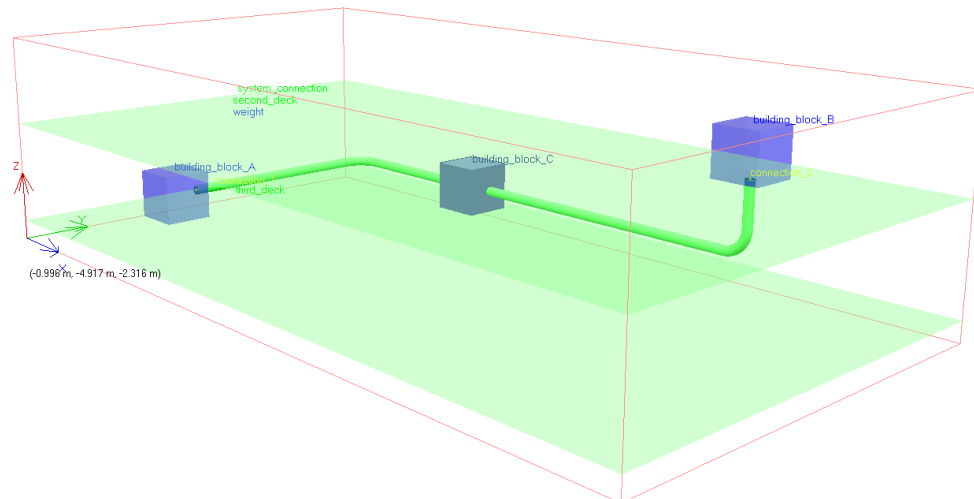


Figure A.30: Automatic routing does not detect clash with component C

Albeit automatic routing exists (Gottschalk et al., 1996; Asmara, 2013; Gongora, 2019), it is for detailed design. Thus, several methods were investigated to avoid such clashes at early-stage design. The first method is using more inputs to define the routing using the “**service_line**” object, which allows segment by segment definition as shown in Figure A.31.

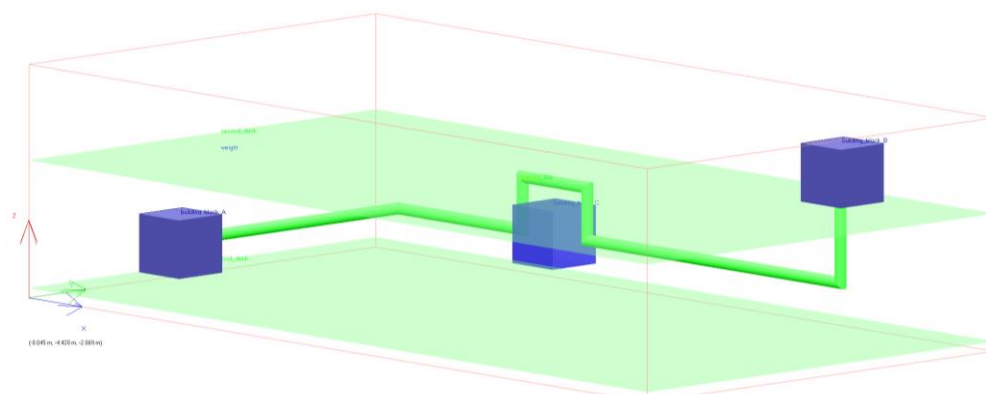


Figure A.31: Segment by segment routing in Paramarine

Another method makes use of “**service_highway**” and “**highway_highway_branch**” objects in Paramarine to set up a highway,

which can be allocated to avoid component C. Thus, the connection is 'pointed' to that highway resulting in a forced route as shown in Figure A.32.

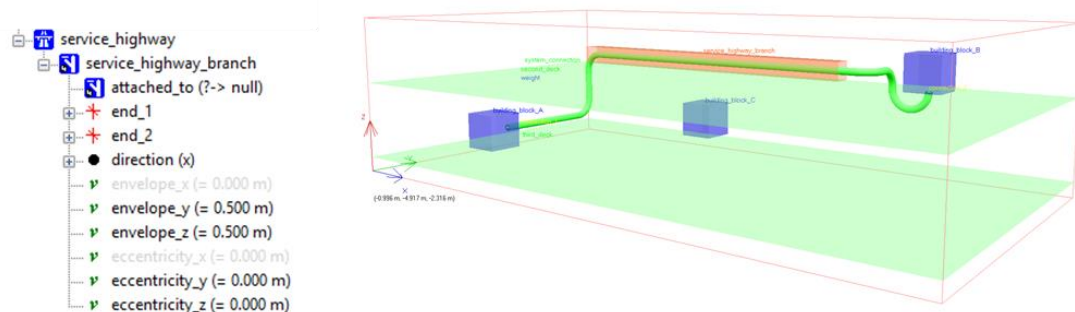


Figure A.32: The use of highway routing (orange) in Paramarine

Various sets of highway configurations were investigated for the submarine DS3 problem as shown in Figure A.33. Figure A.33 (top) provides a more detailed model forcing the automatic routing to follow a set of highways attached to the bulkheads. Figure A.33 (bottom) is less constrained but is sufficient to minimise the number of routing clashes in ESSD.

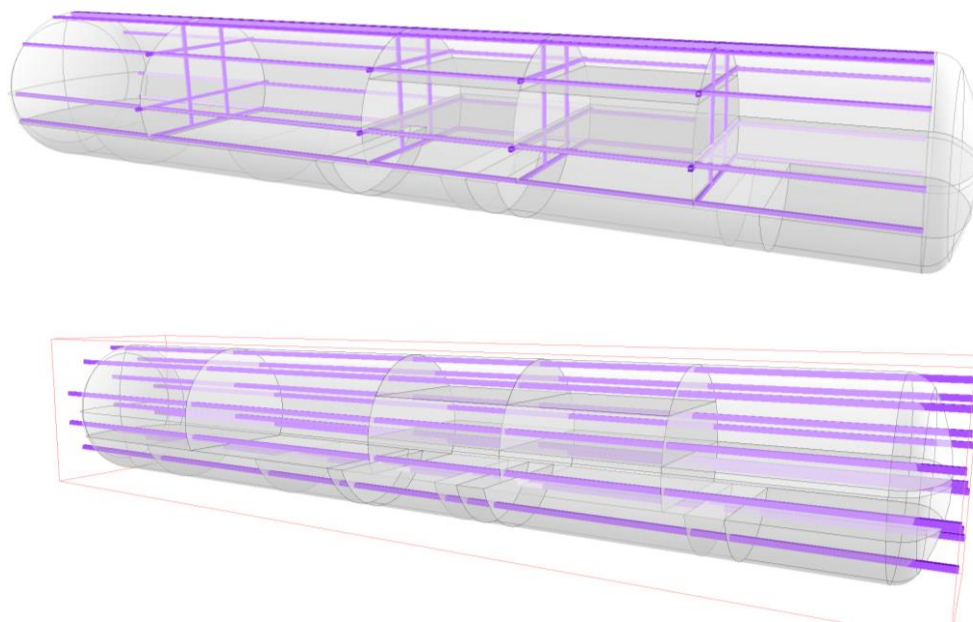


Figure A.33: Multiple DS3 highway networks (purple) in Paramarine, showing a longitudinal highway configuration (bottom) and a complex highway configuration (top)

It is also possible to model a structure duct in Paramarine, which is a connection that follows the curve of the pressure hull as shown in Figure A.34.

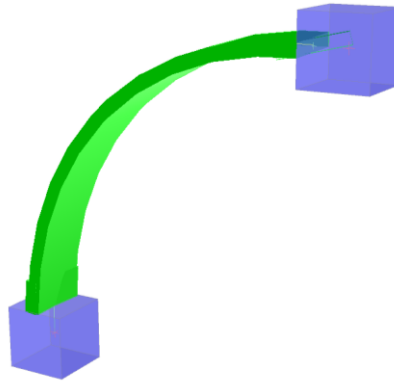


Figure A.34: Structure duct modelling in Paramarine

Having investigated the capability of Paramarine to model DS3 connection using an arbitrary example, this capability was implemented in Case Study 3.3.1.

A 4.4 Further Design Development

Given some modelling approaches have been outlined in previous sections, Case Study 3.3.1 was further developed as shown in Figure A.35. The model had reached 277 DS3 DBB objects with numerical geometric data.

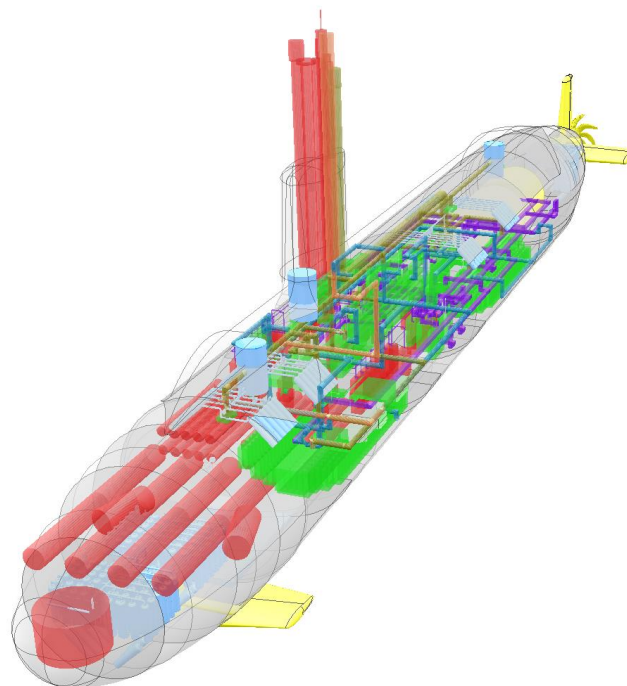


Figure A.35: Refined physical model of Case Study 3.3.1 in Paramarine

Appendix 5

Programs in the Network Block Approach

This appendix provides a more detailed description of the programs in the proposed Network Block Approach (NBA)

A 5.1 Development of the Input Data Centre Tool

This section is divided into two topics, the Physical Loop method and the Logical Loop method.

A 5.1.1 Physical Loop Method

This subsection illustrates the modelling effort required in Paramarine. Normally, to create an object in Paramarine, the designer requires 5 steps as illustrated in Figure A.36 (left), click object, click insert, click the type of the placeholders, click the rename column, and then click OK. Other possible approaches exist e.g., copy, and paste from a pre-defined template. Still, it required at least 3 steps (for renaming each of the relevant objects). This process was considered distractive to the important benefit of the UCL DBB approach, how many clicks would be required if one design consists of hundreds of objects where design exploration aims to explore multiple designs.

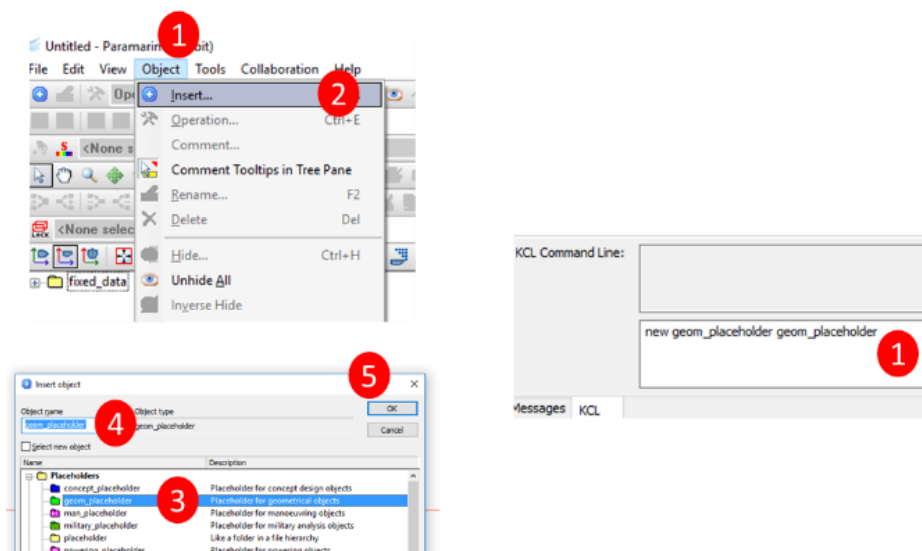
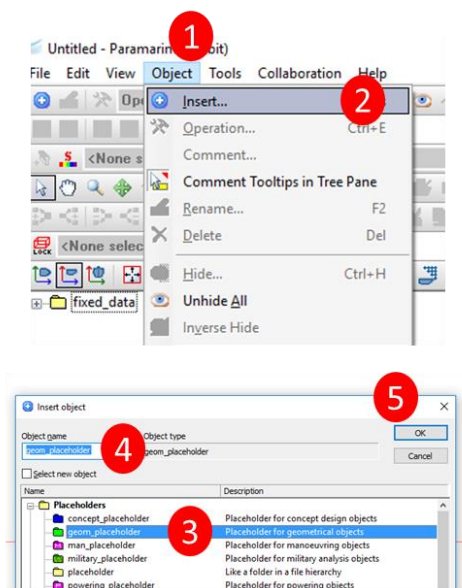


Figure A.36: Illustrative modelling effort in Paramarine showing a manual process (left) and KCL macro line (right)

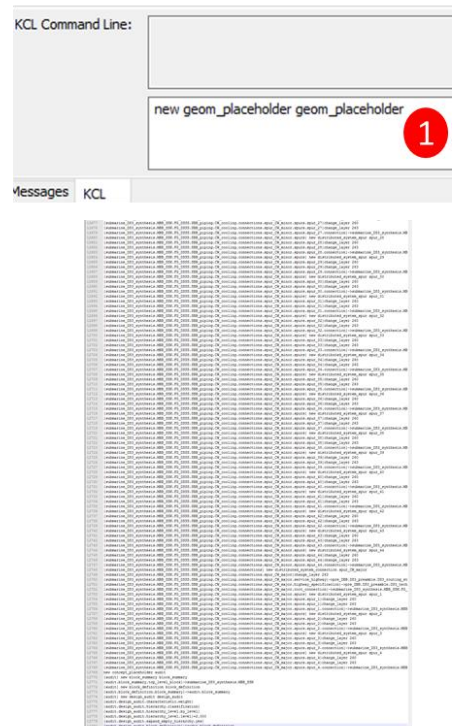
Fortunately, Paramarine has an alternative modelling approach using the KCL programming language (Boscarol and Aiello, 1988) as shown in Figure A.36 (right). Only one step, a one-line KCL command is enough to create an object in Paramarine. This greatly reduced the effort of modelling in Paramarine. Now the question would be how to utilise this feature without constraining the design and retaining the benefits from the UCL DBB approach. Therefore, the Physical Loop method employs programs in Excel to automate the modelling effort using KCL lines.

This was first tested to automate the modelling effort of a refined physical model of Case Study 3.3.1 shown in Figure A.35. The comparison is illustrated in Figure A.37. Figure A.37 (left) shows theoretical modelling required to model 277 Design Building Block (DBB) objects for DS3 components of Case Study 3.3.1. Since each DS3 component would require an equipment object (5 clicks), a geometric object (5 clicks) and then inserted as a SURFCON DBB object (100 clicks). This means if there are 277 DS3 components at the component granularity, the theoretical effort required would be some 30,000 clicks for a single design. Meanwhile, as illustrated in Figure A.37 (right), all numerical input data defined in spreadsheet programs could be converted rapidly to 12,780 KCL lines within 40-50 seconds.

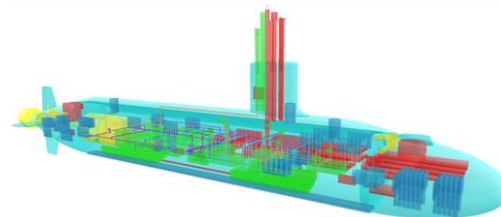
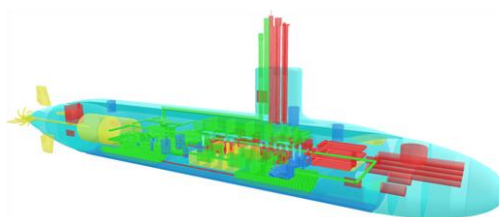
Manual modelling setup in Paramarine



KCL command line



Produced 277 BBs with numerical data



- Assuming per BB requires:
- Geometry modelling (5 clicks)
 - Equip instance modelling (5 clicks)
 - Other pre-setups, audit modelling, and DS3 routing models (100 clicks)

Total of mouse clicks for 277 BBs would be $(5+5+100)*277 = 30,470$ clicks!

This does not include design error/ iteration in the process

Total 12,780 lines of commands can be produced only in 40-50 secs!

- The current novel DS3 tool can facilitate:
- ✓ 80 objects for database
 - ✓ Adjustable hull modelling, including fin and control surfaces
 - ✓ 11 different types of DS3 modelling
 - ✓ 1225 objects for BBs modelling

Only by a SINGLE click from an Excel Macro button!

Figure A.37: Theoretical modelling effort of Case Study 3.3.1 in Paramarine showing the manual process (left) and the KCL macro line (right)

The development of the Physical Loop method was iterative as the nature of the research. As shown in Figure A.38, the depth of BB was initially kept flexible allowing the development of hierarchy complexity up to level 6 depth. However, it was found that flexible depth of hierarchy was not useful when the input data could be compiled in a single sheet. Hence, keeping the BB levels hierarchy was considered disadvantageous for DS3 synthesis.

FUNCTIONAL FOR SPATIAL PHYSICAL ARCHITECTURE														
Call Name	Description	Shape (bo/Levent)	(B/D)(m)	H (m)	Orientation	FG	SAB	BB1	BB2	BB3	BB4	BB5	BB Level (Info only)	Attributes (Weight Gr/Permanent)
1 command_console	command console	box	0.6	0.6	1.9	"Z"	FGHT_database	SUB_consoles_and_cabinets	command_console					4 0.2
2 CPU_cabinet	cabinet CPU SDB 20 box	box	0.6	0.6	1.3	"Z"	FGHT_database	SUB_consoles_and_cabinets	CPU_cabinet					4 0.15
3 mast_communications	communications cylinder	cylinder	0.4	0.4	"Z"	FGHT_database	SUB_communications	mast_communications						4 1.5
4 mast_radar_95	radar SDB pg. cylinder	cylinder	0.2	1	"Z"	FGHT_database	SUB_radar	mast_radar_95						4 1.1
5 mast_ESM	ESM SDB pg. cylinder	cylinder	1	0.8	"Z"	FGHT_database	SUB_electronic_warfare	mast_ESM						4 2.7
6 periscope_attack	periscope	cylinder	1	0.09	"Z"	FGHT_database	SUB_periscopes	periscope_attack						4 3.3
7 periscope_search	periscope	cylinder	1	0.15	"Z"	FGHT_database	SUB_periscopes	periscope_search						4 2.2
8 mast_telescopic	telescopic	cylinder	21	0.6	"Z"	FGHT_database	SUB_periscopes	mast_telescopic						4 0
9 mast_optic	optic	cylinder	13	0.6	"Z"	FGHT_database	SUB_periscopes	mast_optic						4 0
10 countermeasure_small	countermeasure	cylinder	1	0.1	"Z"	FGHT_database	SUB_countermeasures	countermeasure_small						7 0.1
11 sonar_box_cylindrical	sonar	cylinder	1.85	1	"Z"	FGHT_database	SUB_sonars	sonar_box_cylindrical						7 4
12 sonar_stem	sonar stem	box	1.05	0.2	1.65	"Z"	FGHT_database	SUB_sonars	sonar_stem					7 0.2
13 sonar_stem_array_large	sonar stem array	box	24	0.2	0.2	"Z"	FGHT_database	SUB_sonars	sonar_stem_array_large					7 1.6
14 sonar_passive_ranging_PRR	sonar passive ranging	box	2	0.2	1.2	"Z"	FGHT_database	SUB_sonars	sonar_passive_ranging_PRR					7 0.2
15 towed_array_retracted_in_re	towed array	box	2	2.5	3.5	"Z"	FGHT_database	SUB_sonars	towed_array_retracted_in_rectangular_housing					7 0.601
16 torpedo_heavyweight_333mm	torpedo	cylinder	6	0.333	"X"	FGHT_database	SUB_weapon_tubes	torpedo_heavyweight_333mm_MX48_USA						7 1.6
17 torpedo_tube_333mm_forced	torpedo tube	cylinder	10	3.68	"X"	FGHT_database	SUB_weapon_tubes	torpedo_tube_333mm_forced_discharge						7 8.2
18 ATP	ATP	cylinder	2.75	1.25	"X"	FGHT_database	SUB_weapon_tubes	ATP						7 0.6
19 main_electric_motor_PM	propulsion system	cylinder	5.243	5.243	"X"	MOVE_database	propulsion_system	main_electric_motor_PM						2 374.804
20 shaft	shaft	cylinder	15.896	0.432	"X"	MOVE_database	propulsion_system	shaft						2 24.93
21 propeller	propeller	cylinder	2.019	4.2	"X"	MOVE_database	propulsion_system	propeller						2 11.105
22 stem_planes_connector	control system	cylinder	5.75	0.5	"Y"	MOVE_database	control_system	stem_planes_connector						5 0
23 fwd_planes_connector	control system	cylinder	7.25	0.5	"Y"	MOVE_database	control_system	fwd_planes_connector						5 0
24 rudder_connector	control system	cylinder	8.25	0.5	"Z"	MOVE_database	control_system	rudder_connector						5 0
25 aft_actuator	control system	cylinder	5.75	0.5	"X"	MOVE_database	control_system	aft_actuator						5 0
26 fwd_actuator	control system	cylinder	2	0.75	"X"	MOVE_database	control_system	fwd_actuator						5 0
27 joint	control system	box	1	0.5	2.2	"Z"	MOVE_database	control_system	joint					5 0
28 diesel_generators_18_cylinders	power plant system	box	6.31	1.85	2.62	"Z"	INFRASTRUCTURE_database	power_plant_system	diesel_generators_18_cylinders_PG					3 24.92
29 battery_cell_A	battery	box	0.45	0.35	1.25	"Z"	INFRASTRUCTURE_database	power_plant_system	battery_cell_A					3 0.55
30 breaker_generator	breaker	box	1.058	1.058	1.058	"Z"	INFRASTRUCTURE_database	power_plant_system	breaker_generator					3 0.448
31 breaker_battery	breaker	box	2.56	0.896	1.792	"Z"	INFRASTRUCTURE_database	power_plant_system	breaker_battery					3 5.083
32 switchboard	switchboard	box	1.8	0.45	1.8	"Z"	INFRASTRUCTURE_database	power_plant_system	switchboard					3 5.243
33 ID_tank	ID tank	box	1.5	1.5	1.5	"Z"	INFRASTRUCTURE_database	power_plant_system	ID_tank					3 0
34 hydraulic_plant	hydraulic plant	box	1.8	1.8	1.5	"Z"	INFRASTRUCTURE_database	hydraulic_plant_system	hydraulic_plant					5 2.5
35 fan_for_battery	fan	box	0.8	0.4	"Y"	INFRASTRUCTURE_database	HVAC_system	fan_for_battery						5 0.2
36 FCU_2kW_Bronswerk	air system	box	0.94	0.27	0.6	"X"	INFRASTRUCTURE_database	HVAC_system	air_system	FCU_2kW_Bronswerk				5 0.044
37 mast_induction_telescopic	air system	cylinder	13	0.75	"Z"	INFRASTRUCTURE_database	HVAC_system	air_system	mast_induction_telescopic					5 0
38 mast_exhaust_telescopic	air system	cylinder	10	0.65	"Z"	INFRASTRUCTURE_database	HVAC_system	air_system	mast_exhaust_telescopic					5 0
39 head_exhaust	air system	cylinder	1	0.7	"Z"	INFRASTRUCTURE_database	HVAC_system	air_system	head_exhaust					5 0
40 manifold_exhaust	air system	box	0.8	1	1.2	"Z"	INFRASTRUCTURE_database	HVAC_system	air_system	manifold_exhaust				5 0
41 AHJ_15kW_Bronswerk	air system	box	5.19	1.71	1.39	"Z"	INFRASTRUCTURE_database	HVAC_system	air_system	AHJ_15kW_Bronswerk				5 3
42 duct_return	air system	box	0.94	0.6	0.27	"Z"	INFRASTRUCTURE_database	HVAC_system	air_system	duct_return				5 0.044
43 chilled_water_plant_56kW	chilled water system	box	1.8	1.8	1.6	"Z"	INFRASTRUCTURE_database	HVAC_system	chilled_water_plant_56kW					5 3
44 bed	accommodation	box	2	0.8	0.2	"Z"	INFRASTRUCTURE_database	accommodation	bed					6 0
45 bathroom_for_junior	accommodation	box	2	2	1.5	"Z"	INFRASTRUCTURE_database	accommodation	bathroom_for_junior					6 0
46 bathroom_for_senior	accommodation	box	1	1	1.5	"Z"	INFRASTRUCTURE_database	accommodation	bathroom_for_senior					6 0
47 bathroom_for_office	accommodation	box	1.225	1.225	1.5	"Z"	INFRASTRUCTURE_database	accommodation	bathroom_for_office					6 0
48 module_for_captain	accommodation	box	1.225	1.225	1.5	"Z"	INFRASTRUCTURE_database	accommodation	module_for_captain					6 0
49 module_for_galley	accommodation	box	3	2	2.2	"Z"	INFRASTRUCTURE_database	accommodation	module_for_galley					6 0
50 module_for_dining	accommodation	box	3.25	2.5	2.2	"Z"	INFRASTRUCTURE_database	accommodation	module_for_dining					6 0
51 module_for_ward_oom	accommodation	box	3.25	2.5	2.2	"Z"	INFRASTRUCTURE_database	accommodation	module_for_ward_oom					6 0
52 personnel_dumy	accommodation	box	0.25	0.5	1.8	"Z"	INFRASTRUCTURE_database	accommodation	personnel_dumy					6 0.09
53 console_ship_control	console	box	0.6	0.6	1.9	"Z"	INFRASTRUCTURE_database	ship_machinery_control	console_ship_control					4 0
54 console_machinery_control	console	box	0.6	0.6	1.9	"Z"	INFRASTRUCTURE_database	ship_machinery_control	console_machinery_control					4 0

Figure A.38: Initial flexible BB hierarchy in the Physical Loop method

Similarly, as shown in Figure A.39, the early version of the Hull Granularity Program (HGP) adopts a subdivision model using several X, Y, and Z planes. Although this works, this was found to be an inflexible and inefficient model as this required additional effort to individually refer to each subdivided **“solid_body”** as the DBB object in the Component Granularity Program (CGP).

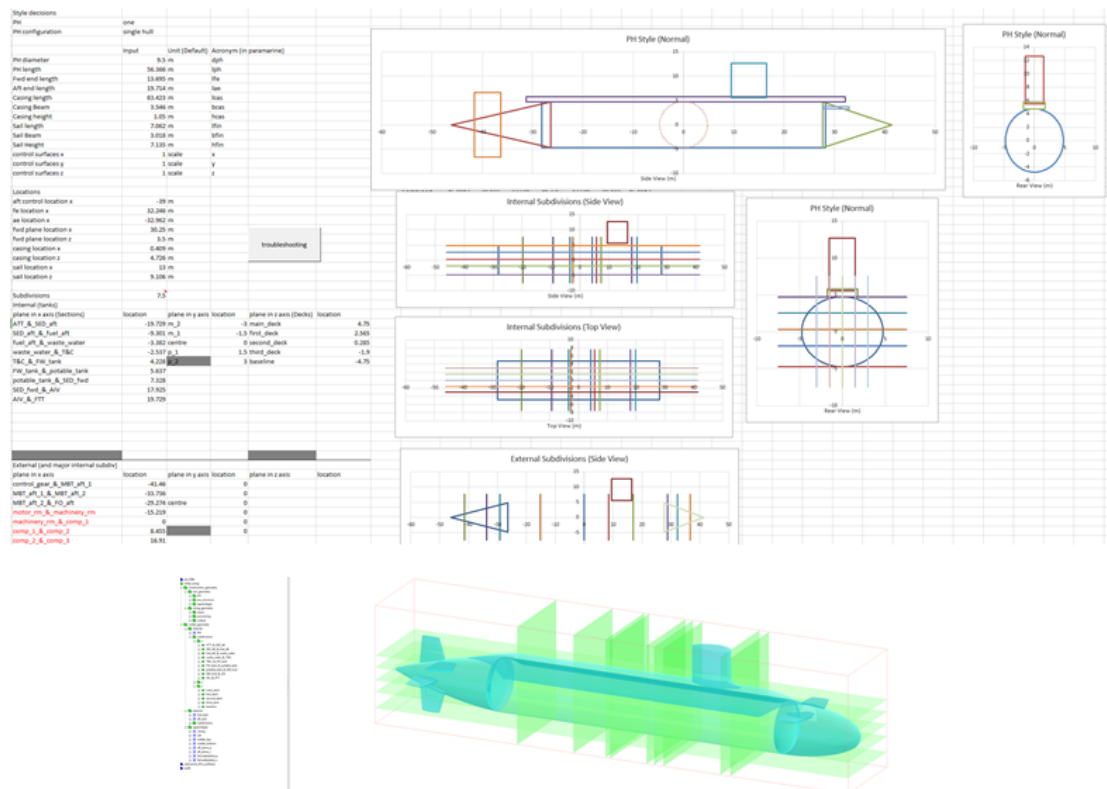


Figure A.39: Initial Hull Granularity Program (HGP), part of Physical Loop method showing the input data in the spreadsheet menu (top) and the output in Paramarine (bottom)

A 5.1.2 Logical Loop Method

On top of the Physical Loop method, the development of the Logical Loop method was also iterative. Given MATLAB can produce automatic network layout, using Case Study 3.3.1, Figure A.40 shows results using circle, forced, layered and 3D forced algorithms.

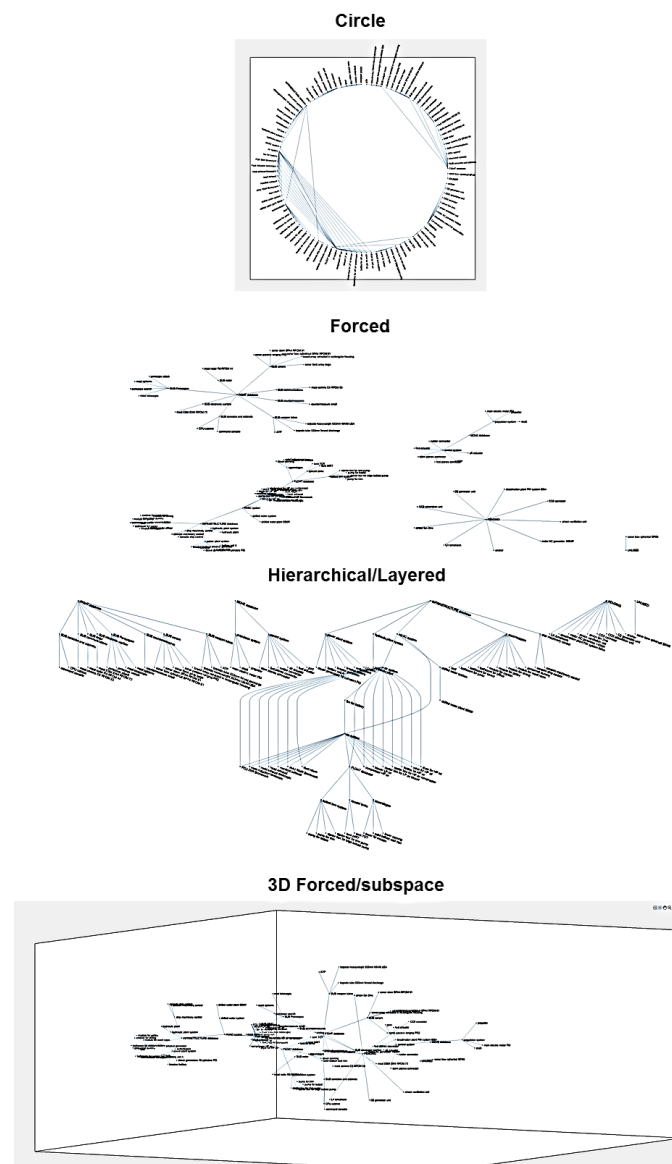


Figure A.40: Various layout algorithms in MATLAB using Case Study 3.3.1, showing circle, forced (Fruchterman and Reingold, 1991), layered (Gansner et al., 1993; Brandes and Köpf, 2002; Barth et al., 2004), and subspace (Koren, 2005) while the label of the nodes is not intended to be readable

Initially, the DS3 network was developed using the layered layout. However, as shown in Figure A.41, the layered layout complicates the appearance of the overall DS3 network, it was difficult to identify, e.g., a ring main configuration.

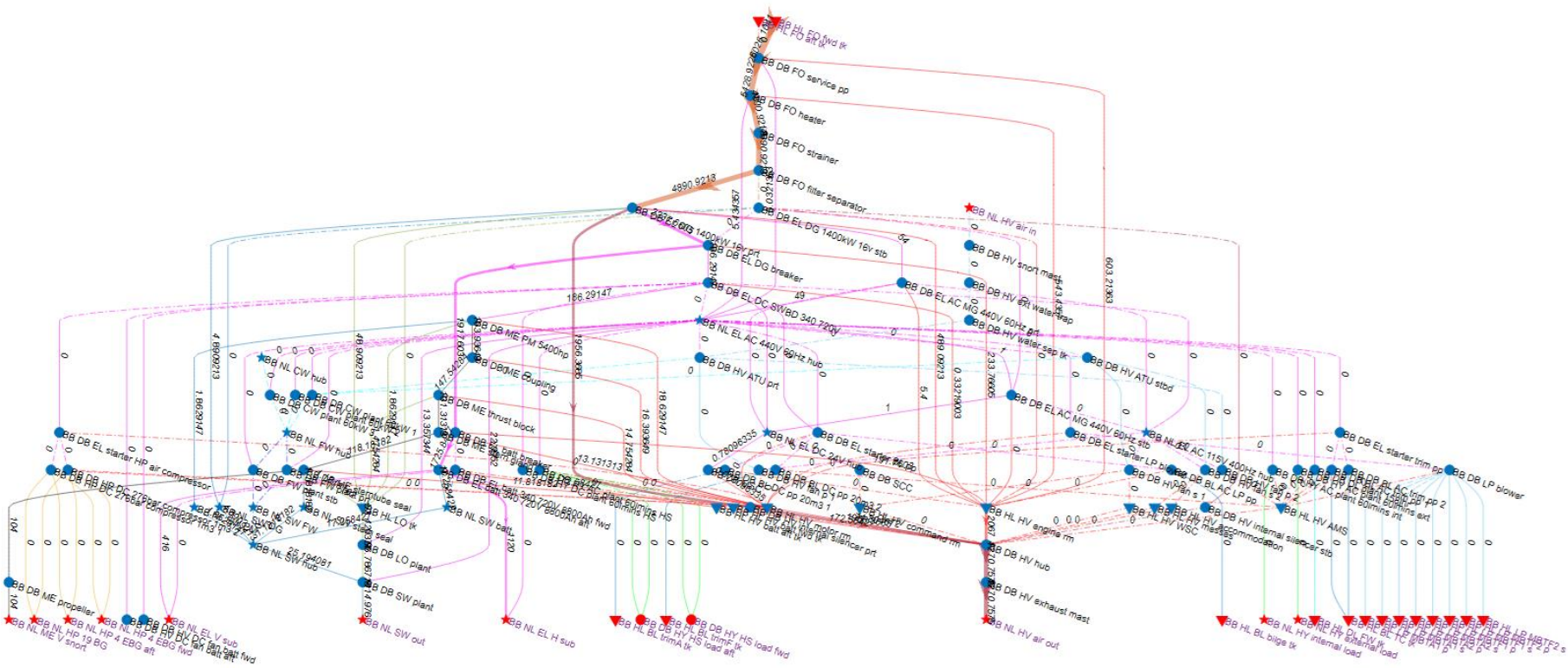


Figure A.41: Initial DS3 network showing various DS3 in different colours using the layered algorithm in MATLAB

A 5.2 Description of the Input Data Centre Tool

This section provides additional detail on the description of the programs within the Network Block Approach (NBA).

A 5.2.1 Main Menu Program

The Main Menu Program (MMP) was developed based on the macro interface that Paramarine (Qinetiq, 2019) has provided. As shown in Figure A.42, it contains several macro buttons: to open software; to open a Paramarine file; to build a KCL script; and to generate the KCL script from all programs and then build; and to generate the KCL script from all programs only.

ip address	127.0.0.1	START PARAMARINE
pm port	2000	
PM Location	C:\Program Files\Qinetiq\Paramarine V19.2\bin	
File location	N:\A DS3T\A TOOL\PREDBB.kcl	OPEN FILE
kcl command	playback N:\A DS3T\A TOOL\PREDBB.kcl	BUILD
opendesign F:\BANK PENDING\SSK 05122019.design		GEN. KCL THEN CLICK BUILD
N:\A DS3T\A TOOL\PREDBB.kcl		GENERATE KCL

Figure A.42: Layout of the MMP

As shown in the compilation sequence of all programs in Figure A.43, the MMP works closely with the Design Analysis Program (DAP) and the Design Preamble Program (DPP), which hardcoded the Gulf of Execution for performing necessary naval architectural analysis in Paramarine. The output of DPP is called DPPO (output) consisting of:

- Weight Group classifications (UCL SUB Weight Groups)
- consumables (seawater, freshwater/ diesel oil, LOX, etc)
- ship conditions (deep/light surfaced/submerged)
- crew types (not used)
- user spec container, costs

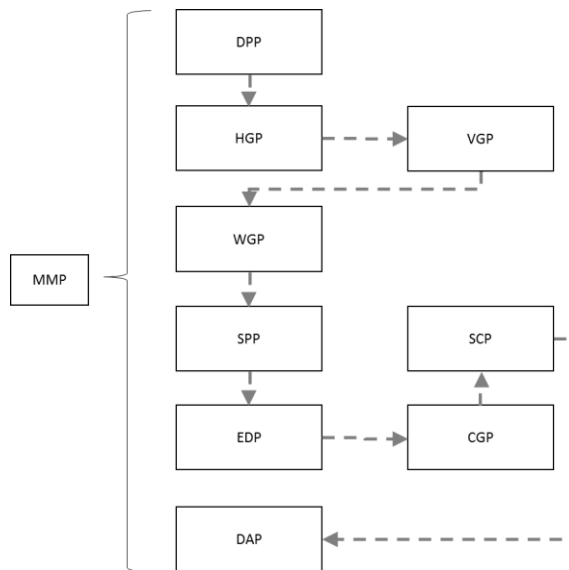


Figure A.43: Compilation sequence of all programs in the NBA

A 5.2.2 Hull Granularity Program

The Hull Granularity Program (HGP), as given in Figure A.44, provides a scalable submarine hull configuration with specific chosen style, which is a single hull with casing configuration. Any different major style will require a new HGP. To develop a new HGP, the designer first manually models the submarine in Paramarine and then create the macro script based on such models.

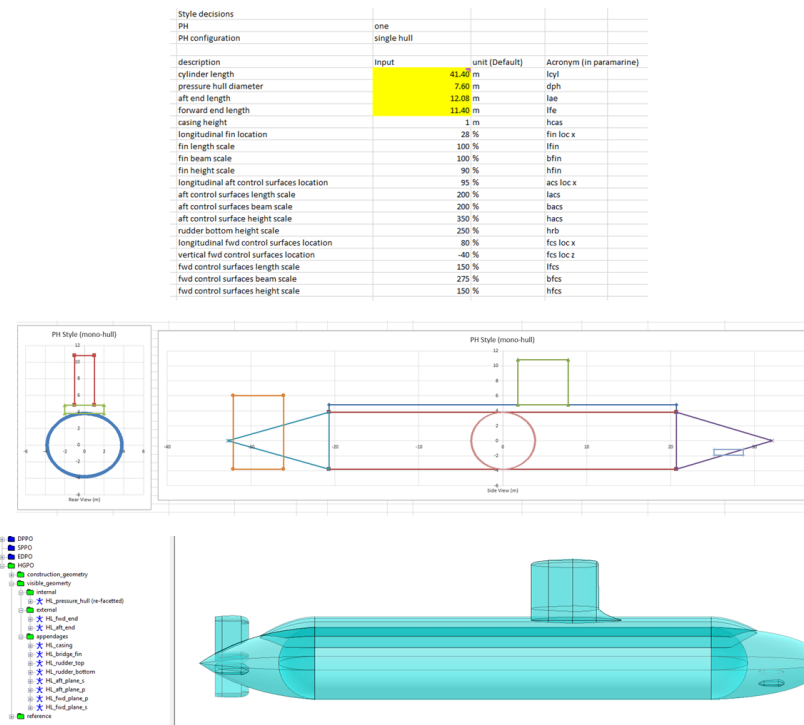


Figure A.44: Layout of the HGP showing the input in Excel (top) and the output in Paramarine (bottom)

A 5.2.3 Volume Granularity Program

The Volume Granularity Program (VGP) consists of inputs to define spaces on the vessel as given in Figure A.45. The DBB objects at the volume granularity were defined based on names, BB hierarchy (to level 4), two points (A and B) defining the boundary of the object, location of the space relative to the hull model defined in VGP, tank definition. This spreadsheet layout reveals the input of Case Study 5.1 reached up to 800 inputs (35 by 23), which includes “string” data input as well as numerical data input.

A 5.2.4 Weight Granularity Program

The Weight Granularity Program (WGP) defines numerical weight on the vessel, as depicted in Figure A.46. This consists of naming convention to reflect the WG number, weight location (“manual” if it is defined in x, y, z coordinates), DBB hierarchy (to the fifth level), volume location defined in VGP, and the numerical weight data. The number of inputs in the WGP for Case Study 5.1 was about 1800 inputs, assuming there are 10 inputs for each weight.

(INFO ONLY)		FUNCTIONAL FOR SPATIAL PHYSICAL ARCHITECTURE (BB management based on functionality >> locations)					start from stbd(-) to port(+)				WG	Permanent Weight %			
Call#	Name	Weight location	1	2	3	4	5	BB Level	initial location	initial			initial location		
1	Ni_2_MCC		M88	WGP	FG	flight	S88	control_data	BB_Ni_2_MCC	0	0	1.47	BB_VI_MV_RM_MK	2	3.3
2	Ni_4_SCC		M88	WGP	FG	flight	S88	control_data	BB_Ni_4_SCC	0	0	2.65	BB_VI_FH_RM_CO	4	0.8
3	Ni_4_miscellaneous_control_instrumentation		M88	WGP	FG	flight	S88	control_data	BB_Ni_4_miscellaneous_control_instrumentation	0	0	1.82	BB_VI_FH_RM_CO	4	2.1
4	Ni_4_data_handling_computer_display		M88	WGP	FG	flight	S88	control_data	BB_Ni_4_data_handling_computer_display	0	0	1.83	BB_VI_FH_RM_CO	4	3.5
5	Ni_4_navigation_equipment		M88	WGP	FG	flight	S88	control_data	BB_Ni_4_navigation_equipment	0	0	0.88	BB_VI_FH_RM_CO	4	2
6	Ni_4_internal_comms		M88	WGP	FG	flight	S88	control_data	BB_Ni_4_internal_comms	0	0	2.88	BB_VI_FH_RM_CO	4	0.9
7	Ni_4_main_passive_sonar_array	manual	M88	WGP	FG	flight	S88	sonar	BB_Ni_4_main_passive_sonar_array	0	0	-6.9	BB_VI_FH_RM_CO	4	5.5
8	Ni_4_main_passive_sonar_dome		M88	WGP	FG	flight	S88	sonar	BB_Ni_4_main_passive_sonar_dome	0	0	-5.3	BB_VI_FF_FF	4	3.9
9	Ni_4_other_sonar_arrays	manual	M88	WGP	FG	flight	S88	sonar	BB_Ni_4_other_sonar_arrays	0	0	5.2	BB_VI_FH_RM_CO	4	2.5
10	Ni_4_other_sonar_windows	manual	M88	WGP	FG	flight	S88	sonar	BB_Ni_4_other_sonar_windows	0	0	4.7	BB_VI_FH_RM_CO	4	2.6
11	Ni_4_sonar_processing_display		M88	WGP	FG	flight	S88	sonar	BB_Ni_4_sonar_processing_display	0	0	2.65	BB_VI_FH_RM_CO	4	1.2
12	Ni_1_periscope_supports_wells		M88	WGP	FG	flight	S88	periscope	BB_Ni_1_periscope_supports_wells	0	0	-0.63	BB_VI_IA_RM_SF	1	7.5
13	Ni_4_periscopes		M88	WGP	FG	flight	S88	periscope	BB_Ni_4_periscopes	0	0	3.27	BB_VI_FF_FF	4	4
14	Ni_4_periscopes_hosts_buffers	manual	M88	WGP	FG	flight	S88	periscope	BB_Ni_4_periscopes_hosts_buffers	0	0	5	BB_VI_FF_FF	4	1.3
15	Ni_4_periscope_bearing_hull_glands		M88	WGP	FG	flight	S88	periscope	BB_Ni_4_periscope_bearing_hull_glands	0	0	4.79	BB_VI_FF_FF	4	1.2
16	Ni_4_wireless_mast_host		M88	WGP	FG	flight	S88	mast	BB_Ni_4_wireless_mast_host	0	0	11.55	BB_VI_FF_FF	4	1.5
17	Ni_4_wireless_RX_TX		M88	WGP	FG	flight	S88	mast	BB_Ni_4_wireless_RX_TX	0	0	2.97	BB_VI_FH_RM_CO	4	2.3
18	Ni_4_radar_mast_host		M88	WGP	FG	flight	S88	mast	BB_Ni_4_radar_mast_host	0	0	8.95	BB_VI_FF_FF	4	2.5
19	Ni_4_radar_set		M88	WGP	FG	flight	S88	mast	BB_Ni_4_radar_set	0	0	1.68	BB_VI_FH_RM_CO	4	0.4
20	Ni_4_EW_mast_host		M88	WGP	FG	flight	S88	mast	BB_Ni_4_EW_mast_host	0	0	8.2	BB_VI_FF_FF	4	2.7
21	Ni_4_EW equip		M88	WGP	FG	flight	S88	mast	BB_Ni_4_EW equip	0	0	2.5	BB_VI_FH_RM_CO	4	1.4
22	Ni_1_torpedo_loading_hatch		M88	WGP	FG	flight	S88	torpedo	BB_Ni_1_torpedo_loading_hatch	0	0	4.15	BB_VI_FH_RM_WS	1	0.7
23	Ni_2_torpedo_tubes		M88	WGP	FG	flight	S88	torpedo	BB_Ni_2_torpedo_tubes	0	0	2.85	BB_VI_FH_RM_WS	7	36
24	Ni_2_torpedo_CP	troubleshooting	M88	WGP	FG	flight	S88	torpedo	BB_Ni_2_torpedo_CP	0	0	1.87	BB_VI_FH_RM_WS	7	1
25	Ni_2_torpedo_stowage_handling_gr		M88	WGP	FG	flight	S88	torpedo	BB_Ni_2_torpedo_stowage_handling_gr	0	0	2.88	BB_VI_FH_RM_WS	7	23.3
26	Ni_2_fluid_torpedo_systems		M88	WGP	FG	flight	S88	torpedo	BB_Ni_2_fluid_torpedo_systems	0	0	1.75	BB_VI_FH_RM_WS	7	7
27	Ni_2_ATP		M88	WGP	FG	flight	S88	torpedo	BB_Ni_2_ATP	0	0	0.81	BB_VI_FH_RM_WS	7	1
28	Ni_2_tube_flood_drain_system		M88	WGP	FG	flight	S88	torpedo	BB_Ni_2_tube_flood_drain_system	0	0	1.83	BB_VI_FH_RM_WS	7	2.5
29	Ni_2_tube_hydraulic_system		M88	WGP	FG	flight	S88	torpedo	BB_Ni_2_tube_hydraulic_system	0	0	2.25	BB_VI_FH_RM_WS	7	6
30	Ni_2_air_landing_jump_system		M88	WGP	FG	flight	S88	torpedo	BB_Ni_2_air_landing_jump_system	0	0	0.84	BB_VI_FH_RM_WS	7	3.4
31	Ni_2_bow_shutters_operating_gr		M88	WGP	FG	flight	S88	torpedo	BB_Ni_2_bow_shutters_operating_gr	0	0	2.73	BB_VI_FH_RM_WS	7	2.7
32	Ni_9_torpedoes		M88	WGP	FG	flight	S88	torpedo	BB_Ni_9_torpedoes	0	0	2.6	BB_VI_FH_RM_WS	9	30
33	Ni_8_vibration_damping		M88	WGP	FG	flight	S88	signature	BB_Ni_8_vibration_damping	0	0	0.18	BB_VI_MV_RM_MK	6	1.8
34	Ni_8_thermal_acoustic_insulation		M88	WGP	FG	flight	S88	signature	BB_Ni_8_thermal_acoustic_insulation	0	0	1.79	BB_VI_IA_RM_SF	6	9.6
35	Ni_8_paint_fillers	manual	M88	WGP	FG	flight	S88	signature	BB_Ni_8_paint_fillers	0	0	1.05	BB_VI_FF_FF	6	12
36	Ni_7_signal_ejectors	manual	M88	WGP	FG	flight	S88	signature	BB_Ni_7_signal_ejectors	0	0	3.2	BB_VI_FF_FF	7	4
37	Ni_3_small_arms_pyrotechnics		M88	WGP	FG	flight	S88	naval_store	BB_Ni_3_small_arms_pyrotechnics	0	0	2.4	BB_VI_FH_RM_WS	9	1
38	Ni_3_naval_store_spare_gear		M88	WGP	FG	flight	S88	naval_store	BB_Ni_3_naval_store_spare_gear	0	0	0.02	BB_VI_IA_RM_SF	9	12
39	Ni_8_captain_windless		M88	WGP	FG	move	S88	mooring_systems	BB_Ni_8_captain_windless	0	0	5.28	BB_VI_FF_CA	6	4.1
40	Ni_8_anchor_cable		M88	WGP	FG	move	S88	mooring_systems	BB_Ni_8_anchor_cable	0	0	1.56	BB_VI_FF_CA	6	4.2
41	Ni_8_bollards_fairleads		M88	WGP	FG	move	S88	mooring_systems	BB_Ni_8_bollards_fairleads	0	0	5.88	BB_VI_FF_CA	6	3.2
42	Ni_8_hoovers_cables		M88	WGP	FG	move	S88	mooring_systems	BB_Ni_8_hoovers_cables	0	0	1.4	BB_VI_FF_CA	6	1.5
43	Ni_1_fed_hydroplanes		M88	WGP	FG	move	S88	manoeuvring_systems	BB_Ni_1_fed_hydroplanes	0	0	-0.25	BB_VI_MV_FF_FF	1	1.6
44	Ni_1_aft_hydroplanes		M88	WGP	FG	move	S88	manoeuvring_systems	BB_Ni_1_aft_hydroplanes	0	0	0.75	BB_VI_MV_FF_FF	1	4.9
45	Ni_1_stabilizers		M88	WGP	FG	move	S88	manoeuvring_systems	BB_Ni_1_stabilizers	0	0	0.75	BB_VI_MV_FF_FF	1	8.7
46	Ni_1_rudders		M88	WGP	FG	move	S88	manoeuvring_systems	BB_Ni_1_rudders	0	0	1.17	BB_VI_MV_FF_FF	1	9.2
47	Ni_5_steering_hydroplane_control_system		M88	WGP	FG	move	S88	manoeuvring_systems	BB_Ni_5_steering_hydroplane_control_system	0	0	1.41	BB_VI_FF_EA	5	1.4
48	Ni_5_steering_diving_hydraulic_plant		M88	WGP	FG	move	S88	manoeuvring_systems	BB_Ni_5_steering_diving_hydraulic_plant	0	0	1.54	BB_VI_MV_RM_MK	5	2.8
49	Ni_3_yarder equip		M88	WGP	FG	move	S88	manoeuvring_systems	BB_Ni_3_yarder equip	0	0	0.88	BB_VI_MV_FF_FF	5	10.6
50	Ni_3_retractable_fed_hydroplane equip		M88	WGP	FG	move	S88	manoeuvring_systems	BB_Ni_3_retractable_fed_hydroplane equip	0	0	-0.25	BB_VI_MV_FF_FF	5	7.5
51	Ni_3_aft_hydroplane equip		M88	WGP	FG	move	S88	manoeuvring_systems	BB_Ni_3_aft_hydroplane equip	0	0	1.61	BB_VI_MV_FF_FF	5	3.9
52	Ni_2_fluid_propulsion_system		M88	WGP	FG	move	S88	propulsion_systems	BB_Ni_2_fluid_propulsion_system	0	0	0.77	BB_VI_IA_DV_LO	2	0.3
53	Ni_2_shafting		M88	WGP	FG	move	S88	propulsion_systems	BB_Ni_2_shafting	0	0	0.76	BB_VI_FF_MK_MA	2	7.4

Figure A.46: Layout of the WGP showing major inputs required in defining items of weight data on the vessel

A 5.2.5 Equipment Database Program

The Equipment Database Program (EDP) defines the input necessary to create a physical model of a DS3 component. As shown in Figure A.47, the input consists of name, shape, dimensions, orientation, BB hierarchy, WG classifications, weight, connection points. For Case Study 5.1, there were 365 equipment objects, which means 5100 input data, assuming each component requires 14 inputs.

(INFO ONLY)		troubleshooting		FUNCTIONAL FOR SPATIAL PHYSICAL ARCHITECTURE			MUST ACC WEIGHT CONDITION/OTHER		LOGICAL ARCHITECTURE						
Call	Name	Shape	L/extent (B/D (m))	H (m)	ation	1 MBB	2 FG	3 SBB	BB Level	Attributes	connection point				
									(info only)	Volume (m ³) /BS Classif/Weight (te)	input	output			
1	DB_FO_VV_TK_a	sphere	0.3	0.3	0.3	Z	DB_DSSS	DB_FO	DB_FO_VV_TK_a	3.0	0.0	9.0	0.0	top	top
2	DB_FO_VV_TK_m	sphere	0.3	0.3	0.3	Z	DB_DSSS	DB_FO	DB_FO_VV_TK_m	3.0	0.0	9.0	0.0	top	top
3	DB_FO_VV_TK_f	sphere	0.3	0.3	0.3	Z	DB_DSSS	DB_FO	DB_FO_VV_TK_f	3.0	0.0	4.0	0.0	top	top
4	DB_DT_CO_AC_a	sphere	0.3	0.3	0.3	Z	DB_DSSS	DB_DT	DB_DT_CO_AC_a	3.0	0.0	4.0	2.6	top	top
5	DB_DT_CO_AC_f	sphere	0.3	0.3	0.3	Z	DB_DSSS	DB_DT	DB_DT_CO_AC_f	3.0	0.0	4.0	2.6	top	top
6	DB_DT_PU_AC	sphere	0.3	0.3	0.3	Z	DB_DSSS	DB_DT	DB_DT_PU_AC	3.0	0.0	4.0	3.0	top	top
7	DB_DT_SA_DC	cylinder	10.0	0.6	0.6	Z	DB_DSSS	DB_DT	DB_DT_SA_DC	3.0	3.6	2.0	2.2	bottom	bottom
8	DB_DT_AK_DC	cylinder	10.0	0.6	0.6	Z	DB_DSSS	DB_DT	DB_DT_AK_DC	3.0	3.6	3.0	1.9	bottom	bottom
9	DB_DT_CN_DC	cylinder	10.0	0.6	0.6	Z	DB_DSSS	DB_DT	DB_DT_CN_DC	3.0	3.6	3.0	1.5	bottom	bottom
10	DB_DT_EW_DC	cylinder	10.0	0.6	0.6	Z	DB_DSSS	DB_DT	DB_DT_EW_DC	3.0	3.6	3.0	2.7	bottom	bottom
11	DB_DT_RA_DC	cylinder	10.0	0.6	0.6	Z	DB_DSSS	DB_DT	DB_DT_RA_DC	3.0	3.6	3.0	2.5	bottom	bottom
12	DB_DT_SO_DC	cylinder	1.9	3.0	3.0	Z	DB_DSSS	DB_DT	DB_DT_SO_DC	3.0	16.7	3.0	4.0	aft	aft
13	DB_DT_SC_DC	sphere	0.8	0.1	0.2	Z	DB_DSSS	DB_DT	DB_DT_SC_DC	3.0	0.0	3.0	0.8	top	top
14	DB_DT_MC_DC	sphere	0.3	0.3	0.3	Z	DB_DSSS	DB_DT	DB_DT_MC_DC	3.0	0.0	3.0	3.3	top	top
15	DB_DT_DD_LC_a	box	2.0	1.0	1.0	Z	DB_DSSS	DB_DT	DB_DT_DD_LC_a	3.0	2.0	3.0	0.2	top	bottom
16	DB_DT_DD_LC_m	box	2.0	1.0	1.0	Z	DB_DSSS	DB_DT	DB_DT_DD_LC_m	3.0	2.0	3.0	0.2	top	bottom
17	DB_DT_DD_LC_f	box	2.0	1.0	1.0	Z	DB_DSSS	DB_DT	DB_DT_DD_LC_f	3.0	2.0	3.0	0.2	top	bottom
18	DB_DT_DD_AN_p	box	2.0	1.0	1.0	Z	DB_DSSS	DB_DT	DB_DT_DD_AN_p	3.0	2.0	3.0	0.2	ftwd	stbd
19	DB_DT_DD_AN_s	box	2.0	1.0	1.0	Z	DB_DSSS	DB_DT	DB_DT_DD_AN_s	3.0	2.0	3.0	0.2	ftwd	port
20	DB_DT_DD_MN_p	box	2.0	1.0	1.0	Z	DB_DSSS	DB_DT	DB_DT_DD_MN_p	3.0	2.0	3.0	0.2	top	stbd
21	DB_DT_DD_MN_s	box	2.0	1.0	1.0	Z	DB_DSSS	DB_DT	DB_DT_DD_MN_s	3.0	2.0	3.0	0.2	top	port
22	DB_DT_DD_FN_p	box	2.0	1.0	1.0	Z	DB_DSSS	DB_DT	DB_DT_DD_FN_p	3.0	2.0	3.0	0.2	aft	stbd
23	DB_DT_DD_FN_s	box	2.0	1.0	1.0	Z	DB_DSSS	DB_DT	DB_DT_DD_FN_s	3.0	2.0	3.0	0.2	aft	port
24	DB_EL_PG_DG_p	box	4.4	1.4	2.0	Z	DB_DSSS	DB_EL	DB_EL_PG_DG_p	3.0	12.2	3.0	19.0	stbd	top
25	DB_EL_PG_DG_s	box	4.4	1.4	2.0	Z	DB_DSSS	DB_EL	DB_EL_PG_DG_s	3.0	12.2	3.0	18.8	port	top
26	DB_EL_PC_DC_p	box	0.5	1.3	1.5	Z	DB_DSSS	DB_EL	DB_EL_PC_DC_p	3.0	1.0	3.0	2.6	aft	ftwd
27	DB_EL_PC_DC_s	box	0.5	1.3	1.5	Z	DB_DSSS	DB_EL	DB_EL_PC_DC_s	3.0	1.0	3.0	2.5	aft	ftwd
28	DB_EL_PD_PG	box	0.5	1.3	1.5	Z	DB_DSSS	DB_EL	DB_EL_PD_PG	3.0	1.0	3.0	0.8	aft	ftwd
29	DB_EL_ND_PG_p	box	0.5	1.3	1.5	Z	DB_DSSS	DB_EL	DB_EL_ND_PG_p	3.0	1.0	3.0	0.9	top	stbd
30	DB_EL_ND_PG_s	box	0.5	1.3	1.5	Z	DB_DSSS	DB_EL	DB_EL_ND_PG_s	3.0	1.0	3.0	1.4	top	port
31	NL_EL_HO_AN	sphere	0.3	0.3	0.3	Z	DB_DSSS	DB_EL	NL_EL_HO_AN	3.0	0.0	3.0	0.0	top	top
32	DB_EL_ND_SE_p	box	0.5	1.3	1.5	Z	DB_DSSS	DB_EL	DB_EL_ND_SE_p	3.0	1.0	3.0	1.4	top	stbd
33	DB_EL_ND_SE_s	box	0.5	1.3	1.5	Z	DB_DSSS	DB_EL	DB_EL_ND_SE_s	3.0	1.0	3.0	1.4	top	port
34	DB_EL_PD_SE	box	0.5	1.3	1.5	Z	DB_DSSS	DB_EL	DB_EL_PD_SE	3.0	1.0	3.0	3.3	top	bottom
35	DB_EL_SE_BD_a	sphere	0.3	0.3	0.3	Z	DB_DSSS	DB_EL	DB_EL_SE_BD_a	3.0	0.0	3.0	0.0	top	top
36	DB_EL_SE_BD_f	sphere	0.3	0.3	0.3	Z	DB_DSSS	DB_EL	DB_EL_SE_BD_f	3.0	0.0	3.0	264.0	top	top
37	NL_EL_EE_SM	sphere	0.3	0.3	0.3	Z	DB_DSSS	DB_EL	NL_EL_EE_SM	3.0	0.0	3.0	0.0	top	top
38	DB_EL_ND_LA_p	box	0.5	1.3	1.5	Z	DB_DSSS	DB_EL	DB_EL_ND_LA_p	3.0	1.0	3.0	0.1	bottom	bottom
39	DB_EL_ND_LA_s	box	0.5	1.3	1.5	Z	DB_DSSS	DB_EL	DB_EL_ND_LA_s	3.0	1.0	3.0	1.4	bottom	bottom
40	DB_EL_PC_AN	box	0.5	1.3	1.5	Z	DB_DSSS	DB_EL	DB_EL_PC_AN	3.0	1.0	3.0	0.0	bottom	bottom
41	DB_EL_PD_LC_a	box	0.5	1.3	1.5	Z	DB_DSSS	DB_EL	DB_EL_PD_LC_a	3.0	1.0	3.0	0.1	top	bottom
42	DB_EL_ND_LM_p	box	0.5	1.3	1.5	Z	DB_DSSS	DB_EL	DB_EL_ND_LM_p	3.0	1.0	3.0	0.1	top	stbd
43	DB_EL_ND_LM_s	box	0.5	1.3	1.5	Z	DB_DSSS	DB_EL	DB_EL_ND_LM_s	3.0	1.0	3.0	0.1	bottom	bottom
44	DB_EL_PC_MN	box	0.5	1.3	1.5	Z	DB_DSSS	DB_EL	DB_EL_PC_MN	3.0	1.0	3.0	0.0	top	bottom
45	DB_EL_PD_LC_m	box	0.5	1.3	1.5	Z	DB_DSSS	DB_EL	DB_EL_PD_LC_m	3.0	1.0	3.0	0.2	top	bottom
46	NL_EL_HO_MN	sphere	0.3	0.3	0.3	Z	DB_DSSS	DB_EL	NL_EL_HO_MN	3.0	0.0	3.0	0.0	top	top
47	DB_EL_ND_LF_p	box	0.5	1.3	1.5	Z	DB_DSSS	DB_EL	DB_EL_ND_LF_p	3.0	1.0	3.0	0.0	bottom	bottom
48	DB_EL_ND_LF_s	box	0.5	1.3	1.5	Z	DB_DSSS	DB_EL	DB_EL_ND_LF_s	3.0	1.0	3.0	0.0	bottom	bottom
49	DB_EL_PC_FN	box	0.5	1.3	1.5	Z	DB_DSSS	DB_EL	DB_EL_PC_FN	3.0	1.0	3.0	0.0	bottom	bottom
50	DB_EL_PD_LC_f	box	0.5	1.3	1.5	Z	DB_DSSS	DB_EL	DB_EL_PD_LC_f	3.0	1.0	3.0	0.2	top	bottom
51	NL_EL_HO_FN	sphere	0.3	0.3	0.3	Z	DB_DSSS	DB_EL	NL_EL_HO_FN	3.0	0.0	3.0	0.0	top	top
52	DB_EL_ND_PM_p	box	0.5	1.3	1.5	Z	DB_DSSS	DB_EL	DB_EL_ND_PM_p	3.0	1.0	3.0	1.4	top	stbd

Figure A.47: Layout of the EDP showing major inputs required in defining spaces on the vessel

A 5.2.6 Component Granularity Program

The Component Granularity Program (CGP) provides input for the Physical Loop method and Logical Loop method. In terms of the Physical Loop method, the inputs for the DS3 components: the type of components, which could be equipment (DB) or numerical (NL) as listed in Table 4.3, Subsection 4.2.6; equipment data defined in EDP; BB hierarchy (up to level 4), relative position in X-, Y-, Z- axes relative to the DBB object at the volume granularity defined in VGP.

Call N	Name	Object Type	Equipment from Database	OPTIONAL FOR SPATIAL PHYSICAL ARCHITECTURE (BB)			management based str from stbd(-) to port(+)			axis ro initial		
				troubleshooting	1	2	3	4	BB Level		(Initial Location	
(INFO ONLY)				MBB	FG	SBB	BB1	X%	Y%	Z%	X/Y/Z	compartment
1	BB_DB_FO_VV_TK_a	equipment	DB_FO_VV_TK_a	MBB	CGP	FO	BB_DB_FO_VV_TK_a	4	0.0	0.0	0.0	BB_VL_JA_DV_OA
2	BB_DB_FO_VV_TK_m	equipment	DB_FO_VV_TK_m	MBB	CGP	FO	BB_DB_FO_VV_TK_m	4	0.0	0.0	0.0	BB_VL_JA_DV_OM
3	BB_DB_FO_VV_TK_f	equipment	DB_FO_VV_TK_f	MBB	CGP	FO	BB_DB_FO_VV_TK_f	4	0.0	0.0	0.0	BB_VL_JA_DV_OF
4	BB_DB_DT_CO_AC_a	equipment	DB_DT_CO_AC_a	MBB	CGP	DT	BB_DB_DT_CO_AC_a	4	0.8	0.0	0.0	BB_VL_FH_RM_CO
5	BB_DB_DT_CO_AC_f	equipment	DB_DT_CO_AC_f	MBB	CGP	DT	BB_DB_DT_CO_AC_f	4	-0.4	0.0	0.3	BB_VL_FH_RM_WS
6	BB_DB_DT_PU_AC	equipment	DB_DT_PU_AC	MBB	CGP	DT	BB_DB_DT_PU_AC	4	0.5	0.0	0.0	BB_VL_FH_RM_CO
7	BB_DB_DT_SA_DC	equipment	DB_DT_SA_DC	MBB	CGP	DT	BB_DB_DT_SA_DC	4	0.1	0.0	0.3	BB_VL_FL_FF_BR
8	BB_DB_DT_AK_DC	equipment	DB_DT_AK_DC	MBB	CGP	DT	BB_DB_DT_AK_DC	4	-0.5	0.0	0.3	BB_VL_FL_FF_BR
9	BB_DB_DT_CN_DC	equipment	DB_DT_CN_DC	MBB	CGP	DT	BB_DB_DT_CN_DC	4	-0.3	0.0	0.3	BB_VL_FL_FF_BR
10	BB_DB_DT_EW_DC	equipment	DB_DT_EW_DC	MBB	CGP	DT	BB_DB_DT_EW_DC	4	-0.2	0.0	0.3	BB_VL_FL_FF_BR
11	BB_DB_DT_RA_DC	equipment	DB_DT_RA_DC	MBB	CGP	DT	BB_DB_DT_RA_DC	4	-0.1	0.0	0.3	BB_VL_FL_FF_BR
12	BB_DB_DT_SO_DC	equipment	DB_DT_SO_DC	MBB	CGP	DT	BB_DB_DT_SO_DC	4	-0.2	0.0	0.0	BB_VL_FL_FF_EF
13	BB_DB_DT_SC_DC	equipment	DB_DT_SC_DC	MBB	CGP	DT	BB_DB_DT_SC_DC	4	0.2	0.0	0.0	BB_VL_FH_RM_CO
14	BB_DB_DT_MC_DC	equipment	DB_DT_MC_DC	MBB	CGP	DT	BB_DB_DT_MC_DC	4	0.7	0.0	0.0	BB_VL_MV_RM_MR
15	BB_DB_DT_DD_LC_a	equipment	DB_DT_DD_LC_a	MBB	CGP	DT	BB_DB_DT_DD_LC_a	4	0.1	0.0	0.5	BB_VL_MV_RM_MR
16	BB_DB_DT_DD_LC_m	equipment	DB_DT_DD_LC_m	MBB	CGP	DT	BB_DB_DT_DD_LC_m	4	-0.8	0.0	-0.3	BB_VL_FH_RM_CO
17	BB_DB_DT_DD_LC_f	equipment	DB_DT_DD_LC_f	MBB	CGP	DT	BB_DB_DT_DD_LC_f	4	-0.1	0.0	0.5	BB_VL_FH_RM_WS
18	BB_DB_DT_DD_AN_p	equipment	DB_DT_DD_AN_p	MBB	CGP	DT	BB_DB_DT_DD_AN_p	4	-0.6	0.4	-0.6	BB_VL_MV_RM_MR
19	BB_DB_DT_DD_AN_s	equipment	DB_DT_DD_AN_s	MBB	CGP	DT	BB_DB_DT_DD_AN_s	4	-0.6	-0.4	-0.6	BB_VL_MV_RM_MR
20	BB_DB_DT_DD_MN_p	equipment	DB_DT_DD_MN_p	MBB	CGP	DT	BB_DB_DT_DD_MN_p	4	-0.5	0.2	-0.4	BB_VL_FH_RM_CO
21	BB_DB_DT_DD_MN_s	equipment	DB_DT_DD_MN_s	MBB	CGP	DT	BB_DB_DT_DD_MN_s	4	-0.5	-0.1	-0.4	BB_VL_FH_RM_CO
22	BB_DB_DT_DD_FN_p	equipment	DB_DT_DD_FN_p	MBB	CGP	DT	BB_DB_DT_DD_FN_p	4	-0.1	0.3	0.3	BB_VL_FH_RM_WS
23	BB_DB_DT_DD_FN_s	equipment	DB_DT_DD_FN_s	MBB	CGP	DT	BB_DB_DT_DD_FN_s	4	-0.1	-0.3	0.3	BB_VL_FH_RM_WS
24	BB_DB_EL_PG_DG_p	equipment	DB_EL_PG_DG_p	MBB	CGP	EL	BB_DB_EL_PG_DG_p	4	0.0	0.4	-0.4	BB_VL_JA_RM_ER
25	BB_DB_EL_PG_DG_s	equipment	DB_EL_PG_DG_s	MBB	CGP	EL	BB_DB_EL_PG_DG_s	4	0.0	-0.5	-0.4	BB_VL_JA_RM_ER
26	BB_DB_EL_PC_DC_p	equipment	DB_EL_PC_DC_p	MBB	CGP	EL	BB_DB_EL_PC_DC_p	4	0.8	0.4	0.1	BB_VL_JA_RM_ER
27	BB_DB_EL_PC_DC_s	equipment	DB_EL_PC_DC_s	MBB	CGP	EL	BB_DB_EL_PC_DC_s	4	0.8	-0.5	0.1	BB_VL_JA_RM_ER
28	BB_DB_EL_PD_PG	equipment	DB_EL_PD_PG	MBB	CGP	EL	BB_DB_EL_PD_PG	4	-0.9	0.4	-0.5	BB_VL_JA_RM_ER
29	BB_DB_EL_ND_PG_p	equipment	DB_EL_ND_PG_p	MBB	CGP	EL	BB_DB_EL_ND_PG_p	4	0.8	0.4	-0.6	BB_VL_JA_RM_ER
30	BB_DB_EL_ND_PG_s	equipment	DB_EL_ND_PG_s	MBB	CGP	EL	BB_DB_EL_ND_PG_s	4	0.8	-0.5	-0.6	BB_VL_JA_RM_ER
31	BB_NL_EL_HO_AN	numerical	NL_EL_HO_AN	MBB	CGP	EL	BB_NL_EL_HO_AN	4				
32	BB_DB_EL_ND_SE_p	equipment	DB_EL_ND_SE_p	MBB	CGP	EL	BB_DB_EL_ND_SE_p	4	-0.8	0.6	0.0	BB_VL_JA_RM_AM
33	BB_DB_EL_ND_SE_s	equipment	DB_EL_ND_SE_s	MBB	CGP	EL	BB_DB_EL_ND_SE_s	4	-0.8	-0.6	0.0	BB_VL_JA_RM_AM
34	BB_DB_EL_PD_SE	equipment	DB_EL_PD_SE	MBB	CGP	EL	BB_DB_EL_PD_SE	4	-0.8	0.0	0.0	BB_VL_JA_RM_AM
35	BB_DB_EL_SE_BD_a	equipment	DB_EL_SE_BD_a	MBB	CGP	EL	BB_DB_EL_SE_BD_a	4	0.0	0.0	0.0	BB_VL_JA_RM_BA
36	BB_DB_EL_SE_BD_f	equipment	DB_EL_SE_BD_f	MBB	CGP	EL	BB_DB_EL_SE_BD_f	4	0.0	0.0	0.0	BB_VL_JA_RM_BF
37	BB_NL_EL_EE_SM	numerical	NL_EL_EE_SM	MBB	CGP	EL	BB_NL_EL_EE_SM	4				
38	BB_DB_EL_ND_LA_p	equipment	DB_EL_ND_LA_p	MBB	CGP	EL	BB_DB_EL_ND_LA_p	4	-0.5	0.4	0.1	BB_VL_MV_RM_MR
39	BB_DB_EL_ND_LA_s	equipment	DB_EL_ND_LA_s	MBB	CGP	EL	BB_DB_EL_ND_LA_s	4	-0.5	-0.4	0.1	BB_VL_MV_RM_MR
40	BB_DB_EL_PC_AN	equipment	DB_EL_PC_AN	MBB	CGP	EL	BB_DB_EL_PC_AN	4	-0.5	0.0	0.0	BB_VL_MV_RM_MR
41	BB_DB_EL_PD_LC_a	equipment	DB_EL_PD_LC_a	MBB	CGP	EL	BB_DB_EL_PD_LC_a	4	-0.7	0.0	0.0	BB_VL_MV_RM_MR
42	BB_DB_EL_ND_LM_p	equipment	DB_EL_ND_LM_p	MBB	CGP	EL	BB_DB_EL_ND_LM_p	4	-0.6	0.6	0.0	BB_VL_JA_RM_AM
43	BB_DB_EL_ND_LM_s	equipment	DB_EL_ND_LM_s	MBB	CGP	EL	BB_DB_EL_ND_LM_s	4	-0.6	-0.6	0.0	BB_VL_JA_RM_AM
44	BB_DB_EL_PC_MN	equipment	DB_EL_PC_MN	MBB	CGP	EL	BB_DB_EL_PC_MN	4	-0.4	0.0	0.0	BB_VL_JA_RM_AM
45	BB_DB_EL_PD_LC_m	equipment	DB_EL_PD_LC_m	MBB	CGP	EL	BB_DB_EL_PD_LC_m	4	-0.6	0.0	0.0	BB_VL_JA_RM_AM
46	BB_NL_EL_HO_MN	numerical	NL_EL_HO_MN	MBB	CGP	EL	BB_NL_EL_HO_MN	4	0.0	0.0	0.0	BB_VL_JA_RM_AM
47	BB_DB_EL_ND_LF_p	equipment	DB_EL_ND_LF_p	MBB	CGP	EL	BB_DB_EL_ND_LF_p	4	-0.9	0.1	-0.4	BB_VL_FH_RM_WS
48	BB_DB_EL_ND_LF_s	equipment	DB_EL_ND_LF_s	MBB	CGP	EL	BB_DB_EL_ND_LF_s	4	-0.9	-0.3	-0.4	BB_VL_FH_RM_WS
49	BB_DB_EL_PC_FN	equipment	DB_EL_PC_FN	MBB	CGP	EL	BB_DB_EL_PC_FN	4	-0.9	-0.1	-0.4	BB_VL_FH_RM_WS
50	BB_DB_EL_PD_LC_f	equipment	DB_EL_PD_LC_f	MBB	CGP	EL	BB_DB_EL_PD_LC_f	4	-0.8	-0.1	-0.4	BB_VL_FH_RM_WS
51	BB_NL_EL_HO_FN	numerical	NL_EL_HO_FN	MBB	CGP	EL	BB_NL_EL_HO_FN	4	0.0	0.0	0.0	BB_VL_FH_RM_WS
52	BB_DB_EL_ND_PM_p	equipment	DB_EL_ND_PM_p	MBB	CGP	EL	BB_DB_EL_ND_PM_p	4	0.5	0.4	0.1	BB_VL_MV_RM_MR

Figure A.48: Physical Loop method of the CGP showing major inputs required in defining DS3 components in the Physical Loop method

The inputs in terms of the Logical Loop method: the type of components as nodes, which were either terminal or hub as outlined in Section 3.3; the equipment load demand or maximum capacity, which was used to define the lower and upper bounds for the SUBFLOW in scenarios snort, sprint, submerged; the objective function coefficient, which was set to zero, based on the formulation discussed in Subsection 4.3.3; the energy coefficients of each component (see Subsection 3.2.5, more specifically, Table 3.11 on page 99) up to 15 different types of DS3; and the logical layout (x, y, z coordinates) to create a multiplex network (Figure 2.7 in Subsection 2.3.4).

The energy coefficients e of each component node are defined as follows:

- The energy that enters a node is expelled 100% outside the node (IN=-1). This option was used for terminal source nodes, such as fuel, or terminal sink nodes, such as propulsion load.
- The energy that enters a node is dispersed to different types of energy in a form of some fraction (IN=fractional OUT). This reflects the Sankey Diagram practice and could have been used for electrical consumer nodes, including energy storage.
- The energy that enters a node is determined by fractions of at least two different nodes in different systems. This option could have been used for modelling the fuel-air ratio of the diesel generator.
- The energy that could have entered a node could have been specified as a fraction of the total heat received at the node and that fraction of energy would have not been forwarded beyond that node (fractional IN=OUT). This choice could be used to describe the 'coefficient of performance' of cooling systems components (see Subsection 5.5).
- A 'daughter' node could receive 100% energy from two parent nodes from different systems and then store 100% energy output to that daughter node. This could have been used to model sink nodes on the vessel, for example, a seawater node.

A 5.2.7 System Preamble Program

The System Preamble Program (SPP) provides an input menu to physically define DS3 connections. As shown in Figure A.50, it consists of the name of the connection, the DS3 technology (e.g., cabling, piping, trunking), the mitred bend assumption, the shape of the connection (circle or rectangle), the cross sectional dimensions, and the UCL submarine weight classification. For Case Study 5.1, there were more than 400 connections and thus 3600 inputs if each connection requires 9 inputs.

GO BACK TO DATABASE AFTER FILLING THIS WORKSHEET								
Service Line Specification (actual/standard piping/cable size from industry that can be used for multiple services)							must larger than Width	(select from c
Call # Name	DS3 Technology	Mitred Bends (yes/no)	Section Shape (Circle/Rectangle)	Width (mm)	Height (mm) (only for rectangle)	Bend Radius (Weight Classification (1 to 9 UCL)		Valid Service 1
1 DT_1	cabling	yes	circle	89	89	98		3 DT
2 DT_2	cabling	yes	circle	89	89	98		3 DT
3 DT_3	cabling	yes	circle	89	89	98		3 DT
4 DT_4	cabling	yes	circle	89	89	98		3 DT
5 DT_5	cabling	yes	circle	89	89	98		3 DT
6 DT_6	cabling	yes	circle	89	89	98		3 DT
7 DT_7	cabling	yes	circle	89	89	98		3 DT
8 DT_8	cabling	yes	circle	89	89	98		3 DT
9 DT_9	cabling	yes	circle	89	89	98		3 DT
10 DT_10	cabling	yes	circle	89	89	98		3 DT
11 DT_11	cabling	yes	circle	89	89	98		3 DT
12 DT_12	cabling	yes	circle	89	89	98		3 DT
13 DT_13	cabling	yes	circle	89	89	98		3 DT
14 DT_14	cabling	yes	circle	89	89	98		3 DT
15 DT_15	cabling	yes	circle	89	89	98		3 DT
16 DT_16	cabling	yes	circle	89	89	98		3 DT
17 DT_17	cabling	yes	circle	89	89	98		3 DT
18 DT_18	cabling	yes	circle	89	89	98		3 DT
19 DT_19	cabling	yes	circle	89	89	98		3 DT
20 DT_20	cabling	yes	circle	89	89	98		3 DT
21 DT_21	cabling	yes	circle	89	89	98		3 DT
22 DT_22	cabling	yes	circle	89	89	98		3 DT
23 DT_23	cabling	yes	circle	89	89	98		3 DT
24 DT_24	cabling	yes	circle	89	89	98		3 DT
25 DT_25	cabling	yes	circle	89	89	98		3 DT
26 DT_26	cabling	yes	circle	89	89	98		3 DT
27 DT_27	cabling	yes	circle	89	89	98		3 DT
28 DT_28	cabling	yes	circle	89	89	98		3 DT
29 DT_29	cabling	yes	circle	89	89	98		3 DT
30 DT_30	cabling	yes	circle	89	89	98		3 DT
31 DT_31	cabling	yes	circle	89	89	98		3 DT
32 DT_32	cabling	yes	circle	89	89	98		3 DT
33 DT_33	cabling	yes	circle	89	89	98		3 DT
34 DT_34	cabling	yes	circle	89	89	98		3 DT
35 DT_35	cabling	yes	circle	89	89	98		3 DT
36 DT_36	cabling	yes	circle	89	89	98		3 DT
37 DT_37	cabling	yes	circle	89	89	98		3 DT
38 DT_38	cabling	yes	circle	89	89	98		3 DT
39 DT_39	cabling	yes	circle	89	89	98		3 DT
40 DT_40	cabling	yes	circle	89	89	98		3 DT
41 DT_41	cabling	yes	circle	89	89	98		3 DT
42 DT_42	cabling	yes	circle	89	89	98		3 DT
43 DT_43	cabling	yes	circle	89	89	98		3 DT
44 DT_44	cabling	yes	circle	89	89	98		3 DT
45 DT_45	cabling	yes	circle	89	89	98		3 DT
46 DT_46	cabling	yes	circle	89	89	98		3 DT
47 DT_47	cabling	yes	circle	89	89	98		3 DT
48 DT_48	cabling	yes	circle	89	89	98		3 DT
49 DT_49	cabling	yes	circle	89	89	98		3 DT
50 DT_50	cabling	yes	circle	89	89	98		3 DT
51 DT_51	cabling	yes	circle	89	89	98		3 DT
52 DT_52	cabling	yes	circle	89	89	98		3 DT
53 DT_53	cabling	yes	circle	89	89	98		3 DT

Figure A.50: Layout of the SPP showing major inputs required in defining physical DS3 connections

In the SPP, the location of system highways can also be adjusted as is shown in Figure A.51. This provides identifications to be used in the System Connection Program (SCP).

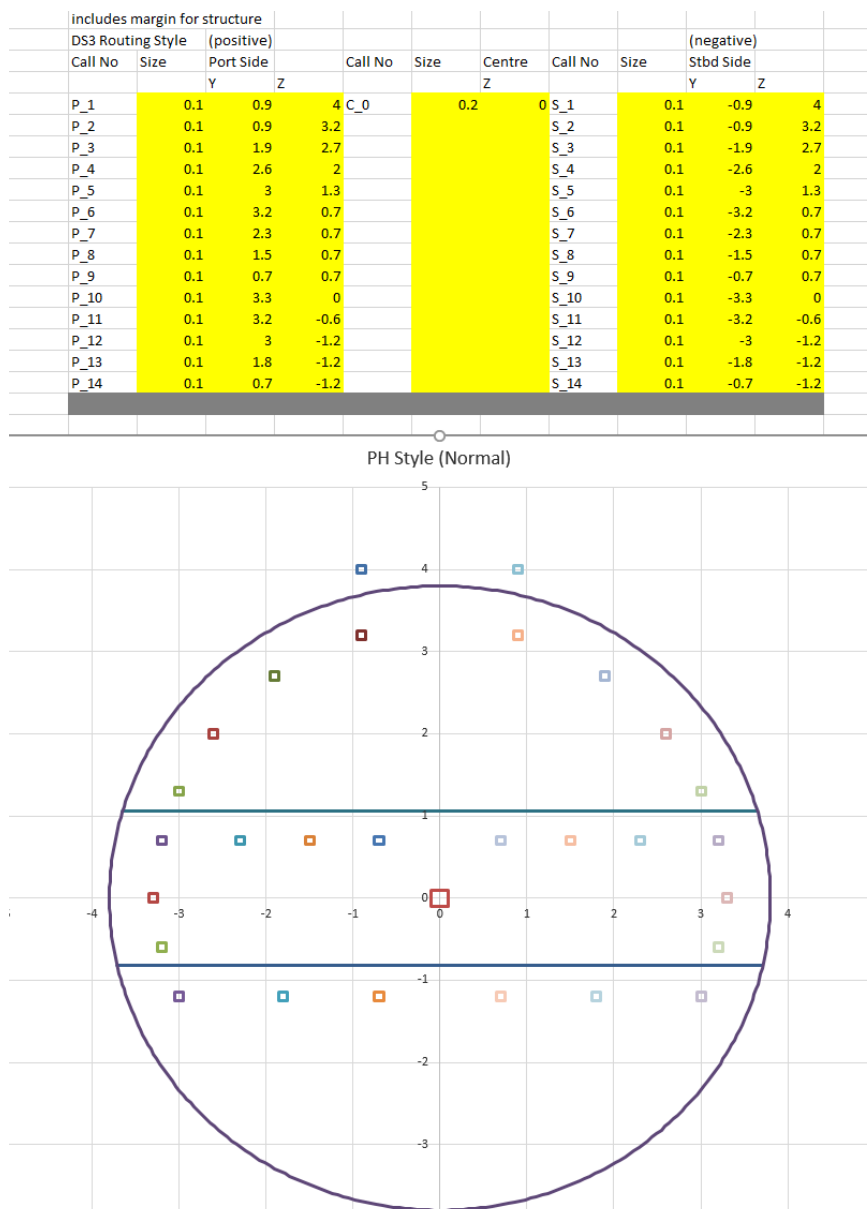


Figure A.51: System highways setup in the SPP showing major inputs required in defining system highways on the vessel

A 5.2.8 System Connection Program

Like the CGP, the System Connection Program (SCP) also provides necessary inputs for the Physical Loop method and Logical Loop method. As shown in Figure A.52, the inputs consist of connection name, physical connection, type of connections, highway defined in SPP, BB hierarchy (up to level 4), the connected DS3 components (source and sink), physical length (calculated from Paramarine). The number of inputs of the SCP in terms of the Physical Loop method for Case Study 5.1 was 4700 as each connection required 10 inputs and there were 470 connections.

ID	Medium (m)	Physical	Type of Connections	Use Set (yes/no)	High	FUNCTIONAL FOR SPATIAL PHYSICAL ARCHITECTURE				LOGICAL ARCHITECTURE		Length (m)				
						1	2	3	4	Direction	Direction		Direction	SELECT FROM ARRANGEMENT TO		
1	DT_1	yes	system_connection	yes	P_9	MBB	FG	SBB	BB1	snort	sprint	sub	BB_DB_DT_CO_AC_a	BB_DB_DT_DD_LC_m	16.9	
2	DT_2	yes	system_connection	yes	P_9	MBB	SCP	DT	BB_DT_2	supply	supply	supply	BB_DB_DT_CO_AC_f	BB_DB_DT_DD_LC_f	9.3	
3	DT_3	yes	system_connection	yes	P_9	MBB	SCP	DT	BB_DT_3	supply	supply	supply	BB_DB_DT_PU_AC	BB_DB_DT_DD_LC_m	14.9	
4	DT_4	yes	system_connection	yes	P_9	MBB	SCP	DT	BB_DT_4	supply	supply	supply	BB_DB_DT_SC_DC	BB_DB_DT_DD_LC_m	12.3	
5	DT_5	yes	system_connection	yes	P_9	MBB	SCP	DT	BB_DT_5	supply	supply	supply	BB_DB_DT_MC_DC	BB_DB_DT_DD_LC_a	8.0	
6	DT_6	yes	system_connection	yes	P_9	MBB	SCP	DT	BB_DT_6	supply	supply	supply	BB_DB_DT_DD_LC_a	BB_DB_DT_DD_AN_p	6.3	
7	DT_7	yes	system_connection	yes	S_9	MBB	SCP	DT	BB_DT_7	supply	supply	supply	BB_DB_DT_DD_LC_a	BB_DB_DT_DD_AN_s	6.3	
8	DT_8	yes	system_connection	yes	P_9	MBB	SCP	DT	BB_DT_8	supply	supply	supply	BB_DB_DT_DD_LC_m	BB_DB_DT_DD_MN_p	6.0	
9	DT_9	yes	system_connection	yes	S_9	MBB	SCP	DT	BB_DT_9	supply	supply	supply	BB_DB_DT_DD_LC_m	BB_DB_DT_DD_MN_s	5.8	
10	DT_10	yes	system_connection	yes	P_9	MBB	SCP	DT	BB_DT_10	supply	supply	supply	BB_DB_DT_DD_LC_f	BB_DB_DT_DD_FN_p	6.2	
11	DT_11	yes	system_connection	yes	S_9	MBB	SCP	DT	BB_DT_11	supply	supply	supply	BB_DB_DT_DD_LC_f	BB_DB_DT_DD_FN_s	6.3	
12	DT_12	yes	system_connection	yes	P_9	MBB	SCP	DT	BB_DT_12	supply	supply	supply	BB_DB_DT_DD_MN_p	BB_DB_DT_DD_AN_p	22.8	
13	DT_13	yes	system_connection	yes	S_9	MBB	SCP	DT	BB_DT_13	supply	supply	supply	BB_DB_DT_DD_MN_s	BB_DB_DT_DD_AN_s	23.0	
14	DT_14	yes	system_connection	yes	P_9	MBB	SCP	DT	BB_DT_14	supply	supply	supply	BB_DB_DT_DD_MN_p	BB_DB_DT_DD_FN_p	21.9	
15	DT_15	yes	system_connection	yes	S_9	MBB	SCP	DT	BB_DT_15	supply	supply	supply	BB_DB_DT_DD_MN_s	BB_DB_DT_DD_FN_s	22.1	
16	DT_16	yes	system_connection	yes	P_9	MBB	SCP	DT	BB_DT_16	supply	supply	supply	BB_DB_DT_DD_AN_p	BB_DB_EL_PG_DG_p	13.6	
17	DT_17	yes	system_connection	yes	S_9	MBB	SCP	DT	BB_DT_17	supply	supply	supply	BB_DB_DT_DD_AN_s	BB_DB_EL_PG_DG_s	13.8	
18	DT_18	yes	system_connection	yes	P_9	MBB	SCP	DT	BB_DT_18	supply	supply	supply	BB_DB_DT_DD_AN_p	BB_DB_EL_PD_PG	11.1	
19	DT_19	yes	system_connection	yes	S_9	MBB	SCP	DT	BB_DT_19	supply	supply	supply	BB_DB_DT_DD_AN_s	BB_DB_EL_PD_PG	12.5	
20	DT_20	yes	system_connection	yes	P_9	MBB	SCP	DT	BB_DT_20	supply	supply	supply	BB_DB_DT_DD_MN_p	BB_DB_EL_PD_SE	6.3	
21	DT_21	yes	system_connection	yes	S_9	MBB	SCP	DT	BB_DT_21	supply	supply	supply	BB_DB_DT_DD_MN_s	BB_DB_EL_PD_SE	6.4	
22	DT_22	yes	system_connection	yes	P_9	MBB	SCP	DT	BB_DT_22	supply	supply	supply	BB_DB_DT_DD_MN_p	BB_DB_EL_SE_BD_a	6.1	
23	DT_23	yes	system_connection	yes	S_9	MBB	SCP	DT	BB_DT_23	supply	supply	supply	BB_DB_DT_DD_MN_s	BB_DB_EL_SE_BD_a	6.2	
24	DT_24	yes	system_connection	yes	P_9	MBB	SCP	DT	BB_DT_24	supply	supply	supply	BB_DB_DT_DD_MN_p	BB_DB_EL_SE_BD_f	20.5	
25	DT_25	yes	system_connection	yes	S_9	MBB	SCP	DT	BB_DT_25	supply	supply	supply	BB_DB_DT_DD_MN_s	BB_DB_EL_SE_BD_f	20.7	
26	DT_26	yes	system_connection	yes	P_9	MBB	SCP	DT	BB_DT_26	supply	supply	supply	BB_DB_DT_DD_AN_p	BB_DB_EL_PC_AN	2.3	
27	DT_27	yes	system_connection	yes	S_9	MBB	SCP	DT	BB_DT_27	supply	supply	supply	BB_DB_DT_DD_AN_s	BB_DB_EL_PC_AN	2.3	
28	DT_28	yes	system_connection	yes	P_9	MBB	SCP	DT	BB_DT_28	supply	supply	supply	BB_DB_DT_DD_MN_p	BB_DB_EL_PC_MN	4.9	
29	DT_29	yes	system_connection	yes	S_9	MBB	SCP	DT	BB_DT_29	supply	supply	supply	BB_DB_DT_DD_MN_s	BB_DB_EL_PC_MN	5.1	
30	DT_30	yes	system_connection	yes	P_9	MBB	SCP	DT	BB_DT_30	supply	supply	supply	BB_DB_DT_DD_FN_p	BB_DB_EL_PC_FN	10.1	
31	DT_31	yes	system_connection	yes	S_9	MBB	SCP	DT	BB_DT_31	supply	supply	supply	BB_DB_DT_DD_FN_s	BB_DB_EL_PC_FN	9.2	
32	DT_32	yes	system_connection	yes	P_9	MBB	SCP	DT	BB_DT_32	supply	supply	supply	BB_DB_DT_DD_AN_p	BB_DB_EL_SG_PM	7.7	
33	DT_33	yes	system_connection	yes	S_9	MBB	SCP	DT	BB_DT_33	supply	supply	supply	BB_DB_DT_DD_AN_s	BB_DB_EL_SG_PM	7.7	
34	DT_34	yes	system_connection	yes	P_9	MBB	SCP	DT	BB_DT_34	supply	supply	supply	BB_DB_DT_DD_AN_p	BB_DB_ME_PM_DC	6.5	
35	DT_35	yes	system_connection	yes	S_9	MBB	SCP	DT	BB_DT_35	supply	supply	supply	BB_DB_DT_DD_AN_s	BB_DB_ME_PM_DC	7.9	
36	DT_36	yes	system_connection	yes	P_9	MBB	SCP	DT	BB_DT_36	supply	supply	supply	BB_DB_DT_DD_AN_p	BB_DB_HY_HS_DC	6.8	
37	DT_37	yes	system_connection	yes	S_9	MBB	SCP	DT	BB_DT_37	supply	supply	supply	BB_DB_DT_DD_AN_s	BB_DB_HY_HS_DC	8.2	
38	DT_38		troubleshooting	ction	yes	P_9	MBB	SCP	DT	BB_DT_38	supply	supply	supply	BB_DB_DT_DD_AN_p	BB_DB_HY_HS_AC	8.2
39	DT_39		troubleshooting	ction	yes	S_9	MBB	SCP	DT	BB_DT_39	supply	supply	supply	BB_DB_DT_DD_AN_s	BB_DB_HY_HS_AC	6.8
40	DT_40		troubleshooting	ction	yes	P_9	MBB	SCP	DT	BB_DT_40	supply	supply	supply	BB_DB_DT_DD_MN_p	BB_DB_HY_IT_AC	4.4
41	DT_41		troubleshooting	ction	yes	S_9	MBB	SCP	DT	BB_DT_41	supply	supply	supply	BB_DB_DT_DD_MN_s	BB_DB_HY_IT_AC	6.0
42	DT_42	yes	system_connection	yes	P_9	MBB	SCP	DT	BB_DT_42	supply	supply	supply	BB_DB_DT_DD_MN_p	BB_DB_HY_ET_AC	5.7	
43	DT_43	yes	system_connection	yes	S_9	MBB	SCP	DT	BB_DT_43	supply	supply	supply	BB_DB_DT_DD_MN_s	BB_DB_HY_ET_AC	6.1	
44	DT_44	yes	system_connection	yes	P_9	MBB	SCP	DT	BB_DT_44	supply	supply	supply	BB_DB_DT_DD_AN_p	BB_DB_TB_PB_AD	18.6	
45	DT_45	yes	system_connection	yes	S_9	MBB	SCP	DT	BB_DT_45	supply	supply	supply	BB_DB_DT_DD_AN_s	BB_DB_TB_PB_AD	17.3	
46	DT_46	yes	system_connection	yes	P_9	MBB	SCP	DT	BB_DT_46	supply	supply	supply	BB_DB_DT_DD_AN_p	BB_DB_TB_PH_DC_a	18.6	
47	DT_47	yes	system_connection	yes	S_9	MBB	SCP	DT	BB_DT_47	supply	supply	supply	BB_DB_DT_DD_AN_s	BB_DB_TB_PH_DC_a	17.2	
48	DT_48	yes	system_connection	yes	P_9	MBB	SCP	DT	BB_DT_48	supply	supply	supply	BB_DB_DT_DD_AN_p	BB_DB_TB_PS_AC_a	16.2	
49	DT_49	yes	system_connection	yes	S_9	MBB	SCP	DT	BB_DT_49	supply	supply	supply	BB_DB_DT_DD_AN_s	BB_DB_TB_PS_AC_a	14.8	
50	DT_50	yes	system_connection	yes	P_9	MBB	SCP	DT	BB_DT_50	supply	supply	supply	BB_DB_DT_DD_FN_p	BB_DB_TB_PH_AC_f	12.8	
51	DT_51	yes	system_connection	yes	S_9	MBB	SCP	DT	BB_DT_51	supply	supply	supply	BB_DB_DT_DD_FN_s	BB_DB_TB_PH_AC_f	11.3	
52	DT_52	yes	system_connection	yes	P_9	MBB	SCP	DT	BB_DT_52	supply	supply	supply	BB_DB_DT_DD_FN_p	BB_DB_TB_PS_AC_f	10.9	

Figure A.52: Physical Loop method of SCP showing major inputs required in defining DS3 connections in the Physical Loop method

In terms of the Logical Loop method, the input consists of the identification of DS3 technologies (see plexus (PL) 0 to 15), the minimum and maximum capacity of the connection based on a given scenario (snort, sprint, submerged), and the objective function coefficient, which was set to zero, based on the formulation discussed in Subsection 4.3.3. Once these inputs had been defined, the CPLEX tool in MATLAB was used to calculate the SUBFLOW solution. For Case Study 5.1, the inputs in the SCP for Logical Loop method were 470, if each connection requires 7 inputs, that meant 3290 inputs.

ID	Medium (m	PL ID	lb	ub snort	ub sprint	ub sub	OFF	OFV
1	DT_1	PL0	0	1.00E+99	1.00E+99	1.00E+99	0	0
2	DT_2	PL0	0	1.00E+99	1.00E+99	1.00E+99	0	0
3	DT_3	PL0	0	1.00E+99	1.00E+99	1.00E+99	0	0
4	DT_4	PL0	0	1.00E+99	1.00E+99	1.00E+99	0	0
5	DT_5	PL0	0	1.00E+99	1.00E+99	1.00E+99	0	0
6	DT_6	PL0	0	1.00E+99	1.00E+99	1.00E+99	0	0
7	DT_7	PL0	0	1.00E+99	1.00E+99	1.00E+99	0	0
8	DT_8	PL0	0	1.00E+99	1.00E+99	1.00E+99	0	0
9	DT_9	PL0	0	1.00E+99	1.00E+99	1.00E+99	0	0
10	DT_10	PL0	0	1.00E+99	1.00E+99	1.00E+99	0	0
11	DT_11	PL0	0	1.00E+99	1.00E+99	1.00E+99	0	0
12	DT_12	PL0	0	1.00E+99	1.00E+99	1.00E+99	0	0
13	DT_13	PL0	0	1.00E+99	1.00E+99	1.00E+99	0	0
14	DT_14	PL0	0	1.00E+99	1.00E+99	1.00E+99	0	0
15	DT_15	PL0	0	1.00E+99	1.00E+99	1.00E+99	0	0
16	DT_16	PL0	0	1.00E+99	1.00E+99	1.00E+99	0	0
17	DT_17	PL0	0	1.00E+99	1.00E+99	1.00E+99	0	0
18	DT_18	PL0	0	1.00E+99	1.00E+99	1.00E+99	0	0
19	DT_19	PL0	0	1.00E+99	1.00E+99	1.00E+99	0	0
20	DT_20	PL0	0	1.00E+99	1.00E+99	1.00E+99	0	0
21	DT_21	PL0	0	1.00E+99	1.00E+99	1.00E+99	0	0
22	DT_22	PL0	0	1.00E+99	1.00E+99	1.00E+99	0	0
23	DT_23	PL0	0	1.00E+99	1.00E+99	1.00E+99	0	0
24	DT_24	PL0	0	1.00E+99	1.00E+99	1.00E+99	0	0
25	DT_25	PL0	0	1.00E+99	1.00E+99	1.00E+99	0	0
26	DT_26	PL0	0	1.00E+99	1.00E+99	1.00E+99	0	0
27	DT_27	PL0	0	1.00E+99	1.00E+99	1.00E+99	0	0
28	DT_28	PL0	0	1.00E+99	1.00E+99	1.00E+99	0	0
29	DT_29	PL0	0	1.00E+99	1.00E+99	1.00E+99	0	0
30	DT_30	PL0	0	1.00E+99	1.00E+99	1.00E+99	0	0
31	DT_31	PL0	0	1.00E+99	1.00E+99	1.00E+99	0	0
32	DT_32	PL0	0	1.00E+99	1.00E+99	1.00E+99	0	0
33	DT_33	PL0	0	1.00E+99	1.00E+99	1.00E+99	0	0
34	DT_34	PL0	0	1.00E+99	1.00E+99	1.00E+99	0	0
35	DT_35	PL0	0	1.00E+99	1.00E+99	1.00E+99	0	0
36	DT_36	PL0	0	1.00E+99	1.00E+99	1.00E+99	0	0
37	DT_37	PL0	0	1.00E+99	1.00E+99	1.00E+99	0	0
38	DT_38	PL0	0	1.00E+99	1.00E+99	1.00E+99	0	0
39	DT_39	PL0	0	1.00E+99	1.00E+99	1.00E+99	0	0
40	DT_40	PL0	0	1.00E+99	1.00E+99	1.00E+99	0	0
41	DT_41	PL0	0	1.00E+99	1.00E+99	1.00E+99	0	0
42	DT_42	PL0	0	1.00E+99	1.00E+99	1.00E+99	0	0
43	DT_43	PL0	0	1.00E+99	1.00E+99	1.00E+99	0	0
44	DT_44	PL0	0	1.00E+99	1.00E+99	1.00E+99	0	0
45	DT_45	PL0	0	1.00E+99	1.00E+99	1.00E+99	0	0
46	DT_46	PL0	0	1.00E+99	1.00E+99	1.00E+99	0	0
47	DT_47	PL0	0	1.00E+99	1.00E+99	1.00E+99	0	0
48	DT_48	PL0	0	1.00E+99	1.00E+99	1.00E+99	0	0
49	DT_49	PL0	0	1.00E+99	1.00E+99	1.00E+99	0	0
50	DT_50	PL0	0	1.00E+99	1.00E+99	1.00E+99	0	0
51	DT_51	PL0	0	1.00E+99	1.00E+99	1.00E+99	0	0
52	DT_52	PL0	0	1.00E+99	1.00E+99	1.00E+99	0	0
53	DT_53	PL0	0	1.00E+99	1.00E+99	1.00E+99	0	0

Figure A.53: Logical Loop method of SCP showing major inputs required in defining DS3 connections in the Logical Loop method

Appendix 6

Codes

The following is a list of abbreviated codes in the NBA. This purpose is to show the format of the VBA and MATLAB codes and to allow reproducing results and facilitating the use of the proposed NBA. The actual code is over 8000 lines long. The full set of source codes is available from the author.

A 6.1 VBA Codes

Table A 2: Summary of codes in the Input Data Centre

Program	Description	Script Identifier	Size (Lines)
MMP	Main Menu Program	A_A_MMP	42
DPP	Design Preamble Program	A_B_DPP	238
DAP	Design Analysis Program	A_C_DAP	537
HGP	Hull Granularity Program	C_A_HGP	1460
VGP	Volume Granularity Program	C_B_VGP	910
		C_C_VGP	254
		C_D_VGP	148
WGP	Weight Granularity Program	B_A_WGP	710
		B_B_WGP	191
EDP	Equipment Database Program	D_A_EDP	556
		D_B_EDP	1200
CGP	Component Granularity Program	D_C_CGP	555
		D_D_CGP	684
		D_E_CGP	81
SPP	System Preamble Program	E_A_SPP	369
SCP	System Connection Program	E_B_SCP	300
		E_C_SCP	756
KCL Output (for Case Study 5.1)			>25000

A_A_MMP (42 lines)

```

'MAIN MENU PROGRAM

Sub MMP ()

Dim StartTime As Double
Dim SecondsElapsed As Double

'Remember time when macro starts
    StartTime = Timer

    Worksheets("MMP").Activate

        Dim myfilepath As String
            myfilepath = Range("J7")
        Dim myFile As Integer
            myFile = FreeFile
        Open myfilepath For Output As #myFile

            Print #1, "newdesign"

'Remember time when macro starts
    'beware of the order of the code!'

    Call DPP 'Design Preamble Program
    Call HGP 'Hull Geometry Program
    Call VGP 'Volume Geometry Program
    Call WGP 'Weight Granularity Program
    Call SPP 'Systems Preamble Program
    Call EDP 'Equipment Database Program
    Call CGP 'Component Granularity Program
    Call SCP 'System Connection Program
    Call DAP 'Design Analysis Program

    Worksheets("MMP").Activate
    Close #myFile

'Remember time when macro starts
    'Determine how many seconds code took to run
    SecondsElapsed = Round(Timer - StartTime, 2)

'Remember time when macro starts
    'Notify user in seconds
    MsgBox "This code ran successfully in " & SecondsElapsed & " seconds",
vbInformation

End Sub

```


A_B_DPP (238 lines)

```

'DESIGN PREAMBLE PROGRAM

Sub DPP()

    'Preamble
    Print #1, "new concept_placeholder DPPO"
    Print #1, "new concept_placeholder SPPO"
    Print #1, "new concept_placeholder EDPO"
    Print #1, "{EDPO} new equipment_container equipment_database"
    'Insert design audit preamble
    Print #1, "set_layer(256, 1.0000000000, 0.0000000000, 0.0000000000, 0,
1.0000000000, 0.0000000000, 0.0000000000, 1, "FIGHT")" 'RED FOR FIGHT
    Print #1, "set_layer(257, 1.0000000000, 1.0000000000, 0.0000000000, 0,
1.0000000000, 1.0000000000, 0.0000000000, 1, "MOVE")" 'YELLOW FOR MOVE
    Print #1, "set_layer(258, 0.0000000000, 1.0000000000, 0.0000000000, 0,
0.0000000000, 1.0000000000, 0.0000000000, 1, "INFRASTRUCTURE")" 'GREEN
FOR INFRASTRUCTURE
    Print #1, "set_layer(259, 0.0000000000, 1.0000000000, 1.0000000000, 0,
0.0000000000, 0.5019607843, 0.7529411765, 1, "FLOAT")" 'LIGHT BLUE FOR
FLOAT
    Print #1, "set_layer(264, 0.3647058824, 0.3647058824, 0.3647058824, 1,
0.1529411765, 0.1529411765, 0.1529411765, 1, "PL0")"

    Print #1, "set_layer(277, 1.0000000000, 0.5019607843, 0.0000000000, 1,
0.5019607843, 0.0000000000, 0.0000000000, 1, "PL13")"
    Print #1, "set_layer(278, 1.0000000000, 0.0000000000, 0.0000000000, 1,
0.6431372549, 0.0000000000, 0.0000000000, 1, "PL14")"
    'weight group classifications
    Print #1, "{DPPO} new concept_placeholder weight_group_classifications"
    Print #1, "{DPPO.weight_group_classifications} new classification
UCL_SUB_weight_groups"
    Print #1,
"{DPPO.weight_group_classifications.UCL_SUB_weight_groups} new
classification group_1_structure"
    Print #1,
"{DPPO.weight_group_classifications.UCL_SUB_weight_groups.group_1_structure
} new classification subgp_10_pressure_hull"
    Print #1,
"{DPPO.weight_group_classifications.UCL_SUB_weight_groups.group_9_variable_
load} new classification subgp_90_variable_load_items"
    Print #1,
"{DPPO.weight_group_classifications.UCL_SUB_weight_groups.group_9_variable_
load} new classification subgp_91_trim_and_compensation_water"
    Print #1,
"{DPPO.weight_group_classifications.UCL_SUB_weight_groups.group_9_variable_
load} new classification subgp_92_main_ballast_water"

    'consumables or densities
    Print #1, "{DPPO} new consumables_container consumables"
    Print #1, "{DPPO.consumables} new density seawater"
    Print #1, "{DPPO.consumables} new density fresh_water"
    Print #1, "{DPPO.consumables} new density dieso"

End Sub

```


B_B_WGP (191 lines)

```
'WEIGHT GRANULARITY PROGRAM

Sub buildingblocknumerical ()

B1 = ActiveCell.Offset(0, Adj1 - 1) 'ADJUSTMENT OBJECT TYPE
B2 = ActiveCell.Offset(0, Adj1) 'ADJUSTMENT equipment from active BB
B4 = ActiveCell.Offset(0, Adj1 + 3) 'ADJUSTMENT colour/layer using SBB
A1 = ActiveCell.Offset(0, Adj2) 'ADJUSTMENT location X
A2 = ActiveCell.Offset(0, Adj2 + 1) 'ADJUSTMENT location Y
A3 = ActiveCell.Offset(0, Adj2 + 2) 'ADJUSTMENT location Z

ITM = ActiveCell 'ADJUSTMENT for item

'If IsEmpty(EI) = False Then 'USELESS BECAUSE ITS A STRING

Print #1, BB; "} new building_block " & ITM
Print #1, BB; "." & ITM; ".attributes.ignore_sub_blocks_use_this}"
Print #1, BB; "." & ITM; ".attributes.initial_geometry.none}"

If A6 = "TBC" Then
Else

    If B1 = "permanent" Then
        Print #1, BB; "." & ITM; ".attributes.characteristics} new char_weight
" & ITM
        Print #1, BB; "." & ITM; ".attributes.characteristics." & ITM;
".permanent_weight}"

        If A5 = 1 Then
            Print #1, BB; "." & ITM; ".attributes.characteristics." & ITM;
".classification}-
>DPPO.weight_group_classifications.UCL_SUB_weight_groups.group_1_structure"
        ElseIf A5 = 2 Then
            Print #1, BB; "." & ITM; ".attributes.characteristics." & ITM;
".classification}-
>DPPO.weight_group_classifications.UCL_SUB_weight_groups.group_2_main_propu
lsion"

'LOCATION

    If B2 = "manual" Then

        Print #1, BB; "." & ITM; ".attributes.datum_point.x}=" & A1; " [m ]"
        Print #1, BB; "." & ITM; ".attributes.datum_point.y}=" & A2; " [m ]"
        Print #1, BB; "." & ITM; ".attributes.datum_point.z}=" & A3; " [m ]"

    Else

        Worksheets("VGP").Activate

    End If
End Sub
```

C_A_HGP (1460 lines)

```
'HULL GRANULARITY PROGRAM
```

```
Sub HGP()
```

```
Worksheets("HGP").Activate
```

```
Print #1, "new geom_placeholder HGPO"
Print #1, "{HGPO} new geom_placeholder construction_geometry"
Print #1, "{HGPO.construction_geometry} new geom_placeholder raw_geometry"
Print #1, "{HGPO.construction_geometry.raw_geometry} new geom_placeholder
internal"
Print #1, "{HGPO.construction_geometry.raw_geometry.internal} new
geom_placeholder construction_geometry"
Print #1,
"{HGPO.construction_geometry.raw_geometry.internal.construction_geometry}
new body_revolved body_revolved"
Print #1,
"{HGPO.construction_geometry.raw_geometry.internal.construction_geometry.bo
dy_revolved.profile.segments} new segment segment"
Print #1,
"{HGPO.construction_geometry.raw_geometry.internal.construction_geometry.bo
dy_revolved.profile.segments} new segment segment_1"
Print #1,
"{HGPO.construction_geometry.raw_geometry.internal.construction_geometry.bo
dy_revolved.profile.segments} new segment segment_4"
Print #1, "{HGPO.construction_geometry.raw_geometry.internal} new
geom_placeholder visible_geometry"
Print #1,
"{HGPO.construction_geometry.raw_geometry.internal.visible_geometry} new
solid body solid_body"
Print #1, "{HGPO.construction_geometry.raw_geometry} new geom_placeholder
external"
Print #1, "{HGPO.construction_geometry.raw_geometry.external} new
geom_placeholder fwd_end"
Print #1, "{HGPO.construction_geometry.raw_geometry.external.fwd_end} new
geom_placeholder construction_geometry"
Print #1,
"{HGPO.construction_geometry.raw_geometry.external.fwd_end.construction_geo
metry} new geom_placeholder input"
Print #1,
"{HGPO.construction_geometry.raw_geometry.external.fwd_end.construction_geo
metry.input} new geom_placeholder boundary"
Print #1,
"{HGPO.construction_geometry.raw_geometry.external.fwd_end.construction_geo
metry.input.boundary} new xt_curve xt_curve"
Print #1, "{HGPO.reference.FS.chopping_points.for_next.by_increment}"
Print #1, "{HGPO.reference.FS.chopping_points.for_next.increment}=0.500
[m]"
Print #1, "{HGPO.reference.FS.chopping_points.for_next.start}=HGPO.con-
struction_geometry.sizing_geometry.output.distances.loa / -2.000"
Print #1, "{HGPO.reference.FS.chopping_points.for_next.stop}=HGPO.construc-
tion_geometry.sizing_geometry.output.distances.loa / 2.000"
Print #1, "{HGPO.reference.FS.solid_geometry.body_pointer}->HGPO.visi-
ble_geomerty.appendages.HL_fwd_plane_s"
Print #1, "{HGPO.reference.FS.section}"
```

```
End Sub
```

C_B_VGP (910 lines)

```

' VOLUME GRANULARITY PROGRAM
Sub VGP() 'Volume Granularity Programme
Print #1, "new concept_placeholder MMPO"
Worksheets("VGP").Activate
Range("A4").Select 'ADJUST HERE, *first line of data*.
' Set Do loop to stop when an empty cell is reached.
CountData = 0
Do Until IsEmpty(ActiveCell)
' Insert your code here.
adj0 = 5 'BB level locations ADJUST RESTORE TOO!
ActiveCell.Offset(0, adj0).Select 'BB level locations ADJUST RESTORE TOO!
'Do Until IsEmpty(ActiveCell)
Do Until CountBB = 8
' Insert your code here.
CountBB = CountBB + 1
'Equipment Countainer Level 2 FOUR
If CountBB = 4 Then
BB = "{MMPO." & ActiveCell.Offset(0, -3) & "." & ActiveCell.Offset(0, -2) &
"." & ActiveCell.Offset(0, -1)
BB0 = "MMPO." & ActiveCell.Offset(0, -3) & "." & ActiveCell.Offset(0, -2) &
"." & ActiveCell.Offset(0, -1)
If CountData > 0 And ActiveCell.Offset(-1, -3) = ActiveCell.Offset(0, -
3) And ActiveCell.Offset(-1, -2) = ActiveCell.Offset(0, -2) And
ActiveCell.Offset(-1, -1) = ActiveCell.Offset(0, -1) And Not
ActiveCell.Offset(-1, 0) = ActiveCell And IsEmpty(ActiveCell.Offset(0, 1))
= False Then
Print #1, BB; "} new building_block " & ActiveCell
Print #1, BB; "." & ActiveCell;
".attributes.use_sub_blocks_ignore_this}"

'Equipment Level
ElseIf CountData = 0 And IsEmpty(ActiveCell) = False And
IsEmpty(ActiveCell.Offset(0, 1)) = True Then

Adj1 = -4 'ADJUSTMENT equipment from SBB in Arrangement Worksheet
Adj2 = 6 'ADJUSTMENT locations in Arrangement Worksheet

Call gtwo 'BBBBBBBBBBBBBBBBBBBBBB' BB PLACEMENT
End If
End If
' Step right 1 row from present location.
ActiveCell.Offset(0, 1).Select
Loop

Restore = CountBB + adj0 'Location of Cell J3 in the sheet ADJUST
HERE TOO
' Step down 1 row from present location.
ActiveCell.Offset(1, -Restore).Select
CountBB = 0
CountData = CountData + 1
'Range("I9").value = CountDATA UNCOMMENT THIS FOR TROUBLESHOOTING

Loop

'Range("I9").value = -Restore
End Sub

```

C_C_VGP (254 lines)

```

' VOLUME GRANULARITY PROGRAM

Sub gtwo()
OT = ActiveCell.Offset(0, Adj1 - 1) 'ADJUSTMENT OBJECT TYPE
(RM/TC/BT/TT/FR)
HC = ActiveCell.Offset(0, Adj1) 'ADJUSTMENT G2 HL from active BB

ITM = ActiveCell 'ADJUSTMENT for item

Print #1, BB; "} new building_block " & ITM
Print #1, BB; "." & ITM; ".attributes.ignore_sub_blocks_use_this}"
Print #1, BB; "." & ITM; ".attributes.initial_geometry.from_construction}"
Print #1, BB; "." & ITM;
".attributes.initial_geometry.construction_geometry} new point AA"
Print #1, BB; "." & ITM;
".attributes.initial_geometry.construction_geometry} new point BB"
Print #1, BB; "." & ITM;
".attributes.initial_geometry.construction_geometry.AA}translate (" & AX;
[m]," & AY; "[m]," & AZ; "[m])"
Print #1, BB; "." & ITM;
".attributes.initial_geometry.construction_geometry.BB}translate (" & BX;
[m]," & BY; "[m]," & BZ; "[m])"
Print #1, BB; "." & ITM;
".attributes.initial_geometry.visible_geometry.solid}cuboid ("; BBO; "." &
ITM; ".attributes.initial_geometry.construction_geometry.AA, "; BBO; "." &
ITM; ".attributes.initial_geometry.construction_geometry.BB)"
Print #1, BB; "." & ITM; ".attributes.datum_point.x="; BBO; "." & ITM;
".attributes.initial_geometry.visible_geometry.solid.attributes.centroid.x"
Print #1, BB; "." & ITM; ".attributes.datum_point.y="; BBO; "." & ITM;
".attributes.initial_geometry.visible_geometry.solid.attributes.centroid.y"
Print #1, BB; "." & ITM; ".attributes.datum_point.z="; BBO; "." & ITM;
".attributes.initial_geometry.visible_geometry.solid.attributes.centroid.z"

Print #1, BB; "." & ITM;
".attributes.initial_geometry.visible_geometry.solid} re_facet (5.000 [m],
0.100 [mm], 5.000 [deg] )"

If SC = "yes" Then
Print #1, BB; "." & ITM; "} intersect (HGPO.visible_geomerty." & IL; "." &
SO; " )"
End If

'COLORING
If HC = "fight" Then
Print #1, BB; "." & ITM; "}change_layer 256"
ElseIf HC = "move" Then
Print #1, BB; "." & ITM; "}change_layer 257"
ElseIf HC = "infrastructure" Then
Print #1, BB; "." & ITM; "}change_layer 258"
ElseIf HC = "float" Then
Print #1, BB; "." & ITM; "}change_layer 18"
End If

End Sub

```

C_D_VGP (148 lines)

```

' VOLUME GRANULARITY PROGRAM

Sub R_VGP()

Dim myFile As String, text As String, textline As String, posLat As
Integer, posLong As Integer
myFile = "C:\Paramarine_data\Macros\OUTPUT.kcl"
Open myFile For Input As #1

Do Until EOF(1)
    Line Input #1, textline
    text = text & textline
Loop

Close #1

Worksheets("VGP").Activate
Range("F4").Select 'ADJUST HERE, *first line of data*.
' Set Do loop to stop when an empty cell is reached.

'OUTPUT = 9 'location of output EARLY STAGE

OUTPUT = 65 'location of output EARLY STAGE

'BB0 = "MMPO." & ActiveCell.Offset(0, -4) & "." & ActiveCell.Offset(0, -3)
& "." & ActiveCell.Offset(0, -2) & "." & ActiveCell.Offset(0, -1)

CountData = 0

Do Until IsEmpty(ActiveCell)
    ' Insert your code here.

'point A x
BB = "{MMPO." & ActiveCell.Offset(0, 0) & "." & ActiveCell.Offset(0, 1) &
"." & ActiveCell.Offset(0, 2) & "." & ActiveCell.Offset(0, 3) &
".attributes.initial_geometry.construction_geometry.AA}translate"
posDATA = InStr(text, BB)
posDATAx = InStr(Mid(text, posDATA, 106), "translate (")
ActiveCell.Offset(0, OUTPUT).value = Mid(text, posDATA + posDATAx + 10, 5)

posDATAy = InStr(Mid(text, posDATA, 110), "[m],")
ActiveCell.Offset(0, OUTPUT + 1).value = Mid(text, posDATA + posDATAy + 3,
5) 'READ KCL DATA

posDATAz = InStr(Mid(text, posDATA + 110, 20), "[m],")
ActiveCell.Offset(0, OUTPUT + 2).value = Mid(text, posDATA + 110 + posDATAz
+ 3, 5) 'READ KCL DATA
' Restore = OUTPUT 'Location of Cell J3 in the sheet ADJUST HERE TOO
' Step down 1 row from present location.
ActiveCell.Offset(1, 0).Select
CountData = CountData + 1
'Range("I9").value = CountDATA UNCOMMENT THIS FOR TROUBLESHOOTING

Loop

End Sub

```

D_A_EDP (556 lines)

```

' EQUIPMENT DATABASE PROGRAM

Public AA As String ' AGAIN IS EMPTY IS NOT WORKING FOR EMPTY CELL
Public AA0 As String

Public Adj1 As String 'ADJUSTMENT shape (see EQUIP)
Public Adj2 As String 'ADJUSTMENT connection point (see EQUIP)

Sub EDP() 'Equipment Database Programme

    Worksheets("EDP").Activate

    Range("A4").Select 'ADJUST HERE, *first line of data*.
    ' Set Do loop to stop when an empty cell is reached.
    CountData = 0

    Do Until IsEmpty(ActiveCell)
        ActiveCell.Offset(0, 8).Select
        'Do Until IsEmpty(ActiveCell)
        Do Until CountBB = 8
            ' Insert your code here.
            CountBB = CountBB + 1
            'Concept Placeholder Level ONE
            If CountBB = 1 Then
                AA = "{EDPO.equipment_database}"
                If CountData = 0 And IsEmpty(ActiveCell) = False Then
                    Print #1, AA; "new equipment_container " & ActiveCell
                ElseIf CountData > 0 And Not ActiveCell.Offset(-1, 0) =
ActiveCell Then
                    Print #1, AA; "new equipment_container " & ActiveCell
                End If
            End If
            'Equipment Countainer Level 1 THREE
            ElseIf CountData = 0 And IsEmpty(ActiveCell) = False And
IsEmpty(ActiveCell.Offset(0, 1)) = True Then
                Print #1, AA; "} new equipment " & ActiveCell
                Adj1 = -7
                Adj2 = 8 'last BB to attributes
                Call equip
            End If
            ' Step right 1 row from present location.
            ActiveCell.Offset(0, 1).Select
            Loop
            Restore = CountBB + 8 'Location of Cell J3 in the sheet
            ActiveCell.Offset(1, -Restore).Select
            CountBB = 0
            CountData = CountData + 1
            'Range("I9").value = CountDATA UNCOMMENT THIS FOR TROUBLESHOOTING
            Loop
            'Range("I9").value = -Restore
        Worksheets("MMP").Activate
        Close #myFile
    End Sub

```


D_B_EDP (1200 lines)

```

' EQUIPMENT DATABASE PROGRAM

Sub equip()

        ii = ActiveCell.Offset(0, Adj1) 'ADJUSTMENT Shape
        jj = ActiveCell.Offset(0, Adj1 + 1) 'ADJUSTMENT L
        kk = ActiveCell.Offset(0, Adj1 + 2) 'ADJUSTMENT B
        ll = ActiveCell.Offset(0, Adj1 + 3) 'ADJUSTMENT H

If ii = "cylinder" Then
    If llo = "X" Then
        Print #1, AA; "." & ActiveCell; ".construction_geometry.H)=" & kk;
        "[m]"
        Print #1, AA; "." & ActiveCell; ".nodes.top.z_offset)=" & AA0; "." &
ActiveCell; ".construction_geometry.B/2"
        Print #1, AA; "." & ActiveCell; ".nodes.bottom.z_offset)=" & AA0; "." &
ActiveCell; ".construction_geometry.B/-2"
        Print #1, AA; "." & ActiveCell; ".nodes.fwd.x_offset)=" & AA0; "." &
ActiveCell; ".construction_geometry.L/2"
        Print #1, AA; "." & ActiveCell; ".nodes.aft.x_offset)=" & AA0; "." &
ActiveCell; ".construction_geometry.L/-2"
        Print #1, AA; "." & ActiveCell; ".nodes.port.y_offset)=" & AA0; "." &
ActiveCell; ".construction_geometry.B/2"
        Print #1, AA; "." & ActiveCell; ".nodes.stbd.y_offset)=" & AA0; "." &
ActiveCell; ".construction_geometry.B/-2"
        ElseIf llo = "Y" Then
            Print #1, AA; "." & ActiveCell; ".construction_geometry.H)=" & kk;
            "[m]"
            Print #1, AA; "." & ActiveCell; ".nodes.top.z_offset)=" & AA0; "." &
ActiveCell; ".construction_geometry.B/2"
            Print #1, AA; "." & ActiveCell; ".nodes.bottom.z_offset)=" & AA0; "." &
ActiveCell; ".construction_geometry.B/-2"
            Print #1, AA; "." & ActiveCell; ".nodes.fwd.x_offset)=" & AA0; "." &
ActiveCell; ".construction_geometry.B/2"
            Print #1, AA; "." & ActiveCell; ".nodes.aft.x_offset)=" & AA0; "." &
ActiveCell; ".construction_geometry.B/-2"
            Print #1, AA; "." & ActiveCell; ".nodes.port.y_offset)=" & AA0; "." &
ActiveCell; ".construction_geometry.L/2"
            Print #1, AA; "." & ActiveCell; ".nodes.stbd.y_offset)=" & AA0; "." &
ActiveCell; ".construction_geometry.L/-2"
            ElseIf llo = "Z" Then
                Else
                    Print #1, AA; "." & ActiveCell; ".nodes.top.z_offset)=" & AA0; "." &
ActiveCell; ".construction_geometry.H/2"
                    Print #1, AA; "." & ActiveCell; ".nodes.bottom.z_offset)=" & AA0; "." &
ActiveCell; ".construction_geometry.H/-2"
                    Print #1, AA; "." & ActiveCell; ".nodes.fwd.x_offset)=" & AA0; "." &
ActiveCell; ".construction_geometry.L/2"
                    Print #1, AA; "." & ActiveCell; ".nodes.aft.x_offset)=" & AA0; "." &
ActiveCell; ".construction_geometry.L/-2"
                    Print #1, AA; "." & ActiveCell; ".nodes.port.y_offset)=" & AA0; "." &
ActiveCell; ".construction_geometry.B/2"
                    Print #1, AA; "." & ActiveCell; ".nodes.stbd.y_offset)=" & AA0; "." &
ActiveCell; ".construction_geometry.B/-2"
                End If
            End If
        End Sub

```

D_C_CGP (555 lines)

```

' COMPONENT GRANULARITY PROGRAM

Public BB As String
Public BB0 As String

Public EI As String 'ADJUSTMENT Equipment Instance string will make IEMPTY
error
Public EX As String
Public EY As String
Public EZ As String
Public ITM As String

Sub CGP() 'Component Granularity Programme

Worksheets("CGP").Activate

Range("A4").Select 'ADJUST HERE, *first line of data*.
' Set Do loop to stop when an empty cell is reached.

CountData = 0

Do Until IsEmpty(ActiveCell)
' Insert your code here.

adj0 = 5 'BB level locations ADJUST RESTORE TOO!
ActiveCell.Offset(0, adj0).Select 'BB level locations ADJUST RESTORE TOO!

'Do Until IsEmpty(ActiveCell)
Do Until CountBB = 8
' Insert your code here.
CountBB = CountBB + 1

'Equipment Level
  ElseIf CountData = 0 And IsEmpty(ActiveCell) = False And
IsEmpty(ActiveCell.Offset(0, 1)) = True Then
    Adj1 = -4 'ADJUSTMENT equipment from SBB in Arrangement Worksheet
    Adj2 = 6 'ADJUSTMENT locations in Arrangement Worksheet
    Call buildingblock '*****' BB PLACEMENT
  ElseIf CountData > 0 And IsEmpty(ActiveCell) = False And
IsEmpty(ActiveCell.Offset(0, 1)) = True Then
    Adj1 = -4 'ADJUSTMENT equipment from SBB in Arrangement Worksheet
    Adj2 = 6 'ADJUSTMENT locations in Arrangement Worksheet
    Call buildingblock '*****' BB PLACEMENT
  End If
End If

Loop

End Sub

```

D_D_CGP (684 lines)

```

' COMPONENT GRANULARITY PROGRAM

Sub buildingblock()

OT = ActiveCell.Offset(0, Adj1 - 1) 'ADJUSTMENT OBJECT TYPE
EI = ActiveCell.Offset(0, Adj1) 'ADJUSTMENT equipment from active BB

ITM = ActiveCell 'ADJUSTMENT for item

If OT = "equipment" Then

Print #1, BB; "} new equipment_instance " & ITM

ElseIf EC = "FH" Then
Print #1, BB; "." & ITM; "}change_layer 256"
ElseIf EC = "MV" Then
Print #1, BB; "." & ITM; "}change_layer 257"
ElseIf EC = "IA" Then
Print #1, BB; "." & ITM; "}change_layer 258"
ElseIf EC = "FL" Then
Print #1, BB; "." & ITM; "}change_layer 18"

If EC = "DT" Then
Print #1, BB; "." & ITM; "}change_layer 264" 'PL0
ElseIf EC = "FO" Then
Print #1, BB; "." & ITM; "}change_layer 265" 'PL1
ElseIf EC = "EL" Then
Print #1, BB; "." & ITM; "}change_layer 266" 'PL2
ElseIf EC = "ME" Then
Print #1, BB; "." & ITM; "}change_layer 267" 'PL3

Worksheets("EDP").Activate

Adj3 = 8 'position of BB level in "EDP" Worksheet COLUMN POS
Adj4 = Application.Match(EI, Range("B4:B1000"), 0) - 1 'ROW POS

Range("A4").Select 'ADJUST HERE, *first line of data*

If Application.VLookup(EI, Range("B4:Q1000"), 16, False) = 3 Then

one = ActiveCell.Offset(Adj4, Adj3) 'AUTOMATIC ADJUSTMENT
TWO = ActiveCell.Offset(Adj4, Adj3 + 1) 'AUTOMATIC ADJUSTMENT
THREE = ActiveCell.Offset(Adj4, Adj3 + 2) 'AUTOMATIC ADJUSTMENT

Print #1, BB; "." & ITM; ".equipment}->EDPO.equipment_database." & one; "."
& TWO; "." & THREE 'MINIMUM
End If

End Sub

```

D_E_CGP (81 lines)

```

' COMPONENT GRANULARITY PROGRAM

Sub R_CGP ()

Dim myFile As String, text As String, textline As String, posLat As Integer, posLong As Integer

myFile = "C:\Paramarine_data\Macros\OUTPUT.kcl"

Open myFile For Input As #1

Do Until EOF(1)
    Line Input #1, textline
    text = text & textline
Loop

Close #1
Worksheets("CGP").Activate
Range("F4").Select 'ADJUST HERE, *first line of data*.
Do Until IsEmpty(ActiveCell)

BB = "{MMPO." & ActiveCell.Offset(0, 0) & "." & ActiveCell.Offset(0, 1) &
"." & ActiveCell.Offset(0, 2) & "." & ActiveCell.Offset(0, 3) &
".datum}translate"

If posDATA > 0 Then

'ActiveCell.Offset(0, OUTPUT).value = Mid(text, posDATA + 1, 68)
posDATAx = InStr(Mid(text, posDATA, 70), "translate ")
'ActiveCell.Offset(0, OUTPUT).value = posDATAx
ActiveCell.Offset(0, OUTPUT).value = ActiveCell.Offset(0, OUTPUT).value +
Mid(text, posDATA + posDATAx + 10, 6)

'ActiveCell.Offset(0, OUTPUT + 1).value = Mid(text, posDATA + 60, 16)
posDATAy = InStr(Mid(text, posDATA + 60, 16), "[m],")
'ActiveCell.Offset(0, OUTPUT + 1).value = posDATAy
ActiveCell.Offset(0, OUTPUT + 1).value = ActiveCell.Offset(0, OUTPUT +
1).value + Mid(text, posDATA + 60 + posDATAy + 3, 7) 'READ KCL DATA

'ActiveCell.Offset(0, OUTPUT + 2).value = Mid(text, posDATA + 70, 16)
posDATAz = InStr(Mid(text, posDATA + 70, 16), "[m],")
'ActiveCell.Offset(0, OUTPUT + 2).value = posDATAz
ActiveCell.Offset(0, OUTPUT + 2).value = ActiveCell.Offset(0, OUTPUT +
2).value + Mid(text, posDATA + 70 + posDATAz + 3, 7) 'READ KCL DATA

End If

    ActiveCell.Offset(1, 0).Select
    CountData = CountData + 1
Loop

End Sub

```

E_A_SPP (369 lines)

```
'Systems Preamble Programme'

Sub SPP()
Worksheets("SPP").Activate

Print #1, "{SPP0} new concept_placeholder DS3_commodities"
Print #1, "{SPP0.DS3_commodities} new service_container cabling"
Print #1, "{SPP0.DS3_commodities} new service_container trunking"
Print #1, "{SPP0.DS3_commodities} new service_container piping"

Range("B4").Select 'ADJUST HERE, *first line of data*.
count = 0
Do Until IsEmpty(ActiveCell) = True ' Set Do loop to stop when an empty
cell is reached.
' Insert your code here.
If IsEmpty(ActiveCell) = False Then
    If ActiveCell.Offset(0, 1) = "cabling" Then
        Print #1, "{SPP0.DS3_commodities.cabling} new service_specification
" & ActiveCell
        If ActiveCell.Offset(0, 2) = "electrical_AC" Then
            Print #1, "{SPP0.DS3_commodities.cabling." & ActiveCell;
".electrical_AC}"
            Print #1, "{SPP0.DS3_commodities.cabling." & ActiveCell;
".voltage}=" & ActiveCell.Offset(0, 3); "[V]"
            Print #1, "{SPP0.DS3_commodities.cabling." & ActiveCell;
".frequency}=" & ActiveCell.Offset(0, 4); "[Hz]"

            ElseIf ActiveCell.Offset(0, 2) = "electrical_DC" Then
                Print #1, "{SPP0.DS3_commodities.cabling." & ActiveCell;
".electrical_DC}"
                Print #1, "{SPP0.DS3_commodities.cabling." & ActiveCell;
".voltage}=" & ActiveCell.Offset(0, 3); "[V]"
            End If
            ElseIf ActiveCell.Offset(0, 1) = "trunking" Then
                Print #1, "{SPP0.DS3_commodities.trunking} new
service_specification " & ActiveCell
                Print #1, "{SPP0.DS3_commodities.trunking." & ActiveCell;
".ventilation}"

            ElseIf ActiveCell.Offset(0, 1) = "piping" Then
                Print #1, "{SPP0.DS3_commodities.piping} new service_specification
" & ActiveCell
                Print #1, "{SPP0.DS3_commodities.piping." & ActiveCell;
".chilled_water}"
            End If
        End If
        count = count + 1
        ActiveCell.Offset(1, 0).Select
    Loop
    Close #myFile

End Sub
```

E_B_SCP (300 lines)

```

' System Connection Program

Public UHW As String 'STRING WILL NOT MAKE ISEMPY WORK!
Public HW As String

Sub SCP()
Worksheets("SCP").Activate

Range("A4").Select 'ADJUST HERE, *first line of data*.
CountData = 0

Do Until IsEmpty(ActiveCell)

If ActiveCell.Offset(0, 12) = "yes" Then 'classify whether it is a physical
or not
adj0 = 17 'BB level locations ADJUST RESTORE TOO!
ActiveCell.Offset(0, adj0).Select 'BB level locations ADJUST RESTORE TOO!
Do Until CountBB = 8
CountBB = CountBB + 1

If CountBB = 4 Then
BB = "{MMPO." & ActiveCell.Offset(0, -3) & "." & ActiveCell.Offset(0, -2) &
"." & ActiveCell.Offset(0, -1) & ".connections"
BB0 = "MMPO." & ActiveCell.Offset(0, -3) & "." & ActiveCell.Offset(0, -2) &
"." & ActiveCell.Offset(0, -1)
If CountData = 0 And IsEmpty(ActiveCell) = False And
IsEmpty(ActiveCell.Offset(0, 1)) = True Then

Adj1 = -6 'ADJUSTMENT yes or no from BB1 in Connections Worksheet
Adj2 = 9 'ADJUSTMENT locations in Connections Worksheet
Call subconnect '*****' BB PLACEMENT
ElseIf CountData > 0 And IsEmpty(ActiveCell) = False And
IsEmpty(ActiveCell.Offset(0, 1)) = True Then
Adj1 = -6 'ADJUSTMENT equipment from SBB in Connections Worksheet
Adj2 = 9 'ADJUSTMENT locations in Connections Worksheet
Call subconnect '*****' BB PLACEMENT
End If
End If

Restore = CountBB + adj0 'Location of MBB? in the sheet ADJUST HERE
TOO
ActiveCell.Offset(1, -Restore).Select
CountBB = 0
CountData = CountData + 1

Loop
End Sub

```

E_C_SCP (756 lines)

```
' System Connection Program

Sub subconnect()

ITM = ActiveCell
TYP = ActiveCell.Offset(0, Adj1 - 1)
UHW = ActiveCell.Offset(0, Adj1)
HW = ActiveCell.Offset(0, Adj1 + 1)
MS = ActiveCell.Offset(0, Adj1 + 2) 'Medium Specification
CLR = ActiveCell.Offset(0, Adj1 + 5) 'SBB for coloring

If TYP = "system_connection" Then

Print #1, BB; "} new system_connection " & ITM
'Print #1, BB; "." & ITM; "}change_layer 261"
Print #1, BB; "." & ITM; ".use_service_highway."; UHW; "}"

If CLR = "DT" Then
Print #1, BB; "." & ITM; "}change_layer 264" 'PL0
ElseIf CLR = "FO" Then
Print #1, BB; "." & ITM; "}change_layer 265" 'PL1
ElseIf CLR = "EL" Then
Print #1, BB; "." & ITM; "}change_layer 266" 'PL2
ElseIf CLR = "ME" Then
Print #1, BB; "." & ITM; "}change_layer 267" 'PL3
ElseIf CLR = "HVIN" Then
End If

If UHW = "yes" Then
'port'
If InStr(HW, "P") > 0 Then
Print #1, BB; "." & ITM; ".service_highway}-
>SPPO.DS3_routing_style_choice.port."; HW
'centre'
ElseIf InStr(HW, "C") > 0 Then
Print #1, BB; "." & ITM; ".service_highway}-
>SPPO.DS3_routing_style_choicecentre."; HW
'stbd'
ElseIf InStr(HW, "S") > 0 Then
Print #1, BB; "." & ITM; ".service_highway}-
>SPPO.DS3_routing_style_choice.stbd."; HW
End If
End If
Worksheets("SCP").Activate

End If

End Sub
```

A 6.2 MATLAB Codes

The use of MATLAB is to perform the proposed Logical Loop method and solve the SUBFLOW analysis. It automates the creation of the adjacency matrix, basic energy conservation (continuity constraints), Operational Matrix, and SUBFLOW network visualisation. The actual code is over 2300 lines.

```

%% NBA codes

tic

filename='E:\NBA.xlsm'; % design file
mode=2; %20=2D without flow 0=auto, 1=layered, for layout using 3-XYZData
sz=10; % label size
vw=[0 90 0 15; 0, 0, 90, 35];
ff=3; % 1 side, 2 front 3 top 4 3D
BC=8; % base color default white

dispfig=0; % 0=no 1=yes NO dispfig for loop
for oo=flip(0:2) % sprint to snort to sub

operational=oo; %
[~,ctr]=xlsread(filename,'SCP','AA4:ZZ1000');

ctr=strrep(ctr,'_',' '); %for plotting purpose/removing (_) underscore
fprintf('stage 0: download file done \n');

ST=[ctr(:,4) ctr(:,5)]; %LOCATION
for ii=1:size(ctr,1)
    if ctr(ii,operational+1)=="return"
        ST(ii,:)=flip(ST(ii,:));
    end
end

G=digraph(ST(:,1),ST(:,2));

lyt={'auto'; %1
     'circle'; %2
     'force'; %3
     'layered'; %4
     'subspace'; %5
     'force3'; %6
     'subspace3'}; %7

[num,ctr]=xlsread(filename,'SCP','A4:HM1000');

ctr=strrep(ctr,'_',' '); %for plotting purpose/removing (_) underscore

if operational==0
ub=6; % see column location of ub in Template/Connections Worksheet and num
SCP
dir=27; % see column location of dir in Template Worksheet and ctr
elseif operational==2
ub=8; % see column location of ub in Template/Connections Worksheet and num
SCP
dir=29; % see column location of dir in Template Worksheet and ctr
else
ub=7; % see column location of ub in Template/Connections Worksheet and num

```



```

dir=28;
end

lb=5; % see column location of lb in Template/Connections/SCP Worksheet and
num
OFF=9; % see column location of OF in Template/Connections/SCP Worksheet and
num
OFV=10; % see column location of OF in Template/Connections/SCP Worksheet and
num

PL=3; % see column location of PL in ctr Template/SCP Worksheet
BI=10; % see column location of BI in ctr Template/SCP Worksheet
SN=29; % see column location of StartNodes in ctr Template/SCP Worksheet
EN=30; % see column location of EndNodes in ctr Template/SCP Worksheet
% DR=21; % column location for direction
Rarcs=[ctr(:,SN) ctr(:,EN)];

G.Edges.OFV=zeros(size(G.Edges,1),1);

G.Edges.OFF=zeros(size(G.Edges,1),1);
G.Edges.PL=strings(size(G.Edges,1),1);
G.Edges.BI=strings(size(G.Edges,1),1);
G.Edges.lb=zeros(size(G.Edges,1),1);
G.Edges.ub=zeros(size(G.Edges,1),1);
for ii=1:size(G.Edges,1)
%   fprintf('processing ii %d of %d... \n',ii,size(G.Edges,1))

    rows= strcmp(ctr(:,SN),G.Edges.EndNodes(ii,1)) &
strcmp(ctr(:,EN),G.Edges.EndNodes(ii,2)); %supply
    rowr= strcmp(ctr(:,EN),G.Edges.EndNodes(ii,1)) &
strcmp(ctr(:,SN),G.Edges.EndNodes(ii,2)); %return

    if ~isempty(ctr(rows))

%       objective function

        G.Edges.OFV(ii)=num(strcmp(ctr(:,SN),G.Edges.EndNodes(ii,1)) &
strcmp(ctr(:,EN),G.Edges.EndNodes(ii,2)),OFV);

        G.Edges.OFF(ii)=num(strcmp(ctr(:,SN),G.Edges.EndNodes(ii,1)) &
strcmp(ctr(:,EN),G.Edges.EndNodes(ii,2)),OFF);
        G.Edges.PL(ii)=ctr(rows,PL);
        G.Edges.BI(ii)=ctr(rows,BI);
        G.Edges.lb(ii)=num(rows,lb);
        if num(rows,ub)==1e99
            G.Edges.ub(ii)=inf;
        else
            G.Edges.ub(ii)=num(rows,ub);
        end

    elseif ~isempty(ctr(rowr)) % ERROR FOR SOME FILES EN=21

        G.Edges.OFV(ii)=num(rowr,OFV);

```

```

G.Edges.OFF(ii)=num(rowr,OFF);
G.Edges.PL(ii)=ctr(rowr,PL);
G.Edges.BI(ii)=ctr(rowr,BI);
G.Edges.lb(ii)=num(rowr,lb);
if num(rowr,ub)==1e99
    G.Edges.ub(ii)=inf;
else
    G.Edges.ub(ii)=num(rowr,ub);
end

end
end

fprintf('stage 2.1: ARCS done \n');

%%%%%%%%%%%%%%%%%%%%%%%%%%%%%%%%%%%%%%%%%%%%%%%%%%%%%%%%%%%%%%%%%%%%%%%%
% READ lb & ub INDEX & MATCH WITH NODES NAME + Objective Function OF

% [num,ctr]=xlsread(filename,'Arrangement','A4:HM1000');
[num,ctr]=xlsread(filename,'CGP','A4:HM1000');

ctr=strrep(ctr,'_',' '); % removing underscore

if operational==0
lb=23; % see column location of lb and ub in arrangement/CGP worksheet and
num
ub=26; % see column location of lb and ub in arrangement/CGP worksheet and
num
elseif operational==1
lb=24;
ub=27; % see column location of lb and ub in arrangement/CGP worksheet and
num
else
lb=25;
ub=28; % see column location of lb and ub in arrangement/CGP worksheet and
num
end

GR=19; %location of granularity in ctr Arrangement/CGP Worksheet
typ=20; %location of type terminal/hub in ctr Arrangement/CGP Worksheet

OFF=29; % see column location of OF in arrangement worksheet and num
OFV=30; % see column location of OF in arrangement worksheet and num
XD=31; % see column location of Xdata in arrangement worksheet and num
YD=32; % see column location of Ydata in arrangement worksheet and num
ZD=33; % see column location of Zdata in arrangement worksheet and num

BB=1; % careful with object location in ctr
Rnodes=ctr(:,BB); % row nodes

G.Nodes.Granularity=strings(size(G.Nodes,1),1);
G.Nodes.Type=strings(size(G.Nodes,1),1);
G.Nodes.lb=zeros(size(G.Nodes,1),1);
G.Nodes.ub=zeros(size(G.Nodes,1),1);
G.Nodes.OFF=zeros(size(G.Nodes,1),1);

```

```

G.Nodes.OFV=zeros(size(G.Nodes,1),1);
G.Nodes.XData=zeros(size(G.Nodes,1),1);
G.Nodes.ZData=zeros(size(G.Nodes,1),1);
G.Nodes.ZData=zeros(size(G.Nodes,1),1);
for ii=1:size(G.Nodes,1)
%     fprintf('processing ii %d of %d... \n',ii,size(G.Nodes,1));

    row=strcmp(ctr(:,BB),G.Nodes.Name(ii));
    G.Nodes.Granularity(ii)=ctr(row,GR);
    G.Nodes.Type(ii)=ctr(row,typ);
    G.Nodes.lb(ii)=num(row,lb);
    if num(row,ub)==1e99
        G.Nodes.ub(ii)=inf;
    else
        G.Nodes.ub(ii)=num(row,ub);
    end
    G.Nodes.OFF(ii)=num(row,OFF);
    G.Nodes.OFV(ii)=num(row,OFV);
    G.Nodes.XData(ii)=num(row,XD);
    G.Nodes.YData(ii)=num(row,YD);
    G.Nodes.ZData(ii)=num(row,ZD);
end
fprintf('stage 2.2: VERTICES done \n');

if dispfig==0
else
%%%%%%%%%%%%%%%%%%%%%%%%%%%%%%%%%%%%%%%%%%%%%%%%%%%%%%%%%%%%%%%%%%%%%%%%
figure(200)

if mode==0
h=plot(G,'NodeLabel',G.Nodes.Name,'NodeFontSize',10,'ArrowSize',10,'ArrowPo
sition',1);
elseif mode==1
h=plot(G,'NodeLabel',G.Nodes.Name,'NodeFontSize',10,'ArrowSize',10,'ArrowPo
sition',1);
layout(h,lyt{4,:},'AssignLayers','alap')
elseif mode==2
h=plot(G,'XData',G.Nodes.XData,'YData',G.Nodes.YData,'NodeFontSize',10,'Arr
owSize',0,'ArrowPosition',1);
set(gca,'XTickLabel',[]);
set(gca,'YTickLabel',[]);
set(gca,'xtick',[])
set(gca,'xticklabel',[])
set(gca,'ytick',[])
set(gca,'yticklabel',[])
axis tight
view(vw(1,ff),vw(2,ff))
axis equal
elseif mode==3
h=plot(G,'XData',G.Nodes.XData,'YData',G.Nodes.YData,'ZData',G.Nodes.ZData,
'NodeFontSize',10,'ArrowSize',10,'ArrowPosition',1);
set(gca,'XTickLabel',[]);
set(gca,'YTickLabel',[]);
set(gca,'ZTickLabel',[]);
set(gca,'xtick',[])
set(gca,'xticklabel',[])
set(gca,'ytick',[])
set(gca,'yticklabel',[])
set(gca,'ztick',[])
set(gca,'zticklabel',[])

```

```

axis tight
view(vw(1,ff),vw(2,ff))
axis equal
end
set(gcf,'units','normalized','outerposition',[0 0 1 1]);
set(gca,'Unit','normalized','Position',[0 0 1 1]);
h.LineStyle = '--';
%%%%%%%%%%%%%%%%%%%%%%%%%%%%%%%%%%%%%%%%%%%%%%%%%%%%%%%%%%%%%%%%%%%%%%%%
end

%%%%%%%%%%%%%%%%%%%%%%%%%%%%%%%%%%%%%%%%%%%%%%%%%%%%%%%%%%%%%%%%%%%%%%%%
%%%%%%%%%%%%%%%%%%%%%%%%%%%%%%%%%%%%%%%%%%%%%%%%%%%%%%%%%%%%%%%%%%%%%%%%
% READ granularity AUTOMATICALLY (CGP Worksheet)

% READ energy
% ADJUST
PLoutC=[ 36 38 40 42 44....
         46 48 50 52 54....
         56 58 60 62 64]; % see column location of PL1 out in
Arrangement Worksheet and num
PLout=zeros;
for jj=1:size(PLoutC,2)
    PLout(1:size(ctr,1),jj)=num(1:size(ctr,1),PLoutC(1,jj));
end

% ADJUST
PLinC=[ 34 36 38 40 42....
        44 46 48 50 52....
        54 56 58 60 62]; % see column location of PL1 out in
Arrangement Worksheet and ctr

PLin=strings;
for jj=1:size(PLinC,2)
    PLin(1:size(ctr,1),jj)=ctr(1:size(ctr,1),PLinC(1,jj)); % ensure all
nodes are modelled
end

PLinNL=zeros;
for jj=1:size(PLoutC,2)
    PLinNL(1:size(ctr,1),jj)=num(1:size(ctr,1),PLoutC(1,jj)-1);
end

fprintf('stage 2: network properties done \n');

G.Nodes.Energy=zeros(size(G.Nodes,1),0);
G.Edges.Energy=zeros(size(G.Edges,1),0);
VERTEX=zeros;
countV=0;
countE=0;
for ii=1:size(ctr,1) % also for PL matrix
    if ctr(ii,typ)=="terminal"
        if ctr(ii,GR)=="G-1" || ctr(ii,GR)=="G-2" || ctr(ii,GR)=="G-3"
            for jj=1:size(PLout,2) % PL
                if PLout(ii,jj)~=0
                    for kk=1:size(PLin,2)
                        if PLin(ii,kk)=="IN" && kk==jj && PLout(ii,jj)==-1
                            %
                                if
                                    isempty(find(strcmp(ctr(ii,BB),G.Edges.EndNodes(:,2)) &
                                        strcmp(strcat({'PL'},num2str(kk)),G.Edges.PL), 1))

```



```

countE=countE+1;

G.Nodes.Energy(strcmp(ctr(ii,BB),G.Nodes.Name),countE)=PLout(ii,jj);
%
G.Edges.Energy(find(strcmp(ctr(ii,BB),G.Edges.EndNodes(:,1)) &
strcmp(strcat({'PL'},num2str(jj)),G.Edges.PL),countE)=1;
G.Edges.Energy(strcmp(ctr(ii,BB),G.Edges.EndNodes(:,1)) &
strcmp(strcat({'PL'},num2str(jj)),G.Edges.PL),countE)=1;

%%%%%%%%%%%%%%%%%%%%%%%%%%%%%%%%%%%%%%%%%%%%%%%%%%%%%%%%%%%%%%%%%%%%%%%%
elseif PLin(ii,kk)=="" %for different input
countE=countE+1;
G.Nodes.Energy(strcmp(ctr(ii,BB),G.Nodes.Name),countE)=-1;
G.Edges.Energy(strcmp(ctr(ii,BB),G.Edges.EndNodes(:,1)),countE)=1; % WORKS
trace origins
for ll=1:size(PLin,2)
if ~isnan(PLinNL(ii,ll))
%
[ii,jj,kk,ll]

countE=countE+1;

G.Nodes.Energy(strcmp(ctr(ii,BB),G.Nodes.Name),countE)=-PLinNL(ii,ll);
%
G.Edges.Energy(find(strcmp(ctr(ii,BB),G.Edges.EndNodes(:,2)) &
strcmp(strcat({'PL'},num2str(ll)),G.Edges.PL),countE)=1;

G.Edges.Energy(strcmp(ctr(ii,BB),G.Edges.EndNodes(:,2)) &
strcmp(strcat({'PL'},num2str(ll)),G.Edges.PL),countE)=1;
if PLout(ii,jj)~=0 && kk==jj % nonzero
same plexus
%
[ii,jj,kk,ll] % row nodes - PLout
col -PLin col - PLin NL
countE=countE+1;

G.Nodes.Energy(strcmp(ctr(ii,BB),G.Nodes.Name),countE)=PLout(ii,jj);
%
G.Edges.Energy(find(strcmp(ctr(ii,BB),G.Edges.EndNodes(:,1)) &
strcmp(strcat({'PL'},num2str(kk)),G.Edges.PL),countE)=1;

G.Edges.Energy(strcmp(ctr(ii,BB),G.Edges.EndNodes(:,1)) &
strcmp(strcat({'PL'},num2str(kk)),G.Edges.PL),countE)=1;

%
break

elseif PLout(ii,jj)~=0 && kk~=jj %
nonzero different plexus
%
[ii,jj,kk,ll]

countE=countE+1;

G.Nodes.Energy(strcmp(ctr(ii,BB),G.Nodes.Name),countE)=PLout(ii,jj);
%
G.Edges.Energy(find(strcmp(ctr(ii,BB),G.Edges.EndNodes(:,1)) &
strcmp(strcat({'PL'},num2str(jj)),G.Edges.PL),countE)=1;

G.Edges.Energy(strcmp(ctr(ii,BB),G.Edges.EndNodes(:,1)) &
strcmp(strcat({'PL'},num2str(jj)),G.Edges.PL),countE)=1;

%
break

```



```

lb = [ zeros(1,size(G.Edges,1))    G.Edges.lb'    -inf(1,size(G.Edges,1))
G.Nodes.lb']; % AUTOMATIC EXCEL
ub = [ ones(1,size(G.Edges,1))    G.Edges.ub'    inf(1,size(G.Edges,1))
G.Nodes.ub']; % AUTOMATIC EXCEL
f = [-G.Edges.OFF'    -G.Edges.OFV'    zeros(1,size(G.Edges,1))
G.Nodes.OFV'    ]; %AUTOMATIC FROM EXCEL

sostype=[];
sosind=[];
soswt=[];

% ctype = repmat('C',1,size(f,2)); %defining binary vs integer vs continous
('B','I','C') based on size f,
ctype = [ ...
    repmat('B',1,size(G.Edges.OFF',2)) ...
    repmat('C',1,size(G.Edges.OFV',2)) ...
    repmat('C',1,size(G.Edges,1)) ...
    repmat('C',1,size(G.Nodes.OFV',2)) ...
    ]; %defining binary vs integer vs continous ('B','I','C') based on
size
fprintf('stage 3.5: CPLEX ready \n');

[x,fval,exitflag,output] =
cplexmip(f,Aineq,bineq,Aeq,beq,sostype,sosind,soswt,lb,ub,ctype,[]);

G.Edges.Weight=round(x(size(G.Edges,1)+1:size(G.Edges,1)*2,:)); % normal
G.Nodes.Weight=round(x(size(G.Edges,1)*3+1:end,:)); % normal

for ii=1:size(G.Edges.Weight,1)
    if G.Edges.Weight(ii)<0.000001
        G.Edges.Weight(ii)=0;
    end
end
for ii=1:size(G.Nodes.Weight,1)
    if G.Nodes.Weight(ii)<0.000001
        G.Nodes.Weight(ii)=0;
    end
end

for ii=1:size(Rarcs,1)
    rows= strcmp(Rarcs(ii,1),G.Edges.EndNodes(:,1)) &
strcmp(Rarcs(ii,2),G.Edges.EndNodes(:,2)); %supply
    rowr= strcmp(Rarcs(ii,2),G.Edges.EndNodes(:,1)) &
strcmp(Rarcs(ii,1),G.Edges.EndNodes(:,2)); %return
    if ~isempty(G.Edges.Weight(rows))
        Rarcs(ii,3)={G.Edges.Weight(rows)};
    elseif ~isempty(G.Edges.Weight(rowr)) %
        Rarcs(ii,3)={G.Edges.Weight(rowr)};
    end
end
% Rnodes=ctr(:,BB);
for ii=1:size(Rnodes,1)
    row=strcmp(Rnodes(ii),G.Nodes.Name);
    Rnodes(ii,2)={G.Nodes.Weight(row)};
end

fprintf('stage 4: LP done \n');

if dispfig==0
Excel = actxserver('Excel.Application');

```

```

Workbooks = Excel.Workbooks;
Excel.Visible=1;
Workbook=Workbooks.Open(filename);
sheetnum=6; % arrangement location - CGP location
data=Rnodes(:,2);
if operational==1 % sprint
range = strcat('BR4:BR',num2str(3+size(Rnodes,1))); %in CGP
elseif operational==2 %sub
range = strcat('BS4:BS',num2str(3+size(Rnodes,1))); %in CGP
elseif operational==0 %sub%snort
range = strcat('BQ4:BQ',num2str(3+size(Rnodes,1)));
end
% range = 'F10:I13';
% Make the first sheet active
Sheets = Excel.ActiveWorkBook.Sheets;
sheet1 = get(Sheets, 'Item', sheetnum);
invoke(sheet1, 'Activate');
Activesheet = Excel.Activesheet;
% Put MATLAB data into Excel
ActivesheetRange = get(Activesheet, 'Range', range);
set(ActivesheetRange, 'Value', data);
% Now read the data from the sheet; you could specify a new range here
Range = get(Activesheet, 'Range', range);
out = Range.value;
sheetnum=8; % connections location - SCP location
data=Rarcs(:,3);
if operational==1 % sprint
range = strcat('AP4:AP',num2str(3+size(Rarcs,1)));
elseif operational==2 %sub
range = strcat('AQ4:AQ',num2str(3+size(Rarcs,1)));
elseif operational==0 %sub
range = strcat('AO4:AO',num2str(3+size(Rarcs,1))); % CAN OVERWRITE
CONNECTIONS LENGTH
end
Sheets = Excel.ActiveWorkBook.Sheets;
sheet1 = get(Sheets, 'Item', sheetnum);
invoke(sheet1, 'Activate');
Activesheet = Excel.Activesheet;
ActivesheetRange = get(Activesheet, 'Range', range);
set(ActivesheetRange, 'Value', data);
Range = get(Activesheet, 'Range', range);
out = Range.value;
invoke(Workbook, 'Save')
invoke(Excel, 'Quit');
delete(Excel);
clear Excel;
fprintf('stage 4.0: Write Excel done \n');
%%%%%%%%%%%%%%%%%%%%%%%%%%%%%%%%%%%%%%%%%%%%%%%%%%%%%%%%%%%%%%%%%%%%%%%%
else
end
highlight(h,G2.Edges.EndNodes(cell2mat(idx(:,1)),1),G2.Edges.EndNodes(cell2
mat(idx(:,1)),2), 'ArrowSize',0, 'LineStyle', '-.') %'-.' | '--' | ':' | '-.' |
'none'.
highlight(h,G2.Edges.EndNodes(cell2mat(idx(:,2)),1),G2.Edges.EndNodes(cell2
mat(idx(:,2)),2), 'ArrowSize',0, 'LineStyle', '--', 'EdgeColor', clr(12,:))
if mode==30
elseif mode==20
else
labeledge(h,G2.Edges.EndNodes(cell2mat(idx(:,2)),1),G2.Edges.EndNodes(cell2
mat(idx(:,2)),2), 'data')

```

```

end
highlight(h,G2.Edges.EndNodes(cell2mat(idx(:,3)),1),G2.Edges.EndNodes(cell2
mat(idx(:,3)),2),'EdgeColor',clr(1,:))
highlight(h,G2.Edges.EndNodes(cell2mat(idx(:,4)),1),G2.Edges.EndNodes(cell2
mat(idx(:,4)),2),'EdgeColor',clr(5,:)) % ELEC
highlight(h,G2.Edges.EndNodes(cell2mat(idx(:,5)),1),G2.Edges.EndNodes(cell2
mat(idx(:,5)),2),'EdgeColor',clr(7,:))
highlight(h,G2.Edges.EndNodes(cell2mat(idx(:,6)),1),G2.Edges.EndNodes(cell2
mat(idx(:,6)),2),'EdgeColor',clr(14,:))
highlight(h,G2.Edges.EndNodes(cell2mat(idx(:,7)),1),G2.Edges.EndNodes(cell2
mat(idx(:,7)),2),'EdgeColor',clr(6,:))
highlight(h,G2.Edges.EndNodes(cell2mat(idx(:,8)),1),G2.Edges.EndNodes(cell2
mat(idx(:,8)),2),'EdgeColor',clr(11,:))
highlight(h,G2.Edges.EndNodes(cell2mat(idx(:,9)),1),G2.Edges.EndNodes(cell2
mat(idx(:,9)),2),'EdgeColor',clr(13,:))
highlight(h,G2.Edges.EndNodes(cell2mat(idx(:,10)),1),G2.Edges.EndNodes(cell
2mat(idx(:,10)),2),'EdgeColor',clr(4,:))
highlight(h,G2.Edges.EndNodes(cell2mat(idx(:,11)),1),G2.Edges.EndNodes(cell
2mat(idx(:,11)),2),'EdgeColor',clr(3,:))
highlight(h,G2.Edges.EndNodes(cell2mat(idx(:,12)),1),G2.Edges.EndNodes(cell
2mat(idx(:,12)),2),'EdgeColor',clr(9,:))
highlight(h,G2.Edges.EndNodes(cell2mat(idx(:,13)),1),G2.Edges.EndNodes(cell
2mat(idx(:,13)),2),'EdgeColor',clr(2,:))
highlight(h,G2.Edges.EndNodes(cell2mat(idx(:,14)),1),G2.Edges.EndNodes(cell
2mat(idx(:,14)),2),'EdgeColor',clr(9,:))
highlight(h,G2.Edges.EndNodes(cell2mat(idx(:,15)),1),G2.Edges.EndNodes(cell
2mat(idx(:,15)),2),'EdgeColor',clr(10,:))
highlight(h,G2.Edges.EndNodes(cell2mat(idx(:,16)),1),G2.Edges.EndNodes(cell
2mat(idx(:,16)),2),'EdgeColor',clr(15,:))

fprintf('stage 7: node label \n');

idx=cell(size(G2.Nodes,1),5);
countA=0;
countB=0;
countC=0;
countD=0;
for ii=1:size(G2.Nodes,1)
%     fprintf('processing ii %d of %d... \n',ii,size(G2.Nodes,1))

    if strcmp('G-1',G2.Nodes.Granularity(ii))
        countA=countA+1;
        idx(countA,1)={ii};

    elseif strcmp('G-2',G2.Nodes.Granularity(ii))
        countB=countB+1;
        idx(countB,2)={ii};
    else
        countC=countC+1;
        idx(countC,3)={ii};
    end

    if strcmp('terminal',G2.Nodes.Type(ii))
        countD=countD+1;
        idx(countD,4)={ii};
    end
end

end

```

```

highlight(h,G2.Nodes.Name(cell2mat(idx(:,1))), 'Marker',MS{12}, 'MarkerSize',
sz) %star shape for G-1
highlight(h,G2.Nodes.Name(cell2mat(idx(:,2))), 'Marker',MS{9}, 'MarkerSize',s
z) %V shape for G-2
highlight(h,G2.Nodes.Name(cell2mat(idx(:,3))), 'Marker',MS{1}, 'MarkerSize',s
z) %circle shape for G-3
highlight(h,G2.Nodes.Name(cell2mat(idx(:,4))), 'NodeLabelColor',clr(12,:), 'N
odeColor',clr(1,:))

if VERTEX~=0
for jj=1:size(VERTEX,2)

highlight(h,G2.Nodes.Name(strcmp(ctr(VERTEX(jj),BB),G2.Nodes.Name)), 'NodeCo
lor',clr(7,:)) % for black node
end
end
%%%%%%%%%%%%%%%%%%%%%%%%%%%%%%%%%%%%%%%%%%%%%%%%%%%%%%%%%%%%%%%%%%%%%%%%
%%%%%%%%%%%%%%%%%%%%%%%%%%%%%%%%%%%%%%%%%%%%%%%%%%%%%%%%%%%%%%%%%%%%%%%% sub network
fprintf('stage 8: sub network \n');

zz_start=min(cellfun(@str2num, regexp(G.Edges.PL, '\d*', 'Match')));
zz_end=max(cellfun(@str2num, regexp(G.Edges.PL, '\d*', 'Match')));
for zz=zz_start:zz_end %full size of plexus
%for zz=zz_start:RAYA %full size of plexus
clear C
SG=strcat({'PL'}, num2str(zz));
% C={};
C=strings(size(G2.Edges,1),2); %setup string array
for ii=1:size(G2.Edges,1)
    if strcmp(SG,G2.Edges.PL(ii))
        C(ii,:)=G2.Edges.EndNodes(ii,:);
    end
end
if ~isempty(C)
    C=C(~any(cellfun('isempty',C),2),:);
end
G3=subgraph(G2,unique([C(:,1); C(:,2)]));

if zz==0
    figure(100) %data
else
figure(zz)
end

set(gcf, 'position', [0 scrsz(1,4)*1/3 scrsz(1,3) scrsz(1,4)*1/2])

if ~isempty(max(G3.Edges.Weight))
LWidths = 5*G3.Edges.Weight/(1+max(G3.Edges.Weight))+1;
AWidths = 5*G3.Edges.Weight/(1+max(G3.Edges.Weight))+15;
OWidths = G3.Edges.Weight/(1+max(G3.Edges.Weight));
else
LWidths = 1;
AWidths = 1;
OWidths = 1;
end
if mode==0
i=plot(G3, 'NodeLabel',G3.Nodes.Name, 'EdgeLabel',G3.Edges.Weight, 'ArrowPosit
ion',1, 'ArrowSize',AWidths, 'LineWidth',LWidths, 'NodeFontSize',sz, 'EdgeFontS
ize',sz);
elseif mode==1

```

```

i=plot(G3, 'NodeLabel', G3.Nodes.Name, 'EdgeLabel', G3.Edges.Weight, 'ArrowPosition', 1, 'ArrowSize', AWidths, 'LineWidth', LWidths, 'NodeFontSize', sz, 'EdgeFontSize', sz);
layout(i, lyt{4, :}, 'AssignLayers', 'alap')
elseif mode==2
h=plot(G, 'XData', G.Nodes.XData, 'YData', G.Nodes.YData, 'NodeFontSize', 10, 'ArrowSize', 0, 'ArrowPosition', 1, 'EdgeColor', clr(BC, :));
h.LineStyle = '--';
h.LineWidth = 0.5;
hold on
i=plot(G3, 'XData', G3.Nodes.XData, 'YData', G3.Nodes.YData, 'NodeLabel', G3.Nodes.Name, 'EdgeLabel', G3.Edges.Weight, 'ArrowPosition', 1, 'ArrowSize', AWidths, 'LineWidth', LWidths, 'NodeFontSize', sz, 'EdgeFontSize', sz);
set(gca, 'XTickLabel', []);
set(gca, 'YTickLabel', []);
set(gca, 'xtick', []);
set(gca, 'xticklabel', []);
set(gca, 'ytick', []);
set(gca, 'yticklabel', []);
set(gca, 'Visible', 'off')
axis tight
axis equal
elseif mode==3
h=plot(G, 'XData', G.Nodes.XData, 'YData', G.Nodes.YData, 'ZData', G.Nodes.ZData, 'NodeFontSize', 10, 'ArrowSize', 0, 'ArrowPosition', 1, 'EdgeColor', clr(BC, :));
h.LineStyle = '--';
h.LineWidth = 0.5;
hold on
i=plot(G3, 'XData', G3.Nodes.XData, 'YData', G3.Nodes.YData, 'ZData', G3.Nodes.ZData, 'NodeLabel', G3.Nodes.Name, 'EdgeLabel', G3.Edges.Weight, 'ArrowPosition', 1, 'ArrowSize', AWidths, 'LineWidth', LWidths, 'NodeFontSize', sz, 'EdgeFontSize', sz);
set(gca, 'XTickLabel', []);
set(gca, 'YTickLabel', []);
set(gca, 'ZTickLabel', []);
set(gca, 'xtick', []);
set(gca, 'xticklabel', []);
set(gca, 'ytick', []);
set(gca, 'yticklabel', []);
set(gca, 'ztick', []);
set(gca, 'zticklabel', []);
set(gca, 'Visible', 'off')
axis tight
axis equal
view(vv(1, ff), vv(2, ff))
elseif mode==30
h=plot(G, 'XData', G.Nodes.XData, 'YData', G.Nodes.YData, 'ZData', G.Nodes.ZData, 'NodeFontSize', 10, 'ArrowSize', 0, 'ArrowPosition', 1, 'EdgeColor', clr(BC, :));
h.LineStyle = '--';
h.LineWidth = 0.5;
hold on
i=plot(G3, 'XData', G3.Nodes.XData, 'YData', G3.Nodes.YData, 'ZData', G3.Nodes.ZData, 'ArrowPosition', 1, 'ArrowSize', sz, 'EdgeFontSize', sz);
set(gca, 'XTickLabel', []);
set(gca, 'YTickLabel', []);
set(gca, 'ZTickLabel', []);
set(gca, 'xtick', []);
set(gca, 'xticklabel', []);
set(gca, 'ytick', []);
set(gca, 'yticklabel', []);
set(gca, 'ztick', []);

```

```

set(gca, 'zticklabel', [])
set(gca, 'Visible', 'off')
axis tight
axis equal
view(vv(1,ff),vv(2,ff))
elseif mode==20
h=plot(G, 'XData',G.Nodes.XData, 'YData',G.Nodes.YData, 'NodeFontSize',10, 'ArrowSize',0, 'ArrowPosition',1, 'EdgeColor',clr(BC,:));
h.LineStyle = '--';
hold on
i=plot(G3, 'XData',G3.Nodes.XData, 'YData',G3.Nodes.YData, 'NodeLabel',G3.Nodes.Name, 'ArrowPosition',1, 'ArrowSize',0, 'NodeFontSize',sz, 'EdgeFontSize',sz);
;
set(gca, 'XTickLabel', []);
set(gca, 'YTickLabel', []);
set(gca, 'xtick', [])
set(gca, 'xticklabel', [])
set(gca, 'ytick', [])
set(gca, 'yticklabel', [])
set(gca, 'Visible', 'off')
i.LineWidth = 1.5;
axis tight
axis equal
end
set(gcf, 'units', 'normalized', 'outerposition', [0 0 1 1]);
set(gca, 'Unit', 'normalized', 'Position', [0 0 1 1]);

idx=cell(size(G3.Edges,1),16);
countA=0;
countB=0;
countC=0;
countD=0;
countE=0;
countF=0;
countG=0;
countH=0;
countI=0;
countJ=0;
countK=0;
countL=0;
countM=0;
countN=0;
countO=0;
countP=0;
for ii=1:size(G3.Edges,1)
%     fprintf('processing ii %d of %d... \n',ii,size(G3.Edges,1))

    if G3.Edges.Weight(ii)==0
        countA=countA+1;
        idx(countA,1)={ii};
    end

    if strcmp('PL0',G3.Edges.PL(ii))
        countB=countB+1;
        idx(countB,2)={ii};
    elseif strcmp('PL1',G3.Edges.PL(ii))
        countC=countC+1;
        idx(countC,3)={ii};
    end
end

```

```

elseif strcmp('PL2',G3.Edges.PL(ii))
    countD=countD+1;
    idx(countD,4)={ii};
elseif strcmp('PL3',G3.Edges.PL(ii))    %mech
    countE=countE+1;
    idx(countE,5)={ii};
elseif strcmp('PL4',G3.Edges.PL(ii))
    countF=countF+1;
    idx(countF,6)={ii};
elseif strcmp('PL5',G3.Edges.PL(ii))
    countG=countG+1;
    idx(countG,7)={ii};
elseif strcmp('PL6',G3.Edges.PL(ii))
    countH=countH+1;
    idx(countH,8)={ii};
elseif strcmp('PL7',G3.Edges.PL(ii))
    countI=countI+1;
    idx(countI,9)={ii};
elseif strcmp('PL8',G3.Edges.PL(ii))
    countJ=countJ+1;
    idx(countJ,10)={ii};
elseif strcmp('PL9',G3.Edges.PL(ii))
    countK=countK+1;
    idx(countK,11)={ii};
elseif strcmp('PL10',G3.Edges.PL(ii))
    countL=countL+1;
    idx(countL,12)={ii};
elseif strcmp('PL11',G3.Edges.PL(ii))
    countM=countM+1;
    idx(countM,13)={ii};
elseif strcmp('PL12',G3.Edges.PL(ii))
    countN=countN+1;
    idx(countN,14)={ii};
elseif strcmp('PL13',G3.Edges.PL(ii))
    countO=countO+1;
    idx(countO,15)={ii};
elseif strcmp('PL14',G3.Edges.PL(ii))
    countP=countP+1;
    idx(countP,16)={ii};
% elseif strcmp('PL15',G3.Edges.PL(ii))
end
end

highlight(i,G3.Edges.EndNodes(cell2mat(idx(:,1)),1),G3.Edges.EndNodes(cell2
mat(idx(:,1)),2),'ArrowSize',0)
highlight(i,G3.Edges.EndNodes(cell2mat(idx(:,2)),1),G3.Edges.EndNodes(cell2
mat(idx(:,2)),2),'ArrowSize',0,'EdgeColor',clr(12,:))
labeledge(i,G3.Edges.EndNodes(cell2mat(idx(:,2)),1),G3.Edges.EndNodes(cell2
mat(idx(:,2)),2),'data')
% elseif zz==2
highlight(i,G3.Edges.EndNodes(cell2mat(idx(:,3)),1),G3.Edges.EndNodes(cell2
mat(idx(:,3)),2),'EdgeColor',clr(1,:))
% elseif zz==3
highlight(i,G3.Edges.EndNodes(cell2mat(idx(:,4)),1),G3.Edges.EndNodes(cell2
mat(idx(:,4)),2),'EdgeColor',clr(5,:)) % ELEC
% elseif zz==4
highlight(i,G3.Edges.EndNodes(cell2mat(idx(:,5)),1),G3.Edges.EndNodes(cell2
mat(idx(:,5)),2),'EdgeColor',clr(7,:))
% elseif zz==5
highlight(i,G3.Edges.EndNodes(cell2mat(idx(:,6)),1),G3.Edges.EndNodes(cell2
mat(idx(:,6)),2),'EdgeColor',clr(14,:))

```

```

% elseif zz==6
highlight(i,G3.Edges.EndNodes(cell2mat(idx(:,7)),1),G3.Edges.EndNodes(cell2
mat(idx(:,7)),2),'EdgeColor',clr(6,:))
% elseif zz==7
highlight(i,G3.Edges.EndNodes(cell2mat(idx(:,8)),1),G3.Edges.EndNodes(cell2
mat(idx(:,8)),2),'EdgeColor',clr(11,:))
% elseif zz==8
highlight(i,G3.Edges.EndNodes(cell2mat(idx(:,9)),1),G3.Edges.EndNodes(cell2
mat(idx(:,9)),2),'EdgeColor',clr(13,:))
% elseif zz==9
highlight(i,G3.Edges.EndNodes(cell2mat(idx(:,10)),1),G3.Edges.EndNodes(cell
2mat(idx(:,10)),2),'EdgeColor',clr(4,:))
% elseif zz==10
highlight(i,G3.Edges.EndNodes(cell2mat(idx(:,11)),1),G3.Edges.EndNodes(cell
2mat(idx(:,11)),2),'EdgeColor',clr(3,:))
% elseif zz==11
highlight(i,G3.Edges.EndNodes(cell2mat(idx(:,12)),1),G3.Edges.EndNodes(cell
2mat(idx(:,12)),2),'EdgeColor',clr(9,:))
% elseif zz==12
highlight(i,G3.Edges.EndNodes(cell2mat(idx(:,13)),1),G3.Edges.EndNodes(cell
2mat(idx(:,13)),2),'EdgeColor',clr(2,:))
% elseif zz==13
highlight(i,G3.Edges.EndNodes(cell2mat(idx(:,14)),1),G3.Edges.EndNodes(cell
2mat(idx(:,14)),2),'EdgeColor',clr(9,:))
% elseif zz==14
highlight(i,G3.Edges.EndNodes(cell2mat(idx(:,15)),1),G3.Edges.EndNodes(cell
2mat(idx(:,15)),2),'EdgeColor',clr(10,:))
% elseif zz==15
highlight(i,G3.Edges.EndNodes(cell2mat(idx(:,16)),1),G3.Edges.EndNodes(cell
2mat(idx(:,16)),2),'EdgeColor',clr(15,:))
% end

idy=cell(size(G3.Nodes,1),5);
countA=0;
countB=0;
countC=0;
countD=0;
for ii=1:size(G3.Nodes,1)
%   fprintf('processing ii %d of %d... \n',ii,size(G3.Nodes,1))

    if strcmp('G-1',G3.Nodes.Granularity(ii))
        countA=countA+1;
        idy(countA,1)={ii};

    elseif strcmp('G-2',G3.Nodes.Granularity(ii))
        countB=countB+1;
        idy(countB,2)={ii};
    else
        countC=countC+1;
        idy(countC,3)={ii};
    end

    if strcmp('terminal',G3.Nodes.Type(ii))
        countD=countD+1;
        idy(countD,4)={ii};
    end
end

end

```


Appendix 7

Analyses of Case Study 5.1

One of the major advantages of the proposed Network Block Approach (NBA) is the use of Paramarine-SURFCON for the 3D based submarine design synthesis. This unlocked the use of readily available naval architectural analyses that Paramarine-SURFCON has provided: producing Flounder Diagram, etc. However, not all Paramarine's comprehensive analysis (object) tools were exploited in this research, only important submarine balance analyses were carried out commensurate with the submarine ESD as outlined in the proposed NBA in Figure 5.44 on page 256. Thus, this appendix provides supporting tables and figures to confirm that the early-stage design undertaken in the current research was realistic.

The submarine balance in this research was divided into several types: weight and space balance; longitudinal and vertical balance (including stability balance); and (DS3) energy balance. Only DS3 energy balance was calculated using SUBFLOW simulation while the rest of the design balance analysis was calculated in Paramarine by first assigning relevant characteristics to various DBB objects, defined in relevant programs (WGP, VGP, CGP, and SCP) and then populated in the DBB hierarchy under a Master Building Block (MBB) object.

A 7.1 Stability

A 7.1.1 Weight and Space Balance

Table A 3 provides the selected numerical algorithms used for initial sizing. As discussed in Section 5.9, some items were refined using the NBA/SUBFLOW process and thus replaced the initial sizing calculations (see Subsection A 7.1.2). The source of the algorithms was based on the annual UCL submarine design and acquisition course data (UCL-NAME 2012; UCL-NAME 2014). Table A 4 shows the summary of calculated volumes of Case Study 5.1.

Table A 3: Summary of numerical sizing for Case Study 5.1

Group	Description	Unit	UCL data (tonne)	Calculated Weight (tonne)	Selected Numerical Algorithm	Notes	Source
1	Hull Structure						
w10	PH plating stiffening		400	402.0	$W_{ph} = \frac{1}{24} \times \frac{DDD}{DYS} \times \Delta \times \rho_{steel}$	Assumed HY80	http://128.40.55.189/mediawiki/index.php/SubGp_10_Pressure_Hull
w103	Dome end bulkheads		50			Minor bulkheads, included in pressure hull	
w104	Conning tower		3	3.0	$3te$	Assumed fixed value	http://128.40.55.189/mediawiki/index.php/SubGp_10_Pressure_Hull
w110	Fore end structure		75	75.0	$\Delta \times 0.03$	Parametric	http://128.40.55.189/mediawiki/index.php/SubGp_11_External_Structure
w111	Aft end structure		25	25.0	$\Delta \times 0.01$	Parametric	http://128.40.55.189/mediawiki/index.php/SubGp_11_External_Structure
w112	Casing		22	25.0	$\Delta \times 0.01$	Parametric	http://128.40.55.189/mediawiki/index.php/SubGp_11_External_Structure
w113	Keel structure		25	75.0	$\Delta \times 0.03$	Parametric	http://128.40.55.189/mediawiki/index.php/SubGp_11_External_Structure
w114	Bridge fin structure		27	17.0	$17te$	Assumed fixed value	http://128.40.55.189/mediawiki/index.php/SubGp_11_External_Structure
w120	Major bulkheads		22	23.1	$0.2 \times D_{ph}^2 \times N_{bh}$	Assumed two bulkheads	http://128.40.55.189/mediawiki/index.php/SubGp_12_Internal_Structure
w121	Decks flats pillars		35	36.8	$0.1 \times \Delta^{\frac{2}{3}} \times N_d$	Assumed two decks	http://128.40.55.189/mediawiki/index.php/SubGp_12_Internal_Structure
w13	Internal structure high			15.0	$0.006 \times \Delta$	Minor bulkheads (steel), Minor bulkheads (partition), Internal non-structural tanks)	http://128.40.55.189/mediawiki/index.php/SubGp_13_Minor_Internal_Structure
	Divisional bulkheads steel		8			Steel included in internal structure high	
	Divisional bulkheads partition		6			Partition included in internal structure high	
	Main non-structural tanks		1			Included in internal structure high	
w13	Internal structure low			62.5	$0.025 \times \Delta$	Internal structural tanks, periscope support wells	http://128.40.55.189/mediawiki/index.php/SubGp_13_Minor_Internal_Structure
	Periscope supports wells		2			Included in internal structure low	
	Internal structural tanks		60			Included in internal structure low	
w14	Access			25.0	$\Delta \times 0.01$	Parametric	http://128.40.55.189/mediawiki/index.php/SubGp_14_Access
w14	Escape towers		2			Included in access	http://128.40.55.189/mediawiki/index.php/SubGp_14_Access
	Torpedo loading hatch		0.7			Included in access	
	Other pressure hull hatches		6			Included in access	
	Manhole covers		6			Included in access	
	Watertight doors		1.7			Included in access	
	Non watertight doors hatches		2			Included in access	
w151	Seats		45	39.6	$0.15 \times M_{battery}$	Included battery support	http://128.40.55.189/mediawiki/index.php/SubGp_15_Seatings
w152	Mounts		15	25.0	$\Delta \times 0.01$	Parametric	http://128.40.55.189/mediawiki/index.php/SubGp_15_Seatings
	Cableways		5				
	Pipe system supports clips		3				
	Gratings ladders		5				
w161	Fwd hydroplanes		1.6	1.7	$\frac{\Delta}{1500}$	Parametric	http://128.40.55.189/mediawiki/index.php/SubGp_16_Control_Surfaces
w162	Aft hydroplanes		4.9	20.8	$\frac{\Delta}{120}$	Parametric	http://128.40.55.189/mediawiki/index.php/SUB_Hydroplane_%26_Rudder_Sizing
	Stabilisers		7				
	Rudders		9.2				
	Total Weight Group 1		875.1	871.3			
2	Propulsion Systems						
w25/28	Fluids propulsion system		0.3	10.0	$\frac{P_s}{400}$		http://128.40.55.189/mediawiki/index.php/SubGp_25_Insulation_and_Fluids_in_Propulsion_Machinery
w26	Shafting	1	7.4	7.4		Scaled from SSK (UCL Submarine Databook 2012) Weight Breakdown Profile	
w26	Thrust block	1	3.2	1.5	$0.8te/m^3$		http://128.40.55.189/mediawiki/index.php/SubGp_26_Main_Machinery

Group	Description	Unit	UCL data (tonne)	Calculated Weight (tonne)	Selected Numerical Algorithm	Notes	Source
w26	Stern seal		1.8	1.8		Taken from UCL Submarine Databook 2012 SSK (pp164 Section 11.1)	
w26	Propeller rope guard cone	1	7.2	8.0	$2 \times 10^{-3} \times P_s$		http://128.40.55.189/mediawiki/index.php/SubGp_26_Main_Machinery
w29	Main motor	1	83	83.0	$MASS(t) = 2.6 \times (\phi(m))^3$	Determined the diameter first then the mass	UCL Submarine Databook 2014 (page 77 Section 5.1.1)
w26	Propulsion switchgear		4.5	4.5		Propulsion Switchboard	UCL Submarine Databook 2014 (page 80 Section 5.1.4)
w29	Main batteries	480	269	264.0		Propulsion system sizing	UCL Submarine Databook 2014 (page 79 Section 5.1.3)
w29	MCC		3.3	3.3		Scaled from SSK (UCL Submarine Databook 2014) Weight Breakdown Profile	http://128.40.55.189/mediawiki/index.php/SubGp_29_Electrical_Propulsion_Equipment_%26_System_s
	Total Weight Group 2		379.7	383.5			
3	Electrical Services						
w30	Cabling		19.5	20.0	$\Delta \times 8 \times 10^{-3}$	Included data cable	http://128.40.55.189/mediawiki/index.php/SubGp_30_Cabling_and_Glands
w30	Electrical glands		2.5	2.5	$\Delta \times 1 \times 10^{-3}$		http://128.40.55.189/mediawiki/index.php/SubGp_30_Cabling_and_Glands
w3	Fluids electrical services		3.7	3.7		Scaled from SSK (UCL Submarine Databook 2012) Weight Breakdown Profile	
w31	140kw 60Hz MG	2	10.7	11.1		Parametric	UCL Submarine Databook 2014 (page 133 Section 6.2.1)
w31	400Hz static frequency changers		1.2	1.2		Parametric	http://128.40.55.189/mediawiki/index.php/SubGp_31_Electrical_Control_and_Conversion
w32	1400kw DG	2	37.9	37.9	$17 \times P_{DG}$	Parametric	UCL Submarine Databook 2014 (page 78 Section 5.1.2)
w32	DG FW system		2	2.0		Scaled from SSK (UCL Submarine Databook 2014) Weight Breakdown Profile	
w32	DG LO system		1.5	1.5		Scaled from SSK (UCL Submarine Databook 2014) Weight Breakdown Profile	
w32	DG air start system		0.5	0.5		Scaled from SSK (UCL Submarine Databook 2014) Weight Breakdown Profile	
w32	DG FO system		1.1	1.1		Scaled from SSK (UCL Submarine Databook 2014) Weight Breakdown Profile	
w32	Diesel exhaust system		12.6	12.6		Scaled from SSK (UCL Submarine Databook 2014) Weight Breakdown Profile	
w32	DG SW system		3.6	3.6		Scaled from SSK (UCL Submarine Databook 2012) Weight Breakdown Profile	
w33	DG breakers	2	0.8	0.8		Parametric generator breaker	UCL Submarine Databook 2014 (page 80 Section 5.1.4)
w33	Main batt breakers	2	3	3.1		Parametric battery breaker	UCL Submarine Databook 2014 (page 80 Section 5.1.4)
w33	Distribution equip 440V 60Hz		1.1	1.1		Scaled from SSK (UCL Submarine Databook 2012) Weight Breakdown Profile	
w33	Distribution equip 115V 60Hz		2.3	2.3		Scaled from SSK (UCL Submarine Databook 2012) Weight Breakdown Profile	
w33	Distribution equip 200 115V 60Hz		0.1	0.1	100 kg	Scaled from SSK (UCL Submarine Databook 2012) Weight Breakdown Profile	http://128.40.55.189/mediawiki/index.php/SubGp_33_Electrical_Distribution
w33	Distribution equip main DC		1	1.0		Calculations are per breaker. Located on the switchboard or near equipment.	
w33	Distribution equip 24V DC		1	1.0		Scaled from SSK (UCL Submarine Databook 2012) Weight Breakdown Profile	
w34	General lighting		1.5	2.5	$\Delta \times 0.001$	Parametric	http://128.40.55.189/mediawiki/index.php/SubGp_34_Lighting
w34	Secondary emergency lighting		0.5				
	Total Weight Group 3		108.1	109.6			
4	Control & Communications						
w40	Periscopes	2	4	4.1	3.3	Payload	http://128.40.55.189/mediawiki/index.php/SubGp_40_Navigation_Equipment
w40	Periscopes hoists buffers		1.3	1.3		Payload	
w40	Periscope bearings hull glands		1.2	1.2		Payload	
w40	Navigation equipment		2.1	2.1	0.8	Assumed fixed value	http://128.40.55.189/mediawiki/index.php/SubGp_40_Navigation_Equipment
w41	Internal comms		0.9	0.9	$0.02 \times Complement$		http://128.40.55.189/mediawiki/index.php/SubGp_41_Internal_Communications
w4	SRE		0.2	0.2	packing density of 0.25 te/m3		http://128.40.55.189/mediawiki/index.php/SubGp_42_Control_Systems
w45	SCC	4	0.8	0.8		Scaled from SSK (UCL Submarine Databook 2012) Weight Breakdown Profile	
w42	Miscellaneous control instrumentation		2	2.0		Assumed fixed value	http://128.40.55.189/mediawiki/index.php/SubGp_43_Command_Spaces_Systems
w44	Sacrificial anodes		2.2	2.2		Cathodic protection	
w40	Wireless mast hoist		1.5	1.5		C5_RFOM53	UCL Submarine Databook 2014 (page 68 Section 2.3.19)
w40	Wireless RX TX		2.3	2.3		Assumed fixed value	

Group	Description	Unit	UCL data (tonne)	Calculated Weight (tonne)	Selected Numerical Algorithm	Notes	Source
w40	Radar mast hoist	1	2.5	2.5		R3 RFOM 100 Payload	UCL Submarine Databook 2014 (page 67 Section 2.3.19)
w45	Radar set		0.4	0.4		Payload	
w40	EW mast hoist	1	2.7	2.7		EW4 RFOM72 Payload	UCL Submarine Databook 2014 (page 68 Section 2.3.19)
w43	EW equip	7	1.4	1.4		Payload	UCL Submarine Databook 2014 (page 54 Section 2.3.10)
w45	Main passive sonar array		5.5	5.5		Payload	UCL Submarine Databook 2014 (page 62 Section 2.3.12)
w45	Main passive sonar dome		3.6	4.0		Payload	UCL Submarine Databook 2014 (page 56 Section 2.3.12)
w45	Other sonar arrays		2.5	2.5		Payload	UCL Submarine Databook 2014 (page 56 Section 2.3.12)
w45	Other sonar windows		2.6	2.6		Payload	
w43	Sonar processing display	37	7.5	7.4		Payload	UCL Submarine Databook 2014 (page 54 Section 2.3.10)
w43	Data handling computer display	23	3.5	3.5		Payload	UCL Submarine Databook 2014 (page 55 Section 2.3.11)
	Total Weight Group 4		50.7	51.1			
5	Ship Services						
w50	MBT vents operating gr		1.6	1.6	1.6 te	Assumed fixed value	http://128.40.55.189/mediawiki/index.php/SubGp_50_Miscellaneous_Services
w50	External drains		1	1.0	$0.0004\Delta_{sub}$	Assumed proportional to displacement	http://128.40.55.189/mediawiki/index.php/SubGp_50_Miscellaneous_Services
w50	FO filling compensating system		3.2	3.5	≈ 3.5	Dependent on the fuel tanks	http://128.40.55.189/mediawiki/index.php/SubGp_50_Miscellaneous_Services
w50	Ship stores refrigeration machinery		0.8	0.3	$(15 \times 10^{-5} \times N \times S)$	Refinement is less accurate	http://128.40.55.189/mediawiki/index.php/SubGp_50_Miscellaneous_Services
w50	Insulation fluid systems		0.4	0.5	0.5-2.5 te	Dependent on length of hydraulic and fuel pipework	http://128.40.55.189/mediawiki/index.php/SubGp_50_Miscellaneous_Services
w50	Fluids ship services		9.6	12.5	$\approx 0.005\Delta_{sub}$	Dependent on size of hydraulic plant	http://128.40.55.189/mediawiki/index.php/SubGp_50_Miscellaneous_Services
w51	Snort induction mast elevating gear		3.3	3.3	0.5-1 te	Dependent on mast height	http://128.40.55.189/mediawiki/index.php/SubGp_51_Ventilation
w51	Snort induction system		4.2	4.2	3-6 te	Dependent on mast height	http://128.40.55.189/mediawiki/index.php/SubGp_51_Ventilation
w52	Oxygen generators candles	280	2.1	2.4	$0.012 \times O_2$	>30 mins fresh air snort gives 12 hrs free (280 candles) candles/man/hr	http://128.40.55.189/mediawiki/index.php/SubGp_52_Atmosphere_Control
w52	CO2 absorption unit canisters	507	3.8	6.1	$0.030 \times CO_2$	>30 mins fresh air snort gives 12 hrs free (507 cannisters) candles/man/hr	http://128.40.55.189/mediawiki/index.php/SubGp_52_Atmosphere_Control
w52	Ventilation trunking		3.5	3.5		Scaled from SSK (UCL Submarine Databook 2012) Weight Breakdown Profile	http://128.40.55.189/mediawiki/index.php/SubGp_52_Atmosphere_Control
w52	Ventilation fans control	6	1.3	1.2		0.2/0.4/0.5 (6 units 0.2 te)	UCL Submarine Databook 2014 (page 136 Section 6.3.2)
w52	Vent valves filters		1.3	1.3		Scaled from SSK (UCL Submarine Databook 2012) Weight Breakdown Profile	
w52	Vent heaters		0.1	0.1		Scaled from SSK (UCL Submarine Databook 2012) Weight Breakdown Profile	
w53	CW plants	2	5.1	6.0		2 unit of 56 kW CW plants	UCL Submarine Databook 2014 (page 131 Section 6.1.8)
w53	CW system		3	7.5	$\approx 0.003\Delta_{sub}$	Dependent on submarine size	http://128.40.55.189/mediawiki/index.php/SubGp_53_Water_Systems
w53	SW cooling system		12.3	12.2	$\approx 0.004\Delta_{sub} - 0.005\Delta_{sub}$	Bigger ratio for smaller submarines	http://128.40.55.189/mediawiki/index.php/SubGp_53_Water_Systems
w53	Trim bilge ballast system		8.8	8.8	8-13 te	Dependent on trim tank size and position	http://128.40.55.189/mediawiki/index.php/SubGp_53_Water_Systems
w53	Trim pp starters	2	0.4	0.5	0.5 te	Assumed fixed value	http://128.40.55.189/mediawiki/index.php/SubGp_53_Water_Systems
w53	HP bilge pp starter	2	1.5	1.5	1.5-2.5 te	Dependent on MBT size	http://128.40.55.189/mediawiki/index.php/SubGp_53_Water_Systems
w53	LP bilge pp starter	2	0.2	0.2	0.2 te	Assumed fixed value	http://128.40.55.189/mediawiki/index.php/SubGp_53_Water_Systems
w53	HP ballast pp starter	2	1.5	1.5	1.5-2.5 te	Dependent on MBT size	http://128.40.55.189/mediawiki/index.php/SubGp_53_Water_Systems
w53	Priming system pp		0.9	1.0	1 te	Assumed fixed value	http://128.40.55.189/mediawiki/index.php/SubGp_53_Water_Systems
w53	Depth gauges		0.2	0.2	0.2-0.5 te	Dependent on design depth	http://128.40.55.189/mediawiki/index.php/SubGp_53_Water_Systems
w53	Hot cold FW system		0.8	0.8			http://128.40.55.189/mediawiki/index.php/SubGp_53_Water_Systems
w54	Sanitary system		1.2	1.2	$\approx 5 \times 10^{-4}\Delta_{sub}$	Dependent on crew size	http://128.40.55.189/mediawiki/index.php/SubGp_54_-_Water_Systems_Continued
w54	Battery cooling system		3	3.0	3 te	Dependent on battery size	http://128.40.55.189/mediawiki/index.php/SubGp_54_-_Water_Systems_Continued
w54	FW cooling system		2.9	2.9	2.5-7 te	Dependent on size of submarine	http://128.40.55.189/mediawiki/index.php/SubGp_54_-_Water_Systems_Continued
w54	Desalination plant	1	1.2	1.2	1-4 te (Dependent on crew size)	Refined in NBA/SUBFLOW sizing	http://128.40.55.189/mediawiki/index.php/SubGp_54_-_Water_Systems_Continued
w54	Domestic plumbing		0.3	0.1	$6 \times 10^{-5}\Delta_{sub}$	Dependent on size of submarine	http://128.40.55.189/mediawiki/index.php/SubGp_54_-_Water_Systems_Continued

Group	Description	Unit	UCL data (tonne)	Calculated Weight (tonne)	Selected Numerical Algorithm	Notes	Source
w55	HP air compressors	2	5	5.4		2 units (320m ³ hr)	UCL Submarine Databook 2014 (page 119 Section 6.1.1) http://128.40.55.189/mediawiki/index.php/SubGp_55_Air_Systems
w55	HP air system		3.9	3.9		Scaled from SSK (UCL Submarine Databook 2012) Weight Breakdown Profile	
w55	HP air bottles	13	6.8	6.5		13 ' 258 litre	UCL Submarine Databook 2014 (page 120 Section 6.1.1) http://128.40.55.189/mediawiki/index.php/SubGp_55_Air_Systems
w55	Hydraulic acc bottles	7	1.6	1.6		SDB shows 106 litre instead (7 ' 108 litre (capacity per bottle))	UCL Submarine Databook 2014 (page 120 Section 6.1.1) http://128.40.55.189/mediawiki/index.php/SubGp_55_Air_Systems
w55	Direct blow system		2.1	2.1		Emergency blow system	
w55	Direct blow bottles	8	4.2	4.0		8 ' 258 litre	UCL Submarine Databook 2014 (page 120 Section 6.1.1) http://128.40.55.189/mediawiki/index.php/SubGp_55_Air_Systems
w55	Aux vent blow system		3.6	3.6		Scaled from SSK (UCL Submarine Databook 2012) Weight Breakdown Profile	
w55	LP blower	1	1.8	2.0		Assumed one blower	http://128.40.55.189/mediawiki/index.php/SubGp_55_Air_Systems
w55	LP blow system		4	4.0		Scaled from SSK (UCL Submarine Databook 2012) Weight Breakdown Profile	
w55	BIBS bottles	6	3.1	3.0		6 units 258 litre	http://128.40.55.189/mediawiki/index.php/SubGp_55_Air_Systems
w55	BIBS system		0.5	0.5		Assumed fixed value	
w55	EBS system		0.3	0.3		Emergency Breathing System assumed fixed value	
w55	Salvage compartment		0.5	0.5		Assumed fixed value	
w57	Main hydraulic system		4.5	4.5	4-7 te	Dependent on main plant	http://128.40.55.189/mediawiki/index.php/SubGp_57_Hydraulic_Systems
w57	External hydraulic system		2.3	2.3	2-6 te	Dependent on external plant	http://128.40.55.189/mediawiki/index.php/SubGp_57_Hydraulic_Systems
w57	Steering hydroplane control system		1.4	1.4	1.5-3 te	Dependent on control plant	http://128.40.55.189/mediawiki/index.php/SubGp_57_Hydraulic_Systems
w57	Steering diving hydraulic plant	1	2.8	2.5	3-4 te	SDB 121 120mins dependent on control surfaces size	http://128.40.55.189/mediawiki/index.php/SubGp_57_Hydraulic_Systems
w57	Main hydraulic plant	1	1.6	1.5		SDB 121 60mins dependent on required capacity	http://128.40.55.189/mediawiki/index.php/SubGp_57_Hydraulic_Systems
w57	External hydraulic plant	1	1.5	1.5		SDB 121 60mins dependent on required capacity	http://128.40.55.189/mediawiki/index.php/SubGp_57_Hydraulic_Systems
w57	Hydraulic oil filling transfer system		0.4	0.4	0.4 te	Assumed fixed value	http://128.40.55.189/mediawiki/index.php/SubGp_57_Hydraulic_Systems
w58	Rudder equip		10.6	10.5	$\approx 0.004\Delta_{sub} - 0.005\Delta_{sub}$	Ram servo etc Dependent on rudder size (bigger ratio for smaller subs)	http://128.40.55.189/mediawiki/index.php/SubGp_58_Steering_and_Planes_Gear
w58	Retractable fwd hydroplane equip		7.5	7.5	$\approx 0.003\Delta_{sub}$	Actuators etc Dependent on hydroplane size	http://128.40.55.189/mediawiki/index.php/SubGp_58_Steering_and_Planes_Gear
w58	Aft hydroplane equip		3.9	4.0	$\approx 0.0016\Delta_{sub}$	Actuators etc Dependent on hydroplane size	http://128.40.55.189/mediawiki/index.php/SubGp_58_Steering_and_Planes_Gear
w59	Garbage ejector		1.2	1.0	1 te	Assumed fixed value	http://128.40.55.189/mediawiki/index.php/SubGp_59_Garbage_Systems
	Total Weight Group 5		154.6	164.8			
6	Outfit & Furnishings						
w60	Indicator buoys	2	1.4	1.4	0.7 per buoy	Assumed 2 buoys	http://128.40.55.189/mediawiki/index.php/SubGp_60_Escape_Equipment
w60	Escape equip		1.8	2.9	6.4te/100men	General guide - escape suits, canisters, candles, barley sugar weight	http://128.40.55.189/mediawiki/index.php/SubGp_60_Escape_Equipment
w61	FF equip systems		2.5	3.0	$\approx 0.0012\Delta_{sub}$	Dependent on size of submarine	http://128.40.55.189/mediawiki/index.php/SubGp_61_Miscellaneous_Outfit
w61	Captans windlass		4.1	4.1	4-5 te	Assumed fixed value. 2 capstans	http://128.40.55.189/mediawiki/index.php/SubGp_61_Miscellaneous_Outfit
w61	Anchor cable		4.2	4.2	4-7 te	Dependent on size of submarine	http://128.40.55.189/mediawiki/index.php/SubGp_61_Miscellaneous_Outfit
w61	Bollards fairleads		3.2	3.2	2-3.5 te	Assumed fixed value	http://128.40.55.189/mediawiki/index.php/SubGp_61_Miscellaneous_Outfit
w61	Hawsers cables		1.3	1.3	1.2-2 te	Dependent on size of submarine	http://128.40.55.189/mediawiki/index.php/SubGp_61_Miscellaneous_Outfit
w61	Lifting beams		0.4	0.5	0.5 te	Assumed fixed value	http://128.40.55.189/mediawiki/index.php/SubGp_61_Miscellaneous_Outfit
w62	Navigation lights		0.2	0.2	0.2-0.5 te	Dependent on length of submarine	http://128.40.55.189/mediawiki/index.php/SubGp_62_Hull_Fittings
w62	Staffs guardrails		1.4	1.4	1.4-2 te	Dependent on number of decks and openings	http://128.40.55.189/mediawiki/index.php/SubGp_62_Hull_Fittings
w62	Ladders		1.2	1.2	1-3.5 te	Dependent on number of decks and openings	http://128.40.55.189/mediawiki/index.php/SubGp_62_Hull_Fittings
w64	Workshop equip		0.5	0.5	0.5-3.5 te	Dependent on size of submarine	http://128.40.55.189/mediawiki/index.php/SubGp_64_Compartment_Equipment
w64	Galley ovens hotplates	2	1.4	1.4	3te/100men	General guideline	http://128.40.55.189/mediawiki/index.php/SubGp_64_Compartment_Equipment
w65	Kit lockers wardrobes		1.2	1.2	2.5te/100men	General guideline	http://128.40.55.189/mediawiki/index.php/SubGp_65_Compartment_Furnishing
w65	Bunks mattresses		3	3.3	7.2te/100men	General guideline	http://128.40.55.189/mediawiki/index.php/SubGp_65_Compartment_Furnishing

Group	Description	Unit	UCL data (tonne)	Calculated Weight (tonne)	Selected Numerical Algorithm	Notes	Source
w65	Office furniture safes		4	3.1	6.7te/100men	General guideline	http://128.40.55.189/mediawiki/index.php/SubGp_65_Compartment_Furnishing
w66	Spear gear lockers		2.4	2.5	2.5-12.5 te	Lower ones for SSKs	http://128.40.55.189/mediawiki/index.php/SubGp_66_Storeroom_Equipment
w66	Battery compartment fittings		5.9	5.9	5-7 te	Lower for SSNs	http://128.40.55.189/mediawiki/index.php/SubGp_66_Storeroom_Equipment
w67	Thermal acoustic insulation		9.6	9.6	8-12 te	Dependent on desired level of signature	http://128.40.55.189/mediawiki/index.php/SubGp_67_Hull_Insulation_and_Tiles
w67	Vibration damping		1.8	2.0	$\approx 8 \times 10^{-4} \Delta_{sub}$	Dependent on power of main propulsion unit	http://128.40.55.189/mediawiki/index.php/SubGp_67_Hull_Insulation_and_Tiles
w68	Paint fillers		12	10.0	$0.004 \Delta_{sub} - 0.005 \Delta_{sub}$	Dependent on external and internal surface area (and number of decks)	http://128.40.55.189/mediawiki/index.php/SubGp_68_General_Finishes_and_Paint
w68	Deck coverings		3.4	3.7	$0.0015 \Delta_{sub} - 0.0025 \Delta_{sub}$	(2 decks lower value, 3 decks higher value)	http://128.40.55.189/mediawiki/index.php/SubGp_68_General_Finishes_and_Paint
	Total Weight Group 6		67.5	66.6			
7	Armaments & Pyrotechnics						
w70	Torpedo tubes	6	36	36.0	6 te	6 units 600mm per tube	UCL Submarine Databook 2014 (page 38 Section 2.3.1)
w70	Bow shutters operating gr	6	2.7	2.7	0.45 te	Per tube	UCL Submarine Databook 2014 (page 38 Section 2.3.1)
w70	Torpedo CP	6	1	1.0	0.167 te	Control panel per tube per tube	UCL Submarine Databook 2014 (page 38 Section 2.3.1)
w70	ATP	2	7.3	7.3	3.65 te	Per unit	UCL Submarine Databook 2014 (page 43 Section 2.3.4)
w70	Tube flood drain system	2	2.5	3.5	1.75 te	Per system	UCL Submarine Databook 2014 (page 43 Section 2.3.4)
w70	Tube hydraulic system	6	6	6.0	1 te	Per tube	UCL Submarine Databook 2014 (page 38 Section 2.3.1)
w70	Air turbine pump system	2	3.4	3.4	1.7 te	Per system	UCL Submarine Databook 2014 (page 43 Section 2.3.4)
w71/72	Torpedo stowage handling gr	12	22.3	22.2	1.85 te	Per weapon carried	UCL Submarine Databook 2014 (page 38 Section 2.3.1)
w73	Signal ejectors	2	4	4.0	2 te	2 units (small countermeasures)	UCL Submarine Databook 2014 (page 38 Section 2.3.17)
w72	Fluids torpedo systems	2	1	1.0	0.5 te	Per system	UCL Submarine Databook 2014 (page 43 Section 2.3.4)
	Total Weight Group 7		86.2	87.1			
8	Fixed Ballast						
w80/81	Fixed ballast, design margin, and growth margins		171.7	149.9	$0.08 \Delta_{ph}$	6-8% solid ballast fraction relative to submerged displacement	http://128.40.55.189/mediawiki/index.php/SubGp_80_Permanent_Ballast
	Total Weight Group 8		171.7	149.9			
9	Variable Items						
w90	Crew effects		5	6.9	0.15te per man	Assumed fixed value	http://128.40.55.189/mediawiki/index.php/SubGp_90_Variable_Load_Items
w90	Small arms pyrotechnics		1	1.0		Payload	http://128.40.55.189/mediawiki/index.php/SubGp_90_Variable_Load_Items
w90	Torpedoes	18	30	29.0	1.61 te each	Payload	UCL Submarine Databook 2014 (page 40 Section 2.3.2.3)
w90	Stores provisions		8.4	9.0	0.004m ³ /man/day with density	Assumed the stores to have an average density of 0.15 te/m ³ .	http://128.40.55.189/mediawiki/index.php/SubGp_90_Variable_Load_Items
w90	Naval stores spare gear		12	12.0	$0.05\% \Delta_{sub}$	Dependent on duration of mission	http://128.40.55.189/mediawiki/index.php/SubGp_90_Variable_Load_Items
w90	Fluids		230	205.8	$0.08 \nabla_{sub} \rho$		http://128.40.55.189/mediawiki/index.php/SubGp_90_Variable_Load_Items
w91	TC water		60	99.6	$0.5 \frac{\delta w_{90}}{0.95 \times 0.95} + \frac{\delta \rho_w \times \Delta_{sub}}{0.95 \times 0.95 \times \rho_w}$		http://128.40.55.189/mediawiki/index.php/subgp_91_Trim_and_Compensation_Water
w92	MBT water		260	241.6	$\frac{r.o.b. \times \Delta_{surf}}{k_{mbt}} = \frac{r.o.b. \times \Delta_{sub}}{(1 + r.o.b.) k_{mbt}}$		http://128.40.55.189/mediawiki/index.php/SubGp_92_Main_Ballast_Water
	Total Weight Group 9		606.4	604.8			
	Total All Weight Groups		2500	2498.4			

Table A 4: Volume summary of Case Study 5.1 showing the balance buoyancy and weight in Table A 5

DBB objects at the volume granularity	Description	Type 2400 (m ³)	% PH Volume	Case Study 5.1 (m ³)	Notes
<i>Zone</i>	<i>Aft</i>	716.2	35.9	760.8	
BB_VL_MV_RM_MR	Motor room	262.2	13.1	275.2	Sized in Paramarine
BB_VL_IA_RM_ER	Engine room	232.9	11.6	244.4	Sized in Paramarine
BB_VL_FL_TB_TA	Trim tank aft	25.5	1.3	26.7	Sized to meet equilibrium balance
BB_VL_FL_RM_BI	Bilge tank	5.2	0.3	5.4	Scaled from Type 2400 SSK
BB_VL_IA_DV_LO	Lubricant oil tank	5.5	0.3	5.8	Scaled from Type 2400 SSK
BB_VL_IA_DV_OA	Fuel tank aft	135.3	6.8	141.9	The total fuel volume must meet the fuel requirement
BB_VL_IA_RM_SA	Storage aft	49.6	2.5	61.4	Covering engineering storage and refrigeration, cold & cool 0.009 m ³ /man/day UCL Submarine Databook page. 143
<i>Zone</i>	<i>Mid</i>	694.5	34.7	675.9	
BB_VL_FH_RM_CO	Control room	227.4	11.4	219.4	Sized in Paramarine based on payload requirement
BB_VL_IA_RM_AM	Auxiliary Machinery Space (AMS)	95.5	4.8	104.4	Sized in Paramarine
BB_VL_IA_RM_MS	Messes, etc.	126.3	6.3	105.8	Calculated covering galley, mess, and passageway based on UCL Submarine Databook page. 141 & 142
BB_VL_IA_DV_OM	Fuel tank mid	8.1	0.4	4.2	The total fuel volume must meet the fuel requirement
BB_VL_IA_RM_BA	Battery aft	116.8	5.8	109.7	The total battery volume must meet the propulsion system calculation
BB_VL_FL_TB_TM	Trim and Compensating tank	53.8	2.7	62.7	Sized to meet equilibrium balance
BB_VL_IA_RM_SF	Storage forward	44.7	2.2	46.8	Provision storage 0.006 m ³ /man/day UCL Submarine Databook page. 143 including personal and communal kit stowage
BB_VL_IA_RM_FW	Fresh water tank	21.9	1.1	22.9	Including desalination water, fresh water 14 litres/man/day UCL Submarine Databook page. 143
<i>Zone</i>	<i>Forward</i>	588.8	29.6	661.3	
BB_VL_FH_RM_WS	Weapon stowage compartment	191.1	9.6	211.4	Sized in Paramarine based on payload requirement
BB_VL_IA_RM_AO	Accommodation	151.7	7.6	170.0	Calculated based on deck area requirement from the UCL Submarine Databook page. 142 covering bathrooms, sleeping area
BB_VL_FH_RM_TR	Space for ATP and WRT	39.6	2	41.5	Sized in Paramarine based on payload requirement, covering space for Water Round Torpedo (WRT) tank so the pressure between the torpedo and the tube can be equalised with sea pressure without changing longitudinal moment
BB_VL_IA_RM_BF	Battery forward	127.3	6.4	133.4	The total battery volume must meet the propulsion system calculation
BB_VL_IA_DV_OF	Fuel tank forward	49.5	2.5	51.9	The total fuel volume must meet the fuel requirement
BB_VL_IA_RM_SG	Sewage tank	3.6	0.2	3.8	Scaled from Type 2400 SSK
BB_VL_FH_RM_TO	Torpedo Operating Tank (TOT)	10.1	0.5	10.6	Sized in Paramarine based on payload requirement, taking all the water required when a full load of torpedoes is discharged
BB_VL_FL_TB_TF	Trim tank forward	15.9	0.8	38.7	
Total	Internal Volume (re-faceted)	1999.6	100	2098	Re-faceted pressure hull volume in Paramarine
BB_VL_FL_FF_EA	Free flood volume aft occupied by equipment	29.6		55.7	Sized in Paramarine
BB_VL_FL_MB_MA	External Main Ballast Tank volume aft	126.4		103.2	Sized in Paramarine
BB_VL_FL_MB_MF	External Main Ballast Tank volume forward	334.3		223.8	Sized in Paramarine
BB_VL_FL_FF_EF	Free flood volume forward occupied by equipment	142.9		181.1	Sized in Paramarine
BB_VL_FL_FF_BR	Bridge fin volume	135.3		102.7	Sized in Paramarine
BB_VL_FL_FF_CA	Casing volume	363.4		296.9	Sized in Paramarine
Total	External Volume	1132		963.4	
BB_VL_MV_FF_RT	Rudder top	9.5		6.6	
BB_VL_MV_FF_RB	Rudder bottom	5.9		3.4	
BB_VL_MV_FF_AP/S	Aft hydroplanes (port & starboard)	24.2		13.2	
BB_VL_MV_FF_FP/S	Forward hydroplanes (port & starboard)	1.8		2.6	
Total	Appendages	41.3		25.8	
Submerged	Buoyant Volume			2437.5	Without freefloods
	Displacement			2496	

A 7.1.2 Longitudinal Moment and Vertical Stability

This subsection provides analyses carried out for surfaced and submerged conditions of Case Study 5.1. Figure A.54 shows the trim condition in a surfaced scenario (surfaced displacement is 2205 tonne) while Figure A.55 shows Case Study 5.1 had adequate righting arms for all anticipated angles of heel and pass relevant criteria for surfaced stability.

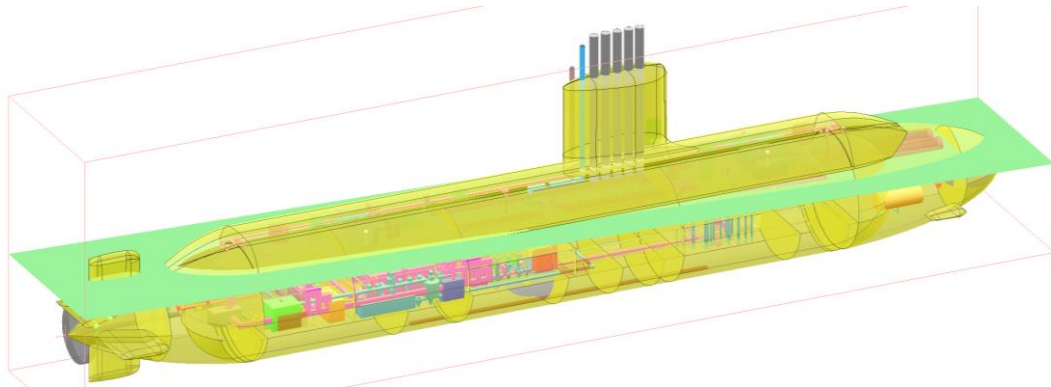


Figure A.54: Visualisation of the trim waterplane in a surfaced condition of Case Study 5.1 using Paramarine-SURFCON

In the submerged operating condition, the weight summary based on DBB functional classification is given in Table A 5. This provides submerged longitudinal centre of gravity (LCG) and vertical centre of gravity (VCG) relative to the centroid (0,0,0), which was set at the mid part and the centre of the pressure hull in Paramarine. Using **char_ballast_shift** object, the submerged BG could then be calculated using Paramarine. The submerged BG of Case Study 5.1 was 0.6 m, which met the criteria based on the UCL submarine design procedure (UCL-NAME, 2012).

Table A 5: Weight summary of Case Study 5.1 based on functional group classification, see Table A 3 for individual items of weight that were sized using parametric approaches and Table A 4 for the total buoyant volume

Functional Group	Design Building Block (DBB) Objects at the Weight Granularity	Weight (tonne)	LCG (m)	VCG (m)
Fight	SBB_control_data	164.9	10.9	1.7
	BB_NL_2_MCC			
	BB_NL_4_SCC			
	BB_NL_4_miscellaneous_control_instrumentation			
	BB_NL_4_data_handling_computer_display			
	BB_NL_4_navigation_equipment			
	BB_NL_4_internal_comms			
	SBB_sonar			
	BB_NL_4_main_passive_sonar_array			
	BB_NL_4_main_passive_sonar_dome			
	BB_NL_4_other_sonar_arrays			
	BB_NL_4_other_sonar_windows			
	BB_NL_4_sonar_processing_display			
	SBB_periscope			
	BB_NL_1_periscope_supports_wells			
	BB_NL_4_periscopes			
	BB_NL_4_periscopes_hoists_buffers			
	BB_NL_4_periscope_bearings_hull_glands			
	SBB_mast			
	BB_NL_4_wireless_mast_hoist			
	BB_NL_4_wireless_RX_TX			
	BB_NL_4_radar_mast_hoist			
	BB_NL_4_radar_set			
	BB_NL_4_EW_mast_hoist			
	BB_NL_4_EW_equip			
	SBB_torpedo			
	BB_NL_1_torpedo_loading_hatch			
	BB_NL_7_torpedo_tubes			
	BB_NL_7_torpedo_CP			
	BB_NL_7_torpedo_stowage_handling_gr			
	BB_NL_7_fluids_torpedo_systems			
	BB_NL_7_ATP			
	BB_NL_7_tube_flood_drain_system			
	BB_NL_7_tube_hydraulic_system			
	BB_NL_7_air_trubine_pump_system			
	BB_NL_7_bow_shutters_operating_gr			
	BB_NL_9_torpedoes			
	SBB_signature			
	BB_NL_6_vibration_damping			
	BB_NL_6_thermal_acoustic_insulation			
BB_NL_6_paint_fillers				
BB_NL_7_signal_ejectors				

Functional Group	Design Building Block (DBB) Objects at the Weight Granularity	Weight (tonne)	LCG (m)	VCG (m)
	SBB_naval_store BB_NL_9_small_arms_pyrotechnics BB_NL_9_naval_stores_spare_gear			
Move	SBB_mooring_systems BB_NL_6_captans_windlass BB_NL_6_anchor_cable BB_NL_6_bollards_fairleads BB_NL_6_hawsers_cables SBB_manoevring_systems BB_NL_1_fwd_hydroplanes BB_NL_1_aft_hydroplanes BB_NL_1_stabilisers BB_NL_1_rudders BB_NL_5_steering_hydroplane_control_system BB_NL_5_steering_diving_hydraulic_plant BB_NL_5_rudder equip BB_NL_5_retractable_fwd_hydroplane equip BB_NL_5_aft_hydroplane equip SBB_propulsion_systems BB_NL_2_fluids_propulsion_system BB_NL_2_shafting BB_NL_2_thrust_block BB_NL_2_stern_seal BB_NL_2_propeller_ropes_guard_cone BB_NL_2_main_motor BB_NL_2_propulsion_switchgear	67.3	-13.3	0.17
Float	SBB_pressure_hull BB_NL_1_PH_plating_stiffening BB_NL_1_dome_end_bulkheads BB_NL_1_conning_tower BB_NL_1_fore_end_structure BB_NL_1_aft_end_structure BB_NL_1_casing BB_NL_1_keel_structure BB_NL_1_bridge_fin_structure BB_NL_1_major_bulkheads BB_NL_1_decks_flats_pillars BB_NL_1_internal_structure_high BB_NL_1_divisional_bulkheads_steel BB_NL_1_divisional_bulkheads_partition BB_NL_1_main_non_structural_tanks BB_NL_1_internal_structure_low BB_NL_1_internal_structural_tanks SBB_water_distribution_systems BB_NL_5_trim_bilge_ballast_system	855.6	1.6	-0.01

Functional Group	Design Building Block (DBB) Objects at the Weight Granularity	Weight (tonne)	LCG (m)	VCG (m)
	BB_NL_5_trim_pp_starters BB_NL_5_HP_bilge_pp_starter BB_NL_5_LP_bilge_pp_starter BB_NL_5_HP_ballast_pp_starter BB_NL_5_priming_system_pp BB_NL_5_depth_gauges BB_NL_9_TC_water BB_NL_9_MBT_water SBB_air_systems BB_NL_5_HP_air_compressors BB_NL_5_HP_air_system BB_NL_5_HP_air_bottles BB_NL_5_hydraulic_acc_bottles BB_NL_5_direct_blow_system BB_NL_5_direct_blow_bottles BB_NL_5_aux_vent_blow_system BB_NL_5_LP_blower BB_NL_5_LP_blow_system BB_NL_5_MBT_vents_operating_gr BB_NL_5_external_drains BB_NL_5_salvage_compartment SBB_outfitting BB_NL_1_seats BB_NL_1_mounts BB_NL_1_pipe_system_supports_clips BB_NL_6_lifting_beams BB_NL_6_navigation_lights SBB_fluids BB_NL_5_fluids_ship_services BB_NL_9_fluids SBB_solid_ballast BB_NL_8_fixed_ballast SBB_broad_margins BB_NL_8_design_margin BB_NL_8_growth_margin BB_NL_4_sacrificial_anodes			
Infrastructure	SBB_power_generations BB_NL_3_1400kW_DG BB_NL_3_DG_breakers BB_NL_3_DG_air_start_system SBB_energy_storage BB_NL_2_main_batteries BB_NL_3_main_batt_breakers BB_NL_6_battery_compartment_fittings	118.8	-0.9	0.7

Functional Group	Design Building Block (DBB) Objects at the Weight Granularity	Weight (tonne)	LCG (m)	VCG (m)
	SBB_power_data			
	BB_NL_1_cableways			
	BB_NL_3_cabling			
	SBB_power_distributions			
	BB_NL_3_electrical_glands			
	BB_NL_3_fluids_electrical_services			
	BB_NL_3_distribution_equip_440V_60Hz			
	BB_NL_3_distribution_equip_115V_60Hz			
	BB_NL_3_distribution_equip_200_115V_60Hz			
	BB_NL_3_distribution_equip_main_DC			
	BB_NL_3_distribution_equip_24V_DC			
	BB_NL_3_140kW_60Hz_MG			
	BB_NL_3_400Hz_static_frequency_changers			
	SBB_fuel_systems			
	BB_NL_3_DG_FO_system			
	BB_NL_5_FO_filling_compensating_system			
	BB_NL_5_insulation_fluid_systems			
	SBB_cooling_cooling_systems			
	BB_NL_3_DG_FW_system			
	BB_NL_3_DG_LO_system			
	BB_NL_3_DG_SW_system			
	BB_NL_5_CW_plants			
	BB_NL_5_CW_system			
	BB_NL_5_SW_cooling_system			
	BB_NL_5_battery_cooling_system			
	BB_NL_5_FW_cooling_system			
	BB_NL_5_hot_cold_FW_system			
	SBB_hydraulics_systems			
	BB_NL_5_main_hydraulic_system			
	BB_NL_5_external_hydraulic_system			
	BB_NL_5_main_hydraulic_plant			
	BB_NL_5_external_hydraulic_plant			
	BB_NL_5_hydraulic_oil_filling_transfer_system			
	SBB_domestic_systems			
	BB_NL_5_garbage_ejector			
	BB_NL_6_indicator_buoys			
	BB_NL_5_sanitary_system			
	BB_NL_5_desalination_plant			
	BB_NL_5_domestic_plumbing			
	SBB_safety_emergency			
	BB_NL_3_secondary_emergency_lighting			
	BB_NL_4_SRE			
	BB_NL_6_FF_equip_systems			
	BB_NL_6_escape_equip			
	BB_NL_5_BIBS_bottles			

Functional Group	Design Building Block (DBB) Objects at the Weight Granularity	Weight (tonne)	LCG (m)	VCG (m)
	BB_NL_5_BIBS_system			
	BB_NL_5_EBS_system			
	SBB_accommodation			
	BB_NL_6_galley_ovens_hotplates			
	BB_NL_6_kit_lockers_wardrobes			
	BB_NL_6_bunks_mattresses			
	BB_NL_6_office_furniture_safes			
	BB_NL_9_crew_effects			
	BB_NL_3_general_lighting			
	SBB_access			
	BB_NL_6_deck_coverings			
	BB_NL_1_access			
	BB_NL_1_escape_towers			
	BB_NL_1_gratings_ladders			
	BB_NL_1_other_pressure_hull_hatches			
	BB_NL_1_manhole_covers			
	BB_NL_1_watertight_doors			
	BB_NL_1_non_watertight_doors_hatches			
	BB_NL_6_staffs_guardrails			
	BB_NL_6_ladders			
	SBB_atmosphere_control			
	BB_NL_3_diesel_exhaust_system			
	BB_NL_5_snort_induction_mast_elevating_gear			
	BB_NL_5_snort_induction_system			
	BB_NL_5_oxygen_generators_candles			
	BB_NL_5_CO2_absorption_unit_canisters			
	BB_NL_5_ventilation_trunking			
	BB_NL_5_ventilation_fans_control			
	BB_NL_5_vent_valves_filters			
	BB_NL_5_vent_heaters			
	SBB_provisions			
	BB_NL_5_ship_stores_refrigeration_machinery			
	BB_NL_6_workshop_equip			
	BB_NL_9_stores_provisions			
	BB_NL_6_spear_gear_lockers			
Summary	Defined in WGP	1406.8	0.7	-0.4
	Defined in VGP	501.7	2.2	-0.9
	Defined in CGP	487.5	1.3	-0.9
	Defined in SCP	91.7	-6.5	0.4
	Ballast shift	8	-0.4	-3.8
	Master Building Block (MBB)	2496	0	-0.6

A 7.1.3 Submerged Equilibrium Analysis

For depth control, the change of buoyancy and weight of the submarine needs to be managed by using various compensating tanks via the Trim and Ballast 'TB' system. As shown in Figure A.56, the trim polygon was constructed from an initial Standard Trim Condition (STC) in the submerged operating condition. The following sequence of events was analysed to determine the case change in weight and moment: lost displacement due to 1% compression of ship's hull; discharge weapons; provisions are consumed; naval stores removed from the ship; and fuel consumptions. Figure A.56 shows the feasible weight changes in weight and moment are covered by the change in weight and moment available via the TB system.

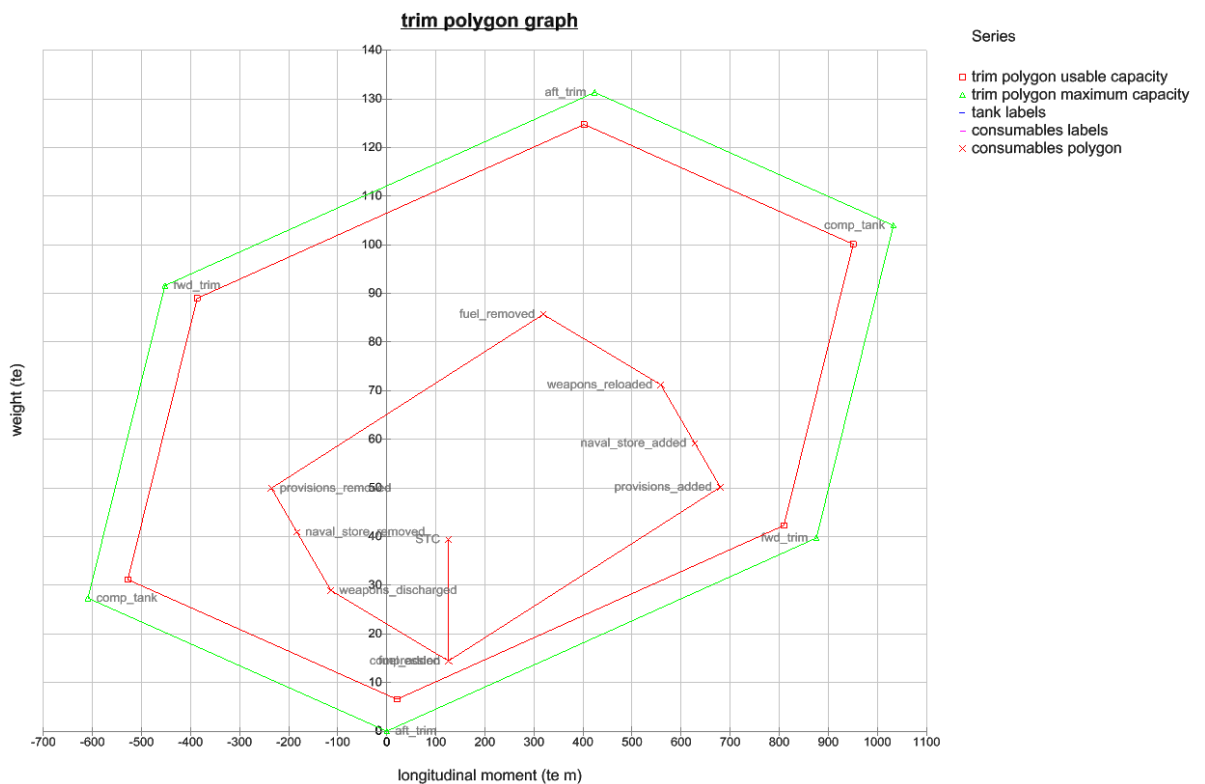


Figure A.56: The trim polygon of Case Study 5.1 using Paramarine-SURFCON

A 7.2 Speed

This section aims to confirm that the chosen propulsion plant of Case Study 5.1 meets speed/power requirements. Figure A.57 shows in the sprint submerged scenario, which is 20 knots (see Table 5.1 on page 174), the effective power calculated is less than 4 MW. Figure A.58 shows in a surfaced scenario, which is 7 knots (see Table 5.1 on page 174), the effective power calculated is less than 500 kW.

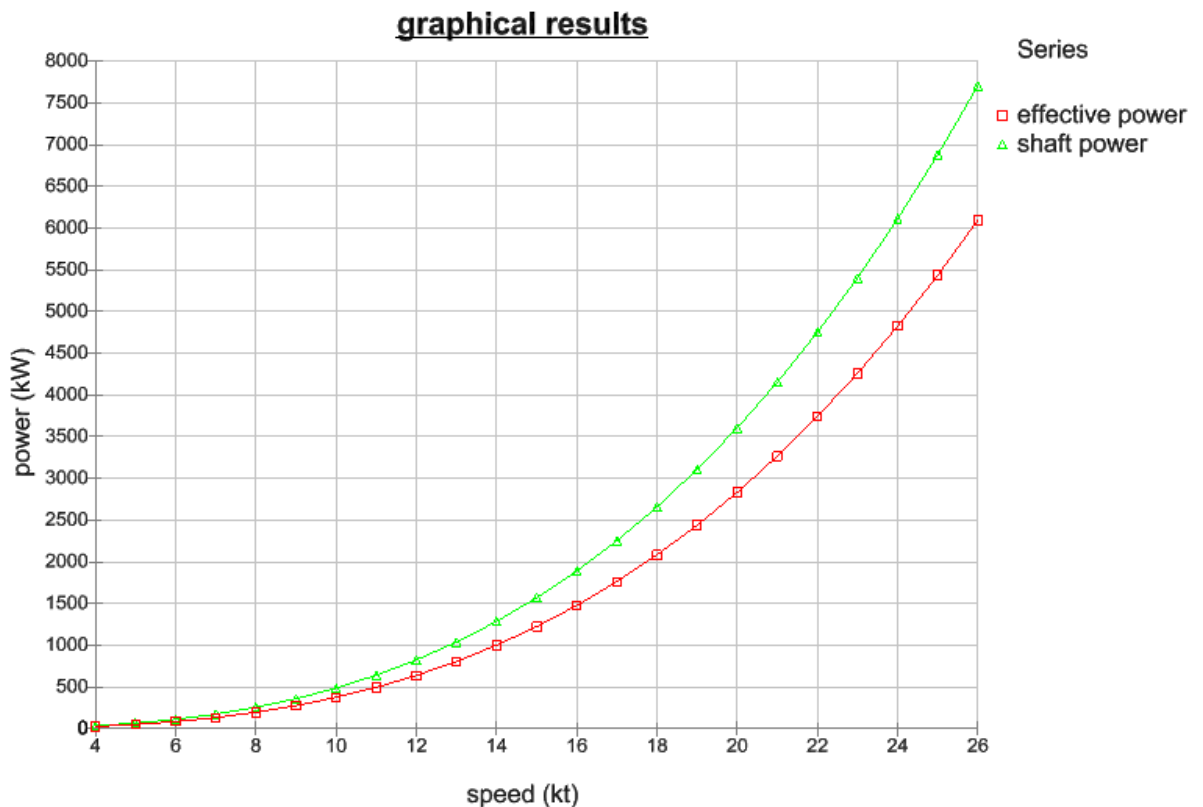


Figure A.57: Power required vs Speed of Case Study 5.1 in the submerged scenario, calculated using Paramarine-SURFCON

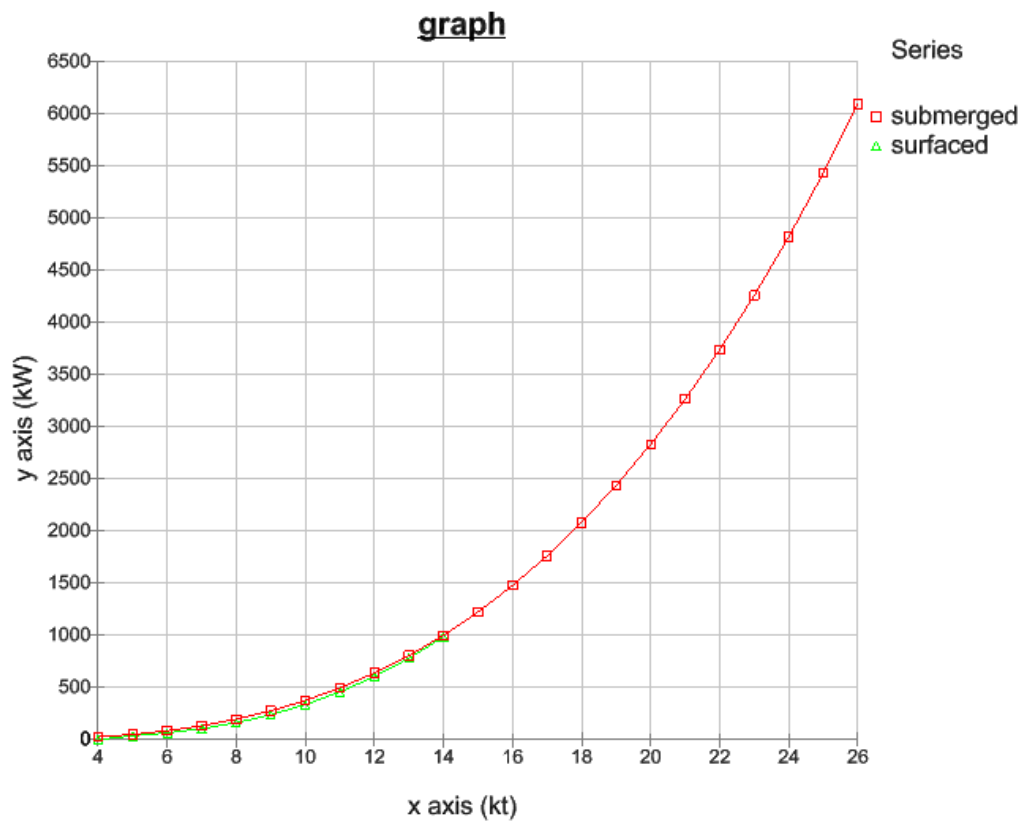


Figure A.58: Power required vs Speed of Case Study 5.1 in a surfaced scenario in green and in the submerged scenario in red, calculated using Paramarine-SURFCON

A 7.3 Strength

This section provides the initial structural analysis of Case Study 5.1 and the model of the required structure into the design. Figure A.59 shows the input of initial pressure hull scantlings to withstand the hydrostatic pressure at the operational depth. This then allows the pressure hull stiffeners to be modelled and visualised with the DS3 components and connections (see Figure A.60) For a 250 m depth, the summary of structural failure is shown in Figure A.61. The lowest safety factor was 1.5 and the theoretical crush depth was 370 m.

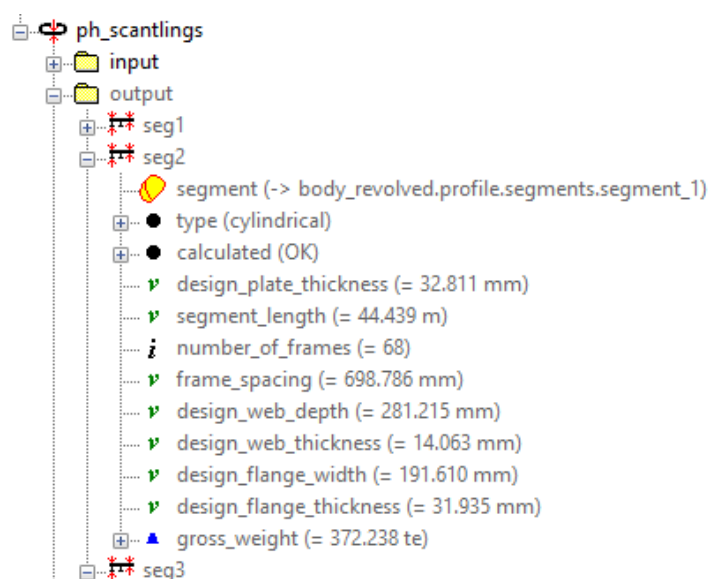


Figure A.59: Initial pressure hull scantling calculation of Case Study 5.1 using Paramarine-SURFCON

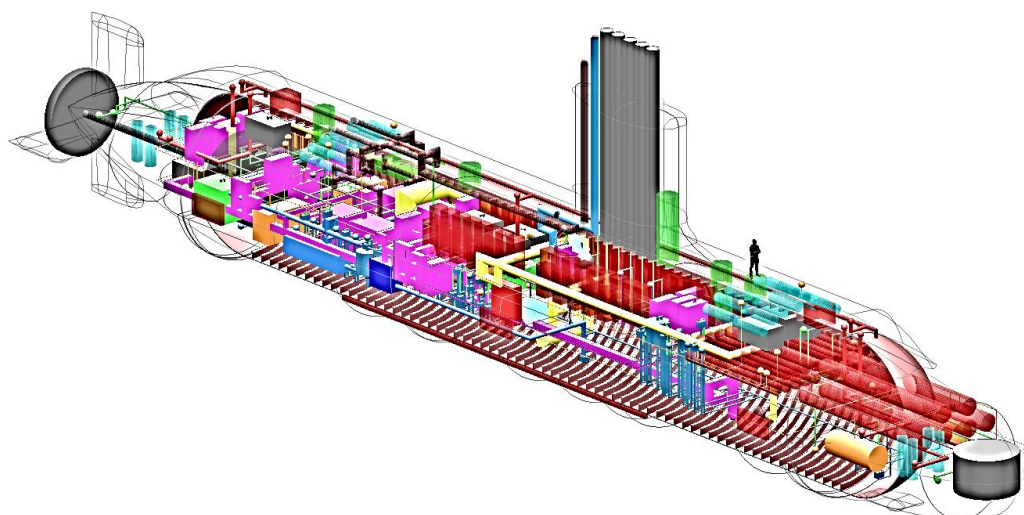


Figure A.60: Initial pressure hull structure modelling of Case Study 5.1 using Paramarine-SURFCON with the DS3 components and connections are shown

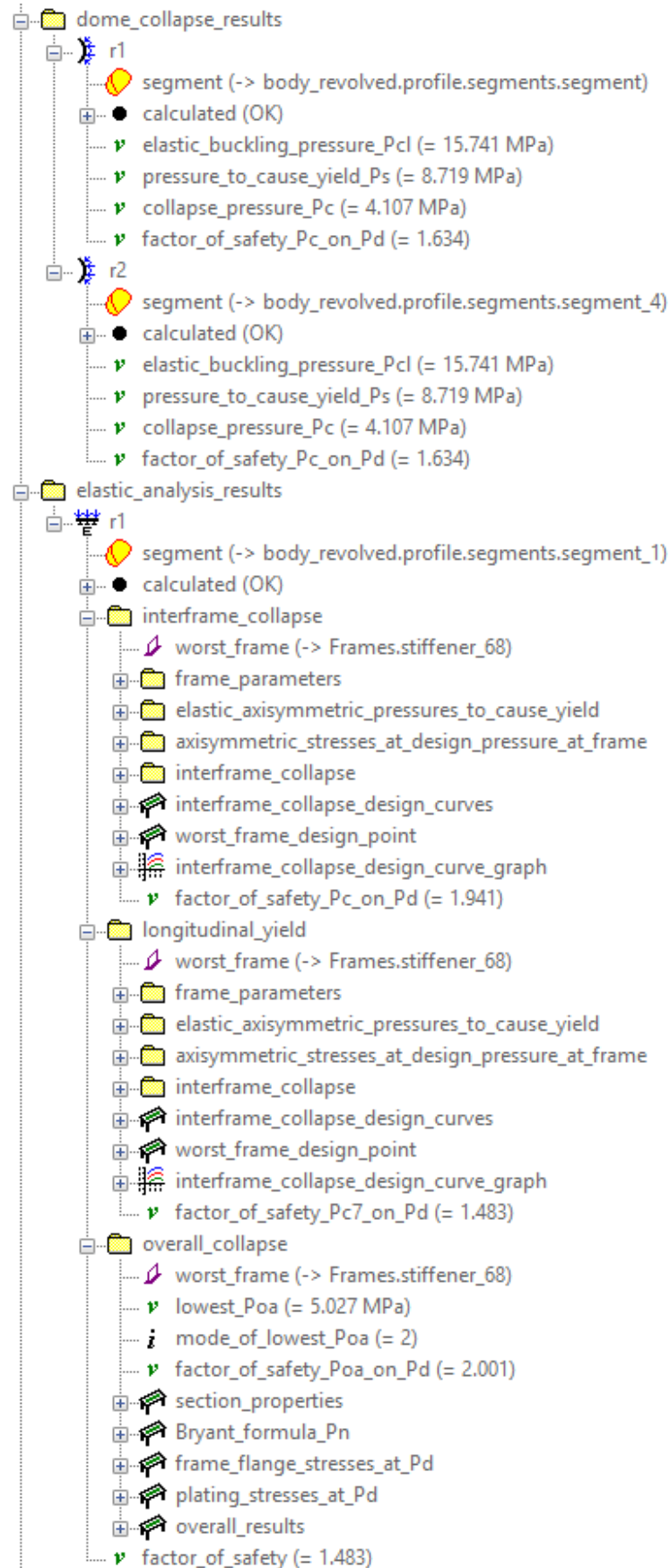


Figure A.61: Summary of initial structural failure analysis of Case Study 5.1 using Paramarine-SURFCON

A 7.4 Manoeuvrability

Initial examination of the manoeuvring performance of the submarine was calculated using Paramarine-SURFCON. Figure A.62 shows the setup for various control surfaces in green with the DS3 components and connections. Using the hull geometry and the weight inputs provided by the Weight Granularity Program (WGP), the Hull Granularity Program (HGP), the Component Granularity Program (CGP), and the System Connection Program (SCP) Paramarine can then estimate the linear and non-linear hydrodynamic coefficients. One of the scenarios examined was circle manoeuvring. At 150 m depth and cruising at a speed of 12 knots, a rudder deflection of 10 degrees was introduced, causing the submarine of Case Study 5.1 to respond with a turning radius of ~180 m and a rise (0.75 m/s) during the turn.

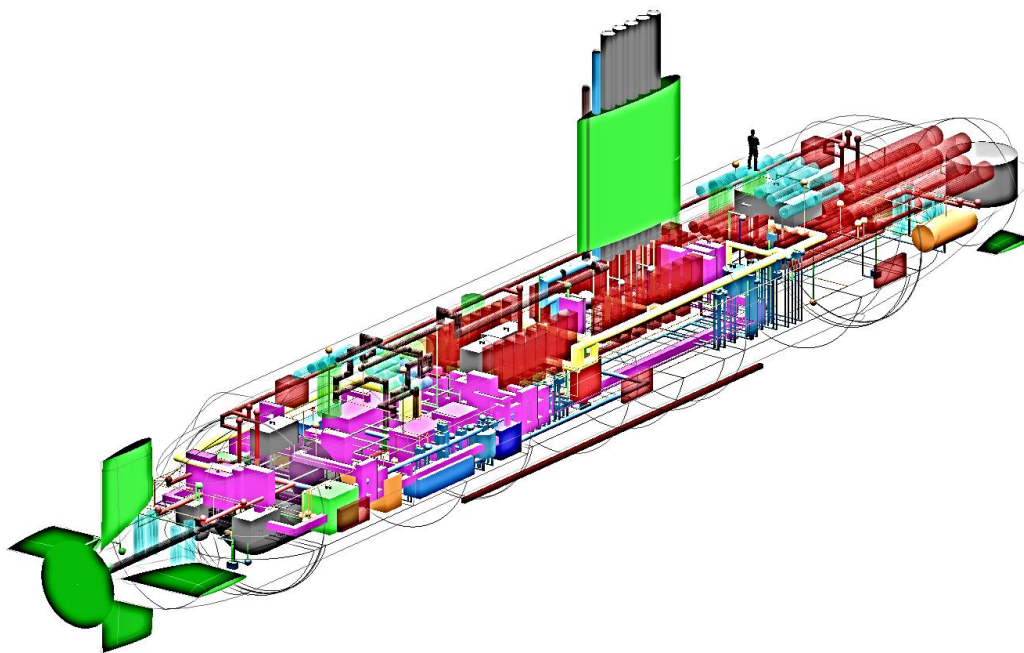


Figure A.62: Control surfaces modelling of Case Study 5.1 using Paramarine-SURFCON showing the setup for control surfaces in green with the DS3 components and connections are shown

Appendix 8

Initial Results and System Diagrams

A feature in Paramarine to visualise individual system diagrams in a hierarchy layout could also be used. This was possible because the new programs produced a script to model the “**system**” object in Paramarine. Although MATLAB could visualise such a system diagram much better with different colour coding and shape, this diagram could be used to check whether the connections between DBB objects in Paramarine are correct as sketched. The diagram also reveals the source of energy as they are located higher than the user nodes in the diagram.

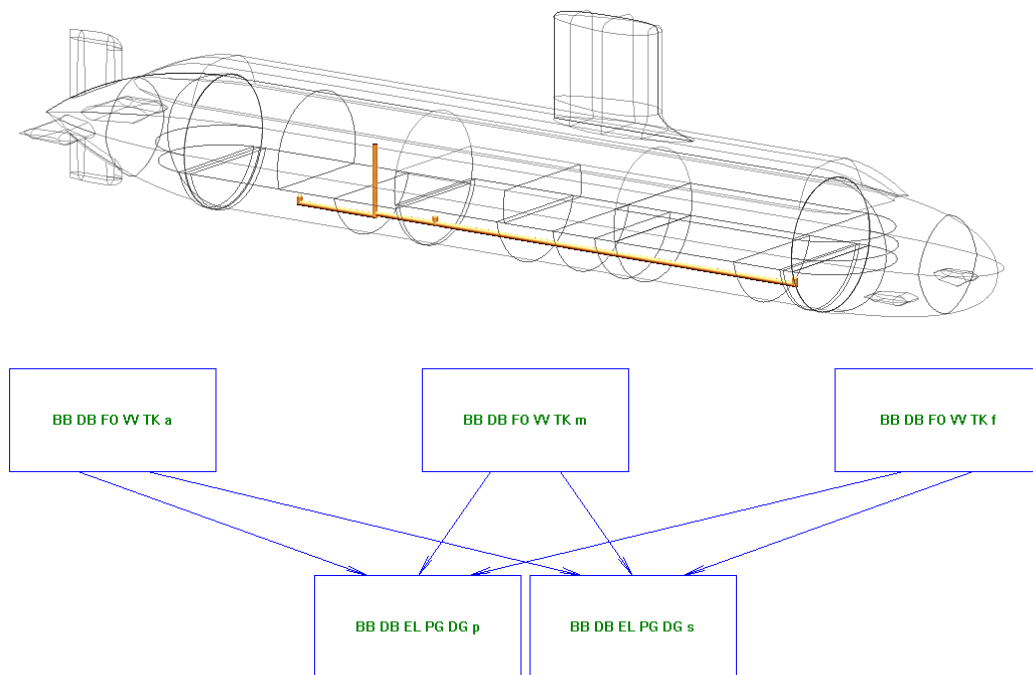


Figure A.63: The initial model of the fuel oil system of Case Study 5.1 in terms of the physical definition (top) and the logical definition (bottom) produced in Paramarine-SURFCON

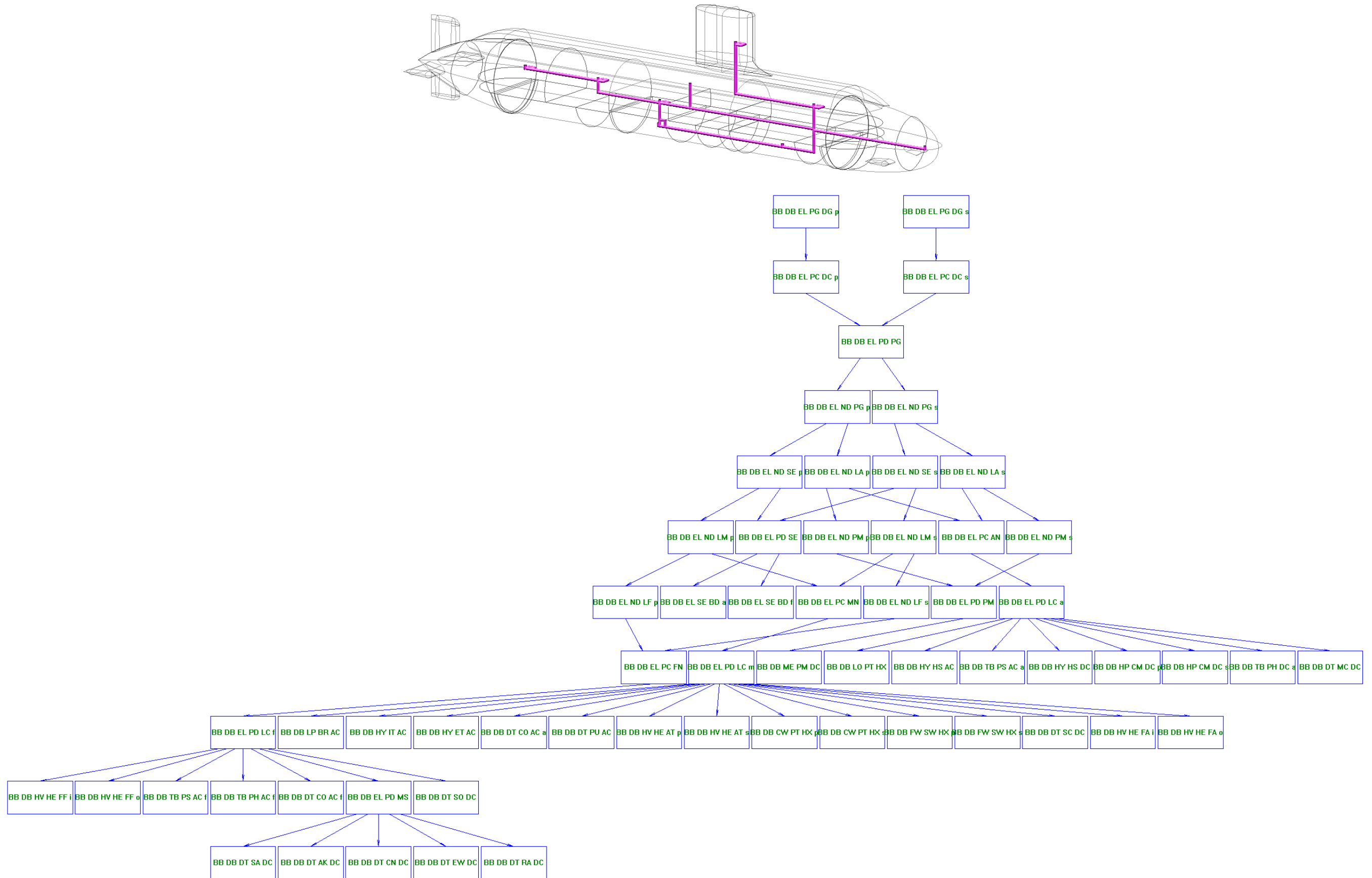


Figure A.64: The initial model of the electrical power distribution system of Case Study 5.1 in terms of the physical definition (shown in purple) (top) and the logical definition (bottom) produced in Paramarine-SURFCON

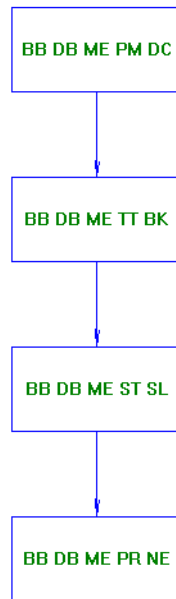
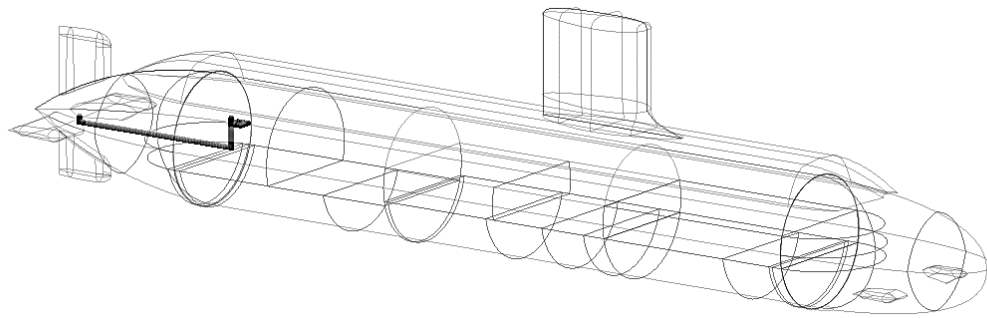


Figure A.65: The initial model of the mechanical system of Case Study 5.1 in terms of the physical definition (top) and the logical definition (bottom) produced using Paramarine-SURFCON

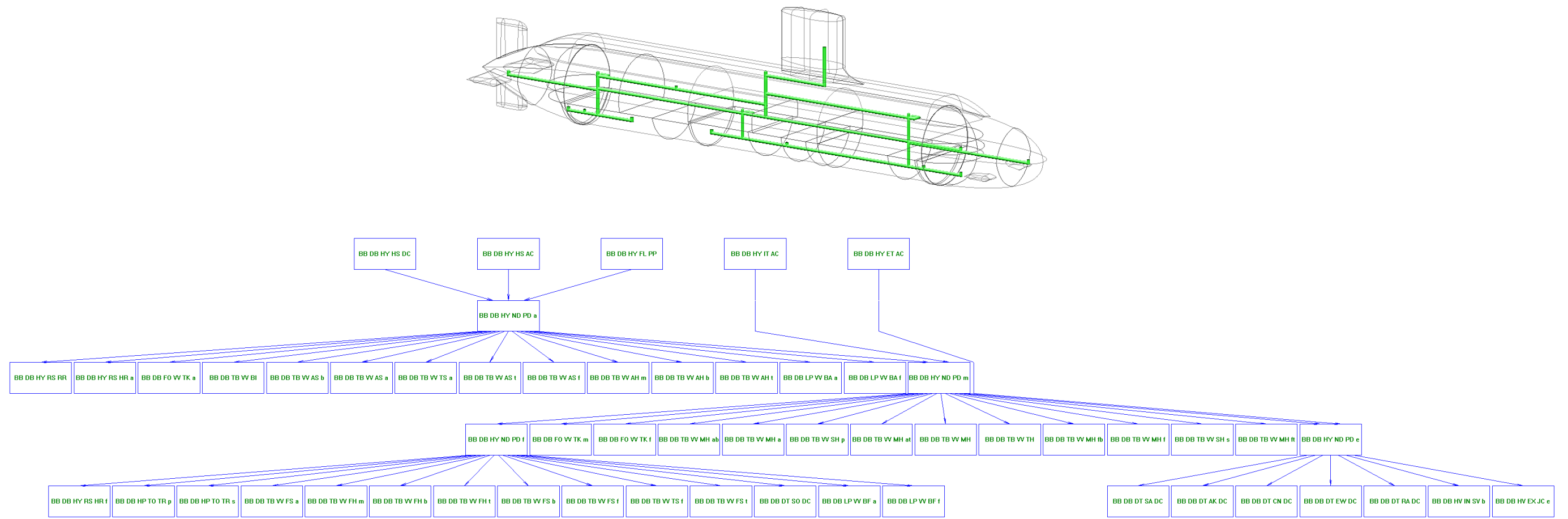


Figure A.66: The initial model of the hydraulic system of Case Study 5.1 in terms of the physical definition (a) and the logical definition (b) produced in Paramarine-SURFCON

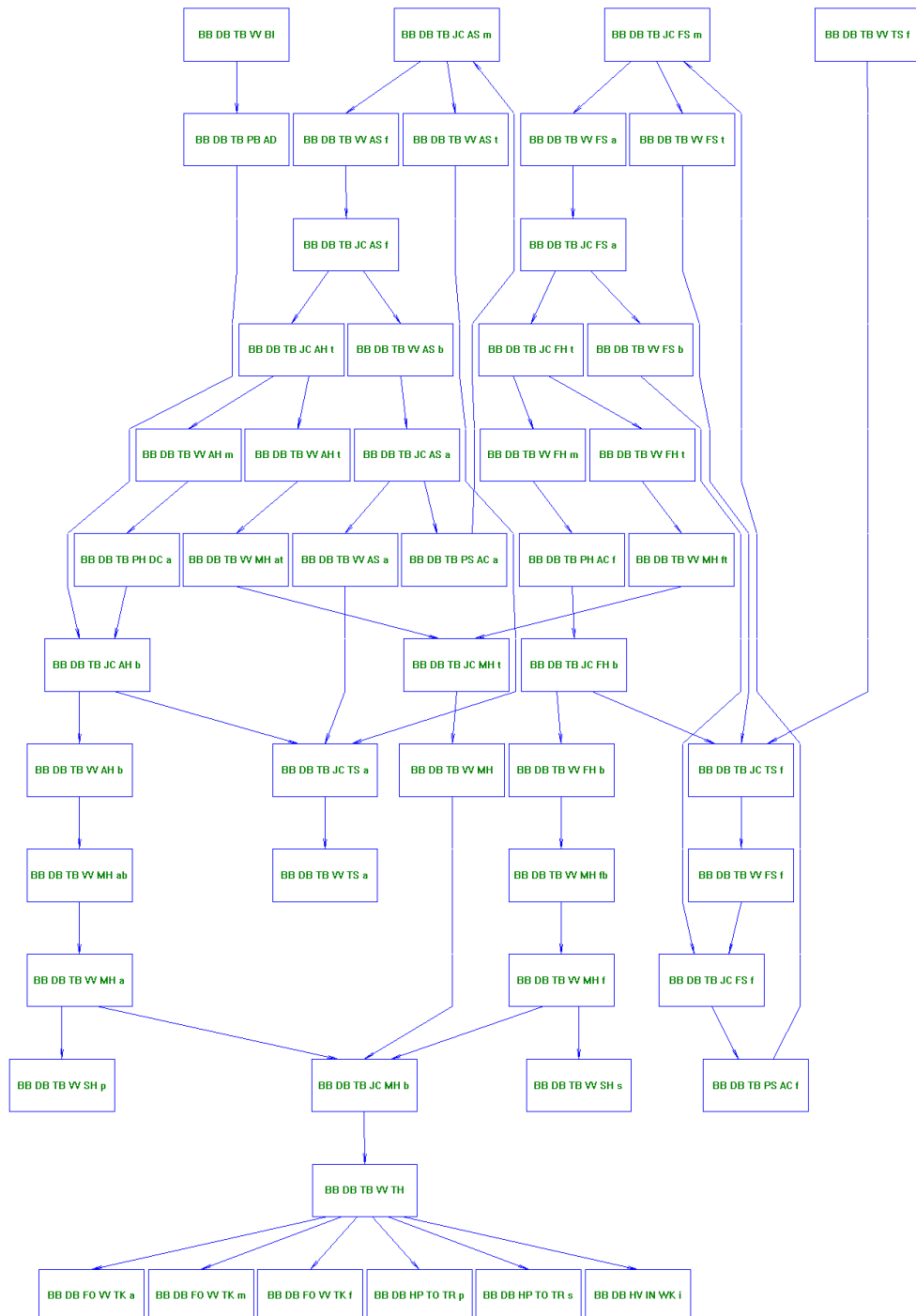
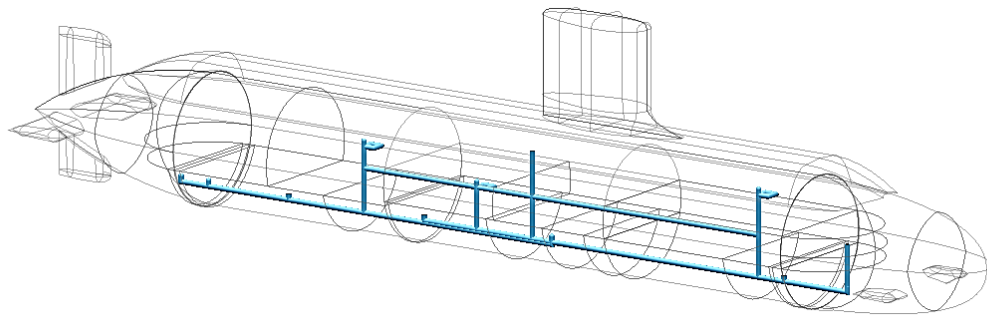


Figure A.67: The initial model of the trim and ballast system of Case Study 5.1 in terms of the physical definition (top) and the logical definition (bottom) produced in Paramarine-SURFCON

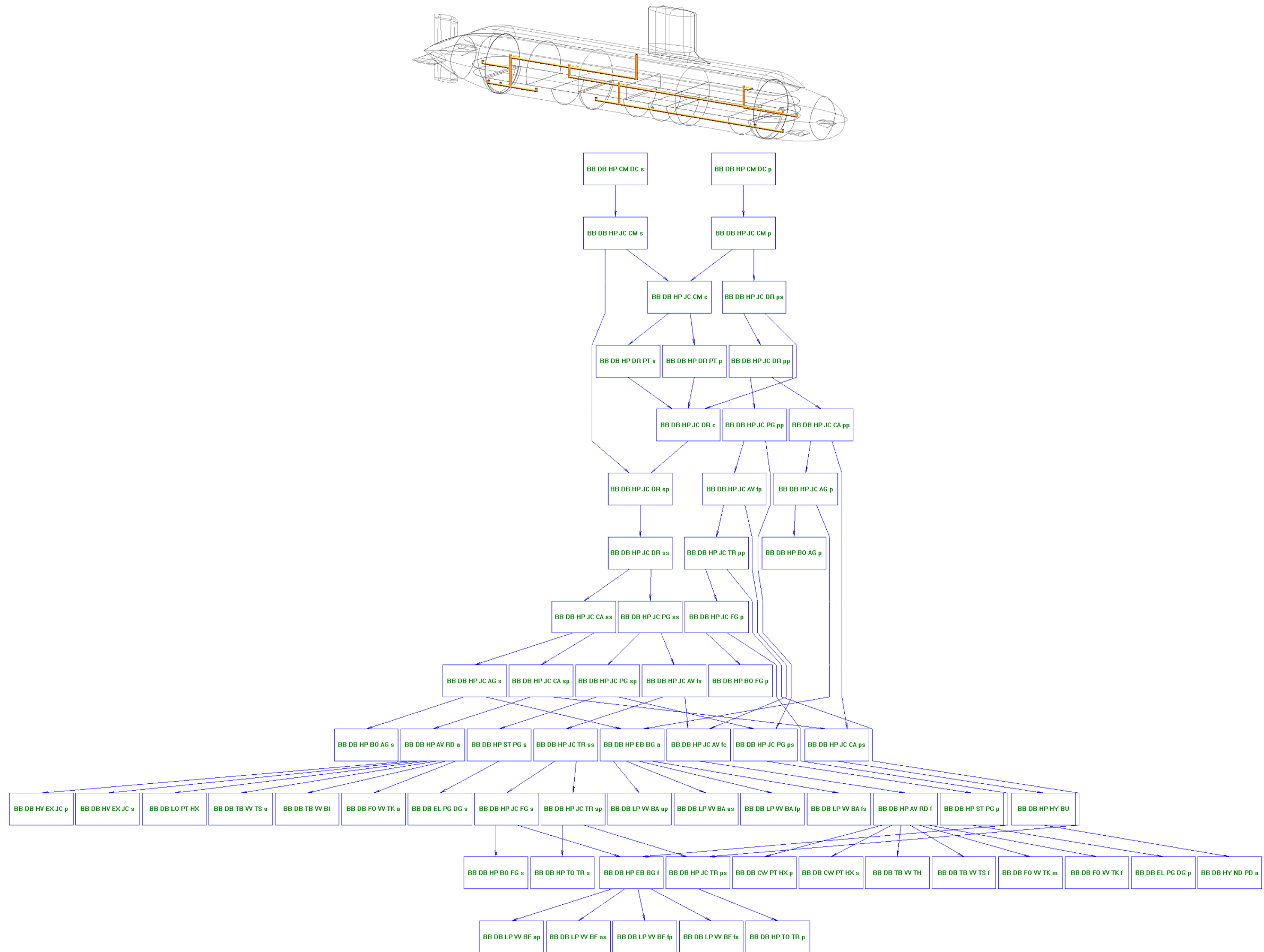


Figure A.68: The initial model of the high-pressure air system of Case Study 5.1 in terms of the physical definition (top) and the logical definition (bottom) produced using Paramarine-SURFCON

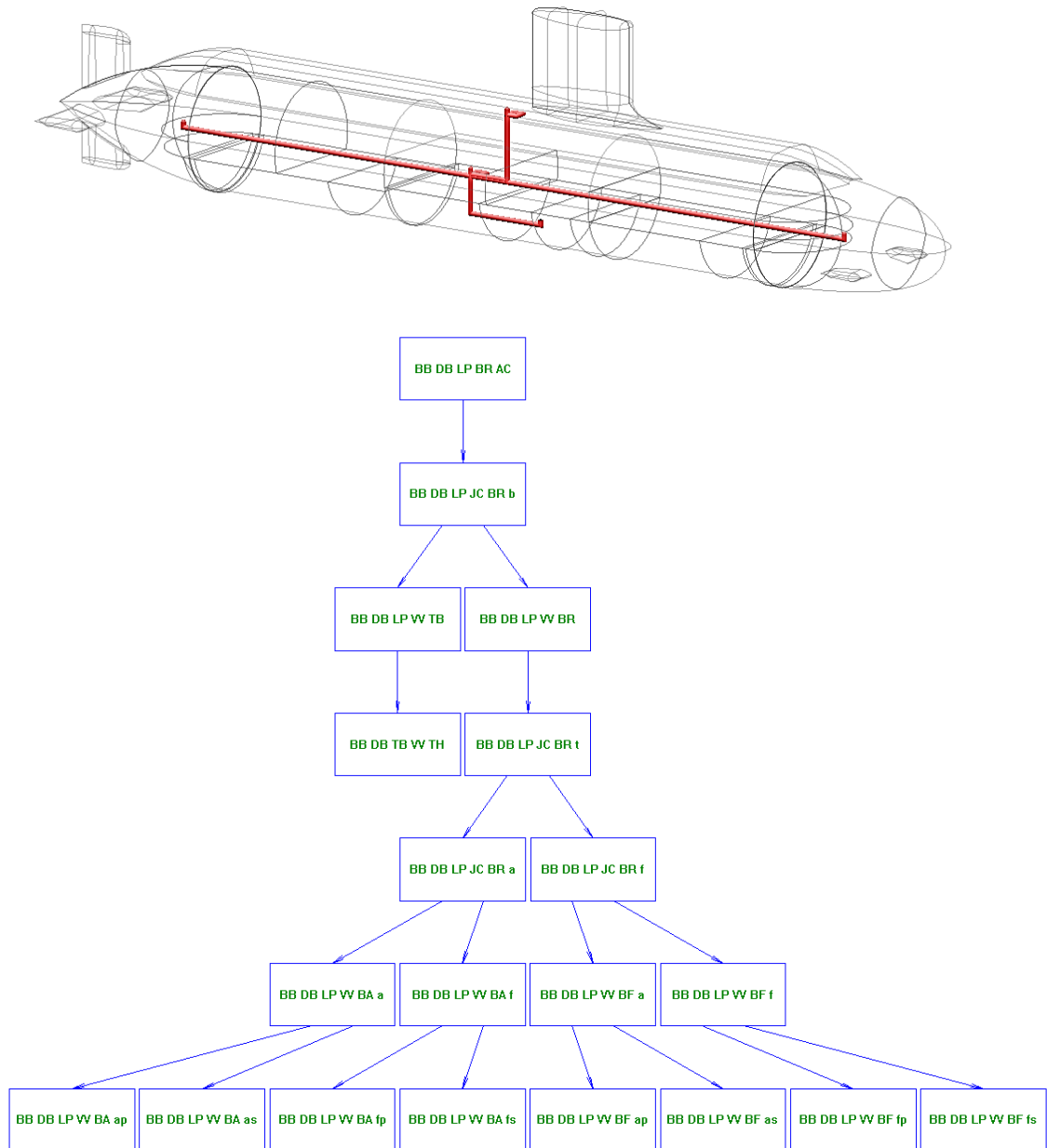


Figure A.69: The initial model of the low-pressure air system of Case Study 5.1 in terms of the physical definition (top) and the logical definition (bottom) produced using Paramarine-SURFCON

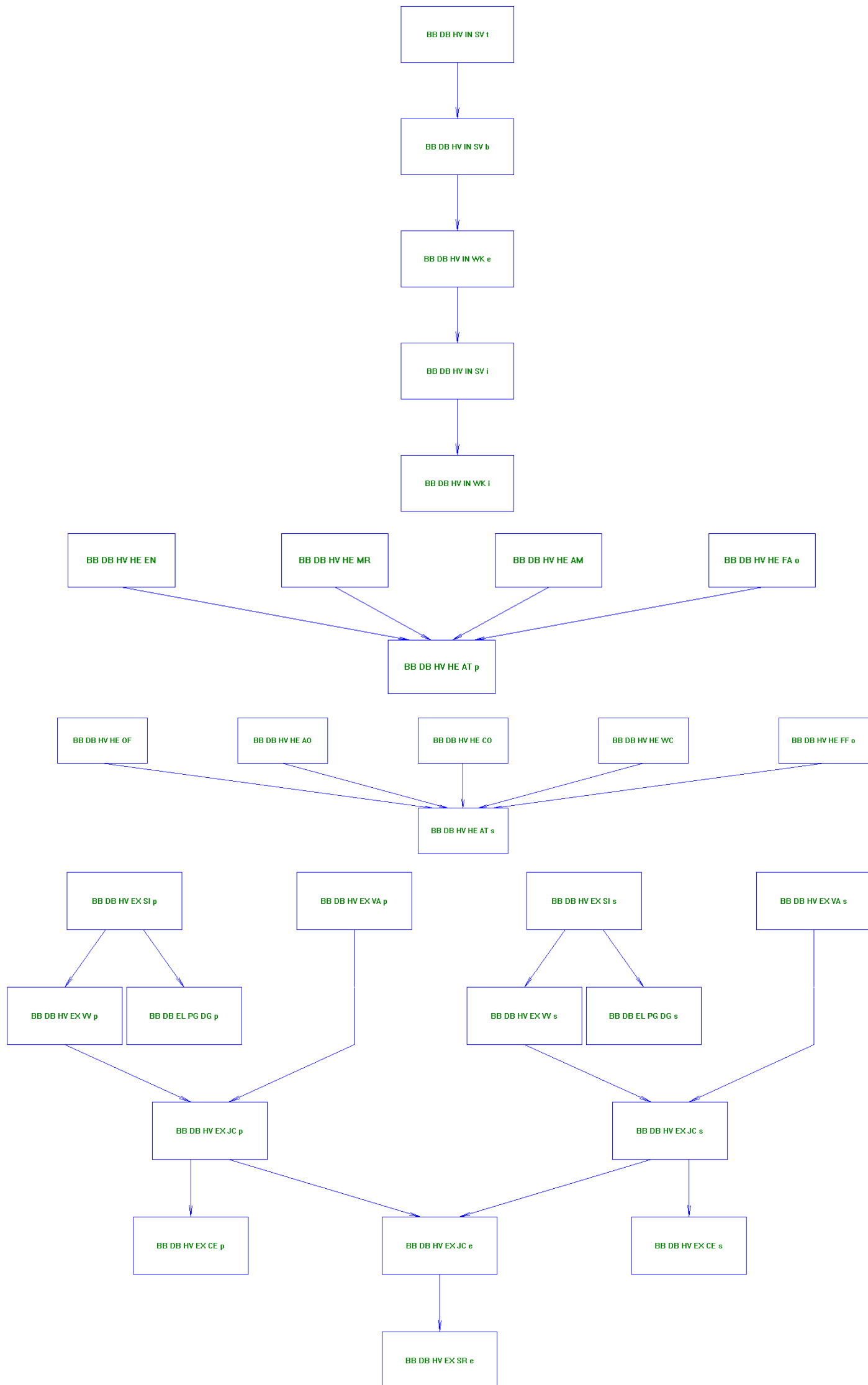
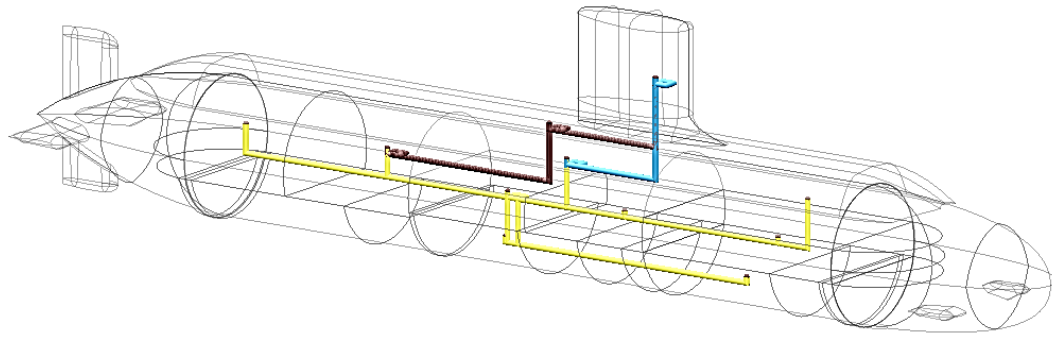


Figure A.70: The initial model of the ventilation of Case Study 5.1 in terms of the physical definition (top) and the logical definition (bottom) produced using Paramarine-SURFCON

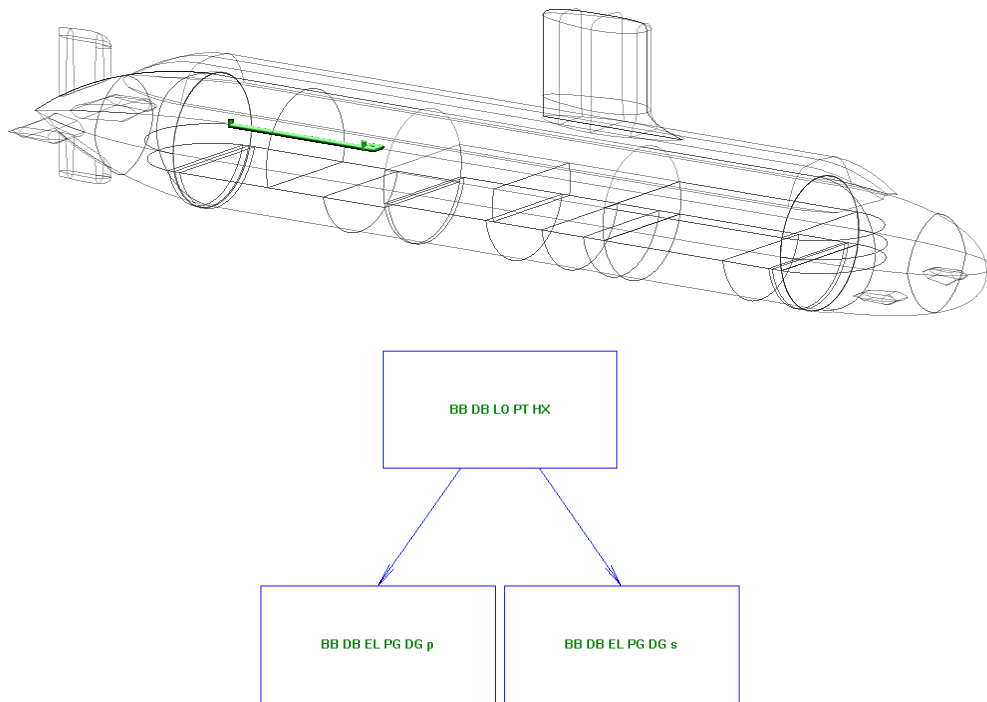


Figure A.71: The initial model of the lubricant oil system of Case Study 5.1 in terms of the physical definition (top) and the logical definition (bottom) produced using Paramarine-SURFCO

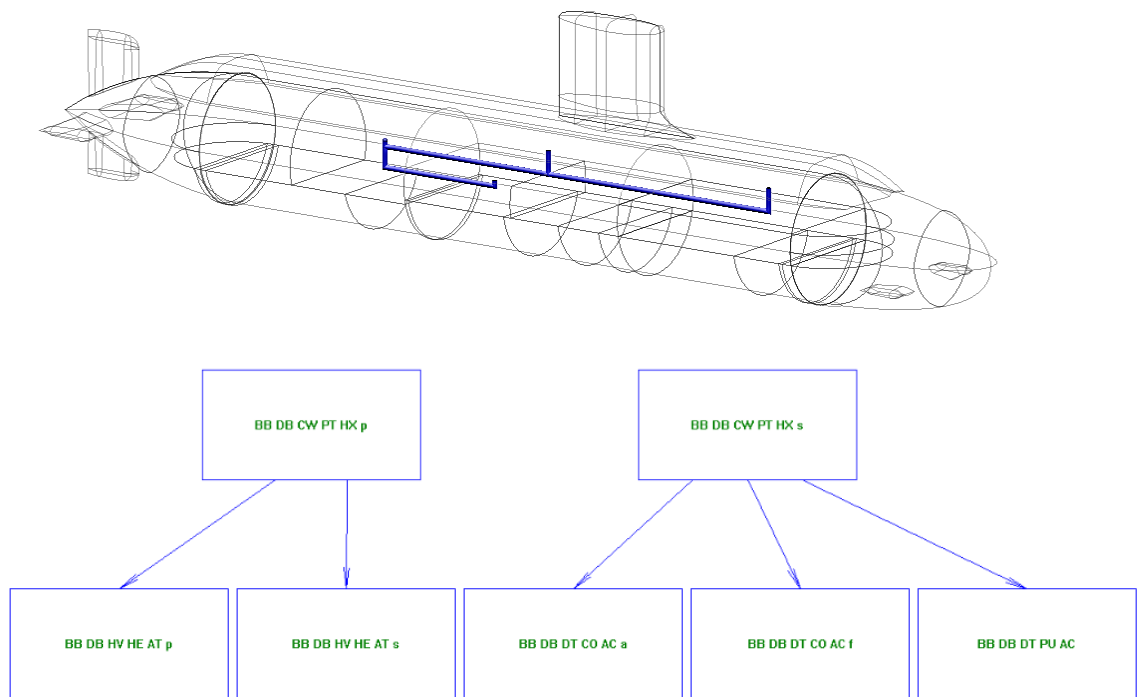


Figure A.72: The initial model of the chilled water system of Case Study 5.1 in terms of the physical definition (top) and the logical definition (bottom) produced using Paramarine-SURFCO

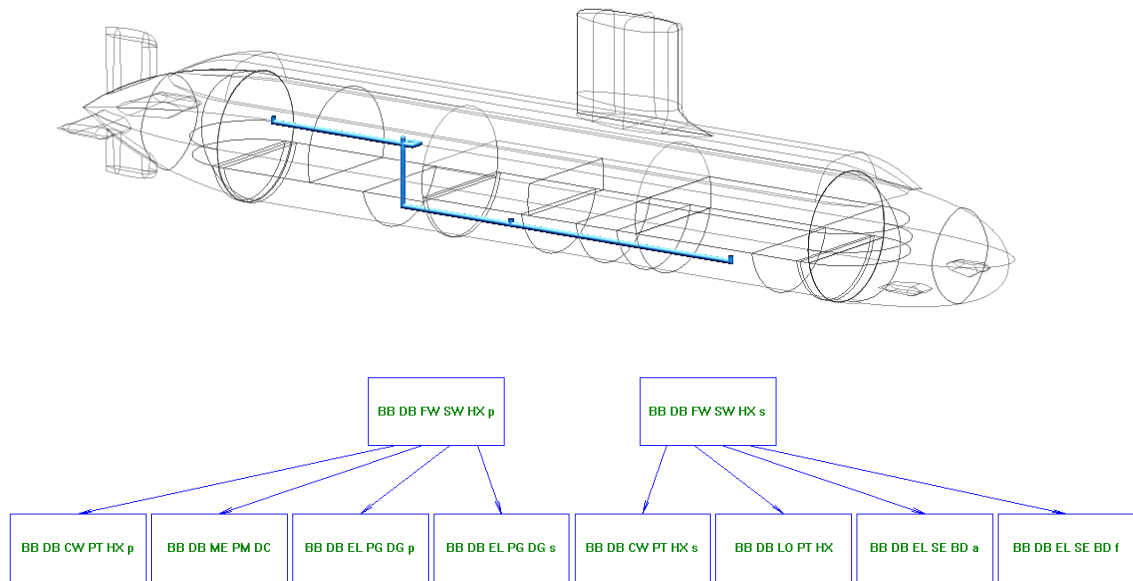


Figure A.73: The initial model of the freshwater cooling system of Case Study 5.1 in terms of the physical definition (top) and the logical definition (bottom) produced using Paramarine-SURFCON

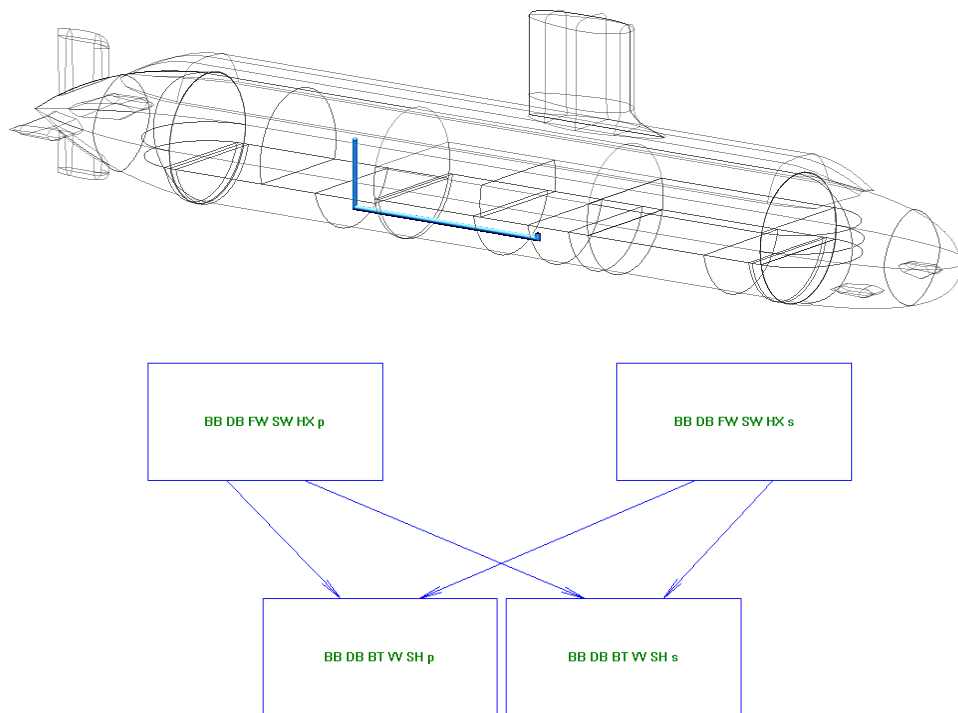


Figure A.74: The initial model of the freshwater seawater cooling system of Case Study 5.1 in terms of the physical definition (top) and the logical definition (bottom) produced using Paramarine-SURFCON

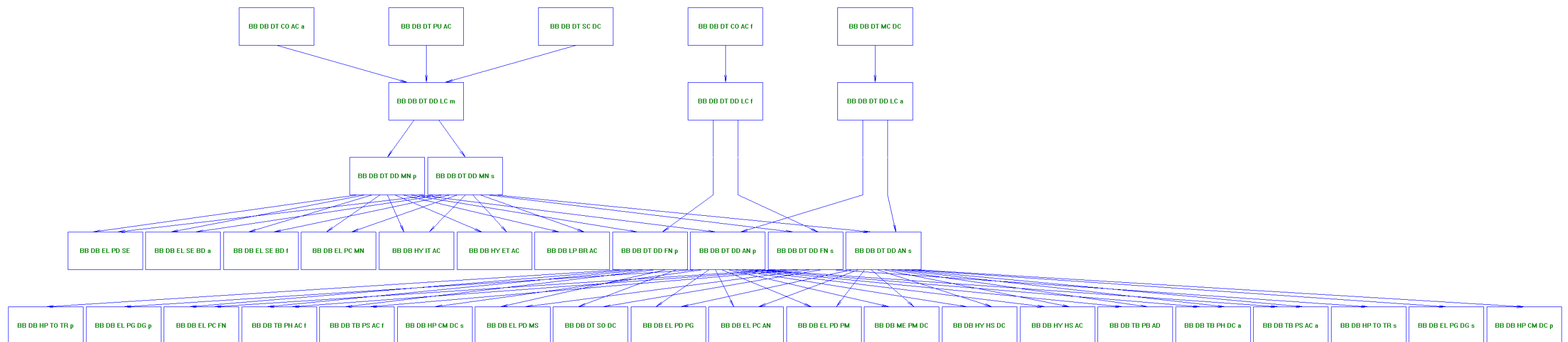
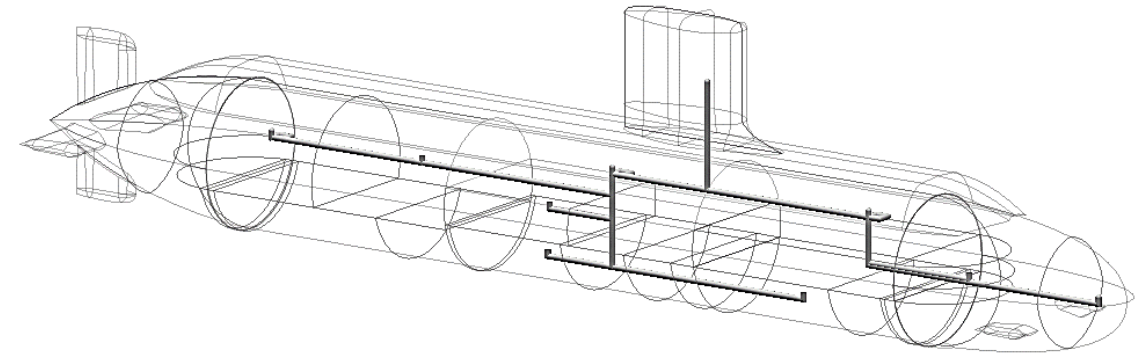


Figure A.75: The initial model of the data system of Case Study 5.1 in terms of the physical definition (a) and the logical definition (b) produced in Paramarine-SURFCON

Appendix 9

Derivation of DS3 of Case Study 5.1

This appendix provides examples of deriving the power to space and weight ratios for various DS3. These ratios were used in Case Study 5.1 and were compared to fictitious yet not unrealistic submarine data, the UCL submarine data (UCL-NAME, 2014).

The derivation of power to space and weight ratio based on various open sources (NAVSEA, 1978; Wrobel, 1984; U.S. Department of Defense, 1989; Harrington, 1992; Burcher and Rydill, 1994; Harbour, 2001; Fiedel, 2011; UCL-NAME, 2014; Trapp, 2015; Robinson, 2018; Stinson, 2019).

The following figures are examples of procedures in deriving various DS3 technologies: piping (fuel oil); cabling (electrical systems); and trunking (ventilation system).

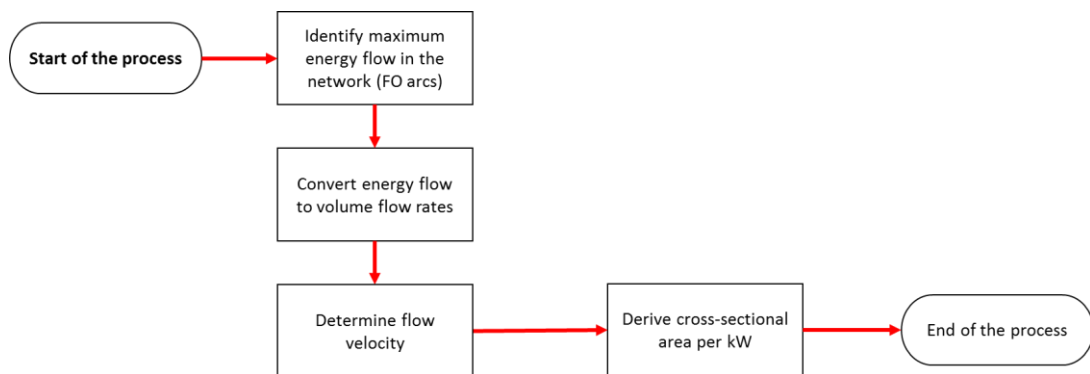


Figure A.76: Fuel oil arc sizing procedure

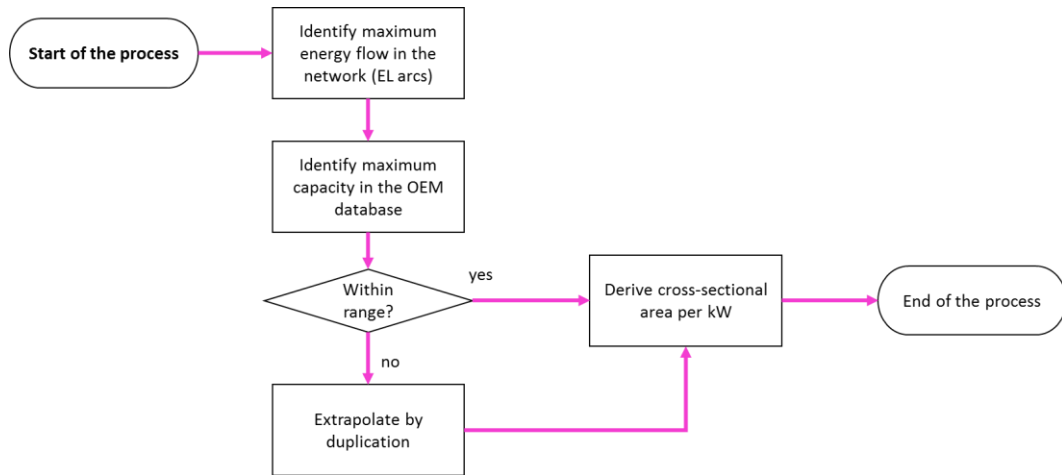


Figure A.77: Electrical arc sizing procedure

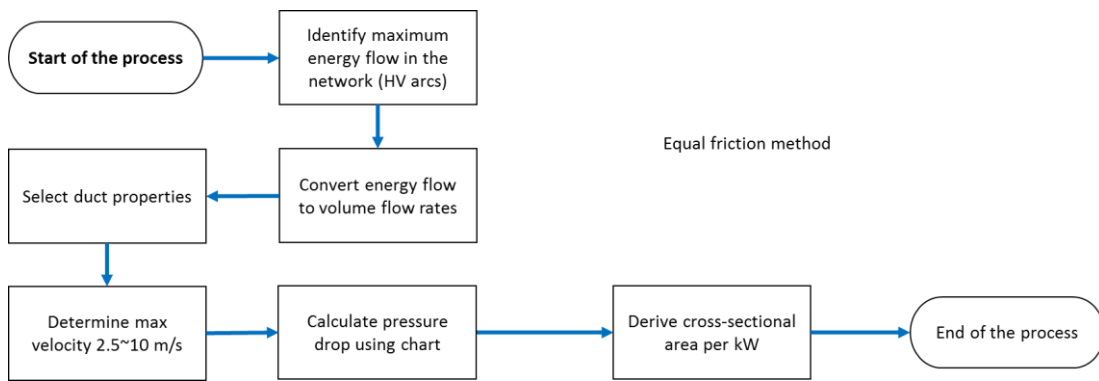


Figure A.78: Ventilation arc sizing procedure

Fuel Oil System

Sankey ratio for fuel at DG node	$\eta_{PG} := 48\%$
Air ratio (assume exhaust heat ratio)	$\eta_{AF} := 38\%$
Fuel ratio	$\eta_{FA} := 100\% - \eta_{AF} = 0.62$
Initial fuel energy assumption at FO arcs	$P_{FO_arc} := 2800 \text{ kW} \cdot \frac{\eta_{FA}}{\eta_{PG}} = 3.617 \text{ MW}$
Power at nominal continuous rating (NCR)	$P_{NCR} := P_{FO_arc} \cdot \frac{\eta_{PG}}{\eta_{FA}} = 2.8 \text{ MW}$
Specific fuel consumption at NCR	$SFC_{NCR} := 0.3 \frac{\text{kg}}{\text{kW} \cdot \text{hr}}$
Fuel oil density	$\rho_{FO} := 0.85 \frac{\text{kg}}{\text{L}}$
Volume flow rate	$V_{FO_arc} := P_{NCR} \cdot SFC_{NCR} \cdot \frac{1}{\rho_{FO}} = 16.752 \frac{\text{in}^3}{\text{s}}$
Design fluid velocity for piping heavy-fuel service suction pg. 796 of Harrington, 1992,	$C_{FO} := 1 \cdot \frac{\text{ft}}{\text{s} \cdot \text{in}^{0.5}} = 1.912 \frac{\text{m}^{0.5}}{\text{s}}$
Initial diameter due to fluid flow	$D_{FO_arc} := \left(\frac{4 \cdot V_{FO_arc}}{\pi \cdot C_{FO}} \right)^{\frac{2}{5}} = 31.97 \text{ mm}$
Margin, to account wall thickness, corrosion allowance, etc.	$m_{OD_FO} := 200\%$
Diameter plus margin	$D_{FO_arc} := \left(\frac{4 \cdot V_{FO_arc}}{\pi \cdot C_{FO}} \right)^{\frac{2}{5}} \cdot (1 + m_{OD_FO}) = 3.776 \text{ in}$
Margin for fittings, pipe support, etc.	$m_{FO_arc} := 30\%$
Cross sectional area plus margin	$A_{FO_arc} := D_{FO_arc}^2 \cdot (1 + m_{FO_arc}) = (1.196 \cdot 10^4) \text{ mm}^2$
Cross sectional area per power flow	$\lambda_{FO_arc} := \frac{A_{FO_arc}}{P_{FO_arc}} = 3.307 \frac{\text{mm}^2}{\text{kW}}$
Pipe density of copper-nickel alloy 715/706 pg. 4 of NAVSEA, 1978	$\rho_{pipe715} := 0.323 \frac{\text{lb}}{\text{in}^3}$
Wall thickness minimum based on calculated OD pg. 5 of NAVSEA, 1978 (round up 4 in, class 700)	$WT_{FO_arc} := 0.18 \text{ in} = 4.572 \text{ mm}$

Pipe weight per meter $AW_{FO_pipe} := \frac{\pi}{4} \cdot \left((2 \cdot D_{FO_arc} \cdot WT_{FO_arc}) - (WT_{FO_arc})^2 \right) \cdot \rho_{pipe715} = 6.012 \frac{kg}{m}$

Fuel weight per meter $AW_{FO_fluid} := \frac{\pi}{4} \cdot (D_{FO_arc} - WT_{FO_arc})^2 \cdot \rho_{FO} = 5.57 \frac{kg}{m}$

FO arc weight per meter $AW_{FO_arc} := (AW_{FO_pipe} + AW_{FO_fluid}) \cdot (1 + m_{FO_arc}) = 15.055 \frac{kg}{m}$

Weight per power flow length $\mu_{FO_arc} := \frac{AW_{FO_arc}}{P_{FO_arc}} = 0.004 \frac{kg}{kW \cdot m}$

Total operating time based on patrol length requirement $\Sigma T_{short} := 5 \text{ hr} \cdot 49$

Fuel margins $m_{FO} := 6\%$

Fuel weight baseline $W_{FO_fluid} := P_{NCR} \cdot SFC_{NCR} \cdot \Sigma T_{short} \cdot (1 + m_{FO}) = 218.148 \text{ tonne}$

Fuel power to weight ratio $\mu_{FO} := \frac{W_{FO_fluid}}{P_{FO_arc}} = 0.06 \frac{\text{tonne}}{kW}$

Fuel volume baseline $V_{FO} := \frac{W_{FO_fluid}}{\rho_{FO}} \cdot (1 + m_{FO}) = 272.043 \text{ m}^3$

Fuel power to volume ratio $\lambda_{FO} := \frac{V_{FO}}{P_{FO_arc}} = 0.075 \frac{\text{m}^3}{kW}$

Information Data system

Various cable properties of LSSSGA-800 Table VI (A)(1) (US DoD 1989)

Maximum current capacity $I_{wire} := 940 \text{ A}$

Maximum voltage $V_{wire_max} := 1000 \text{ V}$

Cable diameter $D_{wire} := 1.535 \text{ in} = 38.989 \text{ mm}$

Cable density $a\rho_{wire} := 3.429 \frac{\text{lb}}{\text{ft}} = 5.103 \frac{kg}{m}$

Cable line redundancy $N_{wire} := 2$

Cross sectional area $A_{DT_arc} := (D_{wire})^2 \cdot N_{wire} = (3.04 \cdot 10^3) \text{ mm}^2$

Cable weight per length $AW_{EL_arc} := N_{wire} \cdot a\rho_{wire} \cdot 2 = 20.412 \frac{kg}{m}$

Electrical System

Various cable properties of LSSSGA-2000 Table VI (A)(1) (US DoD 1989)

Maximum current capacity	$I_{wire} := 1630 \text{ A}$
Maximum voltage	$V_{wire_max} := 1000 \text{ V}$
Cable diameter	$D_{wire} := 2.26 \text{ in} = 57.404 \text{ mm}$
Cable density	$a\rho_{wire} := 7.755 \frac{\text{lb}}{\text{ft}} = 11.541 \frac{\text{kg}}{\text{m}}$
Cable line redundancy	$N_{wire} := 3$
Power to be delivered by cable	$P_{wire} := I_{wire} \cdot V_{wire_max} \cdot N_{wire} = (4.89 \cdot 10^3) \text{ kW}$
Allowance for cable highway uncertainty	$m_{cableway} := 4$
Cable margin	$m_{EL_arc} := 30\%$

Cross sectional area plus margin (assuming each connection required two cables positive and negative)

$$A_{EL_arc} := N_{wire} \cdot (D_{wire})^2 \cdot 2 \cdot (1 + m_{EL_arc}) \cdot (1 + m_{cableway}) = (1.285 \cdot 10^5) \text{ mm}^2$$

Cross sectional area per power flow	$\lambda_{EL_arc} := \frac{A_{EL_arc}}{P_{wire}} = 26.281 \frac{\text{mm}^2}{\text{kW}}$
Cable weight per length	$AW_{EL_arc} := N_{wire} \cdot a\rho_{wire} \cdot 2 \cdot (1 + m_{EL_arc}) = 90.018 \frac{\text{kg}}{\text{m}}$
Cable weight per length power flow	$\mu_{EL_arc} := \frac{AW_{EL_arc}}{P_{wire}} = 0.018 \frac{\text{kg}}{\text{kW} \cdot \text{m}}$
Diesel node power output at NCR	$P_{PG_DG} := 1400 \text{ kW}$
Diesel weight of 1.4 MW NCR (UCL-NAME 2014)	$W_{PG_DG} := 9 \text{ tonne} + 14.8 \text{ tonne} = 23.8 \text{ tonne}$
DG power to weight ratio	$\mu_{PG_DG} := \frac{W_{PG_DG}}{P_{PG_DG}} = 17 \frac{\text{kg}}{\text{kW}}$
Diesel volume of 1.4 MW NCR (UCL-NAME 2014)	$V_{PG_DG} := 5595 \text{ mm} \cdot 1750 \text{ mm} \cdot (1662 \text{ mm} + 838 \text{ mm}) = 24.478 \text{ m}^3$
DG power to volume ratio	$\lambda_{PG_DG} := \frac{V_{PG_DG}}{P_{PG_DG}} = 0.017 \frac{\text{m}^3}{\text{kW}}$
Baseline for a converter (Stinson 2019)	$P_{PC} := 350 \text{ kW}$
	$W_{PC} := 0.64 \text{ tonne}$
	$V_{PC} := 0.32 \text{ m} \cdot 1.25 \text{ m} \cdot 2.5 \text{ m} = 1 \text{ m}^3$

PC power to weight ratio $\mu_{PC} := \frac{W_{PC}}{P_{PC}} = 1.829 \frac{kg}{kW}$

PC power to volume ratio $\lambda_{PC} := \frac{V_{PC}}{P_{PC}} = 0.003 \frac{m^3}{kW}$

Baseline for a bus node
(Stinson 2019)

$$P_{ND_PD} := 2500 \text{ kW}$$

$$W_{ND_PD} := 0.83 \text{ tonne}$$

$$V_{ND_PD} := 0.32 \text{ m} \cdot 1.25 \text{ m} \cdot 2.5 \text{ m} = 1 \text{ m}^3$$

ND power to weight ratio $\mu_{ND_PD} := \frac{W_{ND_PD}}{P_{ND_PD}} = 0.332 \frac{kg}{kW}$

ND power to volume ratio $\lambda_{ND_PD} := \frac{V_{ND_PD}}{P_{ND_PD}} = (4 \cdot 10^{-4}) \frac{m^3}{kW}$

Various baseline equipment based on UCL Submarine Databook (UCL-NAME 2014)

Generator breaker power to weight ratio $\mu_{PD_PG} := 0.7 \frac{m^3}{MW} \cdot 0.4 \frac{\text{tonne}}{m^3} = 0.28 \frac{kg}{kW}$

Generator breaker power to volume ratio $\lambda_{PD_PG} := 0.7 \frac{m^3}{MW} = (7 \cdot 10^{-4}) \frac{m^3}{kW}$

Battery breaker power to weight ratio $\mu_{PD_SE} := 0.01 \text{ m}^3 \cdot \frac{0.65 \text{ tonne}}{m^3} \cdot \frac{1}{1900 \text{ A} \cdot 2.4 \text{ V}} = 1.425 \frac{kg}{kW}$

Battery breaker power to volume ratio $\lambda_{PD_SE} := 0.01 \text{ m}^3 \cdot \frac{1}{1900 \text{ A} \cdot 2.4 \text{ V}} = 0.002 \frac{m^3}{kW}$

Propulsion switchboard power to weight ratio $\mu_{PD_PM} := 1 \frac{m^3}{MW} \cdot 1 \frac{\text{tonne}}{m^3} = 1 \frac{kg}{kW}$

Propulsion switchboard power to volume ratio $\lambda_{PD_PM} := 1 \frac{m^3}{MW} = 0.001 \frac{m^3}{kW}$

Battery cell power to weight ratio $\mu_{SE_BD} := \frac{550 \text{ kg}}{1900 \text{ A} \cdot 2.4 \text{ V}} = 120.614 \frac{kg}{kW}$

Battery cell power to volume ratio $\lambda_{SE_BD} := \frac{1250 \text{ mm} \cdot 450 \text{ mm} \cdot 350 \text{ mm}}{1900 \text{ A} \cdot 2.4 \text{ V}} = 0.043 \frac{m^3}{kW}$

Mechanical System

Max permissible torsional shear stress
(Def Stan 02-304 Part 1 quoted by
UCL Zenith, UCL-NAME 2014)

$$\tau_i := \begin{bmatrix} 90 \\ 155 \\ 70 \end{bmatrix} \text{ N/mm}^2$$

Shaft power baseline pg 165
UCL-NAME 2014

$$P_s := 5500 \text{ hpUK} \cdot \frac{1}{kW} = 4.101 \cdot 10^3$$

Non-dimensionalised shaft speed,
the propeller rotates at 140 rpm
(Harbour 2001)

$$N_s := 140 \frac{\text{rpm}}{\text{rpm}} = 140$$

Shaft outside diameter in the
low torque range

$$D := \left(30 + \sqrt{\frac{304000}{\tau_i} \cdot \frac{P_s}{N_s} - 700} \right) \cdot \text{mm} = \begin{bmatrix} 343.454 \\ 268.237 \\ 385.704 \end{bmatrix} \text{mm}$$

Shaft outside diameter
above the low torque range/
Solid shafting diameter

$$D := \sqrt[3]{\frac{49 \cdot 10^6}{\tau_i} \cdot \frac{P_s}{N_s}} \cdot \text{mm} = \begin{bmatrix} 251.72 \\ 210.001 \\ 273.715 \end{bmatrix} \text{mm}$$

Bore diameter of hollow
bored shafting

$$d := 385 \text{ mm} - 40 \text{ mm} = 0.345 \text{ m}$$

Bearing span and whirling
speed constant

$$k_w := \begin{bmatrix} 121 \cdot 10^6 \\ 108 \cdot 10^6 \\ 94.5 \cdot 10^6 \end{bmatrix}$$

Maximum permissible distance between centrelines of adjacent bearings

For hollow bored shafts

$$L := \sqrt{\frac{k_w \cdot \sqrt{D^2 - d^2}}{1.25 \cdot N_s}} = (471.943 - 471.943i) \text{ m}^{\frac{1}{2}}$$

For solid shafts

$$L := \sqrt{\frac{0.75 k_w}{1.25 \cdot N_s}} \cdot \text{mm} = \begin{bmatrix} 0.72 \\ 0.68 \\ 0.636 \end{bmatrix} \text{ m}$$

Selected characteristics
shaft baseline

$$D_{ME_arc} := 385 \text{ mm} \quad P_{ME_arc} := P_s \cdot \text{kW} = (4.101 \cdot 10^3) \text{ kW}$$

Shaft cross sectional area

$$A_{ME_arc} := \pi \cdot \left(\frac{D_{ME_arc}}{2} \right)^2 = (1.164 \cdot 10^5) \text{ mm}^2$$

Cross sectional area per power flow

$$\lambda_{ME_arc} := \frac{A_{ME_arc}}{P_{ME_arc}} = 28.385 \frac{\text{mm}^2}{\text{kW}}$$

Shafting weight baseline pg. 165
UCL-NAME 2014 with losses

$$W_{ME_arc} := 7.4 \text{ tonne} \cdot \frac{1}{(0.995^2)} = 7.475 \text{ tonne}$$

Assume initial shaft length baseline

$$L_{ME_arc} := 9.3 \text{ m}$$

Shaft weight per meter

$$AW_{ME_arc} := \frac{W_{ME_arc}}{L_{ME_arc}} = 803.716 \frac{\text{kg}}{\text{m}}$$

Shaft weight per length power flow

$$\mu_{ME_arc} := \frac{AW_{ME_arc}}{P_{ME_arc}} = 0.196 \frac{\text{kg}}{\text{kW} \cdot \text{m}}$$

Power baseline

$$P_{PM_DC} := 5400 \text{ hpUK} = (4.027 \cdot 10^3) \text{ kW}$$

Weight baseline

$$W_{PM_DC} := 83.86 \text{ tonne}$$

Volume baseline using parametric algo-
rithm (pg. 77 UCL-NAME 2014) with the
propeller rotates at 140 rpm (Harbour
2001)

$$V_{PM_DC} := \left(0.14 \frac{\text{m}}{\text{kW}} \cdot \frac{\text{rev}}{\text{min}} \cdot \frac{P_{PM_DC}}{140 \frac{\text{rev}}{\text{min}}} \right)^3 = 65.294 \text{ m}^3$$

Main motor power to weight ratio	$\mu_{PM_DC} := \frac{W_{PM_DC}}{P_{PM_DC}} = 20.826 \frac{kg}{kW}$
Main motor power to volume ratio	$\lambda_{PM_DC} := \frac{V_{PM_DC}}{P_{PM_DC}} = 0.016 \frac{m^3}{kW}$
Power at thrust block with loss	$P_{TT_BK} := P_{PM_DC} \cdot 99.5\% = (4.007 \cdot 10^3) kW$
Thrust block weight baseline pg. 165 UCL-NAME 2014	$W_{TT_BK} := 3.2 \text{ tonne}$
Thrust block power to weight ratio	$\mu_{TT_BK} := \frac{W_{TT_BK}}{P_{TT_BK}} = 0.799 \frac{kg}{kW}$
Power at stern seal with losses	$P_{ST_SL} := P_{TT_BK} \cdot 99.5\% = (3.987 \cdot 10^3) kW$
Stern seal weight pg. 165 UCL-NAME 2014	$W_{ST_SL} := 1.8 \text{ tonne}$
Stern seal power to weight ratio	$\mu_{ST_SL} := \frac{W_{ST_SL}}{P_{ST_SL}} = 0.452 \frac{kg}{kW}$
Power at propeller with loss	$P_{PR_NE} := P_{ST_SL} \cdot 99.5\% = (3.967 \cdot 10^3) kW$
Propeller baseline pg. 165 UCL-NAME 2014	$W_{PR_NE} := 7.2 \text{ tonne}$
Propeller, rope guard, and cone power to weight ratio	$\mu_{PR_SB} := \frac{W_{PR_NE}}{P_{PR_NE}} = 1.815 \frac{kg}{kW}$

Ventilation System

Derivation for HVIN and HVEX systems

First approach using SDB algorithm (DG intake requirement)

Power flowing via HVIN arc	$P_{HVIN_arc} := P_{FO_arc} \cdot \frac{\eta_{AF}}{\eta_{FA}} = 2.217 MW$
Cross sectional area based on UCL Submarine Databook pg. 82 (UCL-NAME 2014)	$A_{HVIN_arc0} := P_{NCR} \cdot 45 \frac{mm^2}{kW} = (1.26 \cdot 10^5) mm^2$
Trunking diameter	$D_{HVIN_arc0} := 2 \cdot \left(\frac{A_{HVIN_arc0}}{\pi} \right)^{0.5} = 0.401 m$
Cross sectional area per power flow	$\lambda_{HVIN_arc0} := \frac{A_{HVIN_arc0}}{P_{HVIN_arc}} = 56.842 \frac{mm^2}{kW}$

Second approach using fresh air requirement

Assume a pressure hull volume	$PH_{vol} := 2150 m^3$
-------------------------------	------------------------

Air velocity	$V_{AR} := PH_{vol} \cdot \frac{1}{hr} = 0.597 \frac{m^3}{s}$
Assume a fresh air requirement based on UCL Submarine Databook pg 201	$V_{HVIN_arc} := 43 \frac{m^3}{min}$
Assume air velocity	$v_{HVIN_arc} := 6 \frac{m}{s}$
Wall thickness minimum based on calculated OD pg. 5 of NAVSEA, 1978 (round up 4 in, class 700)	$WT_{HVIN_arc} := 16 \text{ in} - 15.353 \text{ in} = 0.647 \text{ in}$
Trunking diameter	$D_{HVIN_arc_1} := 2 \cdot \left(\frac{V_{HVIN_arc} \cdot 1}{v_{HVIN_arc} \cdot \pi} \right)^{0.5} + WT_{HVIN_arc} = 0.406 \text{ m}$
Cross sectional area	$A_{HVIN_arc_1} := D_{HVIN_arc_1}^2 = (1.652 \cdot 10^5) \text{ mm}^2$
Cross sectional area per power flow	$\lambda_{HVIN_arc_1} := \frac{A_{HVIN_arc_1}}{P_{HVIN_arc}} = 74.512 \frac{mm^2}{kW}$
Summary of trunking diameter	$D_{HVIN_arc} = \begin{bmatrix} 0.401 \\ 0.406 \end{bmatrix} \text{ m}$
Trunking weight per meter	$AW_{HVIN_arc} := \frac{\pi}{4} \cdot ((2 \cdot D_{HVIN_arc} \cdot WT_{HVIN_arc}) - (WT_{HVIN_arc})^2) \cdot \rho_{pipe715} = \begin{bmatrix} 90.545 \\ 91.901 \end{bmatrix} \frac{kg}{m}$
Snort pipe weight per length-power flow	$\mu_{HVIN_arc} := \frac{AW_{HVIN_arc}}{P_{HVIN_arc}} = \begin{bmatrix} 0.041 \\ 0.041 \end{bmatrix} \frac{kg}{kW \cdot m}$
Cross sectional area per power flow	$\lambda_{HVIN_arc} = \begin{bmatrix} 56.842 \\ 74.512 \end{bmatrix} \frac{mm^2}{kW}$
Reverse calculation of heat based on range of air velocity and fan diameter on pg. 135 UCL-NAME 2014	$P_{HVHE_arc} := \begin{bmatrix} 16 \\ 24 \\ 4 \\ 6 \end{bmatrix} kW = \begin{bmatrix} 16 \\ 24 \\ 4 \\ 6 \end{bmatrix} kW$
Initial assumption on energy transferred as heat	$Q_{HE} := P_{HVHE_arc} = \begin{bmatrix} 16 \\ 24 \\ 4 \\ 6 \end{bmatrix} kW$
Specific heat for air	$c_{PAR} := 1026 \frac{J}{kg \cdot K} = (1.026 \cdot 10^3) \frac{J}{kg \cdot K}$
Initial assumption	$\Delta T_{AR} := 10 \Delta C$

Mass flow rate	$\hat{m}_{HE_arc} := \frac{Q_{HE}}{cP_{AR} \cdot \Delta T_{AR}} = \begin{bmatrix} 1.559 \\ 2.339 \\ 0.39 \\ 0.585 \end{bmatrix} \frac{kg}{s}$
Air density at 101.325 kPa, 21 C	$\rho_{AR} := 1.2 \frac{kg}{m^3}$
Air volume flow rate	$V_{HVHE_arc} := \hat{m}_{HE_arc} \cdot \frac{1}{\rho_{AR}} = \begin{bmatrix} 1.3 \\ 1.949 \\ 0.325 \\ 0.487 \end{bmatrix} \frac{m^3}{s}$
Air velocity based on pg. 135 of UCL-NAME 2014	$v_{HVHE_arc} := \begin{bmatrix} 10 \\ 10 \\ 2.5 \\ 2.5 \end{bmatrix} \frac{m}{s}$
Wall thickness minimum based on calculated OD pg. 7 of NAVSEA, 1978 (class 50)	$WT_{HVHE_arc} := 20 \text{ in} - 19.817 \text{ in} = 0.183 \text{ in}$
Trunking diameter	$D_{HVHE_arc} := 2 \cdot \left(\frac{V_{HVHE_arc} \cdot 1}{v_{HVHE_arc} \cdot \pi} \right)^{0.5} + WT_{HVHE_arc} = \begin{bmatrix} 0.411 \\ 0.503 \\ 0.411 \\ 0.503 \end{bmatrix} m$
Supply and return lines	$N_{pipe} := 2$
Cross sectional area (assuming rectangle instead of circular)	$A_{HVHE_arc} := N_{pipe} \cdot D_{HVHE_arc}^2 = \begin{bmatrix} 3.385 \cdot 10^5 \\ 5.057 \cdot 10^5 \\ 3.385 \cdot 10^5 \\ 5.057 \cdot 10^5 \end{bmatrix} mm^2$
Cross sectional area per power flow	$\lambda_{HVHE_arc} := \frac{A_{HVHE_arc}}{P_{HVHE_arc}} = \begin{bmatrix} 2.116 \cdot 10^4 \\ 2.107 \cdot 10^4 \\ 8.463 \cdot 10^4 \\ 8.428 \cdot 10^4 \end{bmatrix} \frac{mm^2}{kW}$
Trunking weight per meter	$AW_{HVHE_arc} := \frac{\pi}{4} \cdot \left((2 \cdot D_{HVHE_arc} \cdot WT_{HVHE_arc}) - (WT_{HVHE_arc})^2 \right) \cdot \rho_{pipe715} = \begin{bmatrix} 26.705 \\ 32.673 \\ 26.705 \\ 32.673 \end{bmatrix} \frac{kg}{m}$
Weight per power flow length	$\mu_{HVHE_arc} := \frac{AW_{HVHE_arc}}{P_{HVHE_arc}} = \begin{bmatrix} 1.669 \\ 1.361 \\ 6.676 \\ 5.446 \end{bmatrix} \frac{kg}{kW \cdot m}$
Calculating air velocity based on air fuel ratio	$AF := 25$
Air volume flow rate	$V_{AR} := P_{NCR} \cdot SFC_{NCR} \cdot AF \cdot \frac{1}{\rho_{AR}} = 4.861 \frac{m^3}{s}$
Air velocity	$v_{AR} := \frac{V_{AR}}{A_{HVIN_arc0}} = 38.58 \frac{m}{s}$

LO system

Initial assumption on energy transferred as heat using Type 2400 (Wrobel 1984) and LO heat ratio (Robinson, 2018)

$$P_{LO_arc} := 2800 \text{ kW} \cdot \frac{8.1\%}{48\%} = 472.5 \text{ kW}$$

$$Q_{LO} := P_{LO_arc}$$

Specific heat for lube oil (Brown 2020)

$$c_{pLO} := 2000 \frac{\text{J}}{\text{kg} \cdot \text{K}}$$

Operating temperature range for lube oil (Brown 2020)

$$\Delta T_{LO} := 11.11 \text{ } \Delta^{\circ}\text{C}$$

Lube oil mass flow rate

$$\hat{m}_{LO_arc} := \frac{Q_{LO}}{c_{pLO} \cdot \Delta T_{LO}} = 21.265 \frac{\text{kg}}{\text{s}}$$

Lube oil density (Brown 2020),

$$\rho_{LO} := 880 \frac{\text{kg}}{\text{m}^3} = 0.88 \frac{\text{tonne}}{\text{m}^3}$$

Lube oil volume flow rate

$$V_{LO_arc} := \hat{m}_{LO_arc} \cdot \frac{1}{\rho_{LO}} = 86.992 \frac{\text{m}^3}{\text{hr}}$$

Design fluid velocity for lube oil pg. 796 of Harrington, 1992

$$C_{LO} := 2 \cdot \frac{\text{ft}}{\text{s} \cdot \text{in}^{0.5}} = 3.825 \frac{\text{m}^{0.5}}{\text{s}}$$

Wall thickness minimum based on calculated OD pg. 5 of NAVSEA,

$$WT_{LO_arc} := 6.625 \text{ in} - 5.719 \text{ in} = 0.906 \text{ in}$$

Diameter of lube oil pipe

$$D_{LO_arc} := \left(\frac{4 \cdot V_{LO_arc}}{\pi \cdot C_{LO}} \right)^{\frac{2}{5}} + WT_{LO_arc} = 6.625 \text{ in}$$

Margin for corrosion, spacing, etc.

$$m_{LO_arc} := 30\%$$

Supply and return lines

$$N_{pipe} := 2$$

Cross sectional area

$$A_{LO_arc} := N_{pipe} \cdot D_{LO_arc}^2 \cdot (1 + m_{LO_arc}) = (7.363 \cdot 10^4) \text{ mm}^2$$

Cross sectional area per power flow

$$\lambda_{LO_arc} := \frac{A_{LO_arc}}{P_{LO_arc}} = 155.834 \frac{\text{mm}^2}{\text{kW}}$$

Trunking weight per meter

$$\text{Pipe} \quad AW_{LO_pipe} := \frac{\pi}{4} \cdot ((2 \cdot D_{LO_arc} \cdot WT_{LO_arc}) - (WT_{LO_arc})^2) \cdot \rho_{pipe715} = 50.668 \frac{\text{kg}}{\text{m}}$$

$$\text{Fluid} \quad AW_{LO_fluid} := \frac{\pi}{4} \cdot (D_{LO_arc} - WT_{LO_arc})^2 \cdot \rho_{LO} = 14.586 \frac{\text{kg}}{\text{m}}$$

$$\text{Total} \quad AW_{LO_arc} := N_{pipe} \cdot (AW_{LO_pipe} + AW_{LO_fluid}) \cdot (1 + m_{LO_arc}) = 169.661 \frac{\text{kg}}{\text{m}}$$

Weight per power flow length

$$\mu_{LO_arc} := \frac{AW_{LO_arc}}{P_{LO_arc}} = 0.359 \frac{\text{kg}}{\text{kW} \cdot \text{m}}$$

CW System

First approach using temperature diff assumption from (NAVSEA 1990) quoted by (Trapp 2015)

Initial assumption on energy transferred as heat using Type 2400 (Wrobel 1984):
3 x 60 kW CW plants

$$P_{CW_arc} := 180 \text{ kW}$$

$$Q_{CW} := P_{CW_arc}$$

Specific heat of CW (Brown 2020)

$$c_{pCW} := 4190 \frac{\text{J}}{\text{kg} \cdot \text{K}}$$

CW density (Brown 2020)

$$\rho_{CW} := 1 \frac{\text{tonne}}{\text{m}^3}$$

Design fluid velocity for CW oil pg. 796 of Harrington, 1992

$$C_{CW} := 5 \cdot \frac{\text{ft}}{\text{s} \cdot \text{in}^{0.5}} = 9.562 \frac{\text{m}^{0.5}}{\text{s}}$$

Standard operating temperature range for CW (NAVSEA 1990) quoted by (Trapp 2015)

$$\Delta T_{CW} := 20 \text{ K}$$

CW mass flow rate

$$\hat{m}_{CW_arc} := \frac{Q_{CW}}{c_{pCW} \cdot \Delta T_{CW}} = 2.148 \frac{\text{kg}}{\text{s}}$$

CW volume flow rate

$$V_{CW_arc} := \hat{m}_{CW_arc} \cdot \frac{1}{\rho_{CW}} = 7.733 \frac{\text{m}^3}{\text{hr}}$$

Wall thickness minimum based on calculated OD pg. 5 of NAVSEA,

$$WT_{CW_arc} := 1.66 \text{ in} - 1.506 \text{ in} = 3.912 \text{ mm}$$

CW pipe diameter (minimum 15 mm (Fiedel 2011))

$$D_{CW_arc0} := \left(\frac{4 \cdot V_{CW_arc}}{\pi \cdot C_{CW}} \right)^{\frac{2}{5}} + WT_{CW_arc} = 42.154 \text{ mm}$$

Margin for corrosion, spacing, etc.

$$m_{CW_arc} := 30\%$$

Supply and return lines

$$N_{pipe} := 2$$

Cross sectional area

$$A_{CW_arc} := N_{pipe} \cdot D_{CW_arc0}^2 \cdot (1 + m_{CW_arc}) = 0.005 \text{ m}^2$$

Cross sectional area per power flow

$$\lambda_{CW_arc0} := \frac{A_{CW_arc}}{P_{CW_arc}} = 25.668 \frac{\text{mm}^2}{\text{kW}}$$

CW connection weight per meter

$$\text{Pipe} \quad AW_{CW_pipe} := \frac{\pi}{4} \cdot \left((2 \cdot D_{CW_arc0} \cdot WT_{CW_arc}) - (WT_{CW_arc})^2 \right) \cdot \rho_{pipe715} = 2.208 \frac{\text{kg}}{\text{m}}$$

$$\text{Fluid} \quad AW_{CW_fluid} := \frac{\pi}{4} \cdot (D_{CW_arc0} - WT_{CW_arc})^2 \cdot \rho_{CW} = 1.149 \frac{\text{kg}}{\text{m}}$$

Total $AW_{CW_arc} := N_{pipe} \cdot (AW_{CW_pipe} + AW_{CW_fluid}) \cdot (1 + m_{CW_arc}) = 8.728 \frac{kg}{m}$

Weight per power flow length $\mu_{CW_arc0} := \frac{AW_{CW_arc}}{P_{CW_arc}} = 0.048 \frac{kg}{kW \cdot m}$

Second approach using temperature diff assumption from (Brown 2020)

Operating temperature range for CW (Brown 2020) $\Delta T_{CW} := 13.89 \Delta^{\circ}C$

CW mass flow rate $\hat{m}_{CW_arc} := \frac{Q_{CW}}{cP_{CW} \cdot \Delta T_{CW}} = 3.093 \frac{kg}{s}$

CW volume flow rate $V_{CW_arc} := \hat{m}_{CW_arc} \cdot \frac{1}{\rho_{CW}} = 11.134 \frac{m^3}{hr}$

Wall thickness minimum based on calculated OD pg. 5 of NAVSEA, $WT_{CW_arc} := 1.9 \text{ in} - 1.742 \text{ in} = 0.158 \text{ in}$

CW pipe diameter (minimum 15 mm (Fiedel 2011)) $D_{CW_arc1} := \left(\frac{4 \cdot V_{CW_arc}}{\pi \cdot C_{CW}} \right)^{\frac{2}{5}} + WT_{CW_arc} = 1.9 \text{ in}$

Cross sectional area $A_{CW_arc} := N_{pipe} \cdot D_{CW_arc1}^2 \cdot (1 + m_{CW_arc}) = 0.006 \text{ m}^2$

Cross sectional area per power flow $\lambda_{CW_arc1} := \frac{A_{CW_arc}}{P_{CW_arc}} = 33.641 \frac{mm^2}{kW}$

CW connection weight per meter

Pipe $AW_{CW_pipe} := \frac{\pi}{4} \cdot \left((2 \cdot D_{CW_arc1} \cdot WT_{CW_arc}) - (WT_{CW_arc})^2 \right) \cdot \rho_{pipe715} = 2.607 \frac{kg}{m}$

Fluid $AW_{CW_fluid} := \frac{\pi}{4} \cdot (D_{CW_arc1} - WT_{CW_arc})^2 \cdot \rho_{CW} = 1.538 \frac{kg}{m}$

Total $AW_{CW_arc} := N_{pipe} \cdot (AW_{CW_pipe} + AW_{CW_fluid}) \cdot (1 + m_{CW_arc}) = 10.776 \frac{kg}{m}$

Weight per power flow length $\mu_{CW_arc1} := \frac{AW_{CW_arc}}{P_{CW_arc}} = 0.06 \frac{kg}{kW \cdot m}$

Third approach using volume rate constant from (NAVSEA 1987) quoted by (Fiedel 2011)

CW volumetric flow rate required for each load (NAVSEA 1987) quoted by (Fiedel 2011) $CV_{CW_arc} := 4.5 \frac{\frac{gal}{min}}{3.51685 \text{ kW}} = 0.291 \frac{m^3}{kW \cdot hr}$

CW volume flow rate $V_{CW_arc} := P_{CW_arc} \cdot CV_{CW_arc} = 0.015 \frac{m^3}{s}$

Wall thickness minimum based on calculated OD pg. 5 of NAVSEA, $WT_{CW_arc} := 3.5 \text{ in} - 3.235 \text{ in} = 6.731 \text{ mm}$

CW pipe diameter (minimum 15 mm (Fiedel 2011))	$D_{CW_arc2} := \left(\frac{4 \cdot V_{CW_arc}}{\pi \cdot C_{CW}} \right)^{\frac{2}{5}} + WT_{CW_arc} = 88.89 \text{ mm}$
Cross sectional area	$A_{CW_arc} := N_{pipe} \cdot D_{CW_arc2}^2 \cdot (1 + m_{CW_arc}) = (2.054 \cdot 10^4) \text{ mm}^2$
Cross sectional area per power flow	$\lambda_{CW_arc2} := \frac{A_{CW_arc}}{P_{CW_arc}} = 114.131 \frac{\text{mm}^2}{\text{kW}}$
CW connection weight per meter	
Pipe	$AW_{CW_pipe} := \frac{\pi}{4} \cdot \left((2 \cdot D_{CW_arc2} \cdot WT_{CW_arc}) - (WT_{CW_arc})^2 \right) \cdot \rho_{pipe715} = 8.085 \frac{\text{kg}}{\text{m}}$
Fluid	$AW_{CW_fluid} := \frac{\pi}{4} \cdot (D_{CW_arc2} - WT_{CW_arc})^2 \cdot \rho_{CW} = 5.301 \frac{\text{kg}}{\text{m}}$
Total	$AW_{CW_arc} := N_{pipe} \cdot (AW_{CW_pipe} + AW_{CW_fluid}) \cdot (1 + m_{CW_arc}) = 34.804 \frac{\text{kg}}{\text{m}}$
Weight per power flow length	$\mu_{CW_arc2} := \frac{AW_{CW_arc}}{P_{CW_arc}} = 0.193 \frac{\text{kg}}{\text{kW} \cdot \text{m}}$

CW Summary

$$P_{CW_arc} = 180 \text{ kW} \quad m_{CW_arc} = 0.3$$

$$D_{CW_arc} = \begin{bmatrix} 42.154 \\ 48.26 \\ 88.89 \end{bmatrix} \text{ mm} \quad \lambda_{CW_arc} = \begin{bmatrix} 25.668 \\ 33.641 \\ 114.131 \end{bmatrix} \frac{\text{mm}^2}{\text{kW}} \quad \mu_{CW_arc} = \begin{bmatrix} 0.048 \\ 0.06 \\ 0.193 \end{bmatrix} \frac{\text{kg}}{\text{kW} \cdot \text{m}}$$

FW/HFC system sizing

Initial assumption on energy transferred as heat	$P_{FW_arc} := P_{CW_arc}$
Specific heat of FW (Brown 2020)	$CV_{FW_arc} := CV_{CW_arc} = 0.291 \frac{\text{m}^3}{\text{kW} \cdot \text{hr}}$
FW volume flow rate	$V_{FW_arc} := P_{FW_arc} \cdot CV_{FW_arc} = 0.015 \frac{\text{m}^3}{\text{s}}$
Design fluid velocity for CW oil pg. 796 of Harrington, 1992	$C_{FW} := 5 \cdot \frac{\text{ft}}{\text{s} \cdot \text{in}^{0.5}} = 9.562 \frac{\text{m}^{0.5}}{\text{s}}$
Wall thickness minimum based on calculated OD pg. 5 of NAVSEA,	$WT_{FW_arc} := 3.5 \text{ in} - 3.235 \text{ in} = 6.731 \text{ mm}$
FW pipe diameter (minimum 15 mm (Fiedel 2011))	$D_{FW_arc} := \left(\frac{4 \cdot V_{FW_arc}}{\pi \cdot C_{FW}} \right)^{\frac{2}{5}} + WT_{FW_arc} = 88.89 \text{ mm}$
Margin for corrosion, spacing, etc.	$m_{FW_arc} := 30\%$

Supply and return lines	$N_{pipe} := 2$
Density of FW	$\rho_{FW} := 1 \frac{\text{tonne}}{\text{m}^3}$
Cross sectional area	$A_{FW_arc} := N_{pipe} \cdot D_{FW_arc}^2 \cdot (1 + m_{FW_arc}) = 0.021 \text{ m}^2$
Cross sectional area per power flow	$\lambda_{FW_arc} := \frac{A_{FW_arc}}{P_{FW_arc}} = 114.131 \frac{\text{mm}^2}{\text{kW}}$
CW connection weight per meter	
Pipe	$AW_{FW_pipe} := \frac{\pi}{4} \cdot ((2 \cdot D_{FW_arc} \cdot WT_{FW_arc}) - (WT_{FW_arc})^2) \cdot \rho_{pipe715} = 8.085 \frac{\text{kg}}{\text{m}}$
Fluid	$AW_{FW_fluid} := \frac{\pi}{4} \cdot (D_{FW_arc} - WT_{FW_arc})^2 \cdot \rho_{FW} = 5.301 \frac{\text{kg}}{\text{m}}$
Total	$AW_{FW_arc} := N_{pipe} \cdot (AW_{FW_pipe} + AW_{FW_fluid}) \cdot (1 + m_{FW_arc}) = 34.804 \frac{\text{kg}}{\text{m}}$
Weight per power flow length	$\mu_{FW_arc} := \frac{AW_{FW_arc}}{P_{FW_arc}} = 0.193 \frac{\text{kg}}{\text{kW} \cdot \text{m}}$
<u>SW system</u>	
Assume baseline heat at SW system	$P_{SW_arc} := P_{CW_arc} + P_{LO_arc} = 652.5 \text{ kW}$
	$Q_{SW} := P_{SW_arc}$
Specific heat of FW (Brown 2020)	$cp_{SW} := 3850 \frac{\text{J}}{\text{kg} \cdot \text{K}}$
Operating temperature range for CW (Brown 2020)	$\Delta T_{SW} := 10 \text{ K}$
SW mass flow rate	$\hat{m}_{SW_arc} := \frac{Q_{SW}}{cp_{SW} \cdot \Delta T_{SW}} = 16.948 \frac{\text{kg}}{\text{s}}$
SW density	$\rho_{SW} := 1.025 \frac{\text{tonne}}{\text{m}^3} = 1.025 \frac{\text{tonne}}{\text{m}^3}$
SW volume flow rate	$V_{SW_arc} := \hat{m}_{SW_arc} \cdot \frac{1}{\rho_{SW}} = 59.525 \frac{\text{m}^3}{\text{hr}}$
Design fluid velocity for seawater pg. 796 of Harrington, 1992	$C_{SW} := 3 \cdot \frac{\text{ft}}{\text{s} \cdot \text{in}^{0.5}} = 5.737 \frac{\text{m}^{0.5}}{\text{s}}$
Wall thickness minimum based on calculated OD pg. 5 of NAVSEA,	$WT_{SW_arc} := 1.385 \text{ in} = 35.179 \text{ mm}$
SW pipe diameter (127-162 mm, pg. 192 UCL-NAME	$D_{SW_arc} := \left(\frac{4 \cdot V_{SW_arc}}{\pi \cdot C_{SW}} \right)^{\frac{2}{5}} + WT_{SW_arc} = 141.308 \text{ mm}$

Margin	$m_{SW_arc} := 30\%$
Supply and return lines	$N_{pipe} := 2$
Cross sectional area	$A_{SW_arc} := N_{pipe} \cdot D_{SW_arc}^2 \cdot (1 + m_{SW_arc}) = (5.192 \cdot 10^4) \text{ mm}^2$

Cross sectional area per power flow $\lambda_{SW_arc} := \frac{A_{SW_arc}}{P_{SW_arc}} = 79.566 \frac{\text{mm}^2}{\text{kW}}$

SW connection weight per meter

Pipe $AW_{SW_pipe} := \frac{\pi}{4} \cdot ((2 \cdot D_{SW_arc} \cdot WT_{SW_arc}) - (WT_{SW_arc})^2) \cdot \rho_{pipe715} = 61.123 \frac{\text{kg}}{\text{m}}$

Fluid $AW_{SW_fluid} := \frac{\pi}{4} \cdot (D_{SW_arc} - WT_{SW_arc})^2 \cdot \rho_{SW} = 9.067 \frac{\text{kg}}{\text{m}}$

Total $AW_{SW_arc} := N_{pipe} \cdot (AW_{SW_pipe} + AW_{SW_fluid}) \cdot (1 + m_{SW_arc}) = 182.495 \frac{\text{kg}}{\text{m}}$

Weight per power flow length $\mu_{SW_arc} := \frac{AW_{SW_arc}}{P_{SW_arc}} = 0.28 \frac{\text{kg}}{\text{kW} \cdot \text{m}}$

Hydraulic system

Control surfaces maximum lift forces (pg. 74 UCL-NAME 2014) for rudders, fore planes, aft planes, respectively, using submerged displacement type 2400 (Wrobel 1984)

$$k := \begin{bmatrix} 0.2 \\ 0.15 \\ 0.1 \end{bmatrix} \quad F_{max} := k \cdot 2400 \cdot 20^2 \cdot \text{kN} = \begin{bmatrix} 192 \\ 144 \\ 96 \end{bmatrix} \text{ MN}$$

Initial estimate hydraulic plant capacity (pg. 123 UCL-NAME 2014) using submerged displacement type 2400 (Wrobel 1984)

$$V_{HY_plant} := 0.024 \cdot 2400 \cdot \frac{L}{\text{min}} = 57.6 \frac{L}{\text{min}}$$

Assume hydraulic volume flow rate, 60 L/min (pg. 9 Type 2400 (Wrobel 1984)) 25 gpm (pg. 188 UCL-NAME 2014)

$$V_{HY_arc} := \begin{bmatrix} 60 \frac{L}{\text{min}} \\ 25 \frac{\text{gal}}{\text{min}} \end{bmatrix} = \begin{bmatrix} 3.6 \\ 5.678 \end{bmatrix} \frac{\text{m}^3}{\text{hr}}$$

Design fluid velocity for seawater pg. 796 of Harrington, 1992

$$C_{HY} := 1.5 \cdot \frac{\text{ft}}{\text{s} \cdot \text{in}^{0.5}} = 2.869 \frac{\text{m}^{0.5}}{\text{s}}$$

Wall thickness minimum based on calculated OD pg. 5 of NAVSEA,

$$WT_{HY_arc} := 1.25 \text{ in} - 1.103 \text{ in} = 3.734 \text{ mm}$$

Diameter hydraulic pipe

$$D_{HY_arc} := \left(\frac{4 \cdot V_{HY_arc}}{\pi \cdot C_{HY}} \right)^{\frac{2}{5}} + WT_{HY_arc} = \begin{bmatrix} 49.326 \\ 58.442 \end{bmatrix} \text{ mm}$$

Margin

$$m_{HY_arc} := 30\%$$

Cross sectional area

$$A_{HY_arc} := N_{pipe} \cdot D_{HY_arc}^2 \cdot (1 + m_{HY_arc}) = \begin{bmatrix} 6.326 \cdot 10^3 \\ 8.88 \cdot 10^3 \end{bmatrix} \text{ mm}^2$$

Assume hydraulic working pressure range (172-207 bar)
pg. 188 UCL-NAME 2014

$$P_{hydraulic} := 207 \text{ bar}$$

Density of XO30 fluid
Renolin [805-913]

$$\rho_{HY} := 913 \frac{\text{kg}}{\text{m}^3}$$

$$P_{HY} := V_{HY_arc} \cdot P_{hydraulic} = \begin{bmatrix} 20.7 \\ 32.649 \end{bmatrix} \text{ kW}$$

HY connection weight per meter

Pipe
$$AW_{HY_pipe} := \frac{\pi}{4} \cdot ((2 \cdot D_{HY_arc} \cdot WT_{HY_arc}) - (WT_{HY_arc})^2) \cdot \rho_{pipe715} = \begin{bmatrix} 2.489 \\ 2.967 \end{bmatrix} \frac{\text{kg}}{\text{m}}$$

Fluid
$$AW_{HY_fluid} := \frac{\pi}{4} \cdot (D_{HY_arc} - WT_{HY_arc})^2 \cdot \rho_{HY} = \begin{bmatrix} 1.491 \\ 2.146 \end{bmatrix} \frac{\text{kg}}{\text{m}}$$

Pipe weight per length
$$AW_{HY_arc} := N_{pipe} \cdot (AW_{HY_pipe} + AW_{HY_fluid}) \cdot (1 + m_{HY_arc}) = \begin{bmatrix} 10.346 \\ 13.293 \end{bmatrix} \frac{\text{kg}}{\text{m}}$$

Trim and ballast system**Hard system**

Assume volume flow rate
- pg. 127 UCL-NAME 2014
- pg. 197 UCL-NAME 2014
- pg. 9 Wrobel 1984

$$V_{TB_H} := \begin{bmatrix} 22 \\ 55 \\ 20 \end{bmatrix} \frac{\text{m}^3}{\text{hr}}$$

Design fluid velocity for seawater
pg. 796 of Harrington, 1992

$$C_{TB} := C_{SW} = 5.737 \frac{\text{m}^{\frac{1}{2}}}{\text{s}}$$

Wall thickness minimum based on
calculated OD pg. 5 of NAVSEA,

$$WT_{TB_H_arc} := 3.5 \text{ in} - 2.701 \text{ in} = 20.295 \text{ mm}$$

Diameter pipe

$$D_{TB_H_arc} := \left(\frac{4 \cdot V_{TB_H}}{\pi \cdot C_{TB}} \right)^{\frac{2}{5}} + WT_{TB_H_arc} = \begin{bmatrix} 3.605 \\ 4.847 \\ 3.5 \end{bmatrix} \text{ in}$$

Margin

$$m_{TB_H_arc} := 30\%$$

Number of pipe

$$N_{pipe} := 1$$

Cross sectional area

$$A_{BT_H_arc} := N_{pipe} \cdot D_{TB_H_arc}^2 \cdot (1 + m_{TB_H_arc}) = \begin{bmatrix} 1.09 \cdot 10^4 \\ 1.971 \cdot 10^4 \\ 1.027 \cdot 10^4 \end{bmatrix} \text{ mm}^2$$

TB hard connection weight per meter

Pipe
$$AW_{TB_H_pipe} := \frac{\pi}{4} \cdot ((2 \cdot D_{TB_H_arc} \cdot WT_{TB_H_arc}) - (WT_{TB_H_arc})^2) \cdot \rho_{pipe715} = \begin{bmatrix} 23.206 \\ 32.199 \\ 22.446 \end{bmatrix} \frac{\text{kg}}{\text{m}}$$

Reference MIL-HDBK class 3300
NAVSEA, 1978

$$17 \frac{\text{lb}}{\text{ft}} = 25.299 \frac{\text{kg}}{\text{m}}$$

Fluid $AW_{TB_H_fluid} := \frac{\pi}{4} \cdot (D_{TB_H_arc} - WT_{TB_H_arc})^2 \cdot \rho_{SW} = \begin{bmatrix} 4.089 \\ 8.512 \\ 3.789 \end{bmatrix} \frac{\text{kg}}{\text{m}}$

Weight per meter $AW_{BT_H_arc} := N_{pipe} \cdot (AW_{TB_H_pipe} + AW_{TB_H_fluid}) \cdot (1 + m_{TB_H_arc}) = \begin{bmatrix} 35.484 \\ 52.924 \\ 34.106 \end{bmatrix} \frac{\text{kg}}{\text{m}}$

Soft system

Assume various flow rates
- pg. 127 UCL-NAME 2014
- pg. 197 UCL-NAME 2014

$$V_{TB_S} := \begin{bmatrix} 5 \\ 22 \\ 14 \end{bmatrix} \frac{\text{m}^3}{\text{hr}}$$

Wall thickness minimum based on
calculated OD pg. 5 of NAVSEA,

$$WT_{TB_S_arc} := 2.5 \text{ in} - 2.342 \text{ in} = 4.013 \text{ mm}$$

Low pressure bilge system diameter
Reference (UCL-NAME 2014):
-44.5 mm pg. 196 discharge line
-57 mm pg. 196 suction line
-108 mm pg. 197 suction line
-76.1 mm pg. 197 discharge line

$$D_{TB_S_arc} := \left(\frac{4 \cdot V_{TB_S}}{\pi \cdot C_{TB}} \right)^{\frac{2}{5}} + WT_{TB_S_arc} = \begin{bmatrix} 43.417 \\ 75.286 \\ 63.498 \end{bmatrix} \text{ mm}$$

Margin

$$m_{TB_S_arc} := 30\%$$

Number of pipe

$$N_{pipe} := 1$$

Cross sectional area

$$A_{BT_S_arc} := N_{pipe} \cdot D_{TB_S_arc}^2 \cdot (1 + m_{TB_H_arc}) = \begin{bmatrix} 2.451 \cdot 10^3 \\ 7.368 \cdot 10^3 \\ 5.242 \cdot 10^3 \end{bmatrix} \text{ mm}^2$$

TB soft connection weight per meter

Pipe $AW_{TB_S_pipe} := \frac{\pi}{4} \cdot ((2 \cdot D_{TB_S_arc} \cdot WT_{TB_S_arc}) - (WT_{TB_S_arc})^2) \cdot \rho_{pipe715} = \begin{bmatrix} 2.334 \\ 4.13 \\ 3.466 \end{bmatrix} \frac{\text{kg}}{\text{m}}$

Fluid $AW_{TB_S_fluid} := \frac{\pi}{4} \cdot (D_{TB_S_arc} - WT_{TB_S_arc})^2 \cdot \rho_{SW} = \begin{bmatrix} 1.25 \\ 4.089 \\ 2.849 \end{bmatrix} \frac{\text{kg}}{\text{m}}$

Weight per meter $AW_{TB_S_arc} := N_{pipe} \cdot (AW_{TB_S_pipe} + AW_{TB_S_fluid}) \cdot (1 + m_{TB_H_arc}) = \begin{bmatrix} 4.659 \\ 10.685 \\ 8.209 \end{bmatrix} \frac{\text{kg}}{\text{m}}$

High pressure air system

Assume volume flow rate - pg. 9 Wrobel 1984	$V_{HP_arc} := 1.7 \frac{m^3}{min} = 0.028 \frac{m^3}{s}$
Assume air velocity	$v_{HP_arc} := v_{AR} = 38.58 \frac{m}{s}$
Wall thickness minimum based on calculated OD pg. 5 of NAVSEA,	$WT_{HP_arc} := 1.315 \text{ in} - 1.204 \text{ in} = 0.111 \text{ in}$
High pressure air pipe diameter	$D_{HP_arc} := 2 \cdot \left(\frac{V_{HP_arc}}{v_{HP_arc}} \cdot \frac{1}{\pi} \right)^{0.5} + WT_{HP_arc} = 33.398 \text{ mm}$
for corrosion, spacing, etc.	$m_{HP_arc} := 30\%$
Ring main configuration	$N_{pipe} := 1$
Cross sectional area	$A_{HP_arc} := N_{pipe} \cdot D_{HP_arc}^2 \cdot (1 + m_{HP_arc}) = (1.45 \cdot 10^3) \text{ mm}^2$
Pipe weight per meter	$AW_{HP_pipe} := \frac{\pi}{4} \cdot ((2 \cdot D_{HP_arc} \cdot WT_{HP_arc}) - (WT_{HP_arc})^2) \cdot \rho_{pipe715} = 1.267 \frac{kg}{m}$
Weight per meter	$AW_{HP_arc} := N_{pipe} \cdot AW_{HP_pipe} \cdot (1 + m_{HP_arc}) = 1.647 \frac{kg}{m}$
Seawater density	$\rho_{SW} = (1.025 \cdot 10^3) \frac{kg}{m^3}$
Assume snorting depth	$Depth_{snort} := 10 \text{ m}$
Hydrostatic pressure at snorting depth	$P_{hydrostatic} := \rho_{SW} \cdot g \cdot Depth_{snort} + 1 \text{ atm} = 1.992 \text{ atm}$
Assume MBT volume from type 2400 (Wrobel 1984)	$V_{mbt} := (163.260 + 469.753 - 35.25 - 139.753) \text{ m}^3 = 458.01 \text{ m}^3$
Assume permeability and blow ability of MBT tanks	$k_{mbt} := 0.9$
Assume submerged dis- placement using type 2400 (Wrobel 1984)	$V_{sub} := 2400 \text{ tonne} \cdot \frac{1}{\rho_{SW}} = (2.341 \cdot 10^3) \text{ m}^3$
Assume reserve of buoyancy	$RoB := 11\%$
Assume MBT volume	$V_{mbt} := \frac{V_{sub}}{k_{mbt}} \cdot \frac{RoB}{1 + RoB} = 257.819 \text{ m}^3$
Assume number of blows un- til subsequent charge	$N_{blow} := 3$
Volume high-pressure air required to fully blow MBT at snorting depth	$V_{HP_req} := V_{mbt} \cdot \frac{P_{hydrostatic}}{1 \text{ atm}} \cdot N_{blow} \cdot k_{mbt} = (1.387 \cdot 10^3) \text{ m}^3$

Assume HP air pressure pg. 200 Burcher and Rydill 1994	$V_{bottle_capacity} := \frac{300 \text{ bar} \cdot 0.26 \text{ m}^3}{1 \text{ atm}} = 76.98 \text{ m}^3$
Number of bottles reference: 21 (UCL-NAME 2014)	$N_{bottle} := \text{round}\left(\frac{V_{HP_req}}{V_{bottle_capacity}}\right) = 18$
Design diving depth	$DDD := 250 \text{ m}$
Assume DDSTP/MED	$DDSTP := DDD \cdot 120\% = 300 \text{ m}$
Hydrostatic pressure at DDSTP	$P_{hydrostatic_DDSTP} := \rho_{SW} \cdot g \cdot DDSTP + 1 \text{ atm} = 30.761 \text{ atm}$
Volume high-pressure air required to fully blow MBT	$V_{HP_req} := V_{mbt} \cdot \frac{P_{hydrostatic_DDSTP}}{1 \text{ atm}} \cdot 1 = (7.931 \cdot 10^3) \text{ m}^3$
Number of bottles required to fully blow MBT at DDSTP (emergency blow)	$N_{bottle} := \text{round}\left(\frac{V_{HP_req}}{V_{bottle_capacity}}\right) = 103$
Assume number of bottles for emergency blow at DDSTP (UCL-NAME 2014 and Wrobel 1984)	$N_{bottle_DDSTP} := 8$
Volume available from the bottles	$V_{air_DDSTP} := N_{bottle_DDSTP} \cdot V_{bottle_capacity} = 615.84 \text{ m}^3$
Volume displaced by the high pressure air at DDSTP	$V_{blow_DDSTP} := V_{air_DDSTP} \cdot \frac{1 \text{ atm}}{P_{hydrostatic_DDSTP}} = 20.02 \text{ m}^3$
Only blow 8% of VMBT at	$\frac{V_{blow_DDSTP}}{V_{mbt}} = 0.078$
<u>Low pressure air system</u>	
Assume volume flow rate pg 201 UCL-NAME 2014	$V_{LP_arc} := 43 \frac{\text{m}^3}{\text{min}} = 0.717 \frac{\text{m}^3}{\text{s}}$
Assume air velocity	$v_{LP_arc} := v_{AR} = 38.58 \frac{\text{m}}{\text{s}}$
Wall thickness minimum based on calculated OD pg. 5 of NAVSEA,	$WT_{LP_arc} := 6.625 \text{ in} - 6.055 \text{ in} = 14.478 \text{ mm}$
Low pressure bilge system diameter Reference SDB 139.7 mm pg. 201 (UCL-NAME 2014):	$D_{LP_arc} := 2 \cdot \left(\frac{V_{LP_arc}}{v_{LP_arc}} \cdot \frac{1}{\pi}\right)^{0.5} + WT_{LP_arc} = 168.269 \text{ mm}$
Number of pipe	$N_{pipe} := 1$
Cross sectional area	$A_{LP_arc} := N_{pipe} \cdot D_{LP_arc}^2 = (2.831 \cdot 10^4) \text{ mm}^2$
Pipe weight per meter	$AW_{LP_pipe} := \frac{\pi}{4} \cdot \left((2 \cdot D_{LP_arc} \cdot WT_{LP_arc}) - (WT_{LP_arc})^2\right) \cdot \rho_{pipe715} = 32.742 \frac{\text{kg}}{\text{m}}$
Weight per meter	$AW_{LP_arc} := N_{pipe} \cdot AW_{LP_pipe} = 32.742 \frac{\text{kg}}{\text{m}}$